UNIVERSITY OF STRATHCLYDE

THE ANALYSIS OF SHEAR WALL STRUCTURES AND THEIR INTERACTION WITH ELASTIC FOUNDATIONS

Norman W. Adams, B.Sc.

Department of Civil Engineering

A thesis presented for the degree of

Doctor of Philosophy in Civil Engineering

1974

SYNOPSIS

The various structural forms commonly adopted for the construction of multi-storey structures are outlined and the advantages of the use of shear walls as the load bearing elements in such structures are indicated. It is shown that, although a considerable amount of research has been devoted to the analysis of multi-storey structures, very little attention has been paid to the effects of foundation deformations on these structures. Three methods for the analysis of shear wall structures are indicated and the suitability of the continuous connection technique for the investigation of the effects of foundation deformations is shown.

Two-dimensional coupled shear wall systems and single walls or box cores, all of which may be based on elastic foundations are analysed subjected to either of two generalised distributions of horizontal forces. The expressions derived for plane coupled shear walls are adapted to produce methods whereby design curves may be drawn for the rapid evaluation of stresses and deflections.

The relationships derived for the two-dimensional analysis are used to derive a method for the analysis of the load distribution in three-dimensional multi-storey shear wall structures subjected to any system of lateral loads which may produce bending and torsion of the structure.

The suitability of the analytical methods for the numerical computation of problems involving shear wall structures is discussed with particular reference to the feasibility of hand calculations and the development of a useful system of programs for computer analysis.

The results of a number of numerical studies, carried out with the aid of the computer programs, are given to illustrate various aspects of the theory. The importance of accurately determining the extent and nature of the lateral load bearing systems within a structure is illustrated. The convergence of solutions obtained using the two load distributions are compared and the applications of each are discussed. The effects of varying the flexibility of

the foundations, both of a two-dimensional coupled wall system and of specific walls in three-dimensional structures are illustrated by examples.

A description is given of an experimental investigation carried out to study the effects of the elastic deformation of foundations on model shear wall structures constructed from "Perspex" sheets. The results of a comprehensive series of tests on the models are compared with the corresponding analytical solutions in order to assess the validity of the assumptions which were made in the derivation of the analytical methods.

ACKNOWLEDGEMENTS

The research reported in this thesis was carried out while the author was a postgraduate student in the Department of Civil Engineering of the University of Strathclyde.

Acknowledgement is due to the Science Research Council for their financial assistance during the period of study.

The author wishes to express gratitude to the following members of staff of the University:-

Professor A. Coull, B.Sc., Ph.D., C.Eng., F.R.S.E., F.I.C.E., F.I.Struct.E., F.A.S.C.E., for suggesting the topic of the research and for his advice and guidance during the course of study.

Douglas M. Logan, B.Sc., for his advice on the development of the computer programs.

The members of the operating staff at the University Computer Centre for their help in the running of the computer programs.

Jack Morrin and the staff of the Structures Laboratory for their assistance in the construction of the experimental apparatus.

Frank Murphy for his work in fabricating the model structures and the foundation mechanism to a high standard.

Miss Catherine Drummond for her neat and diligent typing of the text of the thesis.

CONTENTS

NOTATION

The following symbols, used in this thesis, are introduced under four headings as follows:

1. Dimensions and properties of shear walls

$A_1 A_2$	Cross sectional areas of walls 1 and 2
A_b	Cross sectional area of connecting beam or effective floor slab
b	Clear distance between walls in line
b_c	Effective span of connecting beam or slab
$d_1 d_2 d_3 d_4$	Dimensions from centroids of walls to extreme fibres
$E_1 E_2$	Moduli of elasticity for walls 1 and 2
E_c	Modulus of elasticity for connecting beams or slabs
G_c	Modulus of rigidity for connecting beams or slabs
h	Storey height
H	Total height of walls
$I_1 I_2$	Moments of inertia of walls 1 and 2
I	Moment of inertia of combined section of walls
I_b	Moment of inertia of connecting beam or effective floor slab
I_c	Moment of inertia, I_b, reduced to account for shear deformations
K_θ	Rotational Flexibility Modulus for foundations
K_v	Vertical Flexibility Modulus for foundations
ℓ	Distance between centroids of walls in line
$k\ell$	Distance between centroid of wall 1 and centroid of combined section of walls
ν	Poisson's Ratio for connecting beams or slabs

α μ Dimensionless groups

γ Dimensionless foundation coefficient of rotation

Δ Dimensionless foundation coefficient of vertical deflection

2. Two-dimensional analysis

$a_0 a_1$ -- a_n -- a_m Constant coefficients of shear function series

C_1, C_2, C_3, C_4, D_1, D_2, D_3 Dimensionless constant terms

F_i^q Shear force in i'th connecting beam or slab

F_i^t Axial force in i'th connecting beam or slab

i Suffix denoting storey number

I Total number of storeys, suffix denoting top storey

K_1 to K_8 Constants of integration

L, U Suffices denoting levels below and above level of a point load

M_0 Total base moment

M_{01}, M_{02} Base moments on walls 1 and 2

$M_A(x)$ Moment of applied load at level x

$M(x)$ Sum of bending moments on walls 1 and 2

$M_1(x)$, $M_2(x)$ Bending moments on walls 1 and 2

$M_c(x)$ Moment of the axial forces in connecting medium

$M_{T1}(x)$, $M_{T2}(x)$ Moment of the shear forces in connecting medium about centroids of walls 1 and 2

m Largest exponent in polynomial series,/total number of point loads

n Particular exponent,/suffix of particular point load

p_n Polynomial load coefficient,/point load

$p(x)$ Intensity of applied load at level x

$P_A(x)$	Sum of applied load above level x
$P_C(x)$	Sum of axial forces in connecting medium above level x
$q(x)$	Intensity of shear force in connecting medium
$Q_1(x)$, $Q_2(x)$	Shear forces in walls 1 and 2
Q	Shear force at top of walls
r	Any integer
$t(x)$	Intensity of axial force in connecting medium
T_0	Axial force on base of shear walls
$T(x)$	Axial force at level x
x	Dimensionless level above base, as a proportion of H
x_i	Level of i'th connecting beam
x_n	Level of a particular point load
$y(x)$	Horizontal deflection
δ_1, δ_2, δ_3, δ_4	Partial relative deflections of the 'cut' ends of connecting lamina
δ_θ	Rotation of foundations
δ_v	Relative vertical deflection of foundations
χ	Height above base
η	Supplementary variable of height
π	3.14159
!	Factorial
$\sum$	Summation

3. Design methods

K_1K_2	Wall bending stress factors
K_3	Connecting beam shear force factor
K_4	Maximum wall deflection factor
λ_1	Axial force factor

λ_2	Applied force factor
σ	Stress

4. Analysis of complete structure

$\underline{B}_1, \underline{B}_2, \underline{B}_3$	Constant matrices of stiffness coefficients
C	Torsional stiffness of wall assembly
f_{in}	Flexibility coefficient for deflection
f'_{in}	Flexibility coefficient for rotation
$\underline{F}_j$	Matrix of flexibility coefficients f_{in} for the j'th wall assembly
$\underline{F}'_j$	Matrix of rotation flexibility coefficients f'_{in} for the j'th wall assembly
i	Suffix denoting reference level number
j	Suffix denoting wall assembly number
J	Number of wall assemblies
M_i	Moment of applied load at reference level i, about datum position
$\underline{M}$	Vector of moments M_i
P_i	Shear force on wall at level i
$\underline{P}_j$	Vector of shear forces P_i on wall j
$\underline{p}_j$	Vector of polynomial coefficients/point loads on wall j
s_{in}	Integration coefficient/step coefficient
$\underline{S}$	Matrix of coefficients s_{in}
t_n	Polynomial torque coefficient/point torque
T(x)	Intensity of applied torque at level x
T_i	Total torque on wall at level i
$\underline{T}_j$	Vector of total torquesT_i on wall j
$\underline{t}_j$	Vector of torque coefficients/point torques on wall j

W_i	Sum of loading applied above level i, acting at datum position
$\underline{W}$	Vector of loads W_i
x_i	Relative height of i'th reference level
y_{ij}	Deflection of wall j at reference level i
y_i	Deflection of structure at datum position at level i
$\underline{Y}_j$	Vector of deflections y_{ij} of wall j
$\underline{Y}$	Vector of structure deflections y_i
z_j	Distance of wall j from datum position
θ_i	Rotation of structure at level i
$\underline{\theta}$	Vector of structure rotations θ_i

LIST OF PLATES

LIST OF FIGURES

A list of design charts is included in the Appendix

LIST OF TABLES

CHAPTER 1

INTRODUCTION

1.1 MULTI-STOREY STRUCTURES

In the centres of large industrial cities land for residential and commercial building purposes has for long been at a premium. With the rapid increase of land costs a greater number of multi-storey structures are being built every year, and it is becoming more economical to make use of sites where poor ground conditions formerly ensured their use for low-rise construction. In the suburbs the high price of land linked with the social demands for open recreational space within residential areas and the preservation of "green belts" around cities ensures the continued use of medium- and high-rise construction for residential purposes.

With the increase in the use of light partitioning and high strength concrete and steel reinforcement, resulting in an overall reduction in weight, the effects of wind or seismic loading have become a major factor in the design of tall structures, and some form of bracing must be incorporated to resist these lateral forces. The structural systems currently in use are of several distinct types and the one adopted as most economical in a particular situation depends, to a large extent on the number of storeys and the magnitude of the expected lateral forces.

Within earthquake zones the use of concrete frames as bracing may be restricted to medium-rise buildings. Outwith seismic regions the maximum economic height of concrete frame buildings is generally between fifteen to twenty storeys. Buildings which derive the whole of their lateral strength from shear walls are feasible up to between thirty and forty storeys. Above these heights systems comprising frames interacting with shear walls, framed tube systems, or multiple framed tube systems may be adopted depending on the height and the functional requirements of the building, as discussed by Khan and Iyengar[1].

Structures comprising shear walls may be planned such that these

vertical- and lateral-load bearing elements are so disposed as to simultaneously partition floor areas, enclose stair-wells, lifts and service cores, and provide a degree of both fire resistance and accoustic insulation.

The functional and practical requirements of the planning and construction of multi-storey buildings, (including such aspects as daylighting regulations, access corridors, simplicity of layout, repetition of structural elements to enable the use of industrial building methods, etc.) tend to evolve buildings of long rectangular plan in which the structural elements take the form of similar assemblies of walls coupled by floor slabs or lintel beams with their common planes at right angles to the length of the building. The object of the research embodied in this thesis is to examine the distribution of forces within such structural systems under the action of lateral loads.

1.2 PREVIOUS RESEARCH

In recent years there has been considerable interest in the topic of multi-storey structures, as witnessed by the vast array of published works devoted to various aspects of the subject. The extent of work on shear wall structures published prior to 1965 was reviewed by Coull and Stafford Smith[2]. The majority of the earlier studies and many of the more recent works deal exclusively with two-dimensional systems, with built-in foundations, and subjected to specific, simple lateral load forms in their own plane. Latterly, more attention has been devoted to the problems of analysing complete three-dimensional structures. Present techniques for the analysis of two- and three-dimensional systems were reviewed by a committee of the American Concrete Institute[3] and by Stamato[4]. Both sources give comprehensive lists of the more readily available literature.

1.3 DEFORMATION OF FOUNDATIONS

Published works which deal with the effects of foundation deformations on multi-storey structures are few in number, and deal in the main with two-dimensional systems. Coull investigated the effects of a finite differential settlement between the foundations

of two coupled walls[5], and presented an analysis for coupled shear walls supported on elastic foundations and subjected to the simple lateral load cases of a uniformly and a triangularly distributed load and a point load at the top[6]. In view of the nature of wind and seismic forces the duration of the stressing of foundations will be short and the assumption that the subgrade behaves in an elastic manner will be sufficiently reasonable to give an insight into the effects of foundation movements.

Information on the effects of foundation deformations in three-dimensional shear wall structures, either from measurements of actual buildings or from laboratory tests on models is very limited. There is therefore scope for both analytical and laboratory investigation in this field. The development of a method whereby rapid quantitative solutions to problems of a variety of structures with varying foundation characteristics would enable a qualitative assessment of the effects involved.

1.4 METHODS OF ANALYSIS

The relative merits and the limitations of the three methods which are generally adopted for the analysis of coupled shear walls are well documented in, for example, references (3) and (4). In the frame analogy the coupled wall system is analysed as a frame in which the width of the walls is incorporated by the use of rigid joints of finite dimensions to link the ends of the connecting beams to the columns. The finite element method considers the structure to be divided into a mesh of two-dimensional elements in plane stress which is solved, subject to the appropriate boundary conditions, by matrix techniques. In the third method, the continuum approach, the individual connecting beams are replaced by a continuous connection of laminae of equivalent stiffness, in which it is assumed that the point of contraflexure of each lamina is at its mid-span. The effects of foundation deformations may be incorporated in each of the methods.

Of the three methods, the frame analogy and the finite element technique are basically discrete analyses and are readily adaptable to the variations in geometry encountered in actual structures. However,

the amount of computation involved in these methods increases with height and makes them less suitable for the investigation of the basic behaviour of coupled wall systems. The accuracy of the continuous connection technique, on the other hand, increases with height without additional computation. Although the use is restricted to systems with regular dimensions throughout their height, analysis by hand or with a desk calculator is feasible in many instances, and the method is readily adaptable for use on a digital computer of limited size. The continuous connection technique is therefore adopted in this thesis to develop a method whereby the behaviour of two- and three-dimensional shear wall systems, which are able to undergo foundation deformation, may be assessed both on a general qualitative approach and, in specific cases, as part of the intermediate design prior to a more rigorous analysis.

1.5 SCHEME OF THE THESIS

This thesis is concerned with the investigation of multi-storey structures essentially comprising parallel assemblies of two-dimensional shear walls of various forms, under the action of lateral wind and seismic loads. Particular attention is paid to the effects of foundation deformations which are assumed to be elastic. The material contained in the thesis may conveniently be classified as either analytical or experimental.

The first section of analysis deals with two-dimensional shear wall systems, and covers both isolated and coupled walls, the latter being analysed by means of the continuous connection technique. Walls are loaded in their own plane by horizontal forces of two generalised forms and foundations are assumed to undergo simultaneous rotational and vertical elastic deformations. The expressions derived for plane coupled shear walls are then adapted to produce methods whereby design curves may be drawn for the rapid evaluation of stresses and deflections in the two-dimensional system.

The force-deflection relationships derived for two-dimensional structures are used in the development of two similar methods for the analysis of the distribution of forces amongst the component plane systems of complete multi-storey buildings subjected to any system of lateral wind or seismic forces which causes bending and torsion of the structure, and which has been reduced to a statically

equivalent load form. The two methods differ only in the assumed form of the forces distributed to the plane systems, and the results obtained from both are suitable for use in the further evaluation of the expressions for forces and deformations in the two-dimensional analysis.

Numerical computation of the analytical methods is discussed with reference to the feasibility of hand calculations, the development of a useful system of programs for computer analysis and the convergence of the two methods.

A description is given of an experimental investigation carried out to study the effects of the elastic deformation of foundations on perspex models of shear wall structures. The results of the tests are compared with the relevant analytical solutions in order to assess the validity of the latter.

The results of numerical studies, carried out with the aid of the computer programs, are given to illustrate the effects of varying the flexibility of the foundations, both of a two-dimensional coupled wall system, and of specific walls in complete structures.

1.5.1 LAYOUT OF THE MANUSCRIPT

The expressions derived in the analysis of Chapters 2, 3 and 4 are referred to numerically in eight groups. These and the expressions relevant to each are numbered sequentially throughout. The symbols used in the analysis are defined locally as each is introduced, and a general list of the notation is included at the beginning of the thesis.

Figures, tables and graphs are referred to by chapter number and are included at the end of the relevant chapter.

CHAPTER 2

THE ANALYSIS OF TWO-DIMENSIONAL SHEAR WALL SYSTEMS

2.1 INTRODUCTION

2.1.1 TYPES OF WALLS

The configurations of shear walls for which the analysis is presented fall into three groups..

The first of these consists of a pair of shear walls of equal height,in the plane common to the applied load, and structurally connected throughout their height by a regular array of beams or floor slabs. The individual walls may be of various configurations, typical of which are rectangular walls, walls with flanges, lift shafts and service cores. The two walls need not be of the same configuration.

The second group consists of three shear walls again of equal height and in the same plane. The two outer walls must be of identical section and symmetrically spaced about the centre wall. The outer walls are connected to the inner wall by identical arrays of regularly spaced beams or floor slabs.

Included in the third group are single shear walls, lift shafts and service cores where they cannot be considered as being structurally connected to other elements in the same plane.

2.1.2 FOUNDATIONS

The analysis is basically presented for shear walls which have elastic foundations. Walls are able to undergo rotation and vertical deflection, depending on the elastic properties of the foundation medium. In the limit either rotation or vertical deflection or both may be prevented. In addition to the general elastic foundation, equations are presented for the fully rigid case.

2.1.3 APPLIED LOADING

In general the shear wall system is loaded with any lateral horizontal force distribution in the plane being considered. In

the analysis the load distribution is represented in two ways.

In the first instance the load is expressed by a polynomial series of the general form,

$$P(x) = P_0 + P_1x + P_2x^2 + ... + P_nx^n + ... + P_mx^m \quad (1.1)$$

x is the dimensionless relative height above the base, as given by

$$x = \frac{X}{H} \quad (1.2)$$

X is the absolute height above base datum

H is the total height of the shear wall system.

The non-dimensional height co-ordinate is used throughout the analysis and ensures that all the polynomial coefficients, p have the same dimensional units of force/unit height.

Secondly, the applied load distribution is represented by a suitable array of discrete point loads denoted by

$$P_1, P_2, P_3, ... P_n, ... P_m \quad (1.3)$$

acting at any convenient set of relative heights

$$x_1, x_2, x_3, ... x_n, ... x_m \quad (1.4)$$

respectively.

2.2 GENERAL ASSUMPTIONS

2.2.1 STRUCTURAL

The general assumptions relating to the structural action of all the shear wall systems are as follows:

1. All shear wall elements are of uniform section throughout their height, and perpendicular to the base.
2. All material is both homogeneous and isotropic.
3. No part of any shear wall system is stressed beyond its elastic limit.

4. All sections which are plane initially remain plane under load.

2.2.2 FOUNDATION

The foundation of any shear wall element is assumed to be perfectly elastic in both tension and compression, and is able to deform in two mutually independent ways.

1. VERTICAL DEFORMATION.

The axial force at foundation level of any element is denoted by T_0, tension being assumed positive. T_0 is directly proportional to the vertical deflection, δ_v, which it causes, as given by

$$\delta_v = K_v T_0 \qquad (1.5)$$

K_v will be termed the Vertical Flexibility Modulus of the foundation.

2. ROTATIONAL DEFORMATION

The moment imposed by any element on its foundation is denoted by M_0, clockwise being assumed positive. M_0 causes a rotation of the foundation, δ_θ, to which it is directly proportional, as given by

$$\delta_\theta = K_\theta M_0 \qquad (1.6)$$

K_θ will be termed the Rotational Flexibility Modulus of the foundation.

Both moduli are constant for any given foundation. In the limit either K_v or K_θ are made zero to give complete rigidity in the vertical or rotational sense, respectively. A fully built-in foundation condition is represented by

$$K_v = K_\theta = 0 \qquad (1.7)$$

2.3 PAIR OF COUPLED SHEAR WALLS ON ELASTIC FOUNDATIONS

2.3.1 GENERAL ANALYSIS

The typical configuration of a pair of coupled shear walls, on elastic foundations, as shown in figure 2.1 will be analysed for the general load distribution P(x). The continuous connection technique

is used to derive the differential equations which govern the system.

I CONTINUOUS CONNECTION ASSUMPTIONS

The basic assumptions which are made to enable the use of the continuous connection technique are:-

1. The beams connecting the shear walls are of equal length, area and stiffness, and are regularly spaced throughout the height of the walls.

2. The discrete connecting beams, which have an effective moment of inertia, as reduced for shear deformation, of I_c, are replaced by a continuous system of laminae with the equivalent inertia I_c/h per unit height, where h is the constant storey height.

3. Each connecting beam and each lamina bends with a point of contraflexure midway between the shear walls.

4. The shear forces, F^q and the axial forces, F^t at the points of contraflexure of the discrete beams are replaced by continuous distributions of shear, $q(x)$ and axial force, $t(x)$, acting at the points of contraflexure of the continuous medium.

5. The axial deformation of the connecting beams and of the continuous medium is negligible.

6. At any height the two walls deflect equally and with equal curvatures.

II ACTION OF CONNECTING LAMINA

In order to investigate the action of the connection between the shear walls, the system is assumed to be cut through the points of contraflexure. The shear and axial forces are the only forces acting on the cut ends of the beams or laminae as shown in figure 2.2.

Consider a typical lamina, at an absolute height, χ , relative height, x. The cut ends of the laminae undergo relative deflections due to the forces acting on them, as follows:-

1. ROTATION OF SHEAR WALLS

The elastic rotation of the foundations and the curvature of the shear walls deflect the cut ends of the lamina relative to each other by

$$\delta_1 = \ell \frac{dy}{d\chi} = \frac{\ell}{H} \frac{dy}{dx} \qquad (2.1)$$

2. DEFORMATION OF CONNECTION

The shear, $q(x)$, on the cut ends of the lamina causes deflections due to shear and bending of the laminae, and deformation of the beam- or slab-to-wall connection. The flexibility of the beam- or slab-to-wall connection may be allowed for by assuming the effective span, b_c, of the beam or slab, to be increased from the clear span, b, by the depth of the connecting beams or slabs, as suggested by Michael[7]. The shearing action may be accounted for by reducing the moment of inertia of the connecting beams, I_b, to

$$I_c = \frac{I_b}{1 + 12 \frac{E_c}{G_c} \frac{I_b}{A_b b_c^2}} \qquad (2.2)$$

The relative deflection between the cut ends of the lamina due to the shear and bending of the lamina and deformation of the wall connection is then given by

$$\delta_2 = - \frac{b_c^3 h}{12 E_c I_c} q(x) \qquad (2.3)$$

3. AXIAL DEFORMATION OF SHEAR WALLS

Axial forces, T, in the two walls are, by the condition of vertical equilibrium, equal in magnitude and opposite in sense. Assuming tension positive in wall 1, the relative deflection of the cut ends of the laminae due to the axial forces deforming the walls is

$$\delta_3 = - \left(\frac{1}{A_1 E_1} + \frac{1}{A_2 E_2} \right) H \int_0^x T(\eta) \, d\eta \qquad (2.4)$$

4. VERTICAL DISPLACEMENT OF THE FOUNDATIONS

The axial forces in the two walls cause the foundations to deflect vertically relative to each other by δ_v. The cut ends of the laminae are consequently deflected by

$$\delta_4 = - \delta_v \qquad (2.5)$$

III COMPATIBILITY OF CONNECTING MEDIUM

For continuity at the point of contraflexure there must be no relative deflection at the cut ends of the laminae, thus

$$\delta_1 + \delta_2 + \delta_3 + \delta_4 = 0 \qquad (2.6)$$

Substituting the expressions (2.1), (2.3), (2.4) and (2.5) into (2.6) gives the compatibility condition

$$\frac{\ell}{H}\frac{dy}{dx} - \frac{b_c^3 h}{12E_c I_c} q(x) - \left(\frac{1}{A_1E_1} + \frac{1}{A_2E_2}\right) H \int_0^x T(\eta)\, d\eta - \delta_v = 0 \qquad (2.7)$$

The derivatives of (2.7) with respect to x are used later in the analysis and are

$$\frac{\ell}{H}\frac{d^2y}{dx^2} - \frac{b_c^3 h}{12E_c I_c}\frac{dq}{dx} - \left(\frac{1}{A_1E_1} + \frac{1}{A_2E_2}\right) H\, T(x) = 0 \qquad (2.8)$$

$$\frac{\ell}{H}\frac{d^3y}{dx^3} - \frac{b_c^3 h}{12E_c I_c}\frac{d^2q}{dx^2} - \left(\frac{1}{A_1E_1} + \frac{1}{A_2E_1}\right) H \frac{dT}{dx} = 0 \qquad (2.9)$$

IV EQUILIBRIUM OF SHEAR WALLS

The conditions of equilibrium of the system are firstly considered separately for each wall and then for the wall assembly. The forces acting on the two walls above a section x are as shown in figure 2.3. The force at and the moment about the centroid of the section of the appropriate wall at level x are found for each force action on the wall.

WALL 1

The total force, $P_A(x)$, due to the applied load distribution, $P(x)$, and its moment, $M_A(x)$, are found by integrating $P(x)$ from the section x to the top of the wall as follows

$$P_A(x) = H \int_x^1 P(\eta)\, d\eta \qquad (2.10)$$

$$M_A(x) = H^2 \int_x^1 (\eta - x)\, P(\eta)\, d\eta \qquad (2.11)$$

Differentiating (2.11), with respect to x, gives

$$\frac{d M_A}{dx} = - H \; P_A(x) \qquad (2.12)$$

$$\frac{d^2 M_A}{dx^2} = - H \; \frac{d P_A}{dx} = H^2 P(x) \qquad (2.13)$$

From the condition of vertical equilibrium on wall 1, the total of the shear force distribution, q(x) above the section x is balanced by the axial force, T(x) on the wall at that level, as given by

$$T(x) = H \int_x^1 q(\eta)\, d\eta \qquad (2.14)$$

The derivatives of (2.14) with respect to x are

$$\frac{dT}{dx} = - H\, q(x) \qquad (2.15)$$

$$\frac{d^2 T}{dx^2} = - H \frac{dq}{dx} \qquad (2.16)$$

The moment of the shear distribution about the centroid of wall 1 is

$$M_{T1}(x) = - \left[d_2 + \frac{b}{2} \right] T(x) \qquad (2.17)$$

The total force, $P_c(x)$, and moment, $M_c(x)$, due to the force distribution, t(x), acting axially on the cut ends of the connecting medium above the section x are found by integrating t as follows

$$P_c(x) = H \int_x^1 t(\eta)\, d\eta \qquad (2.18)$$

$$M_c(x) = H^2 \int_x^1 (\eta - x)\, t(\eta)\, d\eta \qquad (2.19)$$

The derivatives of (2.19) with respect to x are

$$\frac{d M_c}{dx} = - H P_c(x) \qquad (2.20)$$

$$\frac{d^2 M_c}{dx^2} = - H \frac{d P_c}{dx} = H^2 t(x) \qquad (2.21)$$

From the conditions of horizontal and rotational equilibrium the shear force, $Q_1(x)$, and bending moment, $M_1(x)$, on wall 1 at level x are respectively

$$Q_1(x) = P_A(x) + P_c(x) + Q \qquad (2.22)$$

$$M_1(x) = M_A(x) + M_{T1}(x) + M_c(x) + QH(1-x) \qquad (2.23)$$

Q is the concentrated interactive force acting between the tops of the walls, which, in general, is required to fulfil the conditions of equilibrium on the individual walls. In the continuous system Q is a discrete axial force at the top of the connecting medium and in the real system it exists as a component of the axial force in the top connecting beam.

WALL 2

The axial force on wall 2, being equal to that on wall 1 is given by (2.14).

The moment of the shear distribution about the centroid of wall 2 is

$$M_{T2(x)} = - \left(\frac{b}{2} + d_3 \right) T(x) \qquad (2.24)$$

The force and moment due to the axial force distribution, t acting on wall 2 are equal and opposite to those on wall 1, as given by (2.18) and (2.19) respectively.

From the conditions of horizontal and rotational equilibrium the shear force, $Q_2(x)$, and bending moment, $M_2(x)$, on wall 2 at level x are respectively

$$Q_2(x) = - P_c(x) - Q \qquad (2.25)$$

$$M_2(x) = M_{T2}(x) - M_c(x) - QH(1-x) \qquad (2.26)$$

The total moment of restraint, $M(x)$, on the two shear walls at level x is given by

$$M(x) = M_1(x) + M_2(x) \qquad (2.27)$$

Substituting the expressions (2.23) and (2.26) for $M_1(x)$ and $M_2(x)$ respectively, subsequently inserting the expressions (2.17) and (2.24) for $M_{T1}(x)$ and $M_{T2}(x)$ respectively and simplifying gives

$$M(x) = M_A(x) - \ell T(x) \qquad (2.28)$$

V MOMENT-CURVATURE RELATIONSHIPS

The curvature at any level is the same for the two walls as given by

$$\frac{d^2y}{d\chi^2} = \frac{1}{H^2} \frac{d^2y}{dx^2} \qquad (2.29)$$

The moments of restraint on the walls are related to the curvature by their respective stiffnesses, E_1I_1 and E_2I_2, as follows,

$$M_1(x) = \frac{E_1I_1}{H^2} \frac{d^2y}{dx^2} \qquad (2.30)$$

$$M_2(x) = \frac{E_2I_2}{H^2} \frac{d^2y}{dx^2} \qquad (2.31)$$

The summation of equations (2.30) and (2.31) gives a second expression for the total moment of restraint as

$$M(x) = \frac{E_1I_1 + E_2I_2}{H^2} \frac{d^2y}{dx^2} \qquad (2.32)$$

Expressions (2.28) and (2.32) are equated to give the moment curvature relationship for the shear wall assembly as

$$M(x) = \frac{E_1I_1 + E_2I_2}{H^2} \frac{d^2y}{dx^2} = M_A(x) - \ell T(x) \qquad (2.33)$$

The derivatives of (2.33) with respect to x are

$$\frac{E_1I_1 + E_2I_2}{H^2} \quad \frac{d^3y}{dx^3} = - H\, P_A(x) - \ell \frac{dT}{dx} \qquad (2.34)$$

$$\frac{E_1I_1 + E_2I_2}{H^2} \quad \frac{d^4y}{dx^4} = H^2\, P(x) - \ell \frac{d^2T}{dx^2} \qquad (2.35)$$

Substituting (2.33) into (2.30) and (2.31) gives the moments on the two walls in the form

$$M_1(x) = \frac{E_1I_1}{E_1I_1 + E_2I_2} \left\{ M_A(x) - \ell\, T(x) \right\} \qquad (2.36)$$

$$M_2(x) = \frac{E_2I_2}{E_1I_1 + E_2I_2} \left\{ M_A(x) - \ell\, T(x) \right\} \qquad (2.37)$$

VI GOVERNING DIFFERENTIAL EQUATIONS

Equations (2.7), (2.14) and (2.33), together with their respective derivatives, interrelate the three functions q(x), T(x) and y(x). By selecting any of the functions as redundant and eliminating the other two a governing differential equation may be set up in terms of the selected function.

Consider q(x) as the redundant function. Substituting (2.15) into (2.34) and rearranging in terms of the third derivative of y gives

$$\frac{d^3y}{dx^3} = \frac{H^3}{E_1I_1 + E_2I_2} \left[\ell\, q(x) - P_A(x) \right] \qquad (2.38)$$

Substituting (2.38) and (2.15) into (2.9) eliminates y(x) and T(x), and by rearranging and simplifying the resultant equation reduces to

$$\frac{d^2q}{dx^2} - \alpha^2\, q(x) = - \frac{\alpha^2}{\mu\, \ell} P_A(x) \qquad (2.39)$$

The dimensionless constants μ and α are defined by

$$\mu = 1 + \frac{E_1I_1 + E_2I_2}{\ell^2} \left(\frac{1}{A_1E_1} + \frac{1}{A_2E_2} \right) \qquad (2.40)$$

$$\alpha^2 = \frac{12\,H^2\,\ell^2}{b_c^3\,h}\quad\frac{E_cI_c}{E_1I_1 + E_2I_2}\cdot\mu \qquad (2.41)$$

Consider $T(x)$ as the redundant function. Rearranging (2.33) in terms of the second derivative of y gives

$$\frac{d^2y}{dx^2} = \frac{H^2}{E_1I_1 + E_2I_2}\left[M_A(x) - \ell\,T(x)\right] \qquad (2.42)$$

Substituting (2.42) and (2.16) into (2.8) eliminates $q(x)$ and $y(x)$. The resultant equation reduces to

$$\frac{d^2T}{dx^2} - \alpha^2\,T(x) = -\frac{\alpha^2}{\mu\,\ell}\,M_A(x) \qquad (2.43)$$

Finally consider $y(x)$ as the redundant function. Rearranging (2.33) in terms of $T(x)$ gives

$$T(x) = \frac{1}{\ell}\left[M_A(x) - \frac{E_1I_1 + E_2I_2}{H^2}\,\frac{d^2y}{dx^2}\right] \qquad (2.44)$$

Rearranging (2.35) in terms of the second derivative of $T(x)$ and substituting into (2.16) gives

$$\frac{dq}{dx} = \frac{1}{H\,\ell}\left[\frac{E_1I_1 + E_2I_2}{H^2}\,\frac{d^4y}{dx^4} - H^2\,P(x)\right] \qquad (2.45)$$

Substituting (2.44) and (2.45) into (2.8) eliminates $q(x)$ and $T(x)$. The resultant equation reduces to

$$\frac{d^4y}{dx^4} - \alpha^2\,\frac{d^2y}{dx^2} = \frac{H^4}{E_1I_1 + E_2I_2}\left[P(x) - \frac{\alpha^2}{H^2}\,\frac{\mu - 1}{\mu}\,M_A(x)\right] \qquad (2.46)$$

Any of the equations (2.39), (2.43) and (2.46) may be solved, subject to the boundary conditions, for any particular load case.

VII BOUNDARY CONDITIONS

The terms in which each of the boundary conditions are best expressed will depend on which of the governing differential equations is chosen, in a particular case. In general there are four boundary conditions as follows

1. At the base of the shear walls there can be no lateral deflection,

$$y(0) = 0 \tag{2.47}$$

2. The slope of the shear walls at the base is equal to the rotation of the foundations,

$$\frac{1}{H} \frac{dy}{dx}(0) = \delta_\theta \tag{2.48}$$

Evaluating (2.33) at $x = 0$ gives expressions for the moment on the walls at the base as

$$M_0 = \frac{E_1 I_1 + E_2 I_2}{H^2} \frac{d^2 y}{dx^2}(0) = M_A(0) - \ell T_0 \tag{2.49}$$

The rotation of the foundations is proportional to the moment at the base of the walls as given in (1.6). The second boundary condition can be expressed by any suitable combination of (1.6) (2.48) and (2.49).

3. The compatibility condition, (2.7), must be fulfilled for all levels. In particular, at the base equation (2.7) reduces to,

$$\frac{\ell}{H} \frac{dy}{dx}(0) - \frac{b_c^3 h}{12 E_c I_c} q(0) - \delta_v = 0 \tag{2.50}$$

At the base the vertical deflection is related to the axial force by (1.5). By using (1.5) together with the relationships of (1.6), (2.48) and (2.49) the third boundary condition can be expressed in the form,

$$q(0) = \frac{\gamma}{H \ell} M_A(0) - \frac{\gamma + \Delta}{H} T_0 \tag{2.51}$$

γ and Δ are dimensionless foundation coefficients of rotation and vertical deflection respectively as defined by

$$\gamma = \frac{12 E_c I_c H \ell^2}{b_c^3 h} K_\theta \tag{2.52}$$

$$\Delta = \frac{12 E_c I_c H}{b_c^3 h} K_v \tag{2.53}$$

4. At the top of the shear walls there can be no bending moment, hence from (2.33)

$$\frac{d^2y}{dx^2}(1) = 0 \qquad (2.54)$$

Also there can be no axial force at the top of the walls. Substituting $T(1) = 0$ and (2.54) into (2.8) evaluated at $x = 1$, the fourth boundary condition may be expressed as

$$\frac{dq}{dx}(1) = 0 \qquad (2.55)$$

VIII FORCES ON THE SHEAR WALLS

Having solved a selected differential equation for $q(x)$, $T(x)$ or $y(x)$, the remaining two functions may be found directly from the relationships previously deduced. Thereafter these functions may be used to evaluate other force actions in the system.

Substituting (2.37) and (2.24) into (2.26) and rearranging the terms gives

$$M_c(x) = -\frac{E_2I_2}{E_1I_1 + E_2I_2} M_A(x) + \left\{\frac{E_2I_2}{E_1I_1 + E_2I_2}\left(\ell - \frac{b}{2} - d_3\right)\right\} T(x) - QH(1 - x) \qquad (2.56)$$

Differentiating (2.56) with respect to x, substituting (2.20), (2.12) and (2.15) into the result and evaluating (2.22) and (2.25) gives the shear forces on the two walls as

$$Q_1(x) = \frac{E_1I_1}{E_1I_1 + E_2I_2} P_A(x) + \left\{\frac{E_2I_2}{E_1I_1 + E_2I_2}\left(\ell - \frac{b}{2} - d_3\right)\right\} q(x) \qquad (2.57)$$

$$Q_2(x) = \frac{E_2I_2}{E_1I_1 + E_2I_2} P_A(x) - \left\{\frac{E_2I_2}{E_1I_1 + E_2I_2}\left(\ell - \frac{b}{2} - d_3\right)\right\} q(x) \qquad (2.58)$$

The shear force Q at the top of the walls may be found by evaluating (2.57) or (2.58) at $x = 1$ to be

$$Q = Q_1(1) = -Q_2(1) = \left\{\frac{E_2I_2}{E_1I_1 + E_2I_2}\left(\ell - \frac{b}{2} - d_3\right)\right\} q(1) \qquad (2.59)$$

Substituting expression (2.25) for $Q_2(x)$ into (2.58), differentiating and substituting (2.21) and (2.13) into the result gives the expression for the axial force distribution in the connecting medium in the form

$$t(x) = - \frac{E_2 I_2}{E_1 I_1 + E_2 I_2} P(x) - \frac{1}{H} \left\{ \frac{E_2 I_2}{E_1 I_1 + E_2 I_2} \ell - \frac{b}{2} - d_3 \right\} \frac{dq}{dx} \qquad (2.60)$$

IX FORCES IN THE CONNECTING BEAMS

Having found the shear and axial force distribution functions in the continuous medium, the discrete forces at the point of contraflexure of any connecting beam may be evaluated.

The action of any beam is assumed to be replaced by that part of the continuous medium contained within half a storey height above and below the level of the beam. It follows that the forces in any beam at level x_i are obtained by integrating the relevant force distributions between these limits, as follows

$$F_i^q = H \int_{x_i - \frac{h}{2H}}^{x_i + \frac{h}{2H}} q(x)\, dx \qquad (2.61)$$

$$F_i^t = H \int_{x_i - \frac{h}{2H}}^{x_i + \frac{h}{2H}} t(x)\, dx \qquad (2.62)$$

By utilising equations (2.14), (2.18) and (2.25) the beam forces may be stated as the differences of the relevant wall forces at the above limits, as

$$F_i^q = - T \left(x_i + \frac{h}{2H} \right) + T \left(x_i - \frac{h}{2H} \right) \qquad (2.63)$$

$$F_i^t = Q_2 \left(x_i + \frac{h}{2H} \right) - Q_2 \left(x_i - \frac{h}{2H} \right) \qquad (2.64)$$

The relevant limits of integration for the top beam are the top

of the walls and half a storey height below. The beam forces, F_I^q and F_I^t in the top beam may be expressed as

$$F_I^q = T \left(1 - \frac{h}{2H} \right) \tag{2.65}$$

$$F_I^t = - Q - Q_2 \left(1 - \frac{h}{2H} \right) \tag{2.66}$$

2.3.2 POLYNOMIAL LOAD CASE

The load distribution on the system is that given in (1.1). For simplicity the action of any particular load term, $p_n x^n$ is considered, that is

$$P(x) = p_n x^n \tag{3.1}$$

Equations (2.10) and (2.11) may be evaluated explicitly as

$$P_A(x) = p_n H \frac{1 - x^{n+1}}{n + 1} \tag{3.2}$$

$$M_A(x) = p_n H^2 \left[\frac{1 - x^{n+2}}{n + 2} - x \frac{1 - x^{n+1}}{n + 1} \right] \tag{3.3}$$

Selecting q(x) as the redundant function and substituting (3.2) into (2.39) gives the governing differential equation as

$$\frac{d^2 q}{dx^2} - \alpha^2 q(x) = - \frac{\alpha^2 H}{\mu \ell} p_n \frac{1 - x^{n+1}}{n + 1} \tag{3.4}$$

The equation (3.4) is a second order linear differential equation with constant coefficients, and may be solved by the method of complementary and particular functions. The complementary function, $q_c(x)$, being the solution of (3.4) with the right hand side made equal to zero, is given by

$$q_c(x) = K_1 \cosh \alpha x + K_2 \sinh \alpha x \tag{3.5}$$

The particular function, $q_p(x)$, is any solution which satisfies (3.4). It is assumed to be of the form

$$q_p(x) = a_0 + a_1 x + a_2 x^2 + \ldots + a_r x^r + \ldots + a_n x^n + a_{n+1} x^{n+1}$$

Substituting for $q(x)$ and its second derivative into (3.4) gives

$$\left(2a_2 + 2(3)a_3x + \ldots + (r-1)r\,a_r x^{r-2} + \ldots + (n-1)n\,a_n x^{n-2} + n(n+1)a_{n+1}x^{n-1} \right) - \alpha^2 \left(a_0 + a_1x + a_2x^2 + \ldots + a_rx^r + \ldots + a_nx^n + a_{n+1}x^{n+1} \right)$$

$$= - \frac{\alpha^2 H}{\mu\ell} \frac{p_n}{n+1} \left(1 - x^{n+1} \right) \qquad (3.6)$$

Equation (3.6) is an identity and must be satisfied for all values of x. It follows that the algebraic sum of the coefficients of each power of x must be zero. Beginning with the highest power the coefficients are systematically evaluated to give

$$a_{n+1} = - \frac{1}{(n+1)} \frac{p_n H}{\mu\ell}, \quad a_n = 0$$

$$a_{n-1} = - \frac{n}{\alpha^2} \frac{p_n H}{\mu\ell}, \quad a_{n-2} = 0$$

$$a_{n-3} = - (n-2)(n-1) \frac{n}{\alpha^4} \frac{p_n H}{\mu\ell}, \quad a_{n-4} = 0 \ldots\ldots$$

By introducing a suitable sine function the zero terms may be included in a general term of the form

$$a_r = - \frac{p_n H}{\mu\ell} \frac{n!}{r!} \frac{\sin^2 \left[\pi(n-r)/2 \right]}{\alpha^{n-r+1}} \qquad (3.7)$$

Using the form of (3.7) the coefficients of the lower powers of x are

$$a_2 = - \frac{p_n H}{\mu\ell} \frac{n!}{2!} \frac{\sin^2 \left[\pi(n-2)/2 \right]}{\alpha^{n-1}}$$

$$a_1 = - \frac{p_n H}{\mu\ell} \frac{n!}{1!} \frac{\sin^2 \left[\pi(n-1)/2 \right]}{\alpha^{n}}$$

$$a_0 = \frac{p_n H}{\mu\ell} \left(\frac{1}{n+1} - \frac{n!}{0!} \frac{\sin^2 \left[\pi n/2 \right]}{\alpha^{n+1}} \right)$$

Consequently the particular function may be expressed in the form

$$q_p(x) = \frac{p_n H}{\mu \ell}\left\{ \frac{1}{n+1} - \sum_{r=0}^{n+1}\left(\frac{n!}{r!} \frac{\sin^2\left[\pi(n-r)/2\right]}{\alpha^{n-r+1}} x^r \right)\right\} \tag{3.8}$$

The general solution for the shear distribution is the sum of the complementary and particular functions as expressed in (3.5) and (3.8) respectively,

$$q(x) = K_1 \cosh \alpha x + K_2 \sinh \alpha x + \frac{p_n H}{\mu \ell}\left\{ \frac{1}{n+1} - \sum_{r=0}^{n+1}\left(\frac{n!}{r!} \frac{\sin^2\left[\pi(n-r)/2\right]}{n-r+1} x^r \right)\right\} \tag{3.9}$$

Two boundary conditions are required to evaluate the constants K_1 and K_2.

Differentiating (3.9) and applying the fourth boundary condition as given by (2.55) gives

$$K_1 \alpha \sinh \alpha + K_2 \alpha \cosh \alpha = \frac{p_n H}{\mu \ell} C_1 \tag{3.10}$$

where $$C_1 = \sum_{r=1}^{n+1}\left(\frac{n!}{(r-1)!} \frac{\sin^2\left[\pi(n-r)/2\right]}{\alpha^{n-r+1}} \right) \tag{3.11}$$

Substituting (3.9) into (2.14) and evaluating the integral for $x = 0$ gives the axial force at the base,

$$T_0 = K_1 \frac{H}{\alpha} \sinh \alpha + K_2 \frac{H}{\alpha}(\cosh \alpha - 1) + \frac{p_n H^2}{\mu \ell} C_2 \tag{3.12}$$

where $$C_2 = \frac{1}{n+1} - \sum_{r=0}^{n+1}\left(\frac{n!}{(r+1)!} \frac{\sin^2\left[\pi(n-r)/2\right]}{\alpha^{n-r+1}} \right) \tag{3.13}$$

Evaluating (3.3) at $x = 0$ gives the moment of the applied load at the base as

$$M_A(0) = \frac{p_n H^2}{n+2} \tag{3.14}$$

Using (3.9), evaluated at $x = 0$, together with (3.12) and (3.14) to apply the third boundary condition, in the form of equation (2.51) gives a second equation relating K_1 and K_2 as

$$K_1 \left(1 + \frac{\gamma + \Delta}{\alpha} \sinh \alpha \right) + K_2 \frac{\gamma + \Delta}{\alpha} \left(\cosh \alpha - 1 \right)$$

$$= \frac{p_n H}{\mu \ell} \left(\frac{\mu \gamma}{n + 2} - (\gamma + \Delta) C_2 + C_3 \right) \qquad (3.15)$$

where $C_3 = \dfrac{n!\, \sin^2 (\pi n/2)}{\alpha^{n+1}} - \dfrac{1}{n + 1}$ (3.16)

Equations (3.10) and (3.15) solve simultaneously to give the constants in the form

$$K_1 = \frac{p_n H}{\mu \ell} D_1$$

and

$$K_2 = \frac{p_n H}{\mu \ell} D_2$$

D_1 and D_2 are dimensionless constants, defined by

$$D_1 = \frac{\dfrac{\gamma + \Delta}{\alpha} C_1 + \left[C_3 - (\gamma + \Delta) C_4 + \dfrac{\mu \gamma}{n + 2} \right] \alpha \cosh \alpha}{\alpha \cosh \alpha + (\gamma + \Delta) \sinh \alpha} \qquad (3.17)$$

$$D_2 = \frac{C_1 - \left[C_3 - (\gamma + \Delta) C_4 + \dfrac{\mu \gamma}{n + 2} \right] \alpha \sinh \alpha}{\alpha \cosh \alpha + (\gamma + \Delta) \sinh \alpha} \qquad (3.18)$$

where $C_4 = \dfrac{C_1}{\alpha^2} + C_2$

$$= \frac{n!\, \sin^2 \left[\pi (n + 1)/2 \right]}{\alpha^{n+2}} + \frac{1}{n + 2} \qquad (3.19)$$

The shear force function can now be written in the explicit form,

$$q(x) = \frac{p_n H}{\mu \ell} \left\{ D_1 \cosh \alpha x + D_2 \sinh \alpha x + \frac{1}{n + 1} - \sum_{r = 0}^{n + 1} \left(\frac{n!}{r!} \frac{\sin^2 (\pi (n - r)/2)}{\alpha^{n-r+1}} x^r \right) \right\} \qquad (3.20)$$

The derivative of (3.20) with respect to x is

$$\frac{dq}{dx} = \frac{p_n H}{\mu \ell} \left\{ \alpha (D_1 \sinh \alpha x + D_2 \cosh \alpha x) - \sum_{r=1}^{n+1} \left[\frac{n!}{(r-1)!} \frac{\sin^2 [\pi (n-r)/2]}{\alpha^{n-r+1}} x^{r-1} \right] \right\} \tag{3.21}$$

Substituting (3.20) into (2.14) and evaluating the integral gives the axial force in the shear walls as

$$T(x) = \frac{p_n H^2}{\mu \ell} \left\{ C_4 - \frac{1}{\alpha} (D_1 \sinh \alpha x + D_2 \cosh \alpha x) - \frac{x}{n+1} - \sum_{r=0}^{n+1} \left[\frac{n!}{(r+1)!} \frac{\sin^2 [\pi (n-r)/2]}{\alpha^{n-r+1}} x^{r+1} \right] \right\} \tag{3.22}$$

Evaluating (3.22) at $x = 0$ gives the axial force at the base as

$$T_0 = \frac{p_n H^2}{\mu \ell} \left\{ C_4 - \frac{D_2}{\alpha} \right\} \tag{3.23}$$

Substituting (3.3) and (3.22) into (2.33) and integrating the latter gives

$$\frac{dy}{dx} = \frac{p_n H^4}{E_1 I_1 + E_2 I_2} \left\{ \frac{x}{n+2} - \frac{x^2}{2(n+1)} + \frac{n!\, x^{n+3}}{(n+3)!} + K_3 - \frac{1}{\mu} \left[C_4 x - \frac{D_1}{\alpha^2} \cosh \alpha x - \frac{D_2}{\alpha^2} \sinh \alpha x - \frac{x^2}{2(n+1)} + \sum_{r=0}^{n+1} \left[\frac{n!}{(r+2)!} \frac{\sin^2 [\pi (n-r)/2]}{\alpha^{n-r+1}} x^{r+2} \right] \right] \right\} \tag{3.24}$$

Combining (1.6), (2.48) and (2.49) gives the second boundary condition in the form

$$\frac{dy}{dx}(0) = HK_\theta \left[M_A(0) - \ell T_0 \right] \tag{3.25}$$

Substituting for $M_A(0)$ and T_0 as in (3.14) and (3.23) respectively and equating (3.25) to (3.24) evaluated at x = 0 gives the constant K_3 as

$$K_3 = \frac{\gamma}{\alpha^2}\left\{ \frac{\mu}{n+2} - C_4 + \frac{D_2}{\alpha} \right\} - \frac{D_1}{\mu\alpha^2}$$

Substituting K_3 into (3.24) gives

$$\begin{aligned}
\frac{dy}{dx} = \frac{p_n H^4}{E_1 I_1 + E_2 I_2} \Bigg\{ & \frac{1}{\mu\alpha^2}\left[D_1(\cosh \alpha x - 1) + D_2 \sinh \alpha x \right] \\
& + \frac{\mu - 1}{\mu}\left[\frac{x}{n+2} - \frac{x^2}{2(n+1)} \right] + \frac{n!\, x^{n+3}}{(n+3)!} \\
& - \frac{1}{\mu} \sum_{r=-1}^{n+1} \left[\frac{n!}{(r+2)!} \frac{\sin^2\left[\pi(n-r)/2\right]}{\alpha^{n-r+1}} x^{r+2} \right] \\
& + \frac{\gamma}{\alpha^2}\left[\frac{\mu}{n+2} - C_4 + \frac{D_2}{\alpha} \right] \Bigg\}
\end{aligned} \tag{3.26}$$

Equation (3.26) is integrated subject to the first boundary condition as given in (2.47) to give the deflection at level x as

$$\begin{aligned}
y(x) = \frac{p_n H^4}{E_1 I_1 + E_2 I_2} \Bigg\{ & \frac{1}{\mu\alpha^3}\left[D_1 \sinh \alpha x + D_2 (\cosh \alpha x - 1) \right] \\
& + \frac{\mu - 1}{\mu}\left[\frac{x^2}{2(n+2)} - \frac{x^3}{6(n+1)} \right] + \frac{n!\, x^{n+4}}{(n+4)!} \\
& - \frac{1}{\mu} \sum_{r=-1}^{n+1} \left[\frac{n!}{(r+3)!} \frac{\sin^2\left[\pi(n-r)/2\right]}{\alpha^{n-r+1}} x^{r+3} \right] \\
& + \frac{x}{\alpha^2}\left[\gamma\left\{ \frac{\mu}{n+2} - C_4 + \frac{D_2}{\alpha} \right\} - \frac{D_1}{\mu} \right] \Bigg\}
\end{aligned} \tag{3.27}$$

The remaining forces in the system may be found by substituting the values of the relevant polynomial actions into the required general expressions.

The total of any force action or deflection due to the complete load distribution is obtained by summing the corresponding actions due to all the load terms of equation (1.1)

2.3.3 POINT LOAD CASE

The load on the system in this case is defined by the array of discrete point loads (1.3) acting at their respective heights (1.4). The action of any particular point load p_n acting at level x_n is considered.

Due to the discrete nature of the load the expressions describing the actions of the system above and below the load point will generally be different. This is accounted for by the use of a suffix notation, U and L denoting the upper and lower regions of the system, respectively.

Other than at the load point the loading on the system can be described by

$$P(x) = 0 \tag{4.1}$$

By inspection equations (2.10) and (2.11) take the form

$$P_{AU}(x) = 0 \tag{4.2}$$

$$P_{AL}(x) = P_n \tag{4.3}$$

$$M_{AU}(x) = 0 \tag{4.4}$$

$$M_{AL}(x) = p_n H (x_n - x) \tag{4.5}$$

Selecting the deflection, $y(x)$, as the redundant function and substituting (4.1), together with one of (4.4) and (4.5) into (2.46) gives the governing differential equations for the upper and lower regions in terms of y_U and y_L respectively as

$$\frac{d^4 y_U}{dx^4} - \alpha^2 \frac{d^2 y_U}{dx^2} = 0 \tag{4.6}$$

$$\frac{d^4 y_L}{dx^4} - \alpha^2 \frac{d^2 y_L}{dx^2} = - \frac{p_n H^3 \alpha^2}{E_1 I_1 + E_2 I_2} \frac{\mu - 1}{\mu} (x_n - x) \tag{4.7}$$

Both the equations (4.6) and (4.7) are fourth order linear differential equations with constant coefficients, and can be solved by the standard method.

The complementary function of (4.6) is also its general solution as given by

$$y_U(x) = K_1 + K_2 x + K_3 \cosh \alpha x + K_4 \sinh \alpha x \quad (4.8)$$

The derivatives of (4.8) with respect to x follow directly as

$$\frac{dy_U}{dx} = K_2 + K_3 \alpha \sinh \alpha x + K_4 \alpha \cosh \alpha x \quad (4.9)$$

$$\frac{d^2 y_U}{dx^2} = K_3 \alpha^2 \cosh \alpha x + K_4 \alpha^2 \sinh \alpha x \quad (4.10)$$

Substituting (4.4) and (4.10) into (2.33) gives the axial force in the walls as

$$T_U(x) = - \frac{E_1 I_1 + E_2 I_2}{H^2 \ell} (K_3 \alpha^2 \cosh \alpha x + K_4 \alpha^2 \sinh \alpha x) \quad (4.11)$$

Differentiating (4.11) with respect to x and substituting the result into (2.15) gives the shear distribution function as

$$q_U(x) = \frac{E_1 I_1 + E_2 I_2}{H^3 \ell} (K_3 \alpha^3 \sinh \alpha x + K_4 \alpha^3 \cosh \alpha x) \quad (4.12)$$

The complementary function for (4.7) takes a similar form to that of (4.6). By assuming a particular function of the form $a_2 x^2 + a_3 x^3$ and using (4.7) to evaluate the coefficients, the general solution of (4.7) is found to be

$$y_L(x) = K_5 + K_6 x + K_7 \cosh \alpha x + K_8 \sinh \alpha x + \frac{p_n H^3}{E_1 I_1 + E_2 I_2} \frac{\mu - 1}{\mu} \left[\frac{x^2 x_n}{2} - \frac{x^3}{6} \right] \quad (4.13)$$

The derivatives of (4.13) with respect to x are

$$\frac{dy_L}{dx} = K_6 + K_7 \alpha \sinh \alpha x + K_8 \alpha \cosh \alpha x + \frac{p_n H^3}{E_1 I_1 + E_2 I_2} \frac{\mu - 1}{\mu} \left[x x_n - \frac{x^2}{2} \right] \quad (4.14)$$

$$\frac{d^2 y_L}{dx^2} = K_7 \alpha^2 \cosh \alpha x + K_8 \alpha^2 \sinh \alpha x + \frac{p_n H^3}{E_1 I_1 + E_2 I_2} \frac{\mu - 1}{\mu} (x_n - x) \quad (4.15)$$

Substituting (4.5) and (4.15) into (2.33) gives the axial force in the walls as

$$T_L(x) = \frac{p_n H}{\mu \ell} (x_n - x) - \frac{E_1 I_1 + E_2 I_2}{H^2 \ell} (K_7 \alpha^2 \cosh \alpha x + K_8 \alpha^2 \sinh \alpha x) \quad (4.16)$$

Substituting $x = 0$ into (4.16) gives the axial force at the base as

$$T_0 = \frac{p_n H x_n}{\mu \ell} - \frac{E_1 I_1 + E_2 I_2}{H^2 \ell} K_7 \alpha^2 \quad (4.17)$$

Differentiating (4.16) with respect to x and substituting the result into (2.15) gives the shear distribution function as

$$q_L(x) = \frac{p_n}{\mu \ell} + \frac{E_1 I_1 + E_2 I_2}{H^3 \ell} (K_7 \alpha^3 \sinh \alpha x + K_8 \alpha^3 \cosh \alpha x) \quad (4.18)$$

BOUNDARY CONDITIONS

Eight boundary conditions are required to evaluate the constants K_1 to K_8. These comprise the four general conditions together with an additional four which refer to the level of the point load, and are as follows.

1. Applying the first condition, (2.47) to equation (4.13) evaluated at $x = 0$ gives

$$K_5 + K_7 = 0 \quad (4.19)$$

2. Combining (1.6), (2.48) and (2.49) gives the second condition in the form

$$\frac{dy_L}{dx}(0) = (E_1I_1 + E_2I_2)\ \frac{K_\theta}{H}\ \frac{d^2y_L}{dx^2}(0) \qquad (4.20)$$

Evaluating (4.14) and (4.15) at $x = 0$, substituting into (4.20) and using the definitions of α and γ gives

$$K_6 - \mu\,\gamma\,K_7 + \alpha\,K_8 = \frac{p_n\ H^3}{E_1I_1 + E_2I_2}\ \frac{\gamma\,x_n}{\alpha^2}(\mu - 1) \qquad (4.21)$$

3. Substituting (4.17), together with (4.5) and (4.18), evaluated at $x = 0$, into (2.51) gives the third boundary condition in the form

$$(\gamma + \Delta)K_7 - \alpha\,K_8 = \frac{p_n\ H^3}{\alpha^2\,\mu(E_1I_1 + E_2I_2)}\ (1 - C_1\,x_n) \qquad (4.22)$$

where

$$C_1 = \gamma(\mu - 1) - \Delta \qquad (4.23)$$

4. Applying the fourth condition in the form of (2.54) to equation (4.10) evaluated at $x = 1$ gives

$$K_3 \cosh\alpha + K_4 \sinh\alpha = 0 \qquad (4.24)$$

5. At the level at which the point load is applied the deflection as given by (4.8) and (4.13) must be the same,

$$y_U(x_n) = y_L(x_n) \qquad (4.25)$$

Substituting $x = x_n$ into (4.8) and (4.13) gives the condition

$$K_1 + K_2\,x_n + K_3 \cosh\alpha\,x_n + K_4 \sinh\alpha\,x_n - K_5 - K_6\,x_n$$
$$- K_7 \cosh\alpha\,x_n - K_8 \sinh\alpha\,x_n = \frac{p_n\ H^3}{E_1I_1 + E_2I_2}\ \frac{\mu - 1}{\mu}\ \frac{x_n^3}{3} \qquad (4.26)$$

6. Also at the load point the slope of the walls as given by (4.9) and (4.14) must be the same,

$$\frac{dy_U}{dx}(x_n) = \frac{dy_L}{dx}(x_n) \qquad (4.27)$$

Substituting $x = x_n$ into (4.9) and (4.14) gives the condition

$$K_2 + K_3 \alpha \sinh \alpha x_n + K_4 \alpha \cosh \alpha x_n - K_6 - K_7 \alpha \sinh \alpha x_n$$

$$- K_8 \alpha \cosh \alpha x_n = \frac{p_n H^3}{E_1 I_1 + E_2 I_2} \frac{\mu - 1}{\mu} \frac{x_n^2}{2} \qquad (4.28)$$

7. A third condition at the load point is that the axial forces as given by (4.11) and (4.16) must be the same,

$$T_U(x_n) = T_L(x_n) \qquad (4.29)$$

Substituting $x = x_n$ into (4.11) and (4.16) gives the condition

$$K_3 \cosh \alpha x_n + K_4 \sinh \alpha x_n - K_7 \cosh \alpha x_n - K_8 \sinh \alpha x_n = 0 \qquad (4.30)$$

8. At the load point the compatibility condition, (2.7) must be satisfied for the expressions which refer to both above and below the load point. (2.7) may be expressed, firstly in terms of y_U, q_U and T_U and then in terms of y_L, q_L and T_L, both sets being evaluated at $x = x_n$. If the difference of the two equations is taken and use made of the previous conditions, (4.27) and (4.29) the resultant equation reduces to

$$q_U(x_n) - q_L(x_n) = 0 \qquad (4.31)$$

Substituting $x = x_n$ into (4.12) and (4.18) gives the final condition

$$K_3 \sinh \alpha x_n + K_4 \cosh \alpha x_n - K_7 \sinh \alpha x_n - K_8 \cosh \alpha x_n$$

$$= \frac{p_n H^3}{\alpha^3 \mu (E_1 I_1 + E_2 I_2)} \qquad (4.32)$$

The equations (4.19), (4.21), (4.22), (4.24), (4.26), (4.28), (4.30) and (4.32) are solved to give the constants $K_1 \ldots K_8$ which are then substituted into the various equations of the system. To simplify the resultant expressions the following dimensionless

constants are defined,

$$C_2 = \gamma (\mu - 1)^2 + \Delta \tag{4.33}$$

$$D_1 = \frac{\sinh \alpha (1 - x_n) - (1 - C_1 x_n) \sinh \alpha}{\alpha \cosh \alpha + (\gamma + \Delta) \sinh \alpha} \tag{4.34}$$

$$D_2 = \frac{\frac{\gamma + \Delta}{\alpha} \sinh \alpha (1 - x_n) + (1 - C_1 x_n) \cosh \alpha}{\alpha \cosh \alpha + (\gamma + \Delta) \sinh \alpha} \tag{4.35}$$

$$D_3 = \frac{\cosh \alpha x_n + \frac{\gamma + \Delta}{\alpha} \sinh \alpha x_n - (1 - C_1 x_n)}{\alpha \cosh \alpha + (\gamma + \Delta) \sinh \alpha} \tag{4.36}$$

The equations for deflection, (4.8) and (4.13) can then be expressed in the form

$$y_U(x) = \frac{p_n H^3}{\alpha^2 \mu (E_1 I_1 + E_2 I_2)} \left\{ \alpha^2 (\mu - 1) \left[\frac{x_n^2 x}{2} - \frac{x_n^3}{6} \right] + D_1 (1 - C_1 x) + x_n (1 + C_2 x) - D_3 \sinh \alpha (1 - x) \right\} \tag{4.37}$$

$$y_L(x) = \frac{p_n H^3}{\alpha^2 \mu (E_1 I_1 + E_2 I_2)} \left\{ \alpha^2 (\mu - 1) \left[\frac{x^2 x_n}{2} - \frac{x^3}{6} \right] + D_1 (1 - C_1 x) + x (1 + C_2 x_n) - D_1 \cosh \alpha x - D_2 \sinh \alpha x \right\} \tag{4.38}$$

The derivatives of (4.37) and (4.38) with respect to x are

$$\frac{dy_U}{dx} = \frac{p_n H^3}{\alpha^2 \mu (E_1 I_1 + E_2 I_2)} \left\{ \alpha^2 (\mu - 1) \frac{x_n^2}{2} - C_1 D_1 + C_2 x_n + D_3 \alpha \cosh \alpha (1 - x) \right\} \tag{4.39}$$

$$\frac{dy_L}{dx} = \frac{p_n H^3}{\alpha^2 \mu (E_1 I_1 + E_2 I_2)} \left\{ \alpha^2 (\mu - 1) \left[x x_n - \frac{x^2}{2} \right] - C_1 D_1 + 1 + C_2 x_n - D_1 \alpha \sinh \alpha x - D_2 \alpha \cosh \alpha x \right\} \tag{4.40}$$

$$\frac{d^2y_U}{dx} = -\frac{p_n H^3}{\mu(E_1I_1 + E_2I_2)} D_3 \sinh \alpha (1 - x) \qquad (4.41)$$

$$\frac{d^2y_L}{dx} = \frac{p_n H^3}{\mu(E_1I_1 + E_2I_2)} \left\{ (\mu - 1)(x_n - x) - D_1 \cosh \alpha x - D_2 \sinh \alpha x \right\} \qquad (4.42)$$

The axial forces in the shear walls are expressed as

$$T_U(x) = \frac{p_n H}{\mu \ell} D_3 \sinh \alpha(1 - x) \qquad (4.43)$$

$$T_L(x) = \frac{p_n H}{\mu \ell} \left\{ x_n - x + D_1 \cosh \alpha x + D_2 \sinh \alpha x \right\} \qquad (4.44)$$

The axial force on the foundations is given by

$$T_0 = \frac{p_n H}{\mu \ell} \left\{ x_n + D_1 \right\} \qquad (4.45)$$

The shear force distribution is given by

$$q_U(x) = \frac{p_n \alpha}{\mu \ell} D_3 \cosh \alpha (1 - x) \qquad (4.46)$$

$$q_L(x) = \frac{p_n}{\mu \ell} \left\{ 1 - D_1 \alpha \sinh \alpha x - D_2 \alpha \cosh \alpha x \right\} \qquad (4.47)$$

The derivatives of (4.46) and (4.47) are

$$\frac{dq_U}{dx} = -\frac{p_n \alpha^2}{\mu \ell} D_3 \sinh \alpha (1 - x) \qquad (4.48)$$

$$\frac{dq_L}{dx} = -\frac{p_n \alpha^2}{\mu \ell} \left\{ D_1 \cosh \alpha x + D_2 \sinh \alpha x \right\} \qquad (4.49)$$

The other forces in the system may be found by substituting the values of the relevant point load actions into the required general expressions.

Any total force or deflection due to the complete array of point loads, (1.3) is obtained by summing the actions of the individual loads.

2.4 PAIR OF COUPLED SHEAR WALLS ON RIGID FOUNDATIONS

2.4.1 INTRODUCTION

The analysis, by the continuous connection technique, of the two-dimensional system of a pair of coupled shear walls with fully built in foundations has been presented by other authors for a variety of load configurations. All these load configurations are definite cases of either of the load cases employed in this thesis.

As outlined in 2.2.2 the conditions for rigid foundations are the limiting case of the general elastic analysis of 2.3. For the foundations to be rigid the relative deflection, δ_v, and the base rotation, δ_θ, must at all times be zero. This is achieved by making the foundation flexibility moduli, K_v and K_θ, both zero, as stated in relations (1.7).

The general analysis of the system is thereafter unchanged, although, if only the rigid foundation analysis was required, considerable simplification of the boundary conditions would be possible. By substitution of (1.7) into the definitions of the dimensionless foundation coefficients, γ and Δ as given in (2.52) and (2.53) it is obvious that

$$\gamma = \Delta = 0 \tag{5.1}$$

The effects which the conditions for rigid foundations have on the various force and deflection expressions are discussed for the two load cases.

2.4.2 POLYNOMIAL LOAD CASE

In the case of a polynomial load distribution the constants C_1, C_2, C_3 and C_4, as defined in (3.11), (3.13), (3.16) and (3.19) respectively, are independent of the foundation conditions.

Constants D_1 and D_2 as given by (3.17) and (3.18) are dependent on the foundations and may be simplified in the rigid case as follows

$$D_1 = C_3 \tag{5.2}$$

$$D_2 = \frac{C_1 - C_3\,\alpha\,\sinh\,\alpha}{\alpha\,\cosh\,\alpha} \tag{5.3}$$

The expressions for the shear distribution in the connecting medium, (3.20), and the axial force in the shear walls, (3.22), are unchanged. The only effect on the slope and deflection functions (3.26) and (3.27) is that the term containing γ may be removed from both.

2.4.3 POINT LOAD CASE

In this case the constants C_1 and C_2 as defined by (4.23) and (4.33) are dependent on foundation conditions and are both found to be zero for the conditions of rigid foundations.

$$C_1 = C_2 = 0 \tag{5.4}$$

Constants D_1, D_2 and D_3 as given by (4.34), (4.35) and (4.36), respectively, are also dependent on the foundation conditions, and may be simplified in the built-in case to give

$$D_1 = \frac{\sinh \alpha (1 - x_n) - \sinh \alpha}{\alpha \cosh \alpha} \tag{5.5}$$

$$D_2 = \frac{1}{\alpha} \tag{5.6}$$

$$D_3 = \frac{\cosh \alpha x_n - 1}{\alpha \cosh \alpha} \tag{5.7}$$

Expressions (4.37) to (4.40), inclusive, for the deflection and slope of the shear walls may be simplified by inspection in that terms containing C_1 and C_2 as multipliers may be removed. Otherwise the expressions for shear distribution and axial force are unchanged.

2.5 THREE SYMMETRICAL COUPLED SHEAR WALLS

In buildings where the functional layout requires that one or more of the two-dimensional shear wall systems contains two bands of openings, it is often the case that these openings will be situated symmetrically about the centre line of the system. In the resultant three wall system the outer shear walls are identical, as are the two bands of connecting beams.

The symmetry of the system requires that the shear distribution, q, is identical in the two connecting systems and that there is no resultant axial force in the central wall. If the procedure of section 2.3.1 is followed it is found that the forms of the governing differential equations, (2.39), (2.43) and (2.46) are the same provided that the dimensionless parameters μ and α are redefined as

$$\mu = 2 + \frac{2E_1I_1 + E_2I_2}{\ell^2 A_1E_1} \qquad (5.8)$$

$$\alpha^2 = \frac{12\,H^2\,\ell^2}{b^3h} \quad \frac{E_cI_c}{2E_1I_1 + E_2I_2}\,\mu \qquad (5.9)$$

In this case suffix "1" refers to the identical outer walls, suffix "2" to the central wall, and ℓ is the distance between the centroid of either outer wall and that of the central wall. In equation (2.46) the additional substitution of $(2E_1I_1 + E_2I_2)$ for the term $(E_1I_1 + E_2I_2)$ must be made. The resultant solutions of the governing differential equations for any particular load case are then identical to the two wall case provided the above substitutions are made where necessary.

The effects of foundation deformations may also be included, as in the two-wall case. The vertical flexibility modulus, K_v, is as defined in (1.5) where, in this case, δ_v is the vertical deflection of an outer wall relative to the central wall, which does not deflect vertically, and T_0 is the axial force at the base of each outer wall. The rotational flexibility modulus, K_θ, is as defined in (1.6) where M_0 is the sum of the base moments on all three walls.

With care, in respect of the correspondence of the dimensions in the two and three-wall systems, the force actions, stresses and deflections of the shear walls and connecting beams may be evaluated as before.

2.6 SINGLE SHEAR WALLS

A shear wall, or an access and service core, which is not coupled to any other shear-bearing element, deforms as a simple

cantilever. The configuration of a single cantilever on an elastic foundation is analysed for the general lateral load distribution P(x).

The moment of restraint on the wall at a section x is equivalent to the moment of the load applied to the wall above x and is given as before in equation (2.11). The moment is related to the curvature of the wall by its stiffness as given by

$$M(x) = \frac{E_1 I_1}{H^2} \frac{d^2 y}{dx^2} \qquad (6.1)$$

Equation (6.1) may be solved for y(x) for any particular load distribution subject to the following boundary conditions:-

1. At the base of the wall there can be no lateral deflection,

$$y(0) = 0 \qquad (6.2)$$

2. The slope of the wall at the base is equal to the notation of its foundation, as given previously in (2.48). Substituting (1.6) into (2.48) gives

$$\frac{dy}{dx}(0) = H K_\theta M_0 \qquad (6.3)$$

The case of a rigid foundation is given by making K_θ zero in (6.3).

2.6.1 POLYNOMIAL LOAD CASE

The action of the particular load term, $p_n x^n$ is again considered. The expression for M(x) is that given in (3.3). Equation (6.1) becomes

$$\frac{d^2 y}{dx^2} = \frac{p_n H^4}{E_1 I_1} \left\{ \frac{1 - x^{n+2}}{n + 2} - x \frac{1 - x^{n+1}}{n + 1} \right\} \qquad (6.4)$$

Evaluating (3.3) at x = 0 and substituting the result into (6.3) gives the second boundary condition in the form

$$\frac{dy}{dx}(0) = \frac{p_n H^3 K_\theta}{n + 2} \qquad (6.5)$$

The solution of (6.4) subject to (6.2) and (6.5) is

$$y(x) = \frac{p_n H^4}{E_1 I_1} \left\{ \frac{\gamma x}{n+2} + \frac{x^2}{2(n+2)} - \frac{x^3}{6(n+1)} + \frac{n!\, x^{n+4}}{(n+4)!} \right\} \qquad (6.6)$$

The dimensionless foundation coefficient of notation, γ , for a single wall is defined as

$$\gamma = \frac{E_1 I_1}{H} K_\theta \qquad (6.7)$$

γ takes zero value in the case of a rigid foundation.

2.6.2 POINT LOAD CASE

The action of any point load, p_n acting at level x_n is again considered. The moments of the applied load at a section x above and below the load point are given by (4.4) and (4.5) respectively. The two forms of (6.1) are thus

$$\frac{d^2 y_U}{dx^2} = 0 \qquad (6.8)$$

$$\frac{d^2 y_L}{dx^2} = \frac{p_n H^3}{E_1 I_1} (x_n - x) \qquad (6.9)$$

Evaluating (4.5) at $x = 0$ and substituting the result into (6.3) gives the second boundary condition in the form

$$\frac{dy_L}{dx}(0) = p_n H^2 x_n K_\theta \qquad (6.10)$$

Two additional boundary conditions which are required to solve equations (6.8) and (6.9), refer to the level of the load point at which the slope and deflection must be continuous. These conditions were stated previously in (4.27) and (4.25) respectively.

The solutions of (6.8) and (6.9) subject to the boundary conditions (6.2), (6.10), (4.27) and (4.25) are

$$y_U(x) = \frac{p_n H^3}{E_1 I_1} \left\{ \gamma x_n x + \frac{x_n^2 x}{2} - \frac{x_n^3}{6} \right\} \qquad (6.11)$$

$$y_L(x) = \frac{P_n H^3}{E_1 I_1} \left\{ \gamma x_n x + \frac{x_n x^2}{2} - \frac{x^3}{6} \right\} \qquad (6.12)$$

where γ is of the form given in (6.7).

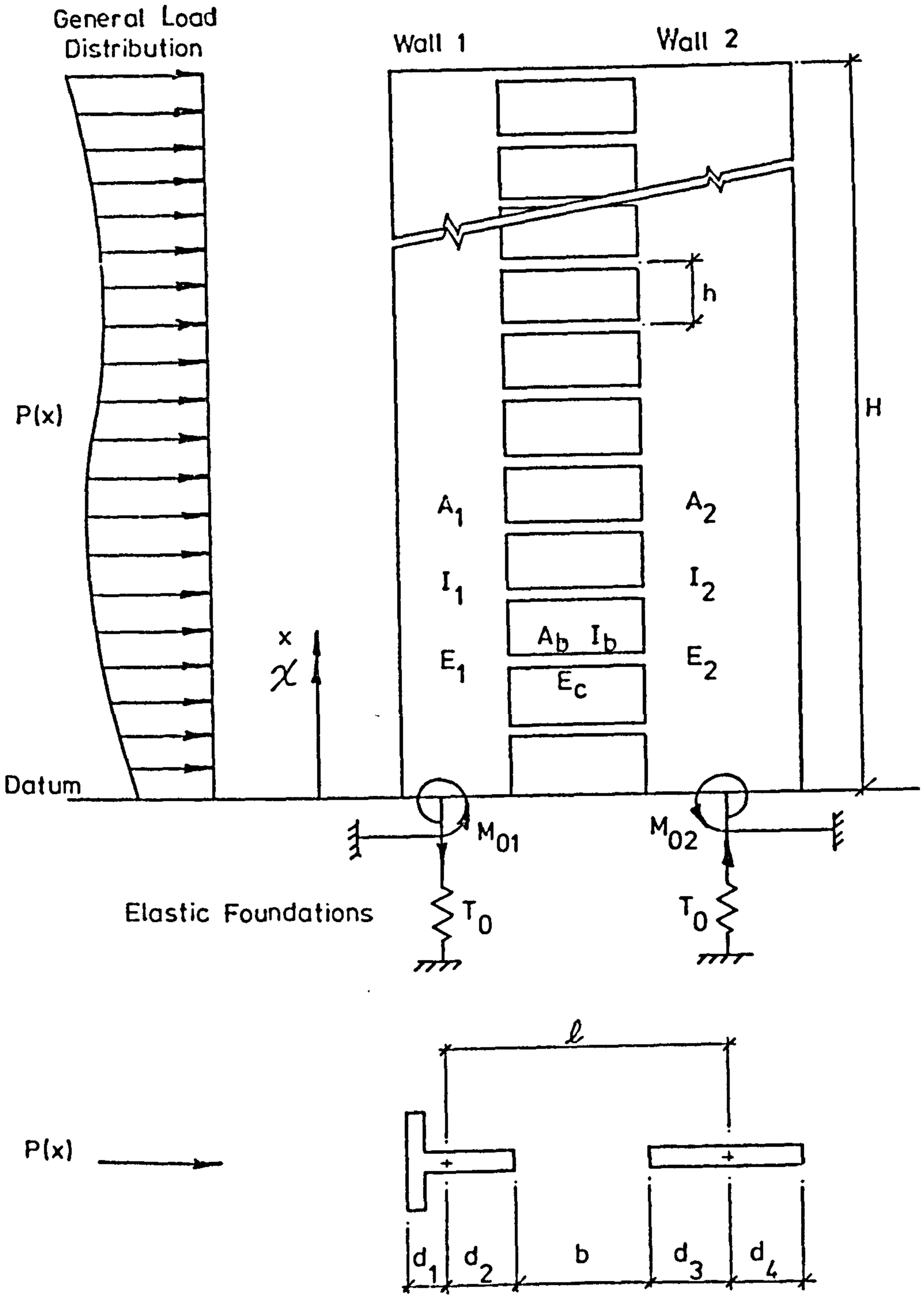

Pair of coupled shear walls on elastic foundations subjected to general load distribution

Figure 2.1

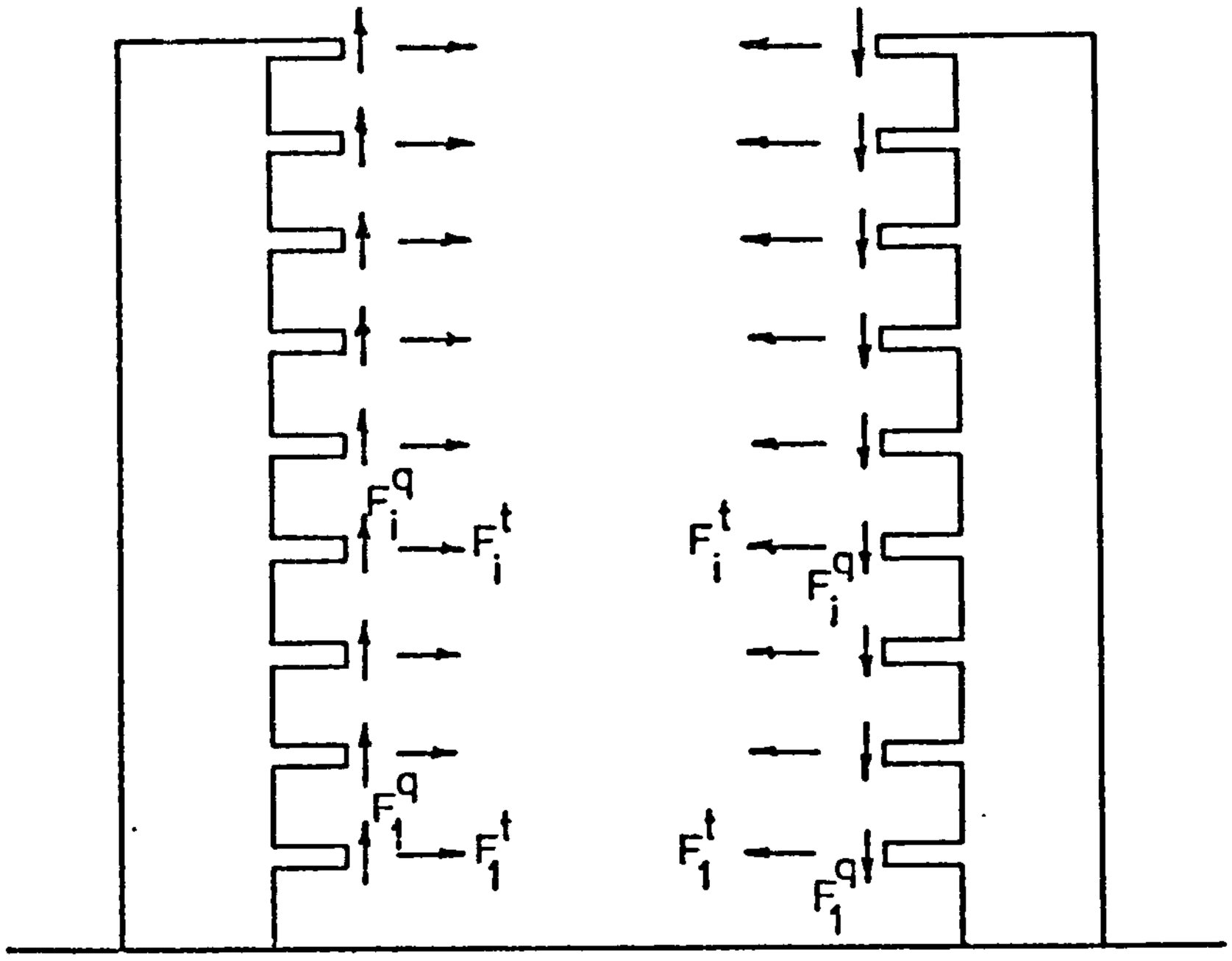

a. Discrete forces on cut ends of connecting beams.

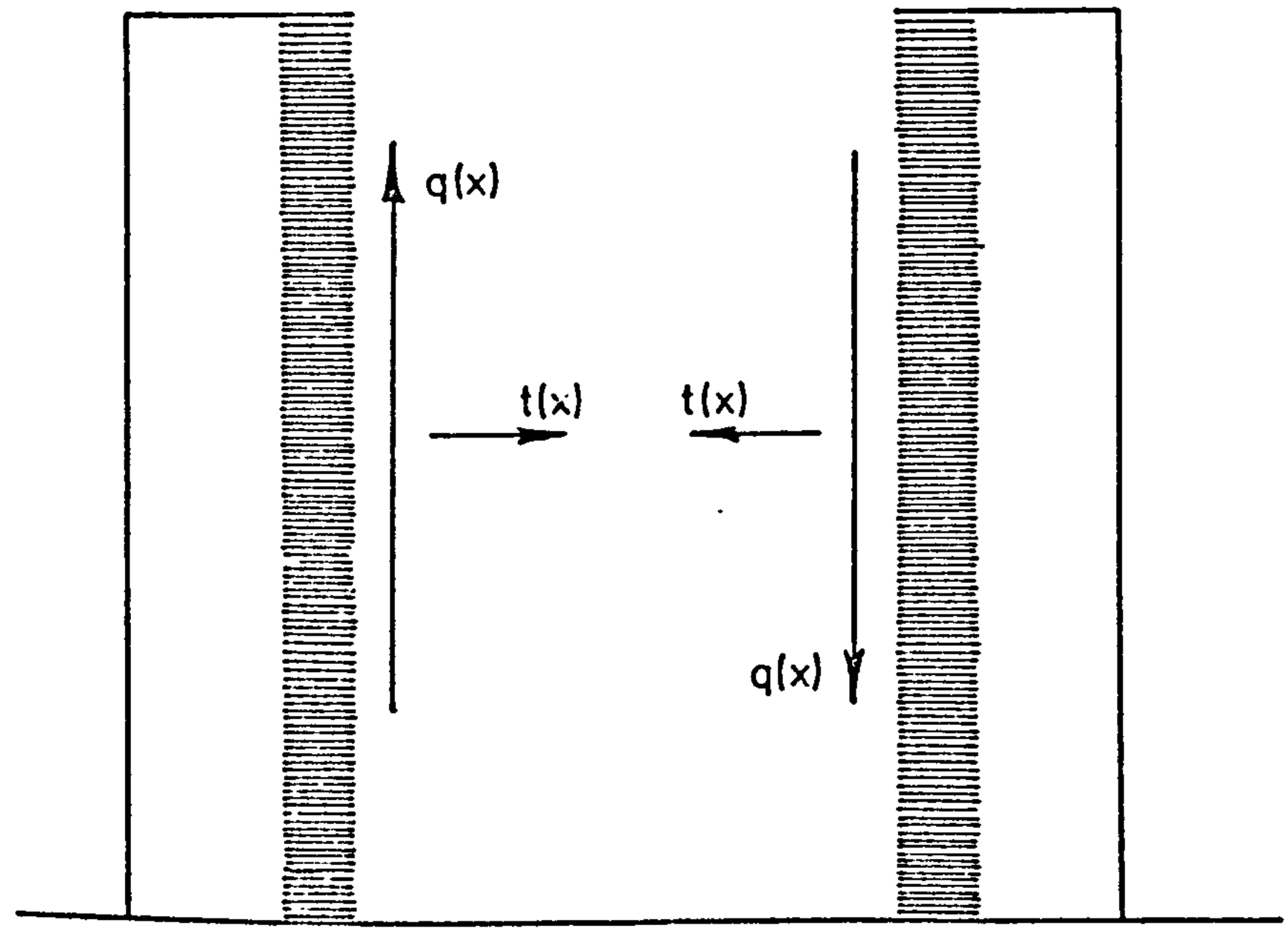

b. Continuous force distributions on cut ends of laminae.

Equivalence of discrete and continuous systems.

Figure 2.2

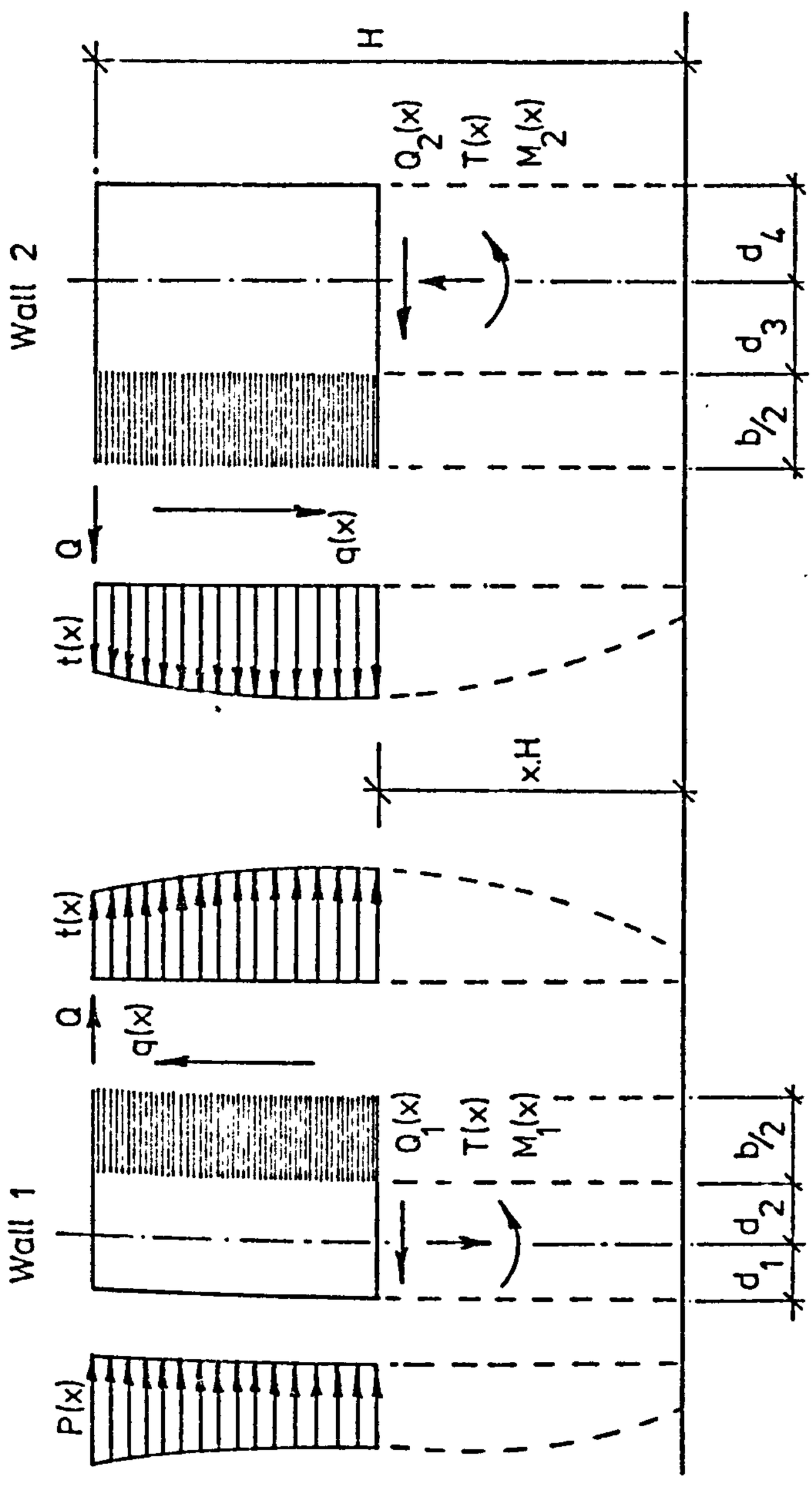

Forces on shear walls above section at level x.

Figure 2.3

CHAPTER 3

DESIGN METHODS FOR COUPLED SHEAR WALLS

3.1 INTRODUCTION

The modern approach to the design of a structure, in particular a multi-storey apartment- or office-style concrete building of the type being considered, demands an overall economy in the function of its constituent parts. The multiple employment of components to bear the dead weight and vertical imposed loading, to resist lateral wind forces, to provide internal partitioning of the floor plan and to give a degree of protection against fire, reduces the quantity of material involved, and leads to an open and more versatile layout.

It is important that an accurate assessment of the effects of the lateral loading is made at an early stage in the design of such buildings. Preliminary outline designs do not justify the cost of using a digital computer and the evaluation of the expressions, presented in Chapter 2, without computer facilities is both tedious and time consuming in all but the most simple cases. There is, therefore, a requirement for procedures for the rapid evaluation of wall stresses, beam shear forces (and hence bending moments), and the maximum deflection in two-dimensional shear wall systems, to be used by the design engineer who possesses an understanding of the limitations of the procedures used.

Methods are presented whereby design curves may be prepared to cover a wide variety of configurations of pairs of coupled shear walls on foundations of known elastic properties. These semi-graphical procedures were used by Coull and Choudhury [8,9] for the cases of uniform and triangular distributed loads and a point load at the top, applied to a pair of coupled walls built in at their bases.

As a greater knowledge of wind behaviour becomes available, a more accurate representation of the loading on tall buildings becomes possible. The pressure distribution may then be represented by a power series. The above graphical techniques are extended to

encompass any lateral load which is representable by a polynomial series, in the height co-ordinate, of the general form (1.1). The general point load case is also included, and the limitations on its use are discussed.

The expressions derived in the present chapter are for the general pair of coupled walls in which the two walls may possess distinct elastic properties which may also be different from those of the connecting beams.

Examples of the curves which may be prepared from the expressions are given in Appendix 1.

3.2 STRESSES IN WALLS

The stress distribution on the section, shown in figure 3.1(a), of a pair of coupled shear walls, at any level x, is shown in figure 3.1(b). The distribution on each of the walls consists of the superposition of a uniform axial stress and a linear bending stress, induced by the axial force $T(x)$ and the bending moment, $M_1(x)$ or $M_2(x)$, respectively. The stresses at points A, B, and C, as shown in figure 3.1(a), may be expressed in terms of the moment of the applied load, $M_A(x)$, and the axial force by substitution of (2.36) for $M_1(x)$ as follows,

$$\sigma_A = \frac{E_1 d_1}{E_1 I_1 + E_2 I_2} \left[M_A(x) - \ell T(x) \right] + \frac{T(x)}{A_1} \qquad (7.1)$$

$$\sigma_B = \frac{T(x)}{A_1} \qquad (7.2)$$

$$\sigma_C = - \frac{E_1 d_2}{E_1 I_1 + E_2 I_2} \left[M_A(x) - \ell T(x) \right] + \frac{T(x)}{A_1} \qquad (7.3)$$

The corresponding expressions may be derived for wall 2 by using equation (2.37).

For the purpose of this design method, the total distribution may be derived from an alternative superposition of two pure bending stress distributions as follows:-

1. Two linear stress distributions obtained on the assumption that the two walls act as independent cantilevers, with a neutral axis at the centroid of each wall as shown in figure 3.1(c).

2. A single bending stress distribution based on the assumption that the wall system acts as a single composite cantilever with the neutral axis at the equivalent centroid of the composite section of the two walls, as shown in figure 3.1(d).

The validity of this procedure is well established[8,9] and may be verified by setting up the constituent linear moment- and axial force-stress relationships for each system, together with the equilibrium conditions relating the externally applied moment and internal stresses. By equating the corresponding stresses at any four points such as the extreme edges of the walls it may be shown that the actual stress distribution may always be achieved by a superposition of the two alternative distributions.

By using this superposition procedure, the solution of the complex coupled structure is reduced, in the general case, to the problem of two simple vertical cantilevers together with one vertical cantilever composed of two parts possessing different elastic properties, for which simple solutions exist[10]. In the case which will most often be encountered, both walls will possess identical material properties and the problem is then that of three simple vertical cantilevers.

Let K_1 and K_2 be the percentages of the applied moment, $M_A(x)$, which are carried by independent and composite cantilever action, respectively, in which case it is a condition that,

$$K_1 + K_2 = 100 \qquad (7.4)$$

For any general lateral loading the applied moment is found from equation (2.11), which, for any polynomial distribution with exponent n is given by (3.3). The latter expression may be stated as,

$$M_A(x) = p_n H^2 \lambda_1 (n, x) \qquad (7.5)$$

where,

$$\lambda_1 = \frac{1 - x^{n+2}}{n + 2} - x \frac{1 - x^{n+1}}{n + 1} \qquad (7.6)$$

Similarly the axial force, T(x), for any polynomial exponent n is given by (3.22), which may be stated in the form,

$$T(x) = \frac{p_n H^2}{\mu \ell} \lambda_2(n, x, \alpha, \mu, \gamma, \Delta) \qquad (7.7)$$

where

$$\lambda_2 = C_4 - \frac{1}{\alpha}(D_1 \sinh \alpha x + D_2 \cosh \alpha x) - \frac{x}{n + 1} + \sum_{r=0}^{n+1} \left[\frac{n!}{(r+1)!} \frac{\sin^2 [\pi(n - r)/2]}{\alpha^{n-r+1}} x^{r+1} \right] \qquad (7.8)$$

1. INDIVIDUAL CANTILEVER ACTION

The total moment carried by this mode is $M_A(x)\ K_1/100$.

Since the two walls are assumed to deflect equally, the bending moment carried by the walls will be in proportion to their flexural stiffnesses. The moment carried by wall 1 is then

$$M_1(x) = M_A(x) \frac{K_1}{100} \frac{E_1 I_1}{E_1 I_1 + E_2 I_2} \qquad (7.9)$$

The stresses at points A, B and C are given by

$$\sigma_A = M_A(x) \frac{K_1}{100} \frac{E_1 d_1}{E_1 I_1 + E_2 I_2} \qquad (7.10)$$

$$\sigma_B = 0 \qquad (7.11)$$

$$\sigma_C = - M_A(x) \frac{K_1}{100} \frac{E_1 d_2}{E_1 I_1 + E_2 I_2} \qquad (7.12)$$

Similar expressions hold for wall 2.

2. COMPOSITE CANTILEVER ACTION

The total moment carried by this mode is $M_A(x)\ K_2/100$.

In the general case being considered the composite cantilever consists of two parts with distinct Young's Moduli, E_1 and E_2. In order to find the neutral axis of the composite section a

transformation is made to both parts such that each sectional dimension at right angles to the plane of the shear wall system is factored by its respective Young's Modulus; a procedure outlined by Timoshenko[10]. The transformed section of wall 1 has an area $A_1 E_1$ and inertia $E_1 I_1$ and, with a Young's Modulus of unity will deform in bending in the plane of the shear-walls, and under axial forces exactly as would the real section. The corresponding statement is valid for wall 2.

The centre of area of the transformed composite section is then found in the normal way, and is such that

$$k = \frac{A_2 E_2}{A_1 E_1 + A_2 E_2} \tag{7.13}$$

where $k\ell$ is the distance from the centroid of wall 1 to the centre of area of the transformed section as shown in figure 3.1(d).

The moment of inertia of the transformed section is given by

$$I = E_1 I_1 + E_2 I_2 + \ell^2 \frac{A_1 E_1 A_2 E_2}{A_1 E_1 + A_2 E_2} \tag{7.14}$$

The stress distribution on the transformed section is linear and the stress at any point is found in the usual way. In transforming back to the real sections the stresses are factored by the relevant Young's Modulus to give the composite stress distribution shown in figure 3.1(d). The stresses at points A, B and C on wall 1 are

$$\sigma_A = \frac{M_A(x)}{I} \frac{K_2}{100} (k\ell + d_1) E_1 \tag{7.15}$$

$$\sigma_B = \frac{M_A(x)}{I} \frac{K_2}{100} k\ell E_1 \tag{7.16}$$

$$\sigma_C = \frac{M_A(x)}{I} \frac{K_2}{100} (k\ell - d_2) E_1 \tag{7.17}$$

Similar expressions may be derived for wall 2

CORRESPONDENCE BETWEEN STRESSES

On equating the actual stress at the extreme fibres of wall 1, (7.1) and (7.3), to the corresponding stresses derived from the

alternative superposition, (7.10), (7.12), (7.15) and (7.17), the composite action proportional function is found to be

$$K_2 = 100 \frac{\lambda_2(n, x, \alpha, \mu, \gamma, \Delta)}{\lambda_1(n, x)} \qquad (7.18)$$

The proportions of individual and composite cantilever action required to produce the true stress distribution at any particular level, for a given exponent n are thus functions of the geometrical parameters α and μ, and of the foundation coefficients γ and Δ.

It is invisaged that in the normal procedure to design such a structure, the initial layout and preliminary design would be made on the assumption that rigid foundation conditions exist. At a later stage the design would be checked to evaluate the effects of possible foundation deformation. Where more information is available as to the nature of the ground conditions and the type of foundations which will be adopted, slab footings, piles, etc. an estimate of γ and Δ may be made at a much earlier stage in the design. In either case where the coefficients γ and Δ have been set the variation of K_2 for any n depends only on the relative height and the geometrical parameters, μ and α. The rigid foundation case is independent of μ and hence a set of curves may be prepared to show the variation of K_2 with α at different levels x, for each relevant exponent n.

The above design procedure has been developed for the case of a polynomial load distribution. The mathematics are the same for the point load case in which only the forms of λ_1 and λ_2 differ. The expressions for λ_1 and λ_2 depend on whether the level concerned is above or below the load point and may be found by referring to (4.4), (4.5), (4.43) and (4.44). From (4.4) it is seen that for levels above the load point λ_1 is zero, and hence K_2 is indeterminate. The alternative superposition procedure is therefore of limited use in dealing with point loads.

Where only the stresses at lower levels are required the majority of an array of point loads will be above these levels and the method may be used with confidence, in which case λ_1 and λ_2 are found from equations (4.5) and (4.44) to be

$$\lambda_1 (x_n, x) = x_n - x \tag{7.19}$$

$$\lambda_2 (x_n, x, \alpha, \mu, \gamma, \Delta) = x_n - x + D_1 \cosh \alpha x + D_2 \sinh \alpha x \tag{7.20}$$

For rigid foundation conditions the variation of K_2 may be plotted for different values of α, for levels below any particular point load. In evaluating stresses by this method the effects of loads applied below the level considered are neglected and it is obvious that the values of stresses found for all but the lowest levels will be unreliable.

Having determined the values of coefficients K_1 and K_2 relevant to the load and wall configuration under investigation the bending stresses in the walls may be obtained by superposition of the individual and composite stresses evaluated from ordinary beam theory.

3.3 FORCES IN CONNECTING BEAMS

In the case of any polynomial exponent n, the shear force per unit height, obtained from equation (3.20), may be expressed in the form

$$q = \frac{p_n H}{\mu \ell} K_3 \tag{7.21}$$

where

$$K_3 = D_1 \cosh \alpha x + D_2 \sinh \alpha x + \frac{1}{n+1} - \sum_{r=0}^{n+1} \left[\frac{n!}{r!} \frac{\sin^2 \left[\pi (n - r)/2 \right]}{\alpha^{n-r+1}} x^r \right] \tag{7.22}$$

Similarly, for a point load at any level, x_n, the shear force distributions of (4.46) and (4.47) may be expressed as

$$q = \frac{p_n}{\mu \ell} K_3 \tag{7.23}$$

where

$$K_{U3} = D_3 \alpha \cosh \alpha (1 - x) \tag{7.24}$$

$$K_{L3} = 1 - D_1 \alpha \sinh \alpha x - D_2 \alpha \cosh \alpha x \qquad (7.25)$$

The form of K_3 depends on whether the level considered lies, respectively, above or below the load point.

The shear force factor, K_3, depends on the relative height, the geometrical parameters, α and μ and the foundation coefficients, γ and Δ, for any polynomial exponent or particular load point. In the initial design, assuming rigid foundations, K_3 depends only on x and α, and a family of curves may be plotted to show its variation for each exponent or load point.

For any particular case the value of the shear force and hence the bending moment in any particular connecting beam is found by evaluating the area under the curve of K_3 between half a storey height above and below the level of the beam and multiplying it by $p_n H^2/\mu\ell$ or $p_n H/\mu\ell$ in the polynomial and point load cases respectively.

The position of the beam which carries the greatest shear force will be obvious from the shape of the relevant curve.

3.4 DEFLECTIONS

The deflection at any level is given by equations (3.27) and (4.27) or (4.28) for the polynomial and point load cases respectively.

The maximum deflection, at the top, in the case of a polynomial distribution may be expressed in the form

$$y_{max} = \frac{p_n H^4}{E_1 I_1 + E_2 I_2} \quad K_4$$

where

$$K_4 = \frac{1}{\mu \alpha^3}\left\{ D_1 \sinh \alpha + D_2 (\cosh \alpha - 1)\right\}$$
$$+ \frac{\mu - 1}{\mu}\left\{\frac{1}{2(n+2)} - \frac{1}{6(n+1)}\right\} + \frac{n!}{(n+4)!}$$
$$- \frac{1}{\mu} \sum_{r=-1}^{n+1} \left[\frac{n!}{(r+3)!} \quad \frac{\sin^2 [\pi (n-r)/2]}{\alpha^{n-r+1}}\right]$$
$$+ \frac{1}{\alpha^2}\left\{\gamma\left[\frac{\mu}{n+2} - C_4 + \frac{D_2}{\alpha}\right] - \frac{D_1}{\mu}\right\} \qquad (7.27)$$

For a point load at any level, the deflection at the top may be stated as

$$y_{max} = \frac{p_n H^3}{\alpha^2 \mu (E_1 I_1 + E_2 I_2)} \quad K_4 \tag{7.28}$$

where

$$K_4 = \alpha^2 (\mu - 1) \left\{ \frac{x_n^2}{2} - \frac{x_n^3}{6} \right\}$$

$$+ D_1(1 - C_1) + x_n (1 + C_2) \tag{7.29}$$

In each case, for any exponent n or a particular load point, the deflection factor K_4 depends on μ , α , γ and Δ . In the initial design approach, with known or assumed foundation conditions K_4 depends on μ and α and curves may be prepared to show its variation for each relevant exponent or load point.

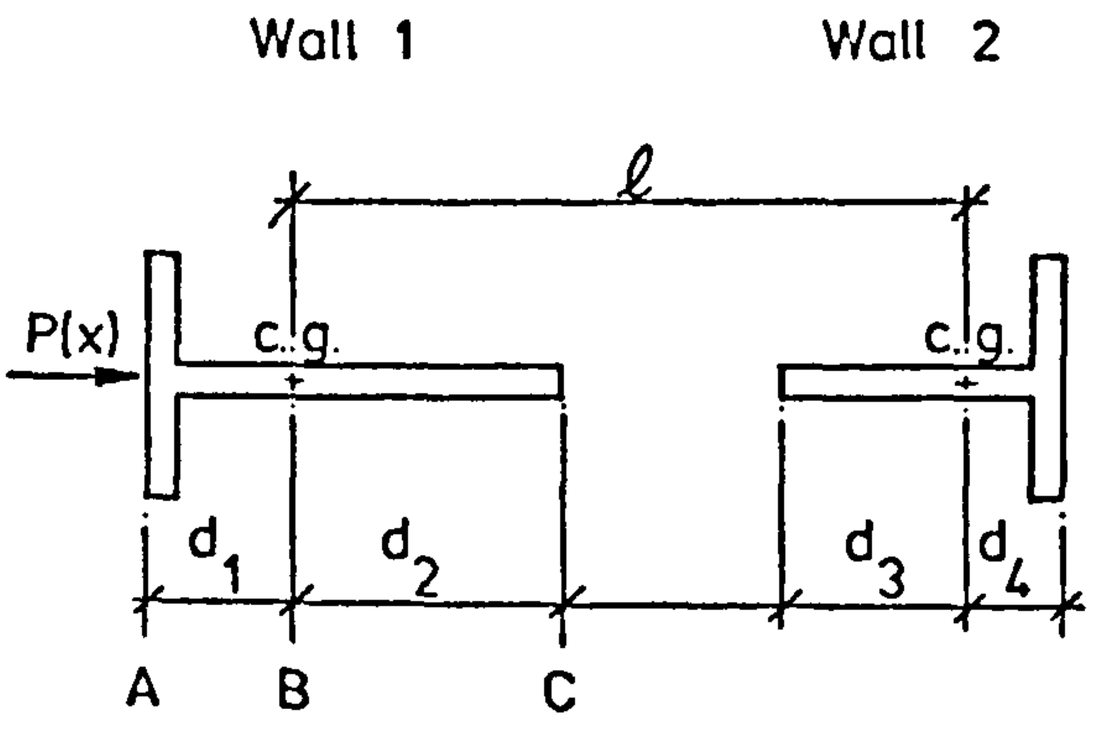

(a) Section through shear walls.

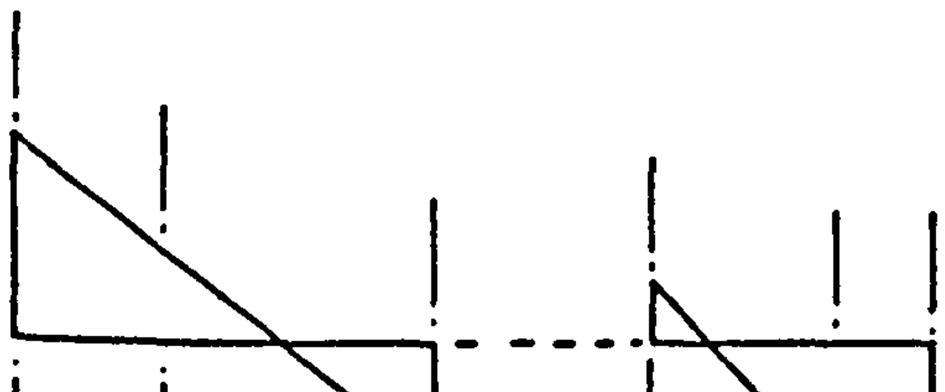

(b) Actual stress distribution.

=

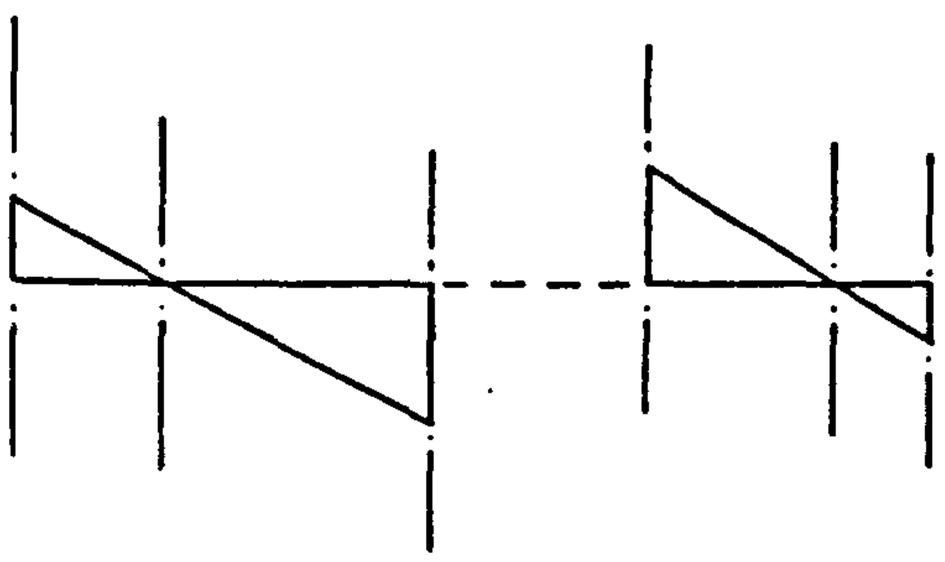

(c) Individual cantilever stresses.

+

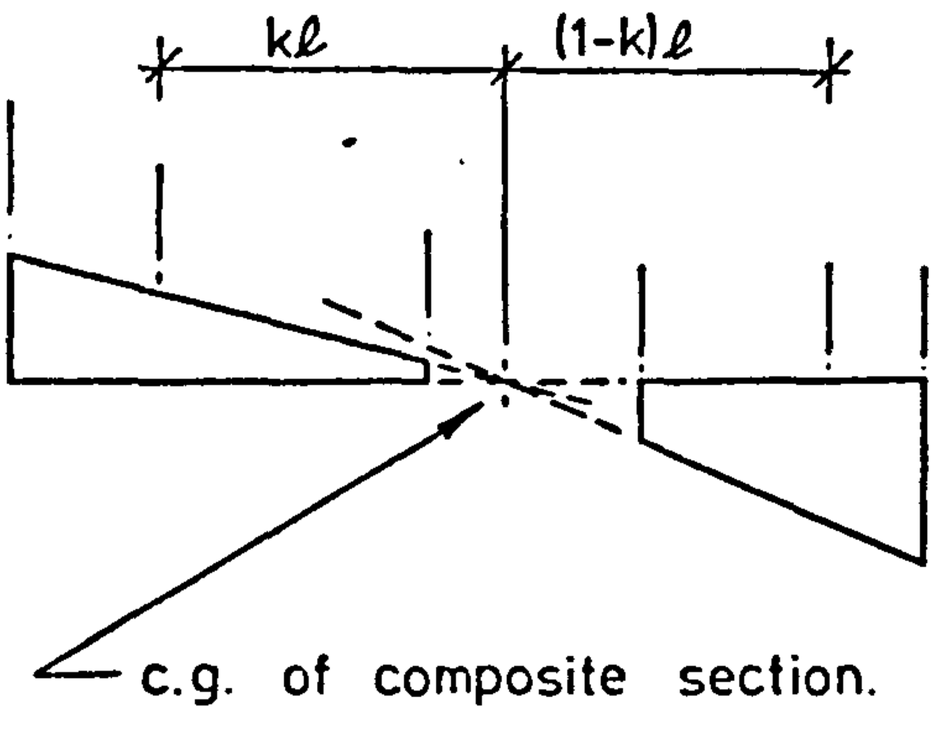

(d) Composite cantilever stresses.

Alternative superposition of stesses.

Figure 3.1

CHAPTER 4

THE ANALYSIS OF COMPLETE STRUCTURES

4.1 INTRODUCTION

The typical three-dimensional structure for which the analysis is presented may consist of various forms of load bearing elements, such as coupled and single shear walls of different dimensions together with cores of box type construction surrounding access and service shafts. In many structures the arrangement of these shear resisting elements in plan is asymmetrical. In the general case the lateral wind loading on the structure may also be asymmetrical.

Except in a symmetrically loaded symmetrical structure comprising parallel wall assemblies possessing identical stiffness matrices, there will be redistribution of the lateral load between the various structural elements throughout the height of the building. The redistribution will be considerable in structures which contain elements which exhibit different modes of deformation, such as coupled shear walls which tend to bend with double curvature and single elements which normally deflect in single curvature. The redistribution of lateral forces may also be considerable where torsional deformations of the walls or elastic deflections in foundations occur.

The analysis puts forward two simple methods of evaluating the distribution of shear loading within a complete multi-storey building whose wind resisting structure essentially consists of parallel systems of plane shear walls and box core elements of the types analysed in Chapter 2. Although basically similar, the two methods differ in respect of the form of distribution which the load is assumed to take on the individual shear resisting structures within the building.

4.2 ASSUMPTIONS

1. The building consists of a number, J , of parallel shear-resisting structures, connected at regularly spaced storey levels by

lintel beams and floor slabs.

2. The stiffness of the floor slabs in their own plane is large enough that they undergo only rigid body displacements. Consequently, under the action of the wind forces, the structure will deform in plan view, at any particular level x_i, as shown in figure 4.1. The movement of that level may be described by the deflection, y_i of any suitable datum position and the rotation θ_i. The displacement, at level x_i, of any wall assembly 'j' at a distance z_j from the datum will consist of a deflection given by

$$y_{ij} = y_i + \theta_i z_j \qquad (8.1)$$

together with the rotation θ_i.

3. Any form of wind pressure distribution may be considered. Since the floor slabs are assumed rigid in their own plane, the effect of the wind load above the level x_i may be represented by a resultant horizontal load W_i and a twisting moment M_i acting at the datum position, as shown in figure 4.1.

4. The resultant force and moment at any level are resisted by a combination of the shearing action and the torsional moment of the J shear wall assemblies. The amount of the total load carried by any particular wall assembly will depend on the load-deflection and moment-rotation characteristics of that assembly.

5. The shear force carried by any wall assembly may be adequately described by either of the load forms (1.1) or (1.3).

4.3 POLYNOMIAL LOAD CASE

For any form of lateral wind loading on the structure it is assumed, in this case, that the direct load distributed to any shear wall assembly is in the form of the polynomial series (1.1), i.e.

$$P(x) = \sum_{n=0}^{m} p_n x^n \qquad (8.2)$$

The distribution of twisting moment on the assembly is assumed

to be of the analogous form

$$T(x) = \sum_{n=0}^{m} t_n x^n \tag{8.3}$$

The total shear force, P_i, and twisting moment, T_i, carried by any particular wall assembly at the level x_i are

$$P_i = H \int_{x_i}^{1} P(x)\, dx = \sum_{n=0}^{m} s_{in} P_n \tag{8.4}$$

$$T_i = H \int_{x_i}^{1} T(x)\, dx = \sum_{n=0}^{m} s_{in} t_n \tag{8.5}$$

s_{in} is an integration coefficient which is independent of any particular wall assembly and is given by

$$s_{in} = H \frac{1 - x_i^{n+1}}{n+1} \tag{8.6}$$

The deflection and rotation of the j'th wall assembly at level x_i can be expressed in the forms

$$y_{ij} = \sum_{n=0}^{m} f_{in} P_n \tag{8.7}$$

$$\theta_i = \sum_{n=0}^{m} f'_{in} t_n \tag{8.8}$$

In expressions (8.7) and (8.8) it is assumed that the direct force produces no rotation of the wall assembly and likewise the twisting moment causes no lateral displacement. This will be a realistic assumption in buildings where the parallel assemblies consist of simple open shapes of the types analysed in Chapter 2.

The influence coefficients f_{in} and f'_{in} depend on the configuration of the wall assembly, including its foundations, to which they refer. The direct load coefficients f_{in} are obtained directly from the relevant equation, (3.27) or (6.6). The torque

coefficients f'_{in} may be evaluated from straightforward "strength of materials" formulae, for example Den Hartog[11] or by a more sophisticated analysis which includes warping effects, for example Michael[12].

The torsional moment on any element is related to the resultant twist by

$$T = C \frac{d\theta}{d\chi} = \frac{C}{H} \frac{d\theta}{dx} \qquad (8.9)$$

where C is the torsional stiffness of the element.

Substituting the torque of equation (8.5) into (8.9) and integrating, subject to the boundary condition that there is zero rotation at the base gives the twisting moment-rotation relationship in the form

$$\theta_i = \frac{H^2}{C} \sum_{n=0}^{m} \left\{ \frac{t_n}{n+1} \left[x_i - \frac{x_i^{n+2}}{n+2} \right] \right\} \qquad (8.10)$$

The influence coefficients for any level x_i are therefore given by

$$f'_{in} = \frac{H^2}{C} \frac{1}{n+1} \left[x_i - \frac{x_i^{n+2}}{n+2} \right] \qquad (8.11)$$

4.4 POINT LOAD CASE

In this case, it is assumed that the direct loading which is distributed to any shear wall assembly is in the form of a series of m point loads, (1.3) which act at any suitable set of m reference levels (1.4). The twisting moment carried by the assembly is assumed to be of the analogous form of a series of m point torques acting at the same set of m reference levels, i.e.

$$t_1, t_2, t_3, \ldots t_n, \ldots t_m \qquad (8.12)$$

The total shear force and twisting moment carried by any particular assembly at the reference level x_i are simply the sum of the point loads and point torques at and above that level as given by

$$P_i = \sum_{n=1}^{m} s_{in} P_n \qquad (8.13)$$

$$T_i = \sum_{n=1}^{m} s_{in}\ t_n \qquad (8.14)$$

In this case s_{in} takes the form of a step function in order to give a single solution for the entire height. s_{in} takes unit value when x_n is greater than or equal to x_i, otherwise it is zero.

The deflection and rotation of the j'th wall assembly at level x_i can be expressed in the forms

$$y_{ij} = \sum_{n=1}^{m} f_{in}\ p_n \qquad (8.15)$$

$$\theta_i = \sum_{n=1}^{m} f'_{in}\ t_n \qquad (8.16)$$

Once again it is assumed that the direct load produces no rotation and the torque no lateral displacement.

In this case the direct load influence coefficients f_{in} are obtained from the relevant equations, (4.37), (4.38), (6.11) or (6.12).

Substituting the torque of equation (8.14) into (8.9) and integrating subject to the boundary conditions that there is zero rotation, in plan, at the base and that there is continuity at each load point gives the twisting moment-rotation relationship in the form

$$\theta_i = \frac{H}{C} \sum_{n=1}^{m} \left\{ x_n - s_{in}\,(x_n - x_i) \right\} \qquad (8.17)$$

The influence coefficients for any level x_i are therefore given by

$$f'_{in} = \frac{H}{C} \left\{ x_n - s_{in}\,(x_n - x_i) \right\} \qquad (8.18)$$

4.5 GENERAL ANALYSIS

The remainder of the analysis of a three-dimensional structure

follows a very similar course for both polynomial and point load cases.

In the polynomial case, the shear forces P_i, on wall j, at any suitable set of $(m + 1)$ reference levels may be related to the $(m + 1)$ load coefficients p_n by the matrix equation

$$\underline{P}_j = \underline{S}\ \underline{p}_j \tag{8.19}$$

Similarly, the twisting moments T_i, on the same wall, at the same set of reference levels are related to the moment coefficients t_n by

$$\underline{T}_j = \underline{S}\ \underline{t}_j \tag{8.20}$$

$\underline{P}_j$ and $\underline{T}_j$ are column vectors of the shear forces and twisting moments on wall j at each reference level.

$\underline{p}_j$ and $\underline{t}_j$ are column vectors of the load and moment coefficients on the wall.

$\underline{S}$ is the square matrix of integration coefficients as given by equation (8.6).

In the point load case, the shear forces and twisting moments, on wall j, at the m load points are related to the m point loads and twisting moments by the same matrix equations (8.19) and (8.20), provided the matrices $\underline{p}_j$, $\underline{t}_j$ and $\underline{S}$ are redefined.

$\underline{p}_j$ and $\underline{t}_j$ are column vectors of the point loads and point torques acting on wall j.

$\underline{S}$ is the square matrix of step coefficients s_{in} as defined in section 4.4.

The load-deflection and moment-rotation relationships for the j'th wall assembly may be expressed in the form of matrix equations as

$$\underline{Y}_j = \underline{Y} + \underline{\theta}\ z_j = \underline{F}_j\ \underline{P}_j \tag{8.21}$$

$$\underline{\theta} = \underline{F}'_j\ \underline{t}_j \tag{8.22}$$

$\underline{Y}_j$ is a column vector of the deflections y_{ij}, of wall j, at each reference level.

$\underline{Y}$ and $\underline{\theta}$ are column vectors of the deflections y_i at the datum position and rotations θ_i of the building, respectively, at each reference level.

$\underline{F}_j$ and $\underline{F}'_j$ are square matrices of the influence coefficients, f_{in} and f'_{in}, respectively, for the j'th wall assembly, found as described in either section 4.3 or 4.4 according to the form of load distribution being considered.

The matrices $\underline{F}$ and $\underline{F}'$ can be evaluated for all the J wall assmeblies comprising the building. In many buildings there are sets of identical wall assemblies which occur more than once. For each set of identical walls the matrices $\underline{F}$ and $\underline{F}'$ are respectively the same and need only be evaluated once.

Equations (8.21) and (8.22) may be solved for $\underline{p}_j$ and $\underline{t}_j$, respectively, to give

$$\underline{p}_j = (\underline{F}_j)^{-1} \quad \underline{Y}_j = (\underline{F}_j)^{-1} \quad (\underline{Y} + \underline{\theta}\, z_j) \tag{8.23}$$

$$\underline{t}_j = (\underline{F}'_j)^{-1} \quad \underline{\theta} \tag{8.24}$$

The conditions of overall equilibrium of the building at level x_i are

$$W_i = \sum_{j=1}^{J} P_{ij} \tag{8.25}$$

$$M_i = \sum_{j=1}^{J} \left\{ P_{ij} \; z_j + T_{ij} \right\} \tag{8.26}$$

For the whole set of reference levels being considered the equilibrium conditions may be written in matrix form as

$$\underline{W} = \sum_{j=1}^{J} \underline{P}_j \tag{8.27}$$

$$\underline{M} = \sum_{j=1}^{J} \left\{ \underline{P}_j \; z_j + \underline{T}_j \right\} \tag{8.28}$$

$\underline{W}$ and $\underline{M}$ are column vectors of the resultant horizontal loads and twisting moments W_i and M_i respectively at each level x_i.

Substituting equations (8.19) and (8.20) into equations (8.27) and (8.28) and subsequently substituting (8.23) and (8.24) into the results gives the equilibrium conditions in the form

$$\underline{W} = \underline{S} \sum_{j=1}^{J} \left\{ (\underline{F}_j)^{-1} \ (\underline{Y} + \underline{\theta} \ z_j) \right\} \tag{8.29}$$

$$\underline{M} = \underline{S} \sum_{j=1}^{J} \left\{ (\underline{F}_j)^{-1} \ (\underline{Y} + \underline{\theta} \ z_j) \ z_j + (\underline{F}'_j)^{-1} \ \underline{\theta} \right\} \tag{8.30}$$

Equations (8.29) and (8.30) are solved simultaneously to give

$$\underline{Y} = \left[\underline{B}_2 - \underline{B}_3 \ (\underline{B}_2)^{-1} \ \underline{B}_1 \right]^{-1} \left[\underline{M} - \underline{B}_3 \ (\underline{B}_2)^{-1} \ \underline{W} \right] \tag{8.31}$$

$$\underline{\theta} = \left[\underline{B}_2 - \underline{B}_1 \ (\underline{B}_2)^{-1} \ \underline{B}_3 \right]^{-1} \left[\underline{W} - \underline{B}_1 \ (\underline{B}_2)^{-1} \ \underline{M} \right] \tag{8.32}$$

The matrices $\underline{B}_1$, $\underline{B}_2$ and $\underline{B}_3$ are defined as follows

$$\underline{B}_1 = \underline{S} \sum_{j=1}^{J} (\underline{F}_j)^{-1} \tag{8.33}$$

$$\underline{B}_2 = \underline{S} \sum_{j=1}^{J} (\underline{F}_j)^{-1} \ z_j \tag{8.34}$$

$$\underline{B}_3 = \underline{S} \sum_{j=1}^{J} \left\{ (\underline{F}_j)^{-1} \ z_j^{\,2} + (\underline{F}'_j)^{-1} \right\} \tag{8.35}$$

Having determined the deflections and rotations of the structure at all the reference levels, the force and moment coefficients in the polynomial case or the point loads and point torques in the point load case may be found, for each of the wall assemblies in the structure, by substituting $\underline{Y}$ and $\underline{\theta}$ into (8.23) and (8.24).

The force coefficients or point loads may then be used to

evaluate the forces and stresses in each individual wall assembly, using the formulae of the relevant sections of Chapter 2. The moment coefficients or point torques may be used to evaluate torsional stresses in the walls, by using established theory.

In many examples of shear wall buildings most of the wall assemblies consist of simple open shapes, often of narrow rectangular form. In such buildings it can be assumed that the torsional moments carried by the individual wall units considered in isolation are small compared to the moments carried by the walls in differential bending, the latter moments being given by the product of the shear force on a wall and its distance from the datum position. This being the case the matrix $\underline{F}'$ is zero and the solution is again given by (8.31) and (8.32) provided $\underline{B}_3$, is redefined as

$$\underline{B}_3 = \underline{S} \sum_{j=1}^{J} (\underline{F}_j)^{-1} \; z_j^{\,2} \qquad (8.36)$$

In cases where both the structure and the applied lateral loading are reasonably symmetrical, the rotations $\underline{\theta}$ will be small. If the torsional deformation can be neglected in comparison with the bending deformations, the $\underline{\theta}$ terms vanish and the equilibrium conditions reduce to

$$\underline{W} = \underline{S} \sum_{j=1}^{J} (\underline{F}_j)^{-1} \; \underline{Y} \qquad (8.37)$$

The solution of (8.37) is then

$$\underline{Y} = (\underline{B}_1)^{-1} \; \underline{W} \qquad (8.38)$$

where $\underline{B}_1$ is as given previously in (8.33).

The force coefficients or the point loads are then found for each wall assembly from equation (8.23) as before, but with $\underline{\theta}$ made equal to zero.

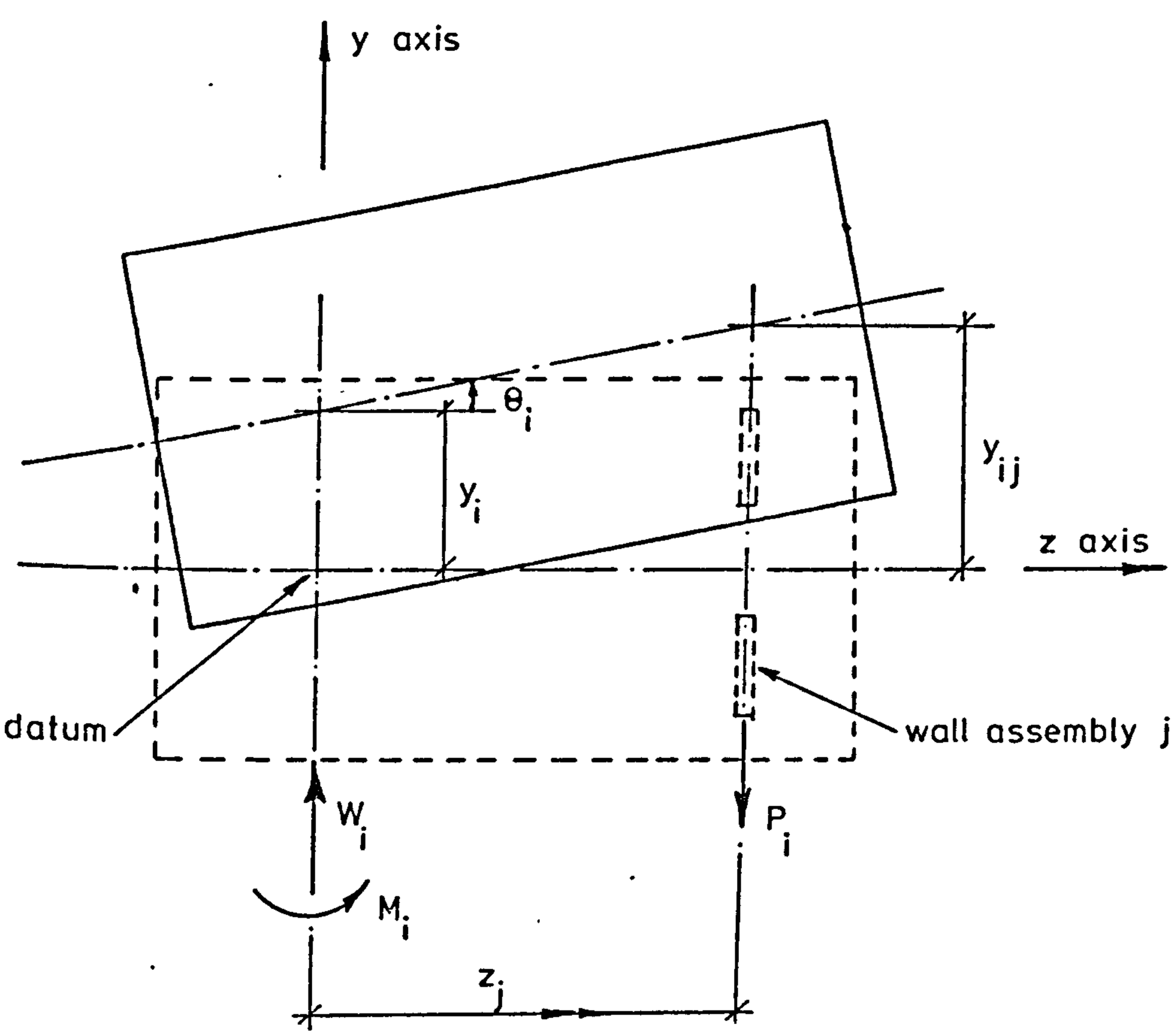

Rigid body movement of floor slab.

Figure 4.1

CHAPTER 5

NUMERICAL COMPUTATION

5.1 INTRODUCTION

Any analysis, no matter how complex, is more readily understood and more simply executed once the various stages of the problem have been defined. Provided that the relationships between the other stages are considered and their effects included, each stage of the analysis may be treated as a separate problem. This is particularly so with the analysis of shear wall structures of the types being considered.

Primarily the design of any structure may be divided into three parts as follows:

1. Planning
2. Structural design to support vertical loads
3. Structural design to resist lateral loads

The three divisions are inter-related to varying degrees depending on the project.

It is normally the responsibility of an architect to plan the structure to fulfil the functional requirements of the client. The structural engineer uses the functional layout, as supplied by the architect, as the basis of the design for vertical and lateral loads. By the utilisation of dividing walls in simple structures it is often unnecessary to introduce additional load bearing members to a structure. However in more complex buildings the structural design often imposes severe restraints on the functional layout and must be considered early in the planning stage. In low-rise buildings the design of the structure to resist vertical forces is the dominant consideration. However, as the height increases, the effects of lateral loads become more important and must be taken into account at an earlier stage in the design.

The present chapter is concerned with the application of the methods of analysis and the analytical expressions presented in

Chapters 2, 3 and 4, to evaluate the forces, stresses and deflections due to lateral loads on a shear wall system. Numerical computations involving the above analyses may be divided into a number of well defined stages which are depicted in the form of a flow chart in Figure 5.1. The various stages and their relationships are discussed in the following section, 5.2.

The application of the computer in the analysis of shear wall structures is discussed and a description is given of a system of programs developed utilising the present analyses.

5.2 STAGES OF COMPUTATION

5.2.1 IDENTIFICATION OF STRUCTURE

The configuration of the lateral load bearing systems within a building is closely linked with the planning and vertical force design stages as indicated on the flow chart, figure 5.1. The evaluation of the lateral load carrying capacity of a building must begin with the identification of those parts of the structure which are capable of resisting such loads. The choice of lateral load resisting systems will depend on the direction of the applied forces and will often be a matter of engineering judgement, based on experience. Although only general effects on the structural elements of the building as a whole are discussed here, the local effects on cladding must also be considered in practice.

In multi-storey shear wall structures of the types being considered, the identification of the general structural systems capable of resisting the lateral loads in any particular direction is reasonably straightforward since, in these buildings, such systems are normally deliberately incorporated in the early stages of planning and design. However difficulties often arise in the determination of the precise strength of these systems. The most commonly encountered problems have been discussed by Popoff[13] and are summarised as follows:

1. In systems which include shear walls with flanges at right angles to the direction of the applied loading, such as the examples of figure 5.2, the portion of the flange which is effective in resisting lateral loads is often uncertain. In figure 5.2,

comparison of the flanges in (a), (b) and (c), each of a common breadth, would indicate different proportions of the seemingly equivalent flanges to be effective in each case. The configuration of neighbouring shear walls may also influence the proportion of a flange which is effective, as illustrated by comparing (d) and (e) in figure 5.2.

2. In shear walls coupled by beams or slabs the beam- or slab-to-wall connection is subject to local deformations which reduce the fixity of the connection and affect the overall stiffness of coupled systems, as discussed by Michael[7]. Provision for inceasing the effective span of connecting beams, as suggested by Michael is incorporated in the analysis in Chapter 2.

3. In systems where the shear walls are coupled wholly or partially by the action of the floor slabs, the stiffness of the system depends on the width of slab which is effective in coupling the walls. One method which has been used to estimate the effective width of a slab coupling is to project lines, on the plan of the slab, from the interior corners of the walls, at 45 degrees to the line of the walls and to consider the width of slab between the intersections of the lines to be effective.

Various experimental investigations have shown that different proportions of the above-defined width of a slab coupling may be effective depending on the configuration. Qadeer and Stafford Smith[14] give proportions less than the above width, Coull[15] shows that proportions greater than the above width may be effective, while tests by Barnard and Schwaighofer[16] show that the entire width is effective under the given circumstances.

An illustration of the effects of different slab widths on the stiffness of a pair of coupled shear walls is given in Chapter 6.

The identification of the precise nature of the lateral load bearing system of a structure is therefore of fundamental importance if the response of the building to wind and seismic forces is to be accurately evaluated.

5.2.2 DESIGN LOADING

The evaluation of the magnitude and distribution of the wind

forces which may be expected to act on a building is normally achieved by the use of the standard code of practice relative to the country in which the building is to be constructed, for example the relevant British Code of Practice[17].

The wind forces generally depend on such factors as the location and exposure of the building, its relationship to surrounding structures, the height and shape of the building and its projected area. All of these factors are direct results of the planning of the building as indicated in figure 5.1.

5.2.3 DISTRIBUTION OF LOADING

The load deflection relationships of the various lateral load bearing systems may be calculated by the use of the relevant equations in Chapter 2. The design forces may then be distributed to the individual wall systems according to their respective stiffnesses by the use of the methods of Chapter 4.

The method entails an initial choice of the number and position of the reference levels which will have an effect, both on the accuracy of the solution and on the amount of computation required. Where a high degree of accuracy is required a large number of reference levels should be used and resort must be made to computer programs, since the matrices, although small compared to those encountered in finite element or frame solutions, are too large for hand computation. However where accuracy is not quite so important, such as during early design work a solution may be obtained using a limited number of reference levels, in which case the matrices are smaller and hand calculations become feasible. The effects of using varying numbers of reference levels are discussed in Chapter 6.

The positions of the reference levels may have an effect on the solution, particularly where the applied forces change rapidly with height. In the normal situation, where the load distribution is reasonably regular, showing no sudden changes, the reference levels are conveniently positioned evenly throughout the height of the building. In cases where rapid variations of applied force occur the accuracy of the solution may be increased by grouping the reference levels more closely in the vicinity of these sudden changes.

The datum position on the plan of the structure, to which all walls and forces are referred, may be selected at any point, within or outwith the bounds of the structure. However, a careful choice of origin, in certain circumstances, may considerably reduce the amount of computation required to reach a solution. For example, in the case of a symmetrical structure, in which the origin is chosen at the centroid of the plan, matrix $\underline{B}_2$, (8.34), is zero and the deflections and rotations at the datum position are independent of each other but dependent, respectively, on the direct load and the twisting moment applied at the datum. The problem may thus be solved and their respective effects superimposed. However, with the same problem, but where the origin is chosen at a position other than the centroid, matrix $\underline{B}_2$ is non-zero and the full computation must be carried through.

In a general unsymmetrical structure it is worth noting that there will be a position of the datum where the terms of matrix $\underline{B}_2$ will be at their smallest; mathematically, the determinant of $\underline{B}_2$ will be at a minimum. It is normally impractical to find the exact position of this "centre of stiffness", however its approximate position may be ascertained by considering the disposition of the various wall assemblies on plan, a good guide being given by the centroid of the areas of the wall sections. Where the datum is chosen in the vicinity of the "centre of stiffness", the numerical values within the matrices $\underline{B}_2$ and $\underline{B}_3$, (8.34) and (8.35) respectively, will tend to be smaller than with other datum positions. The matrix $\underline{B}_1$, (8.33) is unaffected by the position of the datum, and is principally concerned with the bending effects on the structure. Thus, where it is possible to use smaller values in matrices $\underline{B}_2$ and $\underline{B}_3$, besides facilitating the manipulation of the matrix equations, the resultant solution will tend to favour the bending of the walls rather than their torsion. This is especially important in hand computation where rounding errors may have a large effect on the accuracy of the solution.

Having chosen a suitable origin and set of reference levels the load-deflection relationships in the form of the flexibility coefficients, f, are calculated for each wall assembly, at each reference level by using the relevant expressions, contained in Chapter 2. The fact that the flexibility coefficients are the same

for identical wall assemblies allows a considerable reduction in the amount of computation required for buildings in which wall configurations are repeated. The flexibility coefficients for each wall assembly form the flexibility matrix, $\underline{F}$, which is then inverted to give the stiffness matrix for that assembly.

The resultant effects of the applied loading, both the direct forces and the moments about the datum, at each reference level are evaluated by a suitable integration of the load distribution above the relevant level. The vectors of forces and moments, $\underline{W}$ and $\underline{M}$ respectively, together with the stiffness matrices of all the wall assemblies are used to evaluate the deflection and rotation of the datum position at each reference level, by means of the matrix equations (8.31) and (8.32). The deflections of each wall assembly at each reference level follow immediately by employing equation (8.1). The forces or force coefficients relevant to each wall assembly are then found by multiplying the relevant stiffness matrix by the vector of deflections for that assembly as described by equation (8.23).

For general unsymmetrical structures, the evaluation of the loads distributed to each wall assembly involves a number of matrix manipulations. Other than in the specific symmetrical case, all the elements of these matrices are non-zero, and hence none of the techniques developed for manipulating banded matrices are of use in cutting down the amount of computation. However, the size of all the matrices is the same and is identical to the number of reference levels. In consequence, by choosing a small number of levels, the computations may be carried out by hand or by desk calculator, the computer only being resorted to where a high degree of accuracy is required.

5.2.4 EVALUATION OF INDIVIDUAL WALL ACTIONS

Once the forces acting on the wall assemblies are known, each assembly may be considered as a separate unit and its forces, stresses and deflections evaluated directly by the use of those expressions of Chapter 2 which are relevant to the particular configuration of structure and load. These actions may be found at any desired position, irrespective of the positions of the reference levels used in the load distribution stage.

The amount of detail required from any particular analysis will generally dictate the method of computation adopted. In a preliminary design calculation, which employs a small number of reference levels, the distributed load is expressed as the first terms of a polynomial series, or as a small number of point loads. Where stresses and deflections are only required at critical points, for example at the base and top respectively, these may be evaluated by means of the graphical methods of Chapter 3. Otherwise the actions at particular positions may be found by hand or by desk calculator from the relevant expressions. In the light of these outline calculations the projected lateral load bearing structure may require to be modified and the revised system analysed again, as depicted on the flow chart, Figure 5.1.

Once the general outline design has been finalised an accurate load distribution will be carried out using a larger number of reference levels and a comprehensive evaluation of forces, stresses and deflections will be required for the detailed design of the structure. At this stage the amount of computation involved is substantial and hand calculations are tedious, so that it is more practical to make use of the computer programs.

5.3 COMPUTER ANALYSIS

During the course of the present research, much use was made of the available computer facilities and a system of programs was developed for the rapid evaluation of laterally loaded two and three dimensional shear wall systems of a wide variety of configurations. The programs were invaluable when used to study the effects of varying specified parameters of typical systems, where large numbers of similar analyses are required. Although the computer system and the programs themselves were specifically developed for the present study and consequently reflect the purposes for which they were designed, for example the qualitative parameter studies and the tests on the convergence and stability of the solutions discussed later, the end result was a versatile system which is readily usable by the structural engineer with very limited experience of computers.

Since the range of facilities available in the University Computer Centre had a significant effect on the form of the system for

running the programs a brief description of the facilities is included. Discussion of the system and of the programs is limited to a general outline since detailed descriptions would be lengthy and only of interest to a specialist programmer.

5.3.1 COMPUTER FACILITIES

During the earlier part of the present research, the University computer installation consisted of an I.C.L. 1905 machine with a core capacity of 32K, up to 25K of which could be made available for the running of programs. Additional backing storage could be obtained by the use of magnetic discs or magentic tapes. The transfer of programs and data to and from the computer was achieved by punched paper tape, punched cards, line printer or graph plotter, either directly or by the intermediate use of files held on magnetic tape or on an area of magnetic disc. The running of sequences of programs was facilitated by the use of the Lancaster Command Language Processor, a system developed at the University of Lancaster. Files stored on magnetic disc were readily altered by the use of one of a number of teletypes linked either directly or by telephone to the computer system.

Latterly the University has installed an I.C.L. 1904S machine which has a core capacity of 128K words, and is approximately 2.5 times faster than the 1905. Much of the peripheral equipment of the 1905 has been retained, and has been enhanced by, noteably, greater backing storage provided by three additional magnetic disc units and a magnetic drum which give a total on-line storage in the region of 200 million characters.

The computer is currently controlled by the operating system, GEORGE 3 Mark 7 (GEneral ORGanisational Environment). The system allows simultaneous running of a number of programs and the editing of files held in the computer's file store.

5.3.2 PROGRAMMING LANGUAGE

The two languages most widely used for the programming of scientific and engineering problems are Fortran and Algol, both of which are provided on the University computer. Both are "high level" languages, in that the programmer need know nothing of the internal

workings of the computer. Scientific formulae are easily programmed and the program instructions are written using standard words whose actions correspond to their English meanings. Programs written in either language are therefore easy to read and alter.

Both Fortran and Algol have advantages and disadvantages relative to each other. For the present purposes a major consideration was the need to vary the number of reference levels readily in the studies of the convergence and stability of the solutions. The existence in Algol of the facility to change the dimensions of arrays of variables, e.g. matrices, during the running of programs, a facility not available in Fortran, made the former language the obvious choice. Consequently programs were exclusively written in Algol, specifically the I.C.L. implementation of Algol 60.

5.3.3 COMPUTER PROGRAMS

The programs were originally developed on the 1905 computer whose small storage capacity limited the size of programs which could be used. While it is being run, a program, in the form of instructions in machine code, occupies part of the available core, and the remainder may be used to store numerical data. In order to employ the maximum amount of core for the storage of data, thus enabling larger structures to be analysed, it was decided at an early stage to divide the computations into a sequence of small programs. Information could then be transferred between successive programs by utilising the backing storage facilities.

Each program in the sequence closely corresponds to one of the stages of the computation discussed in section 5.2. Where necessary, alternative programs were developed to deal with each of the two forms of load distribution, polynomial and point load, for which the analysis was developed. The general arrangement of the sequence of programs is shown in the form of a flow chart in figure 5.3. The system may be used for the solution both of complete buildings and of individual two-dimensional systems. An advantage of using a number of small programs is that only those programs relevant to any particular problem need be included.

There follows a brief description of each of the programs, together with the approximate core occupied by the program compiled in

machine code, in units of K words. 1 K word is equivalent to 1024 units of core, each capable of storing one real number or two integers.

PROGRAM 1 STRUCTURAL DATA (11K)

Program 1 is used to read in the data which defines the dimensions and elastic properties of the wall assemblies, the foundation conditions for each wall and the layout of the walls in a complete structure. In problems where only a two-dimensional analysis is required the data is identical and is interpreted as a number of separate wall assemblies, each with the same height and number of storeys. In the latter case the data relevant to defining the layout of the walls is read but ignored in subsequent programs.

The program describes and prints each item of data as it is read, firstly to enable a check on the data to be made and secondly to furnish a documented definition of the structure at the head of the results for future reference. The data and structural constants (α, μ, etc.) which are computed from the data, along with a text title, are stored on a backing store file to be read by subsequent programs.

PROGRAM 2 LOADING ON COMPLETE STRUCTURE (10K)

Program 2 is used exclusively in the analysis of complete structures to read in the data relevant to the applied loading. The data is presented in the form of three functions in terms of the height coordinate, χ , whereby almost any type of loading may be represented. Any of the functions may be zero or constant or any mathematical function so long as it is piecewise continuous throughout the height of the structure.

The first function represents the resultant intensity per unit height of the loading throughout the height of the building. The second represents the position of the resultant, which may vary, with respect to the datum position, from which the moment of the resultant about the datum is calculated. As an alternative the third function may be used to represent the applied moment per unit height about the datum, in which case the second function would normally be zero. A pure torque may be represented by the moment function with the load and

position functions both zero. Where all three functions are non zero the total moment is given by the sum of the applied moment function and the moment of the resultant load about the datum.

The data for Program 2 includes a text title which is stored and used to identify the particular load configuration in the output.

Different sets of reference levels may be processed simultaneously in one run of the program, a facility which was used to advantage in the tests on convergence and stability. The program reads the number of sets of levels, the number of levels in each set and the method of positioning the levels, which may be evenly spaced throughout, either including or excluding the top or may be generally placed according to data supplied for each set.

For each set of levels the total direct and moment effects of the force distribution above each level are found by integrating the three functions using a Simpson's rule procedure and the results printed and stored on the backing store file.

PROGRAM 3 LOAD DISTRIBUTION (11K)

There are two versions of Program 3, relevant to the two types of load distribution employed in the analysis. In each version the data stored by Programs 1 and 2 is read and a load distribution is carried out for each of the sets of reference levels defined by the data.

The program deals with the general case of an unsymmetrical structure subjected to unsymmetrical loading. By referring to the flow chart in figure 5.4, it can be seen that the program closely follows the steps outlined in the latter part of section 5.2.3.

During the development of the two versions of Program 3 each matrix was printed out in full as it was calculated. In the final working program only the deflection and rotation of the datum point, at each reference level, are printed out, while the load coefficients are output to the backing store file for use in subsequent programs.

PROGRAM 4 EVALUATION OF WALL ACTIONS (13K)

Once again there are two versions of Program 4, relevant to polynomial and point load cases respectively.

By means of a simple code, supplied as data, the particular levels at which the various wall actions are required are defined. Typical arrangements of levels are; at each storey, evenly throughout the height and at general, specified levels.

The data stored by previous programs is read from the backing store file and the forces, stresses and deflections at the required levels are calculated and printed in a table for each wall assembly subjected in turn to each load function relevant to it. The general sequence of Program 4 is given in the form of the flow chart in figure 5.5.

PROGRAM 5 PERCENTAGE DISTRIBUTION OF LOADING (8K)

Program 5 evaluates the percentages of the total applied load which are carried by each wall assembly in a structure at various levels throughout its height. The loads on all the wall assemblies in the structure for each set of reference levels are read in turn from the backing store file. The shear on each assembly is calculated in the polynomial case by the integration of the load function by Simpson's rule between the level concerned and the top, and, in the case of point loads by simple addition of the load at each level. From the shears at any level the percentage of the applied load carried by each wall is calculated and printed out in the form of a table.

The two versions of the program were developed to give a convenient method of illustrating the load redistribution in shear wall structures and was useful in the consideration of the effects of varying foundation conditions as presented in Chapter 6.

PROGRAM 6 LOADING ON TWO DIMENSIONAL SYSTEMS (9K)

Program 6 was developed so that individual two-dimensional shear wall assemblies could be analysed, subject to known load distributions. The program handles a number of wall assemblies, of equal height and number of storeys, simultaneously. The structural data, as supplied by Program 1, is read from backing store file. The loading data is supplied to the program as a number of load functions on each wall assembly, each in the form of a list of either polynomial or point load coefficients. The lists of load coefficients are placed on the

backing store file for direct use by the relevant form of Program 4.

OTHER PROGRAMS

Various other programs were developed for specific tasks, for example to evaluate the design parameters of Chapter 3 for wide ranges of values of their respective dependent variables, in order to prepare the design curves of Appendix 1.

5.3.4 COMMAND SYSTEM FOR RUNNING PROGRAMS

As indicated in section 5.3.3 the various computer programs may be used for the solution of both two-dimensional wall assemblies and complete three-dimensional structures. Either the polynomial distribution or the point load methods may be used. It was necessary, therefore, to be able to run the programs in the various sequences depicted in figure 5.3.

While the 1905 computer was in operation the Lancaster Command Language was employed to write simple instructions for the running of specific sequences of programs. On the 1904S computer, the GEORGE 3 operating system includes a language called the GEORGE 3 Command Language, in which similar sets of instructions may be written. The greater versatility of the GEORGE 3 Command Language enabled a more general system of instructions to be developed to handle all of the program sequences referred to above.

The general system of instructions, as outlined in figure 5.6, was stored in the computer on a file which then became a command system known as a MACRO. In order to compile and execute any desired program sequence all that was required was to state the MACRO name as a command, followed by a list of parameters which indicated the particular sequence of programs and the sources of all the relevant data. These parameters took the form of keywords which specified the various alternative sequences, such as POLYNOMIAL or POINT, STRUCTURE or WALL, etc. All the programs were stored on files and only those relevant to any particular problem, as defined by the parameters, were compiled using the standard MACRO'S, SALGOL and CONSOLIDATE. The compiled programs, in the form of machine code instructions, were each stored temporarily on files for subsequent execution.

All data was supplied in the form of files, stored in the computer. The names of the files were included in the list of parameters, each prefixed by a code character which identified the type of data contained in each, for example, structural, load, and a code to specify at which levels the wall actions were required.

The compiled programs were executed by the MACRO, in the required sequence, using the data file relevant to each. Results were collected together on a file created by the MACRO, output on the lineprinter as one document and the results file erased.

As indicated on figure 5.6, after the execution of the sequence of programs was complete the parameter specifying the structural data file was deleted from the list. The MACRO then determined if there was another file of structural data specified and continued to execute the sequence of programs until all such files had been used. This ability to recycle the programs for different data enabled a number of structures to be analysed, subjected to the same loads, within one call of the MACRO, and was widely used in the parameter studies of Chapter 6.

Figure 5.6 shows how the MACRO deals with various forms of errors by stopping itself, thus saving valuable computer time. The MACRO also erases all the working files created during each run before it terminates for any reason, thus enabling a series of problems to be run without interference between successive MACRO calls.

The use of the MACRO command system greatly simplified computations using the computer, the workload being reduced to the supply of data on files and single line calls of the MACRO with the relevant parameter list.

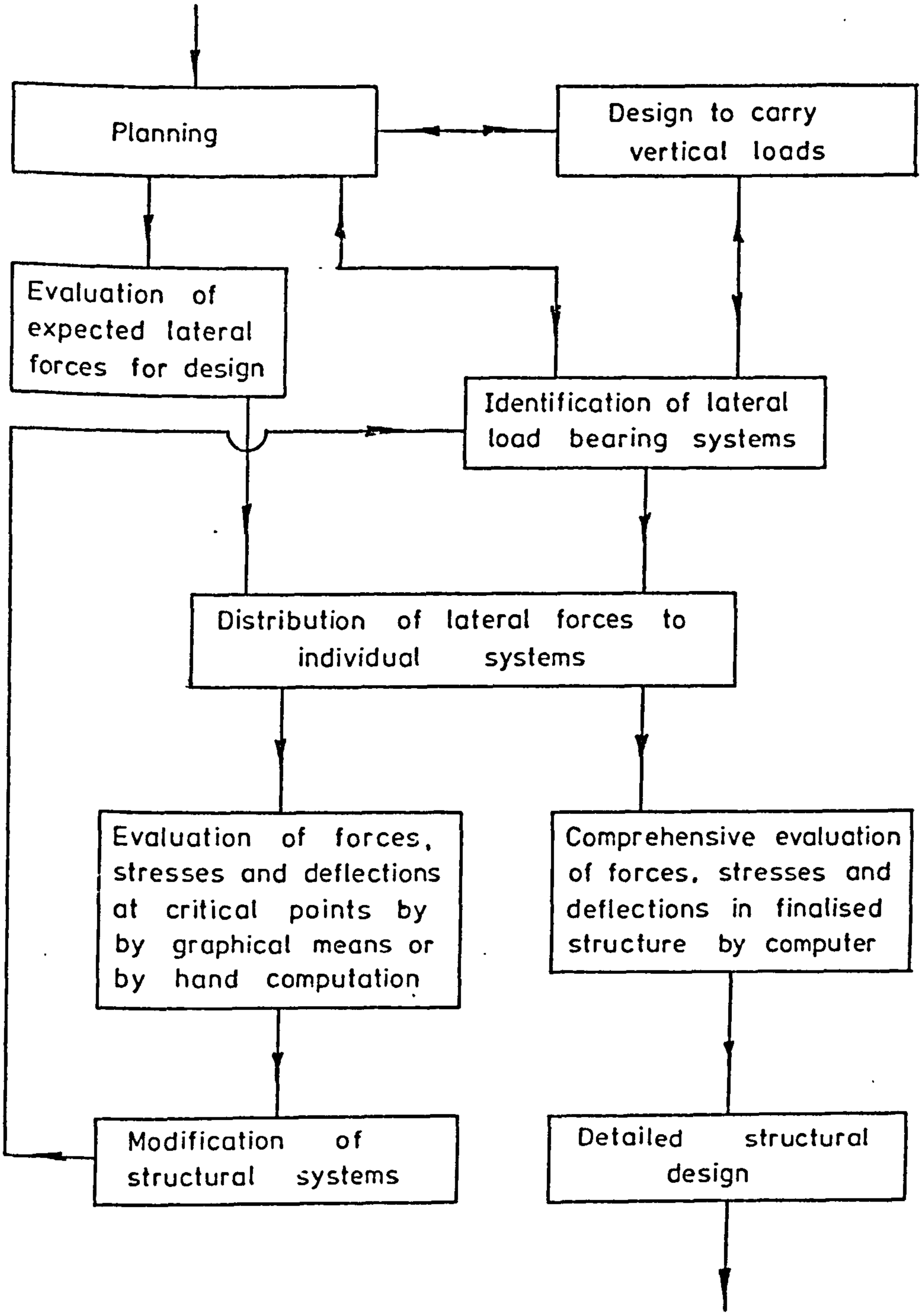

Stages of the design of a structure to resist lateral forces

Figure 5.1

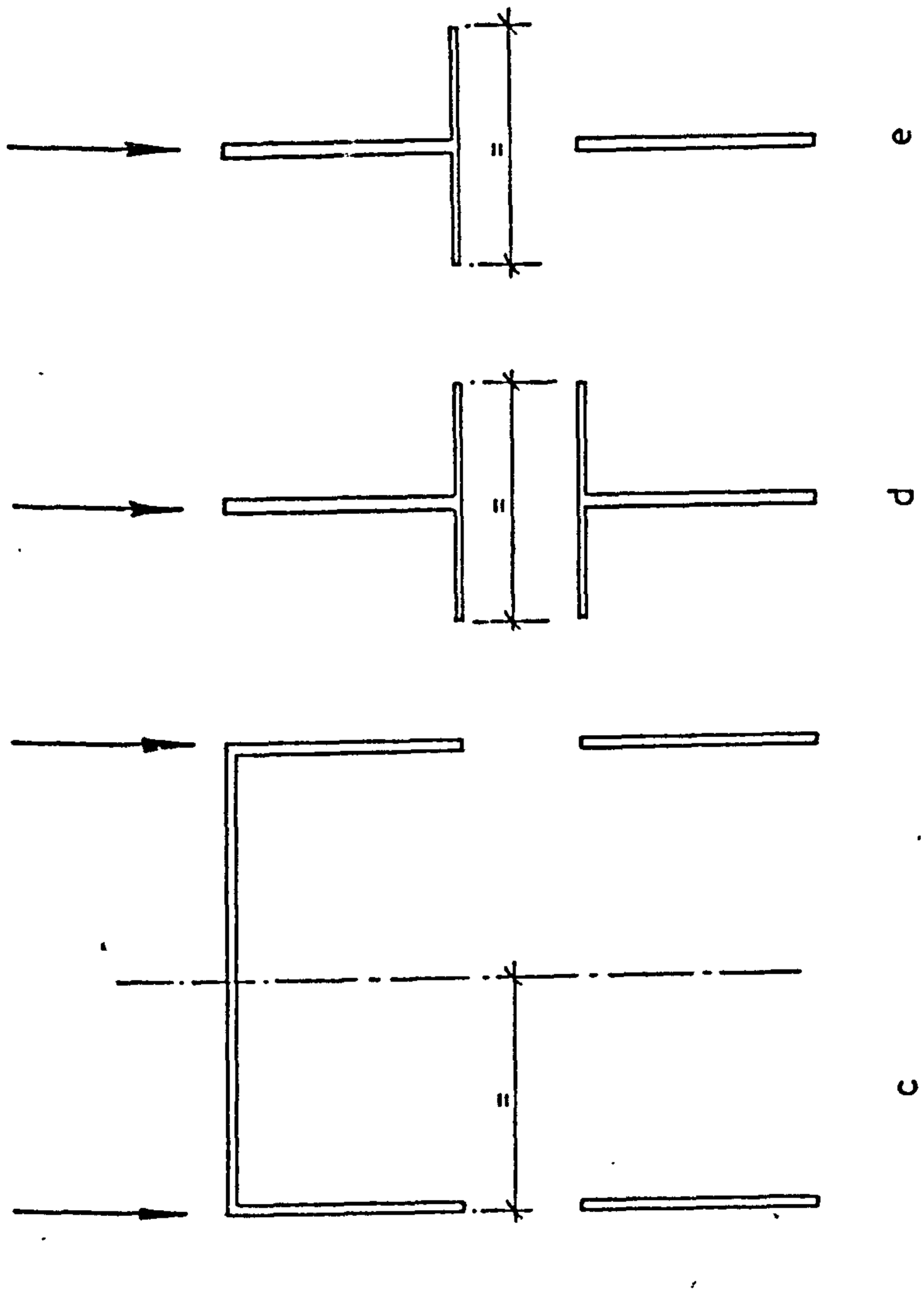
Direction of applied loading
Coupled shear walls incorporating flanges
a
b
c
d
e
h
h
h
h
h

Figure 5.2

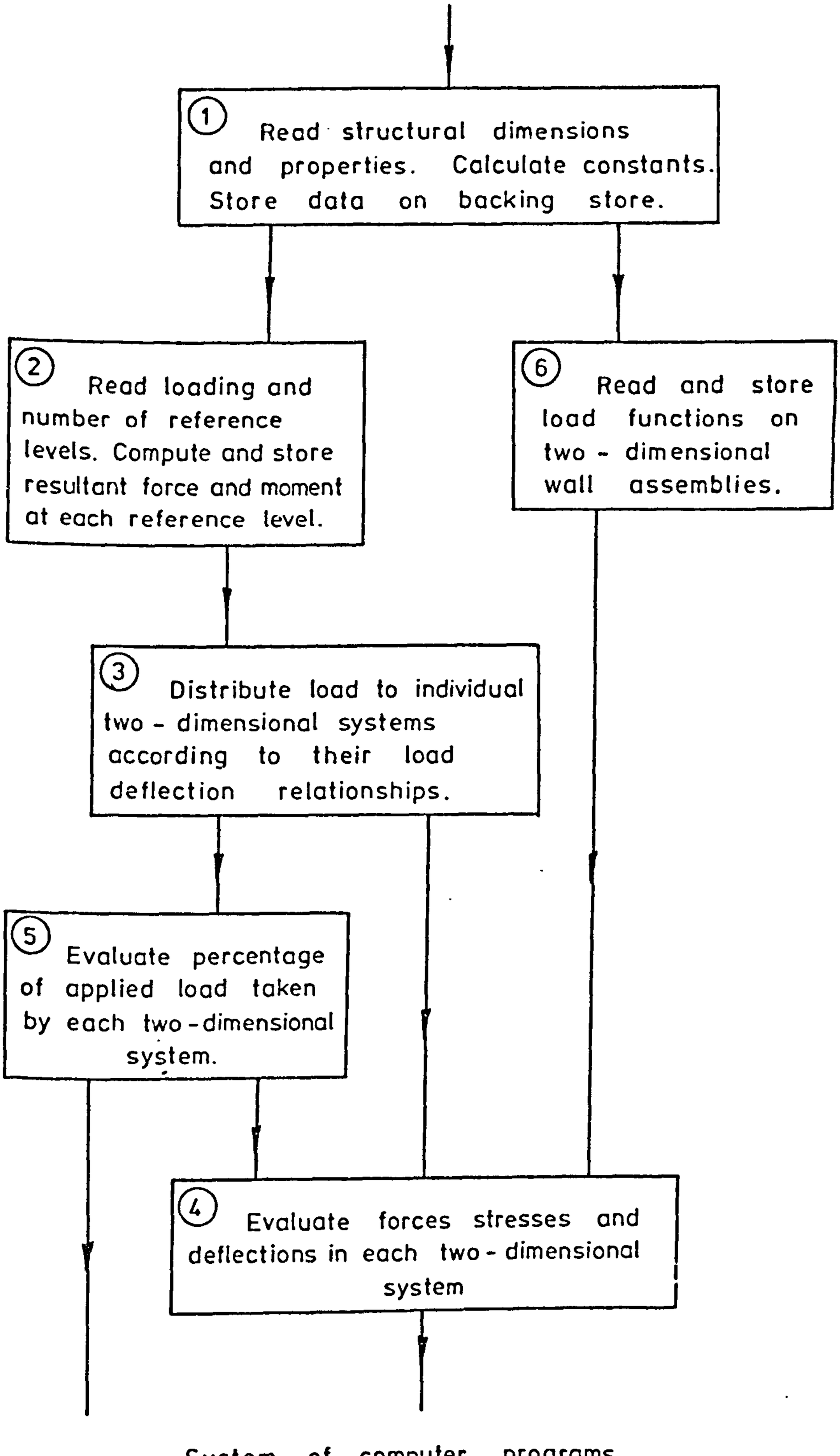

System of computer programs.

Figure 5.3

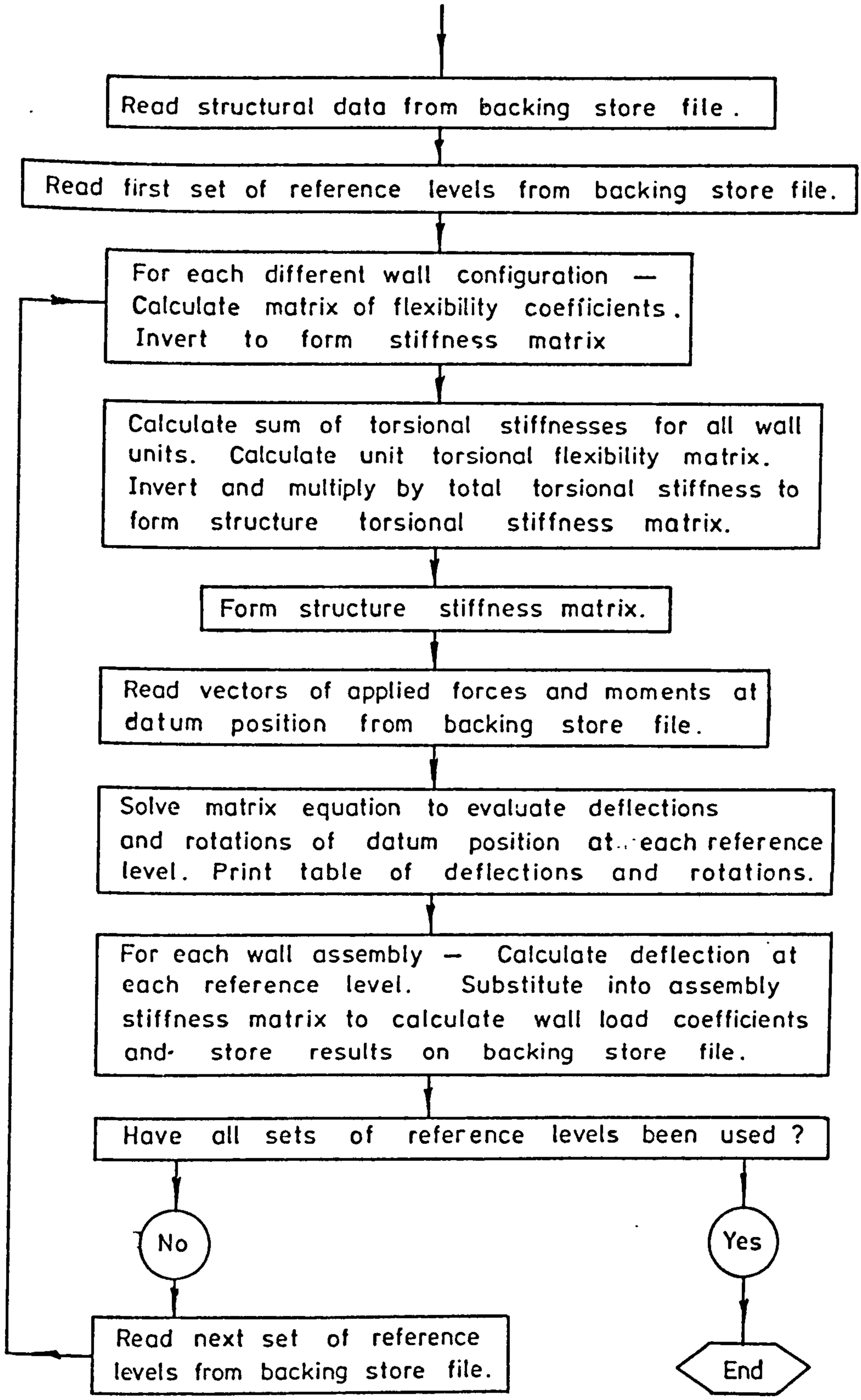

Program 3 - Load distribution

Figure 5.4

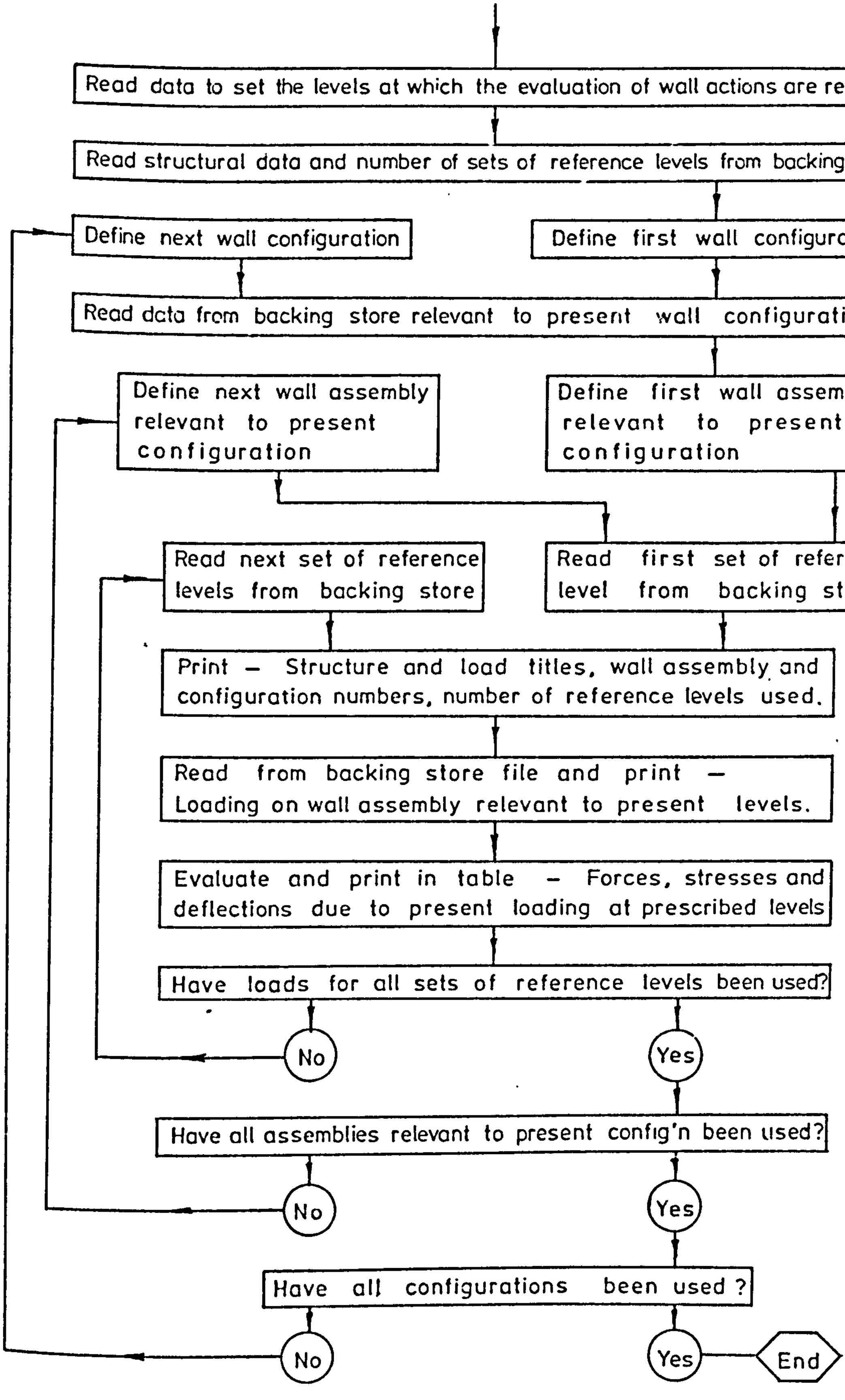

Program 4 – Evaluation of wall actions.

Figure 5.5

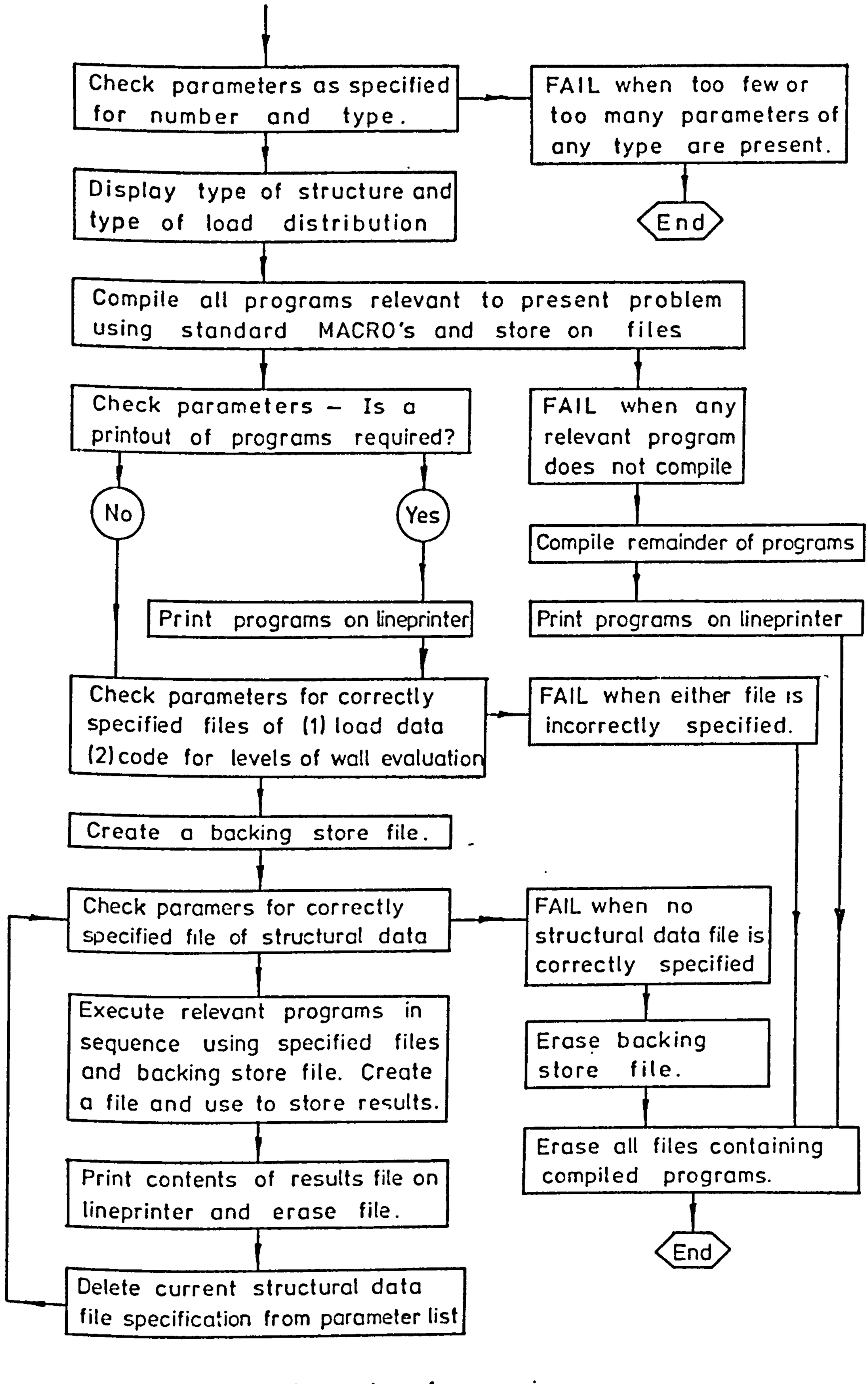

MACRO system for running programs.

Figure 5.6

CHAPTER 6

NUMERICAL PARAMETER STUDIES

6.1 INTRODUCTION

The following sections of the present chapter each contain a numerical investigation into a different facet of the analysis and structural behaviour of shear wall structures. In each section a particular example of coupled shear walls or a shear wall structure is analysed by the methods of Chapters 2 and 4, as incorporated in the computer programs discussed in Chapter 5. A specific parameter, either analytical or structural, is varied and the effects on the results of the analysis presented in graphical form.

In the case of an analytical parameter, namely the number of reference levels used in the analysis, the purpose of the numerical study is to investigate the reliability of the two methods of analysis and to compare the results with those obtained using other methods. The purpose of the structural parameter studies is to illustrate the general behaviour of the structural systems involved and to assess the importance of the particular parameter under investigation.

6.2 EFFECTS OF VARYING THE WIDTH OF A FLOOR SLAB EFFECTIVE AS A COUPLING BETWEEN SHEAR WALLS

As outlined in section 5.2.1 there are discrepancies between the methods available for estimating the width of a floor slab which is effective as a structural coupling between a pair of shear walls.

To illustrate the nature of the errors which may occur in the analysis of a pair of shear walls where the floor slabs are either partly or wholly the means of structural coupling, a series of computations was carried out on the typical connected shear wall system shown in figure 6.1. The example chosen had earlier formed the basis of a three-dimensional model constructed from perspex sheets and tested under the action of lateral loads by Irwin[18]. In a three-dimensional structure the stiffness of the floor slabs depends, in part, on the proximity of the adjoining shear resisting systems.

However, for the purpose of the present study, the coupled walls shown in figure 6.1, were idealised as an independent two-dimensional system.

The width of floor slab effective as the structural coupling was varied in each of a number of calculations and the deflection at the top, the maximum stress at the base and the shear force in the most highly stressed floor slab determined in each case with the system subjected to a uniform loading of 0.5 Kg. per storey (0.0965 N/mm height). The results are presented in graphical form in figures 6.2 and 6.3.

While the curves of figures 6.2 and 6.3 are drawn for the specific example of figure 6.1, they are nevertheless typical and are sufficient to indicate that small differences in an assumed or estimated width of effective floor slab may appreciably influence the calculated values of the force actions and deflections of the entire coupled system. It can be seen, for example, that any overestimation of the slab width effective in such a system gives rise to lower values for stress and deflection in the walls, and would lead to the walls being underdesigned. In such a case, although the total shear in any slab is greater, the shear force per unit width is less, and reinforcement placed across the overestimated width of slab to resist the lower stresses would be ineffective in resisting the larger stresses actually present within a narrower width.

In calculations involving a three-dimensional structure, the effect of overestimating the slab widths of coupled shear wall systems, thus overestimating their capacity to carry load, would be to produce results which would indicate a greater share of the load being carried by the coupled systems and a corresponding reduction in the load calculated as being carried by single wall systems such as access and service cores. Such a core system, designed to carry the calculated loads would consequently be overstressed.

It is thus important, in the analysis and design of structures which incorporate shear walls coupled by floor slabs that the true coupling effect of the slabs be accurately determined.

6.3 EFFECTS OF VARYING THE NUMBER OF REFERENCE LEVELS USED IN THE ANALYSIS

It is possible to solve many engineering problems by a variety of

methods. Often the choice of a particular scheme is made by consideration of the amount and complexity of the calculations involved in its analysis. The chosen scheme may not be the most economical in the use of materials and manpower if there is a sufficient reduction in computation over more sophisticated approaches to the problem. With the wider use of computers and the availability of commercial structural analysis programs it is becoming more common to make use of more sophisticated design techniques where they introduce definite economies. To use the computer in the early design stages is costly, especially where a number of schemes are being compared. There is still a need, therefore, for less complex analytical techniques.

In the present study the complexity of the two methods of analysis depends, almost entirely, on the number of reference levels chosen, as discussed in section 5.2.3. The number of levels chosen in any particular problem in turn depends on a variety of factors amongst which are the required degree of accuracy and the availability and relative costs of the methods of carrying out the calculations, that is by hand, graphical means, desk calculator, etc. Approximate analyses, such as those being considered are only of use if they are reliable, by which is inferred that any inaccuracies, with respect to the true solution, are reasonably predictable for a wide range of problems.

In order to investigate the degree to which and the conditions under which the present methods of analysis are predictable, two simple structures were each analysed by the two methods of distributing the applied loads, with varying numbers of reference levels being used. The reference levels used were spaced throughout the height of the structure such that the distances from the base to the lowest level, between all adjacent levels and from the uppermost level to the top of the structure were equal. The structures considered were the two twenty-storey models which were constructed for the experimental investigation discussed in Chapter 7. The models, the dimensions of which are shown in figures 7.1 to 7.3 inclusive, were considered in their basic form, that is with all the foundations assumed to be fully rigid. Each structure was analysed subjected to a uniform load equivalent to 1 Kg per storey, firstly positioned centrally to produce

no torsion and secondly positioned eccentrically to produce considerable torsion and hence rotation of the structure. The variation of the critical wall actions, namely the deflection at the top of the walls, the maximum rotation (where applicable), the maximum stress at the base of the walls, and the maximum shear force in the connecting beams were considered in each case. The results are presented graphically in figures 6.4 to 6.20 inclusive.

The structures were also analysed by the method given by Coull[19], and the results indicated on the relevant figures. The structures used for the present study are symmetrical and sufficiently regular in form that Coull's analysis yields the exact solution in cases where no torsional deformation of the walls takes place. In addition Coull's solution is not dependent on a system of reference levels and hence furnishes a useful datum for the comparison of the present methods of analyses under the various conditions of the four cases as follows.

Case 1. Model 1, which, for the purposes of this study, consisted of three identical pairs of coupled shear walls, symmetrically disposed in plan, was analysed subject to the symmetrical load described above. The variation of the critical wall actions are plotted in figures 6.4 to 6.6. Since the wall systems are identical and the load is symmetrical each wall pair carries an equal proportion of the load at all levels and there is no redistribution of load within the structure.

In the polynomial case the solution using one reference level produces an equal uniform load distribution on each coupled pair of walls, equivalent to one third of the applied load and is therefore the correct distribution for this case. Using a greater number of reference levels does not alter the solution until eight or more levels are used when the method produces an unstable solution and hence unreliable results.

The graphs of deflection at the top, figure 6.4, and maximum stress at the base, figure 6.5, show that the polynomial solution for these actions using less than eight levels of reference is in exact agreement with Coull's solution. This is to be expected for this symmetrical case and exhibits the validity of Coull's solution as a basis for comparison. Figure 6.6 shows a close agreement between the polynomial solution and Coull's solution for the maximum shear force

in the connecting beams, in this case within one per cent.

In the case of the point load solution it requires a greater number of point loads, and hence more reference levels, to give a reasonable approximation to a uniform load on each wall. It can be seen from the plots of the point load solutions in figures 6.4 to 6.6 that the wall actions shown approach Coull's solution as more reference levels are employed. By using twenty reference levels the results given by the point load analysis are each within six per cent of Coull's solution. Unlike the polynomial analysis the point load method does not become unstable as a greater number of reference levels are employed.

Figure 6.7 was plotted to illustrate the nature of the instability which occurs in higher order solutions using the polynomial method. It can be seen that the use of up to six reference levels produces no perceptable change to the calculated distribution of load. The use of seven reference levels produces a very slight change of distributed load near the base. At eight reference levels the distribution only generally approximates to the true solution except near the base but with more levels the distribution fluctuates widely producing unreliable results for the wall actions. This generally renders the polynomial method of analysis unacceptable when more than seven reference levels are employed.

Case 2. Model 1 was analysed subject to the asymmetrical load and the results are presented in figures 6.8 to 6.11. The rotations, in plan, of the top of the structure were calculated from the deflections of the two outer pairs of walls.

Since all the coupled shear wall systems in the structure are identical there is little redistribution of load between the wall assemblies. Each two-dimensional system assumes a fairly constant proportion of the load at any level depending on its distance from a point of rotation. The results of the polynomial distribution quickly reach stable values until the solution itself becomes unstable, again at eight reference levels. The results of the point load analysis exhibit the same characteristics as those in case 1.

The main difference between the two cases is the degree of agreement with Coull's solution. Since the latter takes no account of the torsional stiffness of the individual elements comprising the

structure it results in a higher value for the rotation of the structure than given by either the polynomial or point load solutions, as shown in figure 6.9. The effects that the differences in rotation between the solutions have on the other wall actions is shown in figures 6.8, 6.10 and 6.11. It can be seen that the results for wall 2 are similar to those for case 1, (identical by Coull's solution). The extra rotation given by Coull's solution gives lower results for wall 1 and higher results for wall 3 than would otherwise be anticipated.

Case 3. Model 2, comprising two identical coupled wall pairs symmetrically disposed about a single shear wall of comparable stiffness was analysed subject to the symmetrical load distribution and the results plotted in figures 6.12 to 6.16.

In this case there is considerable force redistribution between the coupled wall and the single wall systems, due to their different modes of deformation.

In figure 6.12 it can be seen, especially where only a few reference levels are used, that there is a difference between the corresponding values of deflection given for the two types of walls, although the structure is symmetrical and is symmetrically loaded. The fact that the results for the deflection at the top of the two outer coupled walls are the same but differ from those for the central wall appears to suggest a violation of the condition that floor slabs are assumed to be rigid in plane. This apparent anomaly serves to illustrate the limitations of these analyses, in that the condition of in-plane rigidity is only satisfied at the reference levels. Between reference levels wall systems are free to deform naturally. Where few reference levels are used the height of the structure above the uppermost level may be a considerable proportion of the total. In the analyses these parts of the wall systems are not constrained to act with one another hence the differences in the calculated deflections at the top.

In general the results generally follow a similar pattern to case 1, although the values for stresses at the base given by the polynomial solution between four and eight reference levels fluctuate slightly rather than achieve a steady result. There being no torsion involved in this case the results show close agreement with Coull's

solution.

Figures 6.15 and 6.16 firstly illustrate the way in which the force distribution on a shear wall system is represented by a polynomial series and the way in which it is altered by considering successive numbers of reference levels. Secondly the above figures indicate the transfer of lateral forces between the two types of shear wall systems throughout the height of the structure.

Case 4. Model 2 was analysed subject to the asymmetrical load and the results presented in figures 6.17 to 6.20, structure rotations being calculated as for case 2.

Although this is the most complex of the four cases, involving both torsion of the structure and redistribution of forces between walls the results exhibit the same general behaviour as in the other cases and there is good agreement with Coull's solution.

In general the graphs of figures 6.4 to 6.20 show that the polynomial solution rapidly reaches an "optimum" value by using very few, in the order of two to four, reference levels, depending on the complexity of the structure and the amount of load redistribution. By using up to eight levels the solutions fluctuate about this "optimum" while the use of more than eight levels produces an unstable result.

The instability of the polynomial case may be explained by considering the forms of two consecutive polynomial terms. For terms near the beginning of the series, that is with low exponents, the plots of the two terms in non-dimensional height coordinates are of distinct shape, for example, triangular and parabolic, or parabolic and cubic. Similar plots of higher order terms become less distinct, and hence their corresponding load-deflection coefficients tend to be alike. Successive lines in the matrix of flexibility coefficients become increasingly similar for higher order terms, the matrix tends towards singularity and the solution becomes unstable.

The point load solutions generally progress towards an "optimum" value more evenly but more slowly than in the polynomial case. The point load case requires the use of a greater number of reference levels, in excess of ten, to produce results which are reliably within

a few per cent of the "optimum" value. The main reason for this is that a reasonable number of finite point loads are required to give an acceptable approximation to a distributed load form.

It may be concluded that the polynomial solution is generally reliable for solutions using up to eight reference levels. The lowest number of reference levels which are reliable depends on the complexity of the structure and could be determined in any particular case. The point load solution, on the other hand, became more reliable as more reference levels were used and did not exhibit any instability up to twenty levels. This would suggest that the polynomial method is more suitable for rapid approximate evaluation by hand using a small number of reference levels, whereas the point load method is more suited to a more accurate treatment using the computer.

The "optimum" solutions for the polynomial case were generally slightly greater than the corresponding solutions for the point load case. The relationship of the two solutions to each other and to experimental results is discussed in Chapter 8.

6.4 EFFECTS OF FLEXIBLE FOUNDATIONS ON A PAIR OF COUPLED SHEAR WALLS

In a complex structural system it is seldom immediately obvious which actions are most closely related and which of them dominate the behaviour of the system. This is particularly the case in systems, such as those at present under investigation, where the structure may not be supported on completely unyielding foundations. For the purpose of an analysis it is frequently assumed that the foundations of a structure are perfectly rigid. In many cases this may be a valid assumption, especially where precautions are taken during the design to provide a rigid foundation system. However, it is conceivable that particular structures may not be adversely affected by movements of their foundations, in which case the provision of an exceptionally stiff foundation system may not be economic. In order that such a fundamental decision as to the founding of a structure may be taken it is imperative to possess a clear understanding of the effects that a more flexible foundation will have on the structure as a whole.

In order to investigate the effects of foundation deformations on coupled shear walls a series of computations was carried out on the typical system shown in figure 6.21. To reduce the problem to that of a single pair of coupled walls, it was assumed that the walls shown formed part of a structure which consisted of a number of equally spaced identical assemblies based on identical foundation systems. For the case in which the wind load acts in the plane of the coupled walls and is distributed in the same manner throughout the length of the building there will be no redistribution of load between the wall assemblies and hence the problem may be solved as that of one pair of coupled walls acted on by the relevant proportion of the total load on the structure.

Since the particular example of figure 6.21 was devised to be of practical dimensions it was possible to derive a realistic wind pressure distribution for the structure using the relevant British Code of Practice[17]. It was assumed that the building was situated within the built up area at the centre of a city for which the basic wind speed is 51 metres/second, and the dynamic pressure on the building at different heights was calculated using the rules of the Code. The distance between adjacent wall assemblies was taken to be 7 metres and hence the wind force distribution on one pair of shear walls was calculated at a number of heights and expressed as the horizontal force per unit height on the walls. The force distribution is shown graphically in figures 6.22 and 6.23.

Between calculated values the load distribution was assumed to be linear and preliminary computations were carried out with the programs used for three-dimensional structures whereby suitable approximations to the load form were found. The polynomial approximation using the first four terms of the series follows the load distribution very closely as shown in figure 6.22. In the case of the point load method, twenty point loads, equally spaced throughout the height of the walls, were evaluated to approximate the load form. These are shown as a series of uniformly distributed loads in figure 6.23, where it can be seen that the approximation to the load distribution is again reasonable.

The polynomial and point load approximations were used in the relevant programs for analysing two-dimensional systems to carry out a

series of computations on the pair of coupled walls shown in figure 6.21. In the calculations the rotational and vertical flexibility of the foundations of the walls were independently varied over a wide range and the value of a number of critical deflections and force actions was found for each foundation configuration. The results, expressed as the variation of these wall actions, namely the deflection at the top of the walls, the axial force, bending moment and maximum stress at the base of the walls and the maximum shear force in the connecting beams, are shown in graphical form in figures 6.24 to 6.33 inclusively. Each set of results is presented twice in order to illustrate the relationships of the particular wall action to rotational and vertical deformations respectively.

The ranges of the two foundation parameters K_θ and K_v used in the present study are intended to represent the complete spectrum of foundation conditions from the case of perfect rigidity, through rocks, sands and clays to the opposite extreme of a very flexible substrata. In reality both foundation parameters will lie within corresponding regions of their respective ranges for any particular case, since they are principally dependent on the nature of the sub-base material. Their precise relationship will be determined by the configuration of the foundation system. For the present study it has been assumed that K_θ and K_v are mutually independent. This assumption gives rise to the improbable concepts of foundations possessing great vertical stiffness whilst being weak in resisting rotational deformations, and vice versa. However the assumption has merit in as much as it enables the effects that either foundation parameter has on the coupled walls to be more readily illustrated.

In the previous section, 6.3, it was shown that the values of deflections, forces and stresses for a structure based on rigid foundations as calculated using the point load solution were consistently smaller in magnitude by a few per cent compared to the corresponding values calculated by the polynomial solution. The values of the two solutions for the present structure are shown in each of the figures 6.24 to 6.33. In each case it can be seen that the solutions again bear a similar consistent relationship to each other throughout the ranges of both rotational and vertical flexibility considered.

Figures 6.24 and 6.25, respectively, show the effects of

rotational and vertical flexibility of the foundations on the deflection of the walls at the top. As would be anticipated, an increase in either K_θ or K_v produces an increased deflection. It is of note that the deflection produced in a case where rotational and vertical deformations occur simultaneously is considerably greater than the sum of the deflections produced as a result of considering either mode of foundation deformation to take place while the other is held rigid. The explanation for this is that, as the foundation system becomes more flexible to one mode of deformation relative to the second, the latter is comparatively more able to resist the applied lateral load and the proportions of the load carried by the resistance of the foundation system to rotational and vertical deformation changesaccordingly. This effect appears in the figures as a decrease in the slope of the graphs as either K_θ or K_v is increased while the other is held at a constant value.

From consideration of the state of equilibrium of the shear wall assembly, the moment of the applied lateral load about the base is resisted by the sum of the moments at the base due to the bending action of the individual walls and the couple formed by the axial forces induced in the walls by the connecting beams. For any particular load configuration the above sum is constant irrespective of the foundation conditions. This results in the compensating effects which accompany changes in one mode of foundation deformation as described in the preceding paragraph. The effects of changing the relationship between rotational and vertical flexibility are more marked when the axial forces and bending moments in the walls are considered.

Figures 6.26 and 6.27 show the relationship of the flexibility of the foundations to the axial force in the walls at base level. Figure 6.26 shows that, for any particular vertical flexibility, the axial force at the base increases as K_θ increases, while figure 6.27 shows that the axial force decreases with increasing K_v for a constant rotational flexibility. The converse situation is shown in figures 6.28 and 6.29 for the bending moments in the walls at the base. The explanation for these results follows directly from the previous paragraph. Where K_θ is increased with a constant vertical flexibility, the proportion of the load carried by the vertical resistance of the

foundations increases, hence the axial force at the base of the walls is increased (figure 6.26). The proportion of the load carried by the rotational resistance of the foundations correspondingly decreases and the bending moment at the base of the walls decreases (figure 6.28). The situation is reversed where K_v is increased for any constant rotational flexibility.

Figures 6.30 and 6.31 show the effects that varying foundation conditions have on the stresses at the base. Although the stress distribution in the walls is dependent on both the direct axial force and the bending moments it can be seen from the graphs that the stress at the base is affected by changes in foundation flexibility in a similar manner to the bending moments in figures 6.28 and 6.29. This will not be so in every case. In the particular structural system being considered the connecting system, i.e. the lintel beams between the shear walls, is relatively flexible, as shown by the low value of the parameter α (in this case $\alpha = 2.6946$). The major proportion of the load is therefore carried by the bending action of the walls rather than by the axial wall forces induced by the coupling action of the beams. The stress distribution, therefore, is, in this case, more dependent on the bending action of the walls as shown by the form of the graphs.

The shear forces in the connecting beams, as typified by the maximum shear force shown in figures 6.32 and 6.33 follow the same pattern as the axial forces in the shear walls. This is reasonable since it is the shear coupling effect of the beams which induces the axial forces in the walls.

For a pair of coupled shear walls based on perfectly rigid foundations the parameter α gives a good indication as to the way by which the lateral load is resisted. Lower values of α indicate a flexible beam or slab connection and a greater proportion of the load carried by the bending action of the individual walls. As the value of α is increased the connecting action becomes more effective and a greater proportion of the load is carried by the coupling of the axial forces induced in the two walls. The presence of deformable foundations alters the effectiveness of the connecting beams or slabs. Any structural system which is supported elastically is by definition more flexible than its rigid counterpart. However it can be seen

that the two modes of deformation in this case affect the structure in different ways. It was noted earlier that, in reality rotational and vertical deflections generally occur simultaneously. Which of the two is the dominant factor in any structure depends on the configuration of the foundations. Where the foundations are relatively more flexible to rotation the connection between the shear walls becomes more effective and a greater proportion of the load is resisted by the axial forces in the walls than is the case for the same walls based on a rigid foundation system.

6.5 EFFECTS OF FLEXIBLE FOUNDATIONS ON SHEAR WALL STRUCTURES

The preceding section illustrated the effects which flexible foundations have on the interaction between a pair of coupled walls. The two-dimensional system was considered in isolation. In the present section the effects that flexible foundations have on the lateral load bearing units of a three-dimensional structure are investigated by means of two examples.

It can be appreciated that in complex three-dimensional structures the results of there being a number of deformable foundations would be extremely difficult to follow. It was decided therefore to limit the number of walls on elastic foundations to those of a single assembly and to plot the effects on the complete structure of varying the flexibility of those foundations from complete rigidity to extreme flexibility.

The layout and dimensions of the two structures are shown in figures 6.34 and 6.40 respectively. Both structures are of the same overall dimensions and proportions as that which was assumed for the two-dimensional study of section 6.4. The force distribution previously derived is again used, integrated over the larger face of the building (resulting in a total force seven times that used in section 6.4) to represent the lateral wind force on each structure. In their basic form, with the foundations of all walls rigid, both the structures are symmetrical with a regular arrangement of wall assemblies. Since the load is also symmetrical the redistribution of load within the structure is reasonably straightforward. The structures were devised in this manner as a further aid to the clear illustration of the changes brought about by the introduction of flexible foundations.

Since the relationship between the results given using the polynomial and the point load solutions is consistent in previous sections, and in order to simplify presentation of results and avoid confusion, the results of the analyses of the following examples are given only for the polynomial solution.

The first example analysed, as shown in figure 6.34, comprises six identical pairs of coupled shear walls symmetrically disposed about a considerably stiffer central core which consists of two identical channel shaped walls coupled together in a similar manner as are the shear walls. The effects on the structure of increasingly varying the flexibility of the foundations of the central coupled core walls are presented graphically in figures 6.35 to 6.39 inclusively. For the purposes of this study the rotational and vertical flexibility of the central cores are increased simultaneously to give an approximation to the behaviour which could be expected in a real case. On the graphs the flexibility parameters, K_θ and K_v, are plotted to a logarithmic scale whereby one unit on either the rotational or vertical flexibility axis represents a tenfold increase in the relevant parameter.

Figure 6.35 shows the maximum deflection at the top of the structure. As the foundations of the core walls become more flexible the structure undergoes increased deflection. However once a certain stage of flexibility is reached there is a marked tailing off in the rate of increase of deflection.

Figures 6.36 and 6.37 respectively show the effects that the flexible foundations of the core walls have on the axial forces and bending moments at the base of the structure. As the flexibility of their foundations increases the core walls become progressively less effective in resisting the loads on the structure. Both the axial force and the bending moment at base level of the core walls decrease, ultimately to zero while there is a compensating increase in force and moment at the bases of walls on rigid foundations. As was the case in the two-dimensional study of section 6.4 the parameter α for the coupled shear walls is again low (here $\alpha = 2.756$), indicating that a greater proportion of the load is resisted by the bending action of the individual walls rather than through the coupling action of the connecting beams. This factor is apparent from figures 6.36 and

6.37 where the bending moment on the shear walls when the core walls are totally ineffective at the base is approximately twice that when they are rigid, whereas there is only a corresponding increase of less than a third in the axial forces on the shear walls at the base.

As shown in figure 6.38 the effect of a more flexible foundation at the core walls, causing a greater proportion of the load to be carried by the shear walls is to increase the stresses in the latter as the stresses in the core walls decrease. Figure 6.38 is, in effect a combination of the results of the changes shown by figures 6.36 and 6.37.

Although, in the case of extreme flexibility of their foundations, the core walls resist none of the lateral load at the base they have not become entirely useless. Figure 6.39 shows the proportion of the total lateral load carried, throughout the height of the building, both by the coupled cores and by each pair of shear walls, for three particular cases of flexibility of the foundation of the core walls. In the case of intermediate flexibility, the core walls carry a similar proportion of the load above the third storey as they do in the case of rigid foundations. Even in the case of extreme flexibility the core walls carry a considerable proportion of the load for much of their height. The core walls therefore form a strong central spine to the structure even when their foundations are suspect.

The second example of a shear wall structure which was analysed is shown in figure 6.40 and consists of six identical pairs of coupled shear walls regularly spaced with a single channel shaped core wall symmetrically placed at each end. The shear walls are identical to those used for the first example. The effects on the structure of increasing the flexibility of the foundations of one of the end cores, core 1, while the other foundations remain rigid, are presented graphically in figures 6.41 to 6.46 inclusively. As was the case for the first example the flexibilities are plotted to a logarithmic scale.

Figure 6.41 shows the deflection at the top of each wall, plotted against the flexibility of the foundation of core 1. As the foundation flexibility of core 1 increases, the deflection of the core wall increases and, in order to permit this increased deflection the structure undergoes a rotation in the horizontal plane in this case

centred in the vicinity of wall 6. When the foundation of core 1 becomes extremely flexible the core wall no longer resists any of the turning effect of the lateral load at the base level and there is no further change in the deflection of the structure. This effect is similar to that shown for the first example.

Figures 6.42 to 6.44 respectively show the effects that the flexible foundation of core 1 has on the axial force, bending moment and maximum stress at the base of each wall assembly. The results are similar to those for the first example but with the additional factor of the horizontal rotation of the structure. The bending moment at the base of core 1 decreases, eventually to zero, as the flexibility of its foundation increases. There is a net increase in the axial force and bending moment at the base of the other walls to compensate for the reduction in the stiffness of core 1. However, due to the general rotation of the structure, the walls closest to core 1 bear the greater part of the increase while the force and moment on wall 7 and core 8 at the opposite end actually decrease.

Figures 6.45 and 6.46 show the proportion of the total lateral load carried throughout the height of the structure by core 1, walls 2 and 7, and core 8 for three cases of flexibility of the foundations of core 1. Once again the majority of the redistribution of load caused by the flexibility of the foundation at core 1 occurs below the third storey level and, above that level, the load distribution approximately follows that obtained when all the foundations are rigid.

The two preceding examples have been used to yield a general indication of the effects that the presence of elastic foundations have on the behaviour of three-dimensional shear wall structures. Increased flexibility of a foundation system will produce a general increase in the deflection of the structure accompanied by a change of horizontal rotation in cases where the flexible foundation system is not on the centroid or line of symmetry of the structure. The forces, moments and stresses in the vicinity of the base of the walls which have the flexible foundations decrease with increased flexibility accompanied by a compensating increase in the general level of the actions of walls elsewhere in the structure. The proportion of increased action borne by the individual walls depends on the particular configuration and in cases when large rotations occur may

include a reduction in the stresses in some walls, as shown by the second example, although these walls still have rigid foundations. The majority of the redistribution of the lateral load explicitly due to the presence of elastic foundations takes place within the first few storeys. At higher levels the proportion of the total load carried by any wall assembly is largely unaffected by the presence of elastic foundations.

In cases of extreme flexibility a point is reached when any further increase in flexibility of a particular foundation system no longer affects the structure. In cases such as this the foundation may be said to have failed completely as far as resisting the lateral loads by its bending and coupling actions are concerned. However even in this extreme case that particular wall assembly still resists a considerable proportion of the lateral load at higher levels, comparable with that which it would carry had its foundations been rigid and hence the wall assembly itself, as distinct from its foundation cannot be regarded as having failed. It follows that, where foundation conditions beneath a building are suspect, the presence of lintel beams and floor slabs forming couplings between walls and inducing interaction between wall assemblies tie the various elements of the structure together to overcome local weaknesses in the foundations.

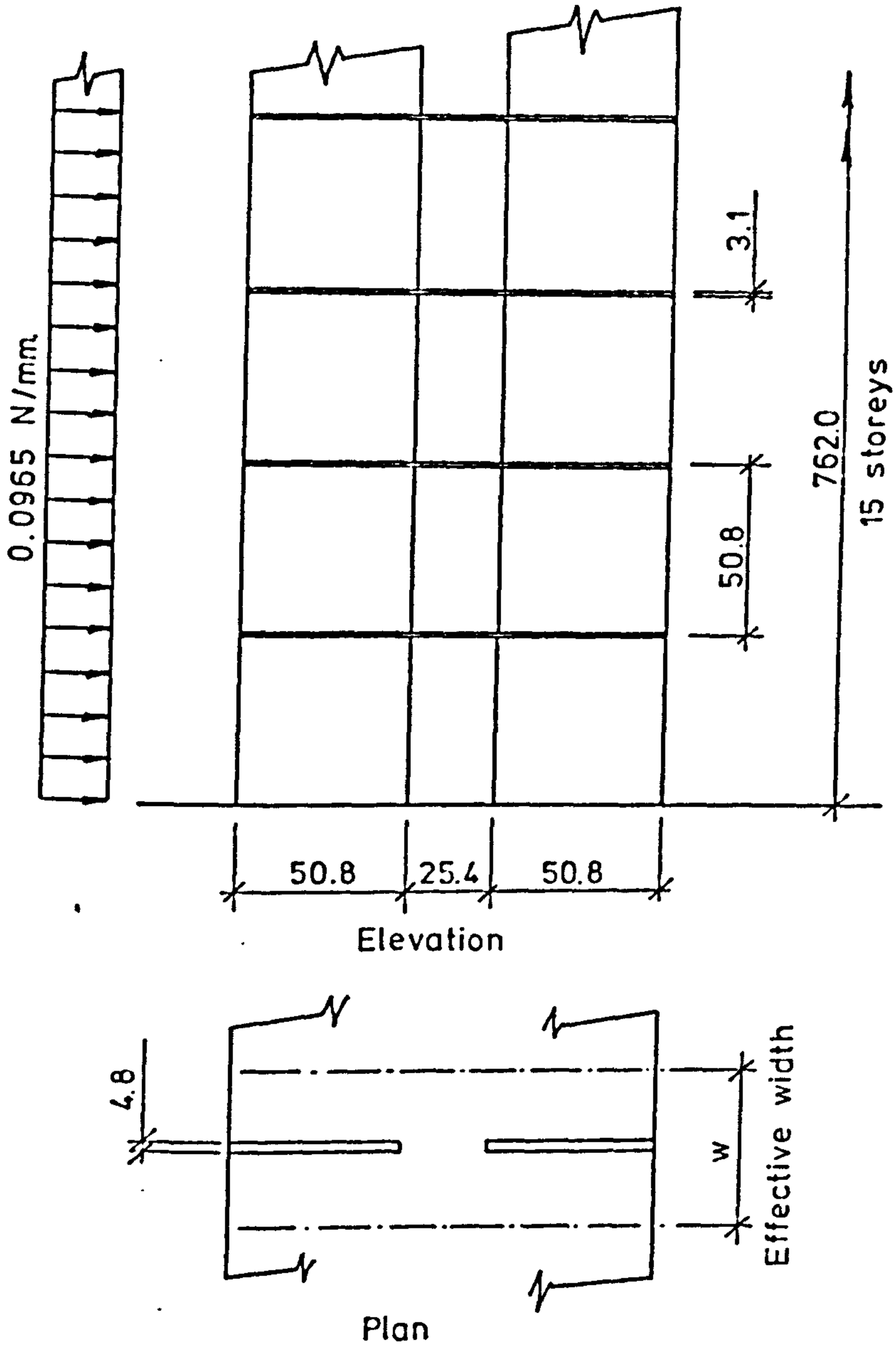

Dimensions in millimetres

$E_1 = E_2 = E_c = 2880\ N/mm^2$

Poisson's Ratio, $\nu = 0.35$

w = 5mm by 5mm increments to 50mm

Shear walls coupled by floor slabs.

Figure 6.1

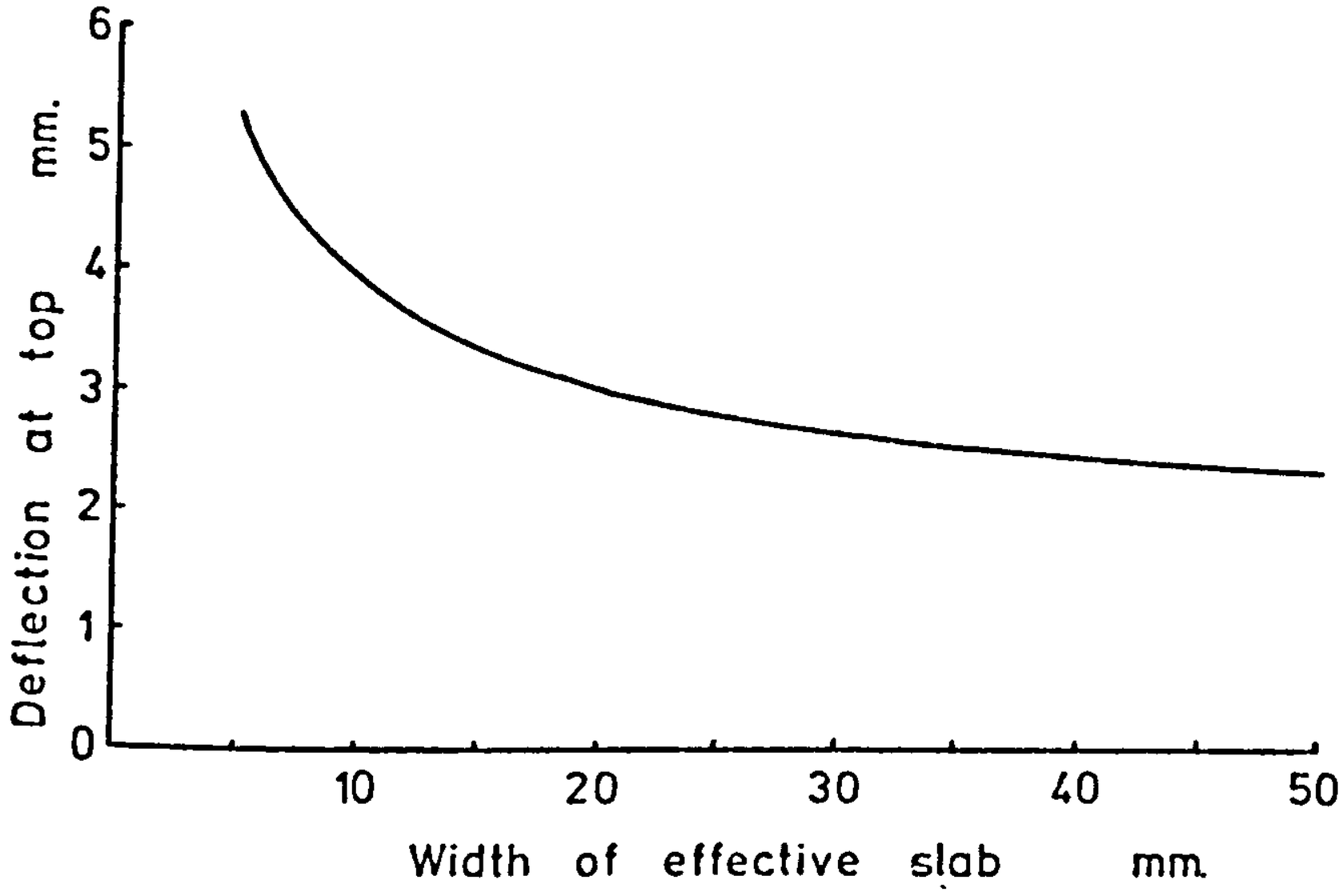

a. Deflection at top of walls.

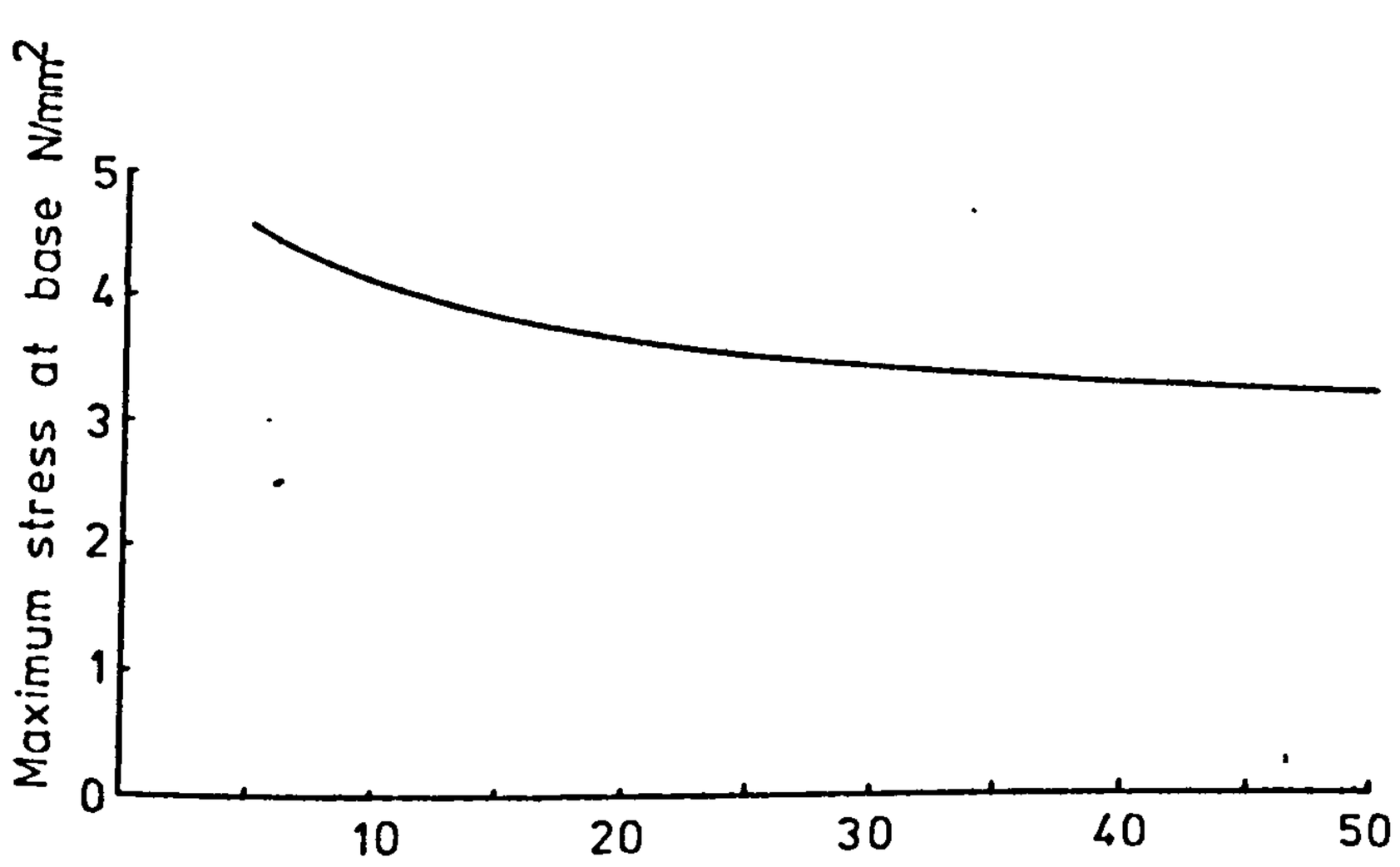

b. Maximum stress at base of walls.

Effects of varying the width of floor slabs effective as a coupling between shear walls (1)

Figure 6.2

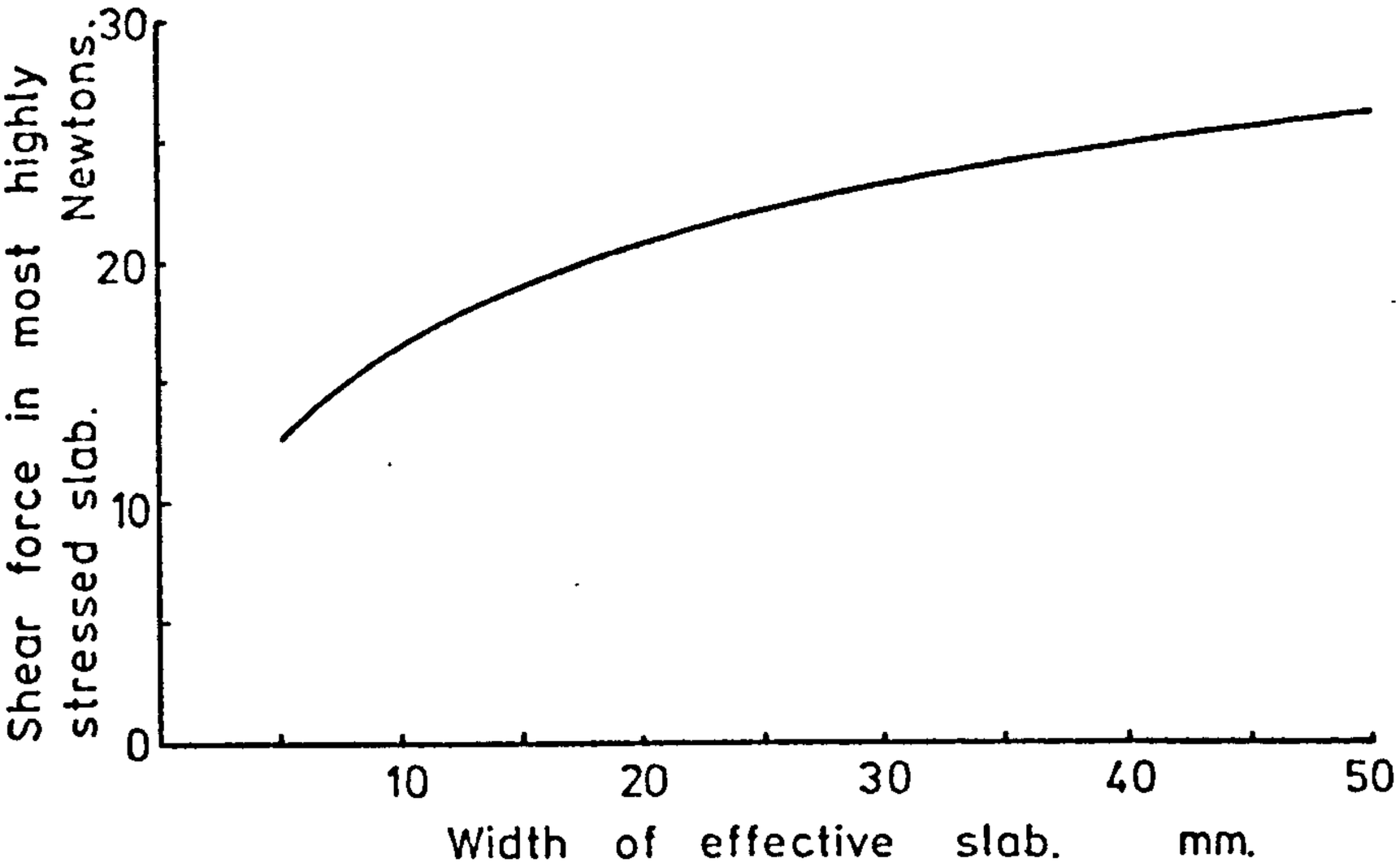

a. Shear force in most highly stressed floor slab.

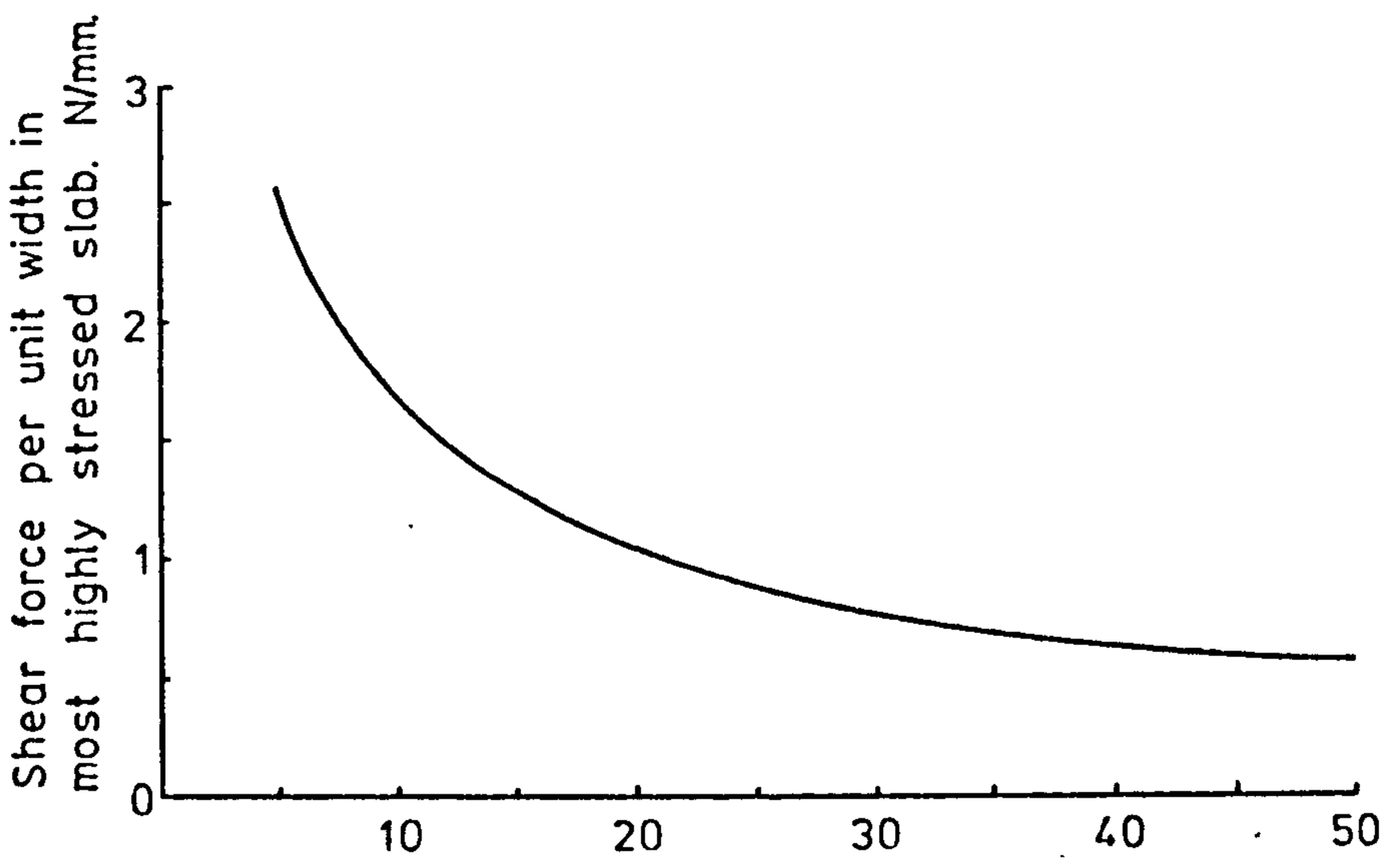

b. Shear force per unit width in most highly stressed floor slab.

Effects of varying the width of floor slabs effective as a coupling between shear walls.

Figure 6.3

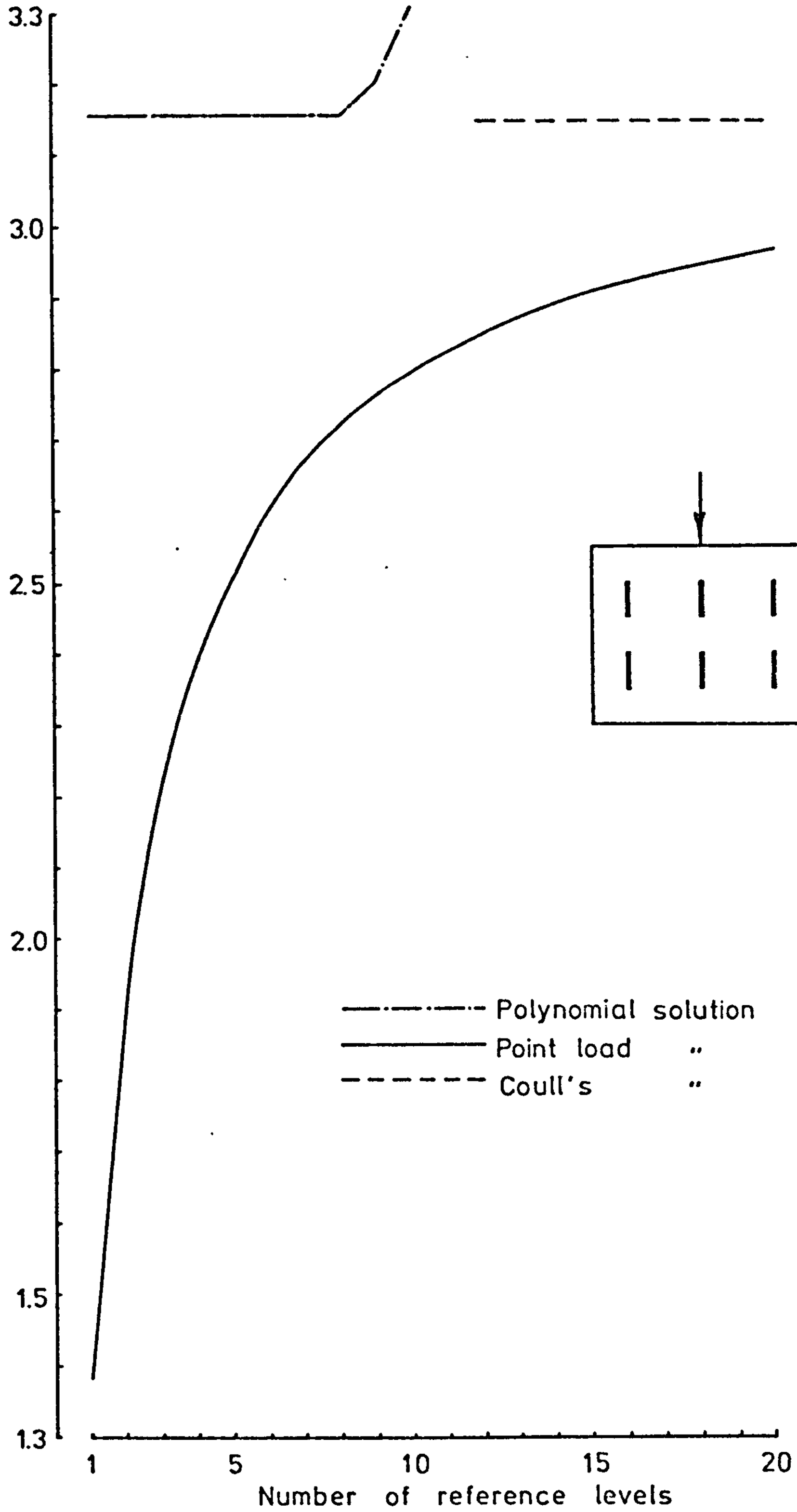

Effect of number of reference levels on deflection at top of walls.
(Case 1)

Figure 6.4

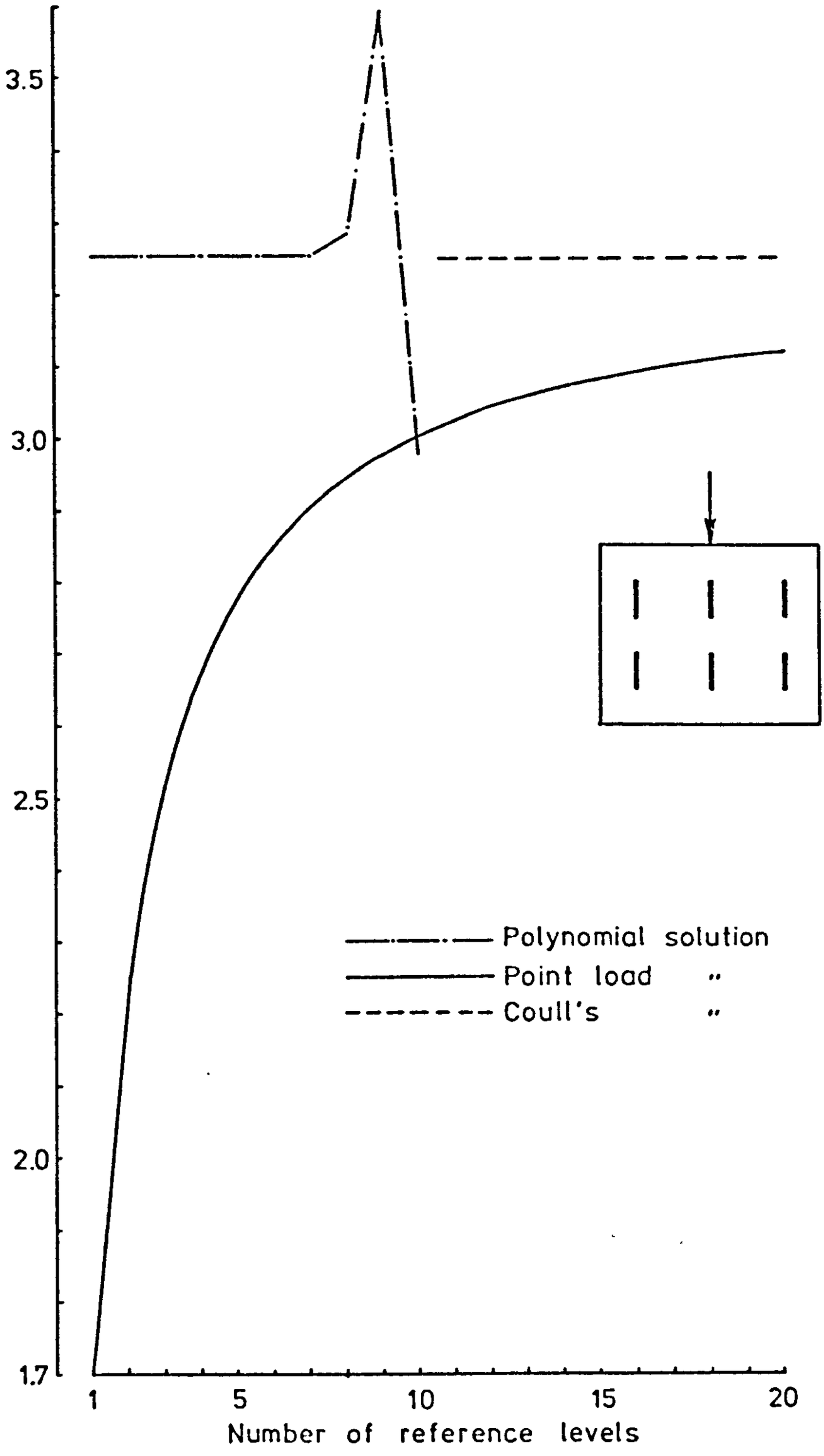

Effect of number of reference levels on stress at base (Case 1)

Figure 6.5

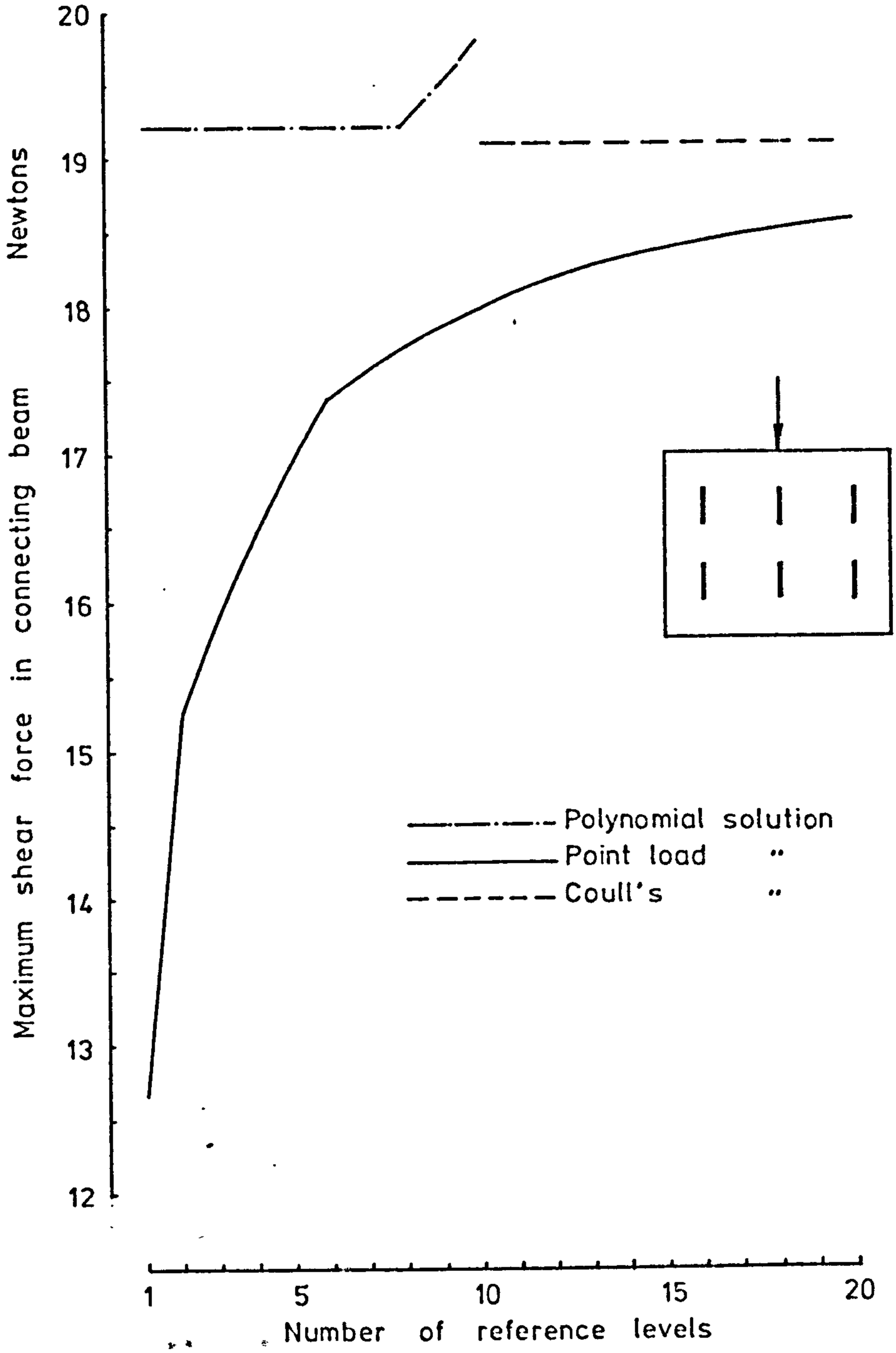

Effect of number of reference levels on shear forces in connecting beams (Case 1)

Figure 6.6

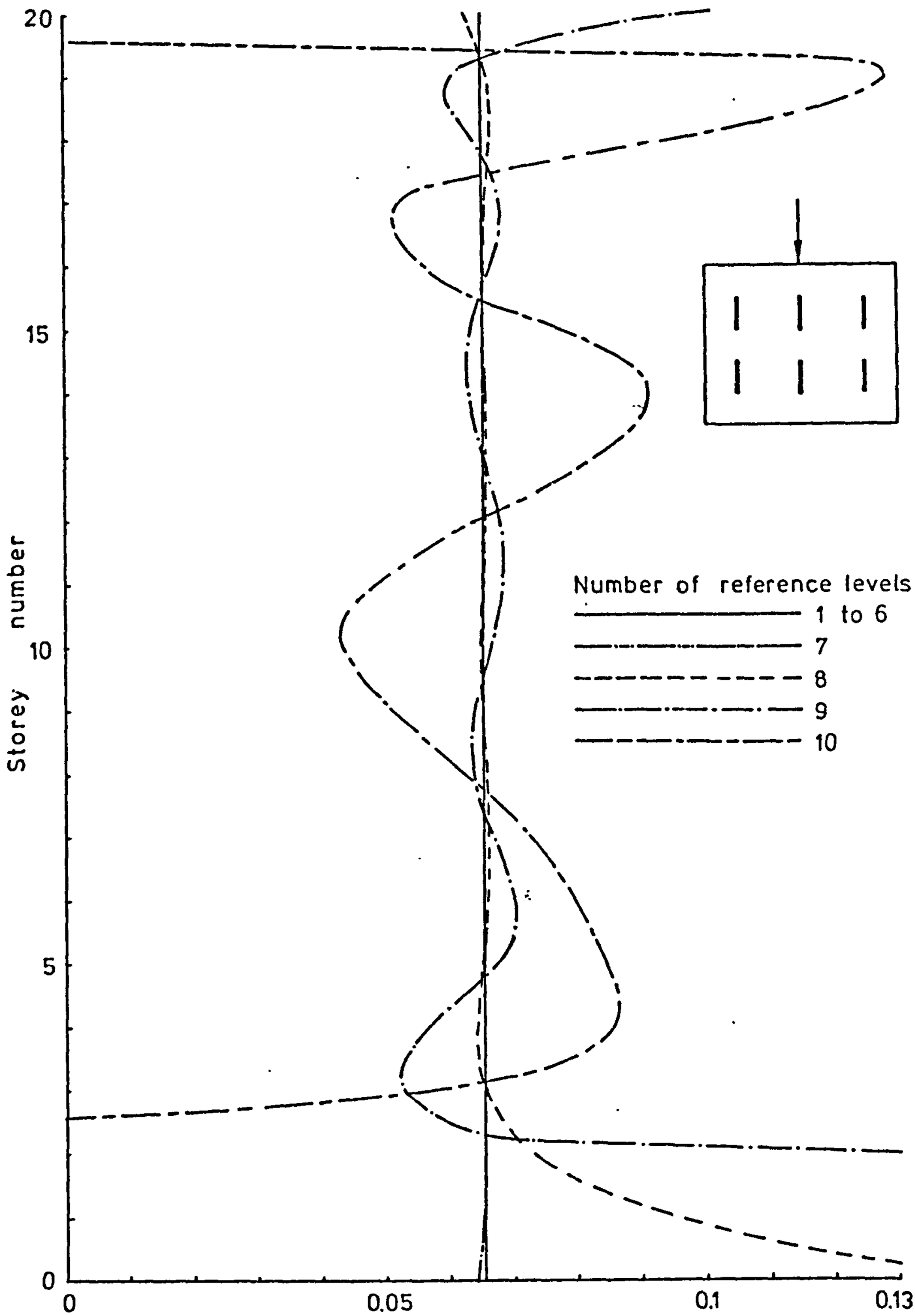

Illustration of break-down of polynomial solution (Case 1)

Figure 6.7

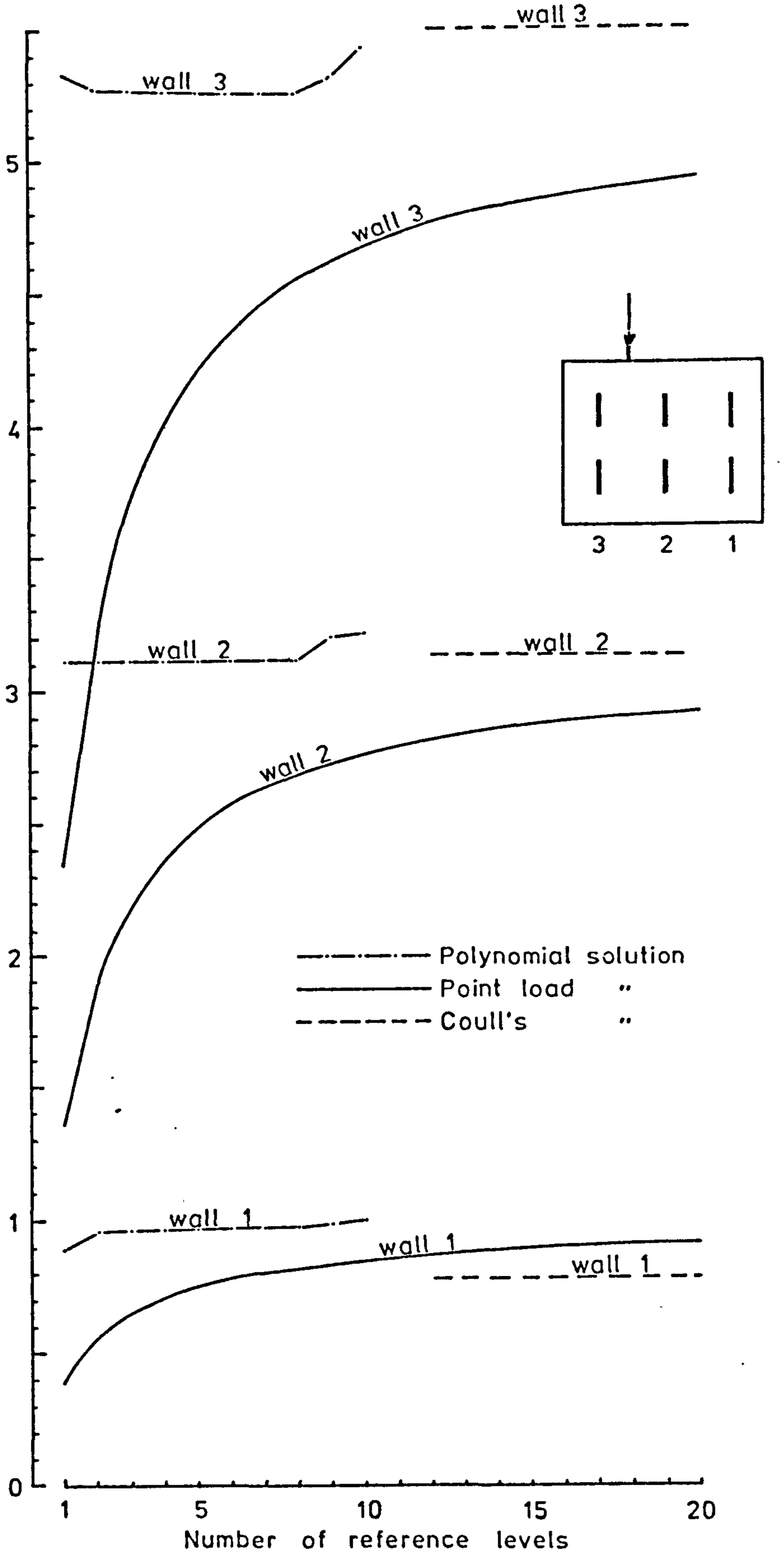

Effect of number of reference levels on deflection at top of walls. (Case 2)

Figure 6.8

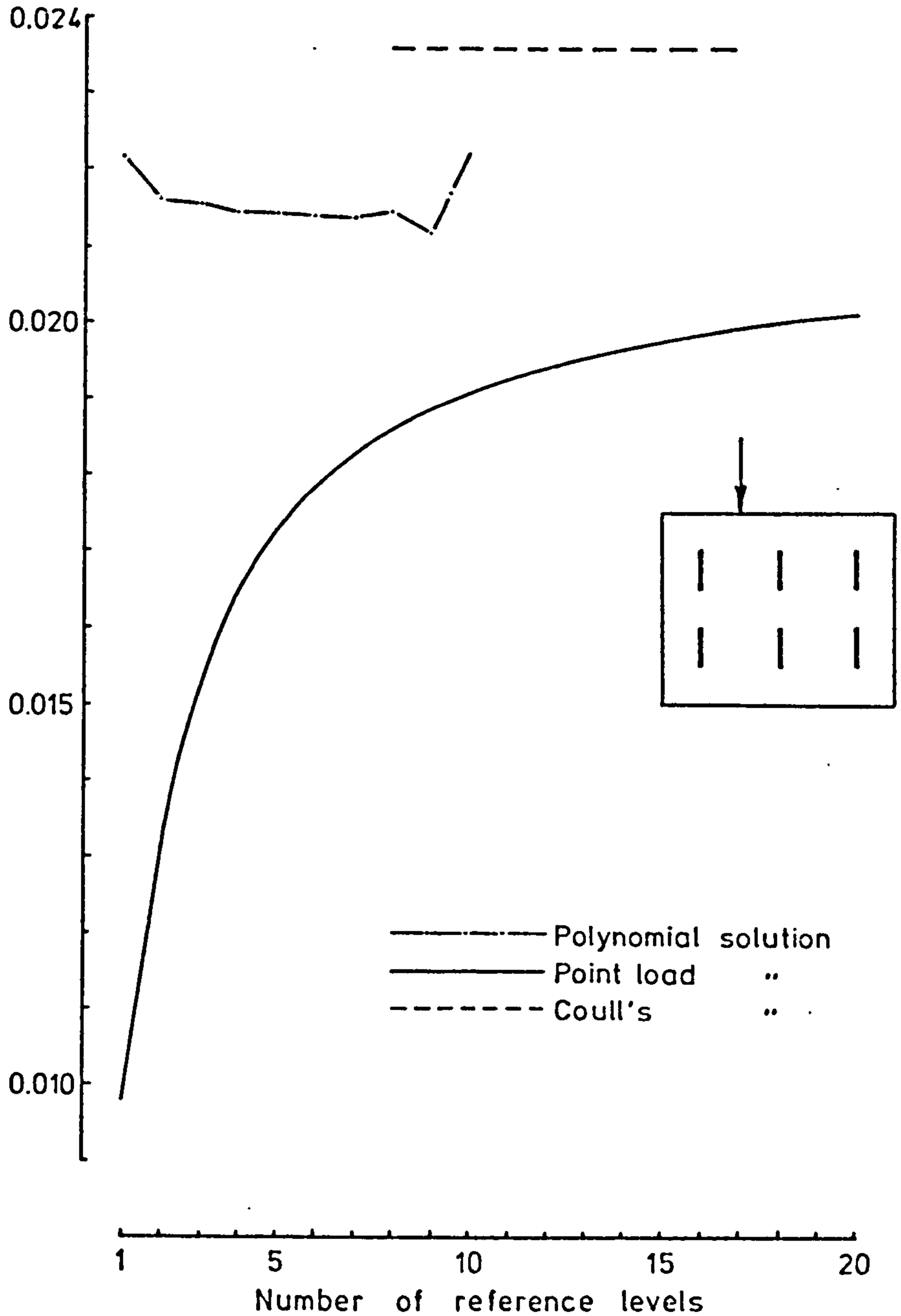

Effect of number of reference levels on rotation at top of structure (Case 2)

Figure 6.9

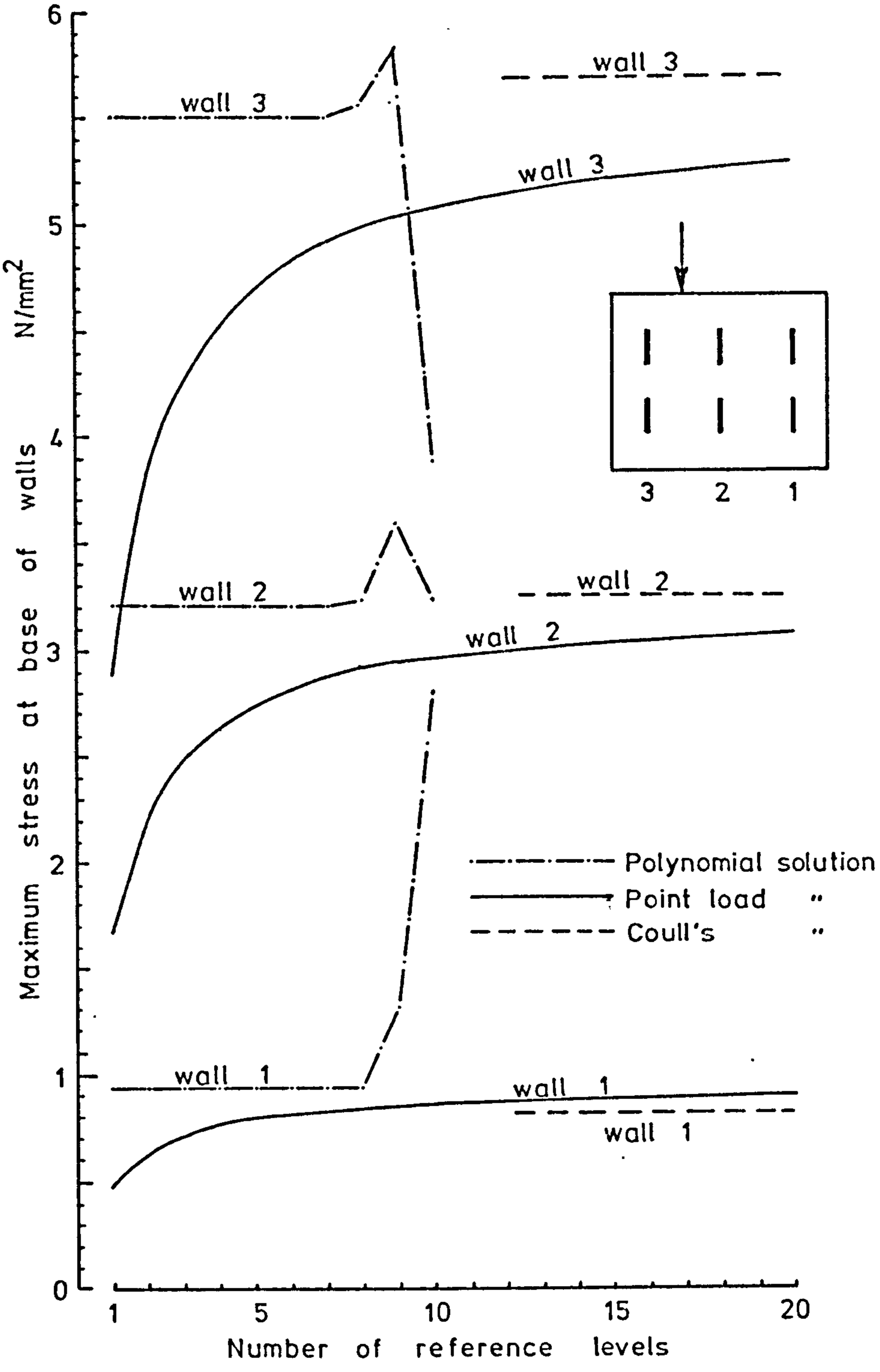

Effect of number of reference levels on stresses at base of walls (Case 2)

Figure 6.10

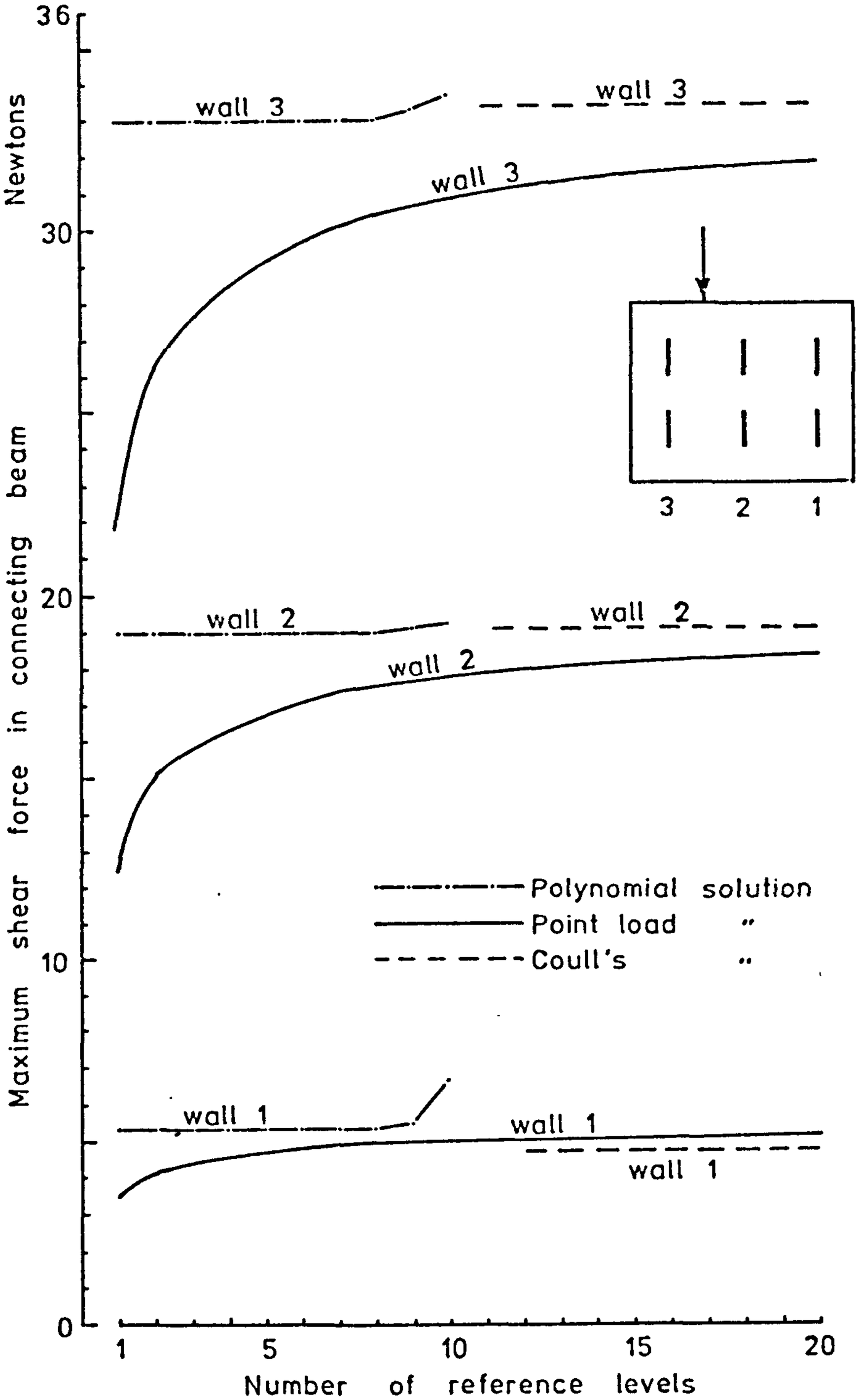

Effect of number of reference levels on shear forces in connecting beams (Case 2)

Figure 6.11

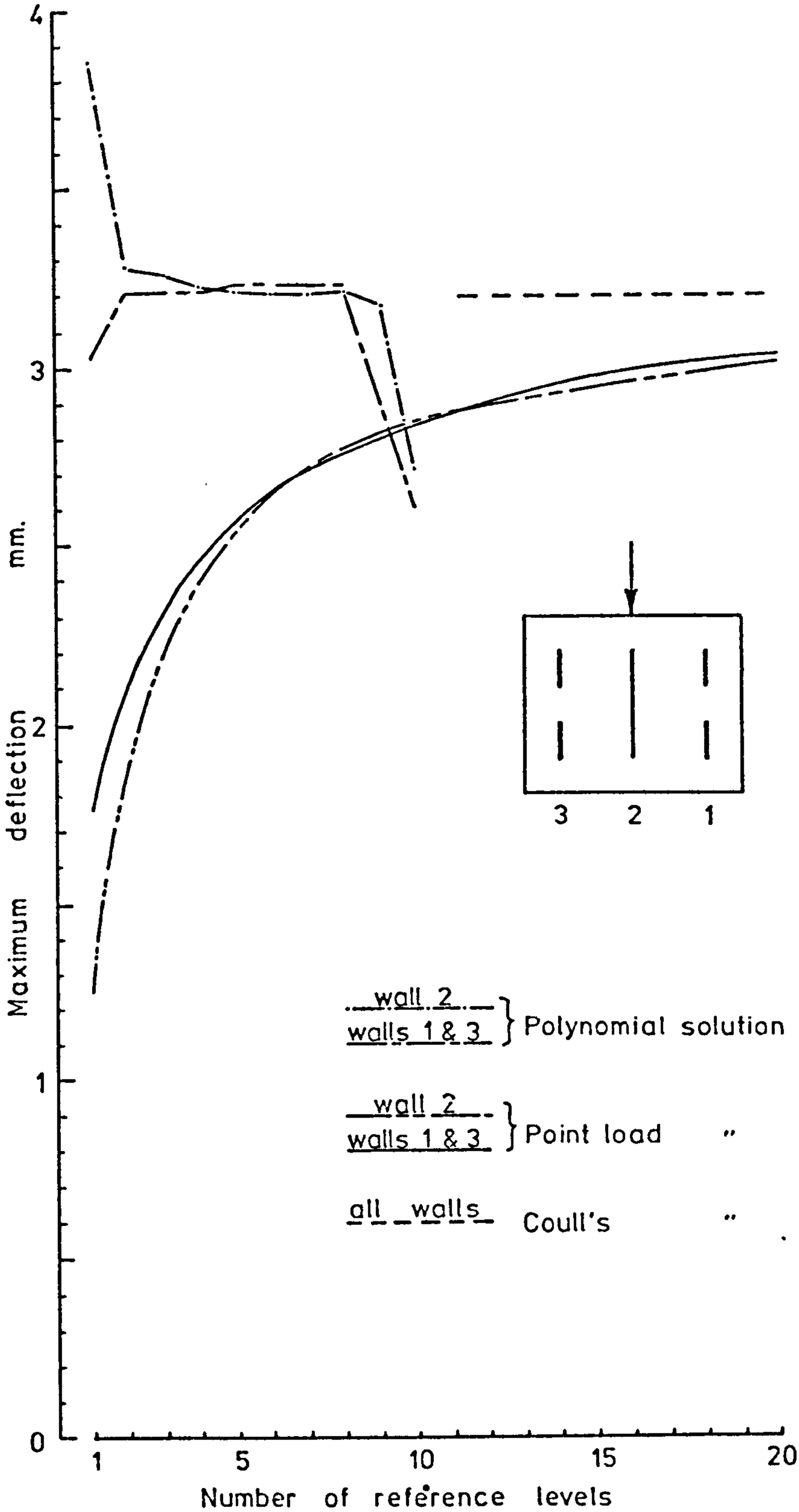

Effect of number of reference levels on deflection at top of walls (Case 3)

Figure 6.12

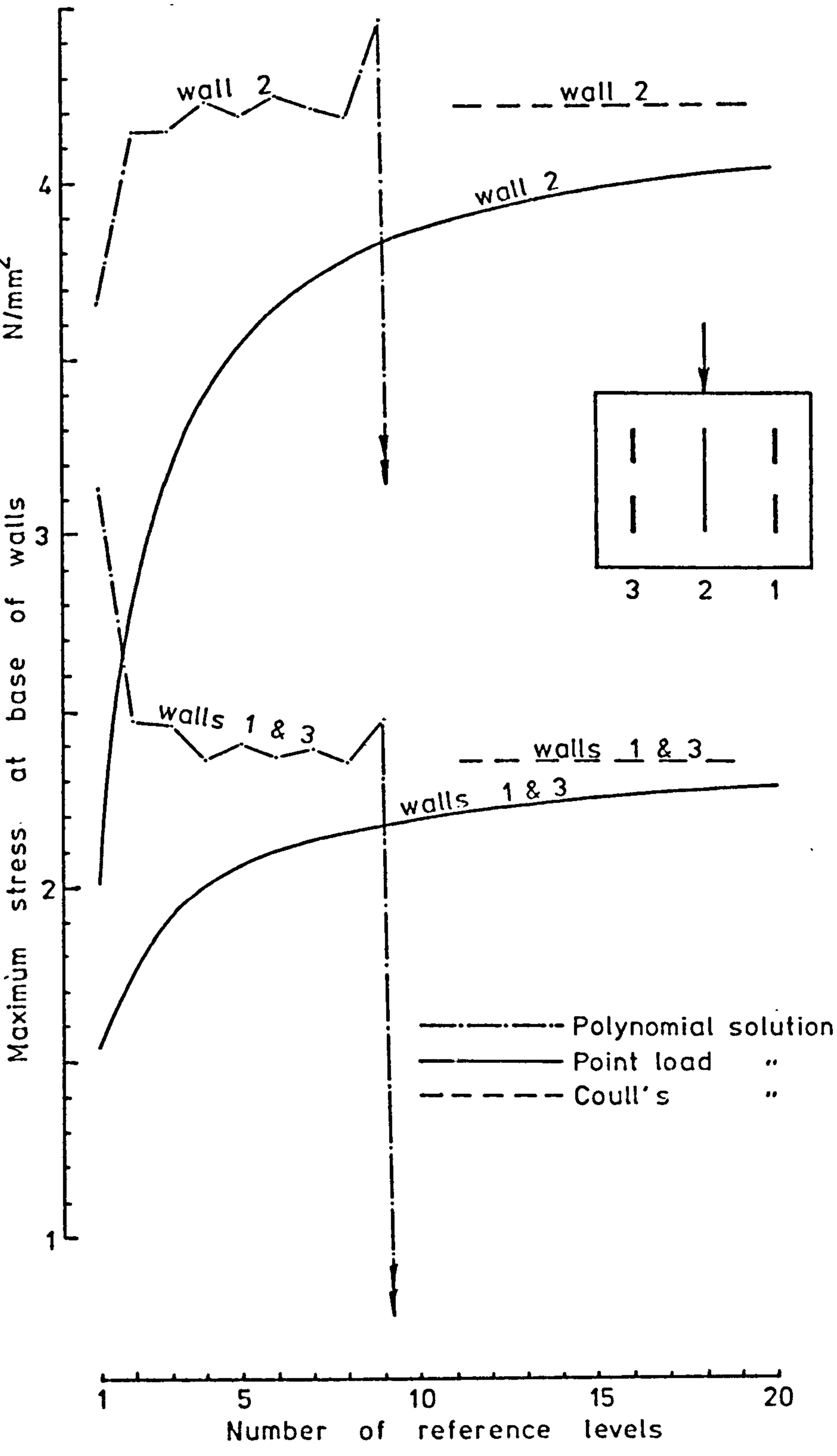

Effect of number of reference levels on stresses at base.
(Case 3)

Figure 6.13

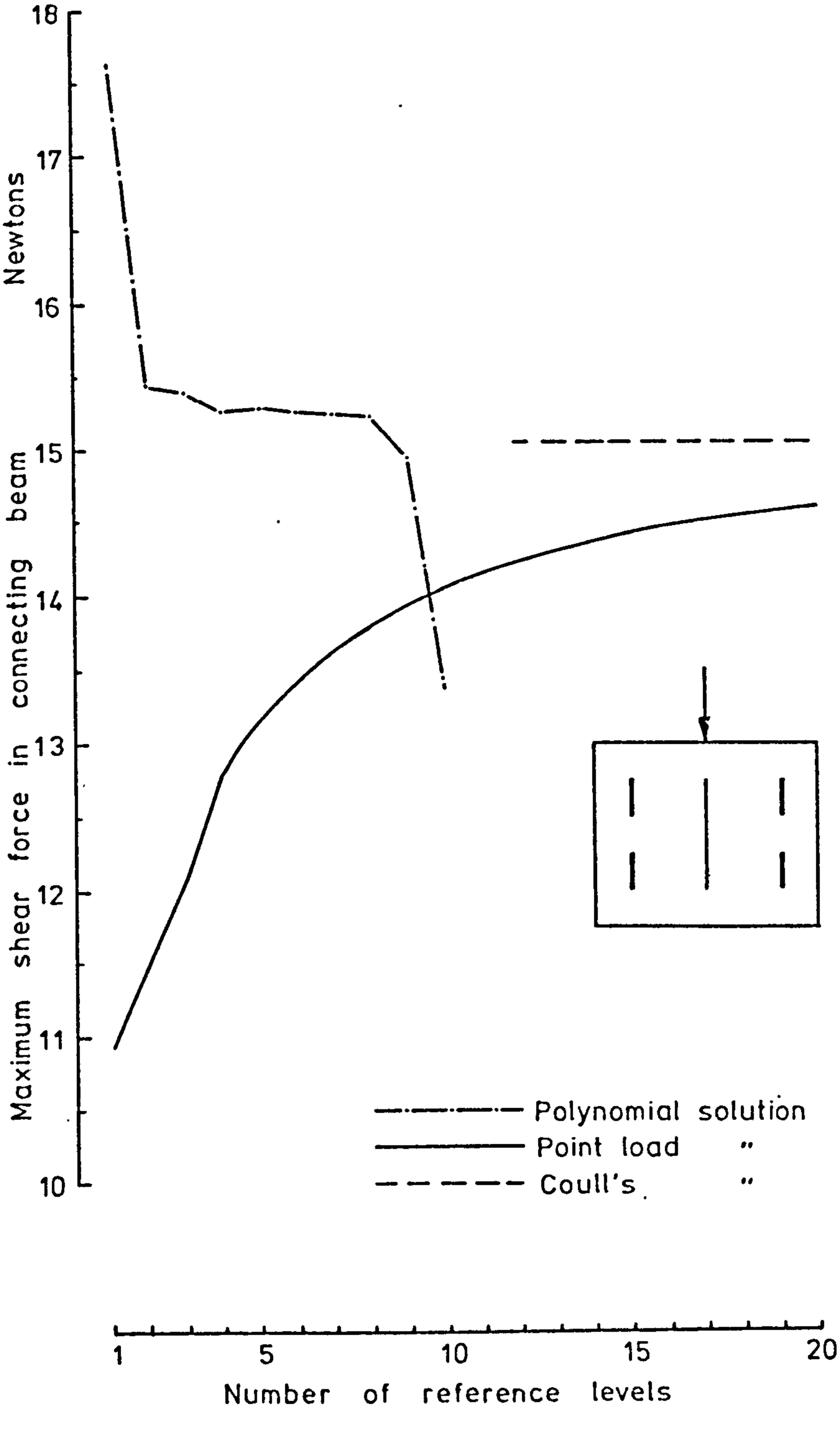

Effect of number of reference levels on shear forces in connecting beams (Case 3)

Figure 6.14

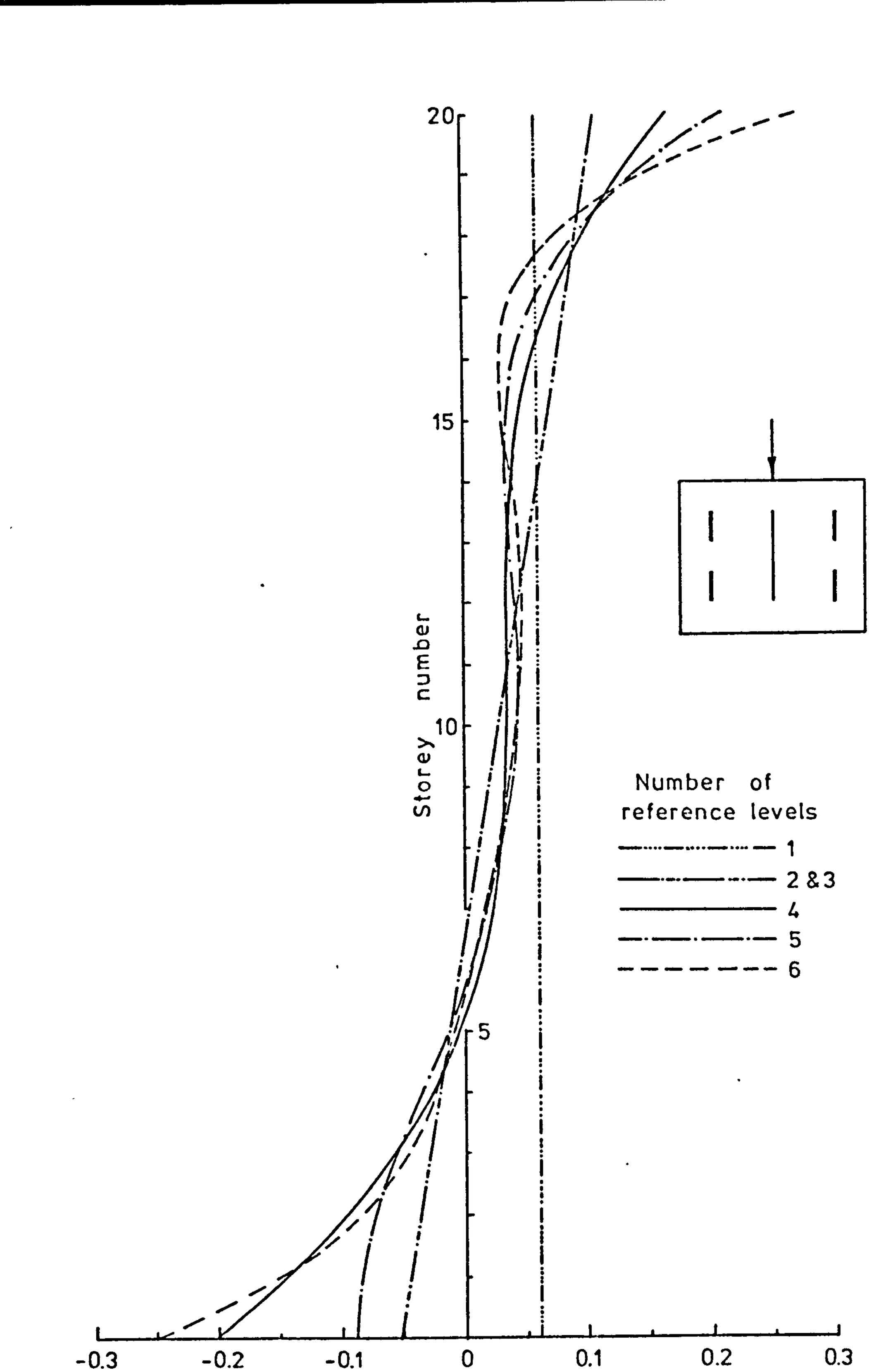

Effect of number of reference levels on polynomial load distribution on coupled shear walls (Case 3)

Figure 6.15

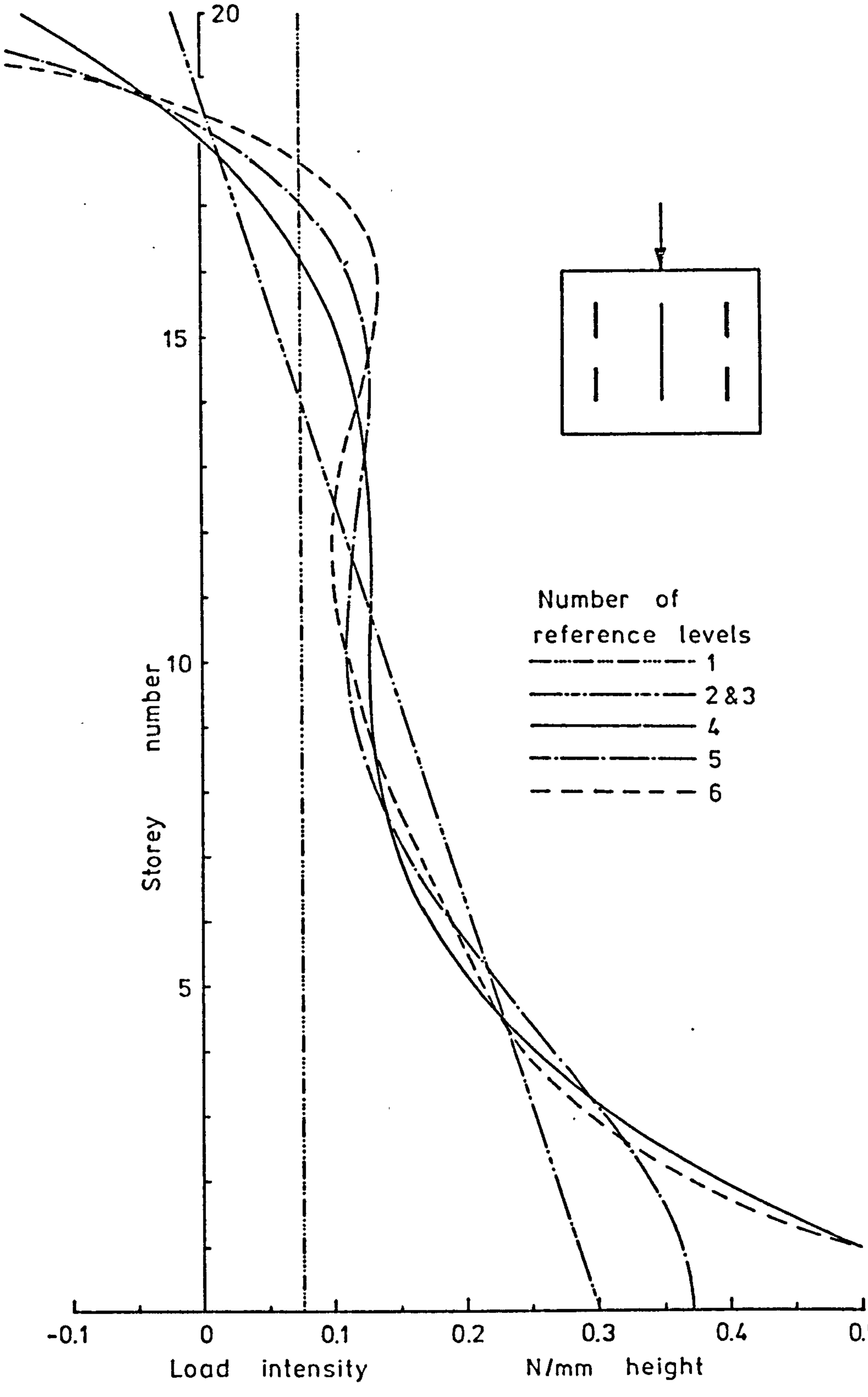

Effect of number of reference levels on polynomial load distribution on single shear wall (Case 3)

Figure 6.16

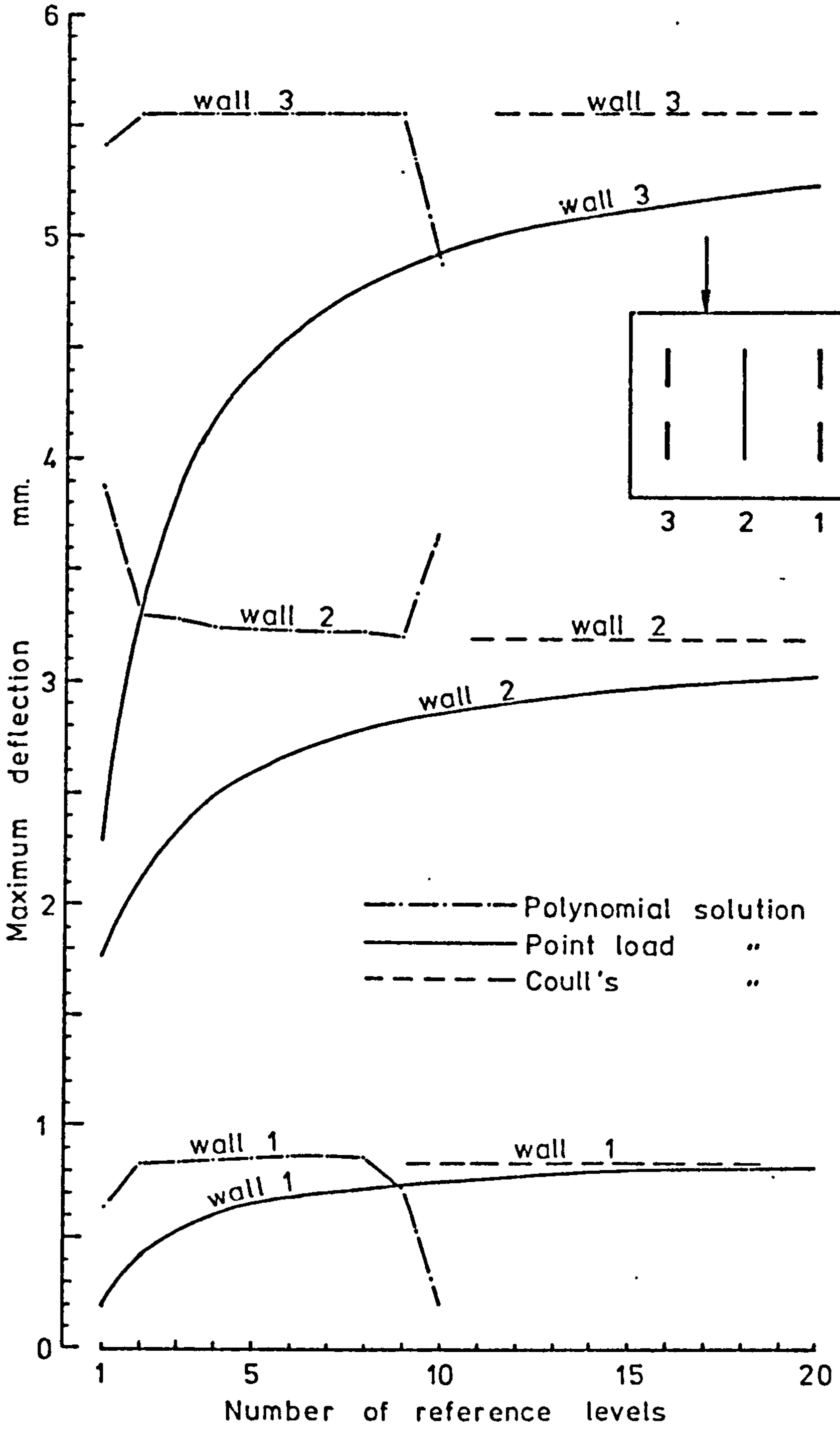

Effect of number of reference levels on deflection at top of walls (Case 4)

Figure 6.17

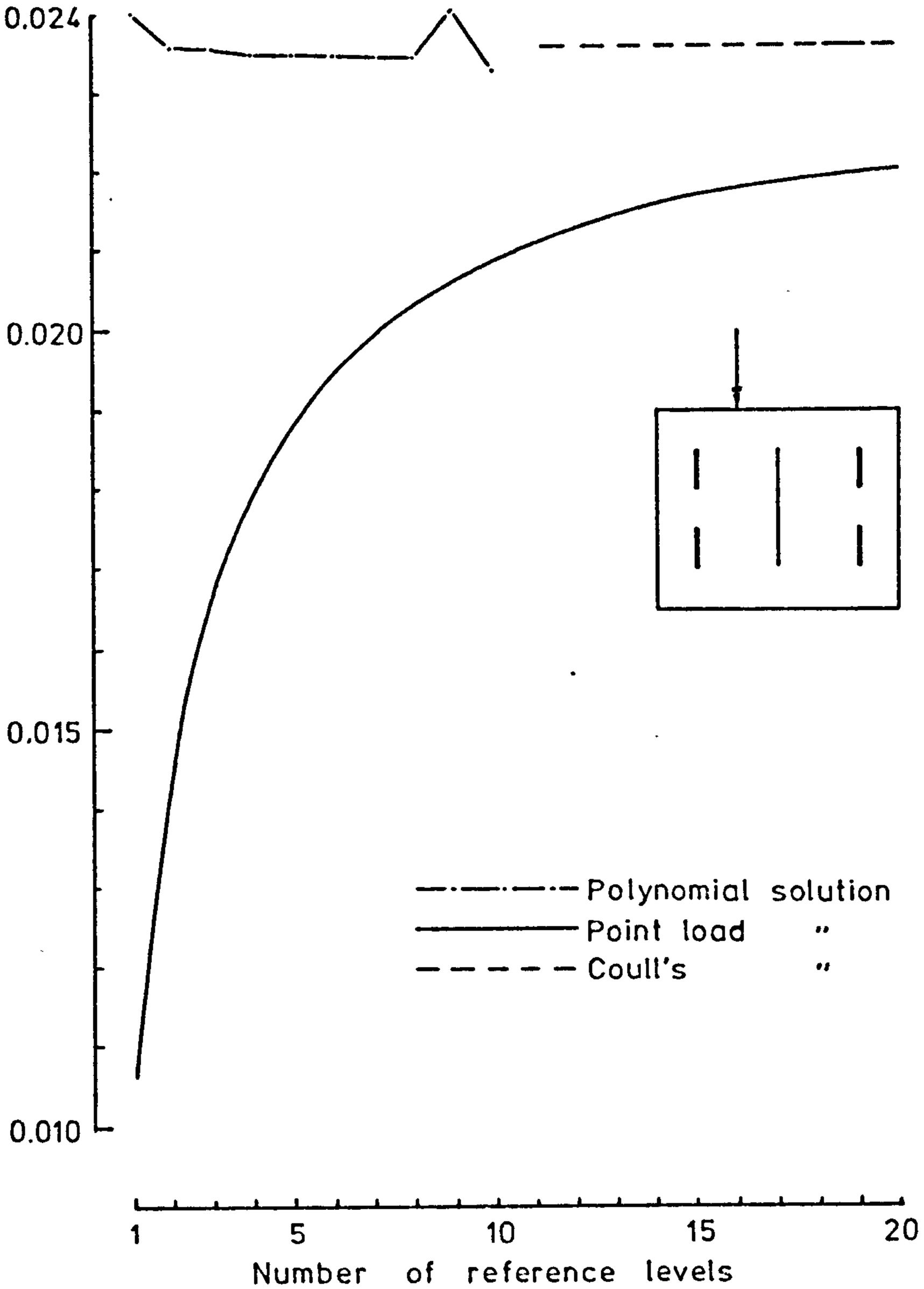

Effect of number of reference levels on rotation at top of structure (Case 4)

Figure 6.18

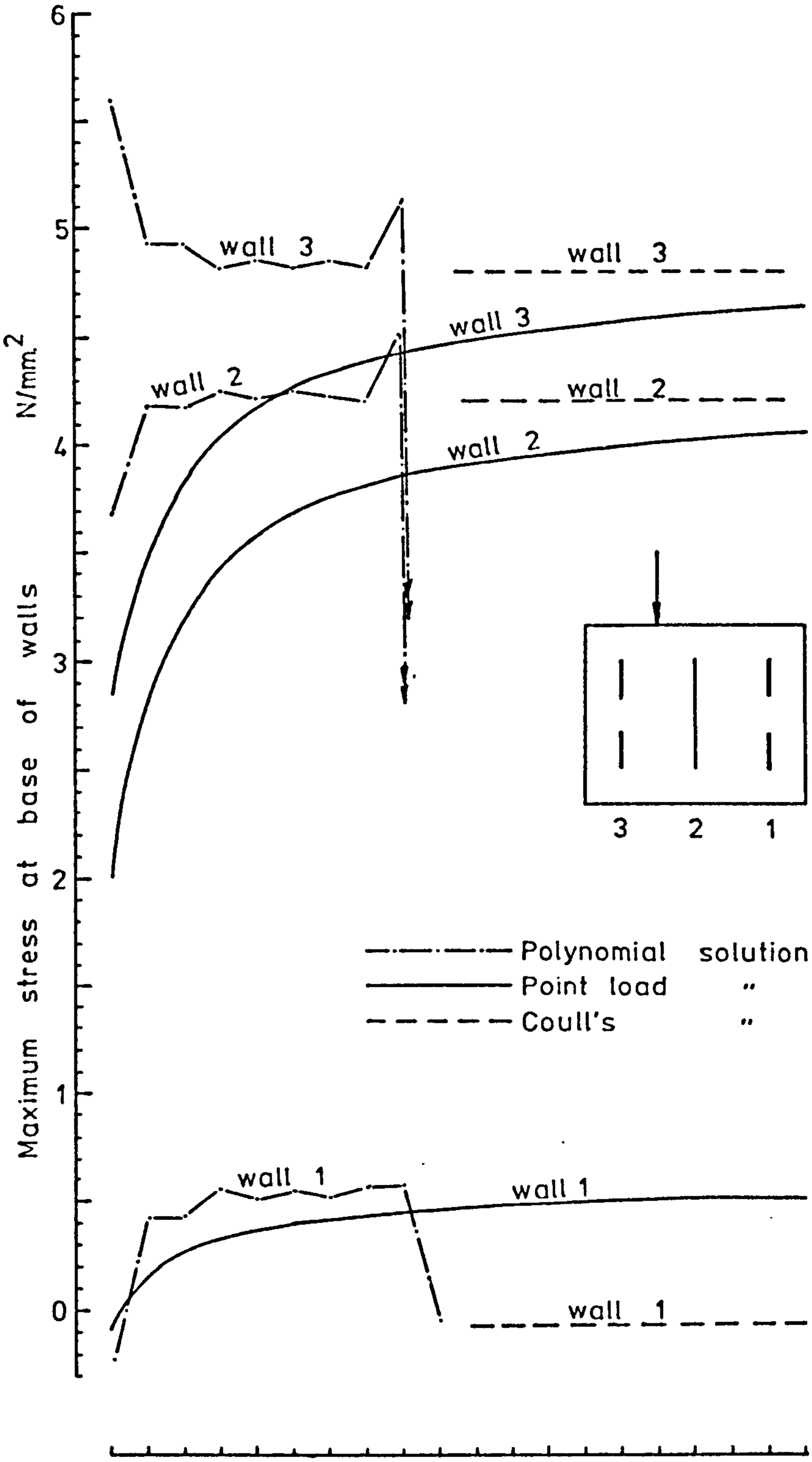

Effect of number of reference levels on stresses at base of walls (Case 4)

Figure 6.19

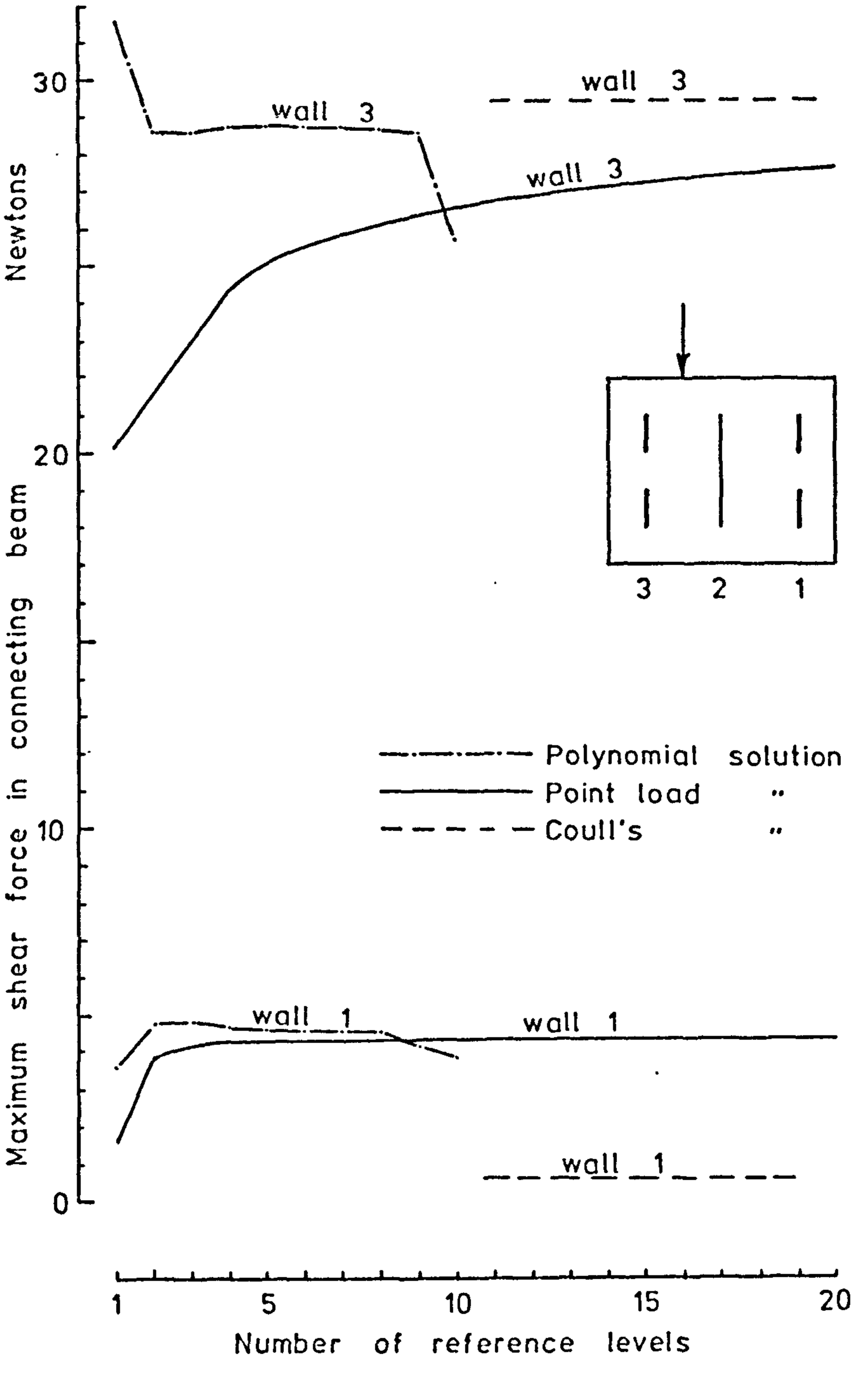

Effect of number of reference levels on shear forces in connecting beams (Case 4)

Figure 6.20

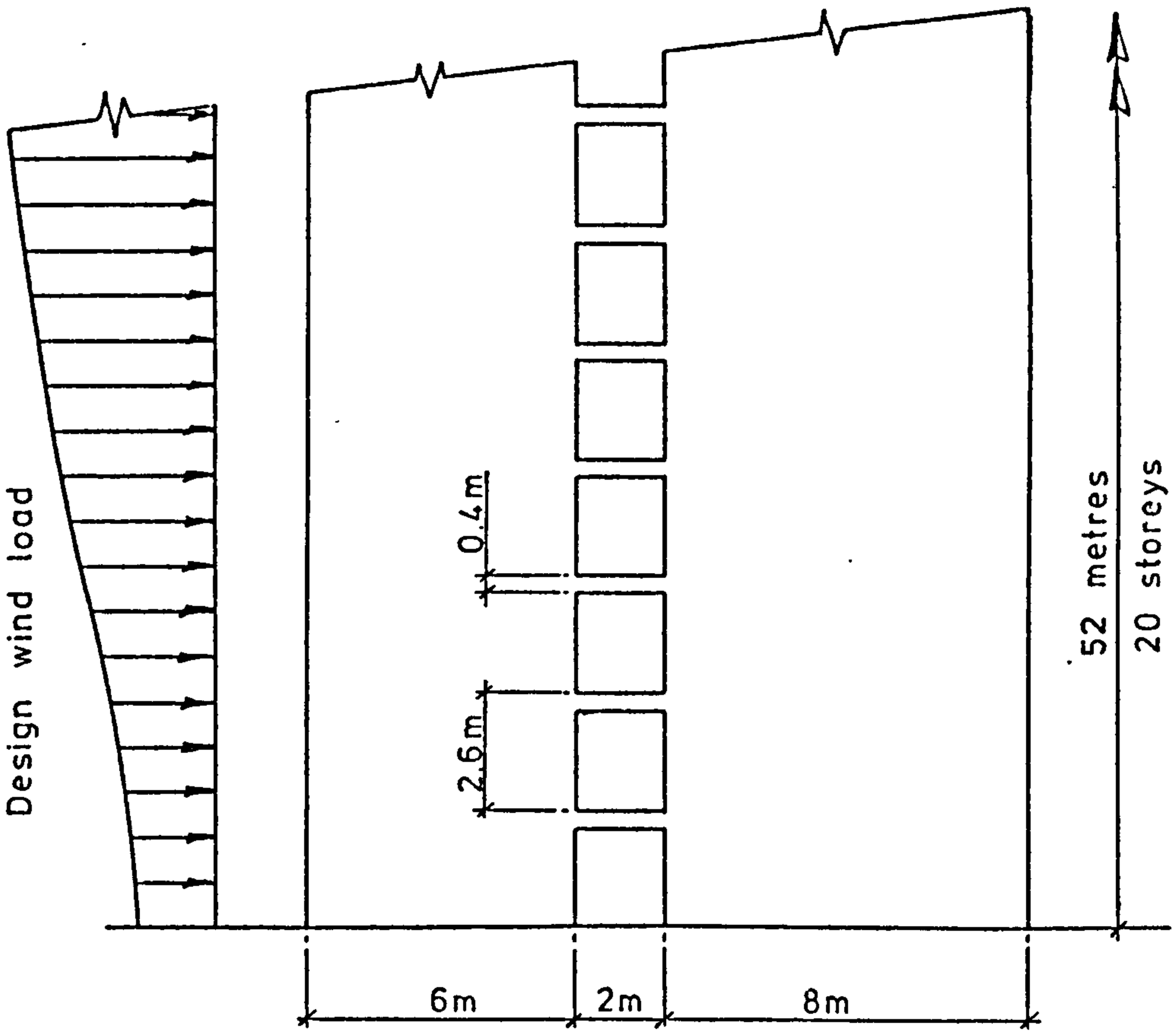

Elevation

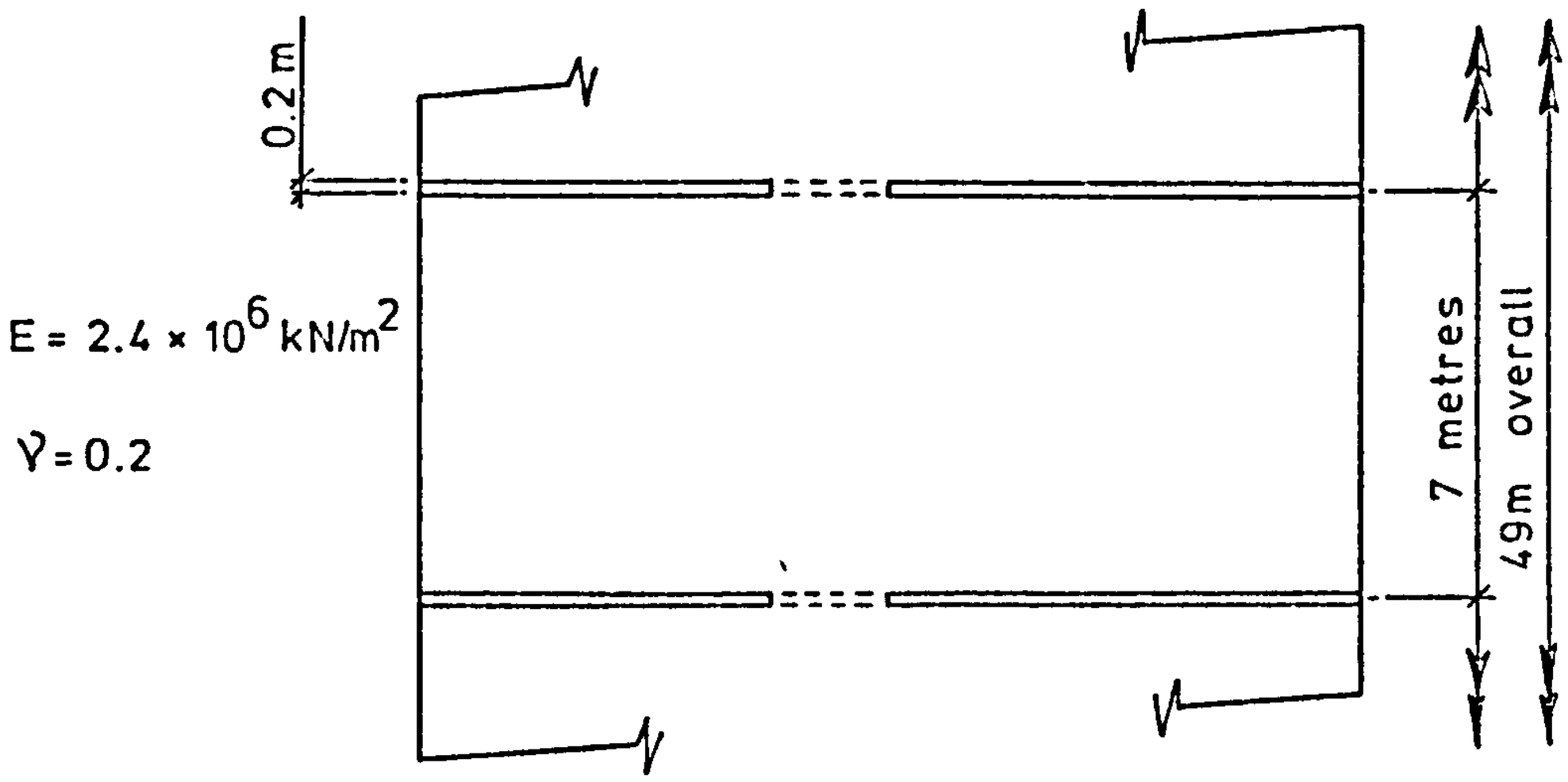

Plan

Shear walls coupled by lintel beams.

Figure 6.21

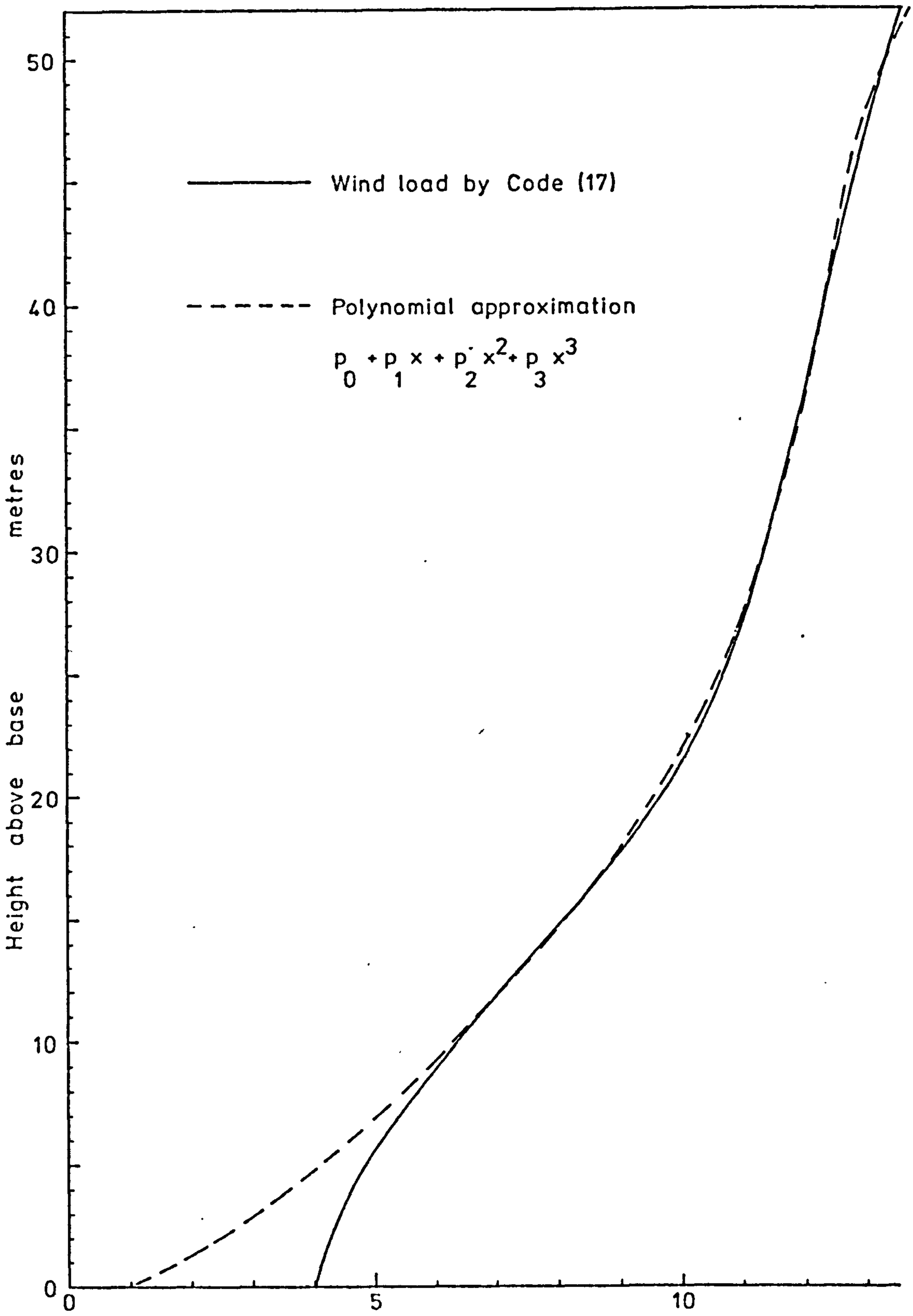

Polynomial approximation to wind load distribution

Figure 6.22

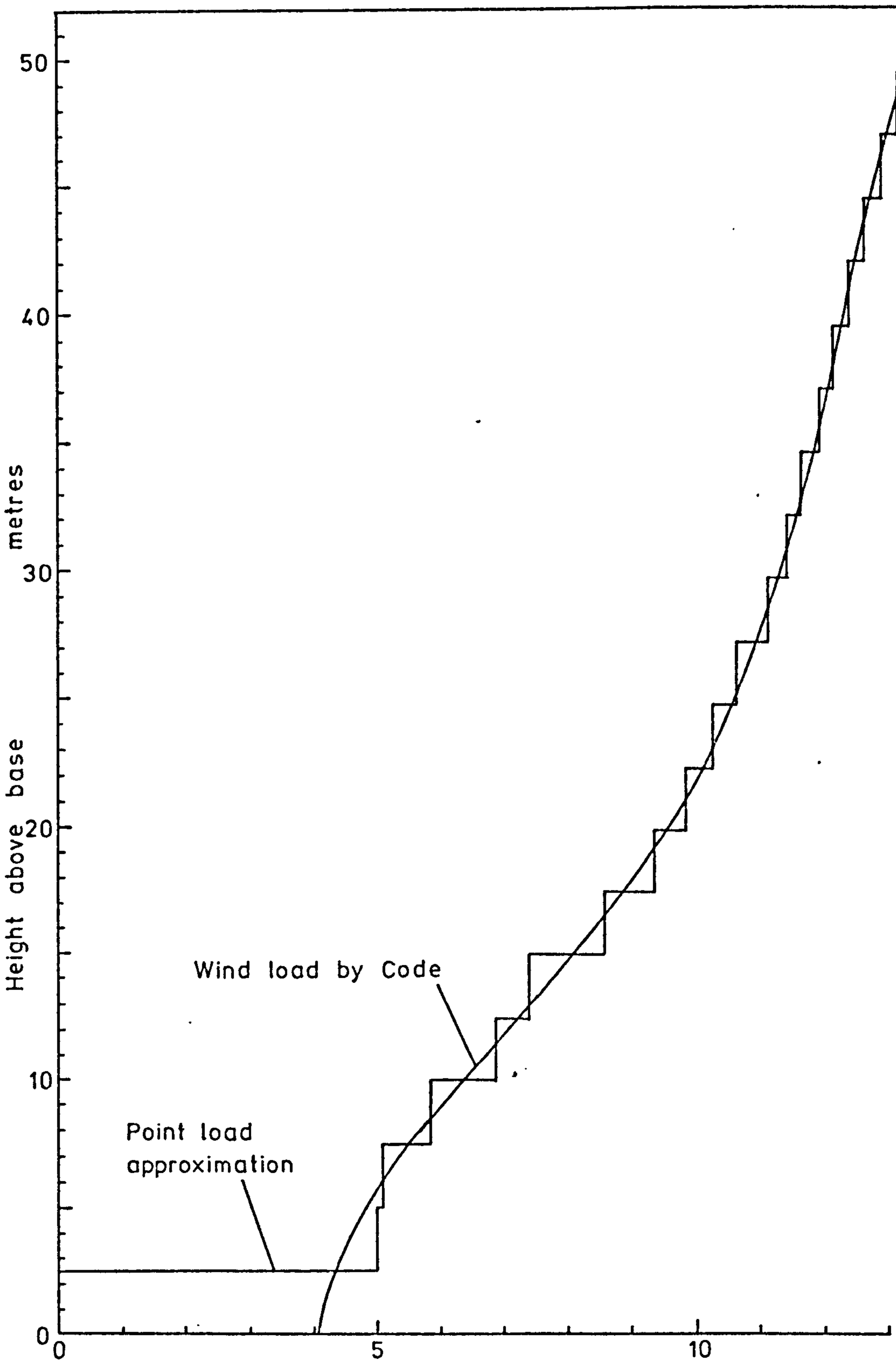

Point load approximation to wind load distribution.

Figure 6.23

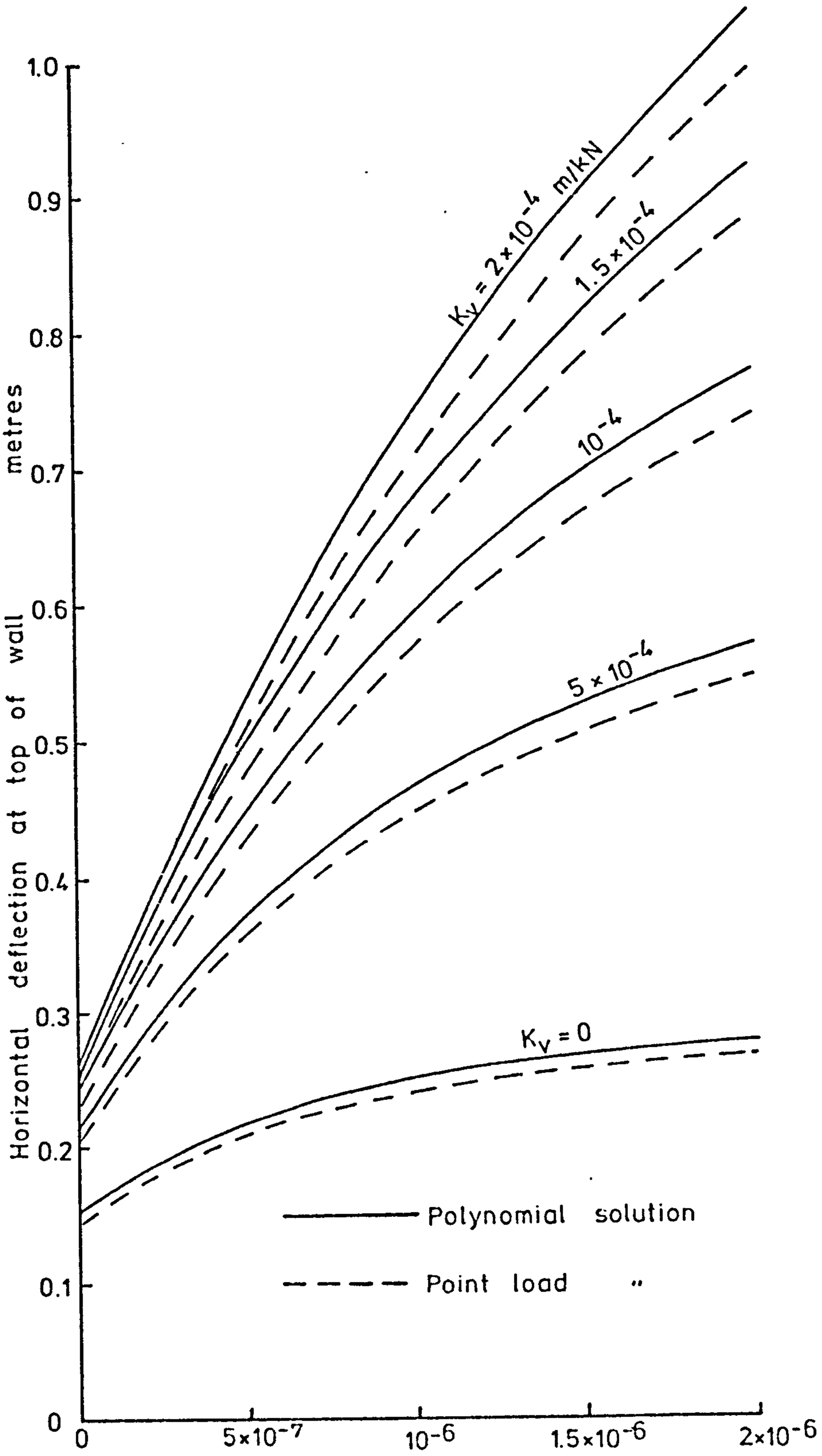

Effect of flexible foundations on deflection at top of walls (1)

Figure 6.24

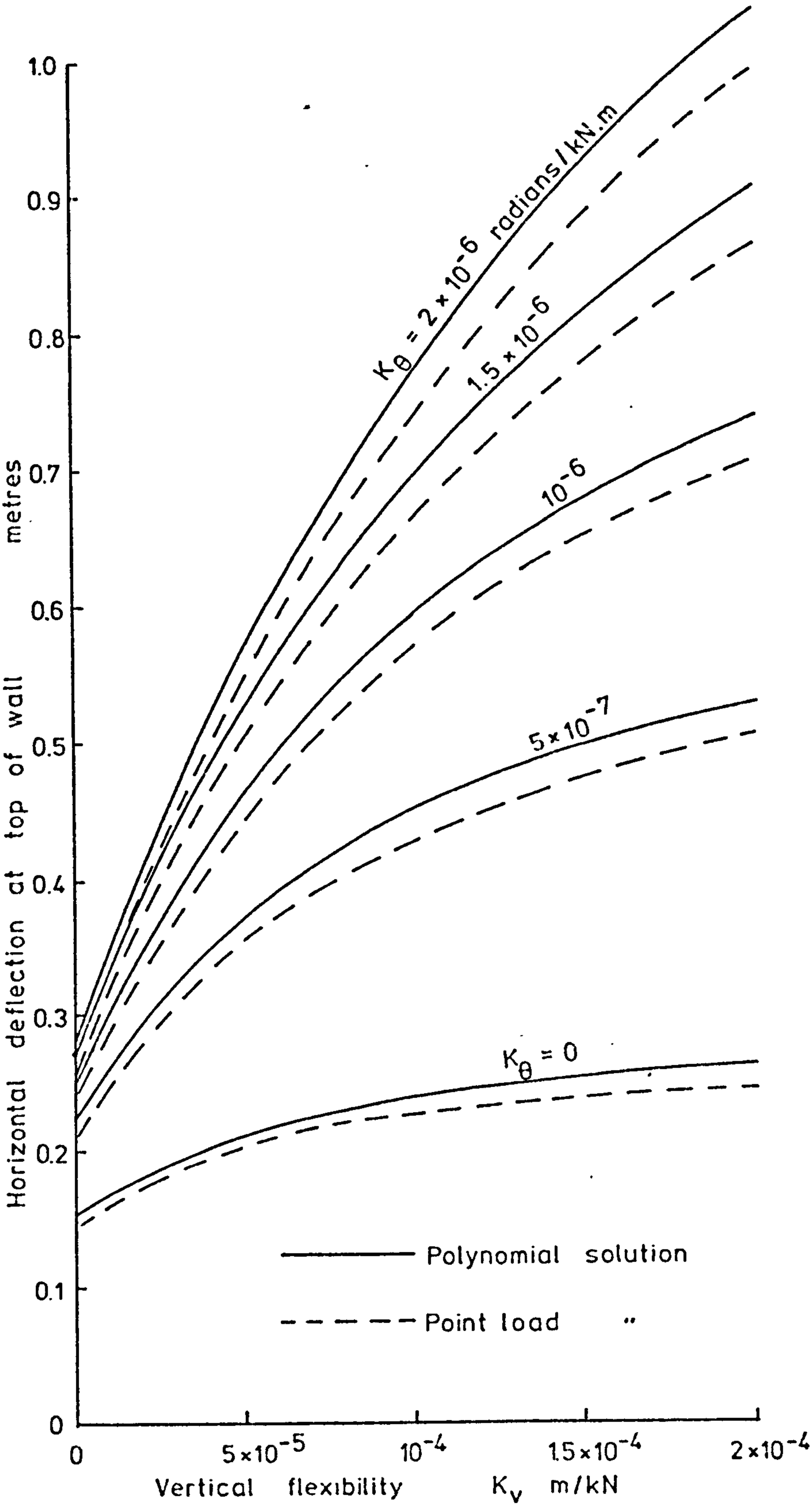

Effect of flexible foundations on deflection at top of walls (2)

Figure 6.25

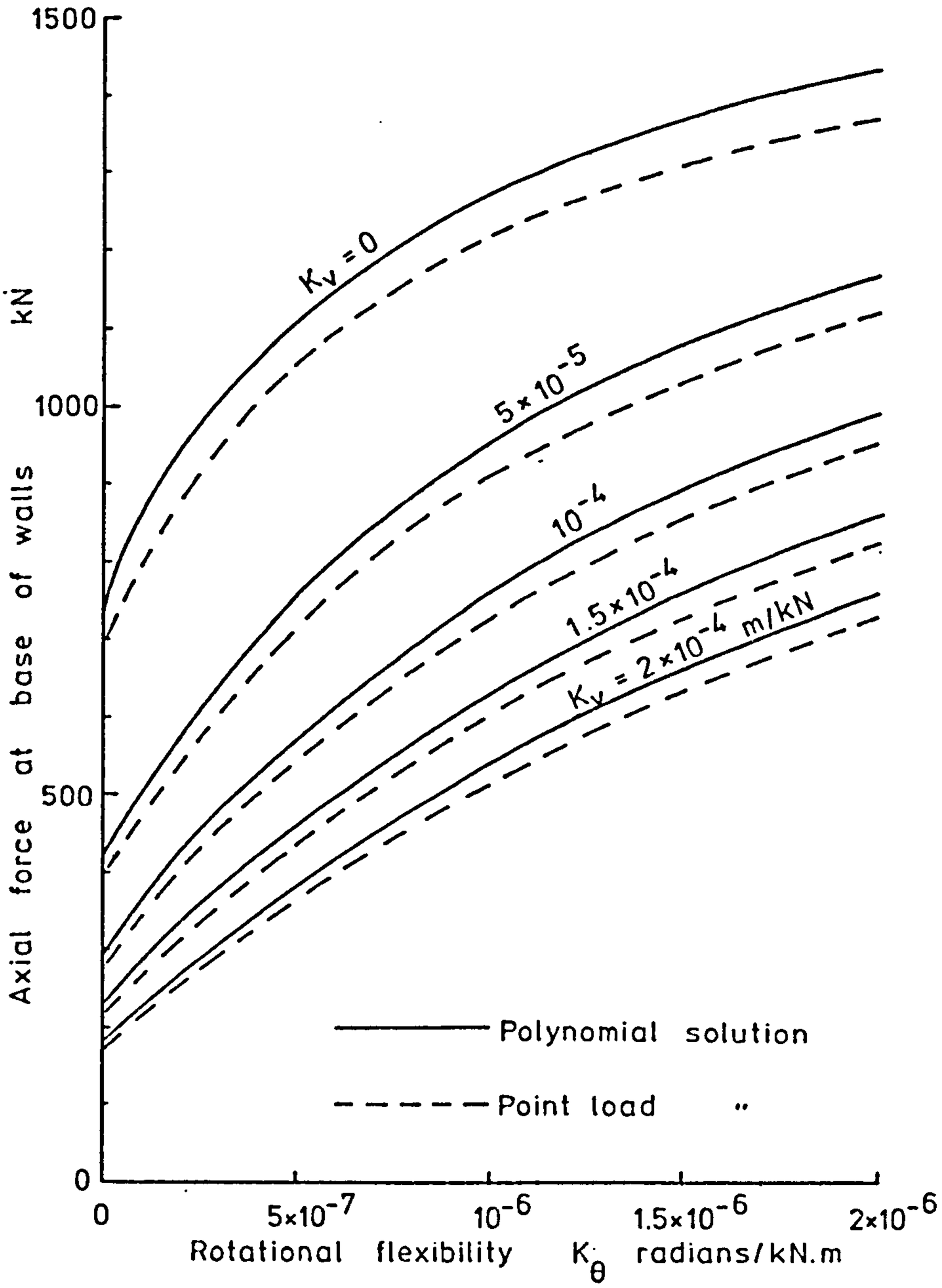

Effect of flexible foundations on axial force at base of shear walls. (1)

Figure 6.26

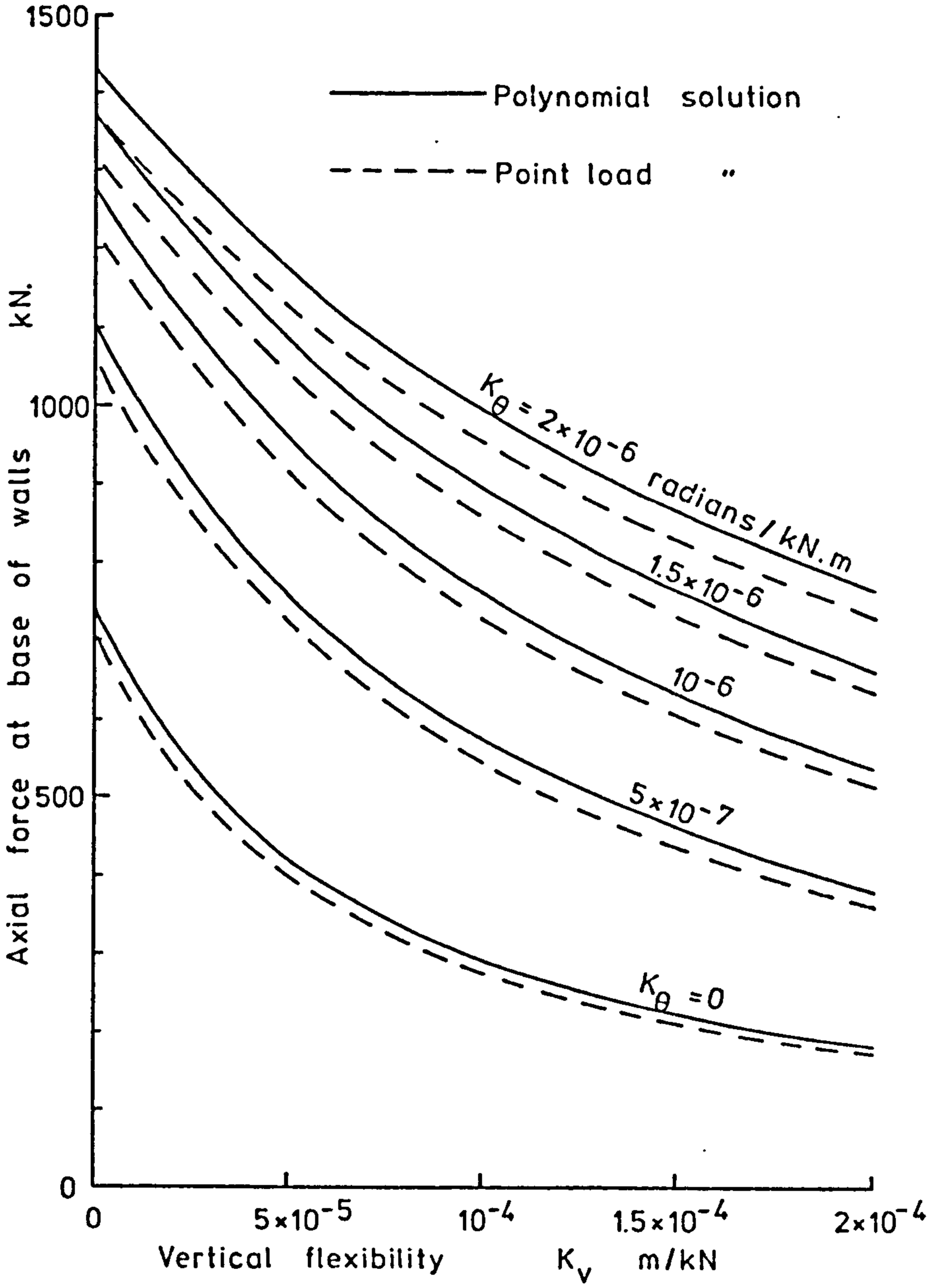

Effect of flexible foundations on axial force at base of shear walls (2)

Figure 6.27

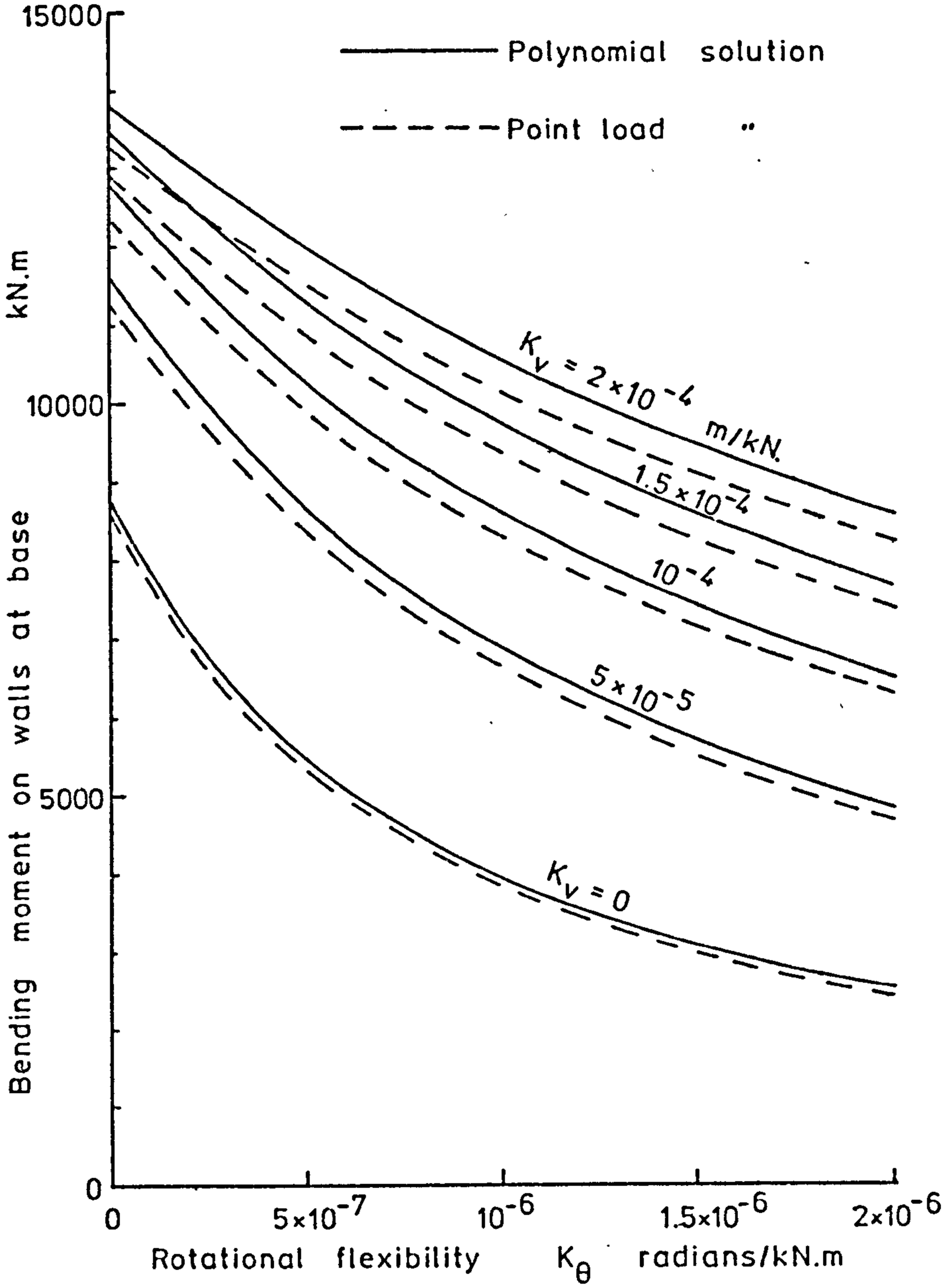

Effect of flexible foundations on bending moment at base of shear walls (1)

Figure 6.28

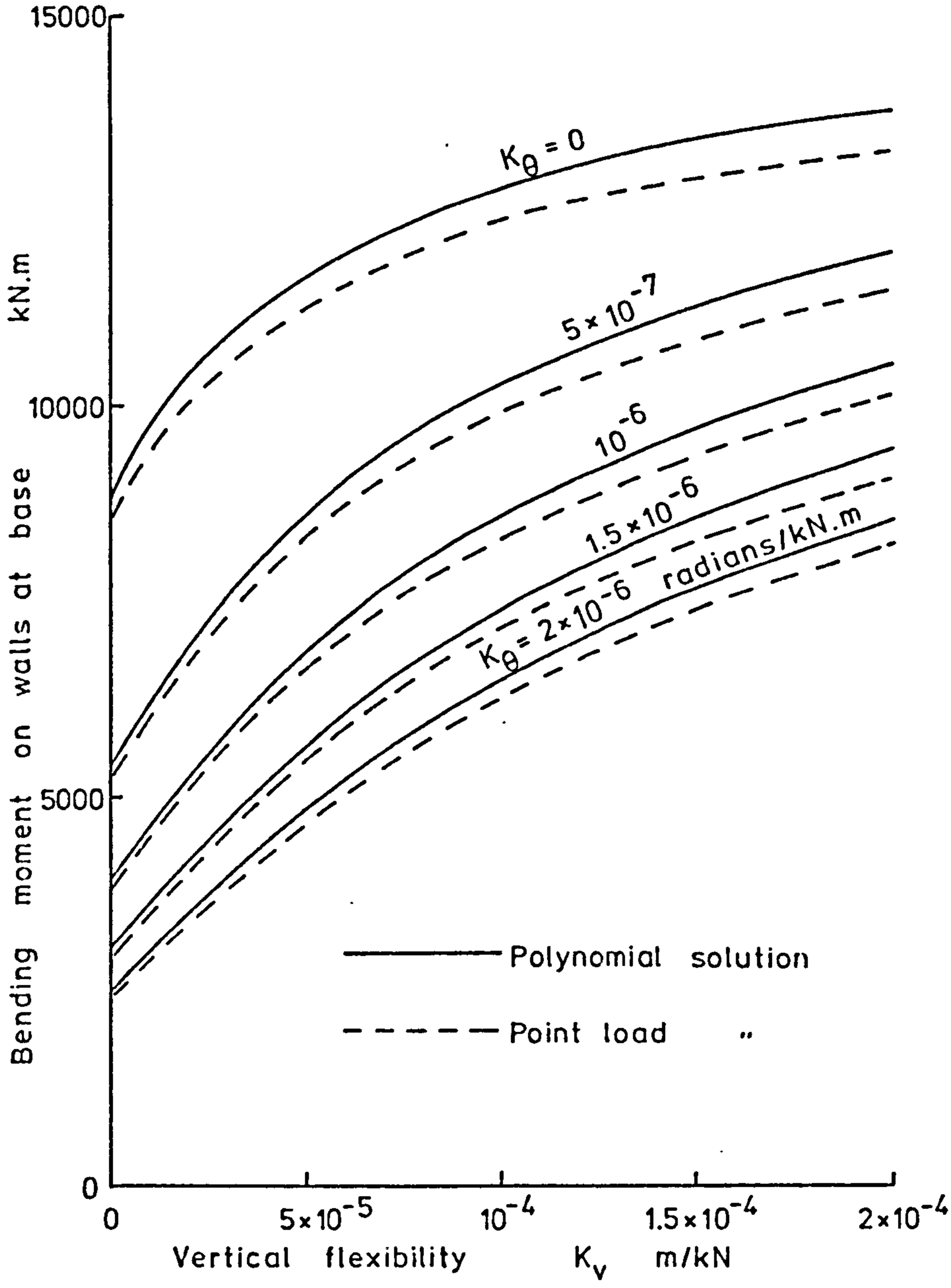

Effect of flexible foundations on bending moment at base of walls. (2)

Figure 6.29

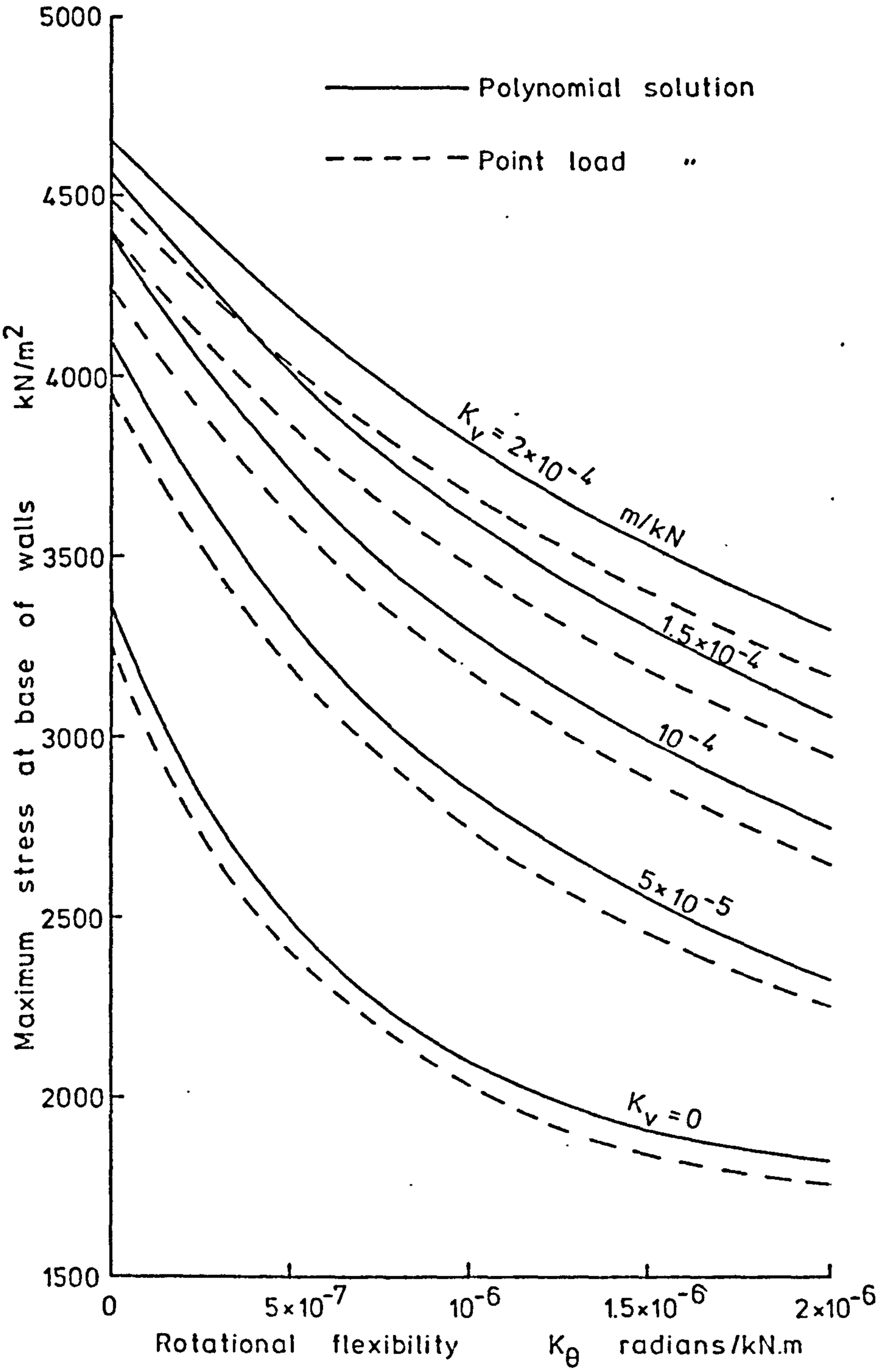

Effect of flexible foundations on stresses at base of shear walls. (1)

Figure 6.30

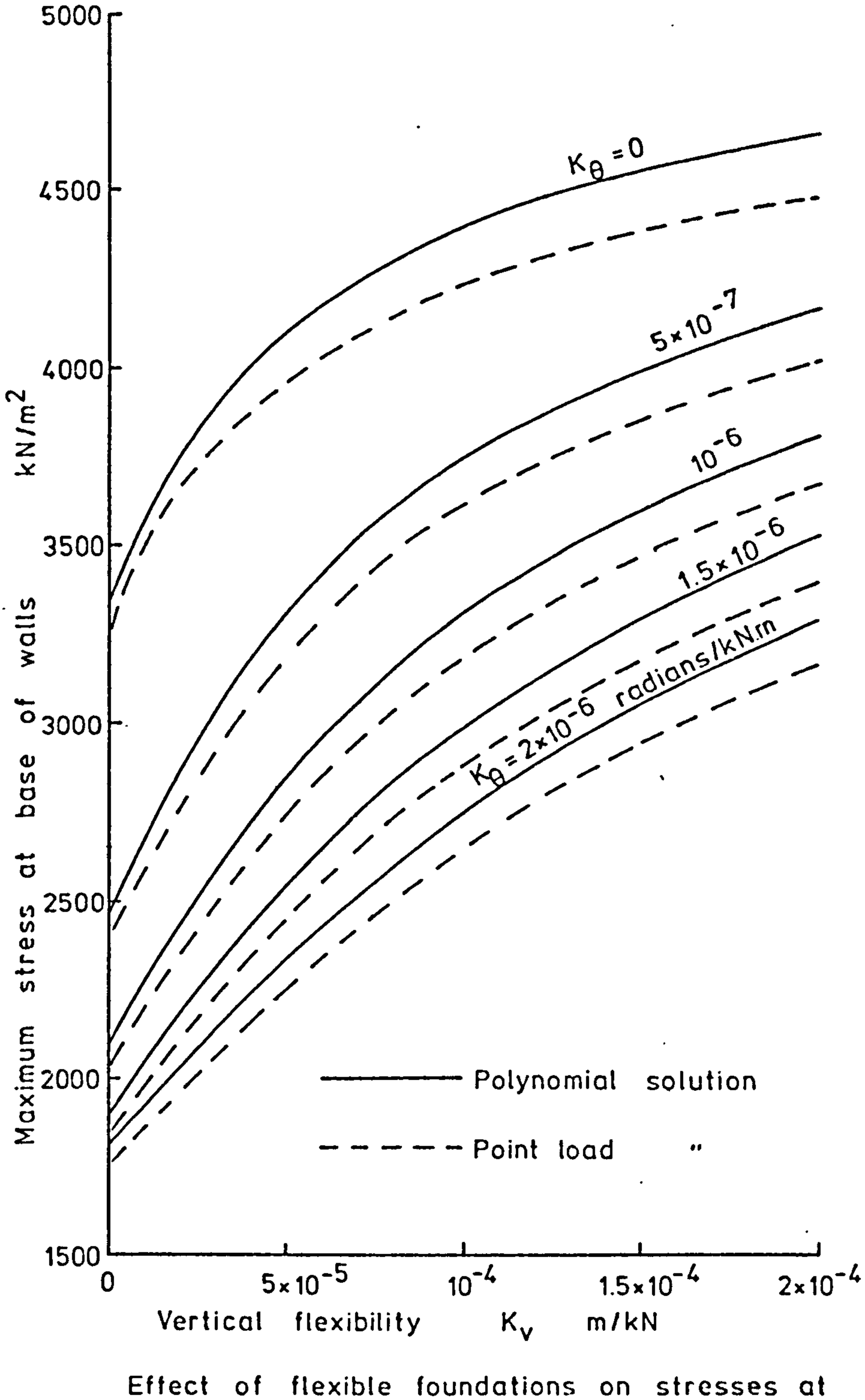

Effect of flexible foundations on stresses at base of shear walls. (2)

Figure 6.31

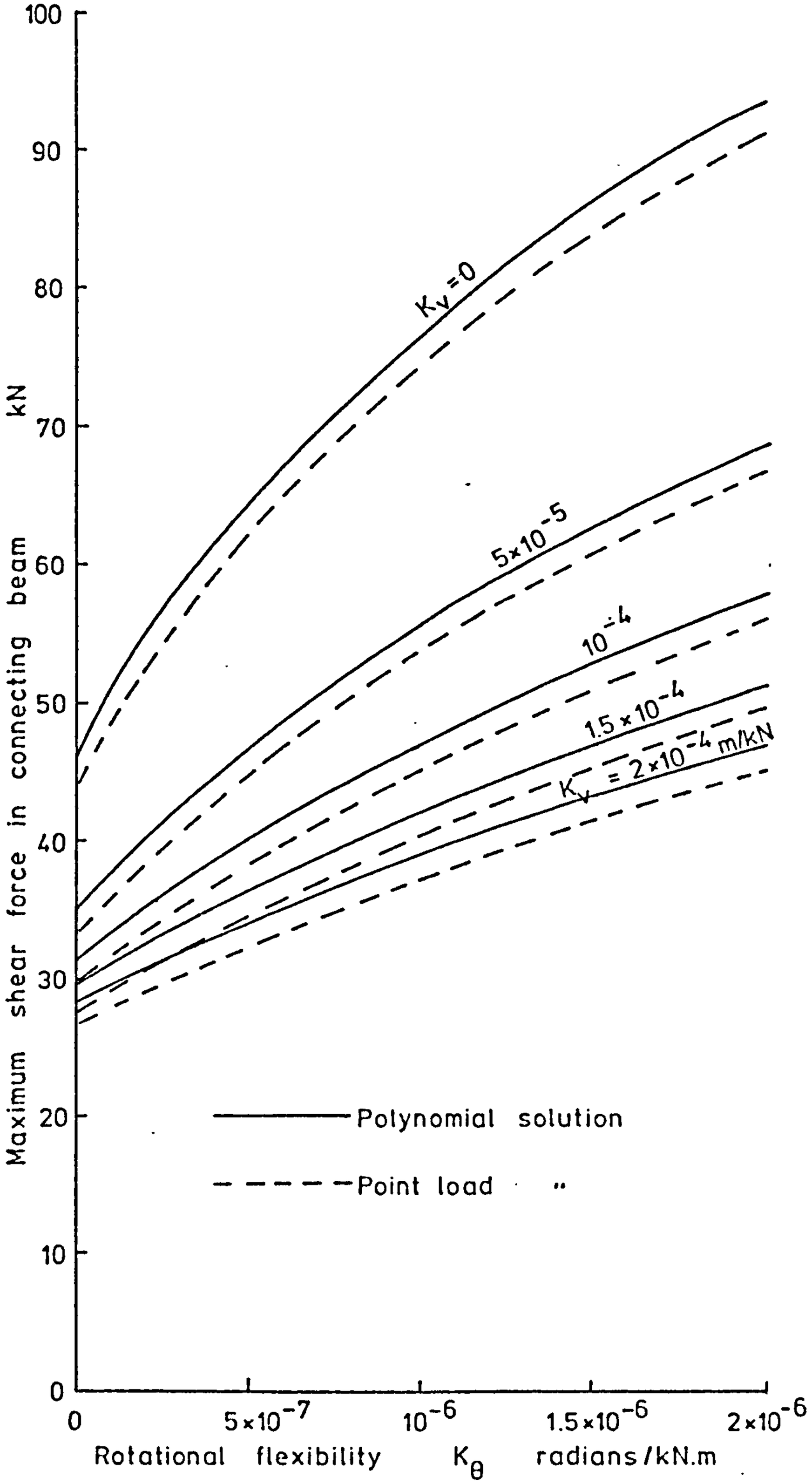

Effect of flexible foundations on shear forces in connecting beams. (1)

Figure 6.32

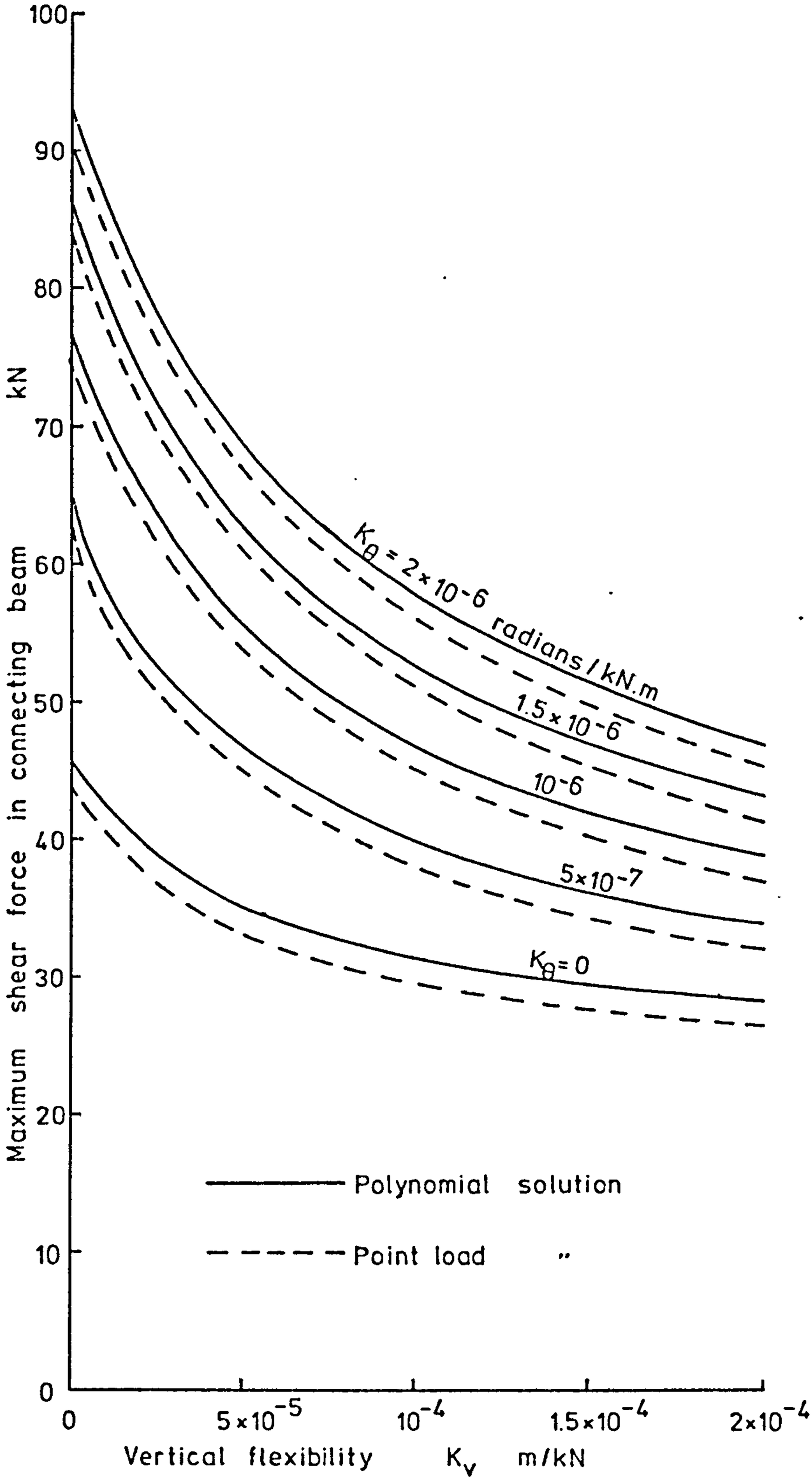

Effect of flexible foundations on shear forces in connecting beams. (2)

Figure 6.33

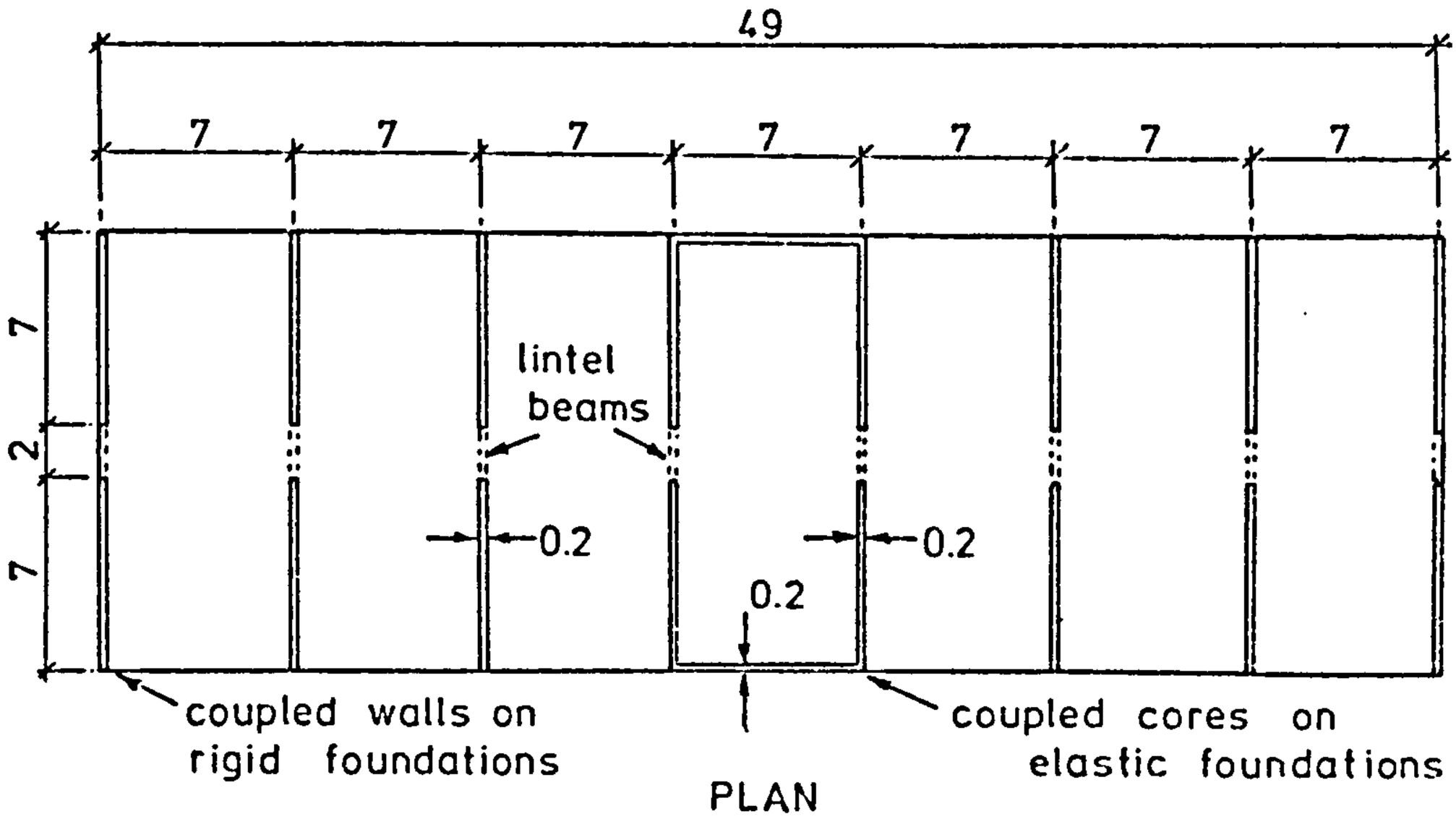

PLAN

Dimensions in millimetres

20 storeys

Height of structure = 52 metres
Storey height = 2.6 "
Young's modulus = 2.4×10^{-6} kN/m^2
Poisson's ratio = 0.2

Lintel beams
built into shear walls and core walls
depth = 0.4 metres
breadth = 0.2 "
effective span = 2.4 "

Shear wall structure with central coupled cores.

Figure 6.34

F 6.35

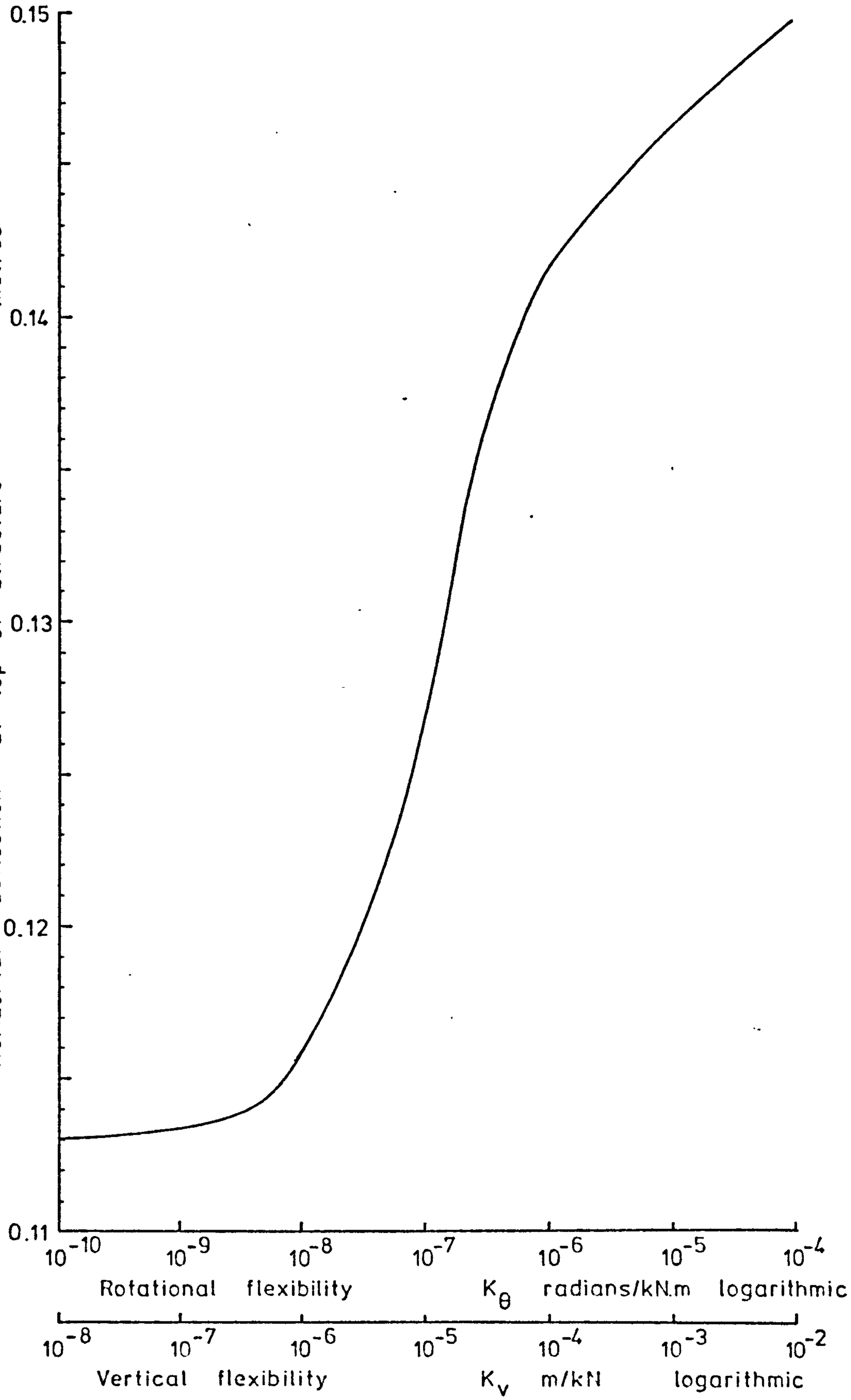

Effect of flexible foundations at core walls on deflection at top of structure.

Figure 6.35

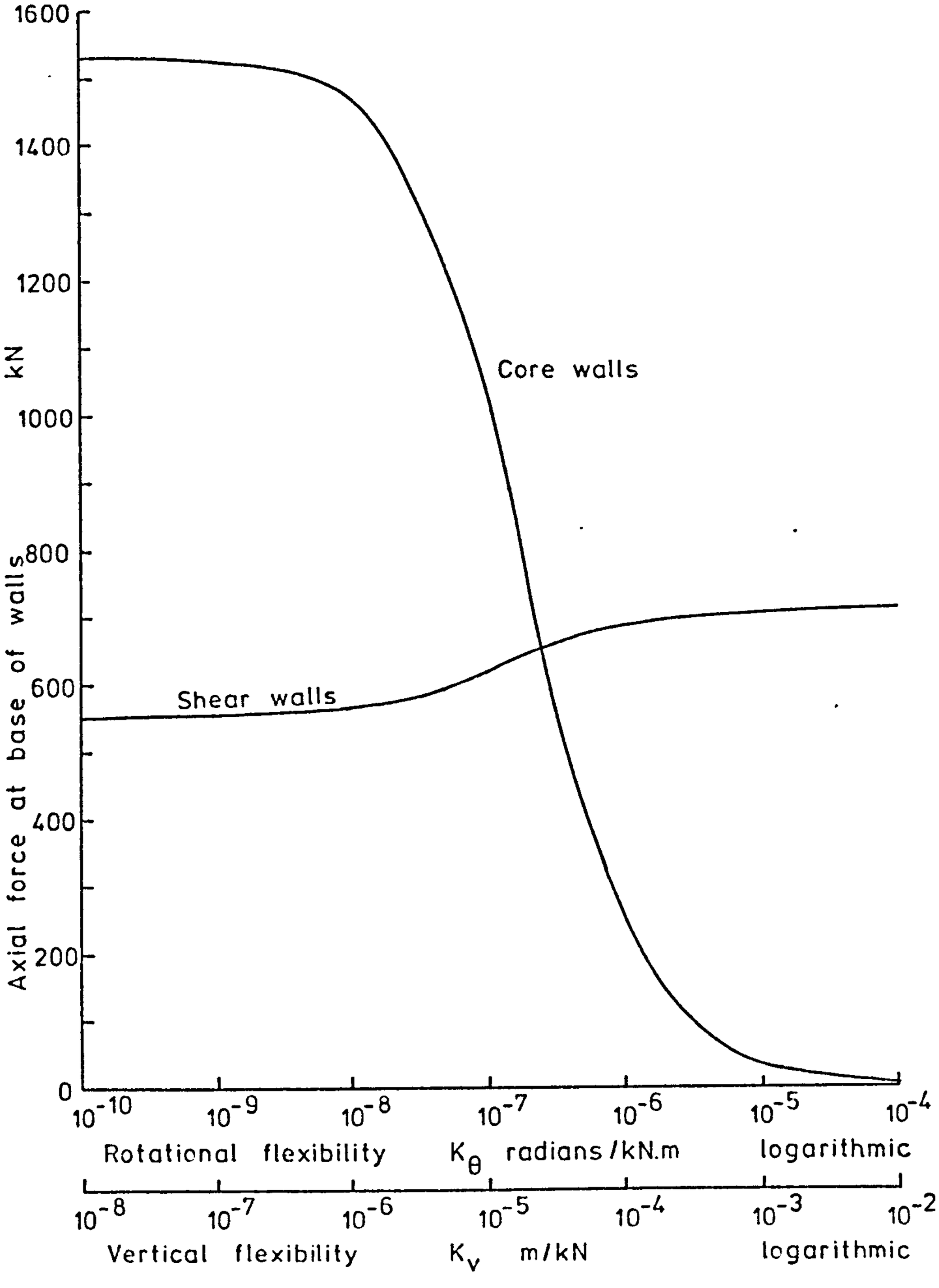

Effect of flexible foundations at core walls on axial forces at base of walls

Figure 6.36

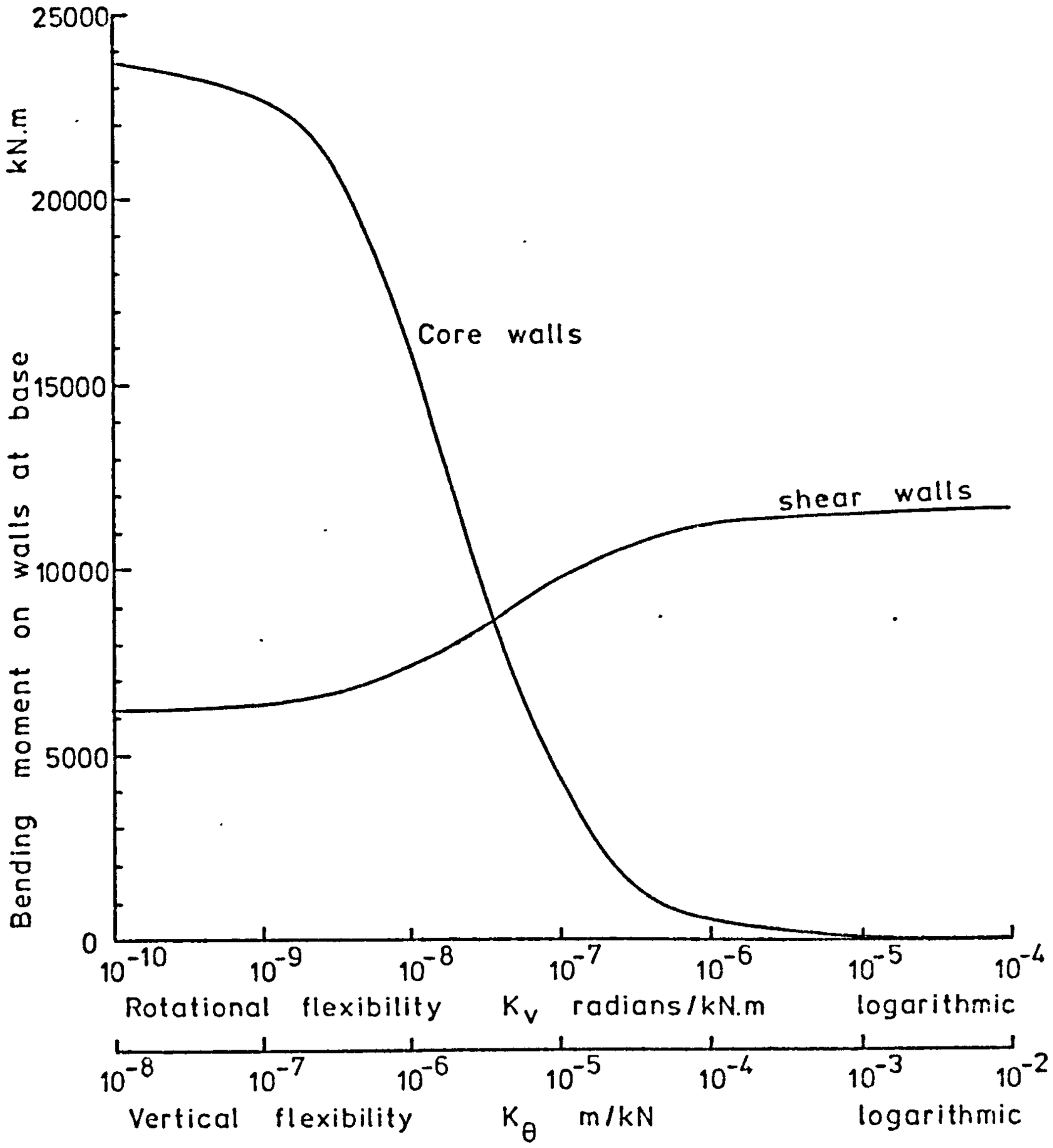

Effect of flexible foundations at core walls on bending moment on walls at the base

Figure 6.37

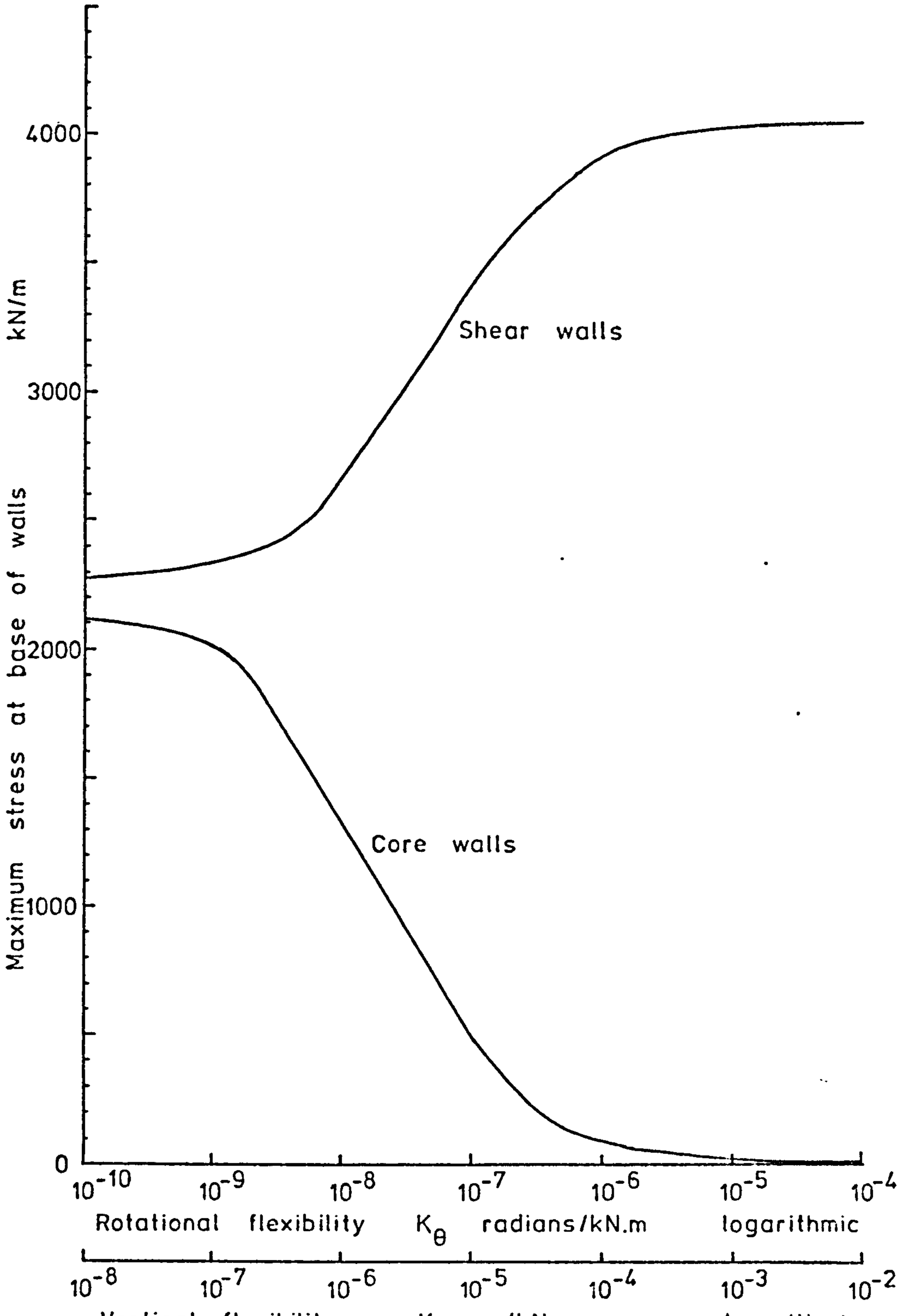

Effect of flexible foundations at core walls on stresses at base of wall

Figure 6.38

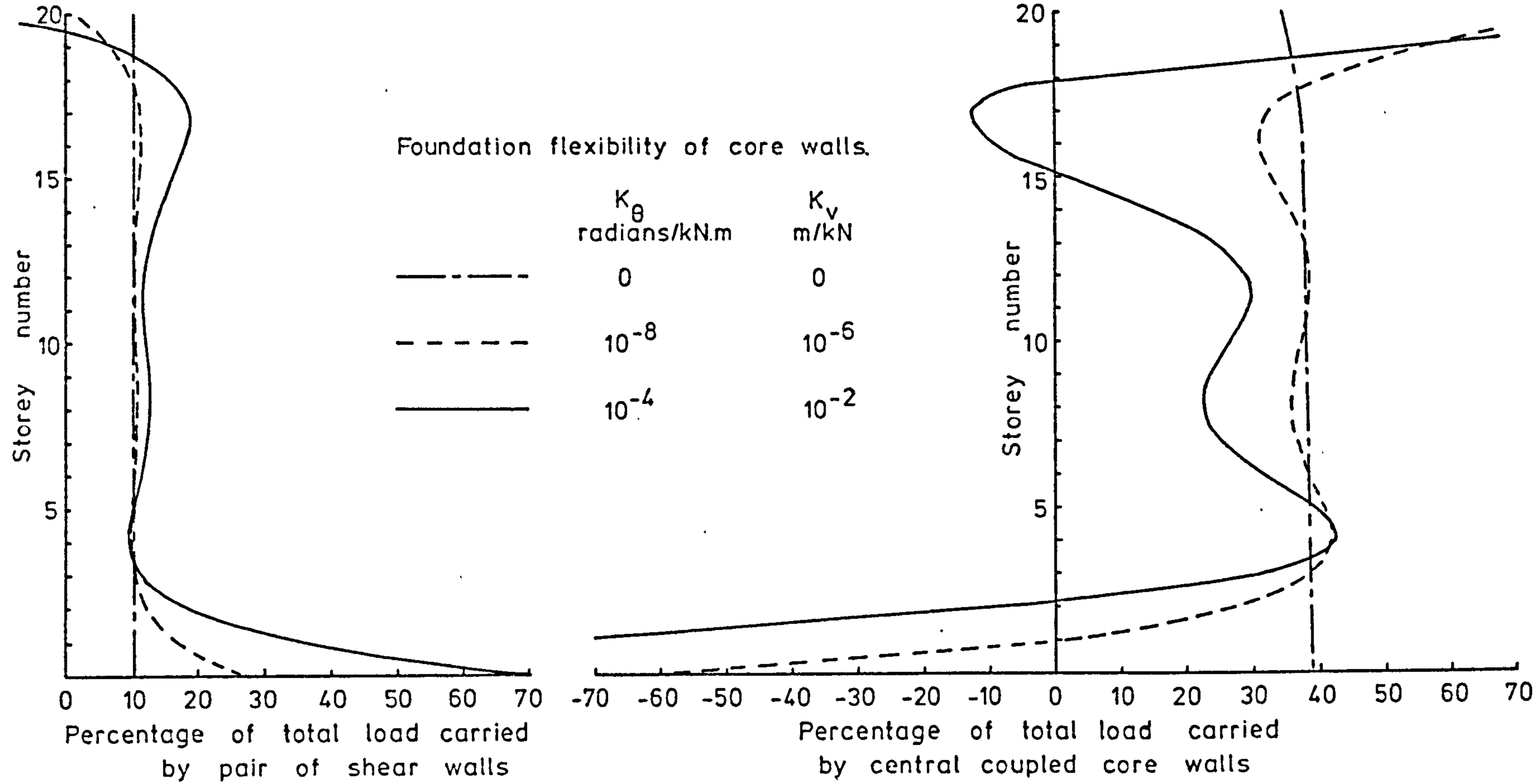

Effect of flexible foundations at core walls on load carried by individual wall assembies.

Figure 6.39

F 6.39

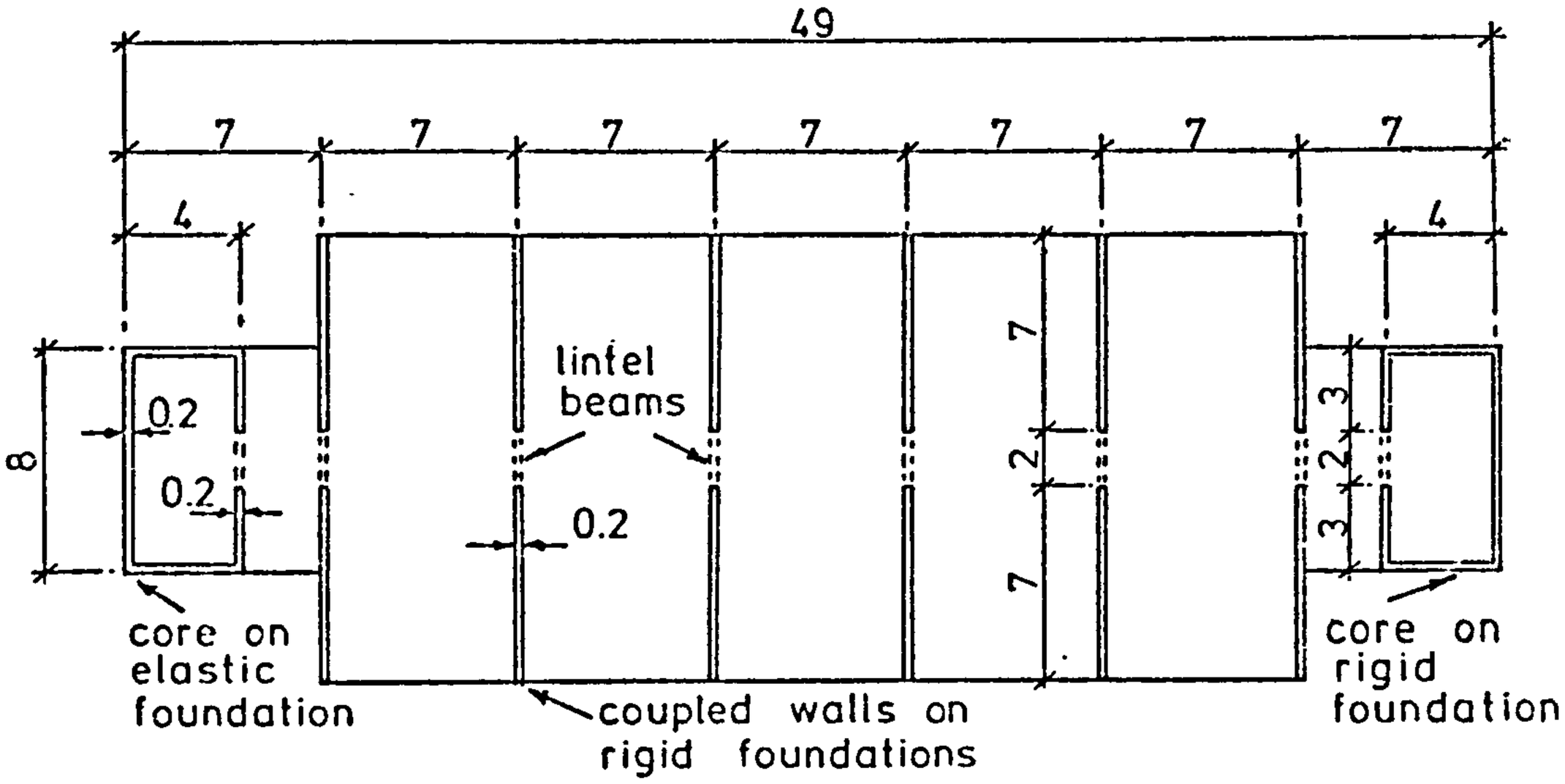

PLAN

Dimensions in millimetres

20 storeys

Height of structure	=	52 metres
Storey height	=	2.6 "
Young's modulus	=	2.4×10^{-6} kN/m^2
Poisson's ratio	=	0.2

Lintel beams

built into walls		
depth	=	0.4 metres
breadth	=	0.2 "
effective span	=	2.4 "

Shear wall structure with end cores

Figure 6.40

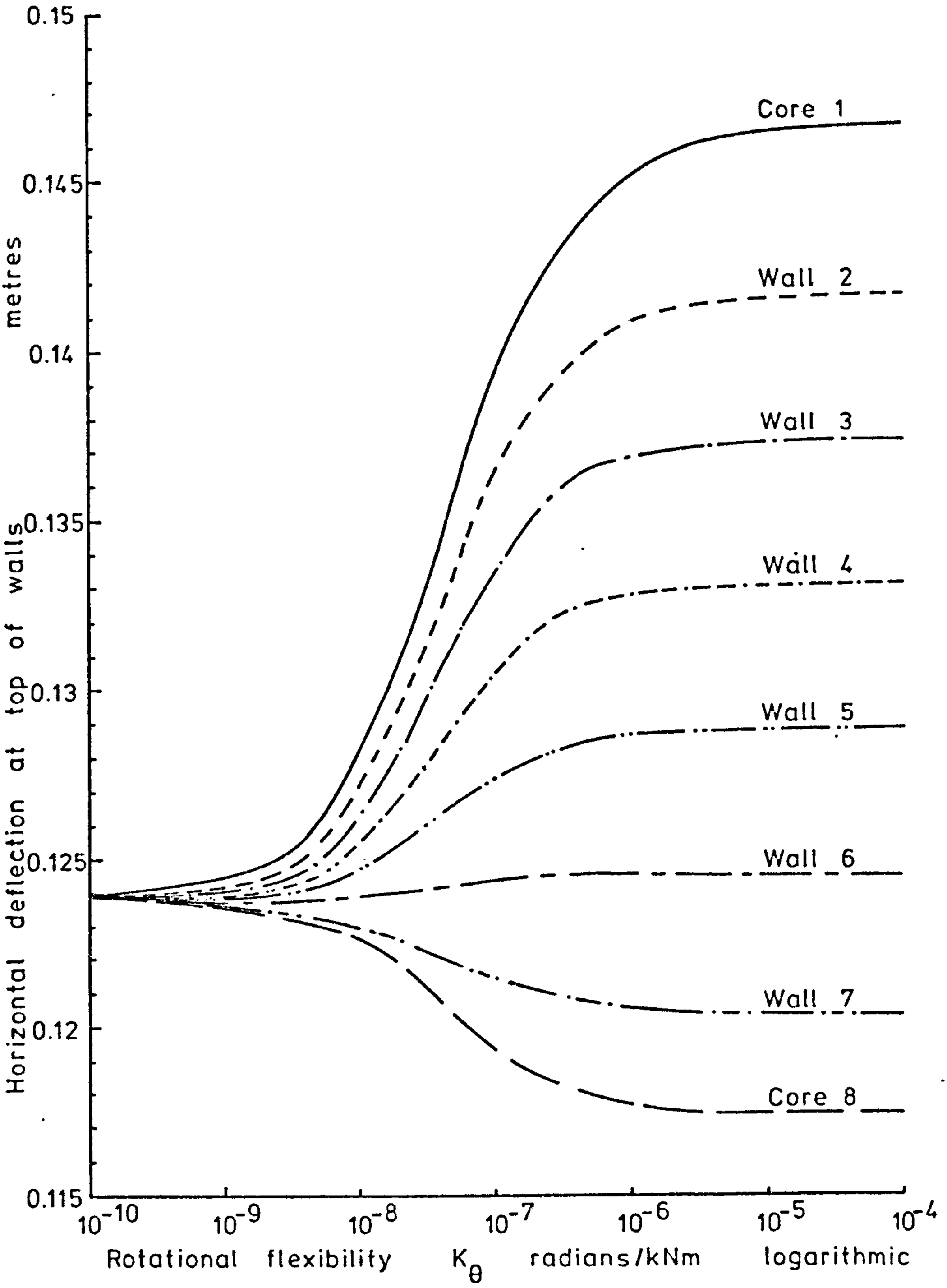

Effect of flexible foundation at end core 1 on deflections at top of structure.

Figure 6.41

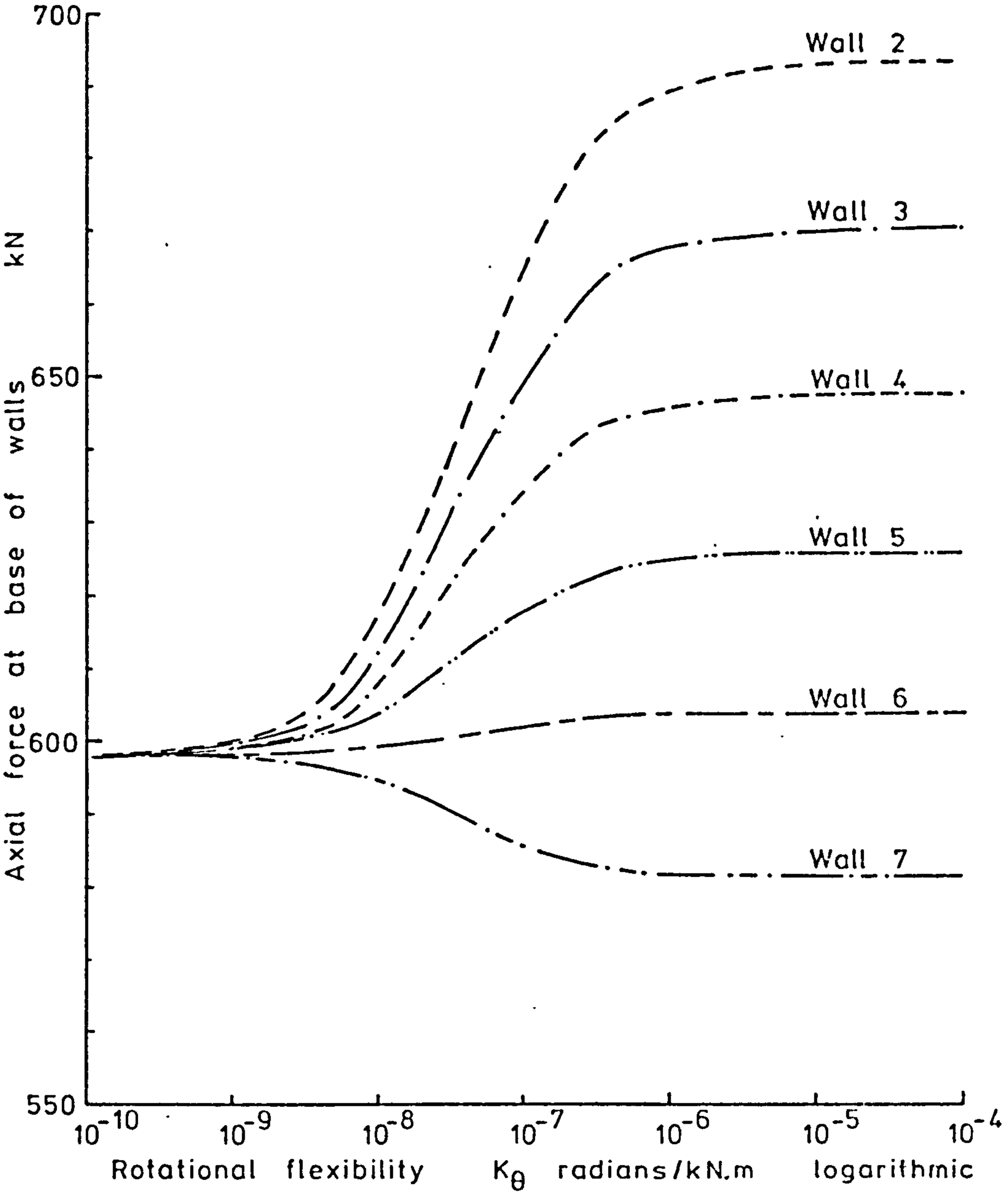

Effect of flexible foundation at end core 1 on axial forces at base of coupled shear walls.

Figure 6.42

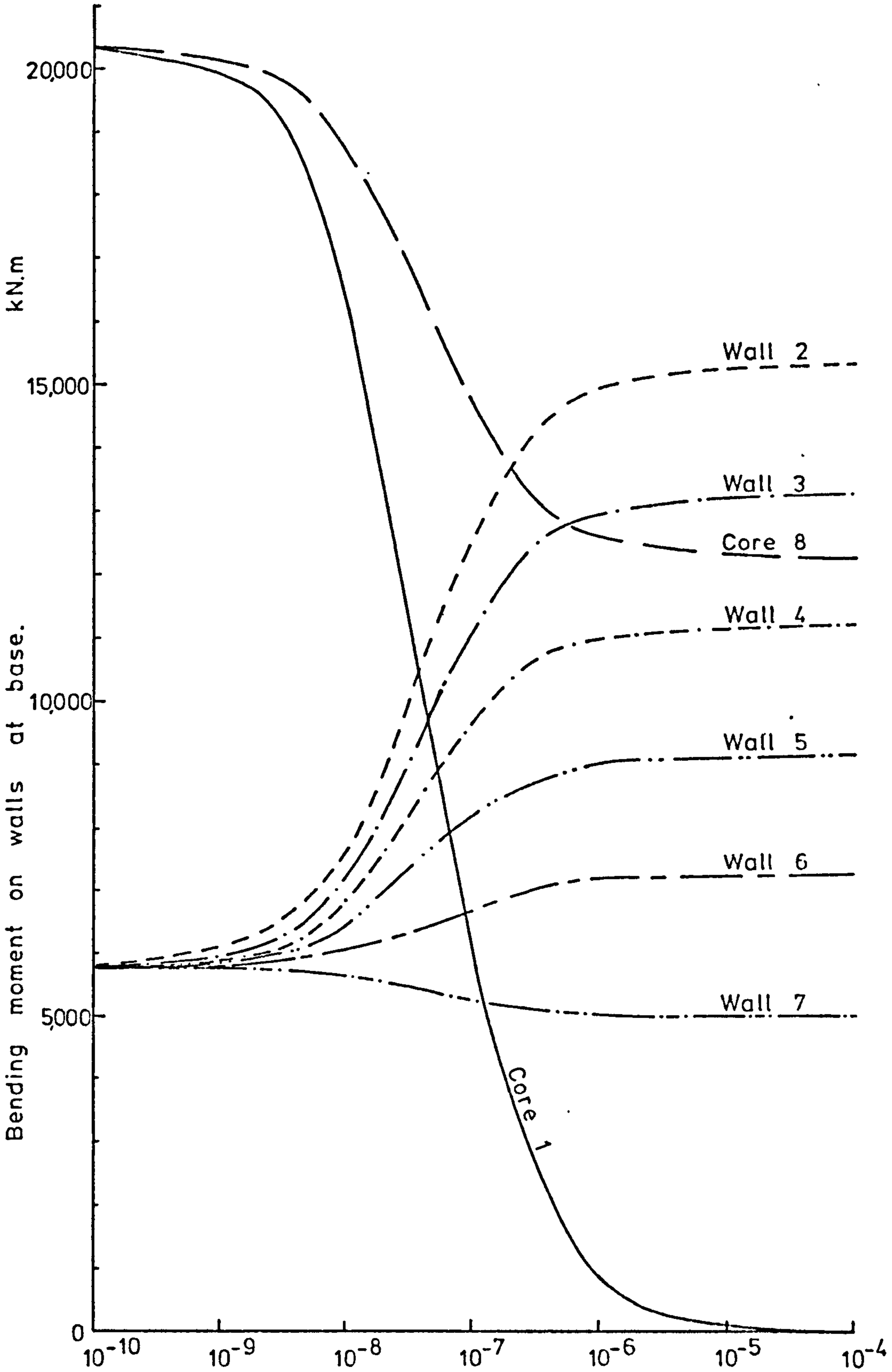

Effect of flexible foundation at end core 1 on bending moments on walls at the base.

Figure 6.43

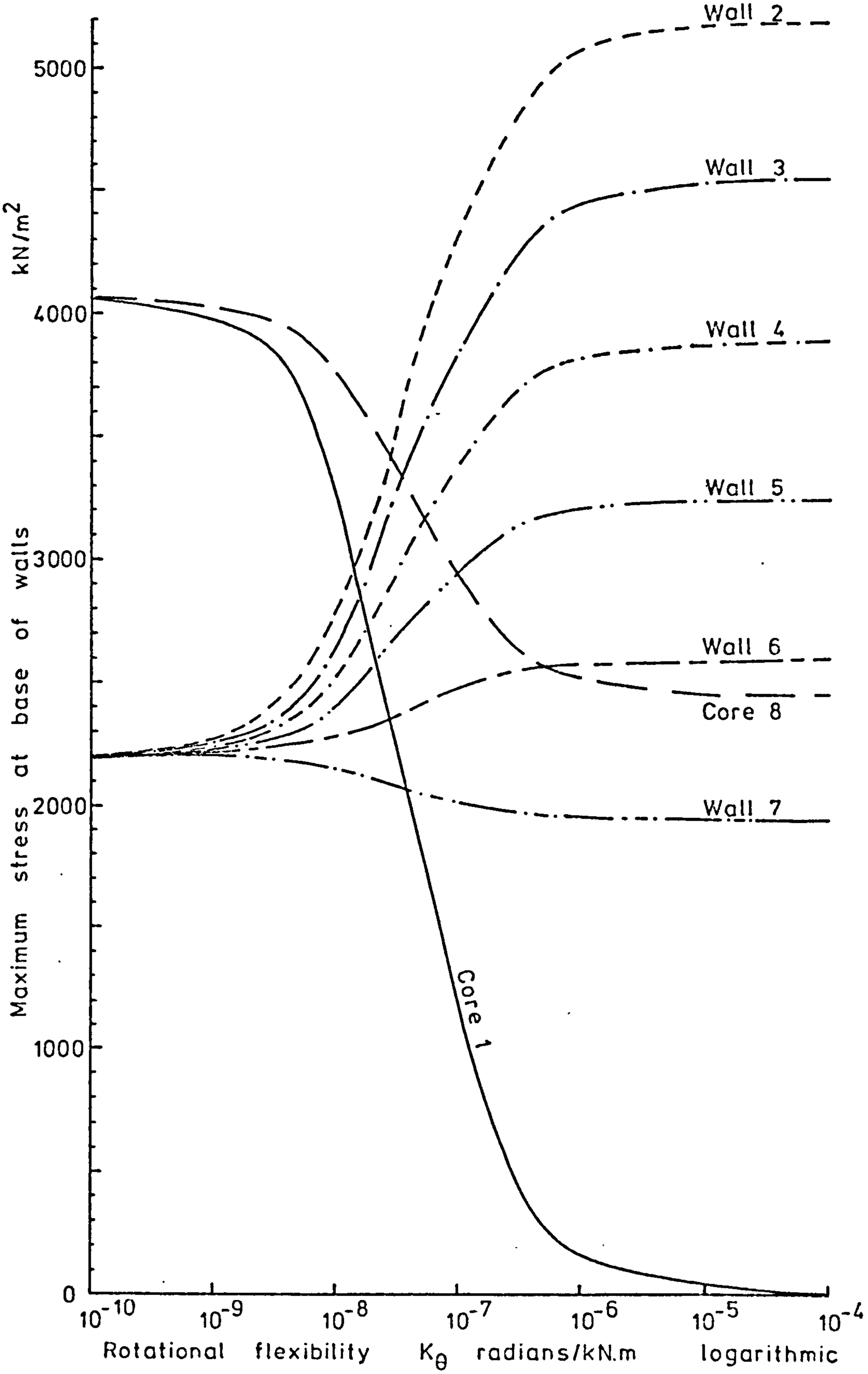

Effect of flexible foundations at end core 1 on on stresses at base of walls.

Figure 6.44

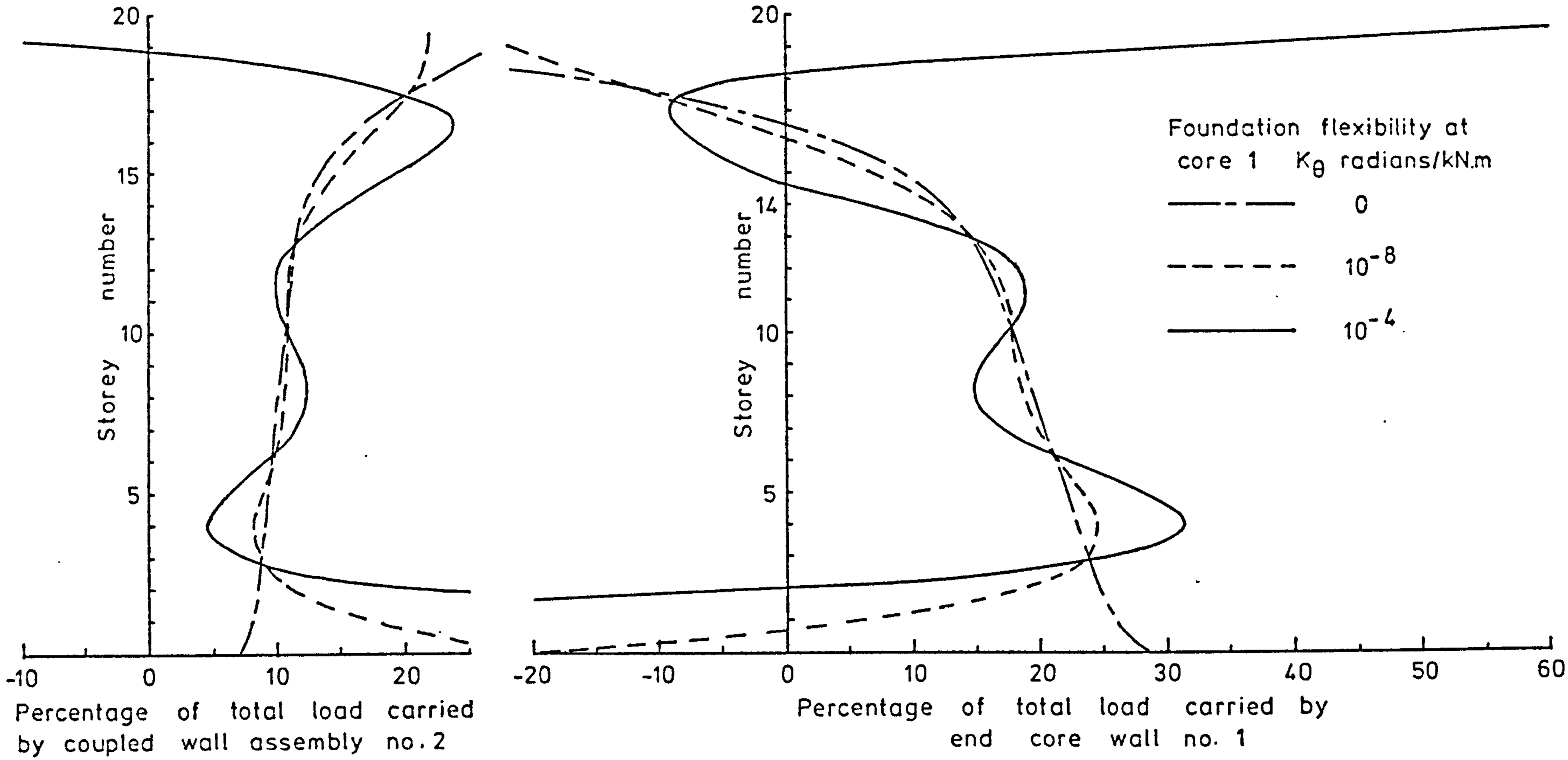

Effect of flexible foundation at end core 1 on load carried by individual wall assemblies. (1)

Figure 6.45

F 6.45

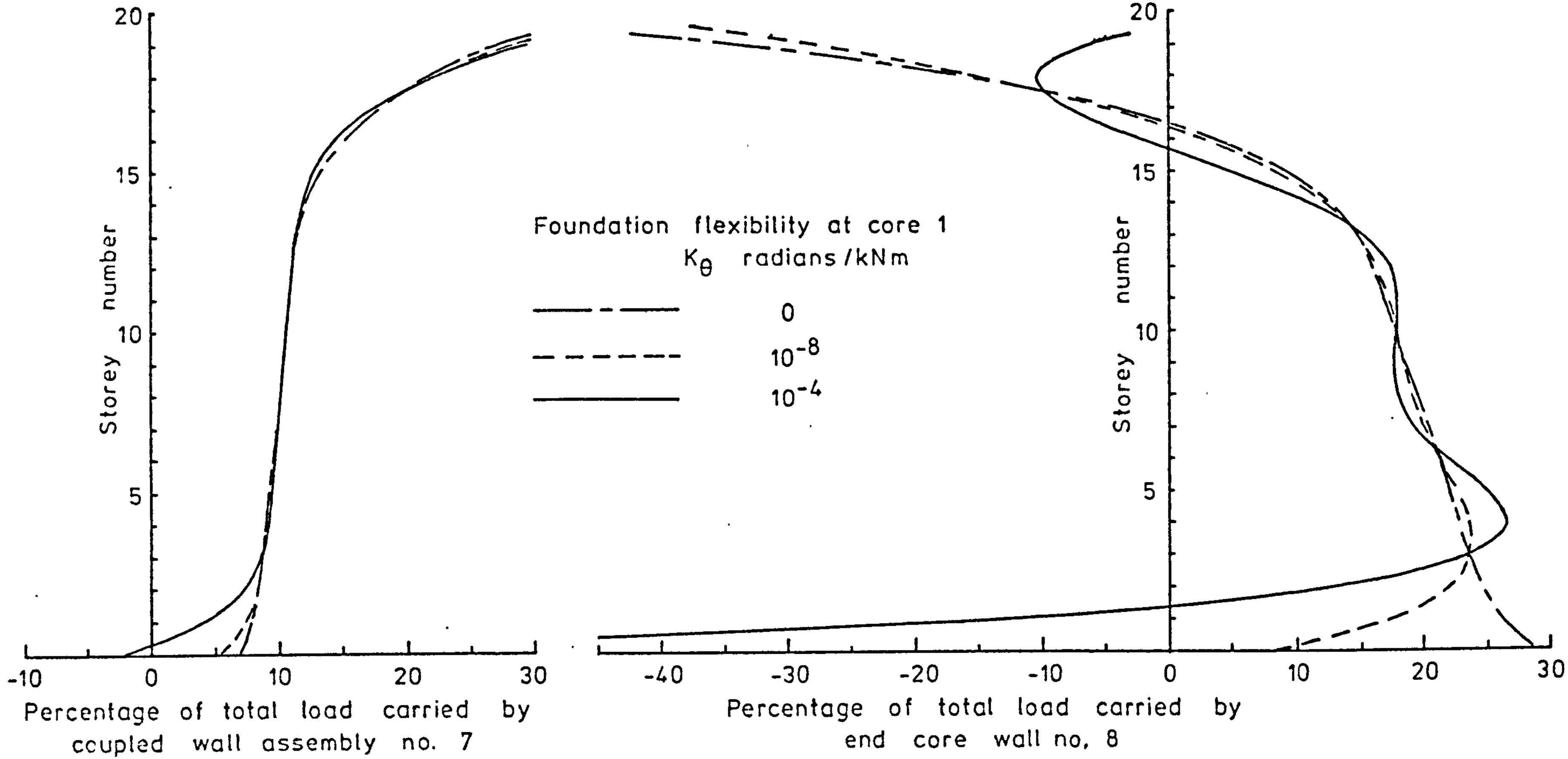

Effect of flexible foundation at end core 1 on load carried by individual wall assemblies. (2)

Figure 6.46

F 6.46

CHAPTER 7

EXPERIMENTAL INVESTIGATION

7.1 INTRODUCTION

The reliability of solutions obtained using either of the methods of analysis was discussed in Chapter 6, section 6.3. It was shown that both methods of distributing the applied lateral load to the shear walls of a multi-storey building gave results which were reasonably consistent for a known range of numbers of reference levels peculiar to each method. These convergence and stability studies gave no indication of the accuracy of the methods as applied to real structures.

The experimental investigation described in the present chapter was undertaken to substantantiate the validity of the assumptions made in the derivation of the methods of analysis of Chapters 2 and 4, in particular where they relate to the effects, on three-dimensional shear wall structures, of the elastic deformation of foundations.

7.2 SCALE OF TESTS

The scope of any program of experimental tests depends on the resources available, both in terms of finance and facilities. Other factors which must be considered include the time available and the uses to which the results will be put. An experimental investigation should be designed to yield sufficient information to enable meaningful conclusions to be drawn as to the behaviour of the subject of the tests in as simple a way as possible by making the best use of the facilities available. There is no merit in designing and testing elaborate systems when a simple test procedure will yield adequate results for the purpose at less expense and with little loss of accuracy.

The costs involved in installing and monitoring equipment within the structure of a building, capable of adequately recording the short term effects of lateral forces on a building are prohibitive. Although there do exist multi-storey buildings which had gauging equipment installed at the time of construction detailed readings from such

buildings are not readily available. Were they available such results would be of limited use due to a number of factors. Lateral forces on buildings, wind or seismic are of a time dependent nature. Difficulties arise in the measurement of such dynamic effects, in their representation as equivalent static forces and in their correlation with the measured strains and deflections of the structure due to time lag in the response of the structure to the transient loading. Due to the complexity of most buildings it is difficult to identify accurately and isolate the extent of the wind resisting systems within them or to evaluate the secondary effects of other systems. There is also a lack of data from such installations which includes information on the effects of short term foundation deformations.

It is of more use in the present study to represent a multi-storey building in the laboratory by its essential wind resisting systems in such a way that there can be as little ambiguity as possible in the measurement of their effects. By the use of static loads many of the difficulties encountered with real wind forces are overcome and greater control may be exercised over the loading on the structure.

Tests on large scale models constructed from similar materials to those used in practice, that is reinforced concrete, would be desirable. However the facilities necessary for such tests are seldom available due to the considerable costs involved.

In studies such as the present one, where a number of tests were invisaged, the only practical and economic solution was to use small-scale models, in this case of an overall height of one metric. However by careful consideration of the design of the models and by taking precautions during tests the results obtained were considered to be of significance.

7.3 MODEL SHEAR WALL STRUCTURES

7.3.1 CHOICE OF MATERIAL

Ideally the models used in an experimental investigation should be constructed from materials which give a good representation, allowing for the effects of scale, of those used in practice. With a

material of the complex nature of reinforced concrete, this scaling down is only possible with relatively large scale models. Concrete was unsuitable for the small scale of the models used in the present study and an adequate substitute had to be chosen.

A major factor affecting the choice of material for an elastic model is the requirement that the deflections and strains induced by a reasonable test load should be of sufficient magnitude to be accurately measured without overstraining the material. High strength materials such as metals, for example steel and aluminium which require both large loads to produce measurable deflections and exceptionally strong test equipment to provide adequate restraint at supports are consequently unsuitable for use in small scale models. Although their properties are far removed from those of concrete, plastic materials manufactured in the form of sheets are often used in the construction of models because of their low elastic stiffness.

Of the available plastic materials "Araldite" and "Perspex" are the most commonly used for shear wall models. Araldite is the more suitable of the two as it is readily machined and exhibits negligible creep under loads which produce stresses in its elastic range. It is however expensive, especially for the construction of complex models which require large amounts of material with considerable wastage. For this reason it was decided to construct the models using the less expensive alternative, Perspex acrylic sheets. The properties of Perspex, which are affected by changes in temperature and humidity, are often anisotropic and vary from sheet to sheet. Perspex sheets may vary in thickness across any sheet; they are difficult to machine; and are subject to creep under load. However, by careful choice of the direction in which sheets are cut to minimise the difference in thickness for any component, by accurate measurement of that thickness, and of the elastic properties of the material, and by taking care during the testing of models, results of reasonable accuracy may be obtained using Perspex.

7.3.2 DESIGN

Previous experimental investigations, for example reference (18), have substantiated the continuous connection technique as a valid method of analysing multi-storey shear wall structures of various

complexities, generally on rigid foundations.

For the present study it was decided to test two twenty-storey models. In order that the effects of varying the foundation flexibilities could be readily identified the models were based on a simple symmetrical layout, each comprising three parallel wall assemblies of small torsional stiffness. Model 1 was designed to exhibit little redistribution of forces within the structure and consisted of three similar pairs of coupled shear walls, while Model 2, which was designed to produce considerable force redistribution between the wall assemblies, consisted of two similar pairs of coupled shear walls symmetrically disposed about a single shear wall of comparable stiffness. Figure 7.1 shows the disposition of the wall units in plan for the two models.

To avoid the difficulties inherent in the evaluation of the width of floor slabs effective as a connection between shear walls, as discussed in section 5.2.1, shear walls in the same assembly were connected by beams rather than by the floor slabs. Figure 7.2 shows the configuration which was used for all coupled wall assemblies in both models. To ensure that the floor slabs had the minimum effect possible in connecting shear walls in the same plane, while retaining their function of maintaining the dimensions of the structure in plan at every storey level, the slab configuration shown in Figure 7.3 was developed. The bending stiffness of the slabs was minimised by the use of thin Perspex, nominally 1/16 inch, and by cutting out the material in the area around the connecting beams. The continuity and general in-plane rigidity of the slabs were ensured by providing a 20 mm. minimum width of material around the perimeter and between the positions of the shear wall assemblies.

To maintain the overall simplicity of the tests on each model, wall assembly numbers 1 and 2, as shown in Figure 7.1, were based on rigid foundations while the flexibility of the foundations of wall assembly number 3 was varied for different tests.

7.3.3 CONSTRUCTION

Two-dimensional components for the models were cut by band saw to their approximate size from Perspex sheets of the required nominal

thickness, 3/16 inch for coupled wall assemblies, 1/8 inch for the single shear wall and 1/16 inch for floor slabs. The sheets were then milled to the correct profile.

Openings in the shear walls were formed with a 5 mm. diameter cutting tool leaving connecting beams of the required depth with 2.5 mm. radius fillets at all internal corners. The fillets help to prevent stress concentrations and the resultant cracks developing at beam-wall connections. All wall components were made with an extra length of material at the base for fixing to their foundations.

The openings in the floor slabs were cut in a similar way to those in the shear walls except that a number of slabs were machined at once, clamped together in a pack to prevent cracking of the thinner Perspex. The slots required to accommodate the shear walls were cut slightly oversize to allow full penetration of cement on assembly.

Tensol No. 7 cement, which has properties similar to those of Perspex once it has cured, was used throughout the assembly of the models.

The rigid foundations required for two wall assemblies of each model were provided by cementing the extra length of each wall into slots cut in 1 inch thick Perspex base plates. The walls were held perpendicular to the base plate and at the correct level while the slots were completely filled with cement and until the cement had hardened.

Starting with the lowest, each floor slab was slid on to the two walls from the top so that the slots for the third wall overhung the edge of the base plate as shown in figure 7.4. Each floor slab was supported from the previous level by spacers which were adjusted to make the slab level and at the correct height, measured from the top of the base, before it was fixed to the two wall assemblies by cementing around the perimeters of the relevant slots.

Once all twenty floor slabs were in place and the cement had hardened the remaining wall assembly was slotted into place and held at the correct level overhanging the Perspex base while it was cemented to each floor slab, which was supported from the previous level so that it was neither bent nor twisted. The longer extensions of the third wall assembly below base level permitted the foundation

mechanism to be firmly fitted during the testing of models incorporating flexible foundations.

Plate 7.1 shows a completed model undergoing a test and plate 7.2 shows the model on the testing frame, with parts of the frame removed to give an unobstructed view of the model.

For the final tests on each model, for which the foundations of all walls were required to be rigid, the base extensions on the third wall assembly were shortened. A 1 inch thick extension piece was cemented to the existing base plate and the shortened bases of the third assembly cemented into slots cut in the extension piece.

7.4 FOUNDATION MECHANISM

7.4.1 DESIGN CONSIDERATIONS

The design of the mechanism for the elastic foundations was developed as a practical simulation of the theoretical conditions used in the analysis. The considerations which influenced the design are summarised as follows:

1. Above base datum level the sectional properties and dimensions of the walls are constant.

2. At base datum level lateral deflection of the shear walls is prevented.

3. Deformations of the foundation, both vertical and rotational are elastic.

4. As a consequence of the assumption that coupled shear walls undergo equal lateral deflections the rotation of their foundations are equal.

5. Each of a pair of coupled shear walls is assumed to rotate about the centroid of its sectional area at base datum level.

6. The vertical deflection of the foundations of a pair of coupled walls is taken as the relative deflection, in a direction perpendicular to the base datum, of the centroids of the two walls at the level of the base datum.

7.4.2 DESCRIPTION

The foundation mechanism is shown in place on the test frame from

three viewpoints in plates 7.3, 7.4 and 7.5. The details of the mechanism are shown in figure 7.5. In figure 7.6 the deformations of the foundations have been greatly exaggerated in order to illustrate the action of the system of levers and restraints for both vertical and rotational movement. In the description which follows the numbers in parenthises are key numbers, all of which appear in figure 7.5. Where applicable the key numbers are repeated on the plates and in figure 7.6.

The direct forces and bending moments at the bases of the coupled shear walls(1) were transmitted by means of four identical components, each of which comprised two steel plates(2) and (3) welded together. They were firmly bolted(4) in pairs to both sides of the extended bases of the shear wall assembly, positioned symmetrically so that the upper edge of each location plate(2) lay along the base datum of the wall assembly. The surface of each location plate which was in contact with the perspex base extension was textured to resist movement between the steel components and the perspex.

At base datum lateral deflection of the shear wall assembly was prevented by a roller bearing(5) supported on the test frame. Due to congestion around the base of the model it was not practical to provide individual lateral restraint to the two walls.

Circular bearings(6), set into the crank plates(3) permitted each shear wall to rotate about its centroid at base datum. The turning effect about this point of rotation caused by the bending moment on the walls at base datum was resisted by a lateral force applied at the lower end of the crank plates, at 80 mm distance from the pivots. This lateral resisting force on each shear wall was transmitted by the shaft(7) and the circular bearing(8) to a common link plate(9). The link plate was held in the plane of the shear walls by ferrule spacers(10) on the shaft(7). The resultant force along the axis of the link plate was transmitted to the steel cantilever bar(11) by two steel ball bearings(12). These were held in position between the link plate and the cantilever bar by a groove cut in each, by virtue of which there was no resistance to "vertical" movement, that is movement perpendicular to the base, between the two components. The axial force in the link plate was resisted by the bending action of the cantilever bar, which deformed in proportion to

the force and therefore to the bending moment in the base of the shear walls. The flexibility of the foundation to rotational deformations therefore depended on the dimensions and properties of the cantilevers.

The axial force in the base of each shear wall was transmitted by the location plates(2), the crank plates(3) and the circular bearings(6) to the half shafts(13) which were each fitted by locknuts to an upper end of one of the vertical link forks(14) and (15). The axial forces in the forks were transmitted by ball bearings(16) to the ends of the cantilever bars(17) and (18) respectively. The ball bearings were held in position between the base of the link fork and the end of the cantilever bar by a small circular depression set symmetrically in each. The axial force at the base of each shear wall was therefore resisted by the bending action of the relevant cantilever bar, which in turn deformed in proportion to the force.

By changing the configurations of the three cantilevers(11), (17) and (18), it was possible to alter the rotational flexibility and the vertical flexibility of the shear wall assembly independently.

7.4.3 CONSTRUCTION

The components of the foundation mechanism were manufactured from pieces of mild steel cut from standard 1/4 inch thick bars (1" x 1/4", 1-1/4" x 1/4" and 2" x 1/4"). The inner face of each location plate(2) was ground flat before being centre-punched to provide the plane textured surface with which to grip the perspex shear walls. The location plates were welded to their respective crank plates before the holes in the latter were drilled, in case any distortion of the bars occurred due to the heat of welding. The holes in the crank plates were accurately set out and drilled on a milling machine to ensure that the lever arm for the rotational restraint force was precisely the required 80 mm. The holes to take the bearings(6) and (8) in the crank plates(3) and in the link plate(9) respectively were drilled accurately to provide a press tight fit to the outer race. The shafts(7) and (13) were turned on a lathe to provide a similar fit to the inner race of the bearings. The vertical link forks(14) and (15) were each formed by welding two steel bars to the ends of a short piece of 2" x 1" rectangular hollow section.

The complete mechanism was assembled, using two separate pieces of scrap Perspex in place of the base extensions of the shear walls in the models, to ensure that all the bearings turned freely.

The three cantilever bars(11), (17) and (18) forming the elastic restraints were made from 1" x 1/4" thick mild steel bar. The profile of each bar was made perfectly rectangular and identical to the others by grinding all three symultaneously by machine. A datum line was lightly scribed close to one end of each bar and similar lines were set out and scribed at intervals along the bar by a vernier gauge. The groove in the bar(11) and the circular depression in the bars(17) and (18) were centred on the datum line at the end of each.

The cantilever action of the vertical restraints was achieved by placing one end of the bar between two ground plates and bolting the outer plate to a 1/2 inch thick steel backing plate thereby holding the bar firmly with its free end forming the cantilever. The flexibility of the cantilever was adjusted by altering the free length of the bar, as measured from the scribed datum line to the leading edge of the clamping plates.

The cantilever bar forming the rotational restraint was similarly clamped between the ground flanges of two pieces of steel angle section , the other flanges being bolted to a 1/2 inch steel backing plate. The backing plates were each provided with a number of holes to allow adjustment of the positions of the cantilevers and for mounting the plates on the test frame.

7.5 TEST FRAME

The frame on which the models were mounted during the tests is shown in plate 7.1. Although constructed for the present test program it was designed as a modular system which could be easily adapted for other purposes and could be dismantled to save storage space.

The modular system consisted of a pair of vertical mounting units which could be set parallel at any desired distance apart and connected by horizontal and inclined bracing to form a stiff self supporting box frame. Since the model was mounted within the box, the system was very stable and the model was protected from accidental

damage by the frame. By the use of additional mounting units and bracing a series of such boxes could be built up for testing models back to back, etc.

Mounting units consisted of two 1/2 inch thick by 6 inch wide steel plates, provided with a regular array of holes for use in fixing models and other equipment to the frame. The plates were set near the upper ends of their supporting legs to provide adequate clearance below models to hang weights and at different distances apart on the various units to enable models with a wide range of base size to be used. The ends of each plate were welded to the vertical legs which consisted of 3" x 1-1/2" steel channels welded to 6" square base plates. The bracing consisted of cut lengths of 2" x 1" rectangular hollow section with welded end plates which were tapped for bolting to the vertical channels.

The configuration in which the frame was used in the present study, as shown in plate 7.1, comprised two mounting units braced together a short distance apart to which the model and the backing plates of the foundation mechanism could be attached and a third unit placed one metre distant and braced to the other two to form the box and give the frame its stability.

The frame was itself tested prior to mounting the model by loading up a jib arrangement fixed to the mounting unit to be used in the tests, in order to investigate the effects which the loaded model would have on the frame. No general movement of the frame could be detected, but there was a slight local deflection of the two plates to which the model would be bolted, just detectable on a dial gauge reading to 0.002 mm.

To strengthen these plates similar 1/2 inch plates were placed vertically across them before the base of the model was positioned. The model was orientated using a plumb line so that the planes of its walls were exactly vertical and the base extensions for fixing to the foundation mechanism projected through between the plates of the mounting unit. The Perspex base was further strengthened by placing pieces of hollow section vertically between the walls and horizontally above and below the model in the form of a grillage. The hollow sections, the base of the model and the steel plates were firmly attached to the mounting unit by 1/2 inch diameter screwed rods to

form an inflexible foundation for the walls of the models assumed to be built in at the base.

The foundation mechanism was assembled on to the base extensions and lay within the space between the two mounting units at the base of the model. The backing plates for the cantilever restraints were bolted in place and the three cantilever bars were clamped to them. Care was taken that the datum lines on the bars were correctly lined up with the foundation mechanism and the precise unsupported length of each cantilever bar required for the particular test was obtained by lining up the relevant scribed mark on the bar with the edge of the clamp plates. Finally the ball bearings were inserted between the ends of the cantilever bars and their corresponding positions on the foundation mechanism. By using oversized bearings, any play in the mechanism and the initial rotation and deflection of the base of the third wall assembly were removed to ensure that all three wall assemblies were level before each test.

7.6 MEASUREMENT OF STRAIN AND DEFLECTION

7.6.1 STRAIN

The strains induced in the model by the applied loads were measured by electrical resistance strain gauges. The gauges were placed 5 mm from, and parallel to the edge of each wall of the model at a height of 175 mm above the base. This position was selected close to the base to give measurable strains but far enough above the base to be outwith any local effects caused by the base-to-wall connection. The position of the gauges was also midway between floors, the third and fourth, in order to minimise distortions caused locally by wall-beam interaction. Gauges were generally placed on one side of a wall assembly, but at one position on each wall an extra gauge was placed on the opposite side to provide a check that bending occurred in the plane of the wall.

The strain gauges, Japanese type PL.10, and the terminal strips for the wire leads were glued to the Perspex by Eastman 710 adhesive and varnished over for insulation and protection. The resistance of each gauge was measured prior to use to ensure that the leads were correctly connected and there was no fault in the gauge.

Each strain gauge was wired to the indicator equipment with an identical gauge, provided by the model not under test, to compensate both for temperature changes in the laboratory during tests and for local heating of the Perspex caused by the current passing through the gauge during the actual measurement of strain.

Baldwin-Lima-Hamilton BLH 1200 series strain indicator equipment was used to measure the change of resistance of the gauges and hence the strain of the Perspex during the tests. Each gauge and its compensator were wired to one channel of a ten-gang switching unit, each channel of which was provided with a control whereby the initial value of strain could be set to zero. The switching units were in turn connected to the indicator unit which measured the resistance of the channel selected by the switching unit and provided an instant digital display directly in units of microstrains. The power required for the indicator equipment was supplied from the mains to the indicator unit which converted the 240 volt A.C. source to a low voltage controlled direct current suitable for the strain gauges.

7.6.2 DEFLECTION

Deflections were measured by "John Bull" dial gauges, manufactured by British Indicators Ltd. The deflections of the model under test were measured by gauges supported on a light "Dexion" framework bolted to the test frame. The gauges were positioned directly above the walls, midway between floor slabs at five positions on each wall assembly. At the lower three positions, half a storey above the third, seventh and eleventh floors, the gauges used were type 2U which incorporated jewelled pivots and were sensitive to 0.002mm per division of the dial, with a maximum travel of 12.7mm. The gauges at the upper positions, above the fifteenth and nineteenth floors, were type 2S with a longer range, 25.4 mm, and a sensitivity of 0.01 mm per division.

The deflections of the foundation restraint cantilevers were measured by gauges type 2U held in position by magnetic stands clamped to their respective backing plates. Gauges type 2U were also used to detect any deformation of the Perspex base plate at the positions of the built in walls. In this case the gauges were supported by magnetic stands positioned close to each other on the

outer mounting unit of the test frame in order to include any local rotation of the plates of the unit on which the model was mounted.

7.7 DETERMINATION OF ELASTIC PROPERTIES OF PERSPEX

In order to evaluate the stresses induced in the models from the strain gauge readings, and to compare the experimental results with those calculated using the theoretical analyses, the elastic constants, namely Young's Modulus, E, and Poisson's Ratio, ν , were evaluated for the two thicknesses of Perspex, nominally 3/16 inch and 1/8 inch, used to construct the shear walls of the models.

Two rectangular specimens, nominally 1.5 inches by 10 inches, of each thickness were cut from the same sheets of perspex as were the walls. Their long edges were milled parallel and two electrical resistance strain gauges, as used on the models, were fixed near the mid point of each specimen. On one speciman of each size of Perspex the gauges were both positioned longitudinally on opposite faces, while on the other specimens the gauges were placed, one longitudinally and one transversely, on the same face. The precise width and thickness of the specimens in the region around the gauges were measured by means of a vernier and a micrometer respectively.

The specimens were each tested in bending, between level supports, 240 mm apart, equal loading being applied at the third points of the span to produce constant bending, with no shear, in the region of the strain gauges. During tests on one specimen the gauges on the other specimen of the same thickness were used as dummy temperature compensators.

Specimens were loaded and unloaded progressively by small increments, the maximum loading in any test being that which produced a strain similar to those encountered in tests on the models. The best linear strains were evaluated for the loading and the unloading processes by the procedure outlined in section 7.10. Each specimen was tested four times, twice on each face, the specimen being turned end for end between successive tests in an attempt to avoid errors due to misalignment of the specimen, the supports or the strain gauges.

The stress at the position of the longitudinal gauges was found

by statics using the accurate dimensions of each specimen. The average of the strain results for each specimen was evaluated and the Young's Modulus for each thickness of Perspex found. Poisson's Ratio was evaluated by dividing the strain of the lateral gauge by the corresponding strain of the longitudinal gauge and an average found for each thickness of Perspex.

The average values of Young's Modulus and Poisson's ratio, which were used in the computer analysis of the model structures and for the evaluation of stresses in the tests are given in Table 7.1.

7.8 CALIBRATION OF FOUNDATION CANTILEVERS

In order to relate the deflections measured at the foundation mechanism to the forces and bending moments on the base of the shear walls, the flexibility of the steel cantilever bars were determined for each of the settings, i.e. free length, at which the models were tested.

Each cantilever bar was tested with the same clamping arrangement as would be used in the tests. The rotational cantilever was placed, with the groove for the ball bearings upwards, between the two angle pieces and clamped in position on the tests frame. The backing plate for the vertical restraint cantilevers was removed from the frame and bolted horizontally to a firm support. The relevant cantilevers were clamped in their positions on the plate with the circular recess in each facing upwards.

The bars were each tested, bending in the same direction as would occur during the model tests, by suspending weights on a hanger centred on the datum line of each. The bars were loaded and unloaded progressively by one kilogramme increments. The maximum load depended on the length at which the bar was set. The deflection caused by a 10 Kg weight was found by the method outlined in section 7.10 for the loading and unloading processes. Each specimen was tested five times at each setting and an average deflection for each bar at each setting was evaluated.

The flexibility of each bar at each setting was found as the deflection in millimetres caused by a force of one Newton applied at the datum line. The rotational flexibility coefficient, K_θ, for the

shear wall assembly follows directly by considering the geometry of the foundation mechanism as shown in figure 7.5 and is given on dividing the flexibility of the rotational restraint cantilever by the square of the effective lever arm (80 mm) of the crank plates. The vertical flexibility coefficient, K_v, being the relative deflection between the bases of the two walls caused by an equal axial force of one Newton in the two walls is given as the sum of the individual flexibilities of the two vertical cantilevers at the setting considered. The values of K_θ and K_v for the lengths used in the model tests are shown in table 7.2.

7.9 TEST PROCEDURE

The model was bolted to the test frame, the foundation mechanism assembled and the cantilever bars set at the lengths required for the particular tests, as described in section 7.5. Uniform loads were simulated by applying a point load at each storey in the form of 100 gramme and 200 gramme weights on light alloy hangers suspended by "Terylene" cord from the floor slabs. The cord was accurately positioned relative to the shear walls and held by adhesive tape to prevent accidentally changing its position when weights were placed on the hangers.

Prior to each test the model was loaded and unloaded to ensure that all the components, particularly the foundation mechanism had fully settled after being mounted or reset.

With no weight on the hangers the reading for each strain gauge was set approximately to zero and noted and the dial gauges read. The load was applied in increments of 0.2 Kg per storey to a maximum equivalent to 1 Kg per storey. A standard time, 10 minutes, was allowed after the addition of each load increment before the readings were taken to permit the gauges to settle to reasonably stable values. A set order of reading the gauges was adopted throughout the test program.

In an attempt to eliminate errors due to creep in the Perspex the model was unloaded by increments and a separate set of readings taken. The mean of the results obtained from the loading and unloading procedures was used in the comparison of the experimental

and the analytical results.

7.10 EVALUATION OF TEST RESULTS

In all the loading tests on the models, the perspex specimens and the cantilever bars, the results were evaluated by the same method. The readings taken from any gauge during a test were plotted to scale against the load increments and the best straight line was drawn by eye, ignoring any obvious misread points and the typical non-linear portion at the beginning of each plot. The value of strain or deflection for the total applied load was evaluated from the slope of the line.

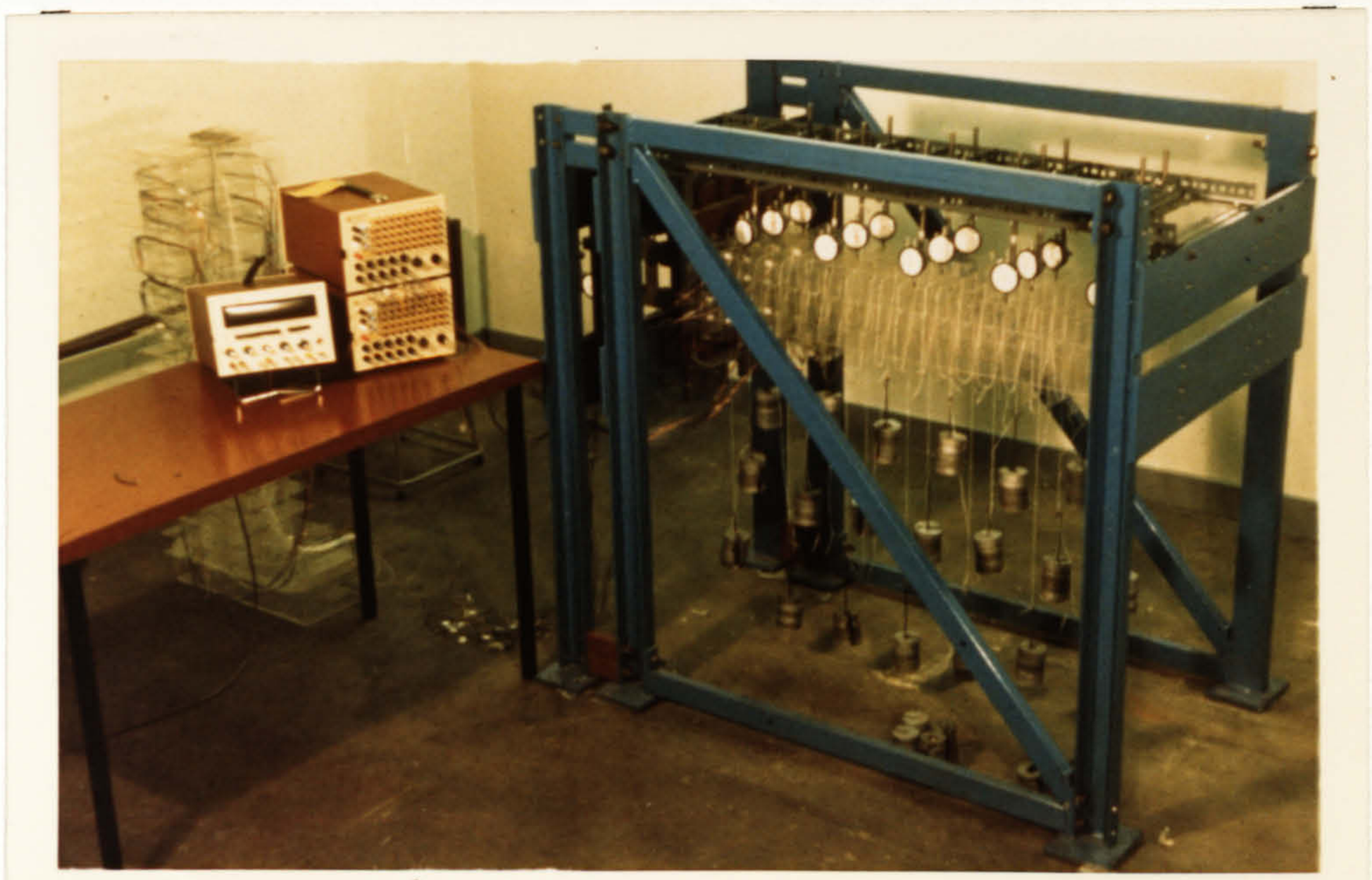

Shear wall model undergoing test.

Plate 7.1

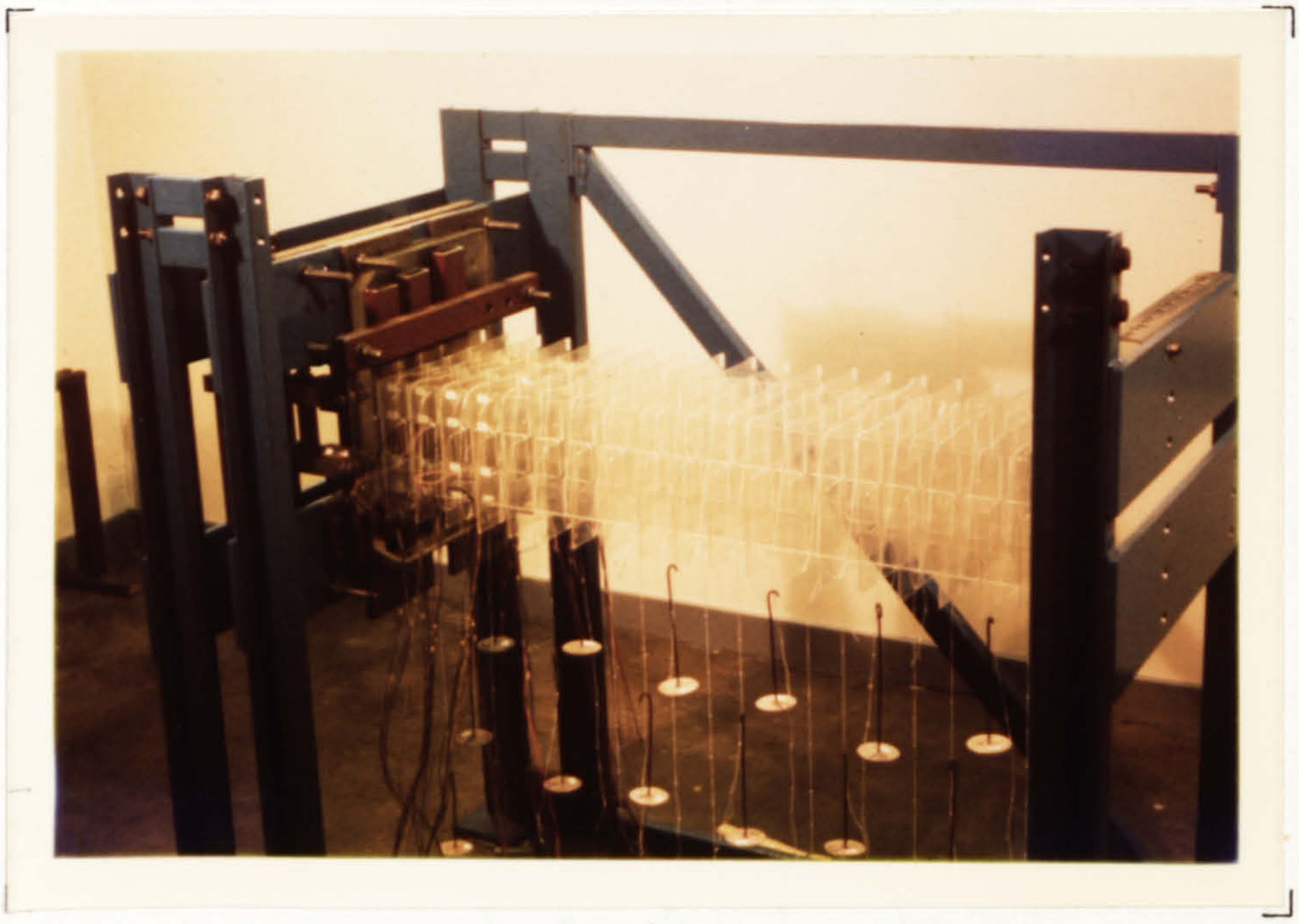

Shear wall model mounted on test frame.

(Bracing of frame removed to give unobstructed view of model)

Plate 7.2

BEST COPY

AVAILABLE

Variable print quality

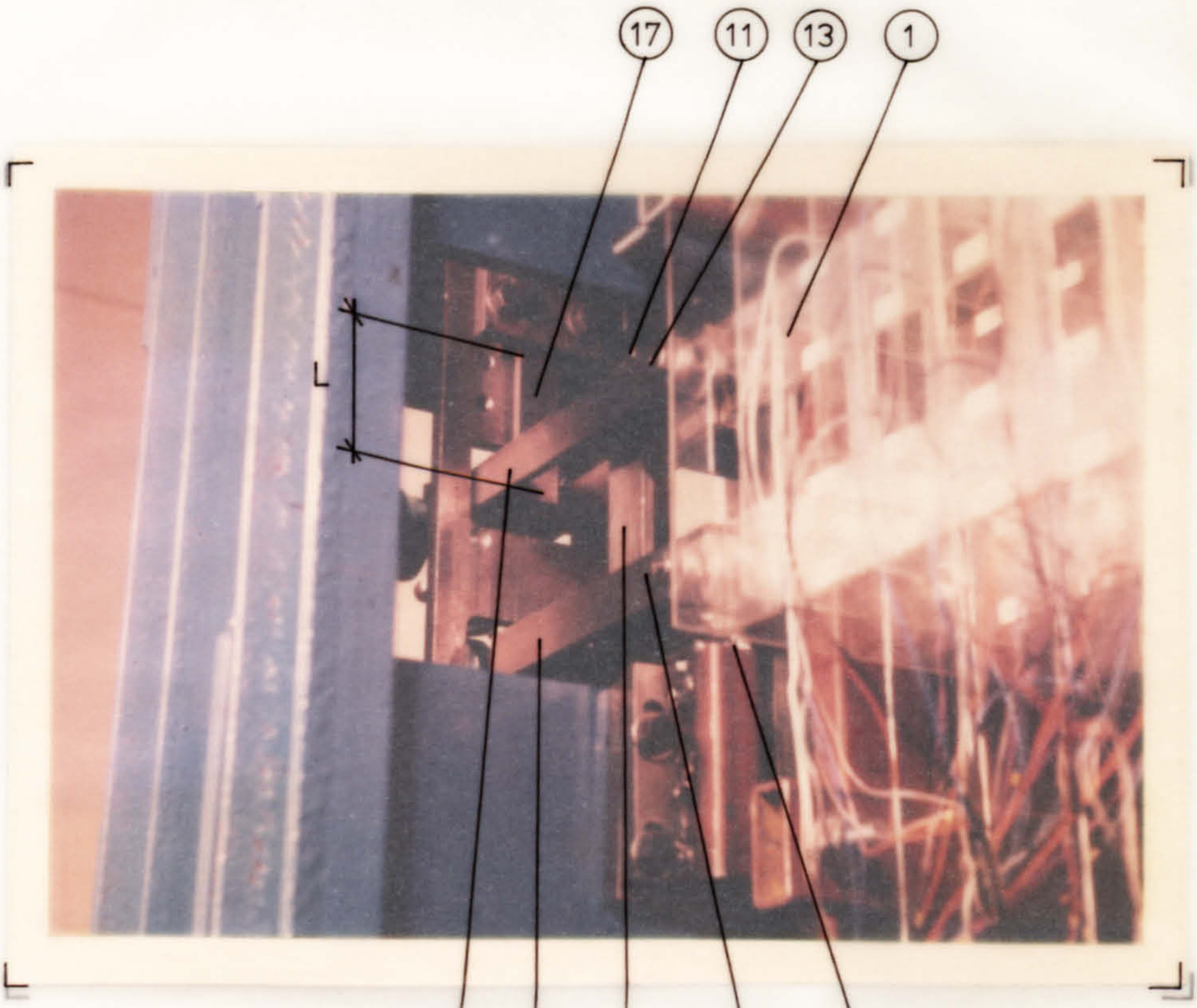

Foundation mechanism viewed from the front of the test frame

Plate 7.3

BEST COPY

AVAILABLE

Variable print quality

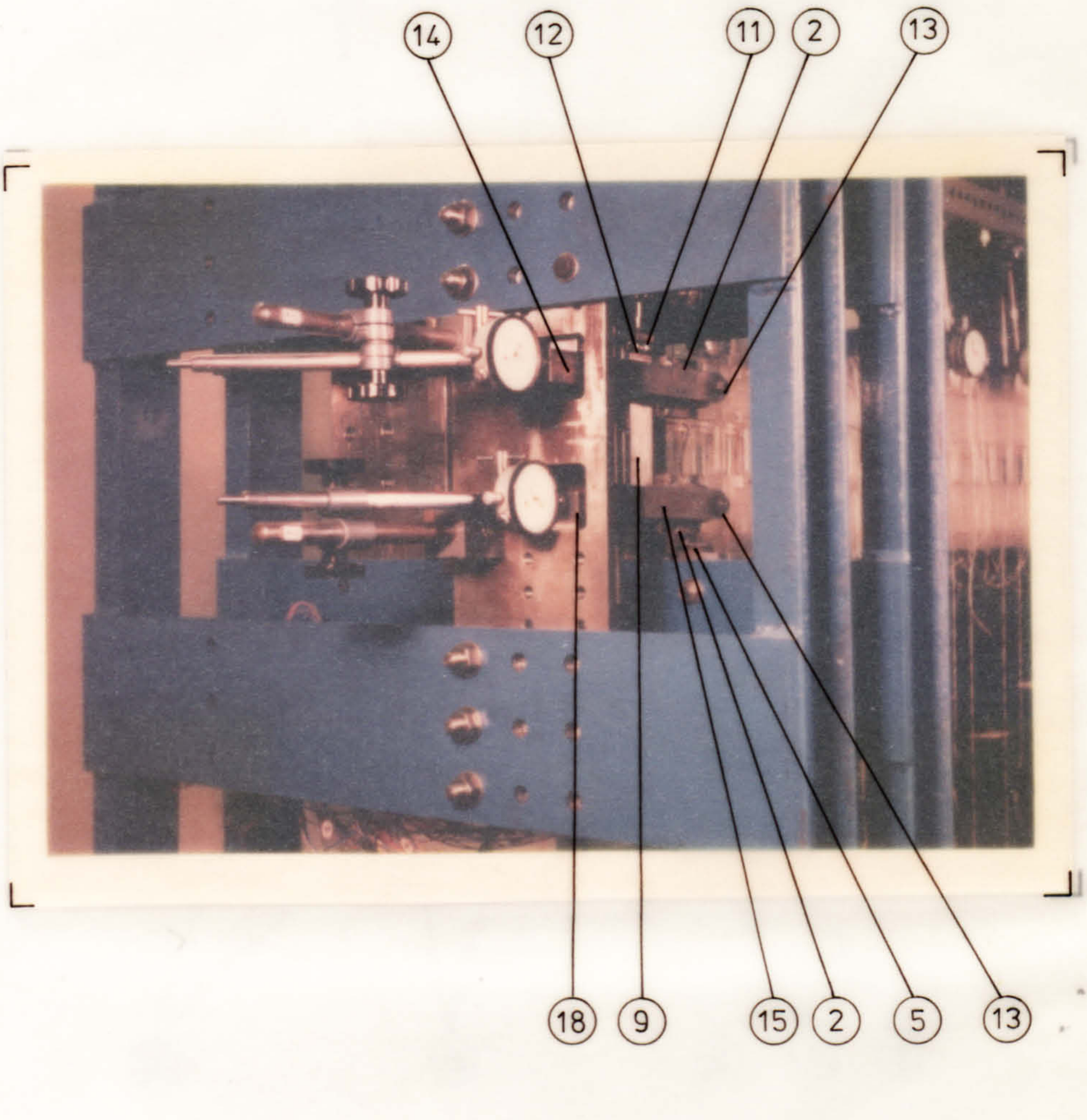

Foundation mechanism viewed from behind the test frame.

Plate 7.4

BEST COPY

AVAILABLE

Variable print quality

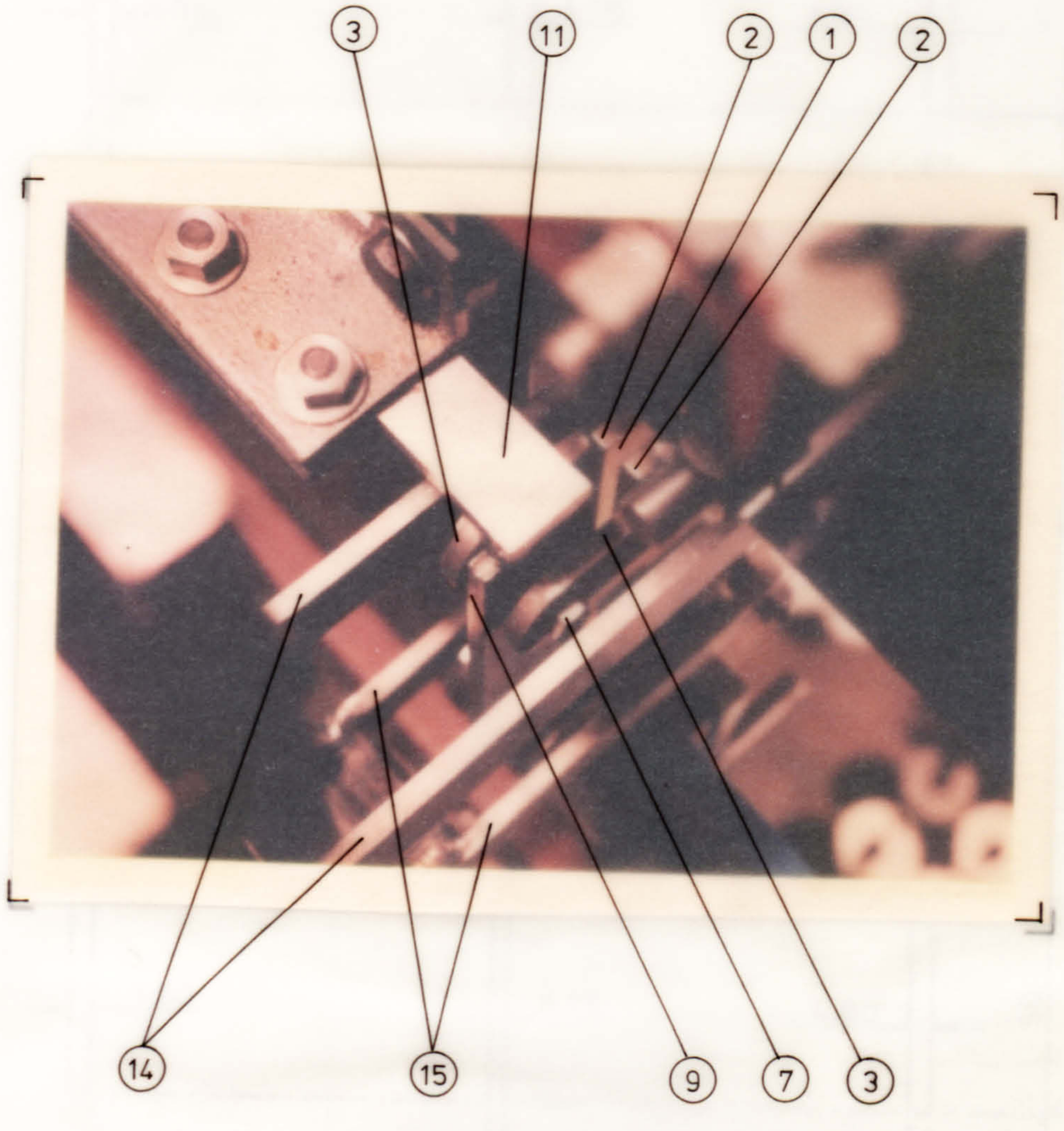

Foundation mechanism viewed from above the test frame.

Plate 7.5

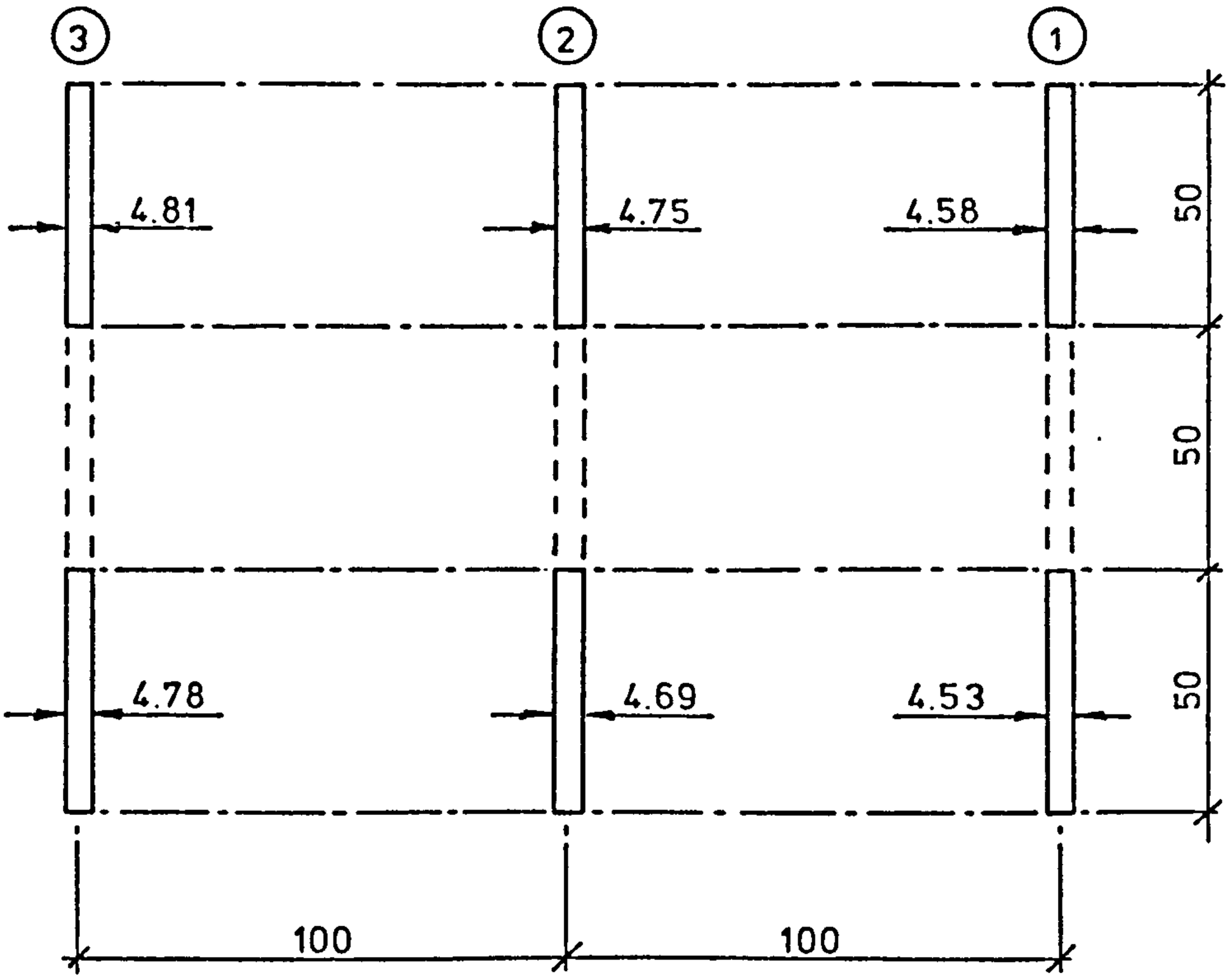

Model 1

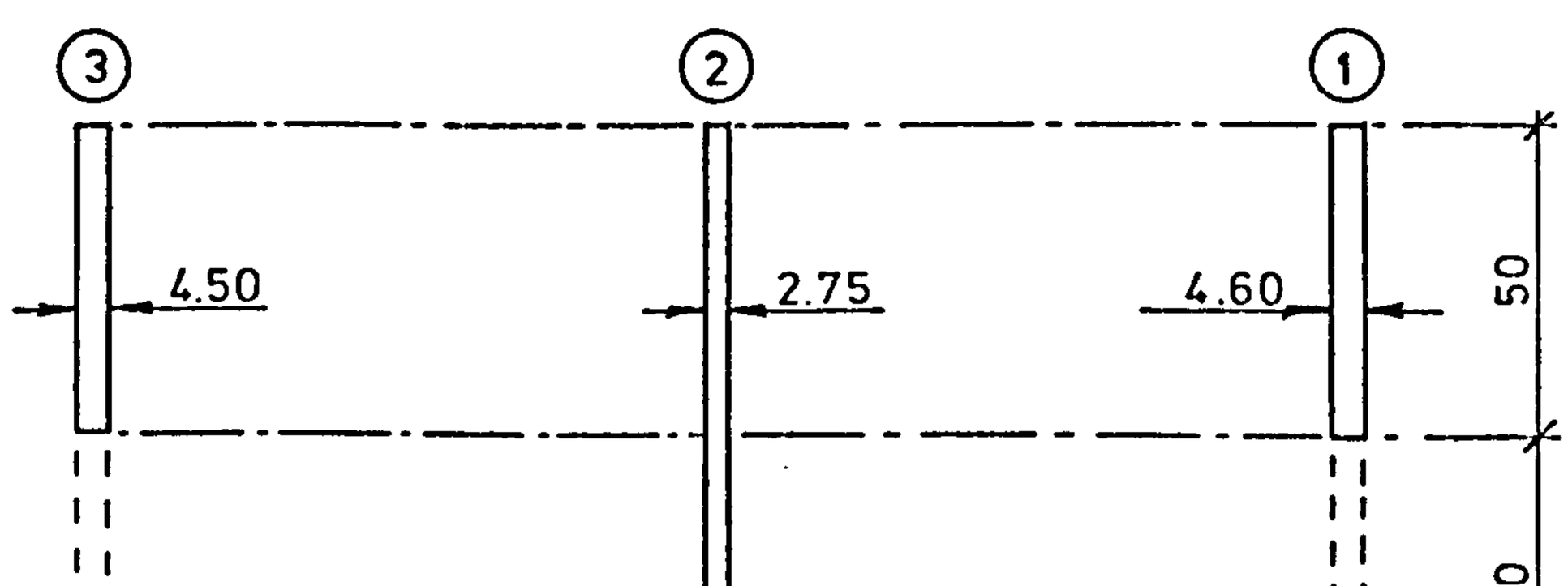

Model 2

Layout of shear walls in models.

Figure 7.1

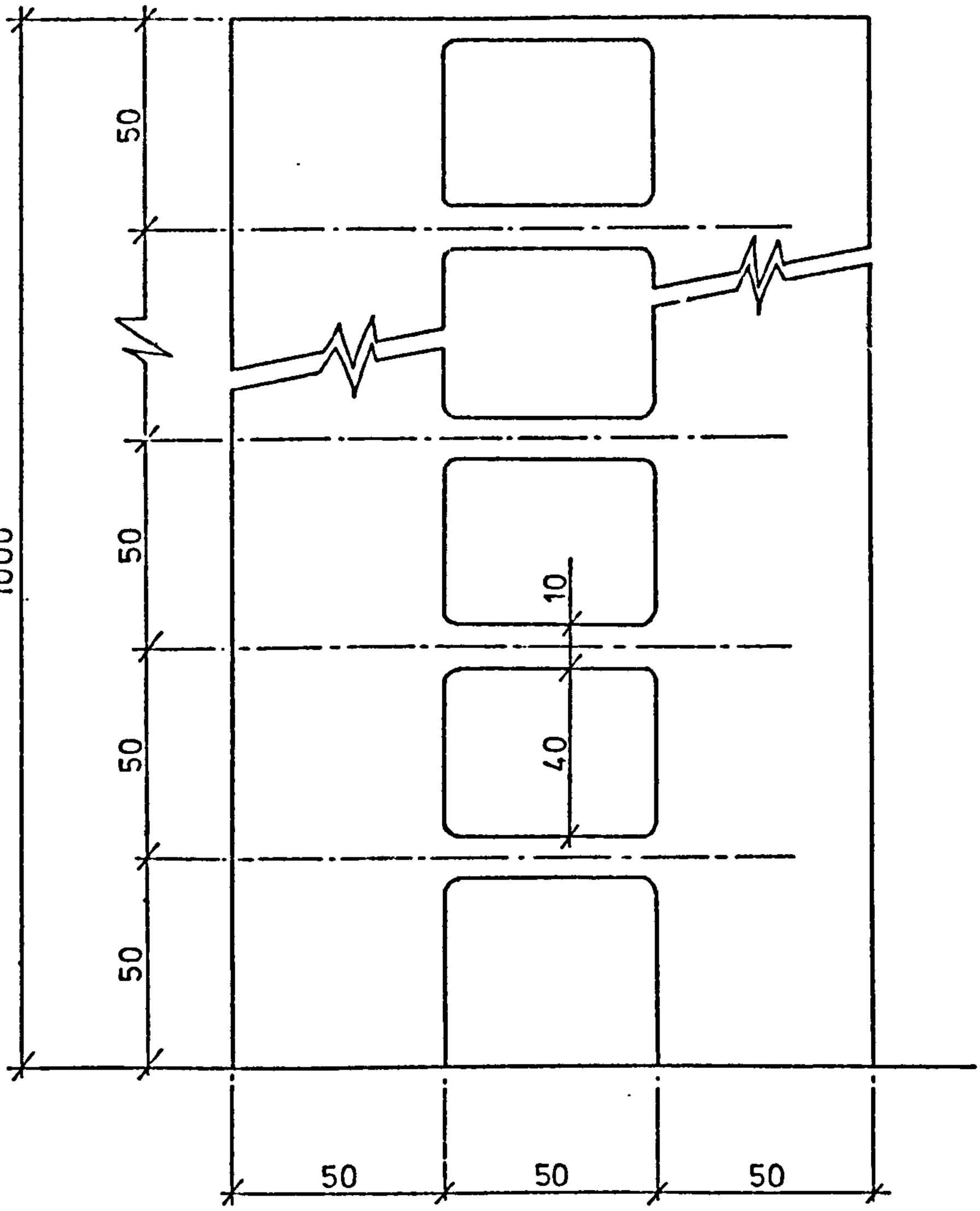

Pair of coupled shear walls as used in models

Figure 7.2

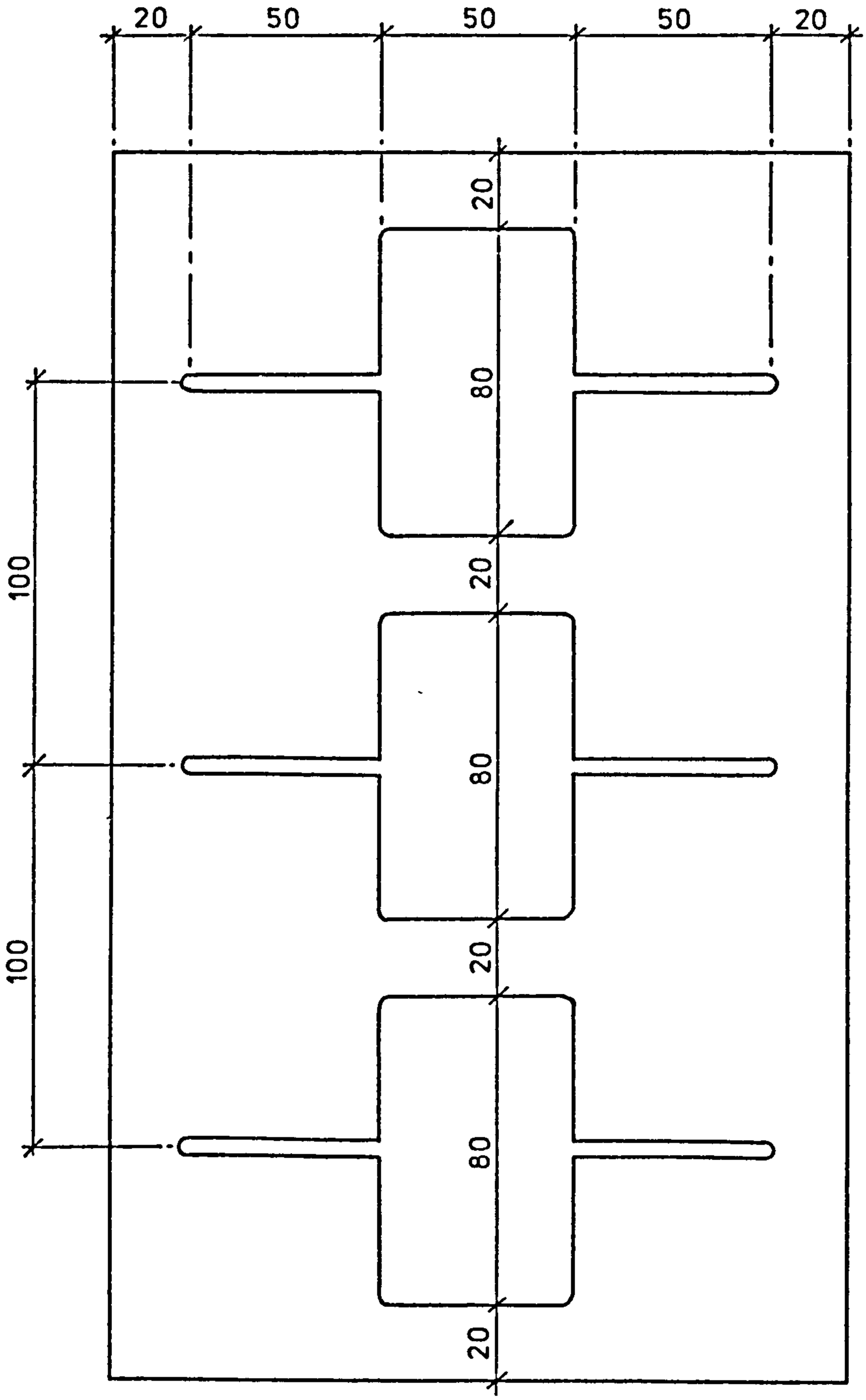

Floor slab

Figure 7.3

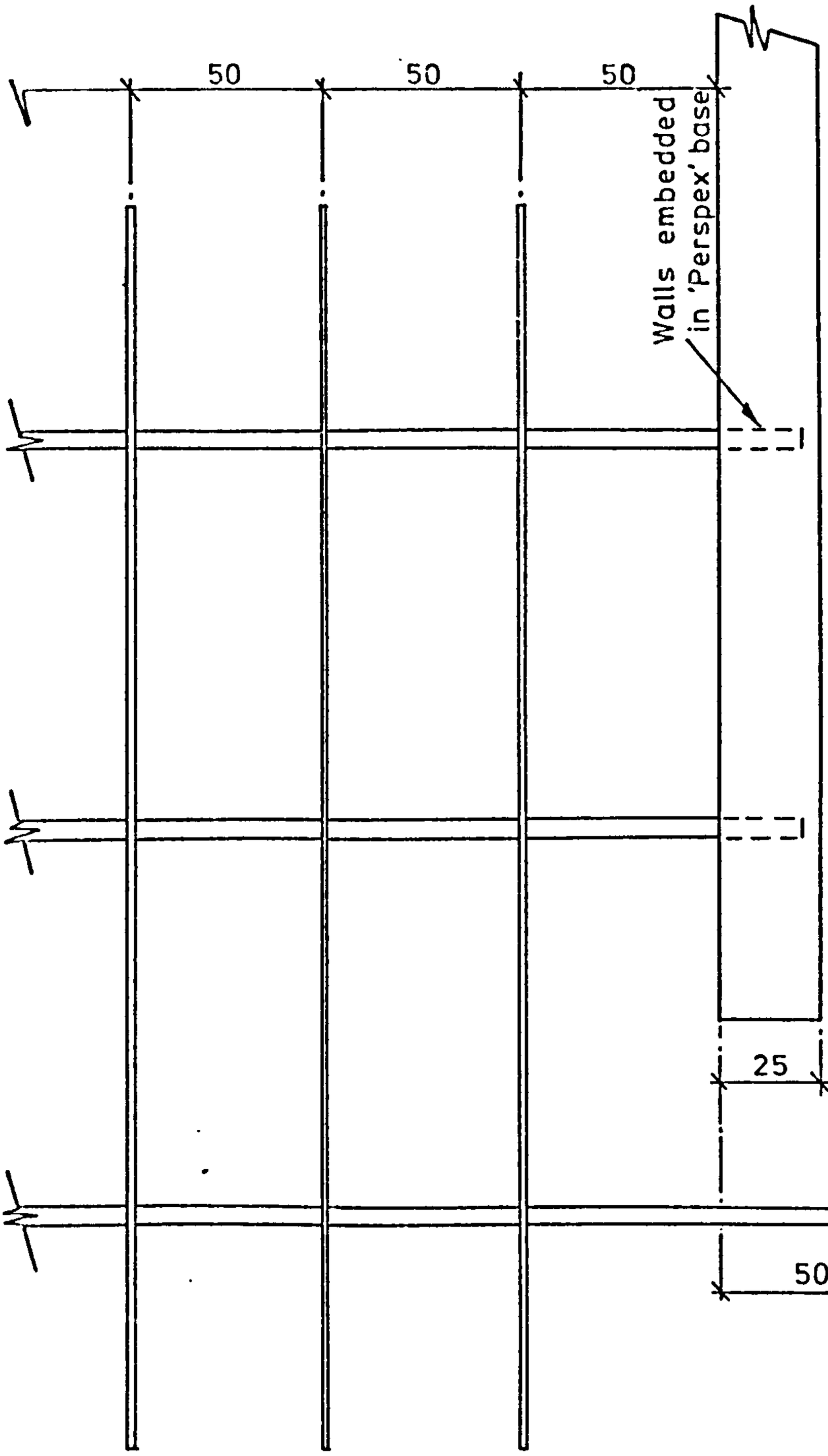

Arrangement of walls at base

Figure 7.4

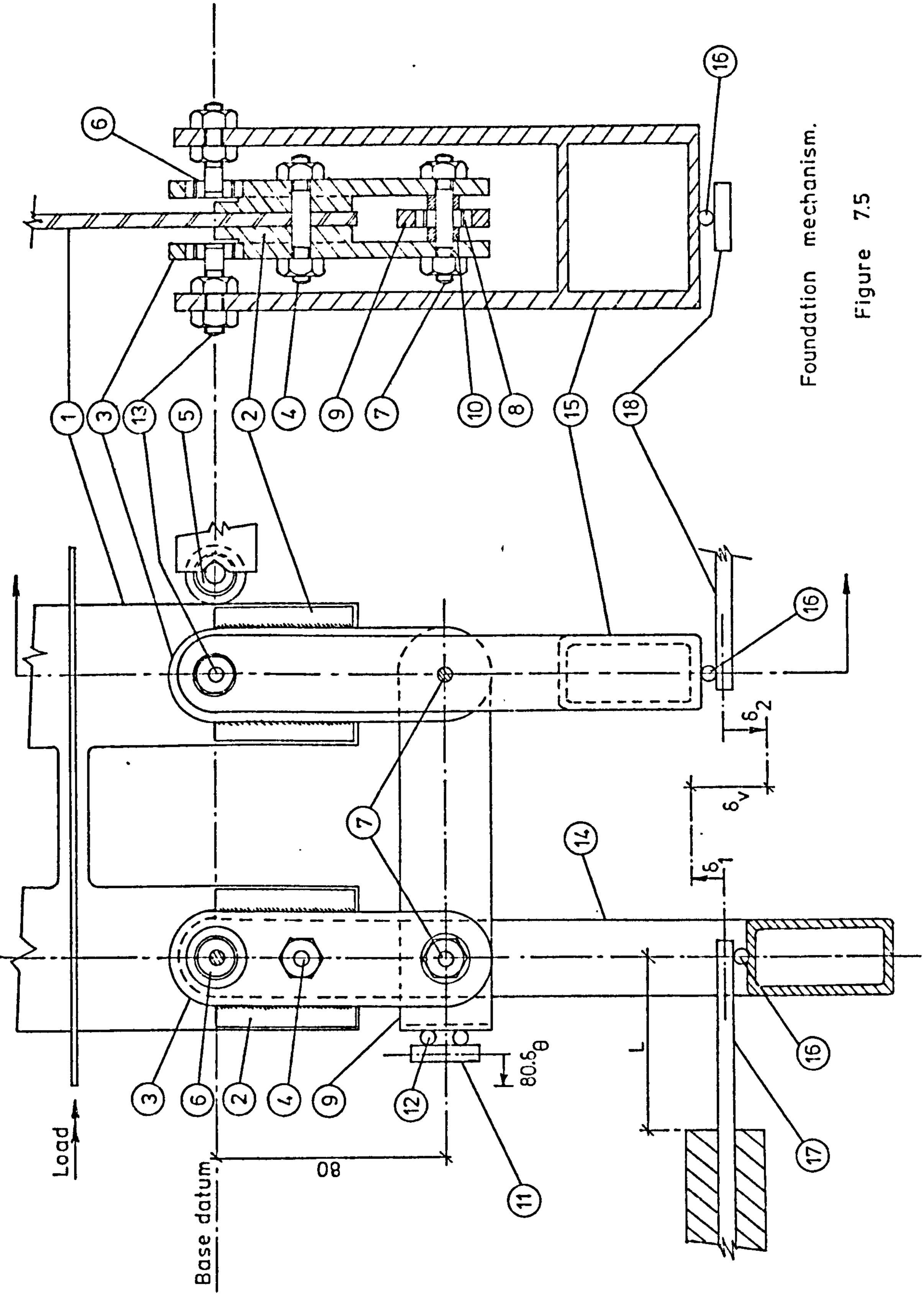
Foundation mechanism.
Figure 7.5
Load
Base datum
08
L
80.5_B
6_2
6_V
6_1
1
3
13
5
2
4
9
7
10
8
15
18
16
6
12
11
14
17

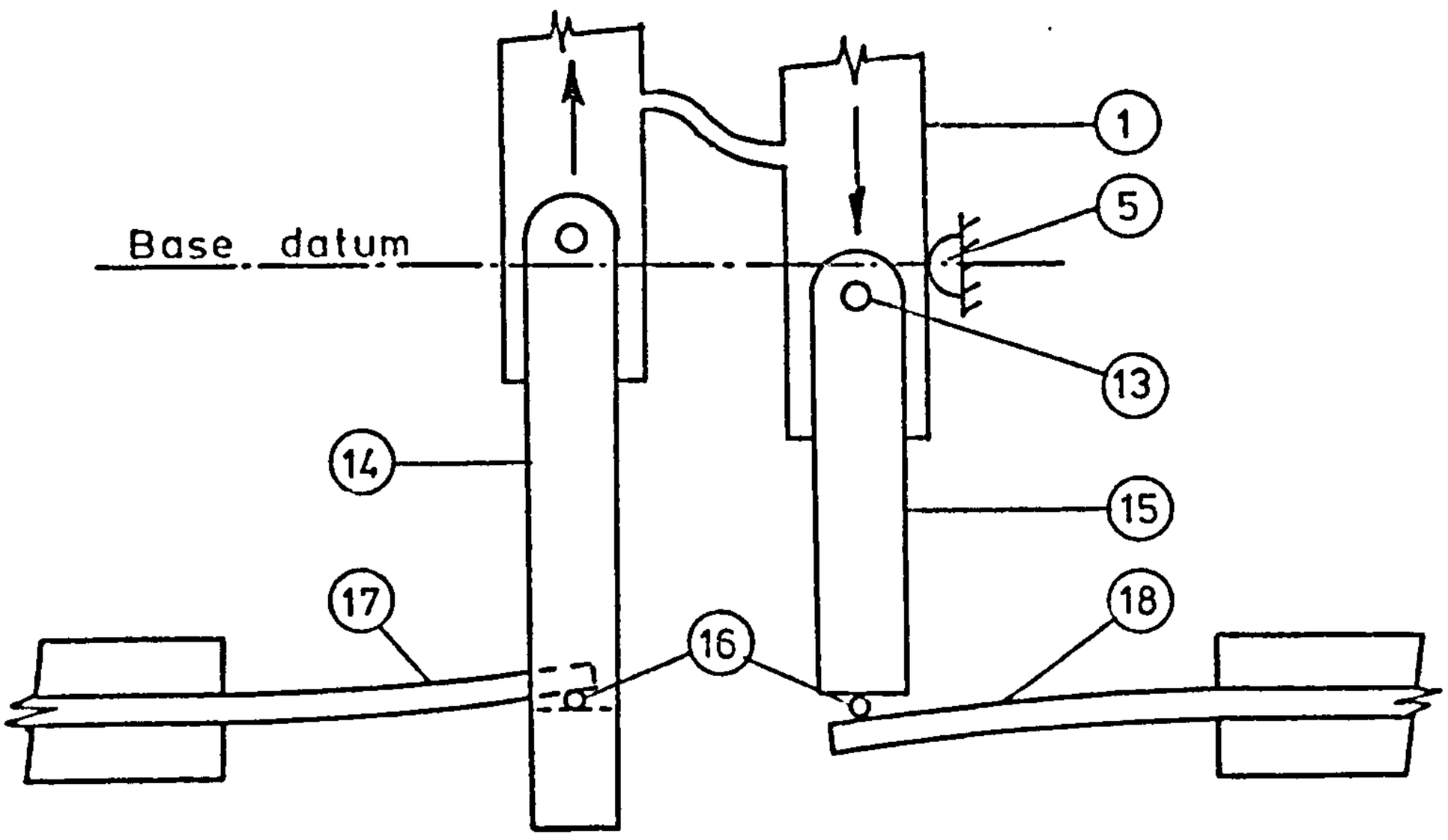

(a) Vertical foundation movement

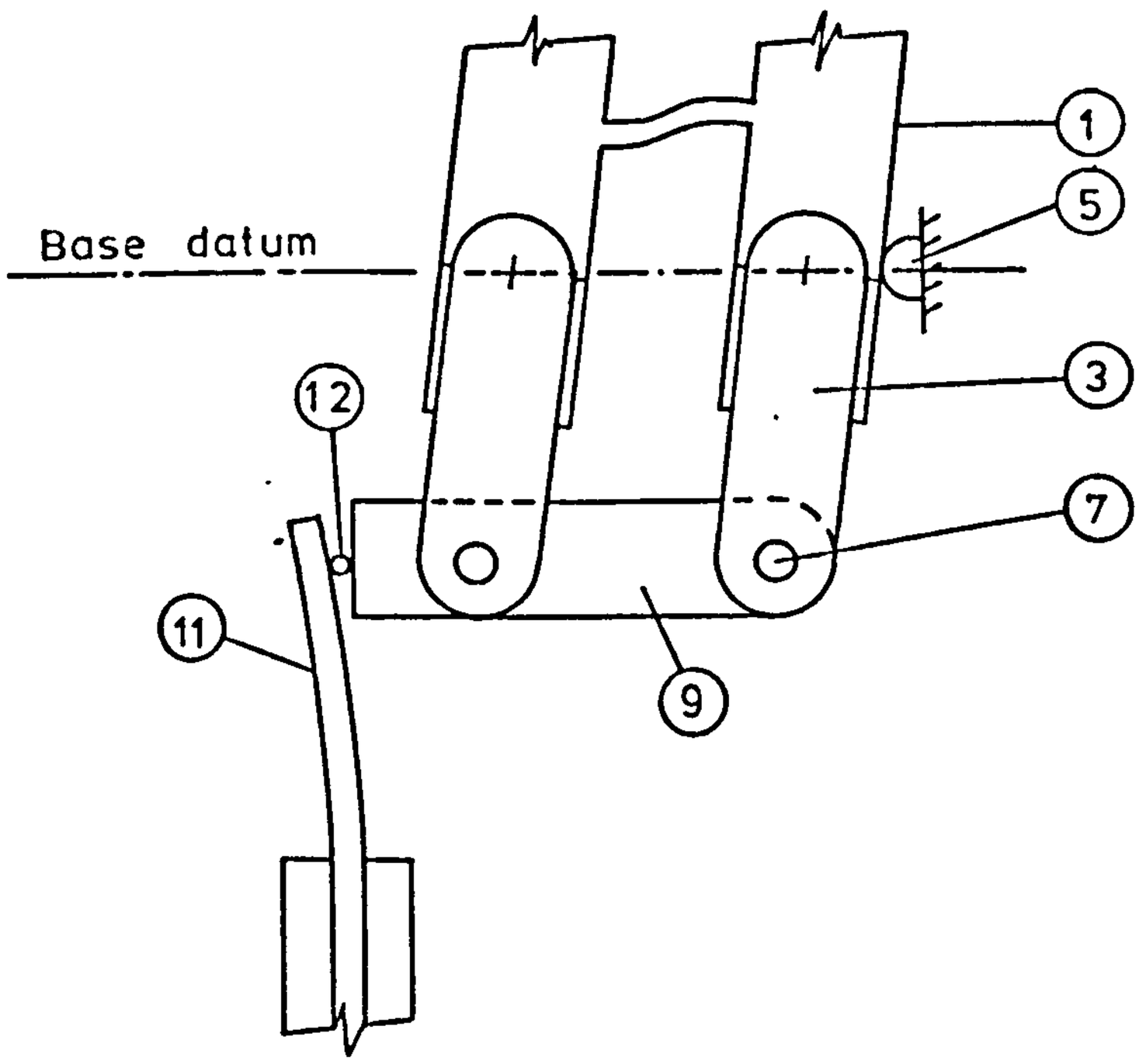

(b) Foundation rotation

Action of foundation mechanism

Figure 7.6

Nominal Sheet Thickness	Young's Modulus N/mm^2	Poisson's Ratio
3/16 inch	3103	0.366
1/8 inch	3155	0.352

Elastic properties of Perspex used for Models

Table 7.1

Effective length of cantilever mm	Rotational Flexibility Coefficient K_θ radians/N.mm	Vertical Flexibility Coefficient K_v mm/N
30	-	0.370×10^{-3}
40	0.0607×10^{-6}	-
80	0.364×10^{-6}	4.586×10^{-3}

Values of the Foundation Flexibility Coefficients used in the Model Tests

Table 7.2

CHAPTER 8

EXPERIMENTAL RESULTS

8.1 INTRODUCTION

The present chapter deals with the presentation of the results of the experimental investigation carried out as described in Chapter 7. The results of the series of tests on the two three-dimensional shear-wall models are given in comprehensive tabular form for reference purposes. In addition, the results are presented graphically together with the analytical solutions corresponding to each particular test. The experimental results are discussed and are compared with the analytical solutions by referring to the graphs.

8.2 PRESENTATION OF RESULTS

The two models, the layout and dimensions of which are shown in figures 7.1 to 7.3 inclusive, were each tested under the action of the uniformly distributed load, simulated as described in section 7.9. The two alternative positions adopted for the load are shown relative to the walls of the models in figure 8.1. Load position number 1 was symmetrical with respect to the plan layout of the models while load position number 2 was asymmetrical, placed midway between wall assemblies numbers 2 and 3.

A detailed account of the load position and the setting of the foundation mechanism at the base of wall assembly number 3, as used for each of the twenty tests is given in table 8.1. Each of the models was tested under the action of the distributed load in each of its two positions, with five different foundation conditions at the base of wall assembly number 3. These foundation conditions were chosen to simulate the following combinations of rotational and vertical flexibility:-

1. Relatively stiff to both rotational and vertical deformations - as used in tests 1, 2, 11 and 12.

2. Relatively flexible to rotation and stiff to vertical deformations - as used in tests 3, 4, 13 and 14.

3. Relatively flexible to both rotational and vertical deformations - as used in tests 5, 6, 15 and 16.

4. Relatively stiff to rotation and flexible to vertical deformations - as used in tests 7, 8, 17 and 18.

5. "Rigidly" built in to the 'Perspex' base plate - as used in tests 9, 10, 19 and 20.

The deflection of each wall assembly at the positions of the dial gauges, as derived from the experimental readings, are given in tables 8.2 to 8.5 inclusive. The values given have been adjusted where applicable to allow for the measured deflections of the steel base plates supporting the models. The rotation of the models in plan at the levels of the dial gauges, as calculated from the relevant results of deflection of wall assemblies 1 and 3, are also given in the above tables.

The vertical stress at each of the positions shown on plan in figure 8.1, at a height of 175mm above the base, as derived from the results of the strain gauge readings taken during the tests, is given in tables 8.6 to 8.9 inclusive. The convention that tensile stresses are considered positive is adopted throughout the tables.

The measured deformations of the foundation system of wall assembly number 3 are given in table 8.10 for those tests where the flexible foundation mechanism was used.

The computer programs discussed in Chapter 5 were used to evaluate analytical solutions corresponding to the conditions of each test. The measured dimensions of the individual walls and the relevant flexibility coefficients of the foundation mechanism of wall assembly number 3 were used to define the structure. The bases of wall assemblies 1 and 2 were assumed to be rigid in all analytical computations. The load used in the programs was a uniform line load equivalent to 1 Kg per storey at the relevant position. Six reference levels were used for the polynomial solution and twenty for the point load solution. The results of the computer evaluations of the deflections of the wall assemblies throughout the height of the models are presented graphically with polynomial and point load results for any one test being shown on the same graph onto which the experimental results are superimposed. With the exception of tests numbers 9 and 19, where theoretically there should be no

rotation of the model in plan, a graph of the rotation of the model throughout its height is given for each test, again with the two analytical solutions and the experimental results being shown on the one graph. A third graph is given for each test which shows the two analytical stress distributions at the level of the strain gauges, together with the experimental stresses derived from the strain gauge readings.

The percentage of the total shear load distributed to each wall assembly throughout its height, as evaluated by the analytical methods, is shown on separate graphs for the two methods, for each test, with the exception of test number 9 where each of the three wall assemblies carries an equal proportion of the load at all heights.

The graphs described above are presented in figures 8.2 to 8.97 inclusive at the end of the chapter. They are arranged according to the numerical order of the tests, with all the graphs relating to a particular test appearing in consecutive figures.

The analytical solutions for the rotation and relative vertical deflection of the bases of the walls of assembly number 3 are compared with the corresponding experimental results in table 8.10.

8.3 DISCUSSION OF RESULTS

8.3.1 EXPERIMENTAL RESULTS

In any practical experimental investigation it is inevitable that a number of sources of error are present, for example deficiencies in the apparatus or in the model materials.

The experimental apparatus described in Chapter 7 was designed to be as inflexible compared to the models as the practical considerations of available techniques and materials would permit. Nevertheless, the apparatus could not be considered rigid. The test procedure described in section 7.9 was adopted to reduce any loss of accuracy of the results arising from deficiencies in the apparatus or in the model material. The same procedure was adhered to throughout the test program in order that any residual errors which were not determinable would be relatively consistent, thus enabling meaningful comparisons to be drawn between the results of the various tests.

Random errors, such as the misreading of gauges, and systematic errors, in this case for example the typically small changes of strain and deflection found during the first load increments of each test, occur in any experimental program. The method of evaluating the test results described in section 7.10, was used to enable such errors to be eliminated. However the experimental results were derived by drawing the best straight line by eye through the test readings, excluding those eliminated above. This procedure, although enabling many errors in the readings to be eliminated, relies on the judgement of the individual and inevitably there is some degree of error involved. However, a full mathematical treatment of the results whereby the best straight line is found by a "least squares" method would not be able to eliminate the random and systematic errors described above. A more ideal treatment of the test readings might be to subject them to an initial graphical plot whereby the obviously erroneous points may be eliminated and thereafter the best straight line through the remaining points could be found by mathematical methods. In the present case it was considered that the large amount of work involved in the latter two-part technique did not justify the small increase in accuracy which might be achieved.

When the individual weights were placed on the hangers the model underwent rapid changes of deflection. Great care was taken to ensure that each load increment was applied as smoothly as possible to minimise any impact effect of the load on the model. The weights were placed on or taken off the hangers, as applicable, in the same order throughout all the tests, beginning in each case with the hanger at the top of the model and working towards the base. By adopting this procedure it was intended that any over-reaction of the model caused by the addition of weights near the top, where a unit increment of load has the largest effect, would be compensated for when the weights were added near the base, where they have a relatively small effect. The impact of adding and removing weights to the model during the tests should not be of importance provided that the material of the model is elastic and its yield stress is nowhere exceeded during the tests. However 'Perspex' is prone to creep under load and is hence imperfectly elastic, so that some error in the results may be expected from this source.

The dial gauges are precision instruments and any error introduced by them will be negligible, especially in the relatively large deflections encountered at the higher levels of the models. Small errors may be introduced where the ball at the point of the gauge bears on an uneven surface. However, the components of the model were machined to close tolerances and given a good finish to avoid such errors. The dial gauges used to record the deflections of the model were mounted on a framework consisting of 'Dexion' angles, securely bolted to the test rig. The 'Dexion' is comparatively flexible and could lead to errors were it to be disturbed during a test. The dial gauges are constructed so that the spring force exerted by the point of the gauge on the model is constant throughout the travel of the gauge. Therefore the resultant force of the gauges on the mounting frame and on the model should remain constant throughout the tests and provided that the frame is not disturbed by, for example, an accidental jolt, little error should be introduced as a consequence of the flexibility of the 'Dexion' frame.

The electrical resistance strain gauges and the indicator equipment are once again items of precision scientific equipment, designed to give results of high accuracy. However, to take advantage of their potential great care must be taken in the application and use of the gauges. To this end compensating gauges were used as described in section 7.6.1. To avoid any errors in the readings of the strain gauges caused by the wires connecting the gauges to the indicator equipment straining under their own weight these wires were hanked together and supported at close centres throughout their length.

The conditions at the bases of those walls which are considered to be rigid introduce a further source of error encountered in all experimental studies where rigid conditions of fixity are required. During each test the deflection of the underside of the 'Perspex' base plate of the model was measured at the position of the centre of each built-in wall, whereby the rotation of the base between the two walls of each assembly was calculated. From this the deflection at the height of each dial gauge position caused by the base rotation was calculated and the results for the deflection of the walls adjusted accordingly. The presence of elastic foundations at wall

assembly number 3 caused some difficulty in this respect. Obviously the rotation at the bases of the "built-in" walls must have an effect on the deflections of assembly number 3. The corrections applied to the deflections of the wall assemblies with "built-in" bases were extrapolated to give an estimate of that part of the deflection of wall assembly number 3 caused by the rotation of the base under the other "built-in" walls. This "rule of thumb" method was used to adjust the results for the deflections of wall assembly number 3. The adjustments made using the above procedure were comparable with those obtained from measurements of the base rotation of wall assembly number 3 in those tests where the latter walls were built in to the "Perspex" base plate.

Deformations occur within the depth of the "Perspex" base, local to the foot of each wall. It was not practical to position gauges on the "Perspex" base plate from above so that these deformations are not accounted for in the measurements taken below the base and must have an effect on the accuracy of the results. The tendency will be to produce results for deflection and rotation of the model rather larger than would be the case if the bases were truly rigid.

During the tests the models were not prevented from moving at right angles to the planes of the shear wall assemblies. Although the applied load was in every case parallel to the planes of the walls some movement at right angles must be expected, particularly where a large rotation of the model is present. This movement will tend to produce different strains on opposing faces of the same wall. However, at those positions where gauges were fixed to both sides of a wall at the same position, the difference in results was in no instance greater than three percent.

The floor slabs were designed to be flexible in bending, particularly in the locality of the lintel beams connecting shear walls, while maintaining a high degree of stiffness in their own plane. The configuration used is largely justified by the results obtained, namely that the deflections of the three wall assemblies at any level bear a close linear relationship throughout the tests. However it was not practical to measure deflections at the levels of the lowest floor slabs where the largest redistribution of forces between wall assemblies may be expected., The greatest tendency for

the floor slabs to deform, therefore, exists at the lowest levels and some inaccuracy must be expected from this source.

When the applied load is asymmetrical the structure undergoes rotation in plan and the deflected forms of the wall assemblies are unequal. At any height above the base the slopes of the wall assemblies are thus unequal. It follows that the inclination of a floor slab to the horizontal, as determined by the walls to which it is fixed, varies across its length. This warping effect of floor slabs will mobilise the torsional stiffness of the slabs which was assumed negligible in the analysis, thus introducing a further source of inaccuracy between the experimental results and the analytical solutions.

As noted in section 7.3.1, one of the disadvantages encountered in using "Perspex" to construct model structures is that this material is subject to considerable creep under sustained loading conditions. Since the model creeps in the same direction as the applied load the procedure of repeating each test during the unloading of the model was adopted. During the loading sequence the creep is in the same direction as the changes of deflection of the model, while during the subsequent unloading sequence the creep is in the opposite direction to the changes of deflection of the model. Since the average load on the model during the loading sequence was the same as that during the unloading sequence and the length of time required to carry out each operation was approximately equal, it can be argued that the magnitude of the creep would be approximately the same in each case. Hence, by taking the mean of the results for deflections obtained for the loading and unloading of the model, the errors contributed by creep in the "Perspex" will be accounted for to a considerable extent.

The value of the modulus of elasticity, as used to evaluate the stresses in the model from the results of the strain gauge readings, was assumed to be constant in tension and compression throughout Perspex cut from a common sheet. This assumption will introduce errors in the results since the elastic properties of "Perspex" are known to differ in tension and compression and also to vary within single sheets.

As indicated at the beginning of this section the apparatus and procedure adopted for this experimental investigation were designed

to reduce or eliminate as many of the sources of error as practical considerations permitted. The precise degree of accuracy of the experimental results achieved for any particular test is very difficult to estimate. Any figures quoted would be a matter of conjecture. However, the fact that a rigorous test procedure was adhered to throughout the program ensures that errors in the results of the various tests are consistent and that the results may be used with confidence for comparative purposes.

8.3.2 ANALYTICAL SOLUTIONS

The analytical solutions presented in graphical form at the end of this chapter were derived using the physical dimensions and structural conditions which most accurately represented the models within the limitations of the assumptions used in the derivation of the analytical methods. The fact that these assumptions were carefully considered in the design of the models ensures that analytical representation of the models is well defined. However it cannot be considered complete for a number of reasons.

As indicated previously each "Perspex" sheet comprising the components of the models varies in thickness. For the analysis the mean thickness of each shear wall was used. Differences in thickness local to the foot of any wall will have a greater influence on the results for the deflection of the wall than would differences near the top. The analytical methods assume that the walls are of constant cross section throughout their height, and the analytical solutions, therefore, fail to represent the model completely in this respect. In order to represent the model as accurately as possible the dimensions of each component as used in the analytical solutions were those found as the mean of a number of measurements on the components.

A similar discrepancy in the representation of the models by the theory arises from the assumption of constant elastic properties throughout any component of the models. The analytical methods are again unable to accommodate the undefined variations of these properties in the model material.

Factors which increase the accuracy of the analytical representation of the behaviour of the models have been considered in

the analysis. Amongst these is the inclusion in the analysis of the effects of shear deformations in the connecting beams. The flexibility of the beam to wall connections in the shear wall assemblies had also been taken into account by using an effective span for the connecting beams greater than the clear span by the depth of the beams, as suggested by Michael[7].

8.3.3 COMPARISON BETWEEN EXPERIMENTAL RESULTS AND ANALYTICAL SOLUTIONS

DEFLECTIONS

Generally, the experimental results for the deflections of the models throughout the twenty tests follow a consistent pattern which is in close agreement with the two analytical solutions. A relationship between the polynomial and point load solutions similar to that discussed in Chapter 6 is again shown in the graphs; that is, the polynomial solution is consistently larger than the corresponding point load solution.

The graphs are largely self explanatory and hence only general features are indicated as follows:-

1. The plots of the experimental deflections closely follow the characteristic form of curve obtained from the analytical solutions.

2. The experimental results are generally greater than both analytical solutions.

3. In any particular test the difference between the experimental deflection of a wall assembly and the corresponding analytical solution is approximately proportional to the height above base datum.

4. In those tests where the applied load was symmetrical and hence the deflected forms of the three wall assemblies were approximately the same the difference between the experimental deflection of each wall assembly at a particular height and either corresponding analytical solution tended to be in proportion to the deflection of that wall measured at the relevant height. However, the difference between experimental results and analytical solutions varied from test to test. The difference between the experimental results and the polynomial solutions was generally less than 10%, while the

difference between the experimental results and the point load solution was generally less than 16%.

5. In the tests where the applied load was asymmetrical and hence the deflections of the wall assemblies at any height were greatly different, the differences between the experimental results and the analytical solutions were not generally in proportion to the deflection of the wall assembly at that height. The differences between the experimental results for wall assembly number 3 and the polynomial and point load solutions were generally in the same range as those for the symmetrical loading, that is below 10% and 16% respectively. The experimental results for wall assembly number 1 were, in many instances, many times larger than the corresponding analytical solutions. However the maximum deflection of wall assembly number 1, under asymmetrical load was small compared to the deflection of wall assembly number 3 and the numerical magnitude of the differences between the experimental results and the analytical solutions for wall assembly number 1 were comparable to the corresponding differences for wall assembly number 3.

ROTATIONS

Both the experimental results and the analytical solutions for the rotations of the models in plan under the various combinations of load and foundation conditions are related directly to the corresponding deflections of the wall assemblies. Since the relationship between experimental deflections and the corresponding analytical solutions was reasonably close and consistent it is logical to expect a similar relationship to exist between experimental and analytical rotations. The graphs of rotations relevant to the various tests generally show this to be the case.

The general comments on the graphs of rotation which follow are, in cases, necessarily similar to the comments made in the previous section on deflections:-

1. The plots of the experimental results of rotations of the models are of similar form to the graphs obtained from the analysis.

2. Although the majority of the experimental results for rotation are again greater than both analytical solutions, there is a

significant number of instances where the experimental results lie between the polynomial and point load solutions.

3. Whereas it was the case that the difference between experimental and analytical deflections was generally proportional to the height above the base, the corresponding differences in rotations are not generally proportional in all the tests. Although there are cases where the difference between the experimental rotation and the analytical solution increases with height, there are also cases where the above difference is numerically constant or even decreases with height.

4. Where either the asymmetrical loading case or the more flexible foundation conditions produced larger rotations of the models the agreement between the experimental results for rotation and the analytical solutions was generally better than the figures of 10% and 16% as quoted for the polynomial and point load deflection respectively.

5. Where symmetrical loading combined with less flexible foundation conditions produced little rotation of the models as shown in figures 8.3, 8.13, 8.50 and 8.60, the percentage agreement between experimental results and analytical solutions was in cases markedly poor, the experimental results being up to approximately 50% in excess of the analytical solution on occasion. However, in such cases the rotations were very small in magnitude and the actual numerical discrepancy between experimental and analytical results was also numerically small compared to those encountered in other tests.

STRESSES

The stresses in the walls of the models, as derived from the strain gauge readings taken during the tests, yield a general form of stress distribution which bears a very consistent relationship to the stress distributions predicted by the analytical solutions. The maximum stresses in each wall assembly at the level of the strain gauges are invariably at the outer extreme fibres of the walls, that is adjacent to gauge positions A and D, as defined in figure 8.1. The experimental stresses at positions A and D are in very close agreement with the analytical solutions throughout the series of twenty

tests. The stresses at the inner extreme fibres of the walls, that is adjacent to gauge positions B and C, are generally much smaller than the corresponding values at positions A and D, and in this instance the agreement between experimental results and the analytical solutions is not so marked. There is however a consistent relationship between experimental results and analytical solutions namely, that the experimental results for stresses at positions B and C invariably lie to that side of the analytical solutions which is towards the result at the outer edge of the same wall. In cases where there is a reversal of stress across an individual wall the above relationship is shown as a smaller experimental stress than, or one of opposite sense to that predicted by the analytical solutions at positions B and C. In cases where there is no stress reversal the experimental stresses at B and C are invariably larger in magnitude than the corresponding analytical solutions.

The lack of agreement between the experimental results and the analytical solutions for stresses at the inner extreme fibres of coupled wall assemblies may be a result of, firstly, the assumptions made in the development of the analyses or, secondly, the estimation of the flexibility of the connections between beams and shear walls, or, finally, local stiffening of the Perspex by the strain gauges. In the first alternative the analysis was developed on the assumption that the connection between the walls was of a continuous nature whereas, in reality, it consists of a number of discrete beams, whose presence will necessarily affect the distribution of stress in particular near the inner edges of the walls. In a similar fashion an error in the estimation of the flexibility of the beam-to-wall connections will affect the stress distributions predicted by the analytical solutions. The presence of a strain gauge on the Perspex surface thickens the material in the vicinity of the gauge thus stiffening it locally. The strain reading taken by means of the gauge will be correspondingly affected. The effect becomes more important on thinner sheets of Perspex.

FOUNDATION DEFORMATIONS

The experimental results for the rotation and relative vertical deflection of the bases of wall assembly number 3 are compared with the corresponding analytical solutions in table 8.10. The general

level of agreement is very close considering the extremely small movements encountered in the tests. The analytical solutions take no account of deformations of the bases of wall assemblies 1 and 2 which are considered rigid throughout the analysis but which do tend to deform under test conditions as discussed in section 8.3.1.

8.3.4 LOAD DISTRIBUTION

The load distribution graphs are included as a further illustration of the effects of flexible foundations as previously discussed in section 6.5. As was the case in the previous section one wall assembly, in this case number 3, is considered to have flexible foundations and the effects of different foundation configurations on the distribution of the applied load are shown in the graphs.

The general conclusions drawn from the previous examples are again valid in the present case. The majority of the redistribution of load within the structure caused by changes in foundation conditions again takes place within the lowest storeys, and the proportion of load resisted by the walls at higher levels is not so dependent on the foundation conditions. The latter effect is not so marked in the present cases as in the previous examples. In the examples of section 6.5 the wall assembly considered to have elastic foundations was one of seven or eight assemblies in the structure and even under rigid foundation conditions assumed a small proportion of the total load. However, in the case of the experimental models there are only three wall assemblies in each structure and individually they play a proportionally larger part. In the present case, therefore, flexible foundations at the base of one wall assembly will have a greater effect on the distribution of load in the upper storeys.

It is of note that, although the polynomial and point load solutions give similar values for the load distribution in each case, the form of the load function used is reflected in the resultant graphs. The distributions in the polynomial case follow smooth curves of a polynomial nature whereas the point load graphs are angular, reflecting the discrete nature of the solution.

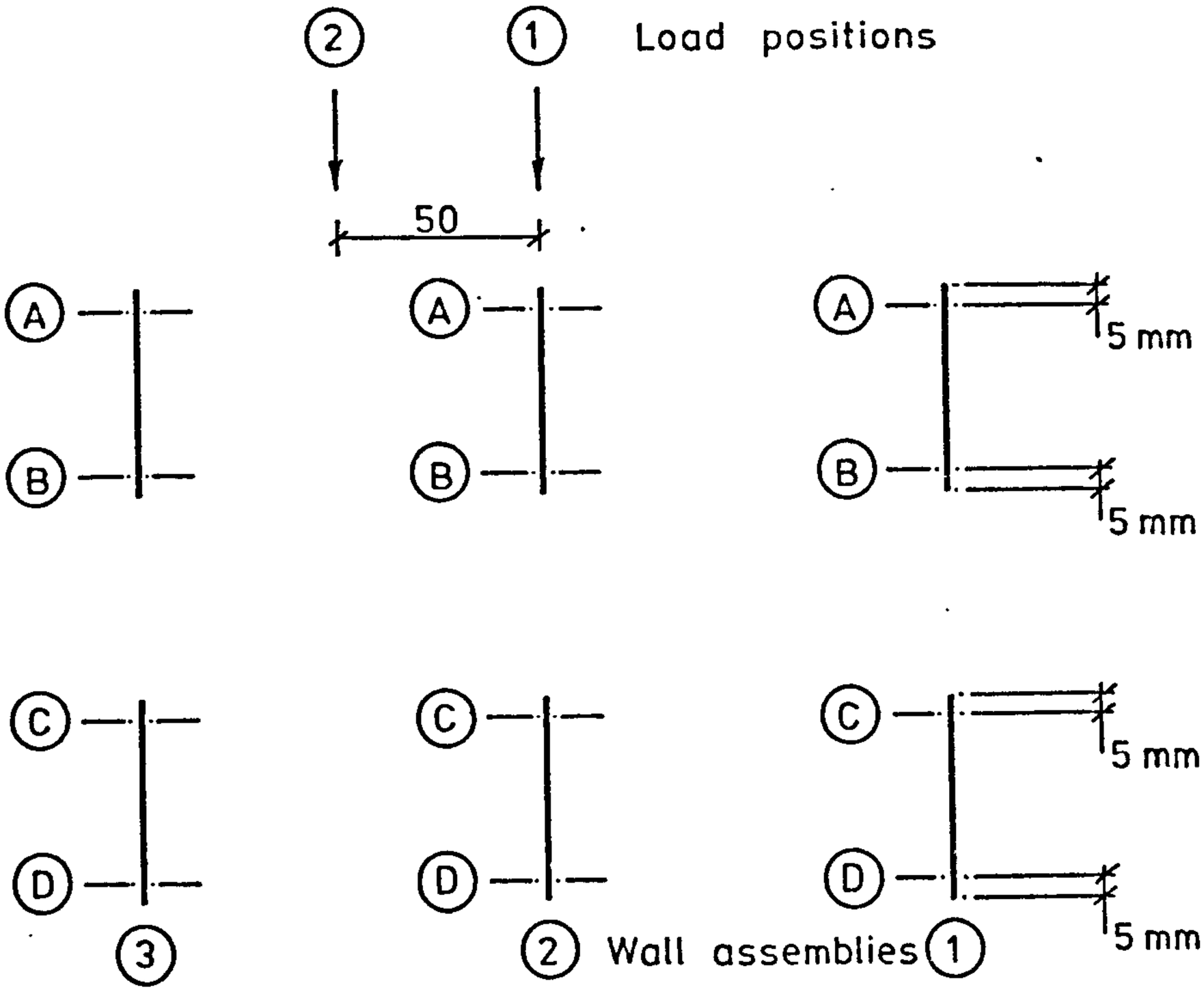

Model 1

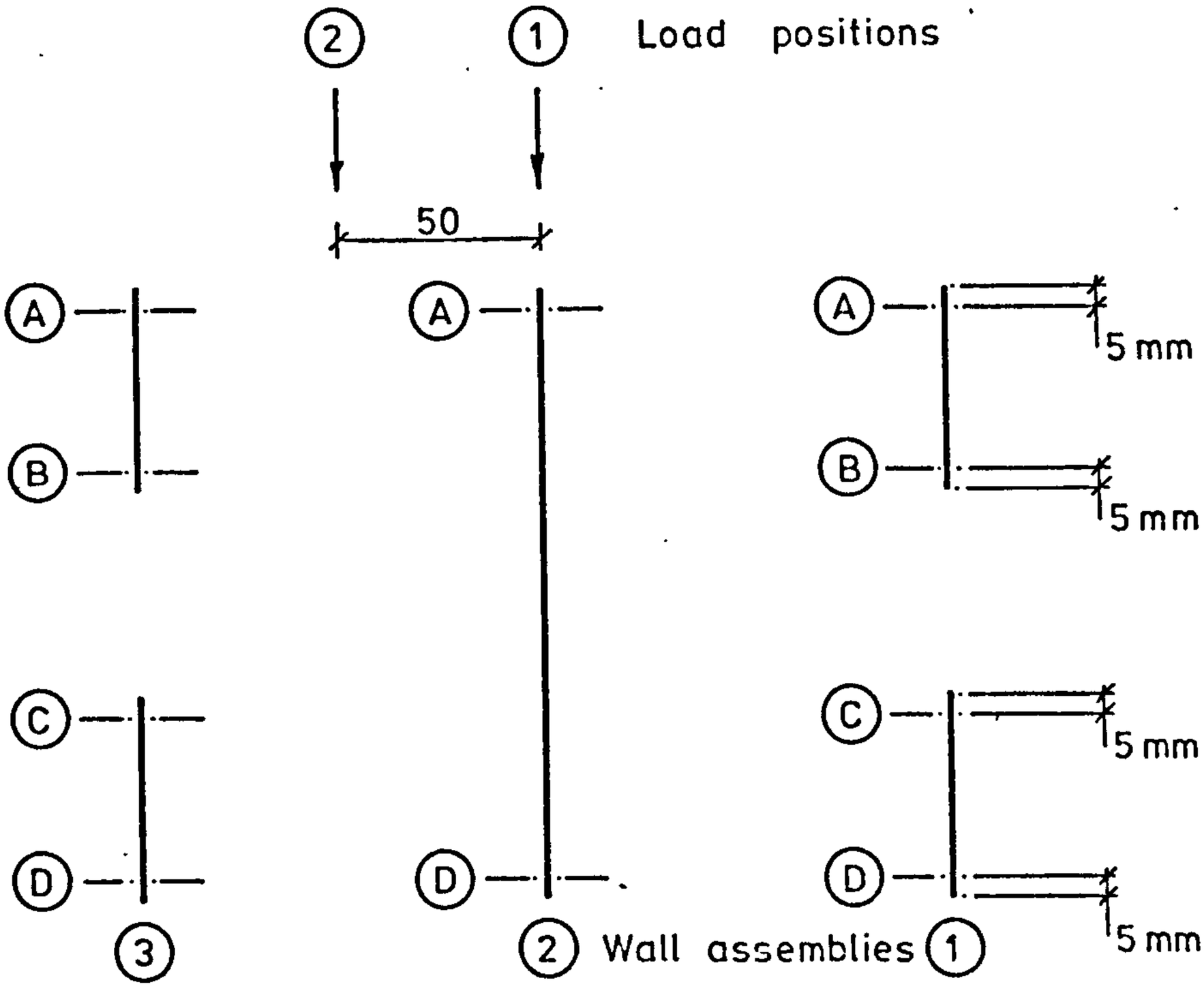

Model 2

Key plans for positions of applied loads and strain gauges on models

Figure 8.1

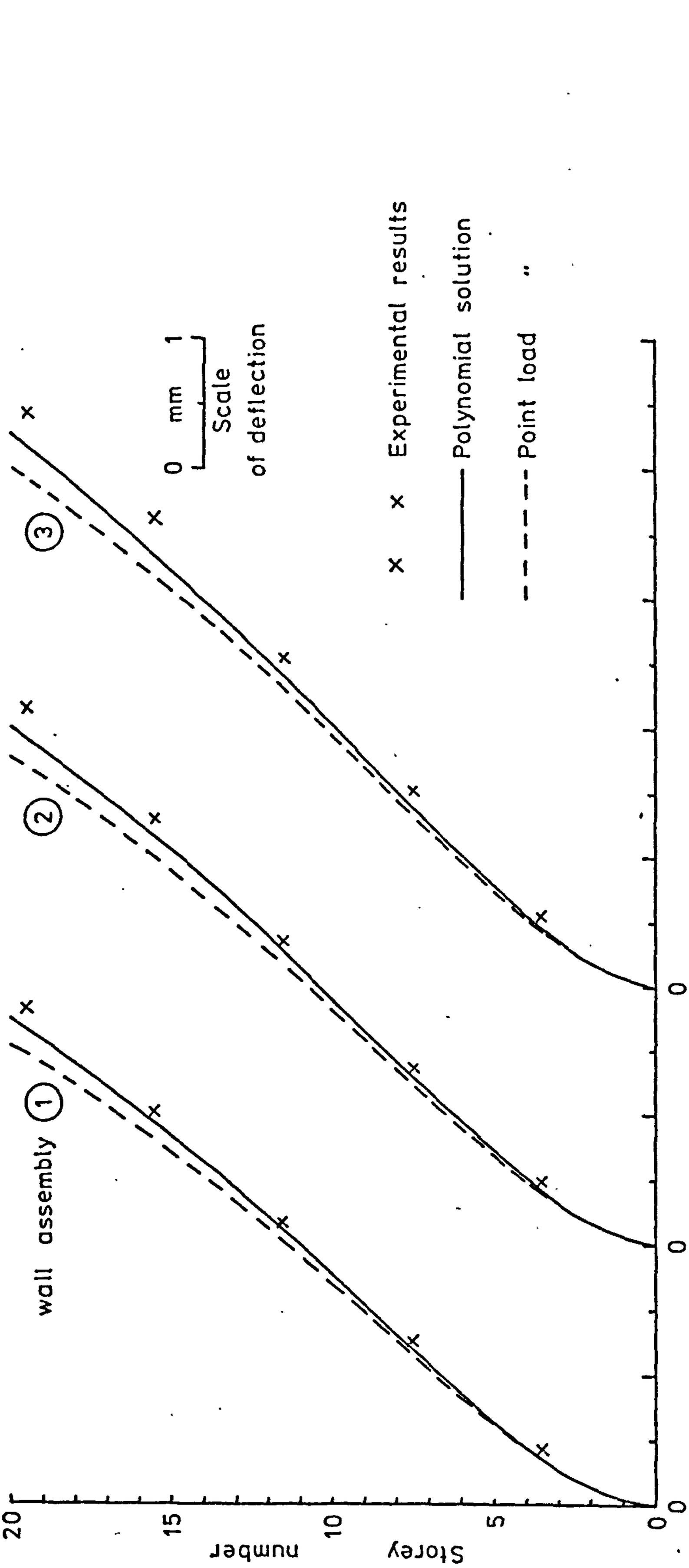
Storey number
20
15
10
5
0
wall assembly ①
②
③
x
Deflections
mm
0
Test number 1 - Deflection
Scale of deflections
0 mm
Experimental results
Polynomial solution
Point load "

Figure 8.2

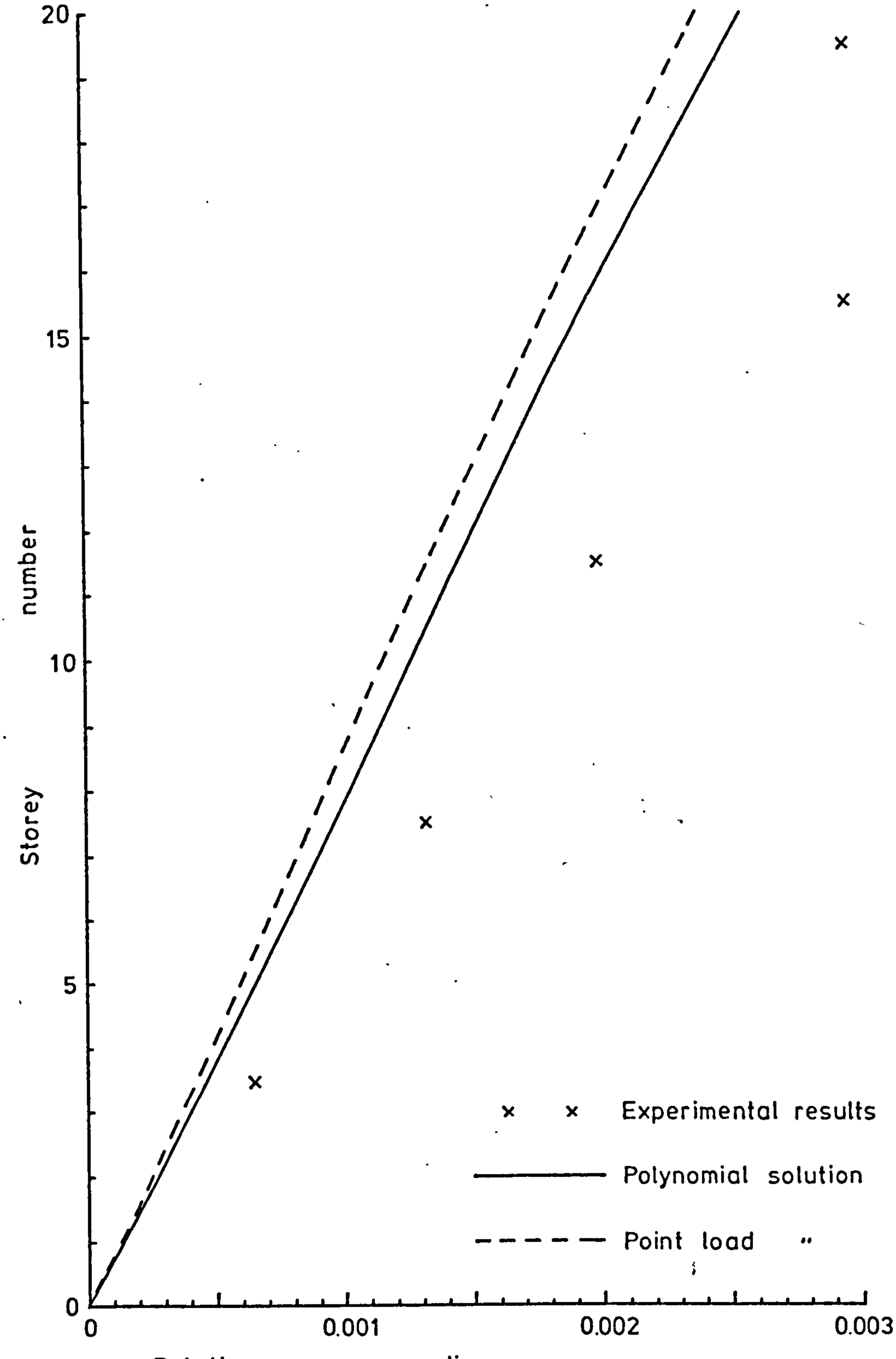

Test number 1 - Rotations

Figure 8.3

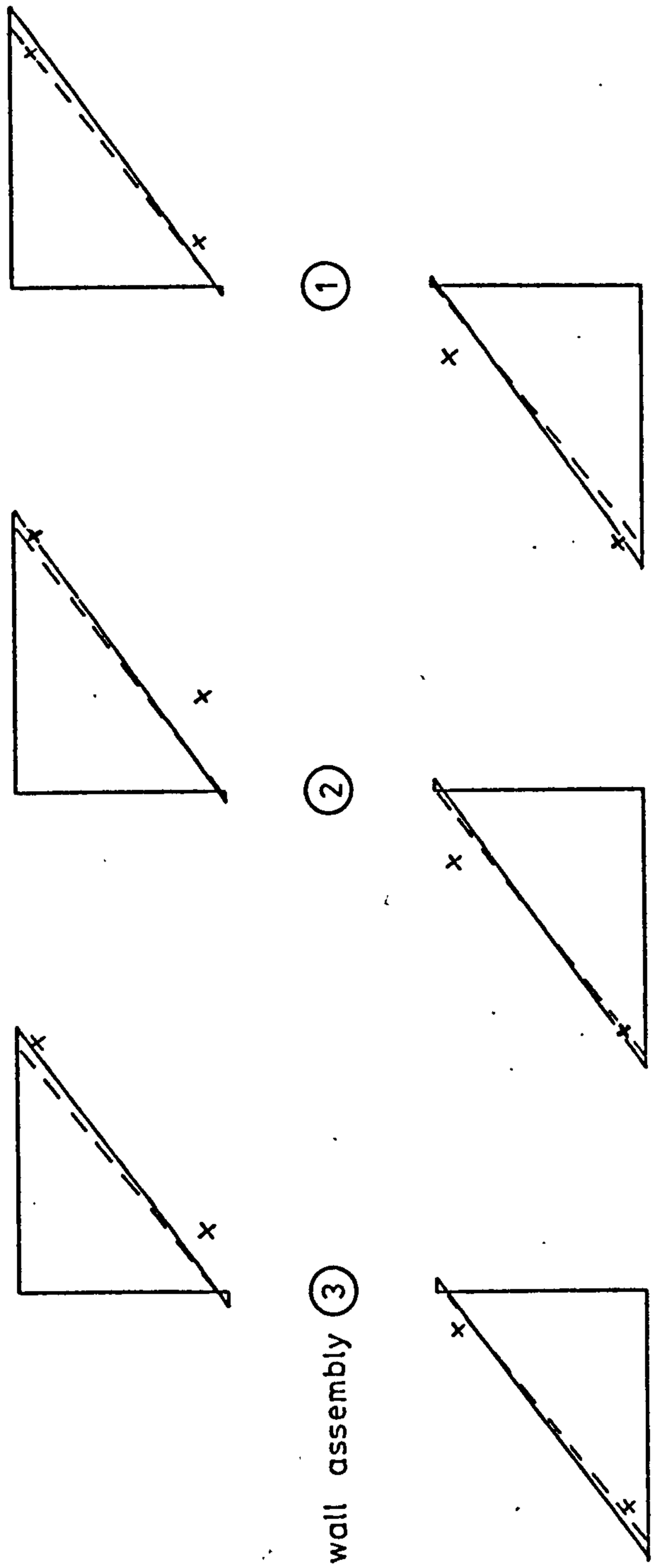
1 Comp. 0 Tens. 1
Scale N/mm2
1
2
3
Wall assembly
Stresses
Experimental results
Polynomial solution
Point load
"
Test number 1

Figure 8.4

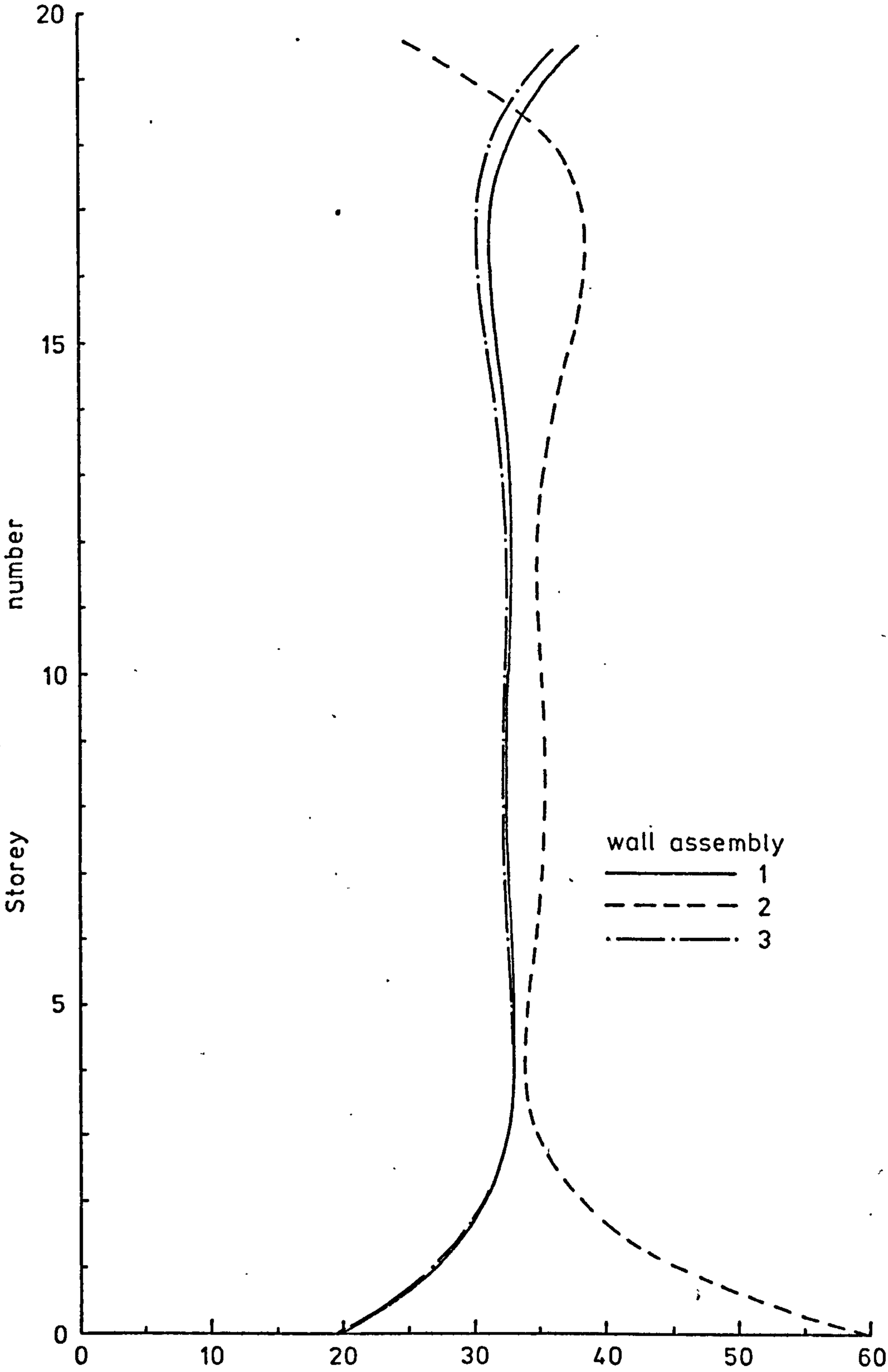

Test number 1 - Load distribution - Polynomial solution

Figure 8.5

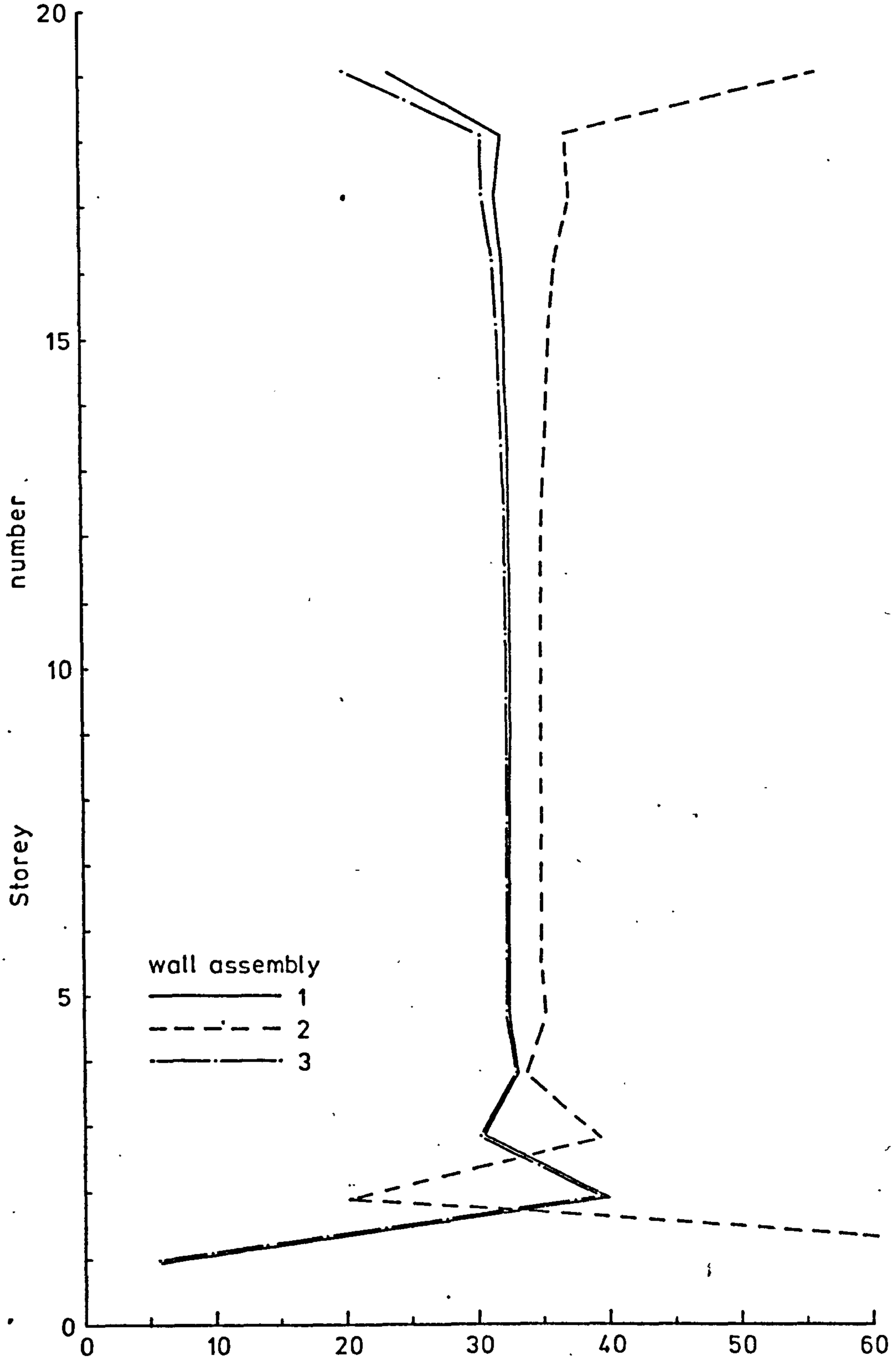

Test number 1 – Load distribution – Point load solution

Figure 8.6

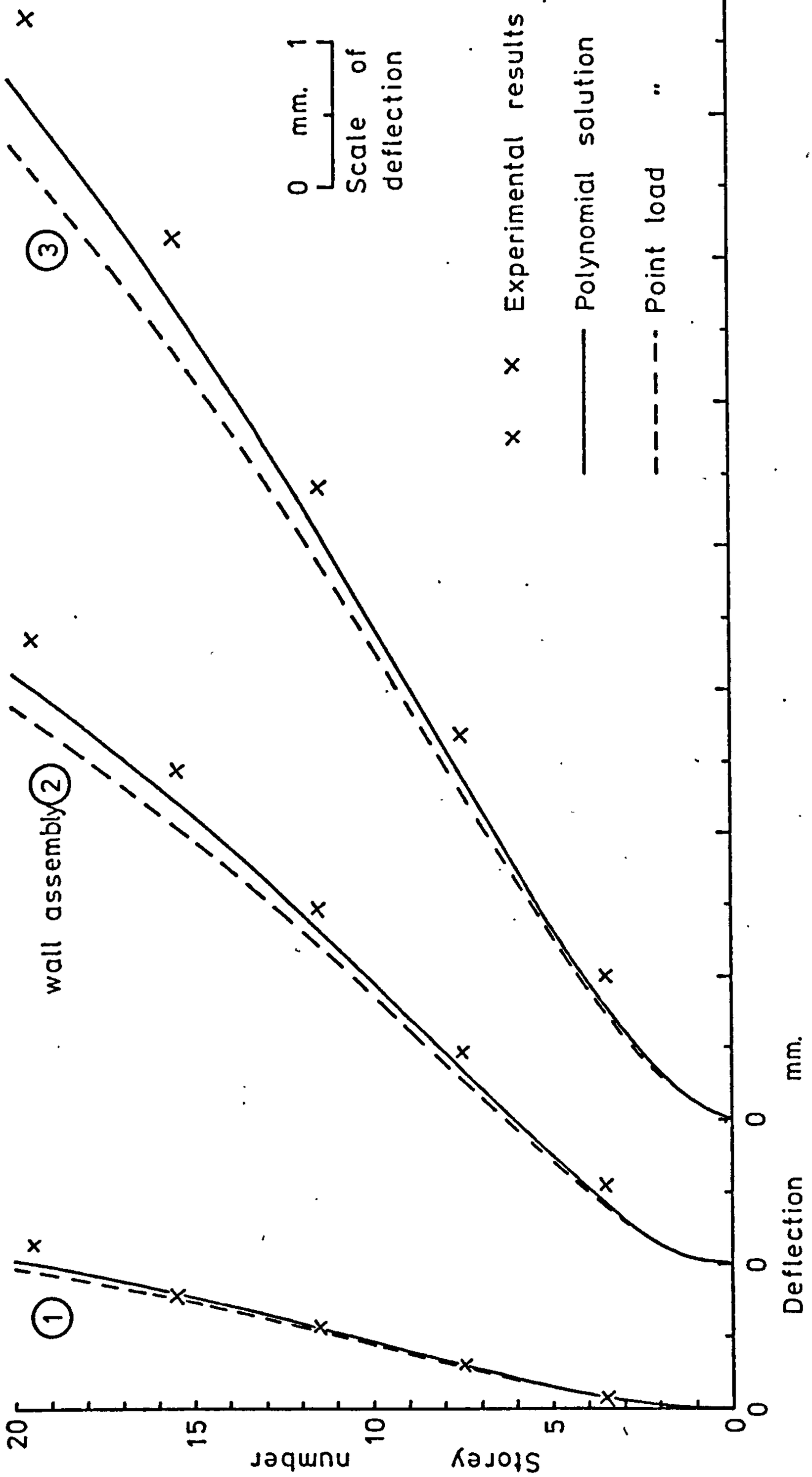
0 mm. 1
Scale of deflection
x Experimental results
Polynomial solution
Point load "
Deflections
8.7
Test number 2
wall assembly (2)
(3)
(1)
Deflection mm.
0
0
5
10
15
20
Storey number

Figure

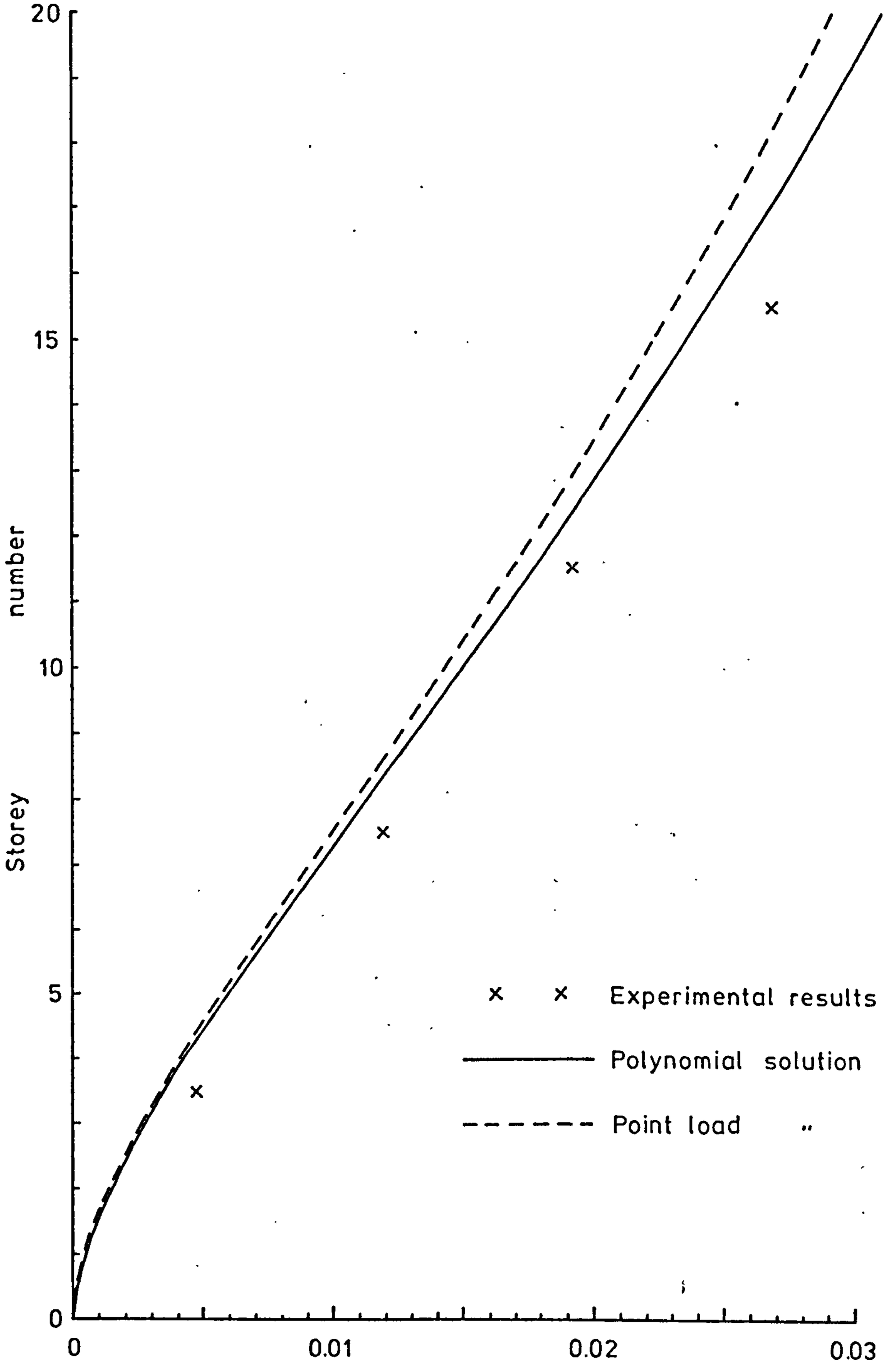

Test number 2 - Rotations

Figure 8.8

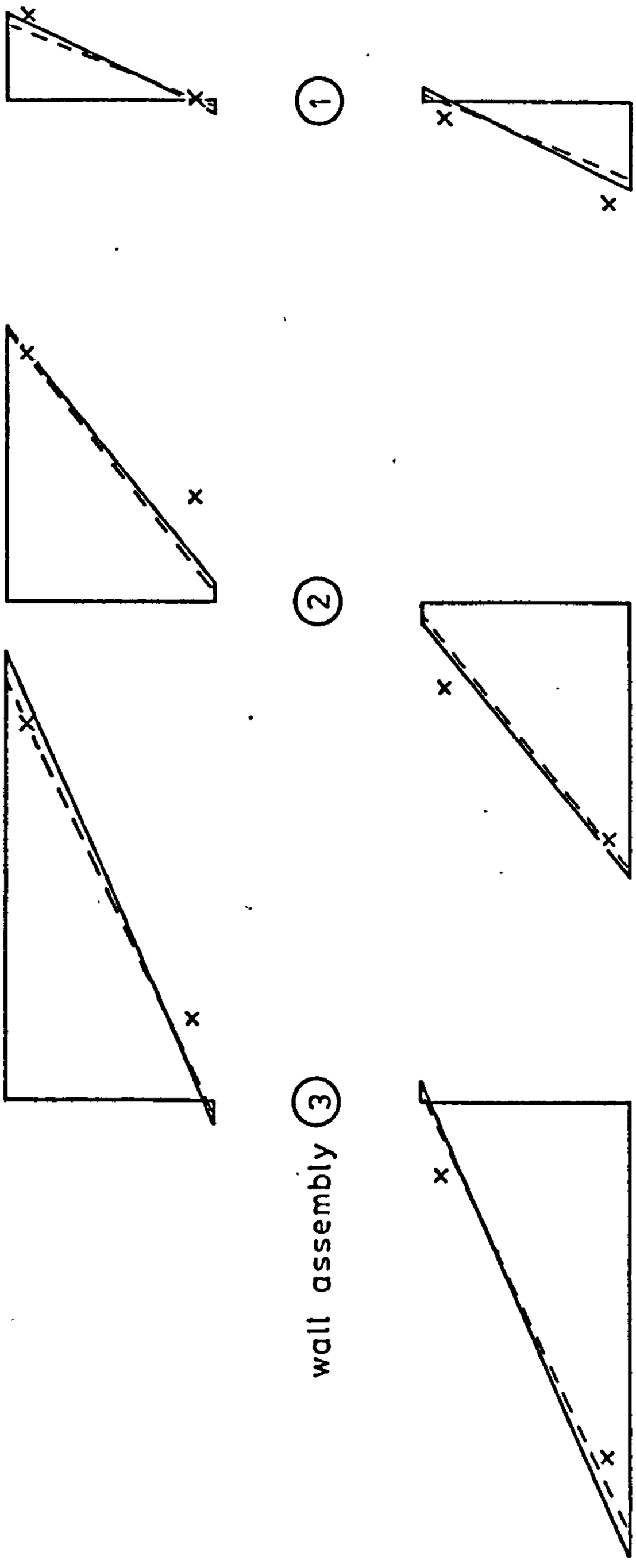
1 Comp. 0 Tens. 1
Scale N/mm2
1
2
3
wall assembly
Stresses
x Experimental results
Polynomial solution
Point load "
Test number 2 —

Figure 8.9

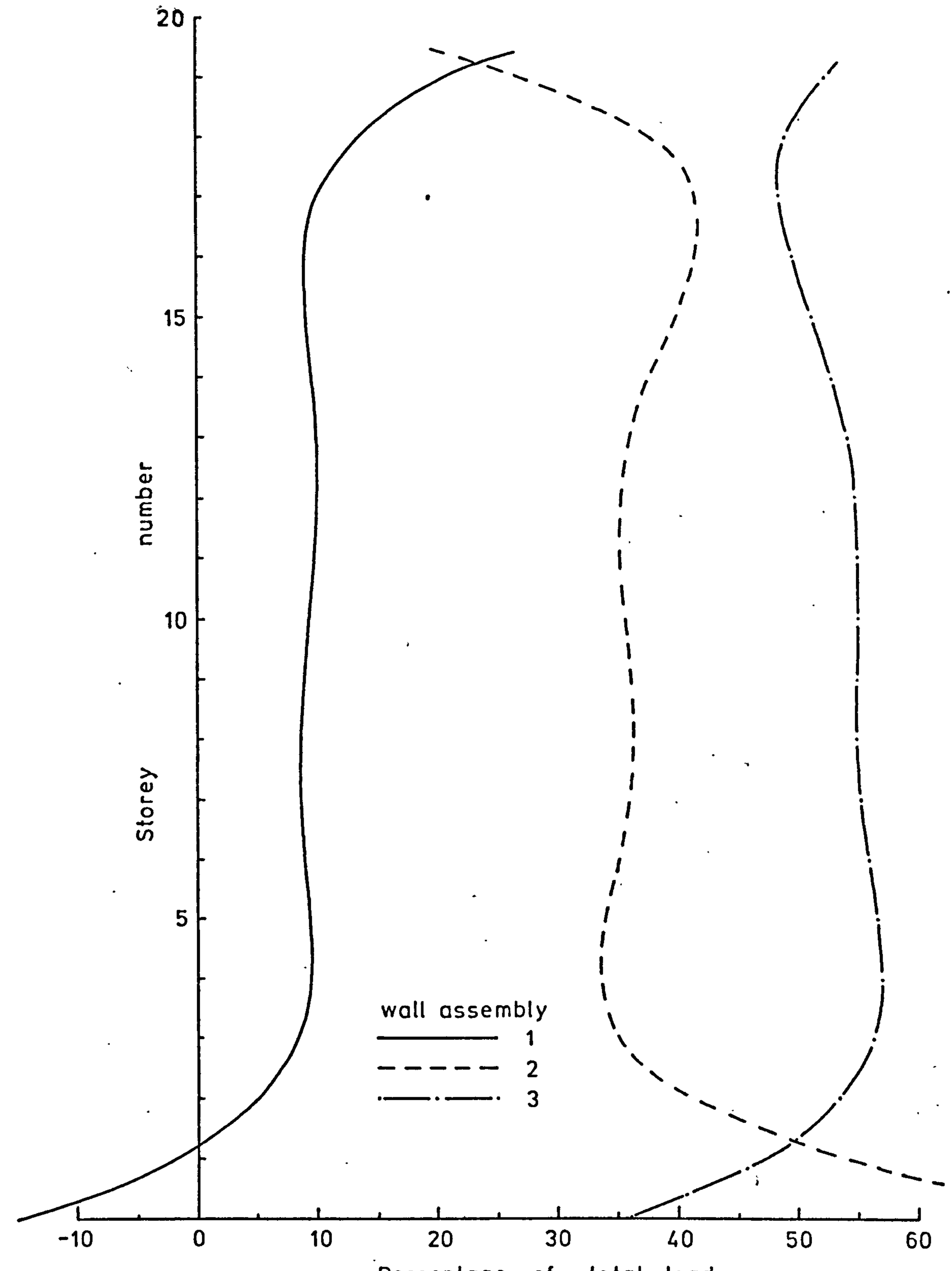

Test number 2 - Load distribution - Polynomial solution

Figure 8.10

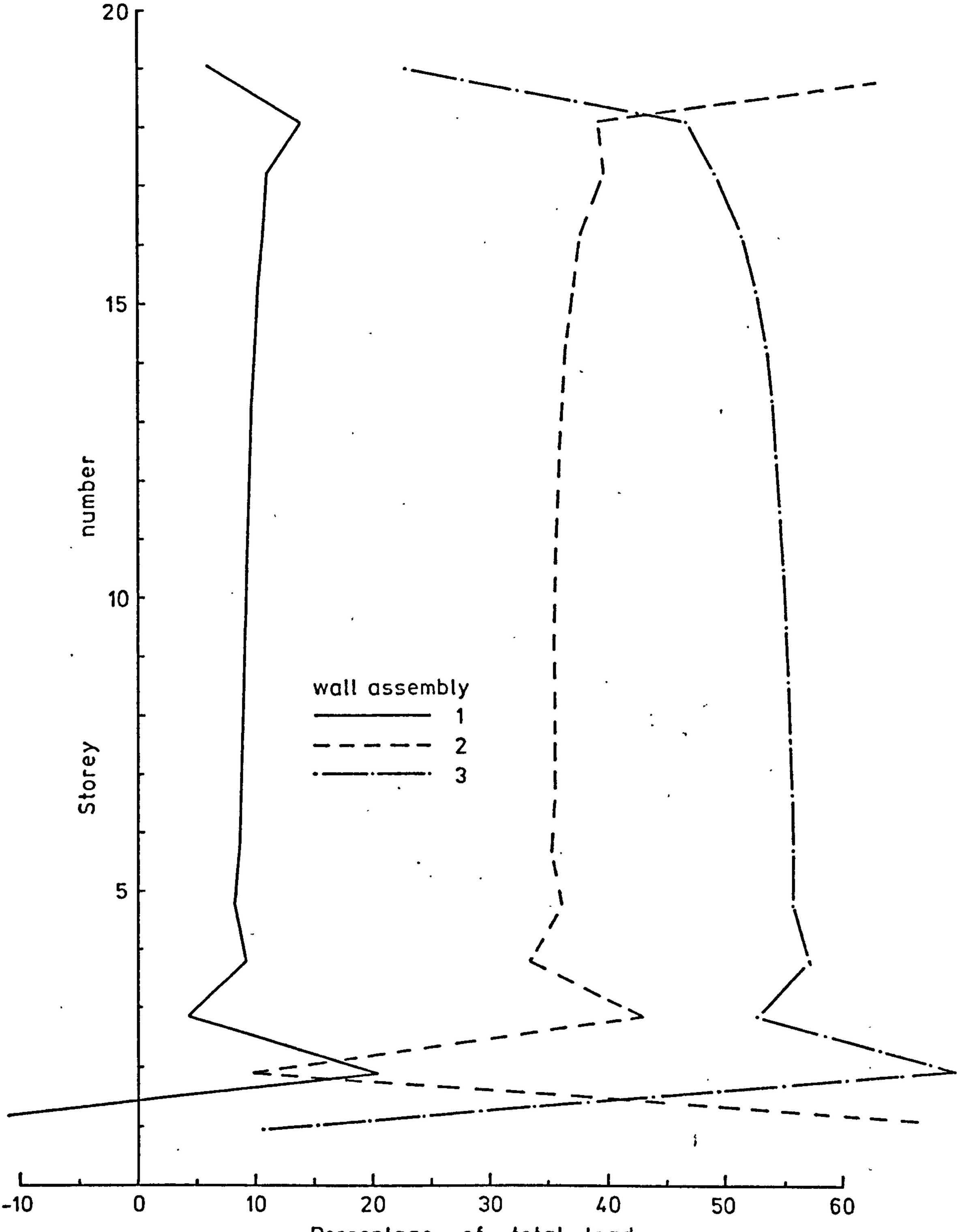

Test number 2 - Load distribution - Point load solution

Figure 8.11

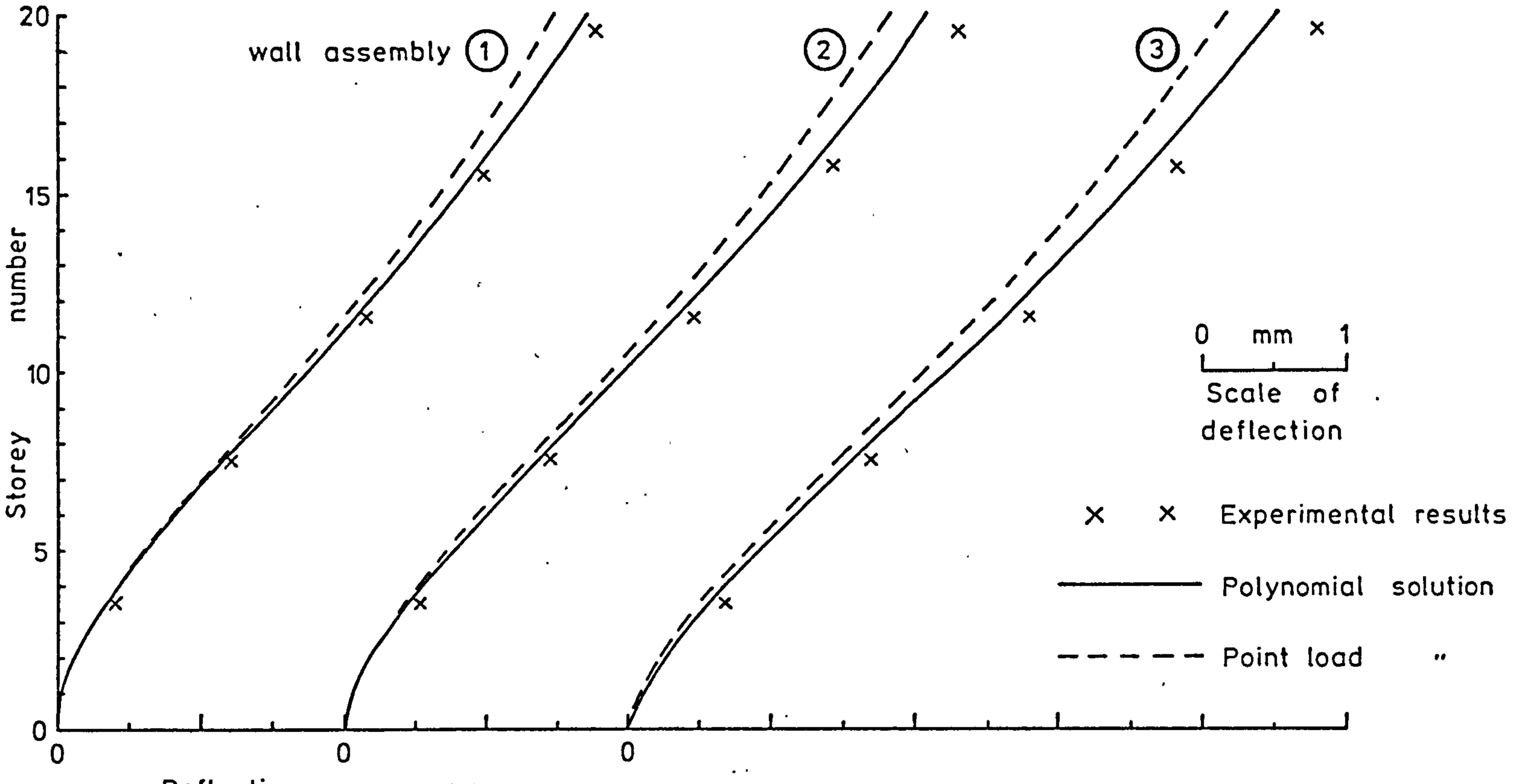

Test number 3 – Deflections

Figure 8.12

F 8.12

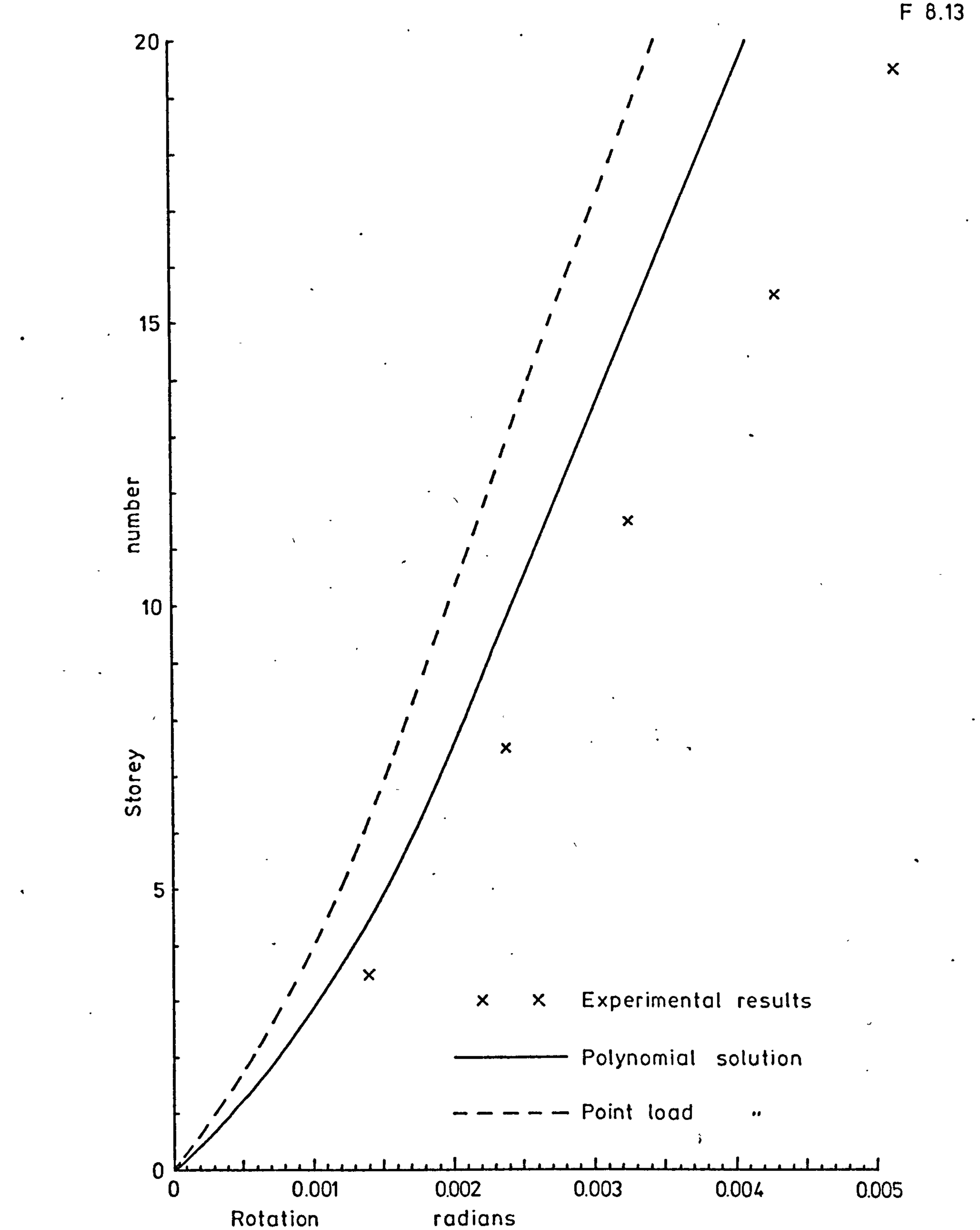

Test number 3 - Rotations

Figure 8.13

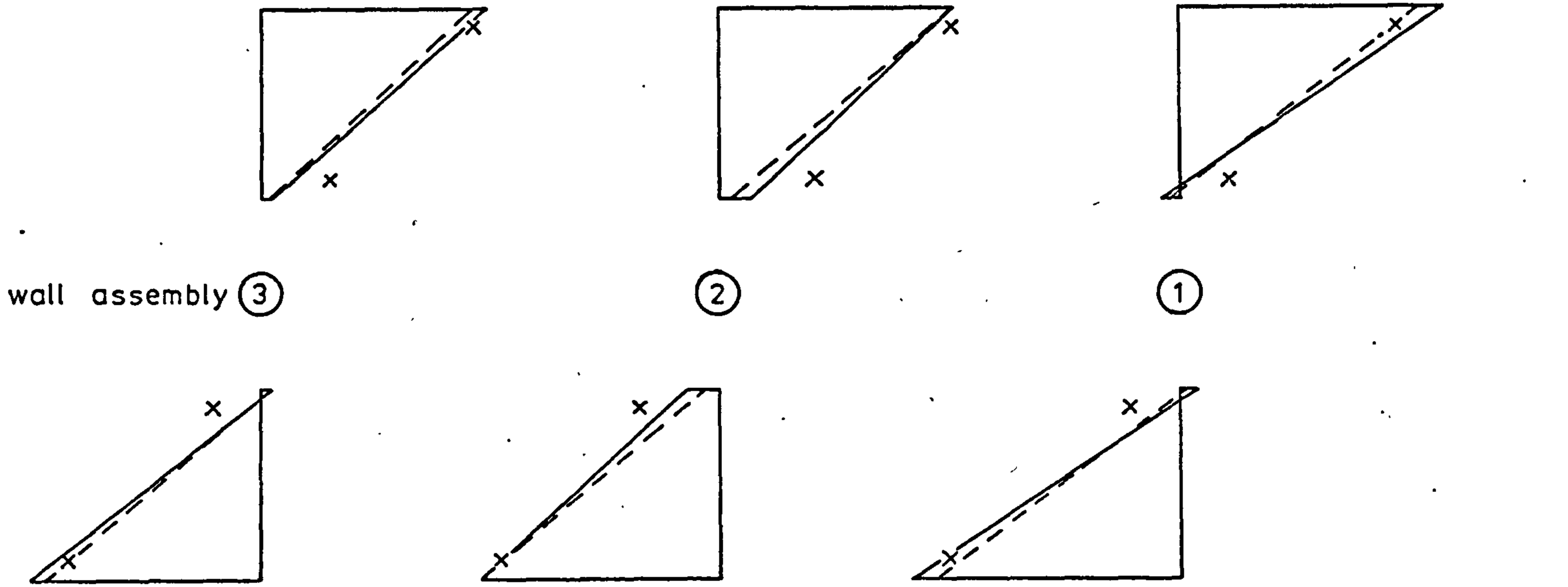

Test number 3 - Stresses

Figure 8.14

F 8.14

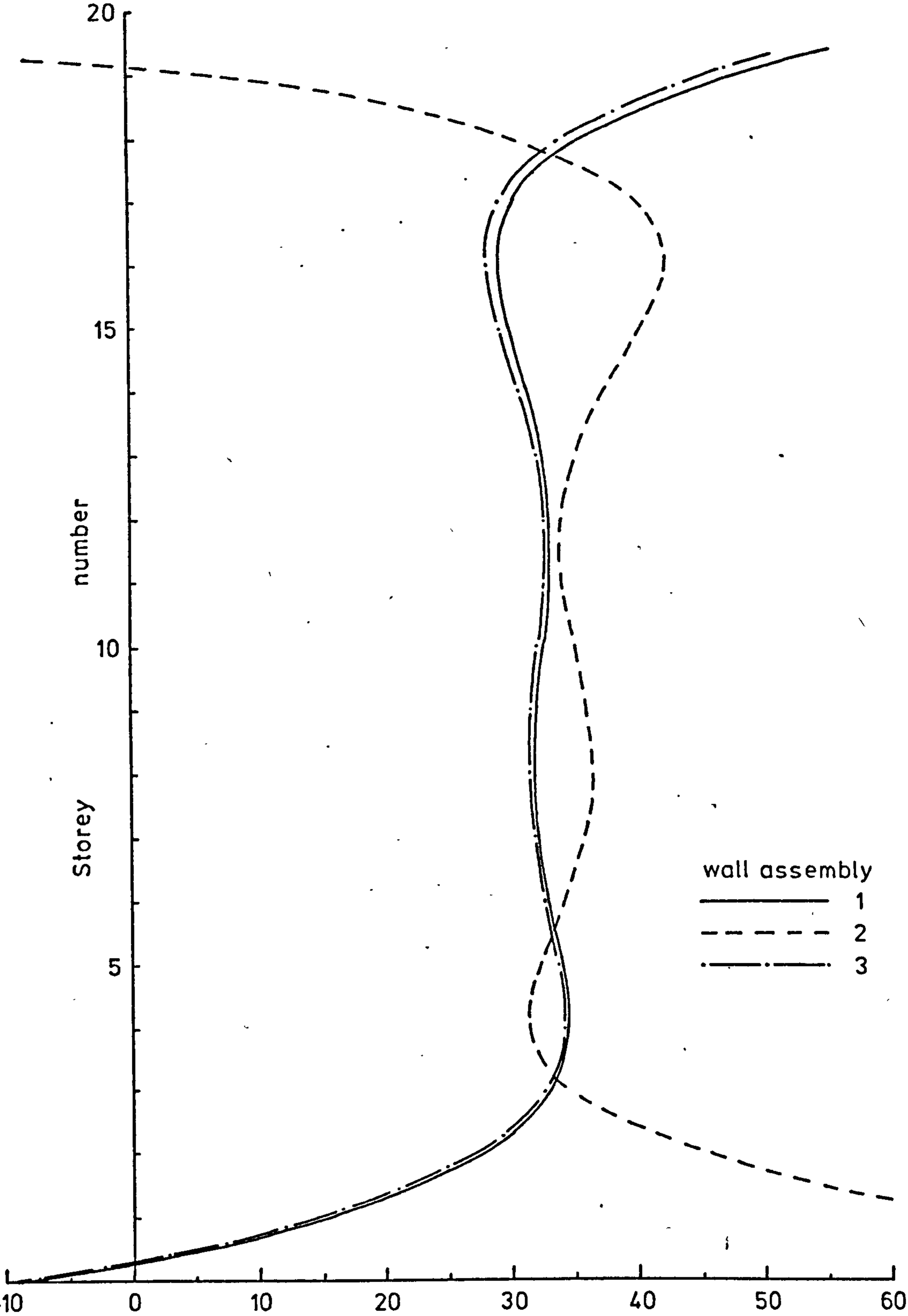

Test number 3 - Load distribution - Polynomial solution

Figure 8.15

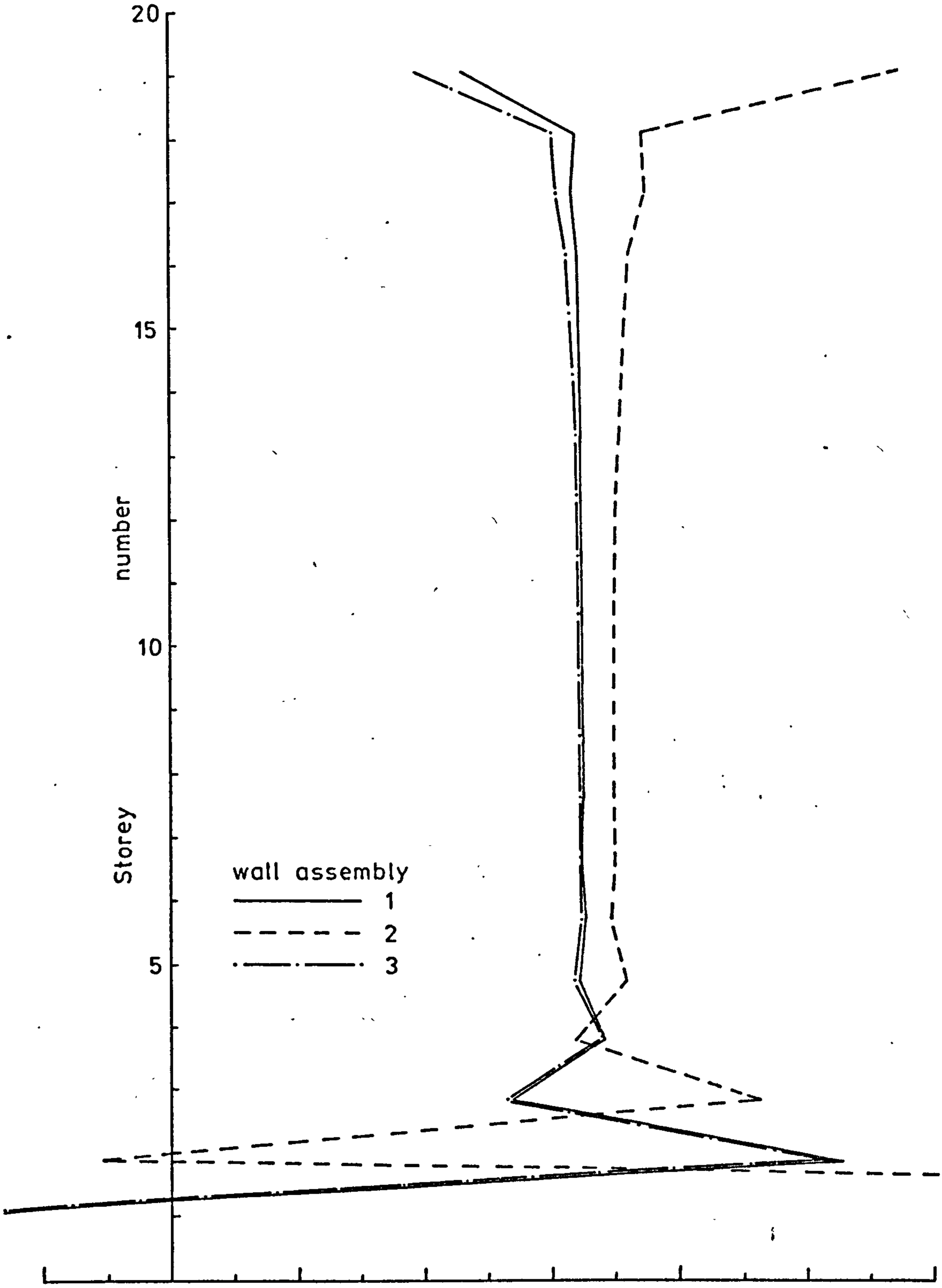

Test number 3 - Load distribution - Point load solution

Figure 8.16

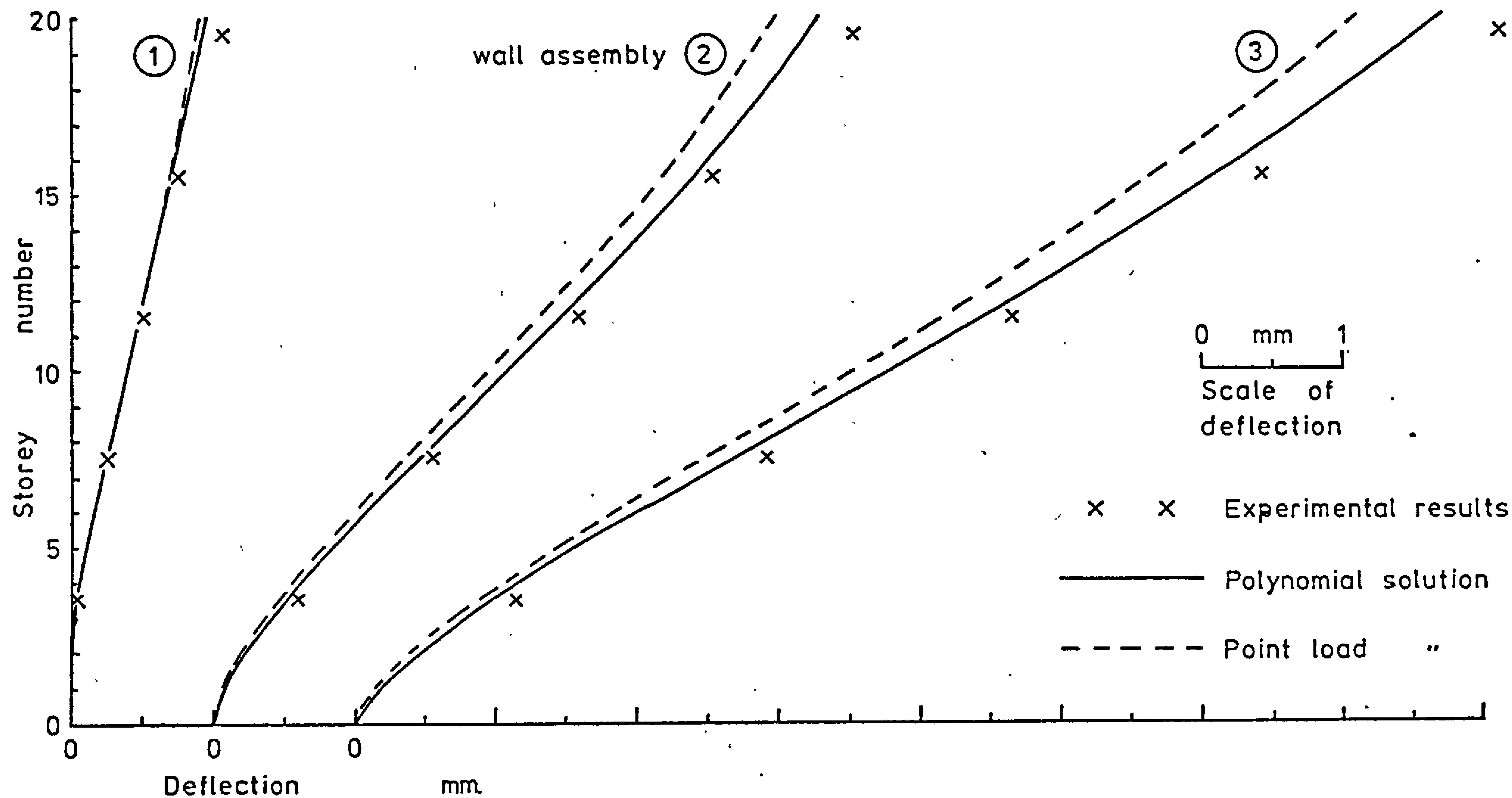

Test number 4 - Deflections

Figure 8.17

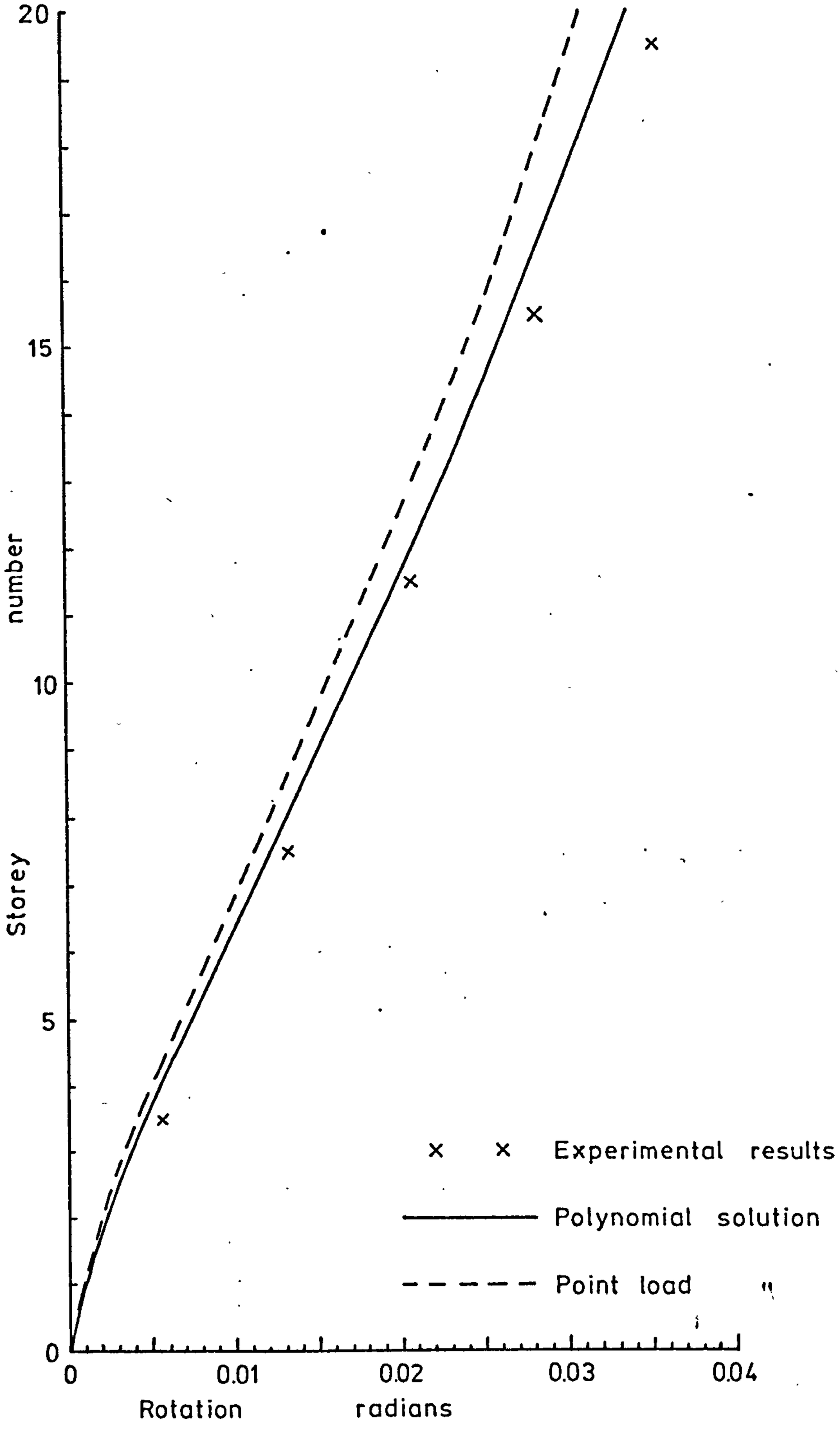

Test number 4 - Rotations

Figure 8.18

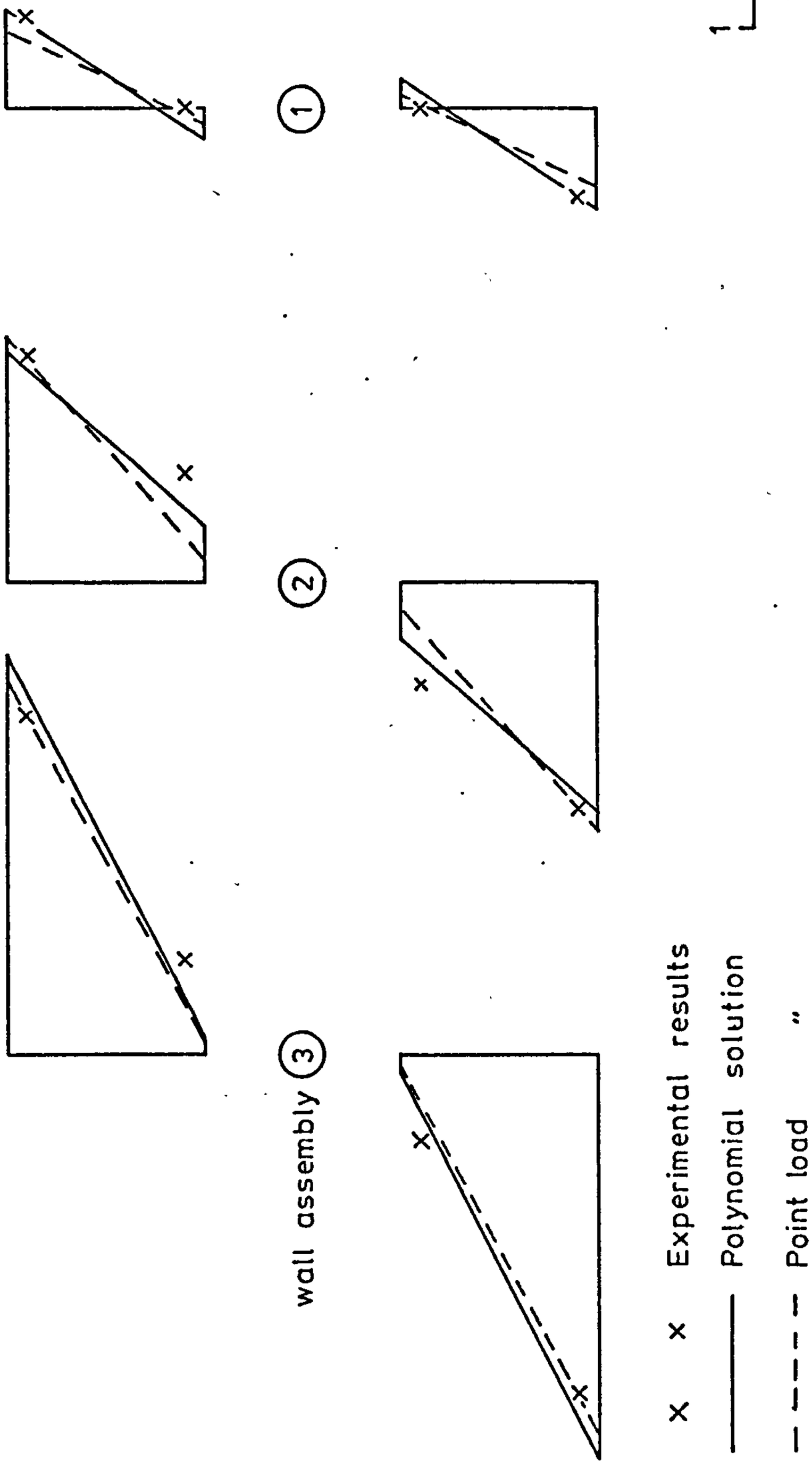

Test number 4 - Stresses

Figure 8.19

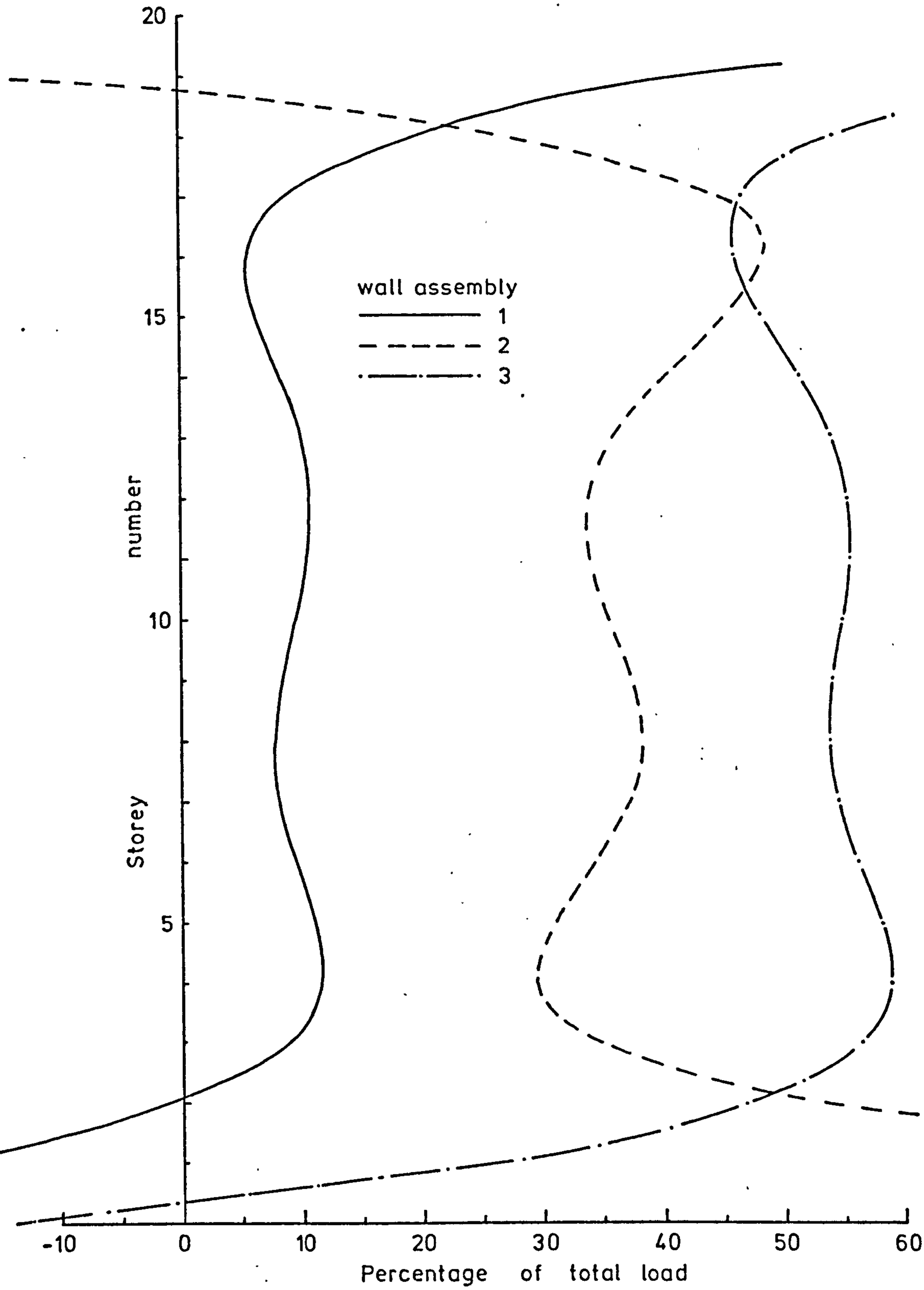

Test number 4 - Load distribution - Polynomial solution

Figure 8.20

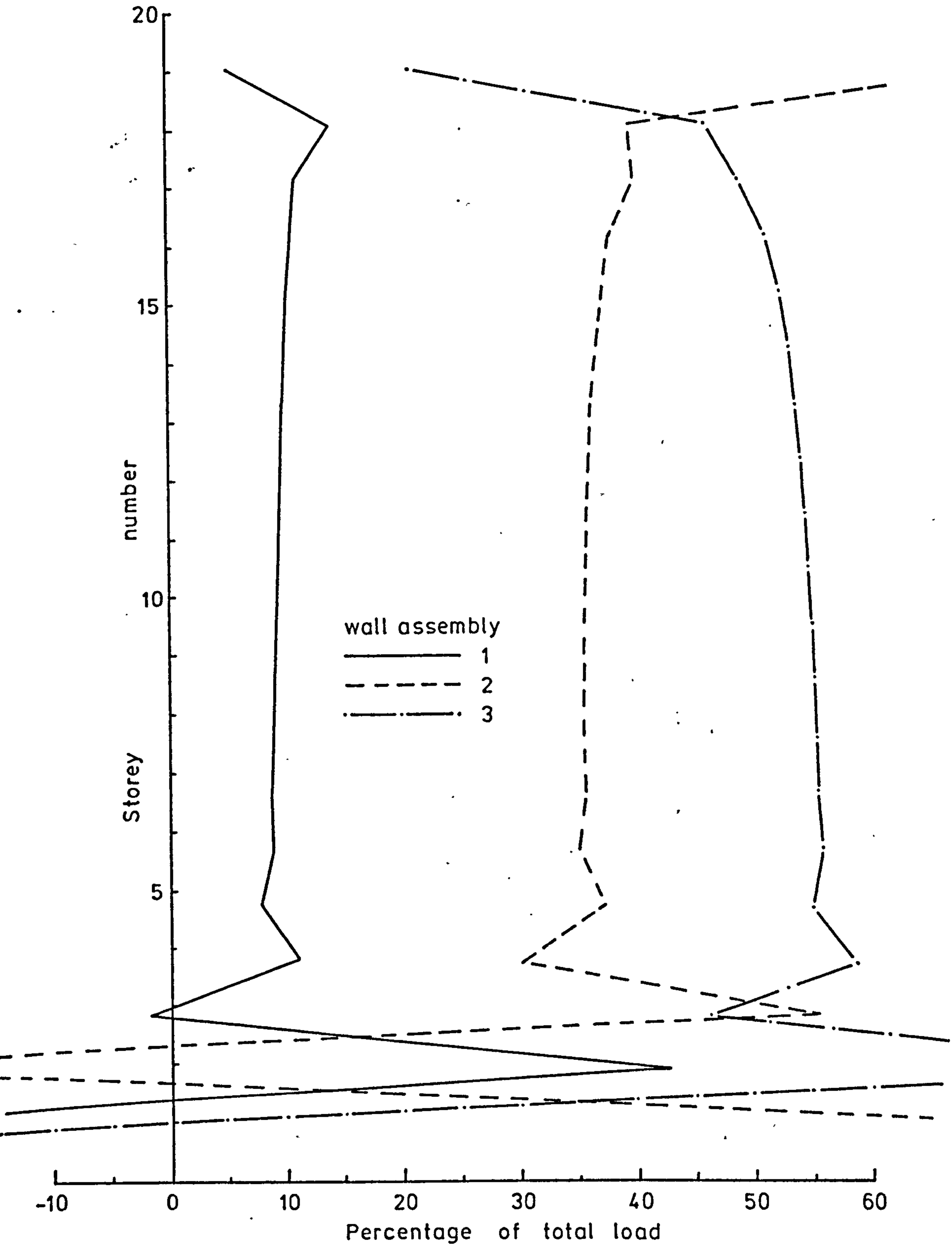

Test number 4 - Load distribution - Point load solution

Figure 8.21

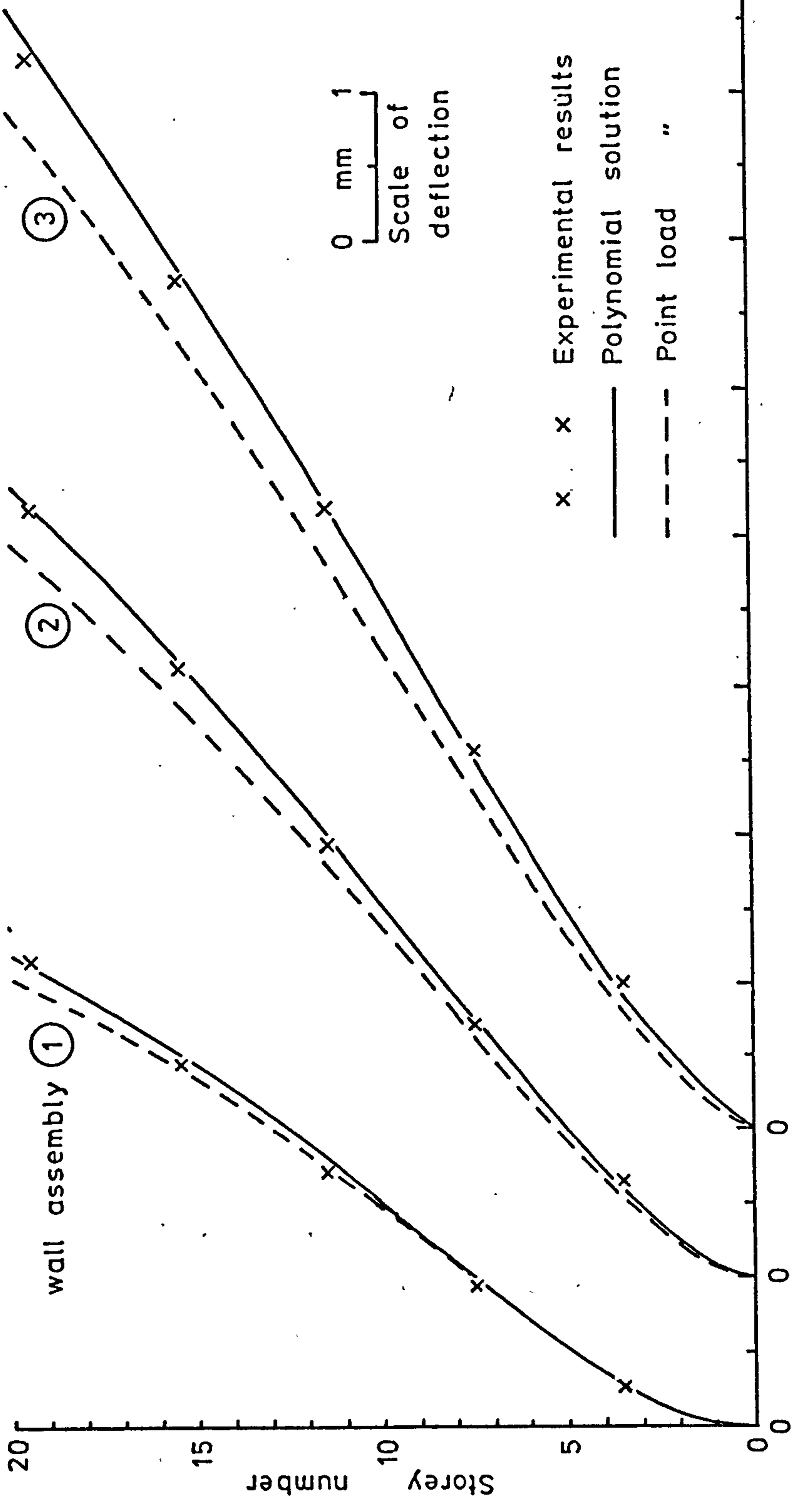

Test number 5 - Deflections

Figure 8.22

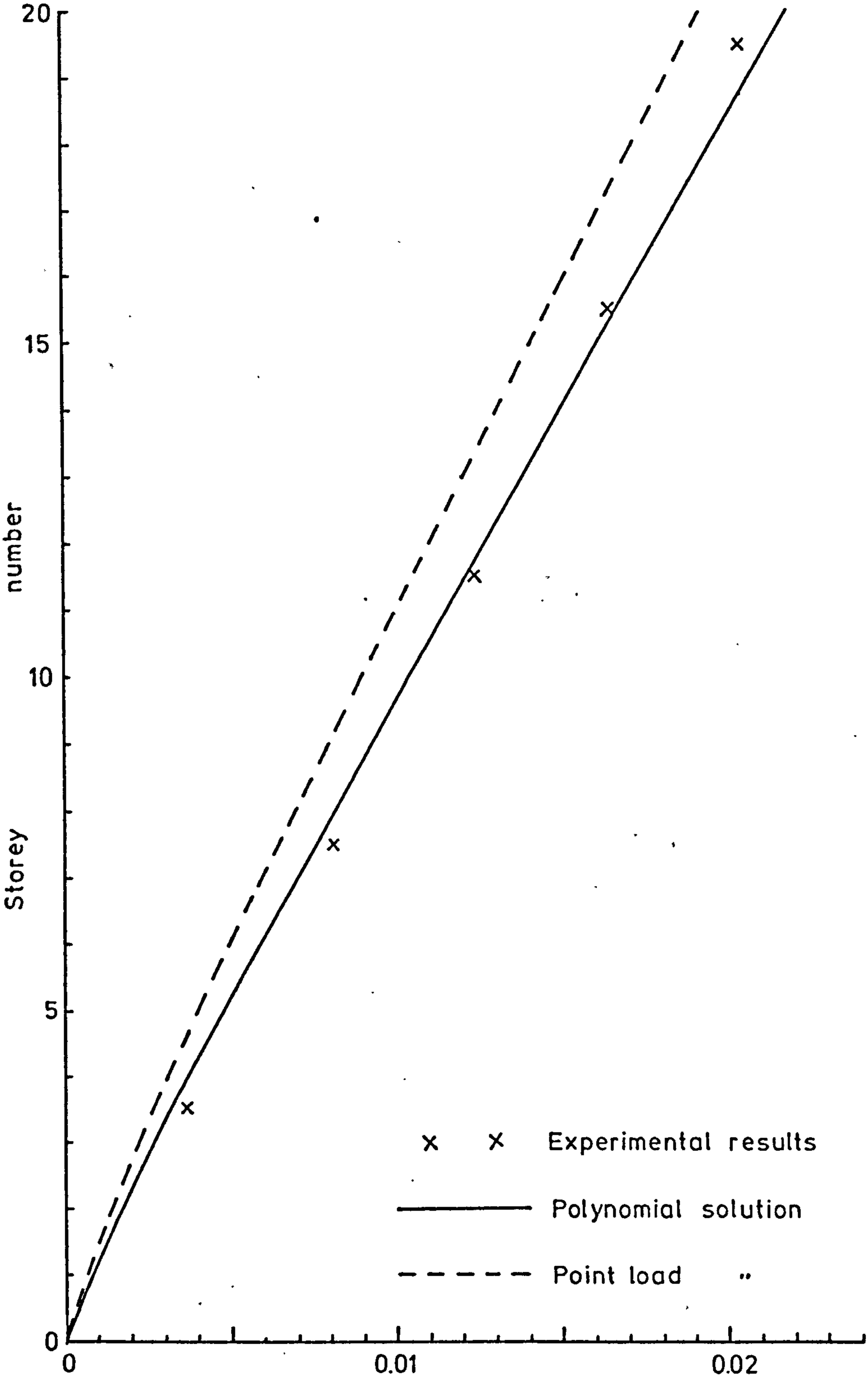

Test number 5 - Rotations

Figure 8.23

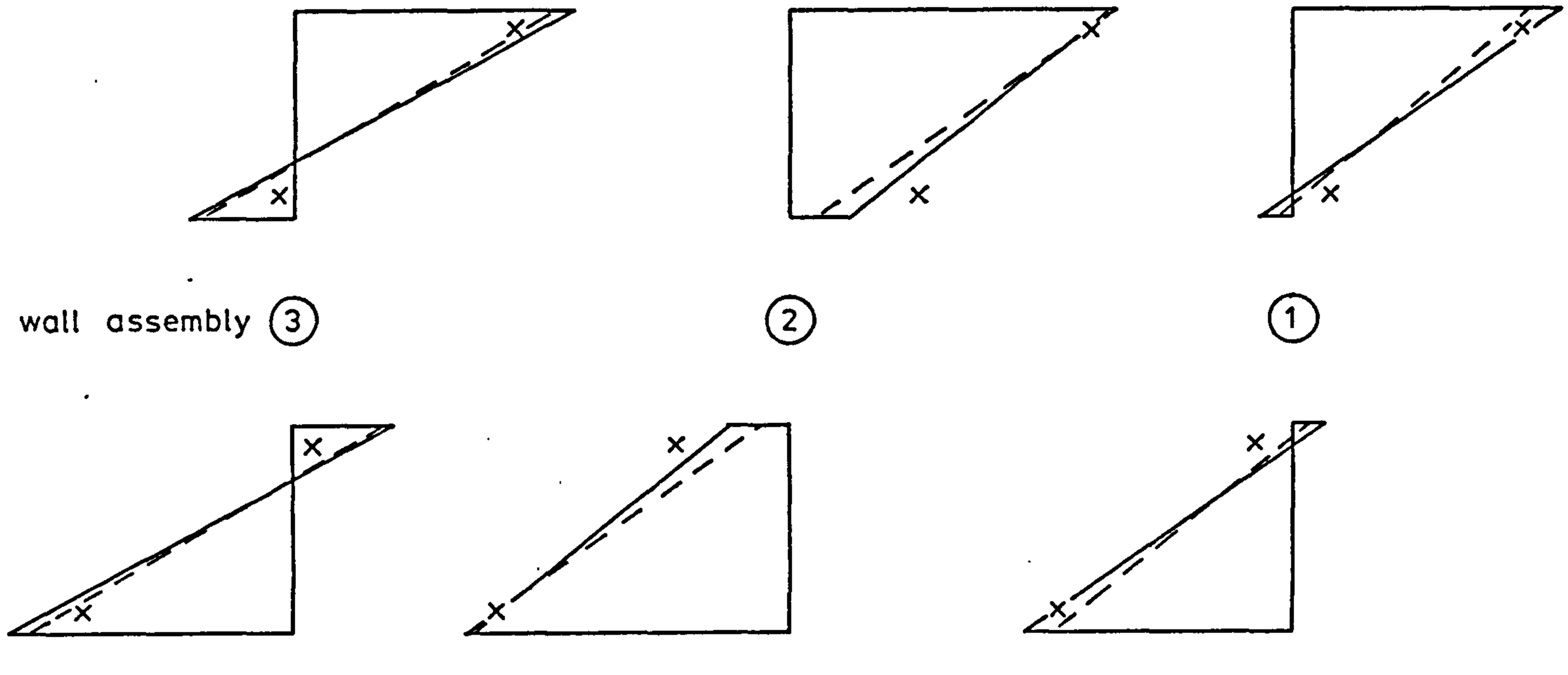

Test number 5 - Stresses

Figure 8.24

F 8.24

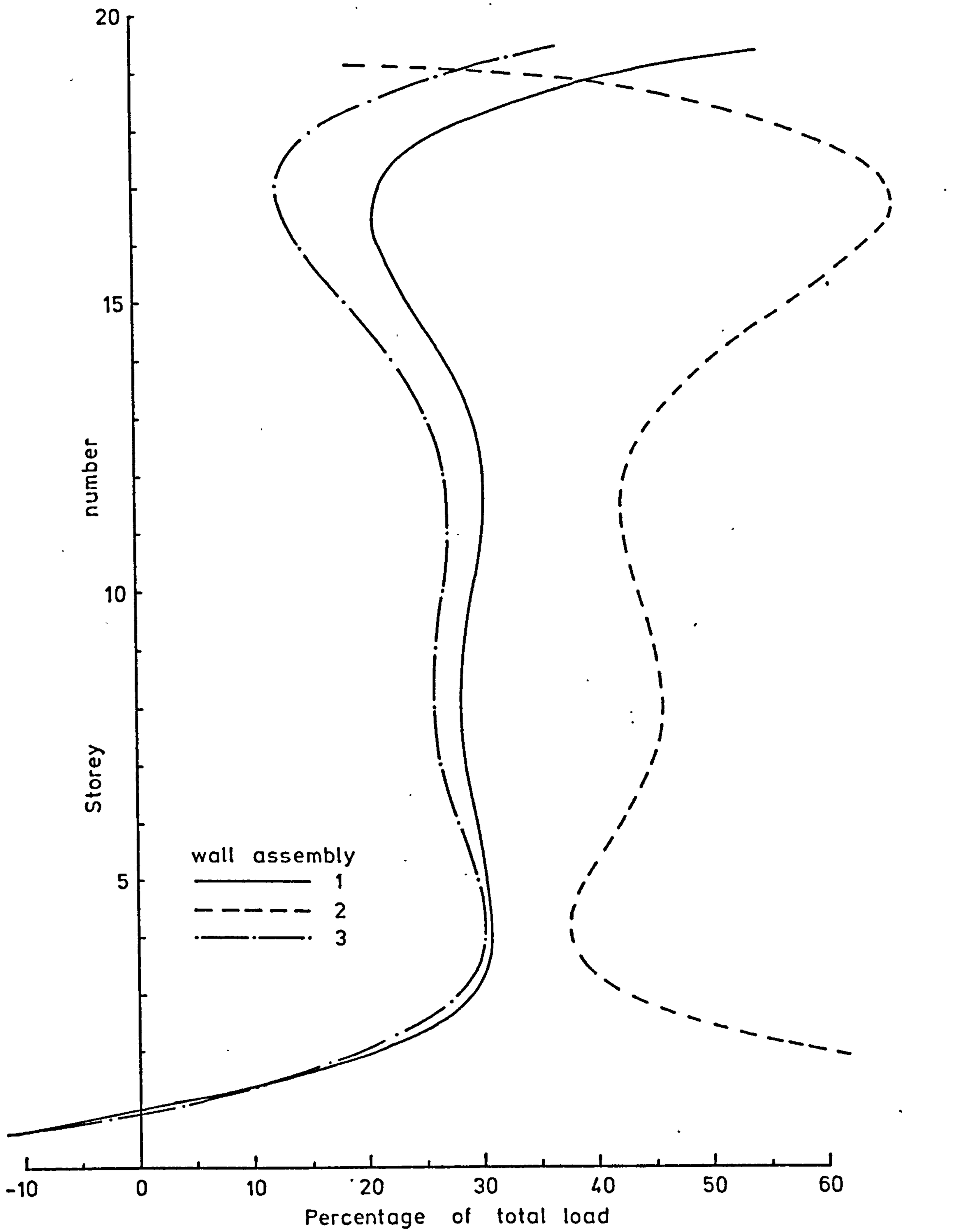

Test number 5 - Load distribution - Polynomial solution

Figure 8.25

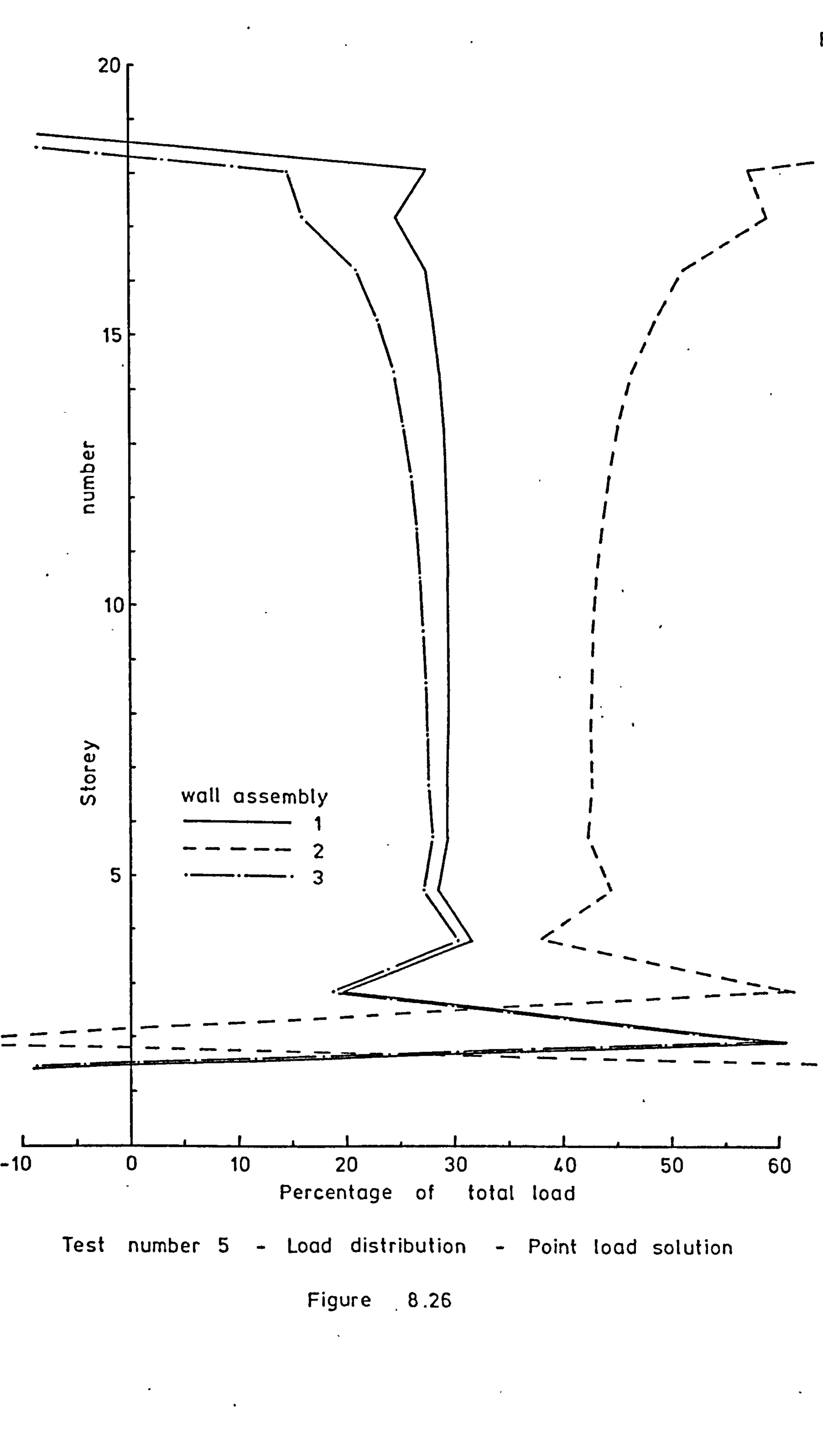

Test number 5 - Load distribution - Point load solution

Figure 8.26

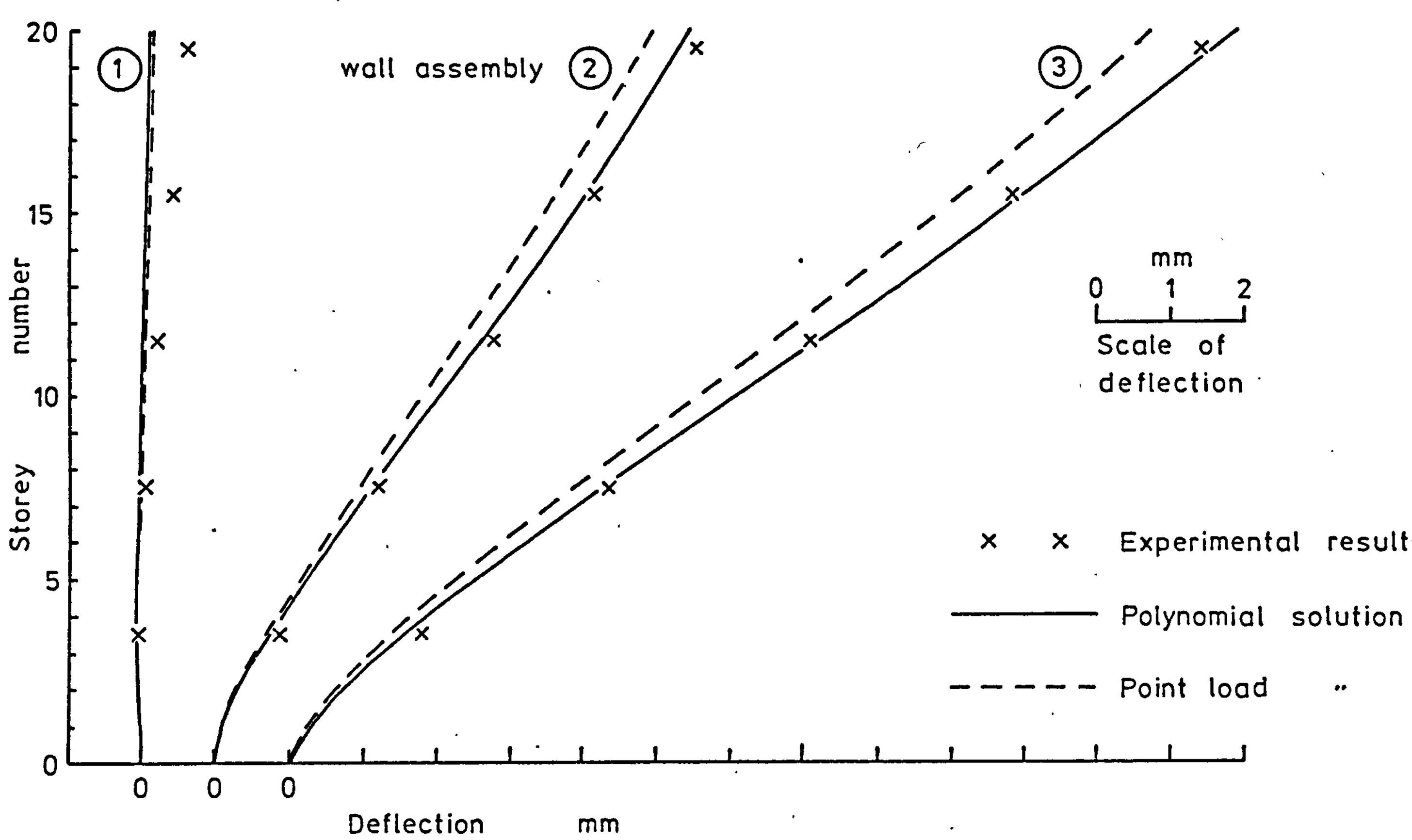

Test number 6 - Deflections

Figure 8.27

F 8.27

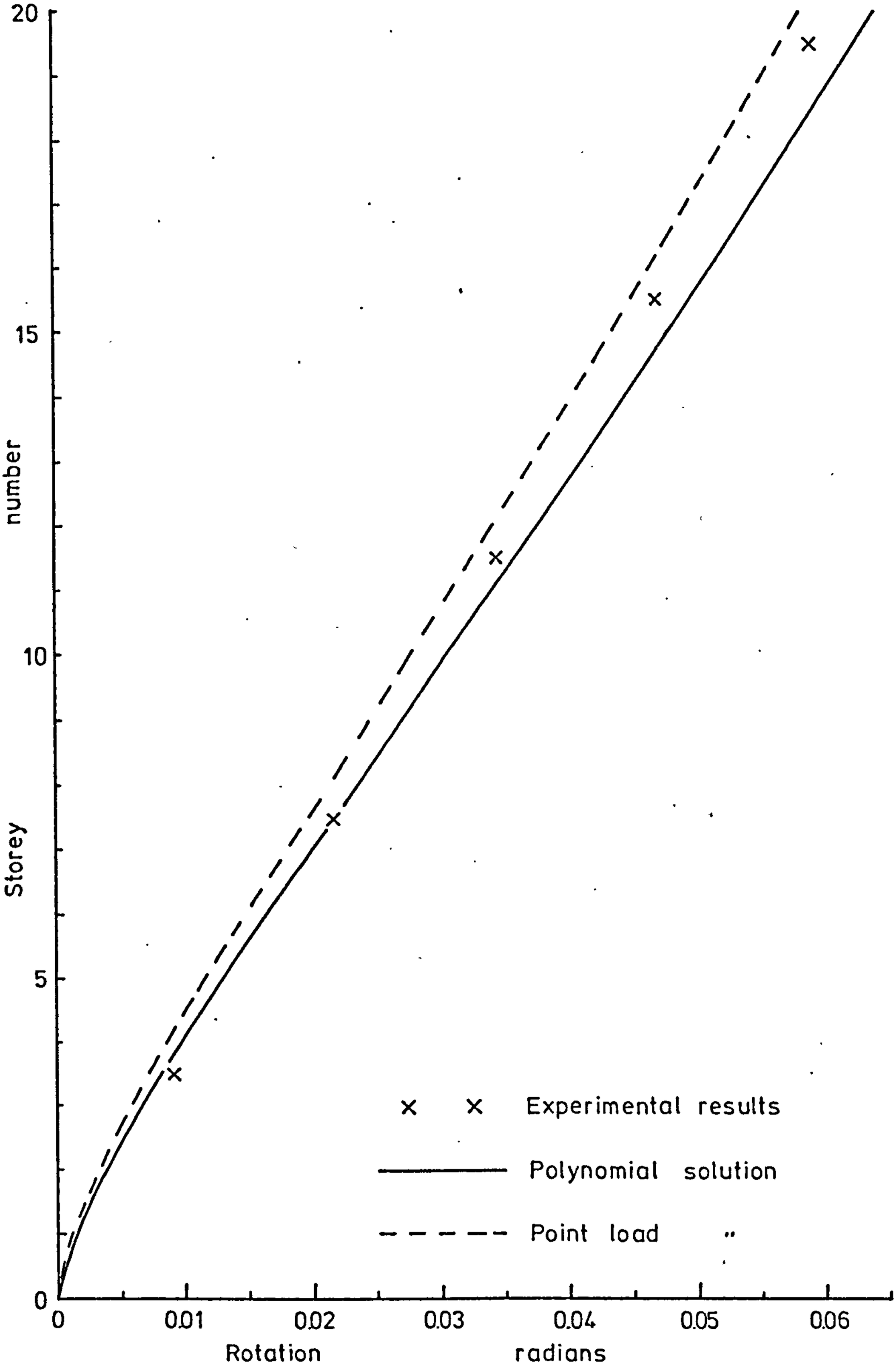

Test number 6 - Rotations

Figure 8.28

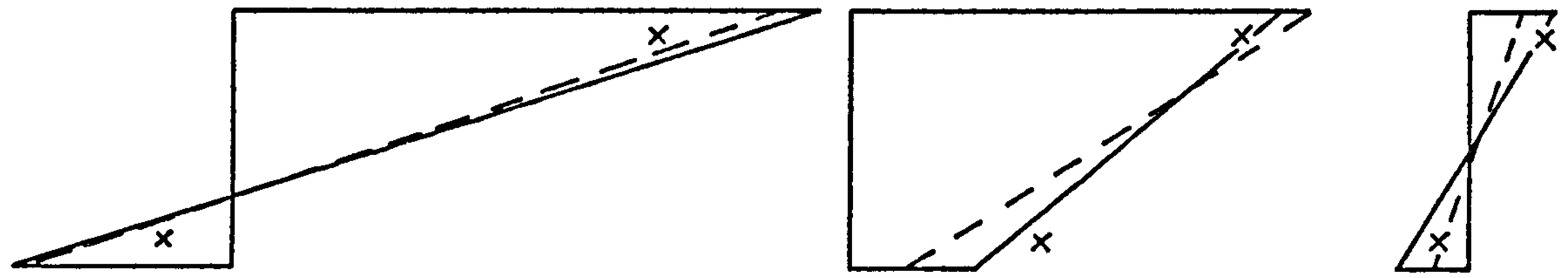

wall assembly ③ ② ①

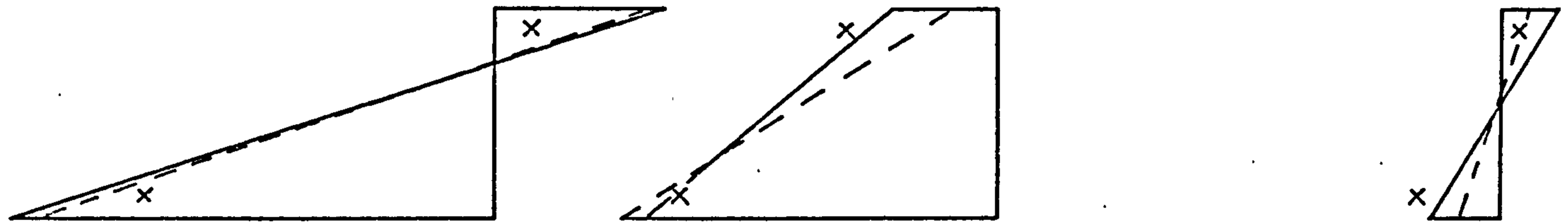

× × Experimental results

——— Polynomial solution

– – – – – Point load "

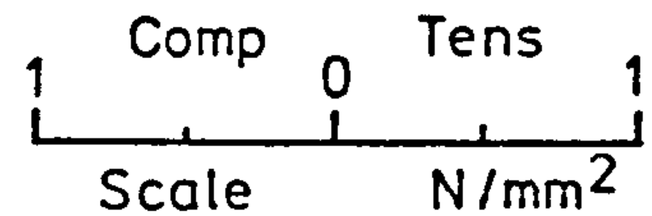

Test number 6 - Stresses

Figure 8.29

F 8.29

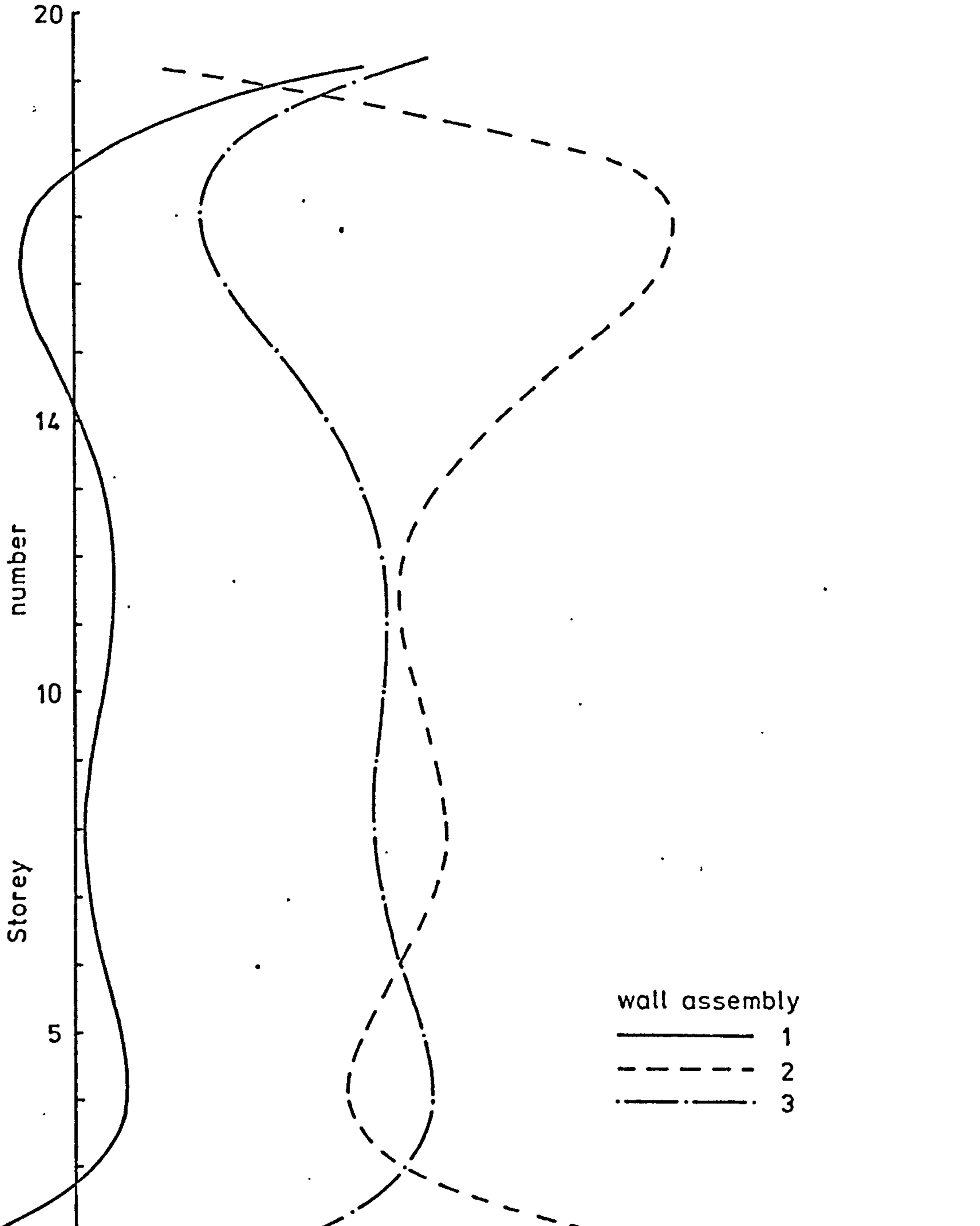

Test number 6 - Load distribution - Polynomial solution

Figure 8.30

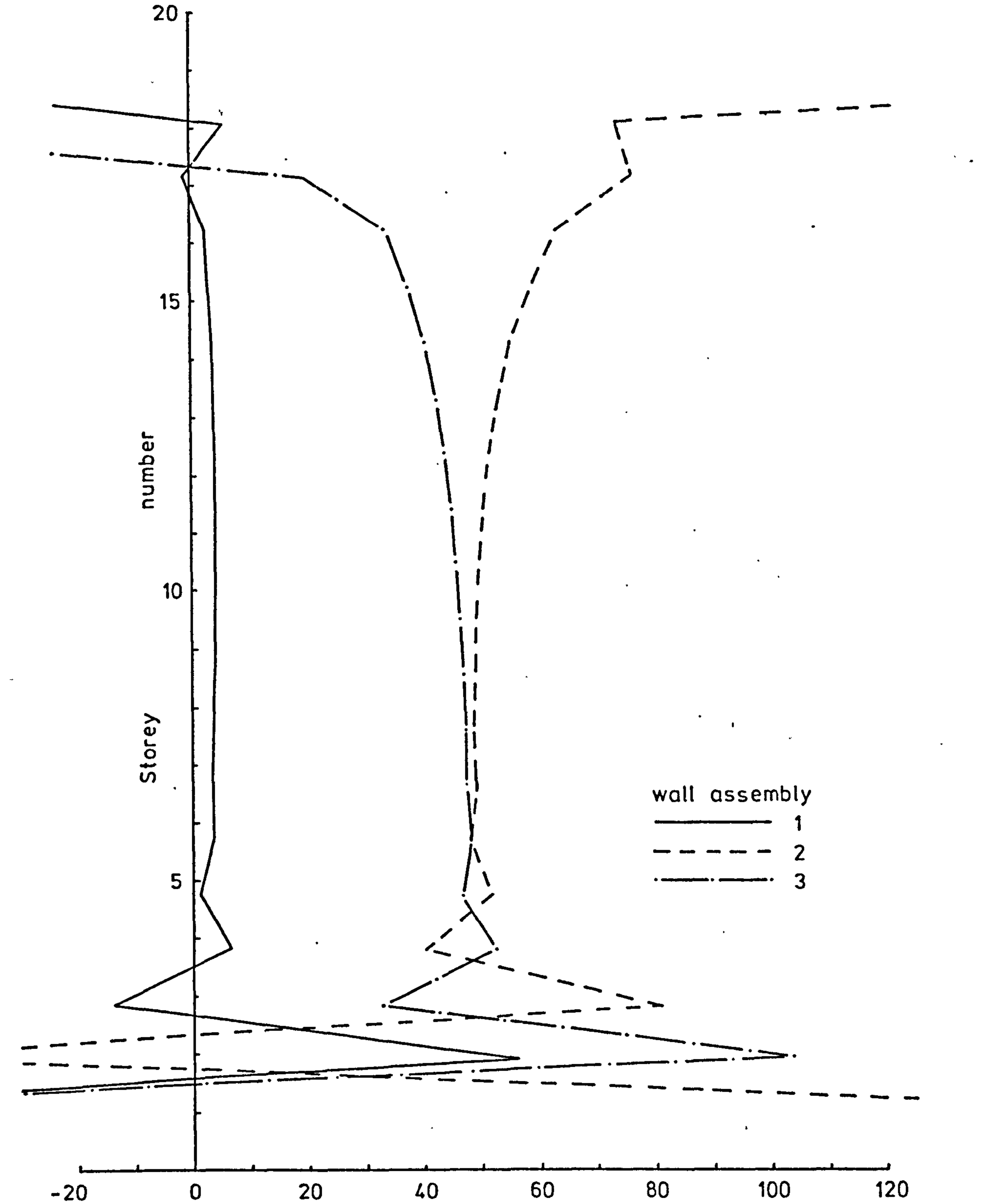

Test number 6 - Load distribution - Point load solution

Figure 8.31

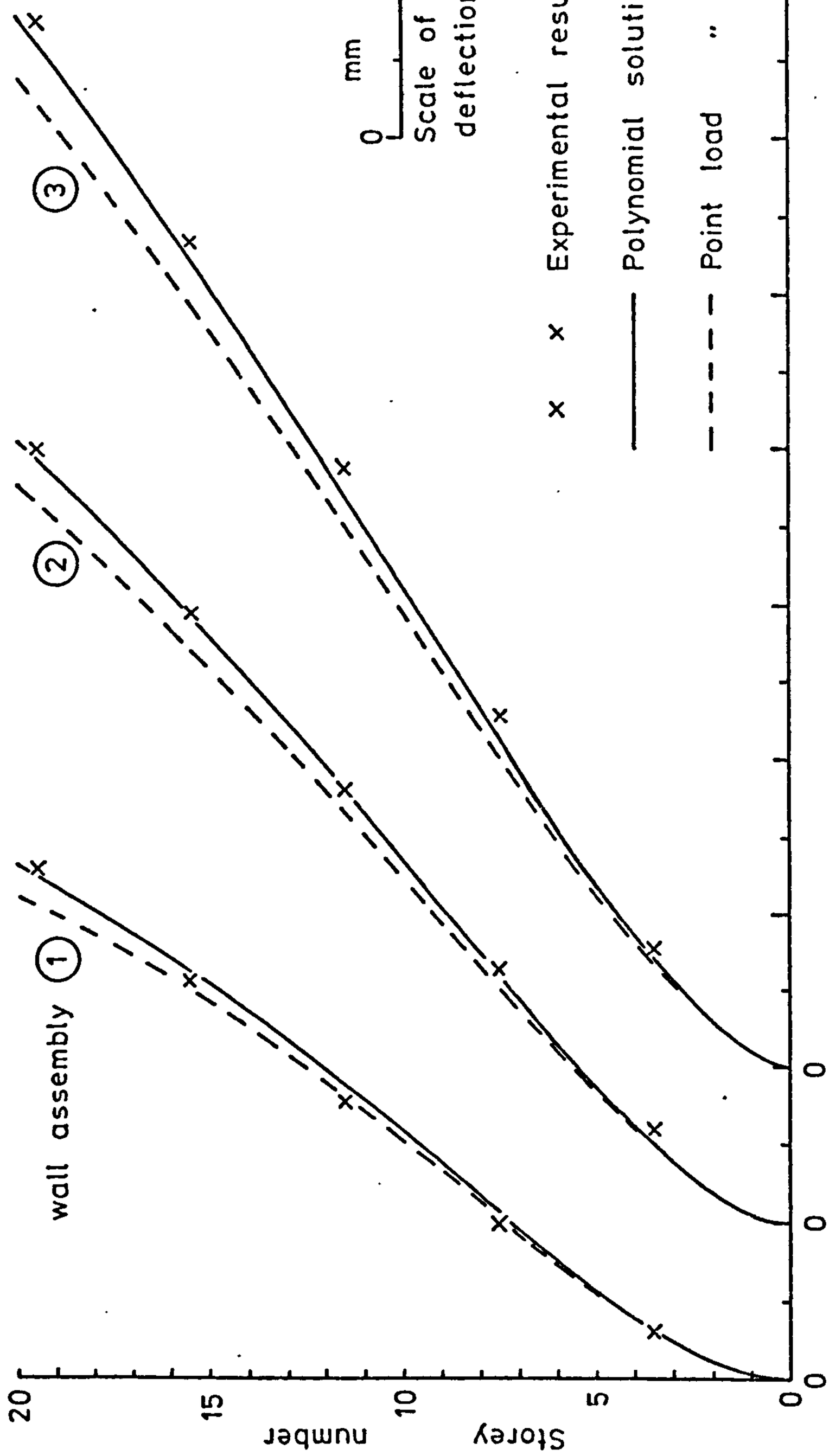
wall assembly
1
2
3
Storey number
20
15
10
5
0
0
Deflection
mm
Test number 7 - Deflections
0
mm
1
Scale of deflection
x Experimental results
Polynomial solution
Point loads

Figure 8.32

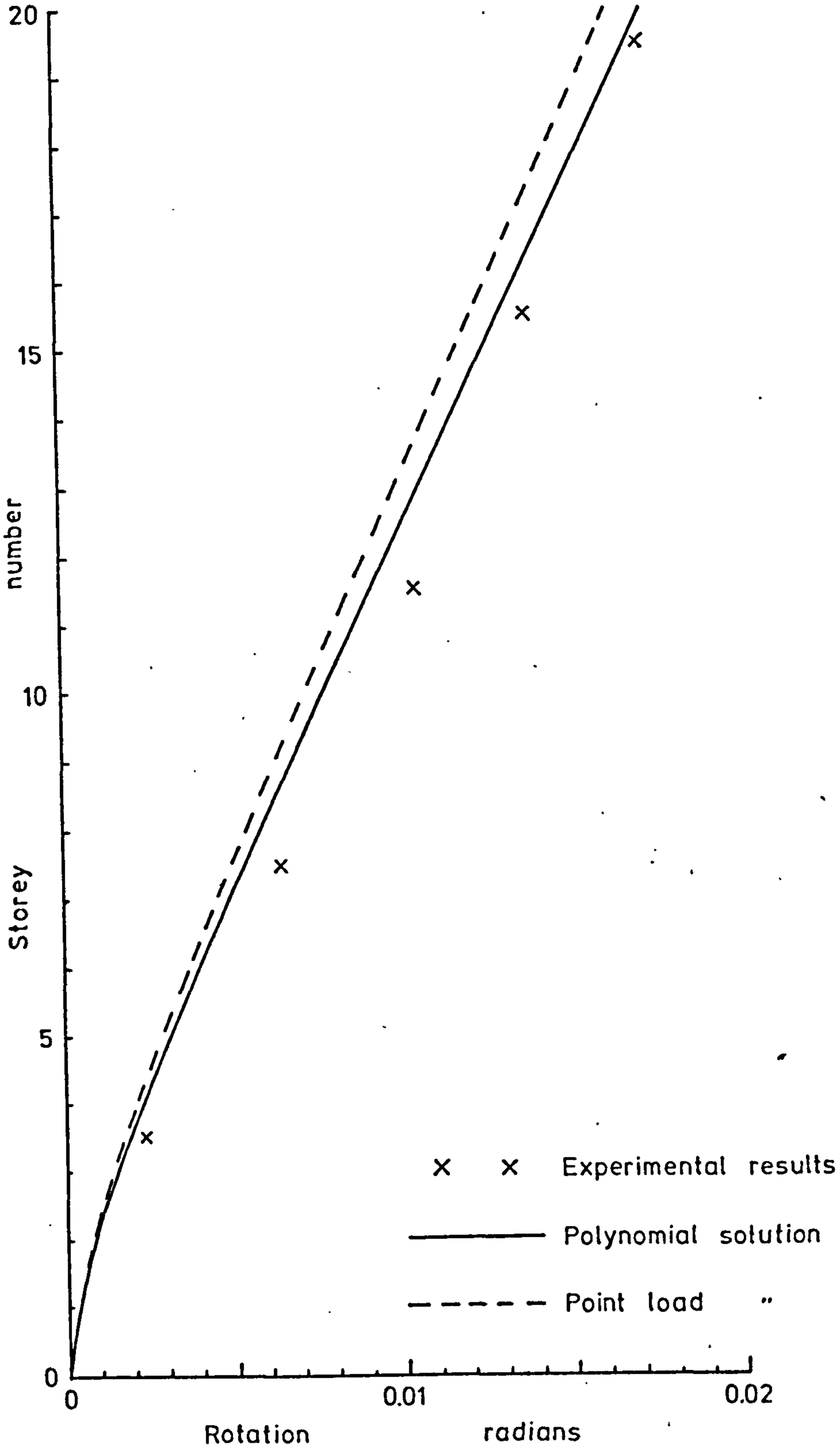

Test number 7 - Rotations

Figure 8.33

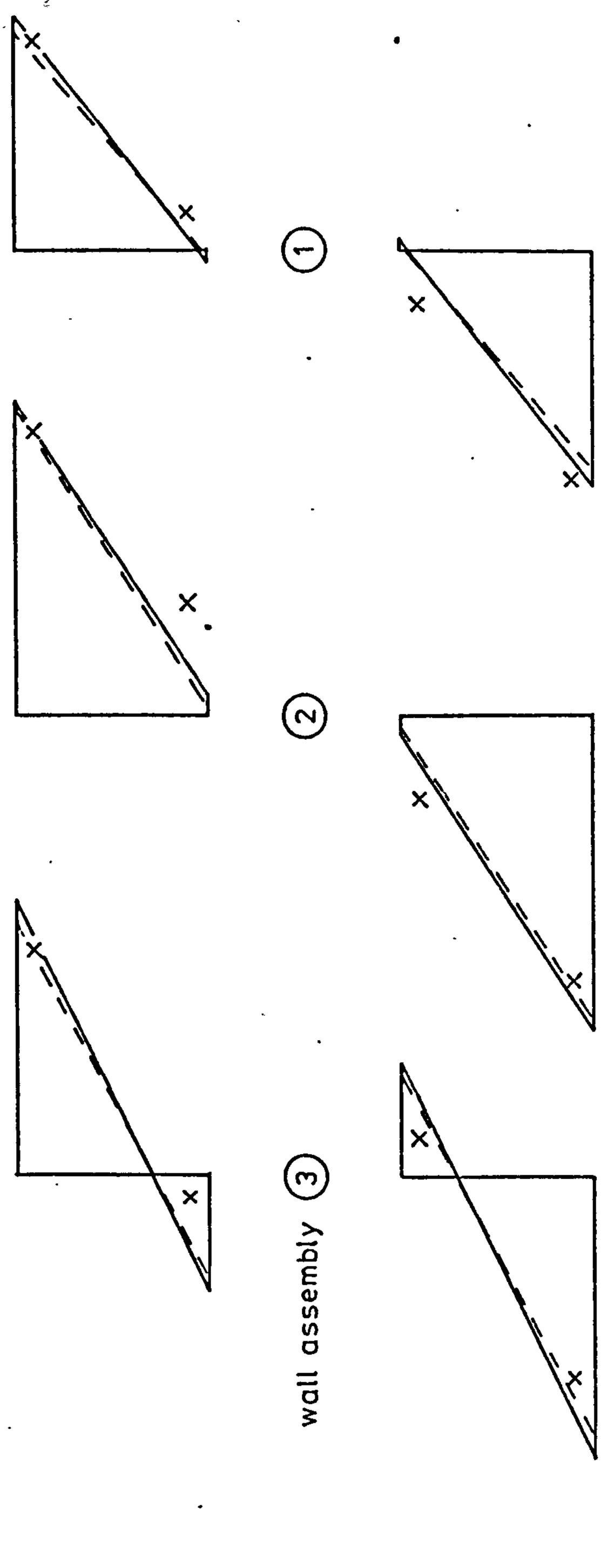
Comp. 0 Tens.
1 1
Scale N/mm2
1
2
3
Wall assembly
Stresses
8.34
Experimental results
Polynomial solution
Point load
Test number 7

Figure 8

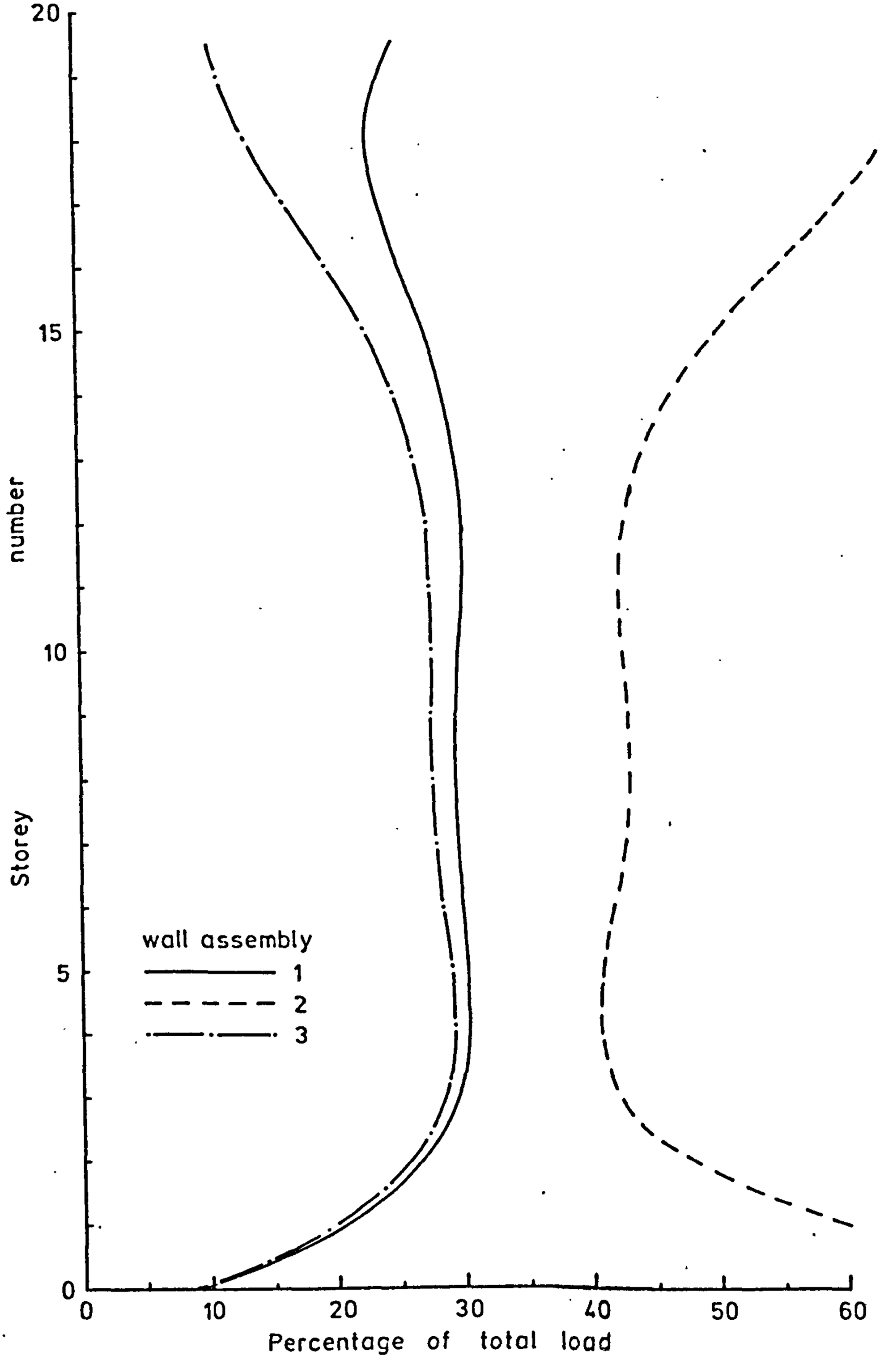

Test number 7 - Load distribution - Polynomial solution

Figure 8.35 .

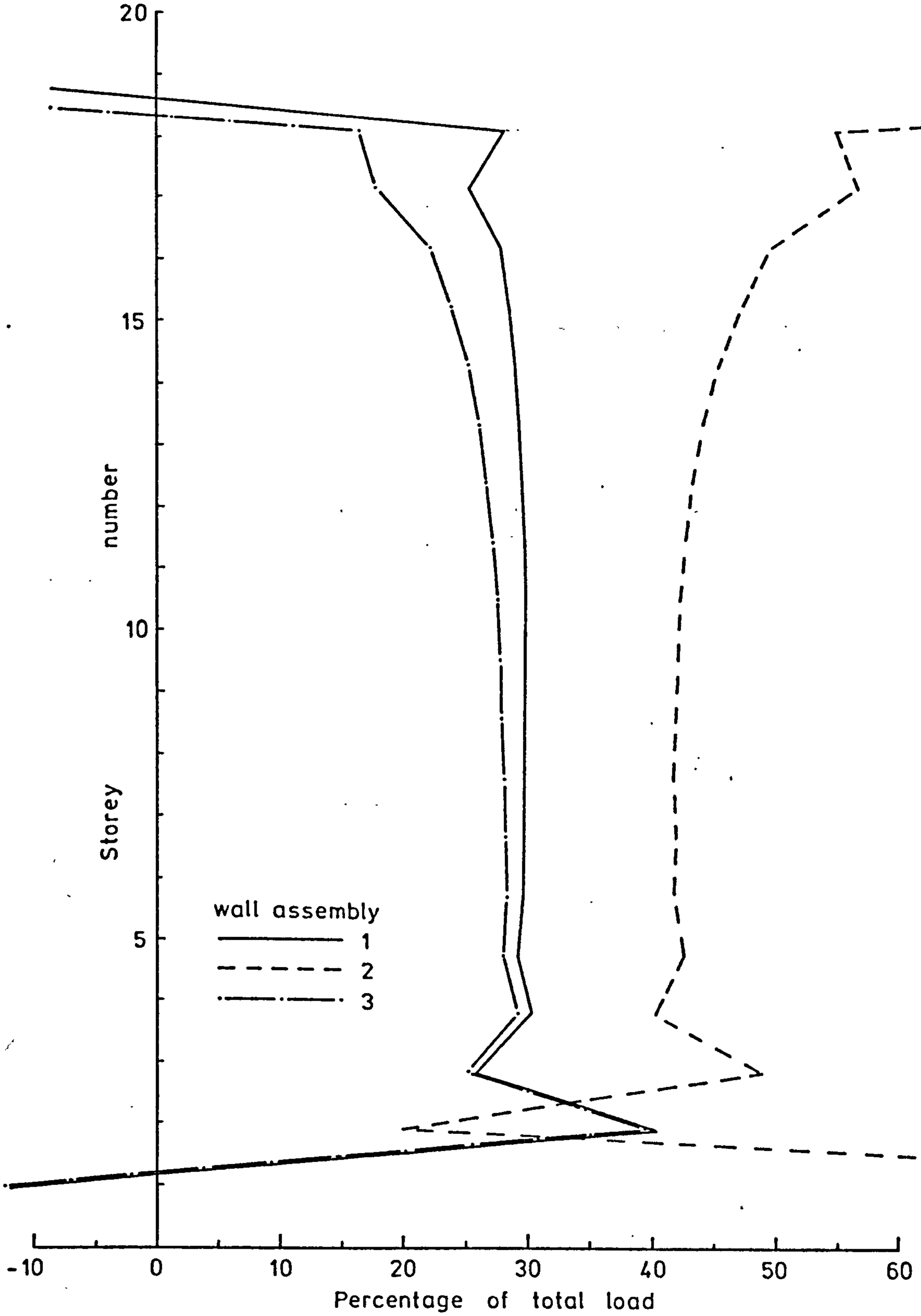

Test number 7 - Load distribution - Point load solution

Figure 8.36

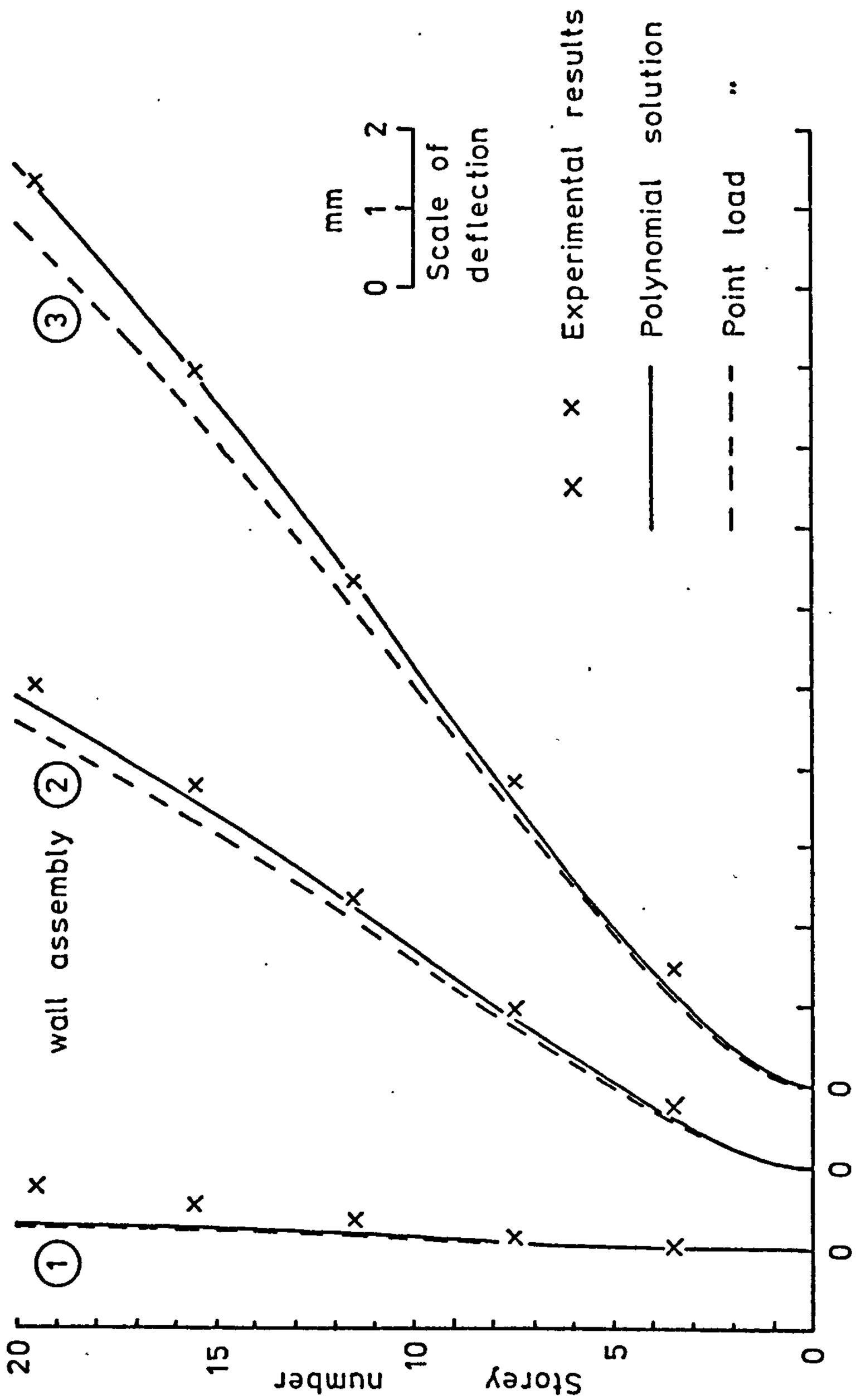
Storey number
20
15
10
5
0
Deflections
Deflection mm
0
0
Test number 8 - wall assembly
1
2
3
Scale of deflection
0 1 2 mm
X X Experimental results
Polynomial solution
Point load "

Figure 8.37

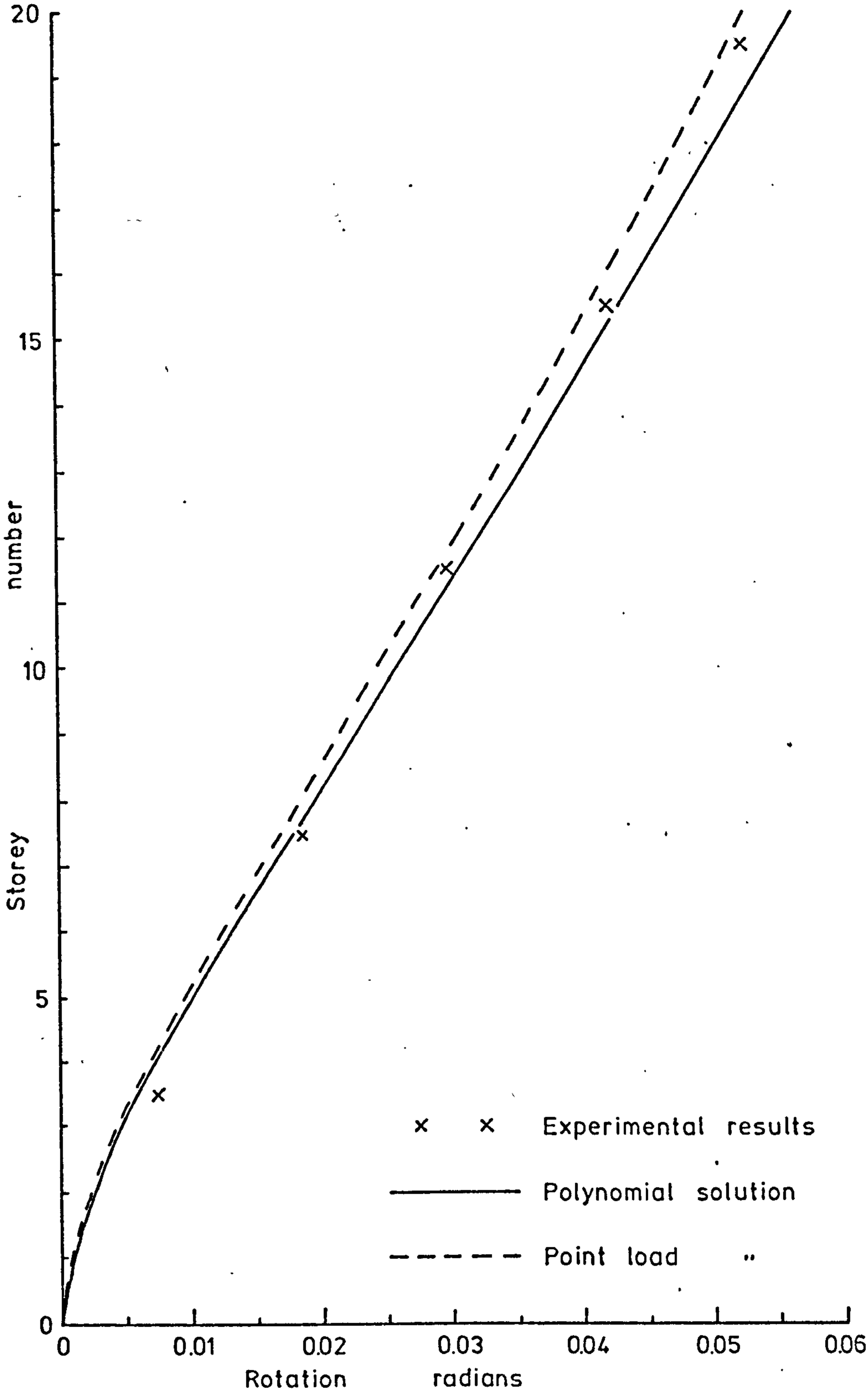

Test number 8 - Rotations

Figure 8.38

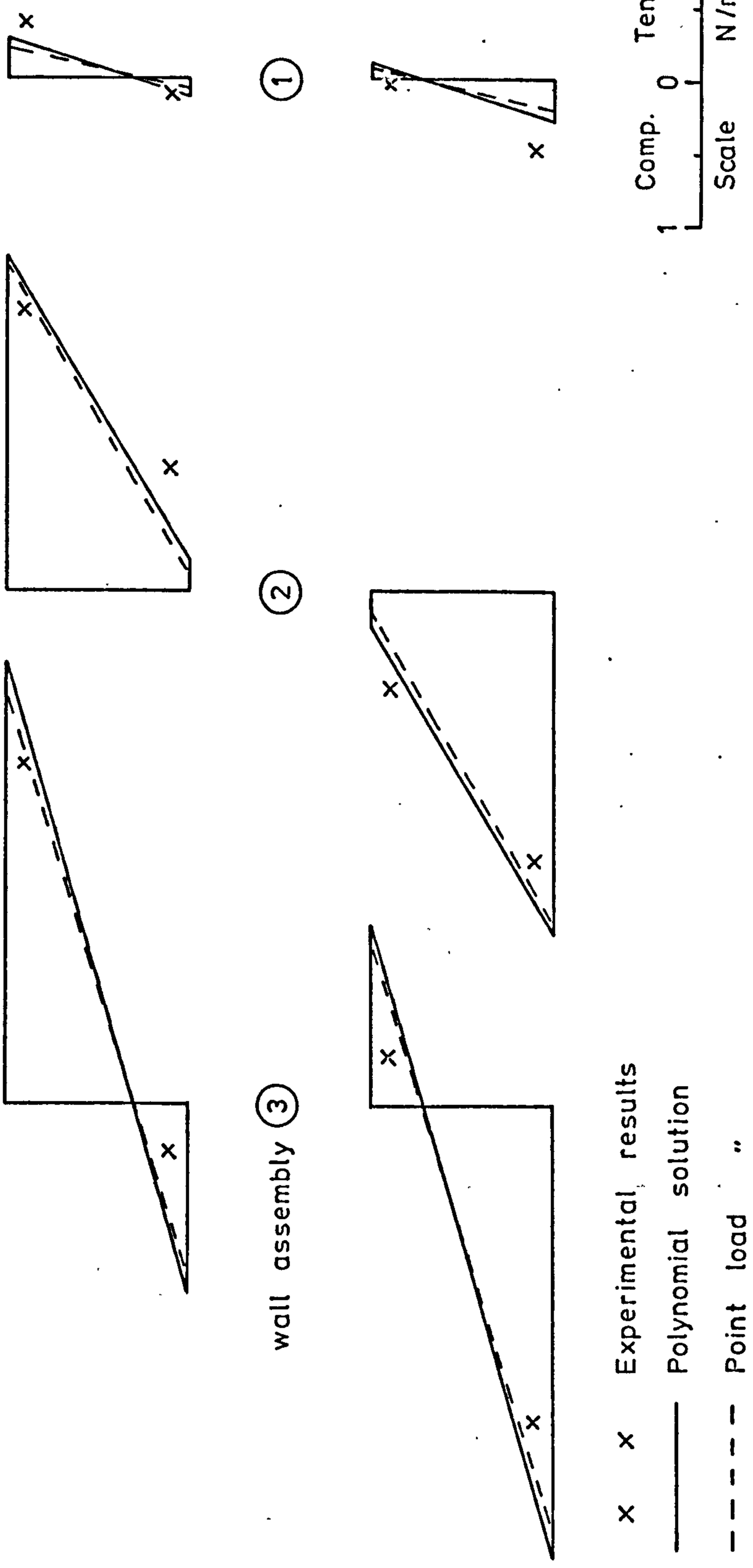

Test number 8 – Stresses

Figure 8.39

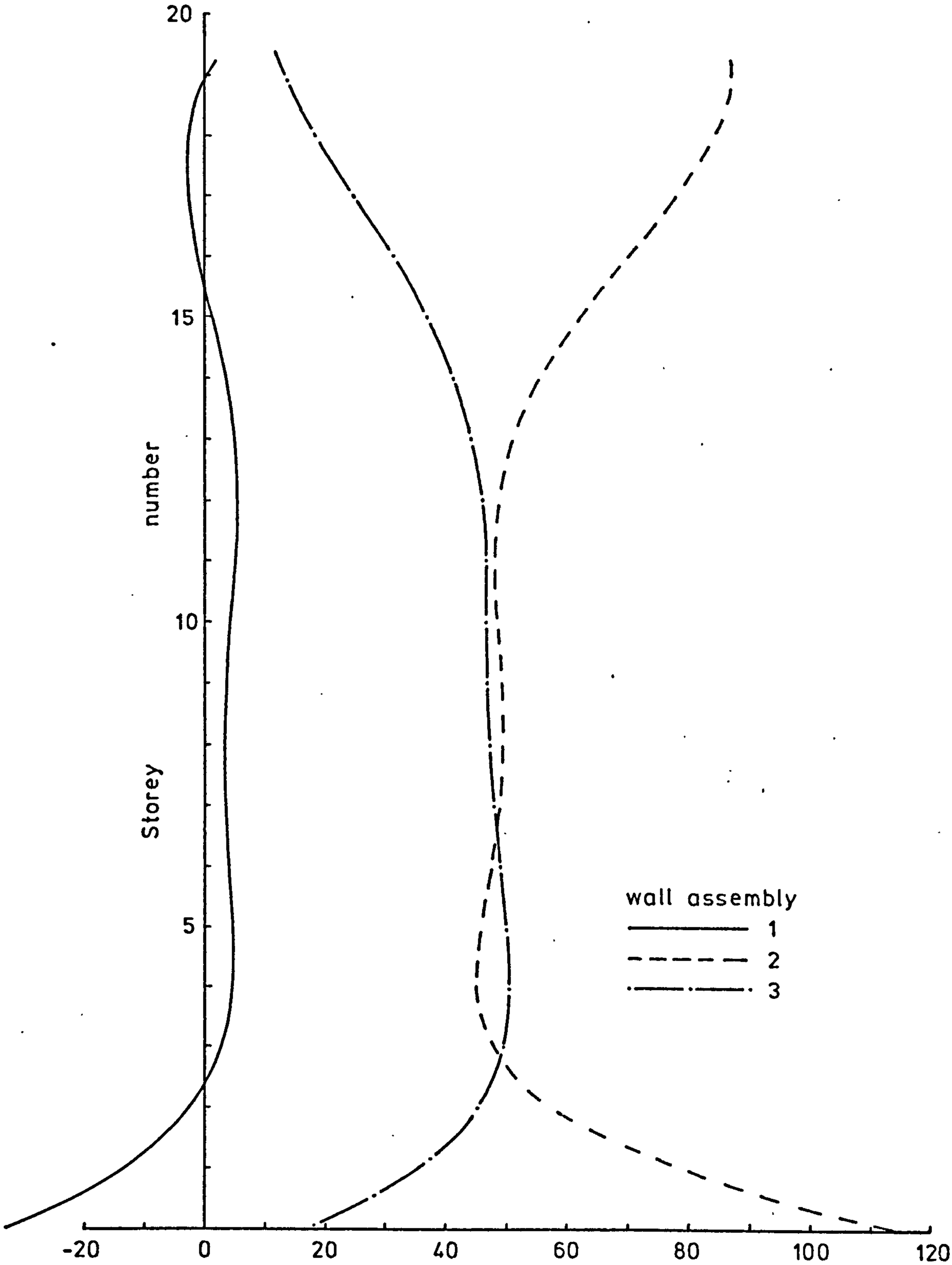

Test number 8. - Load distribution - Polynomial solution

Figure 8.40

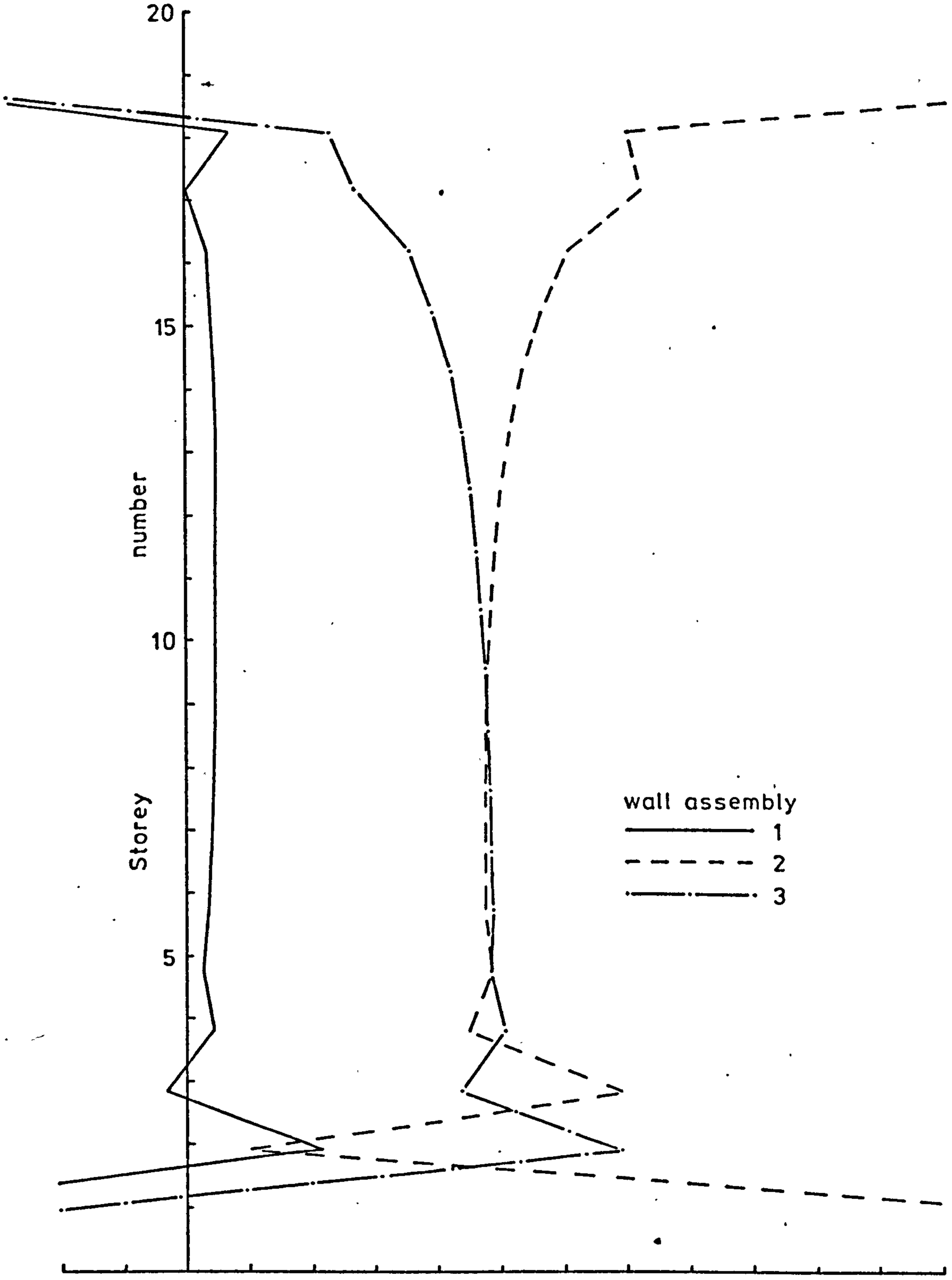

Test number 8 - Load distribution - Point load solution

Figure 8.41

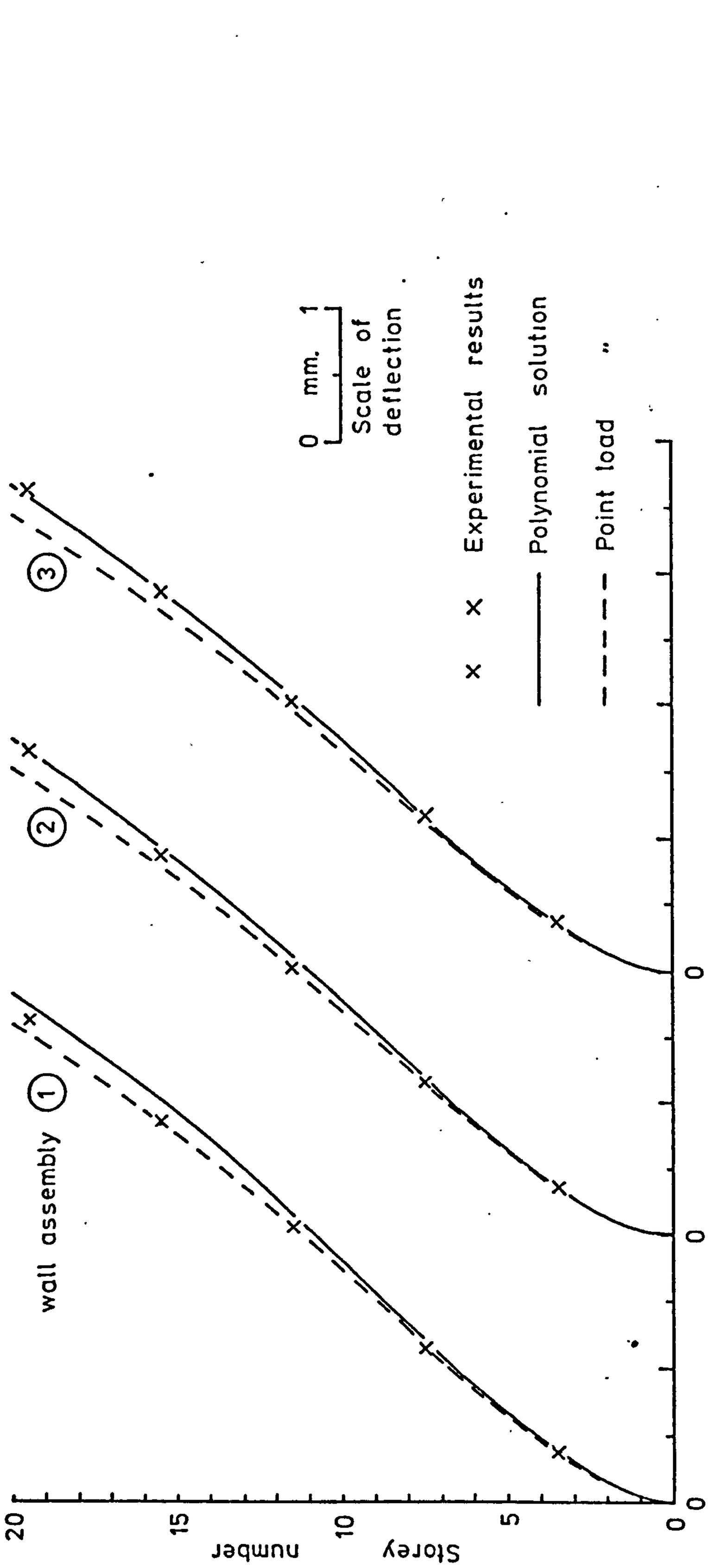
0 mm. 1
Scale of deflection
x x Experimental results
Polynomial solution
Point load "
Deflections
8.42
Test number 9
Figure
wall assembly ①
②
③
0
Deflection mm.
0
5
10
15
20
Storey number

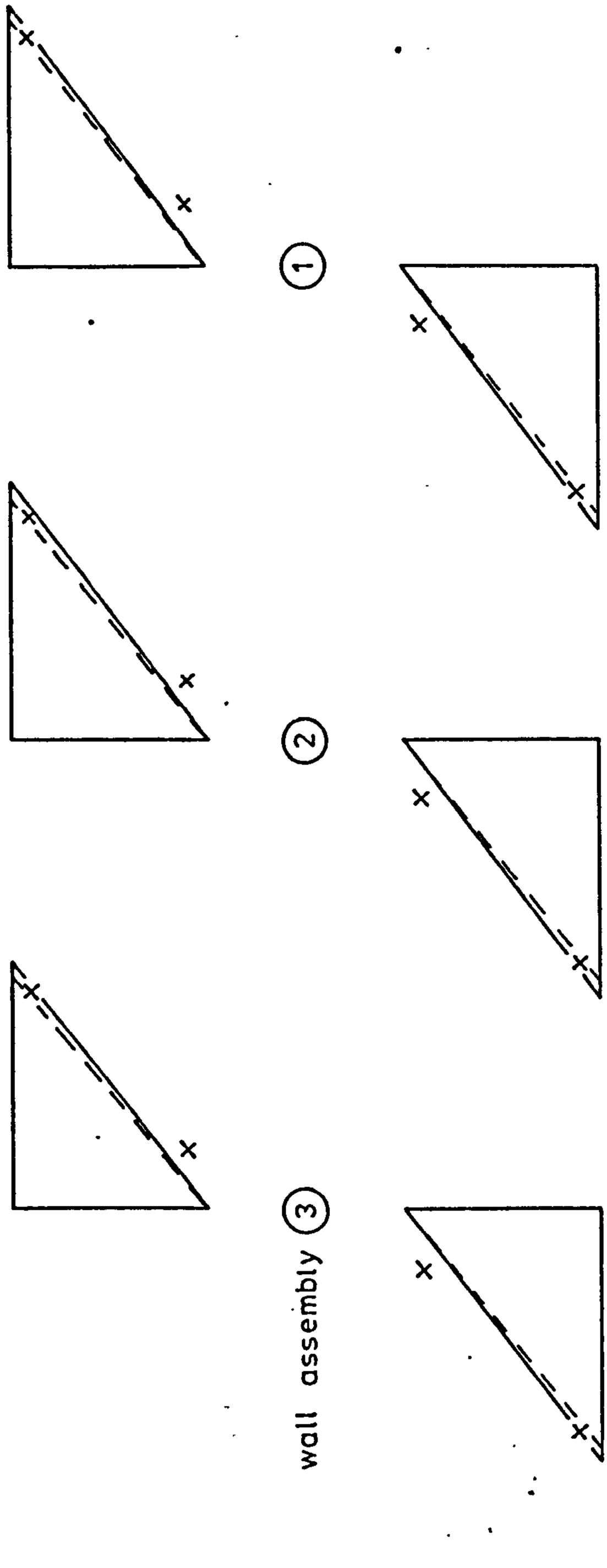

Test number 9 - Stresses

8.43

Figure

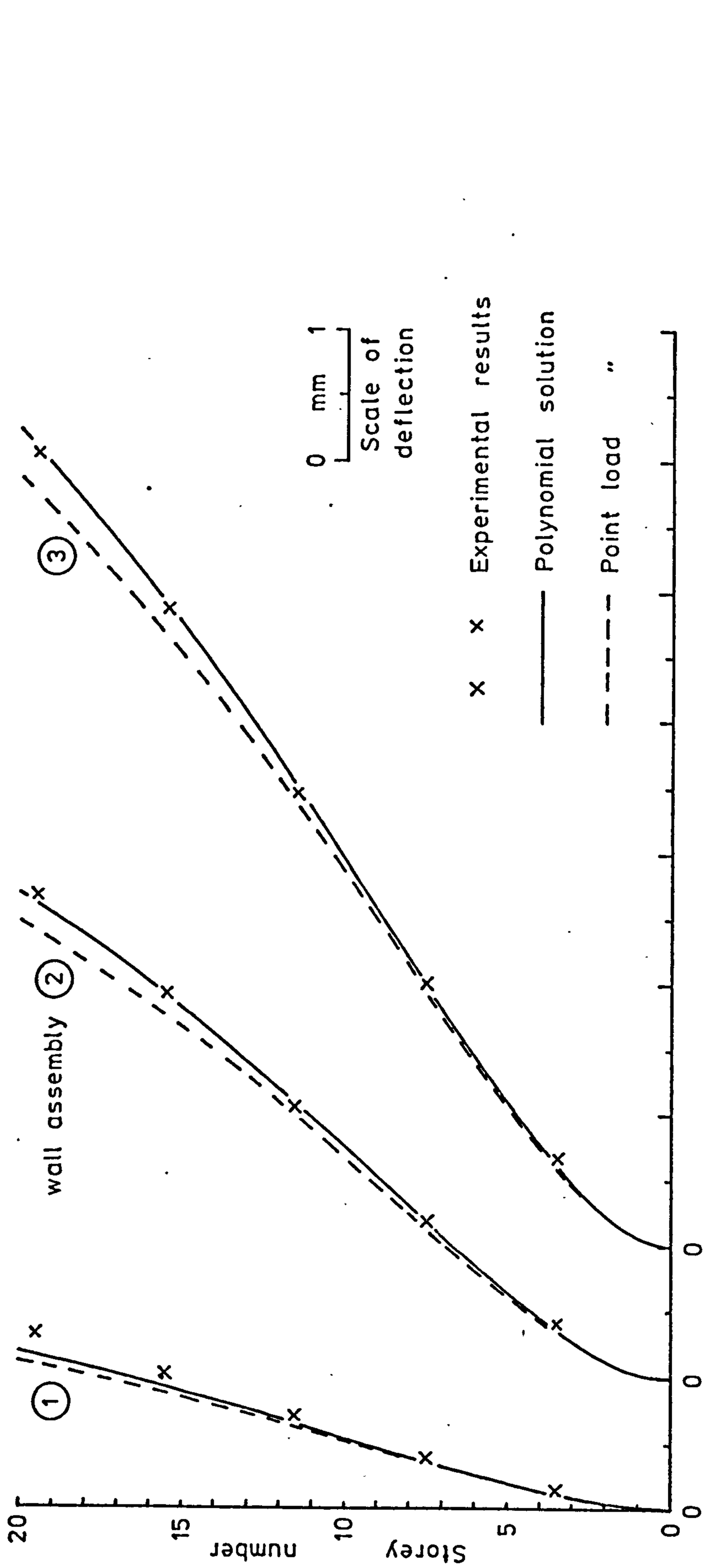
Deflections
mm.
Test number 10 - wall assembly ② ③ ① ④
Deflection
0
0
Storey number
20
15
10
5
0
Scale of deflection
0 mm 1
x Experimental results
Polynomial solution
Point load "

Figure 8.44

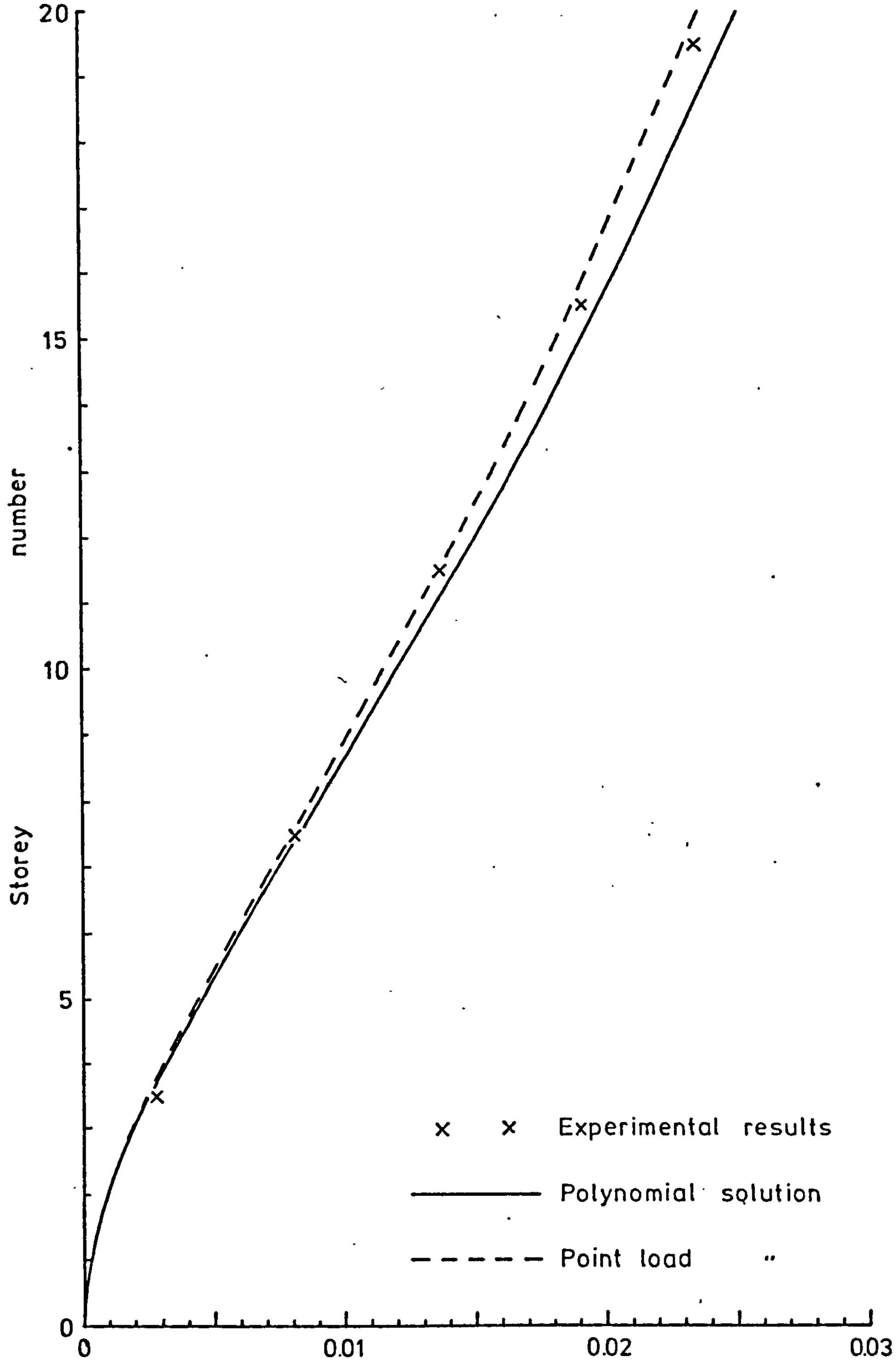

Test number 10 - Rotations

Figure 8.45

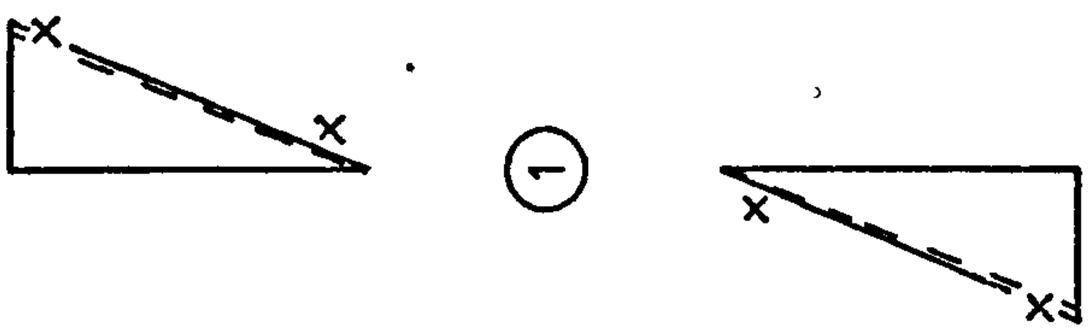
Comp. 0 Tens.
1 1
Scale N/mm2
1
2
3
Experimental results
Polynomial solution
Point load "
Test number 10 - Stresses

Figure 8.46

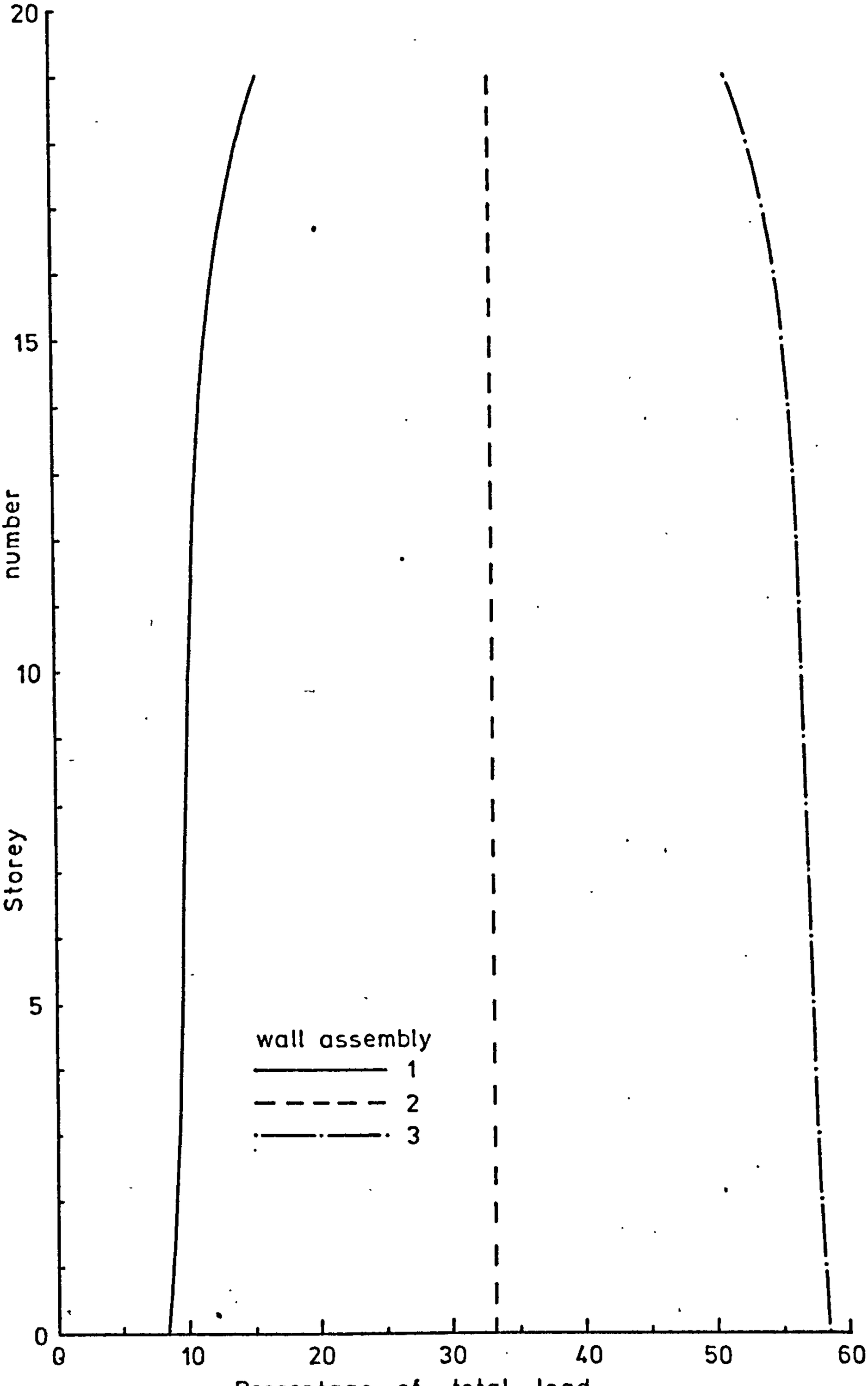

Test number 10 - Load distribution - Polynomial solution

Figure 8.47

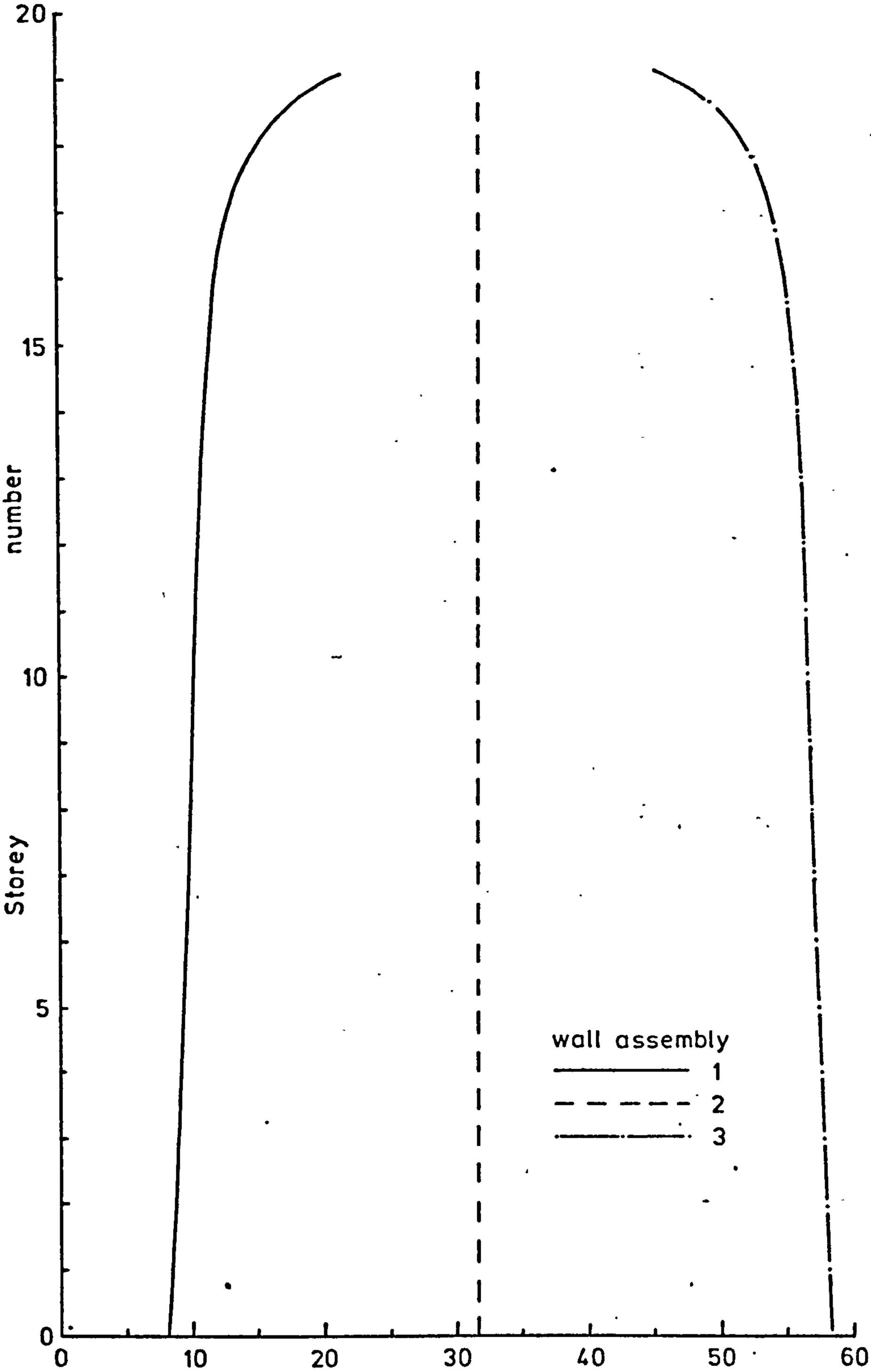

Test number 10 - Load distribution - Point load solution

Figure 8.48

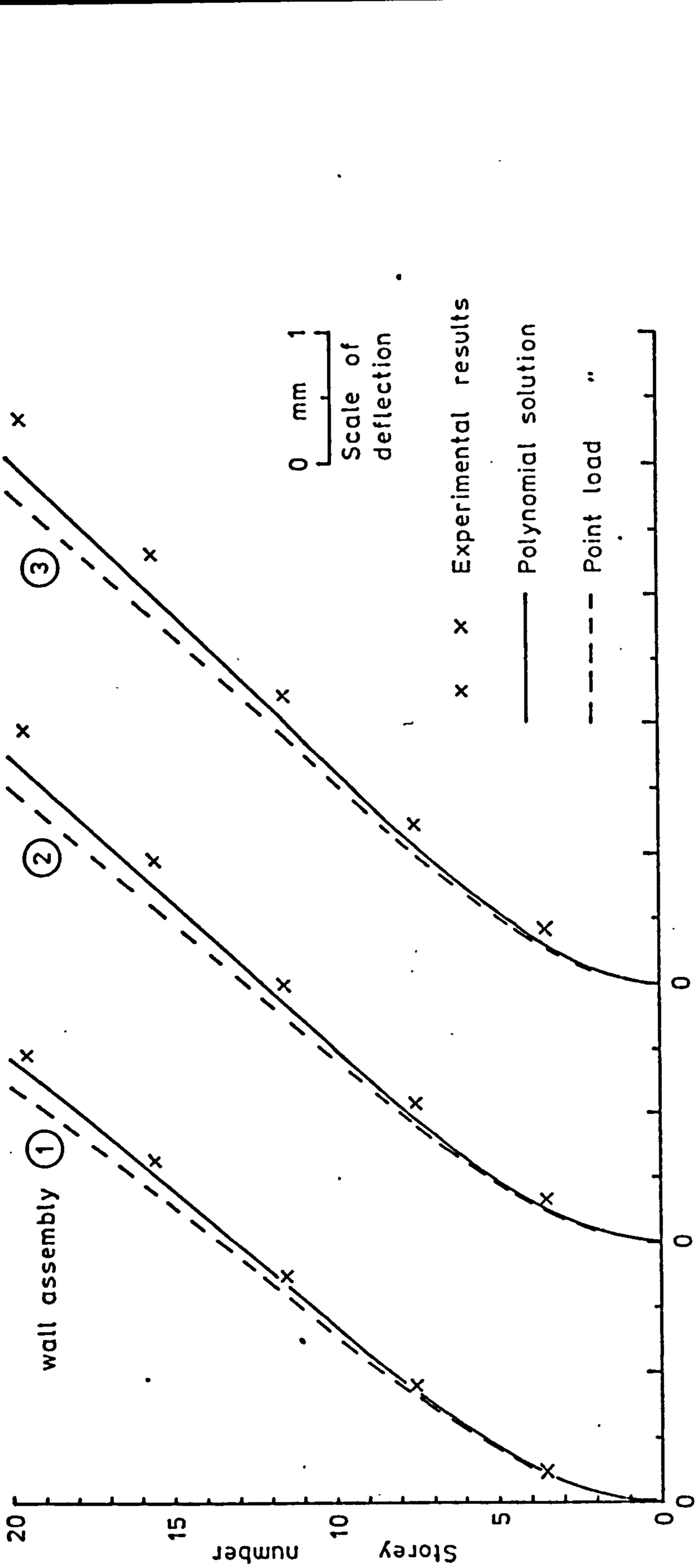

Test number 11 - Deflections

Figure 8.49

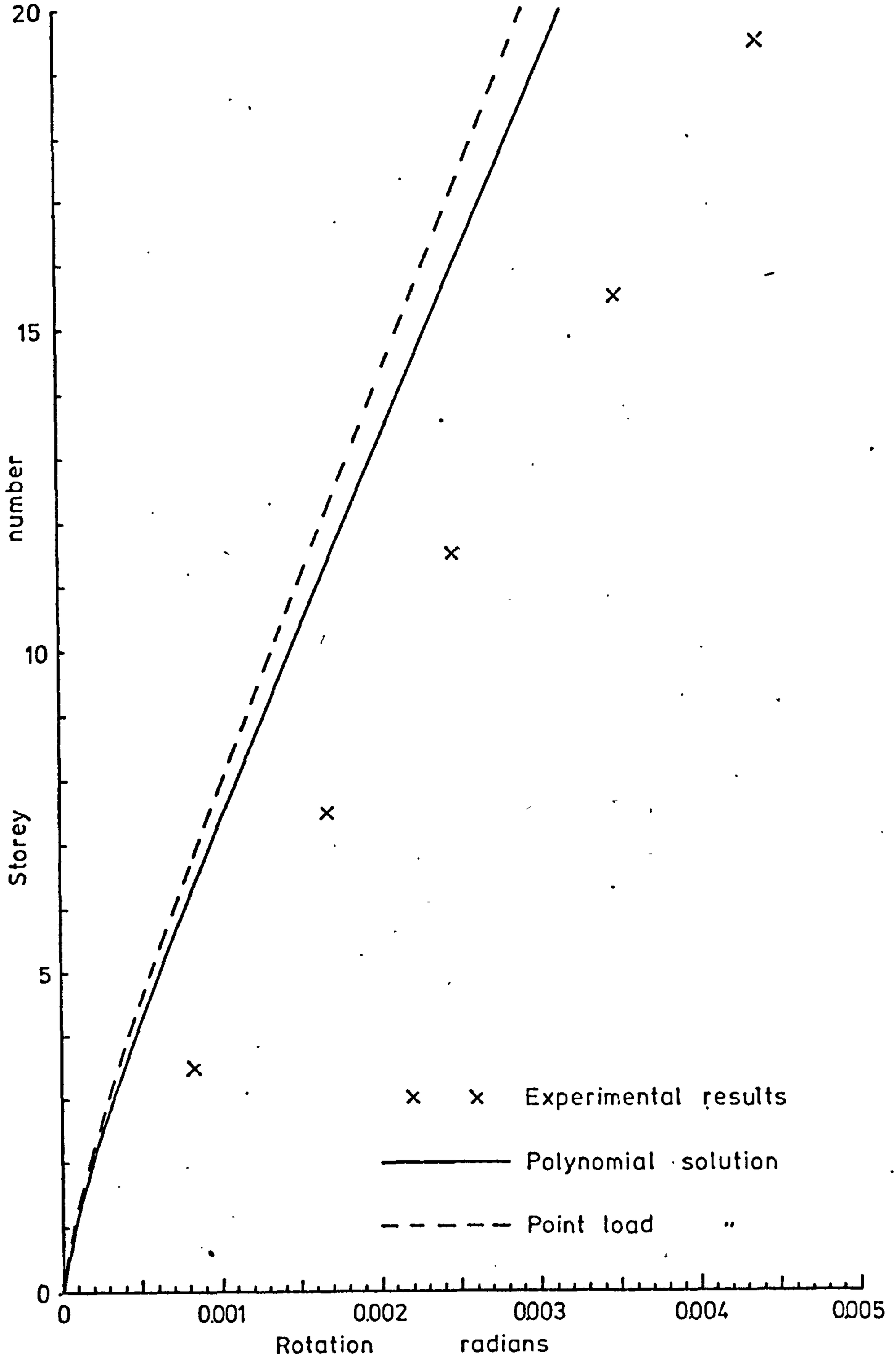

Test number 11 - Rotations

Figure 8.50

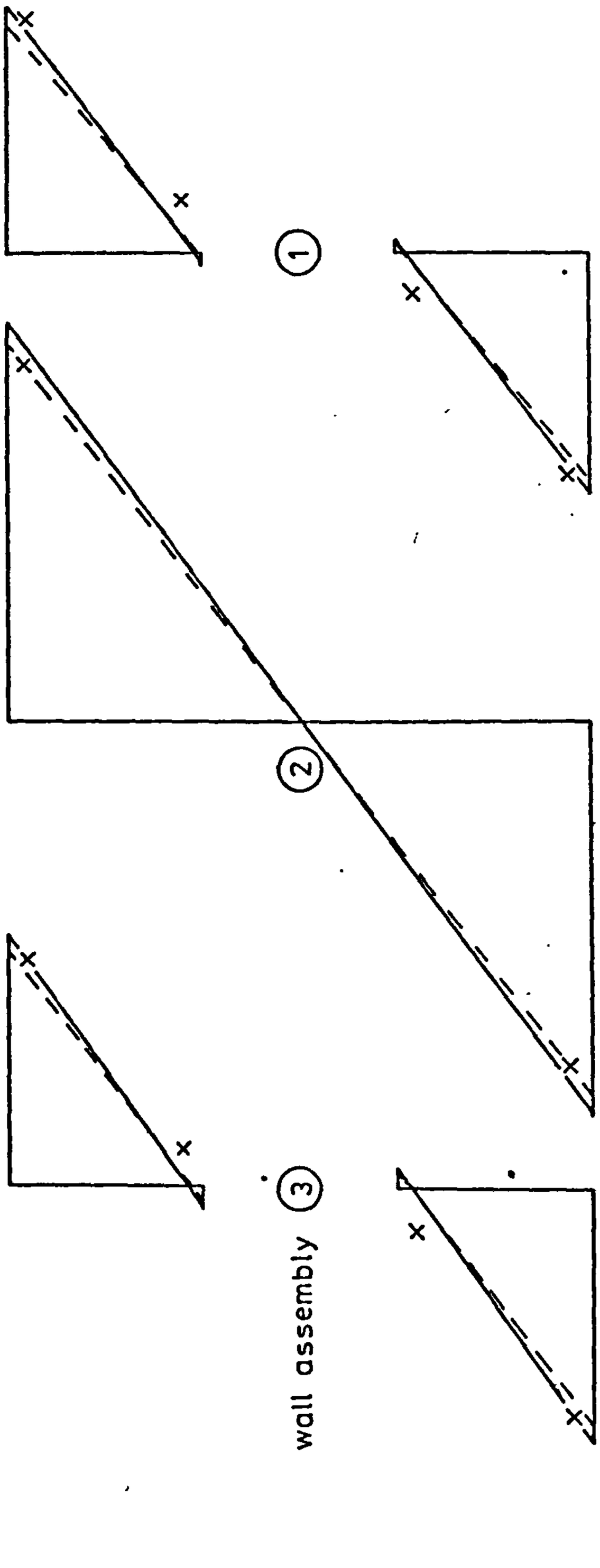
Comp.
Tens.
0
1
1
Scale N/mm2
Test number 11 - Stresses
Figure 8.51
X Experimental results
—— Polynomial solution
- - - - Point load "
wall assembly ①
wall assembly ②
wall assembly ③

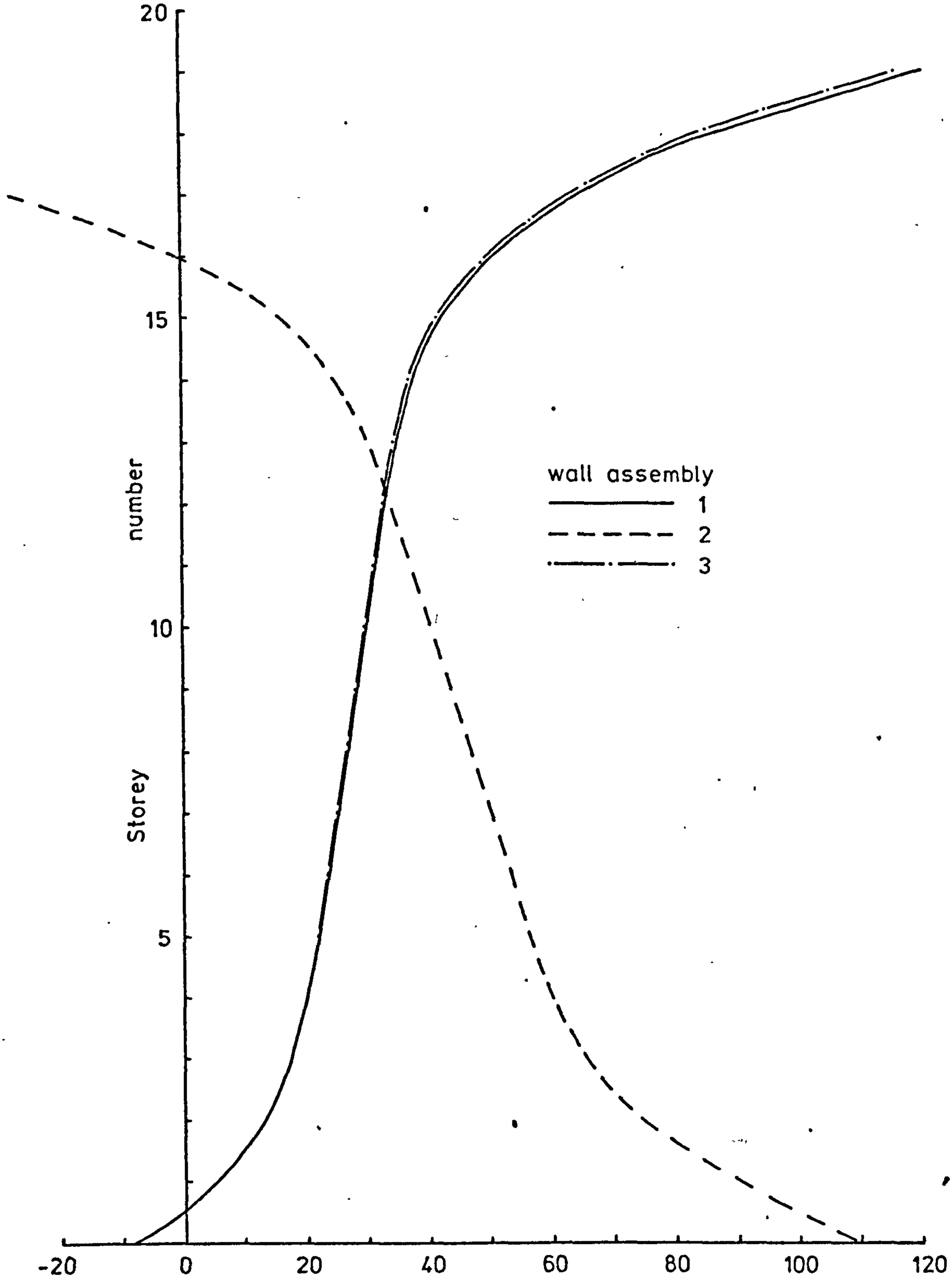

Test number 11 - Load distribution - Polynomial solution

Figure 8.52

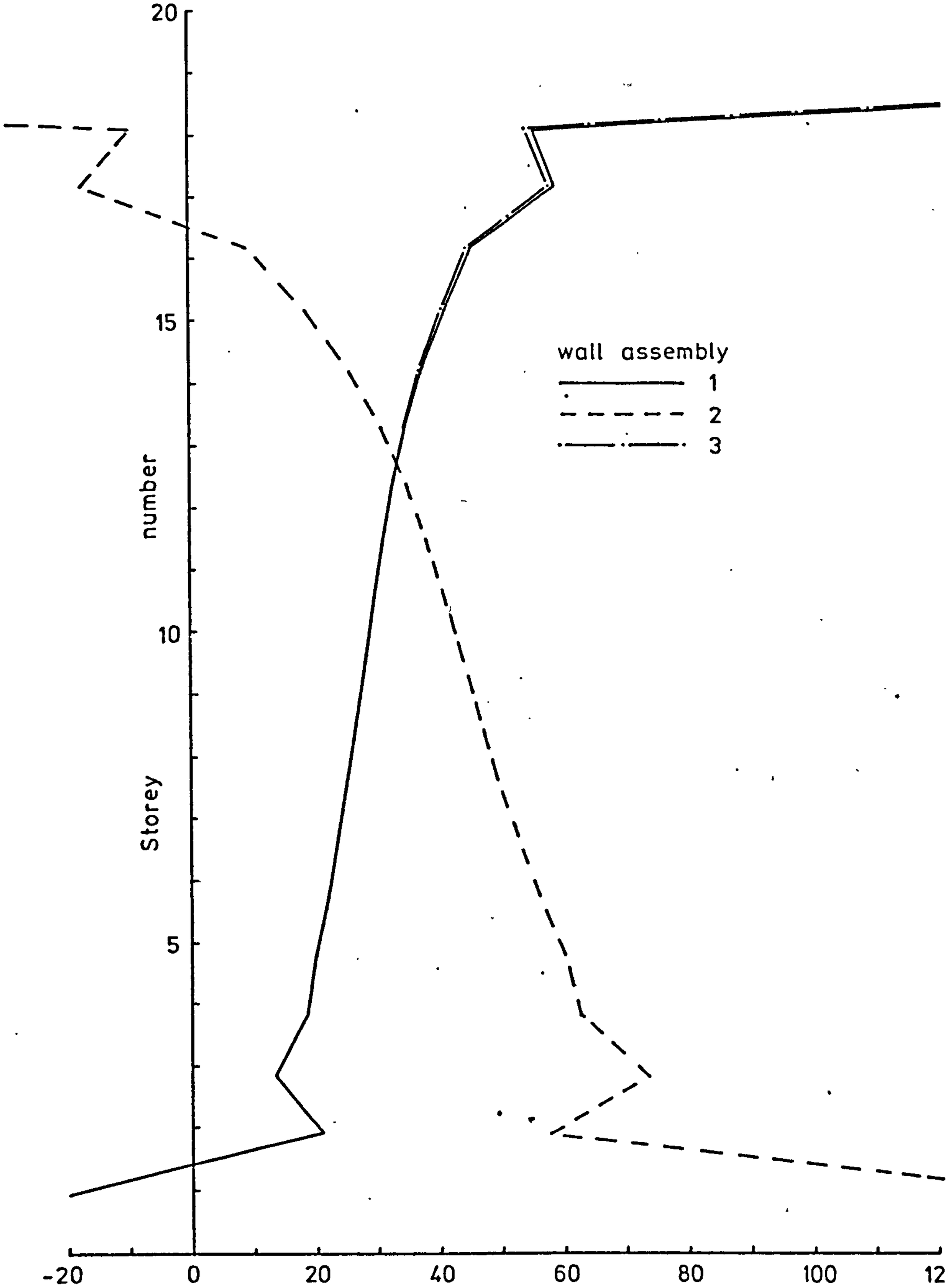

Test number 11 - Load distribution - Point load solution

Figure 8.53

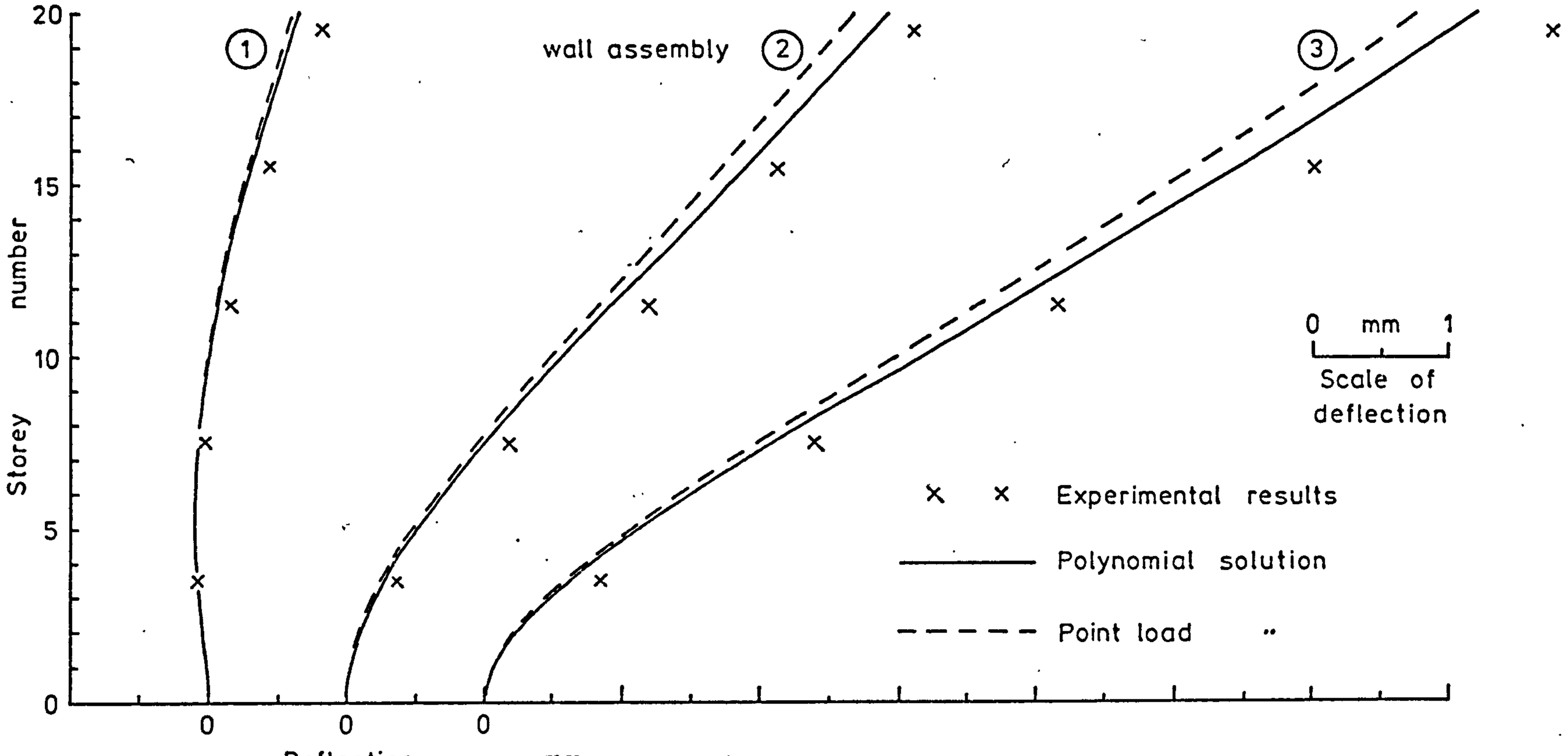

Test number 12 - Deflections

Figure 8.54

F 8.54

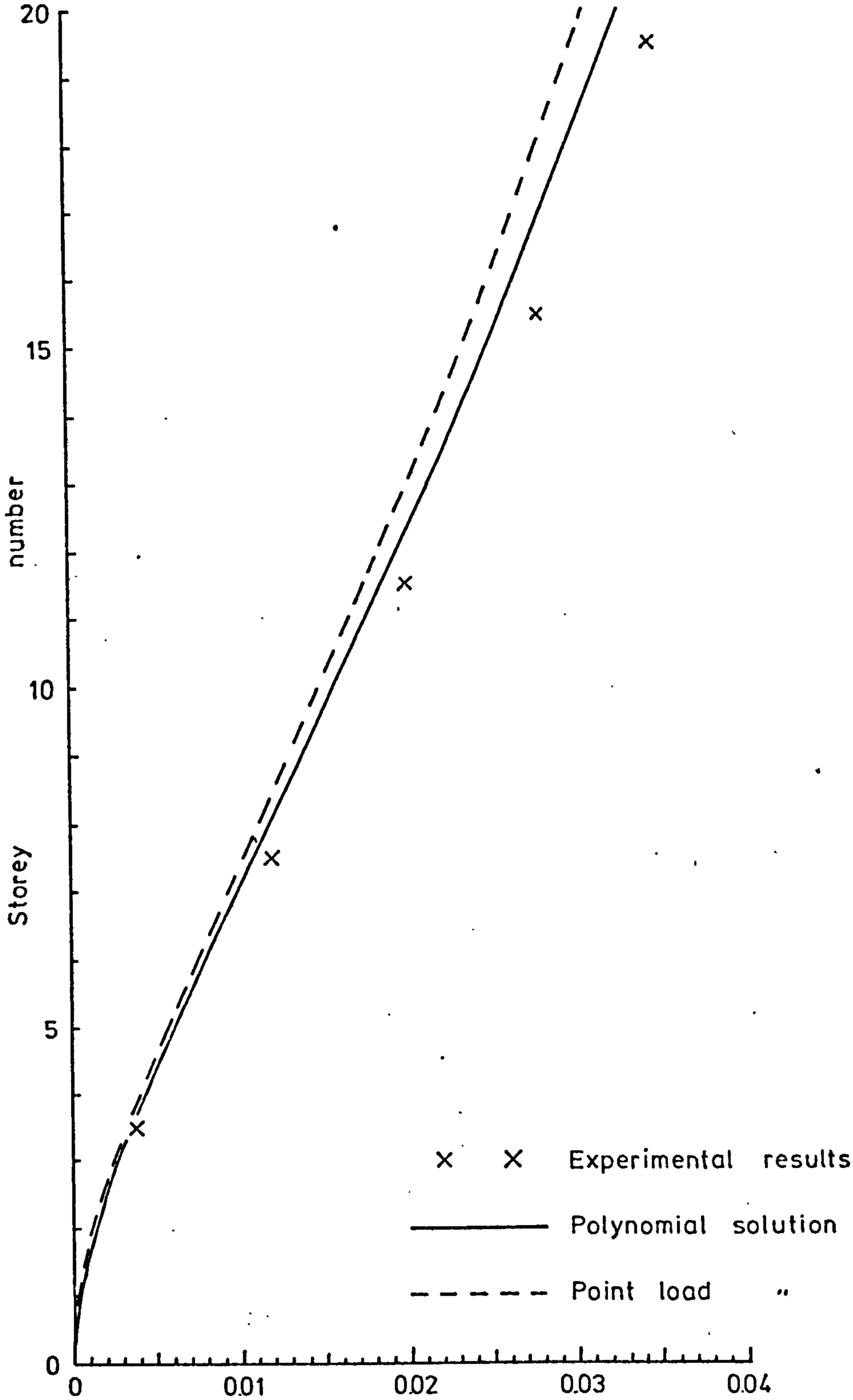

Test number 12 - Rotations

Figure 8.55

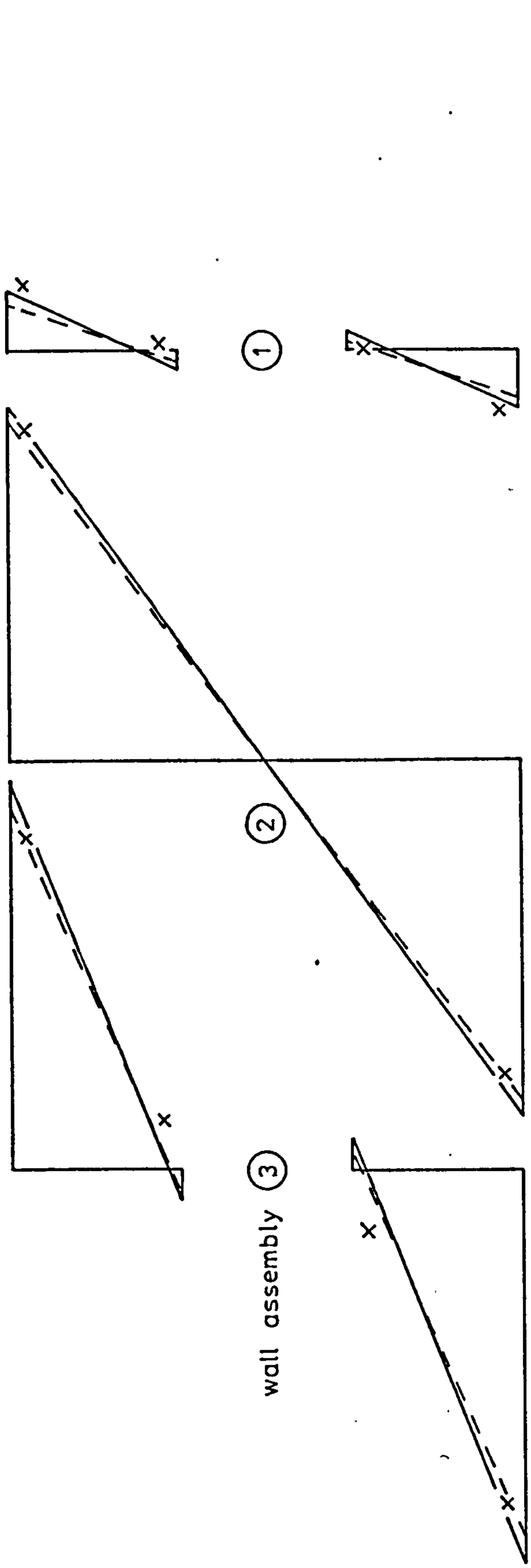

Test number 12 - Stresses

Figure 8.56

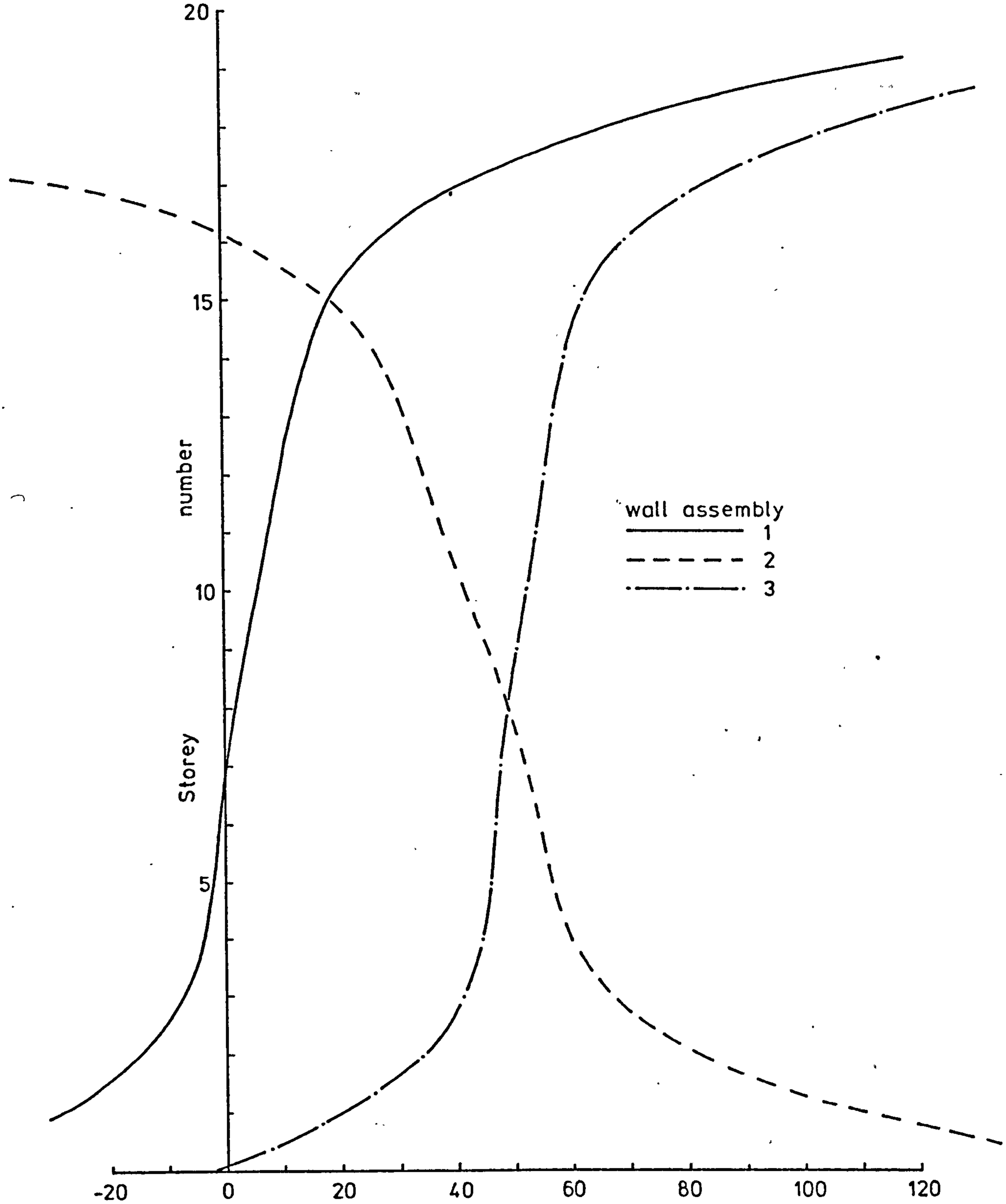

Test number 12 - Load distribution - Polynomial solution

Figure 8.57

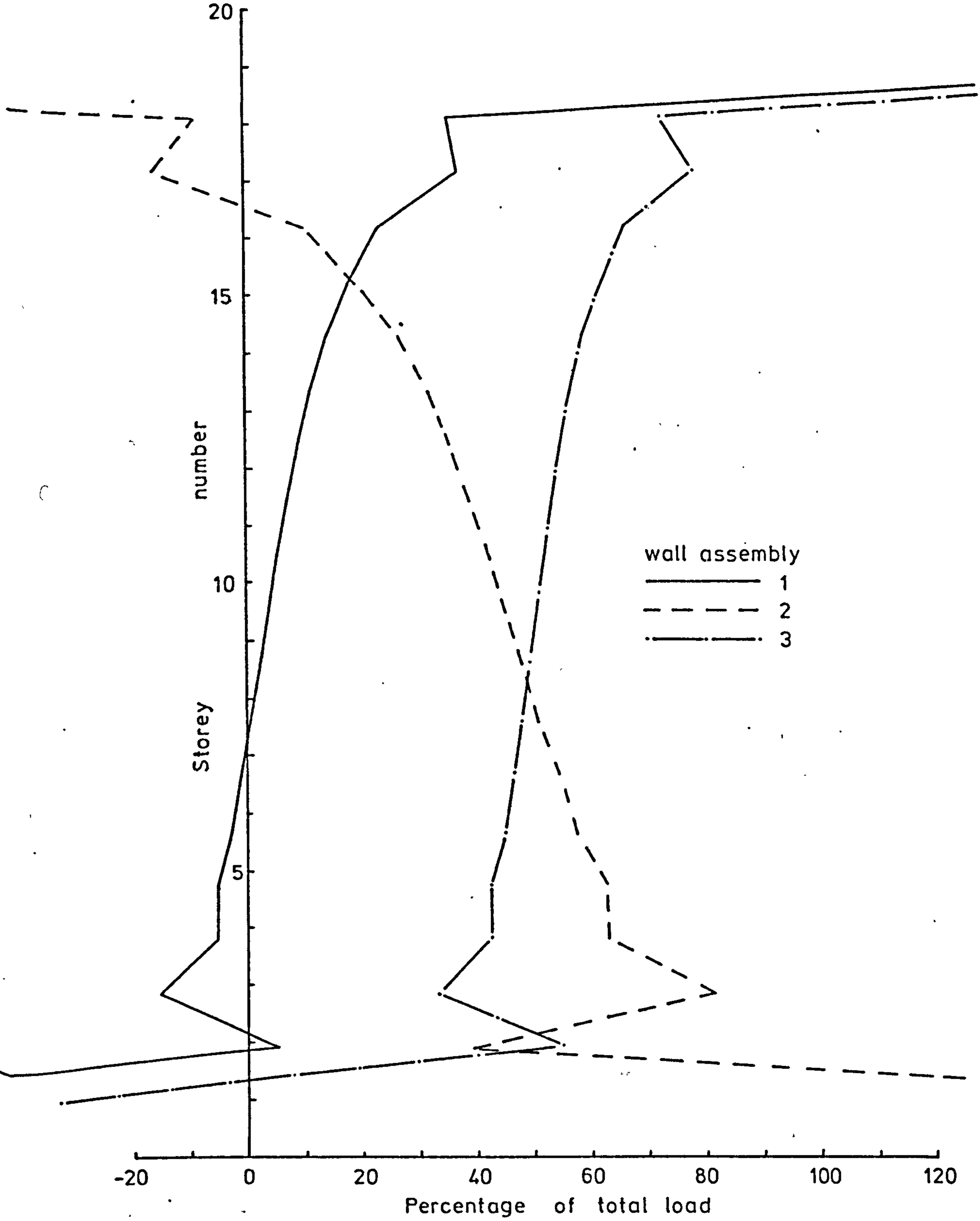

Test number 12 - Load distribution - Point load solution

Figure 8.58

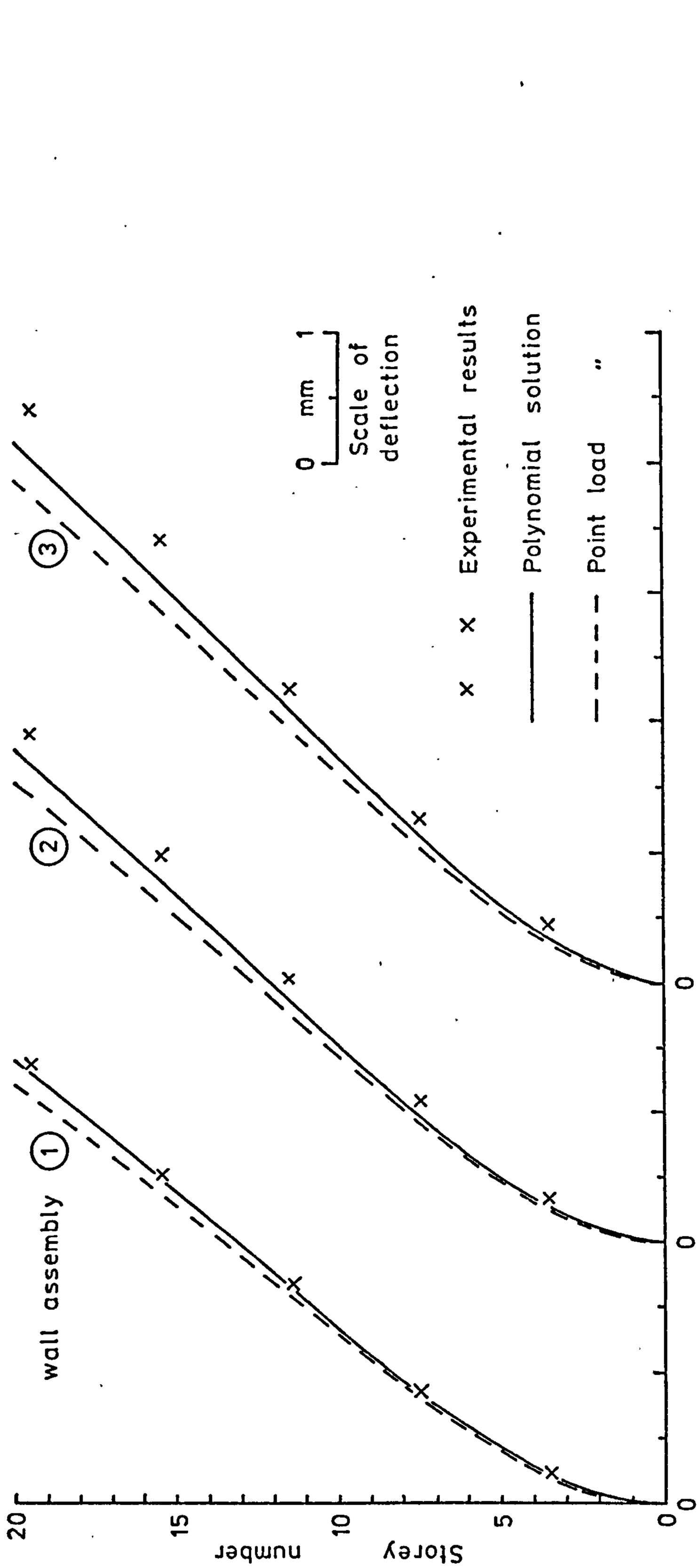
Storey number
20
15
10
5
0
Deflection
0
0
mm.
Test number 13 - Deflections
Figure 8.59
wall assembly ①
②
③
0 mm 1
Scale of deflection
x Experimental results
Polynomial solution
Point load "

F 8.60

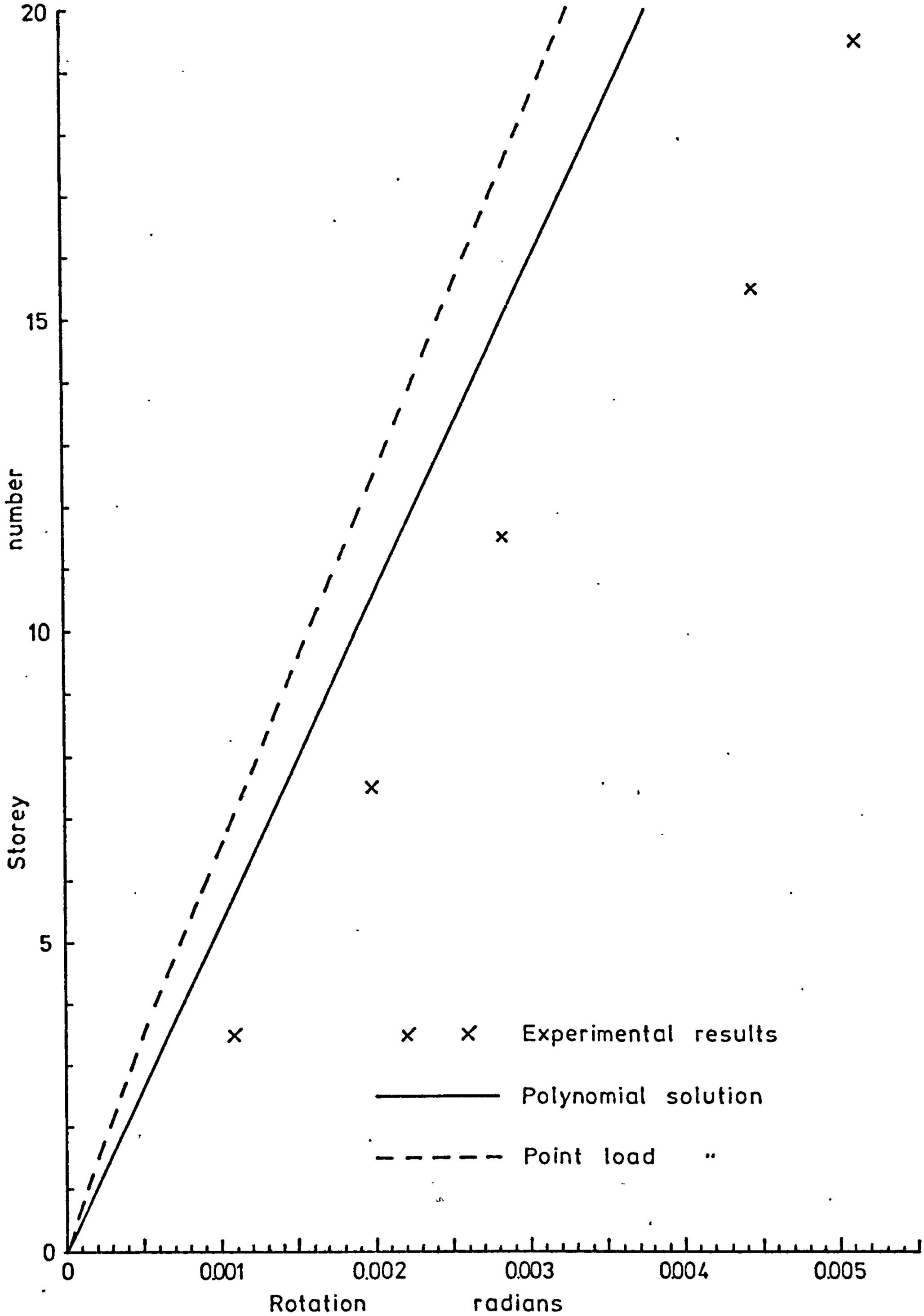

Test number 13 - Rotations

Figure 8.60

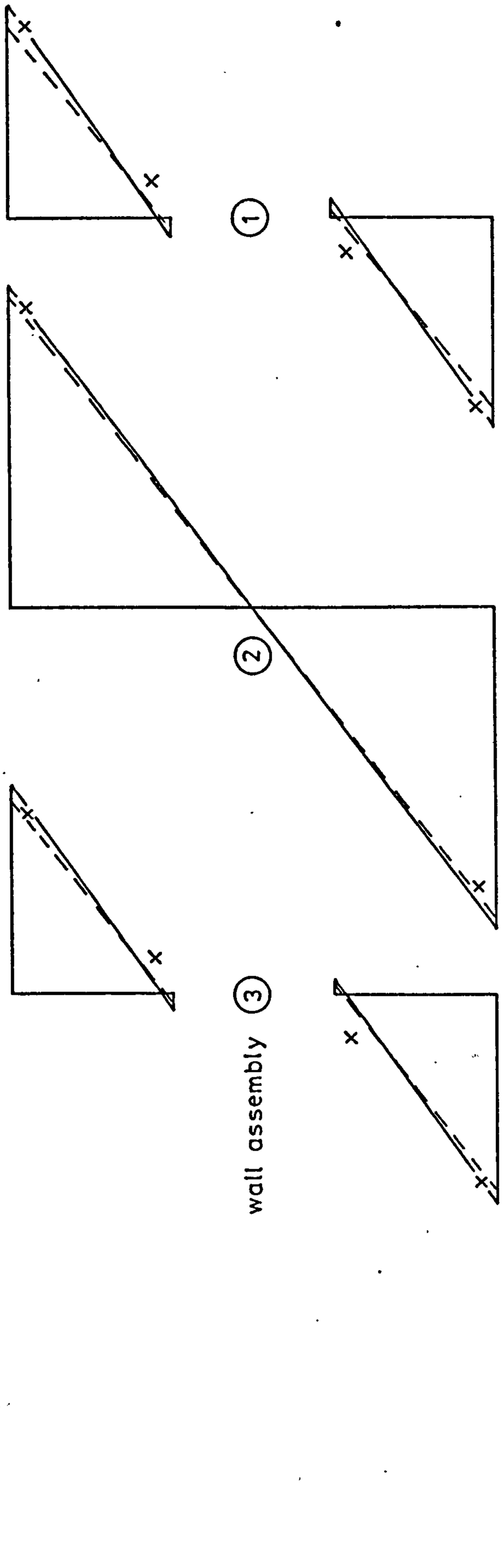

Test number 13 -

Figure 8.61

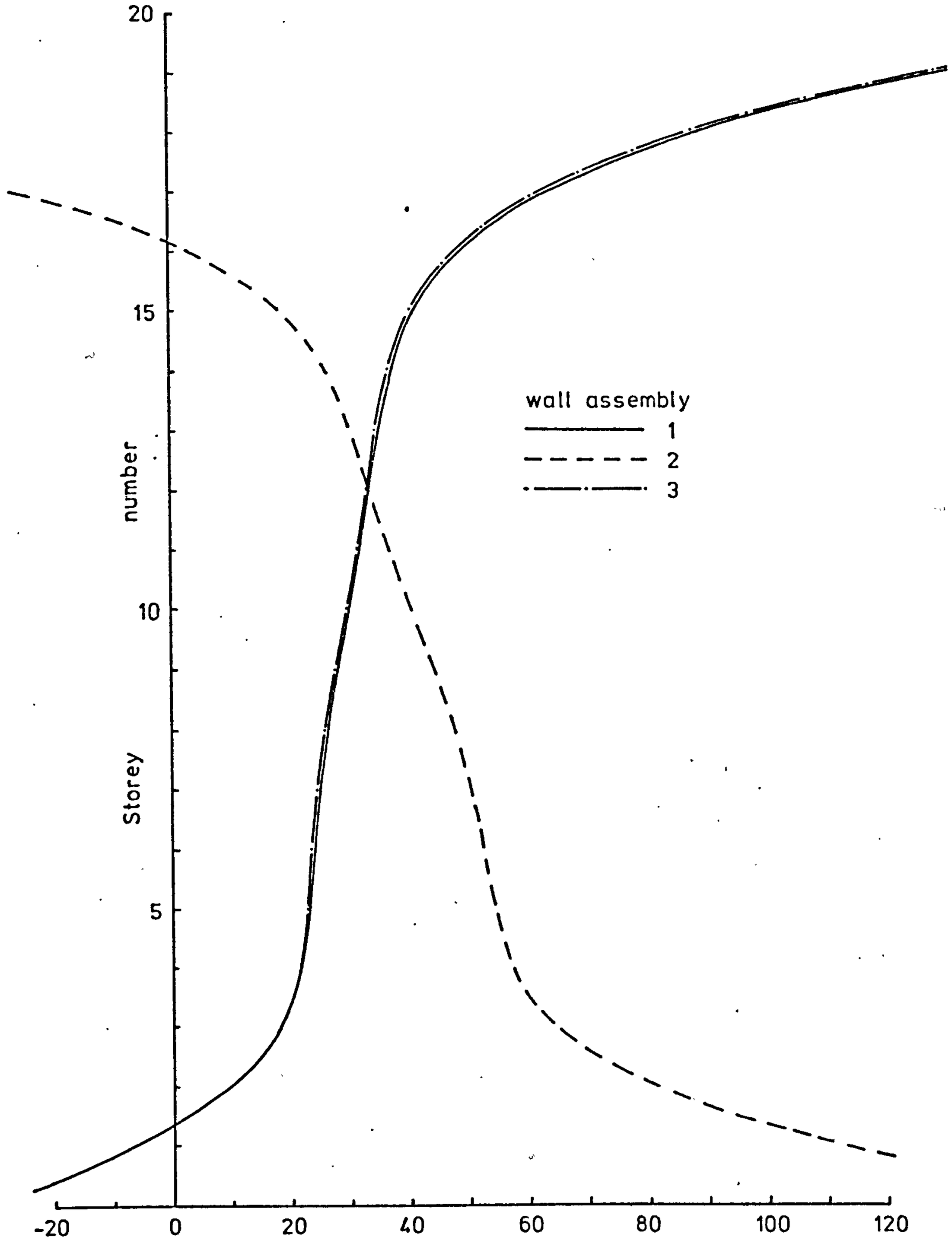

Test number 13 - Load distribution - Polynomial solution

Figure 8.62

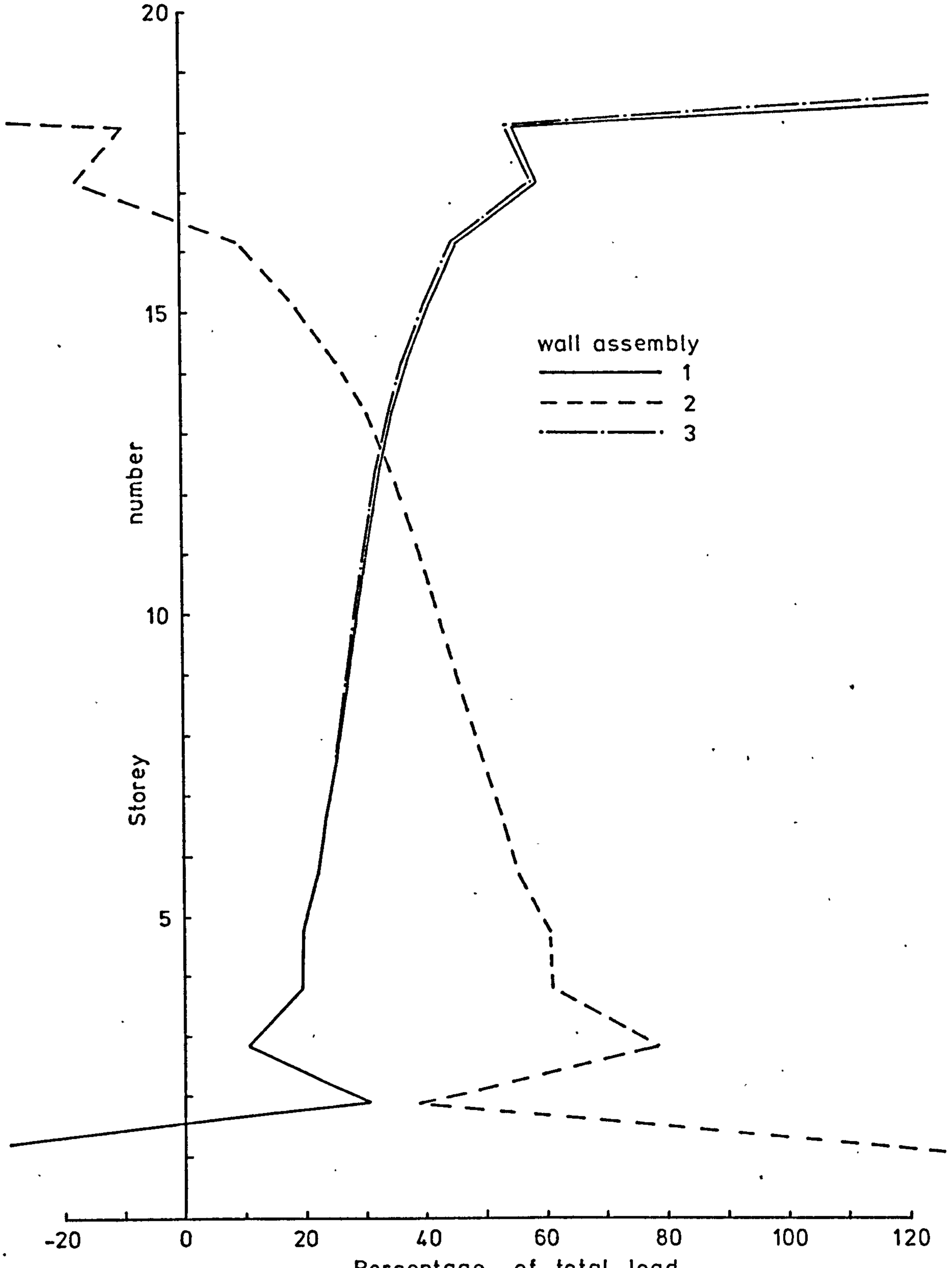

Test number 13 - Load distribution - Point load solution

Figure 8.63

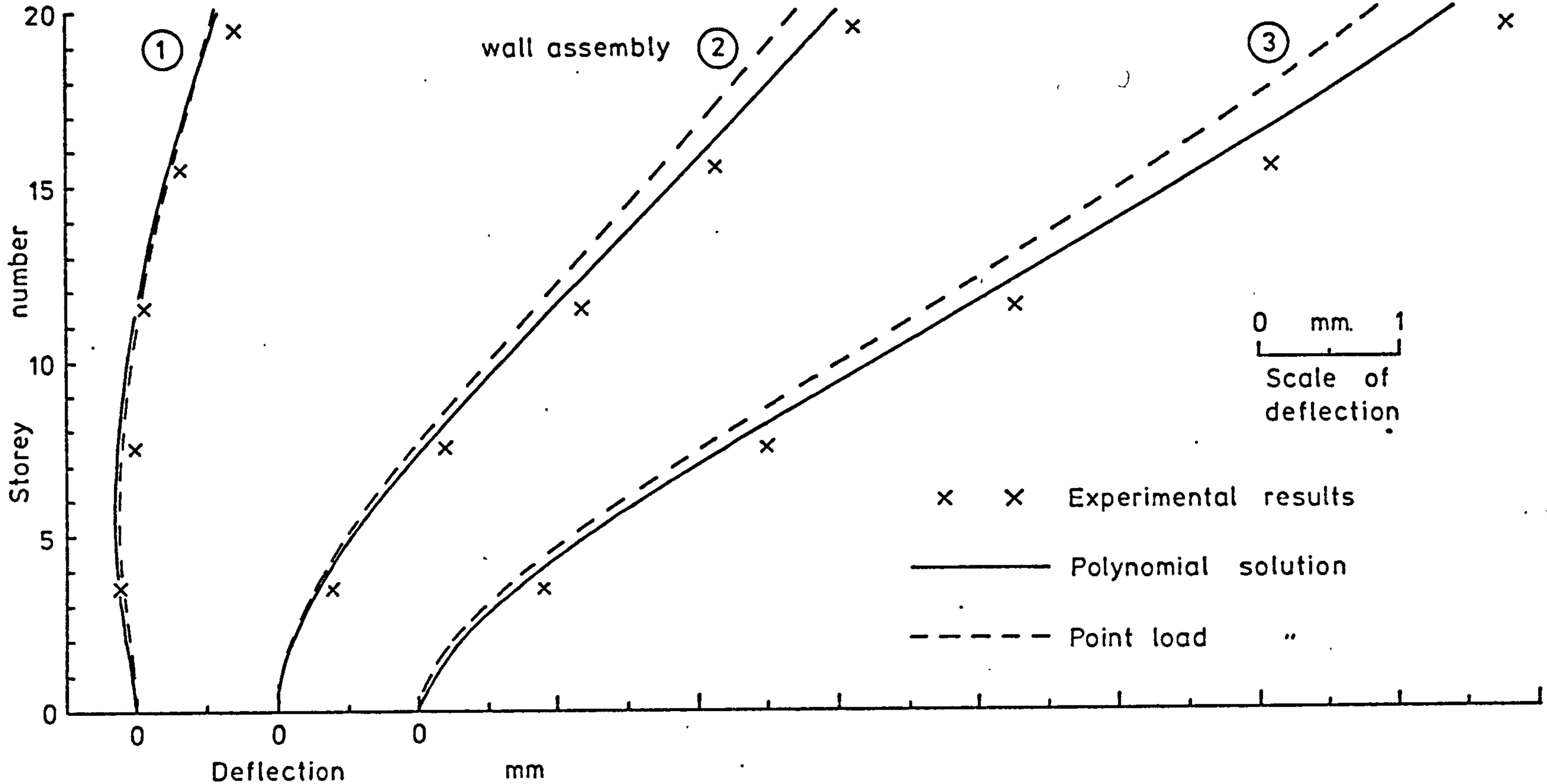

Test number 14 - Deflections

Figure 8.64

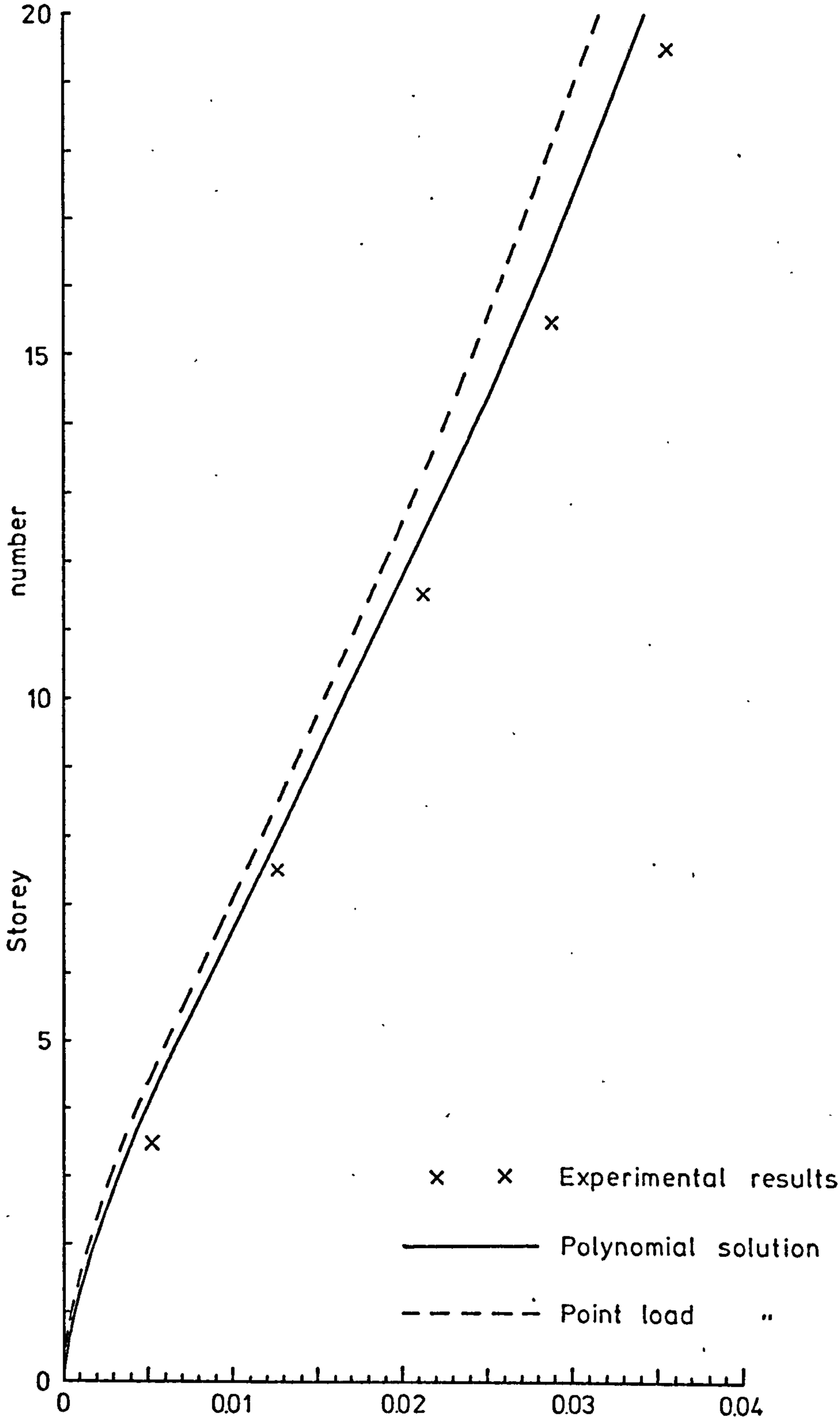

Test number 14 - Rotations

Figure 8.65

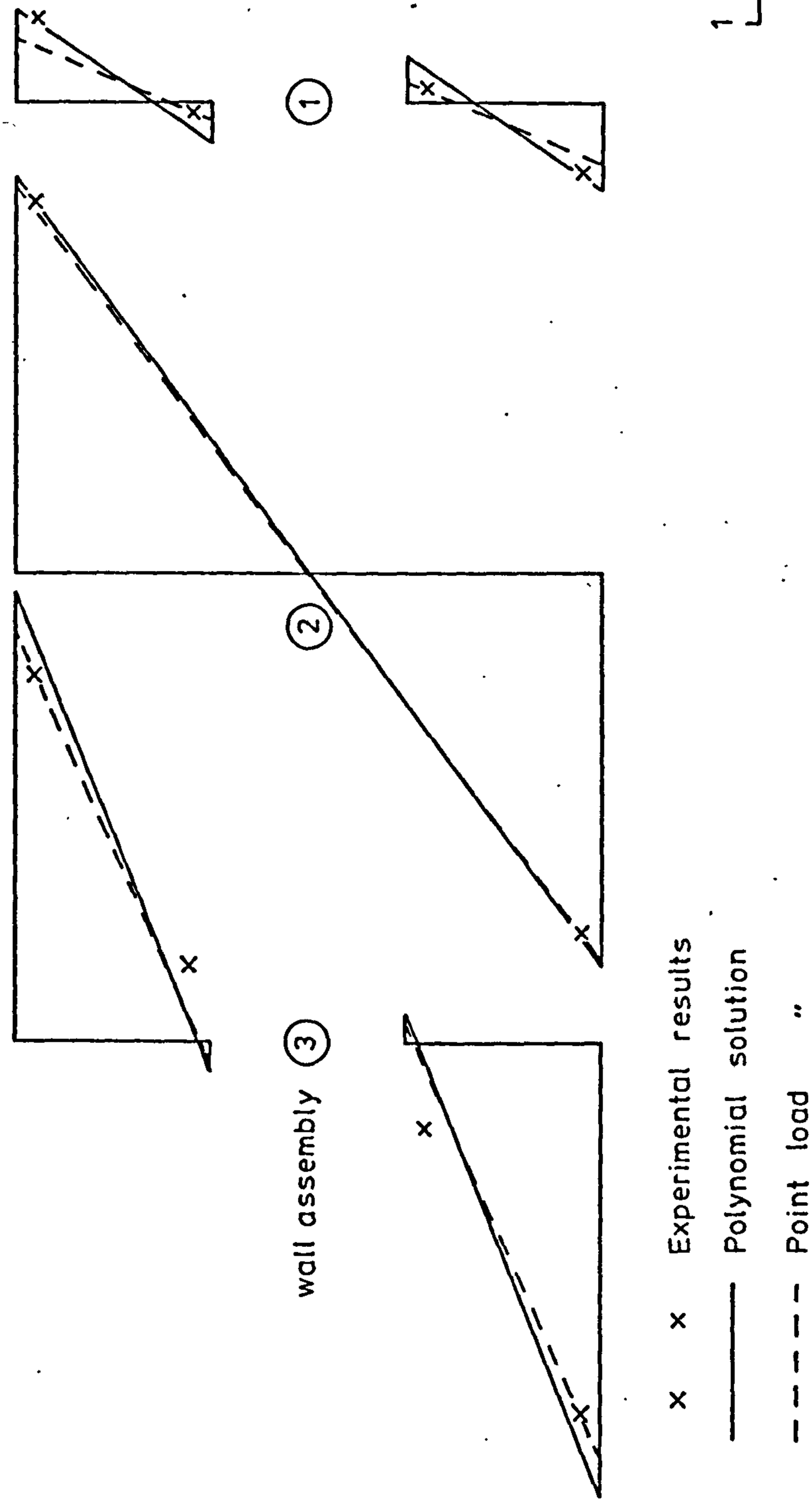

Test number 14 - S

Figure 8.66

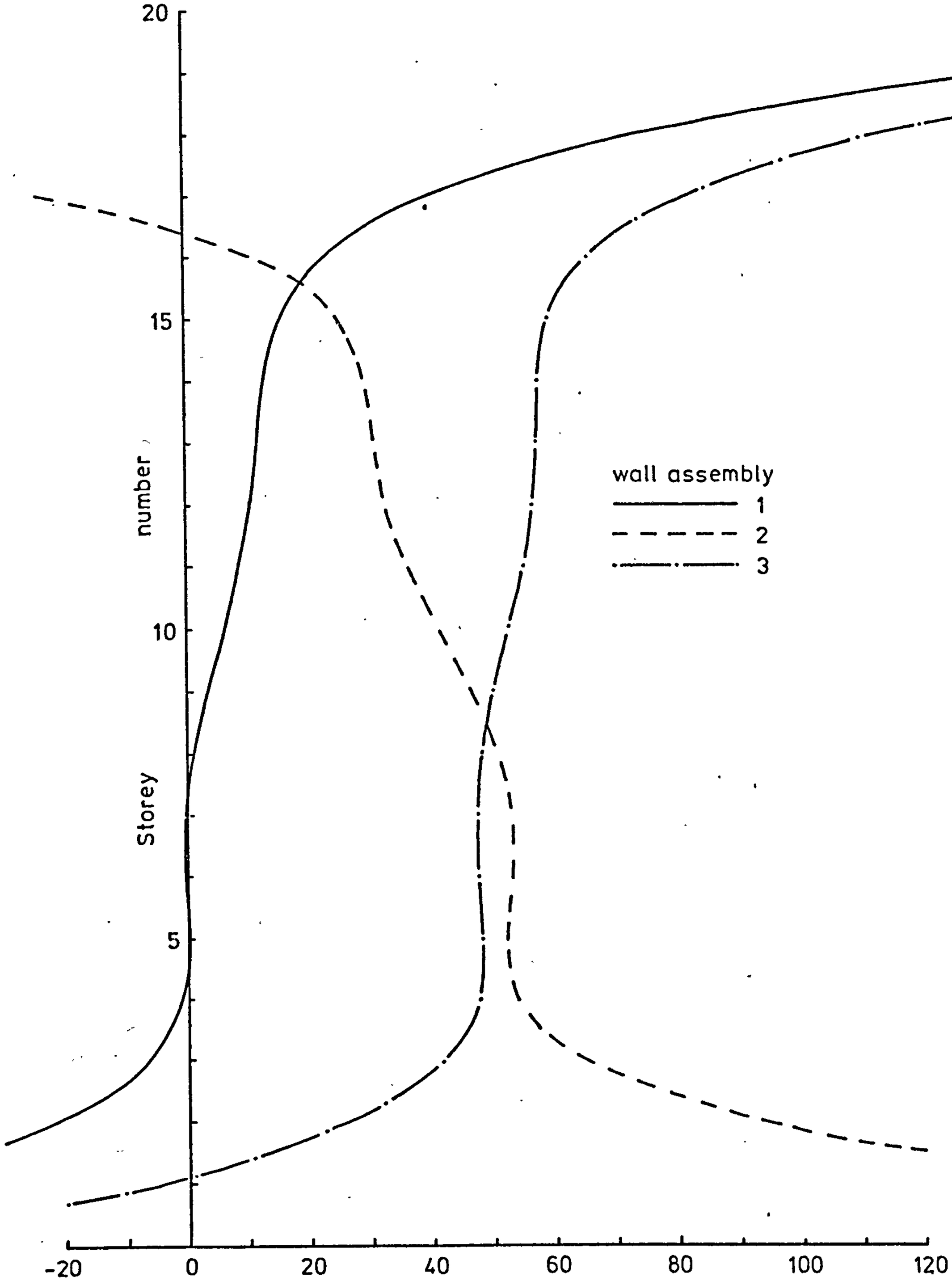

Test number 14 - Load distribution - Polynomial solution

Figure 8.67

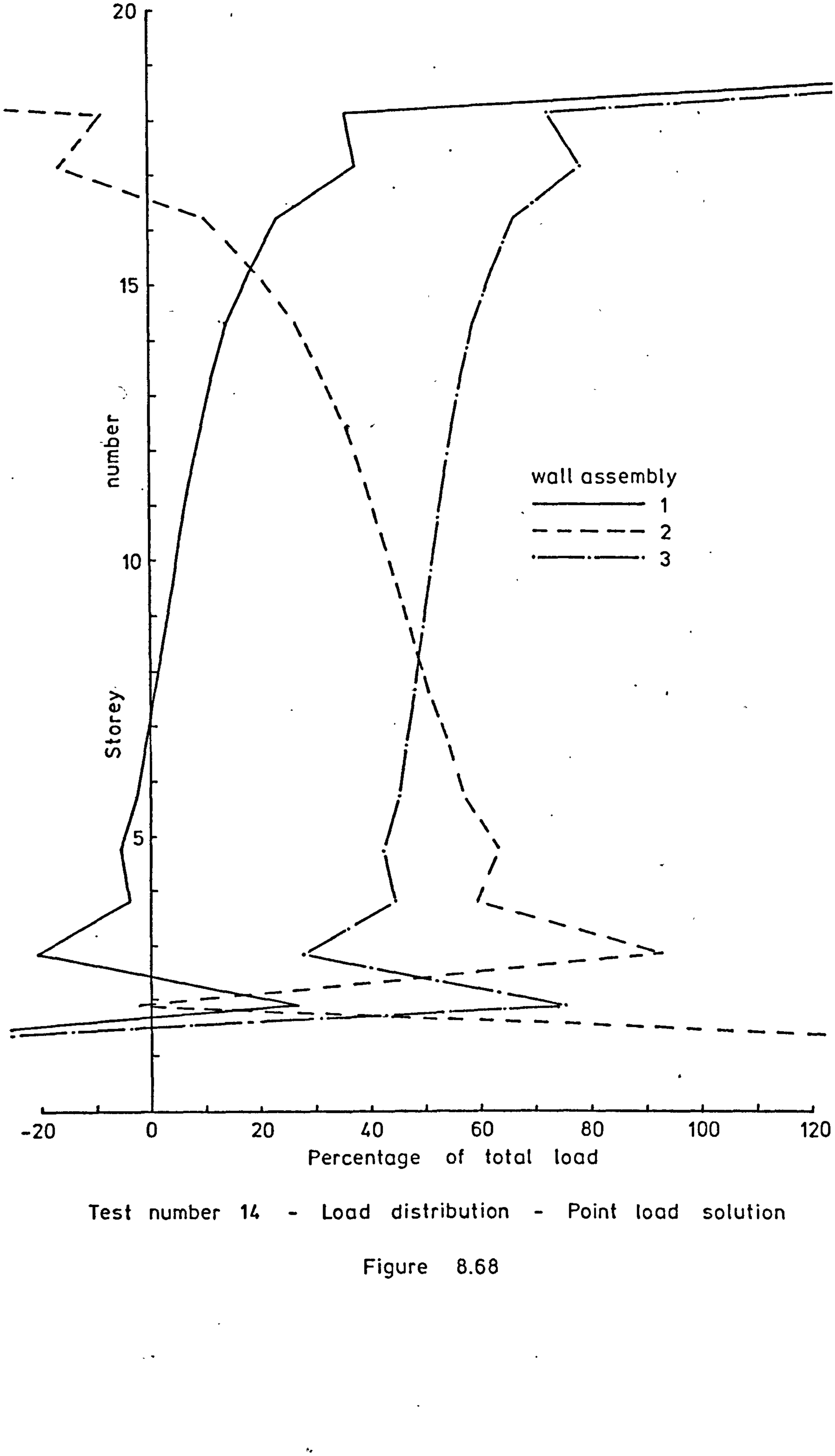

Test number 14 - Load distribution - Point load solution

Figure 8.68

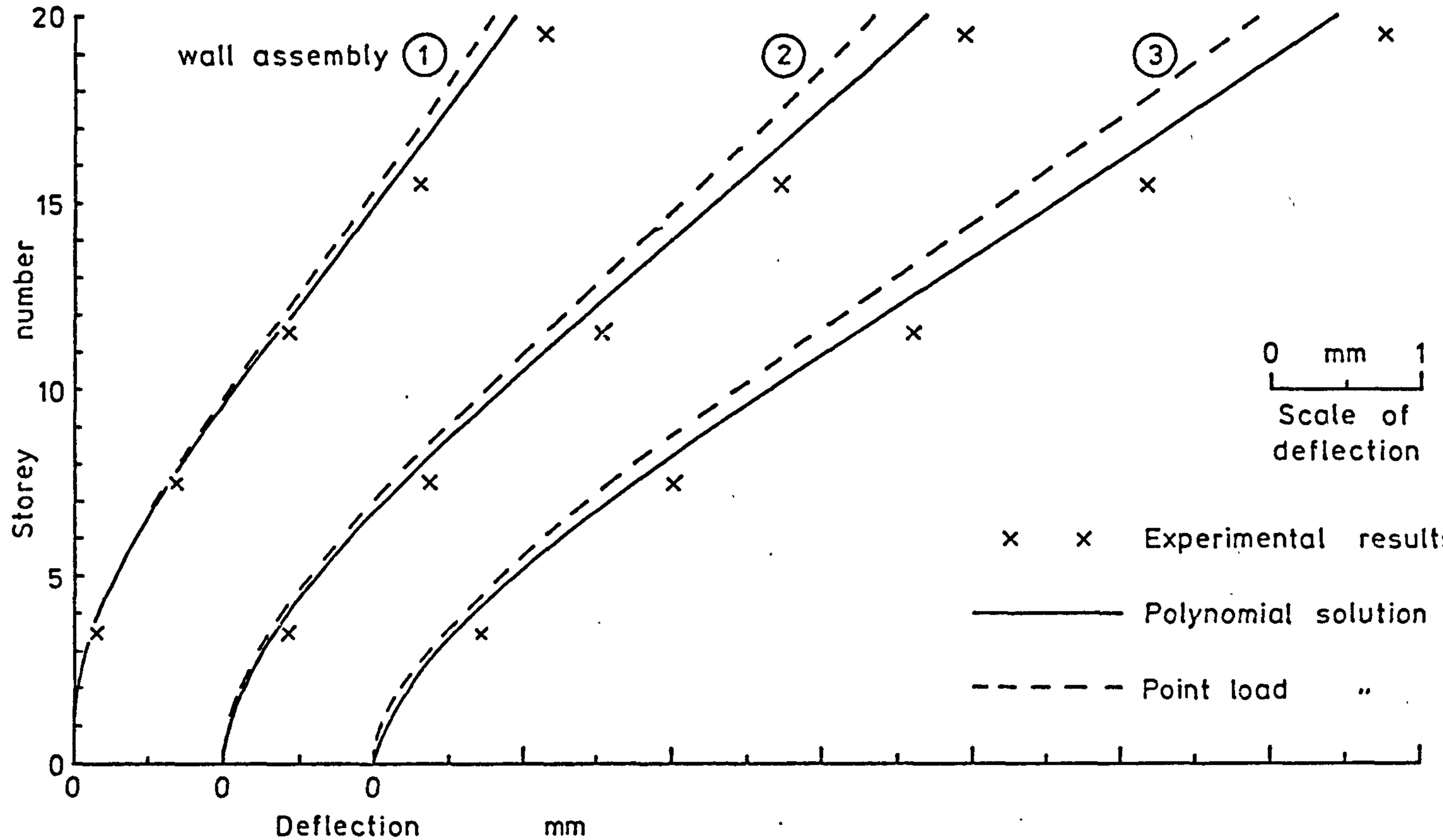

Test number 15 - Deflections

Figure 8.69

F 8.69

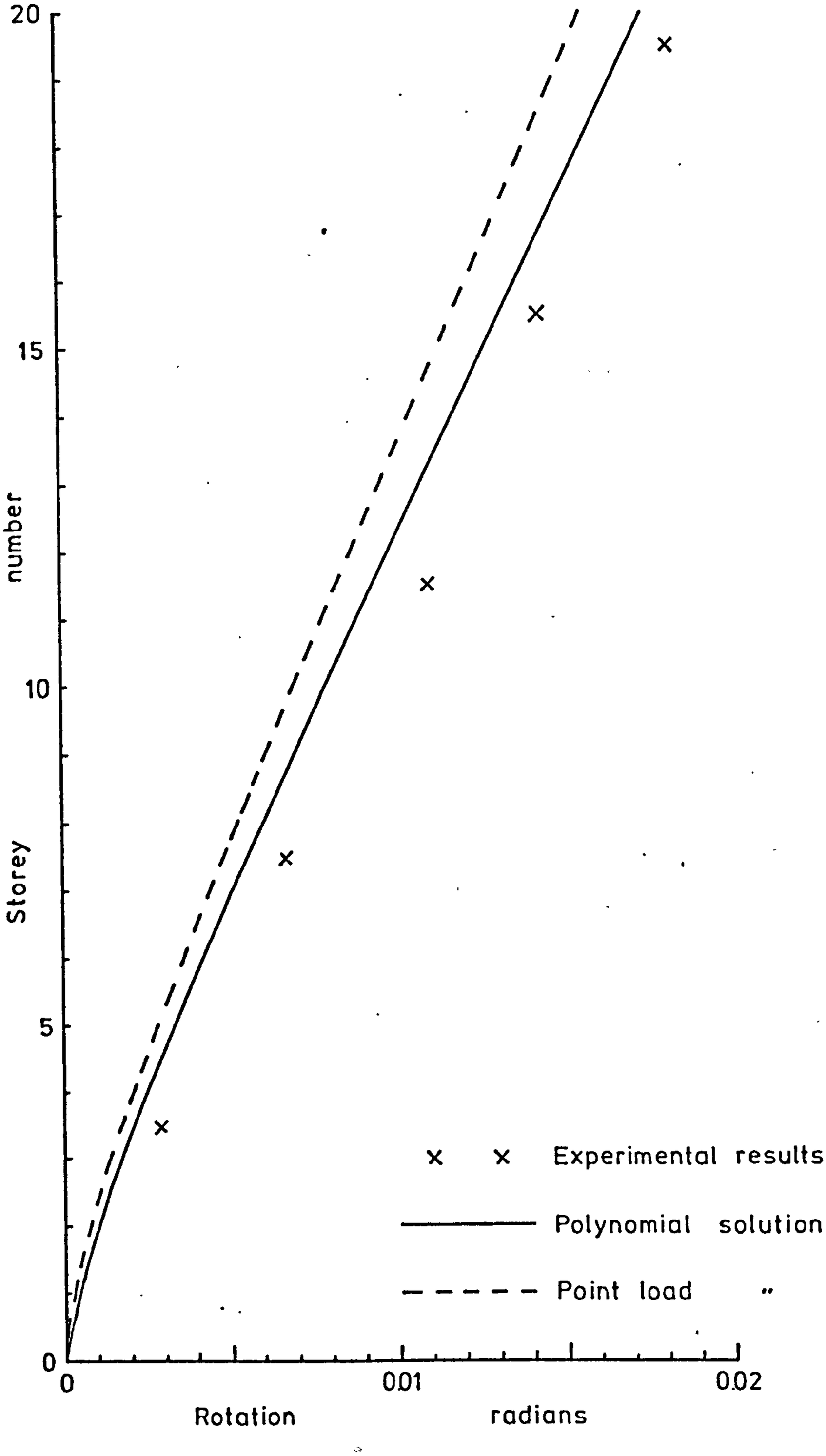

Test number 15 - Rotations

Figure 8.70

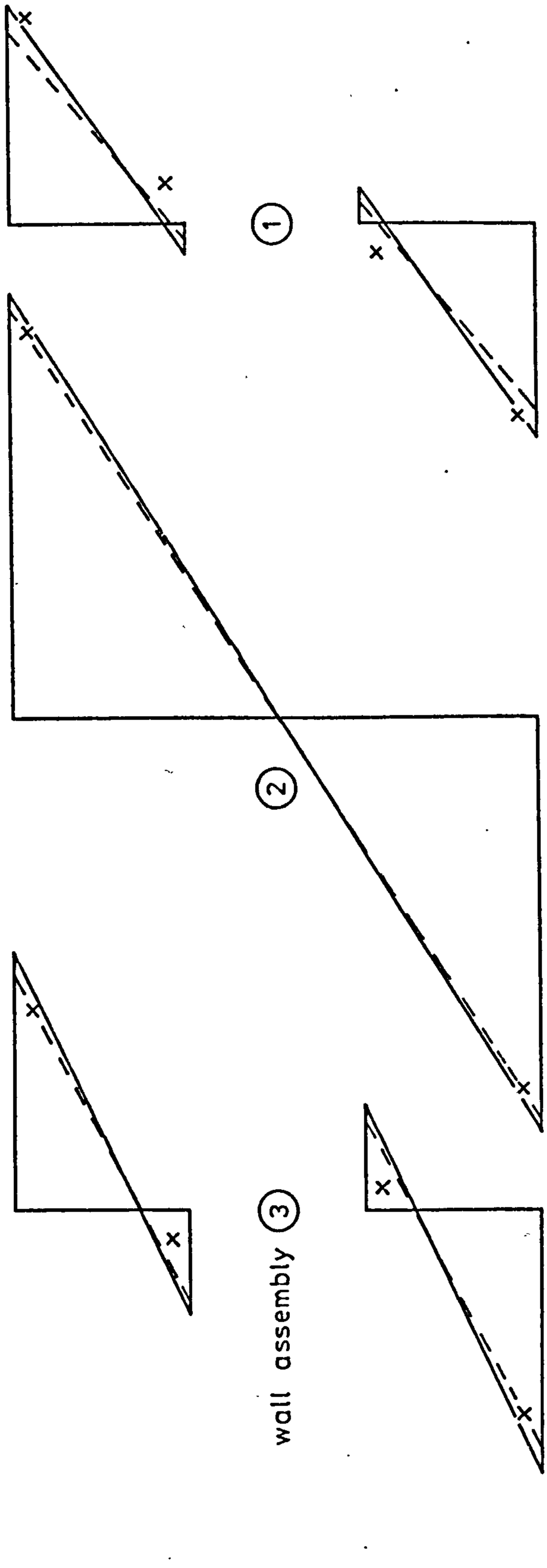
Comp. 0 Tens.
1 1
Scale N/mm2
1
2
3
wall assembly
x Experimental results
Polynomial solution
Point load "
Test number 15
Figure 8.71 - Stresses

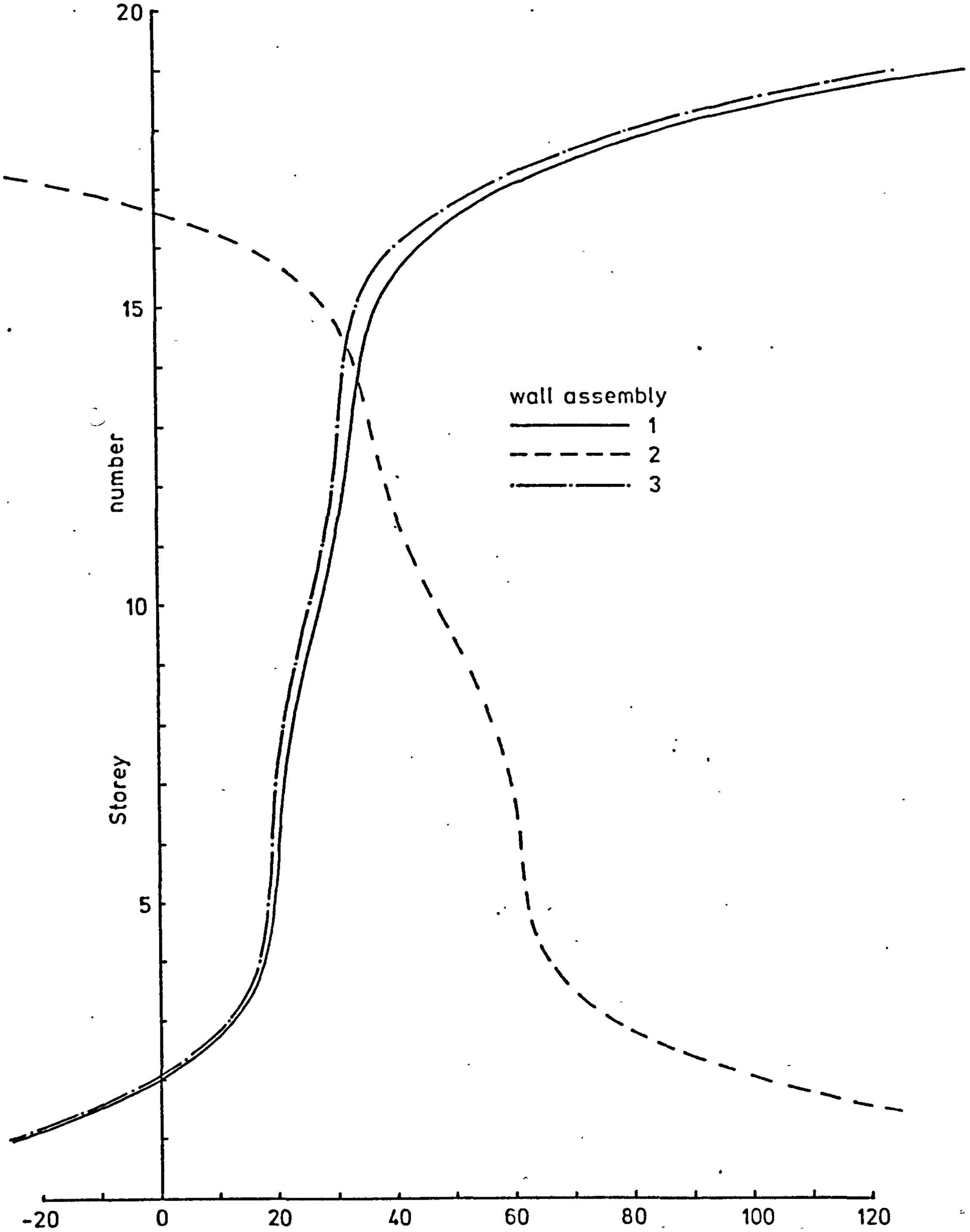

Test number 15 - Load distribution - Polynomial solution

Figure 8.72

Test number 15 - Load distribution - Point load solution.

Figure 8.73

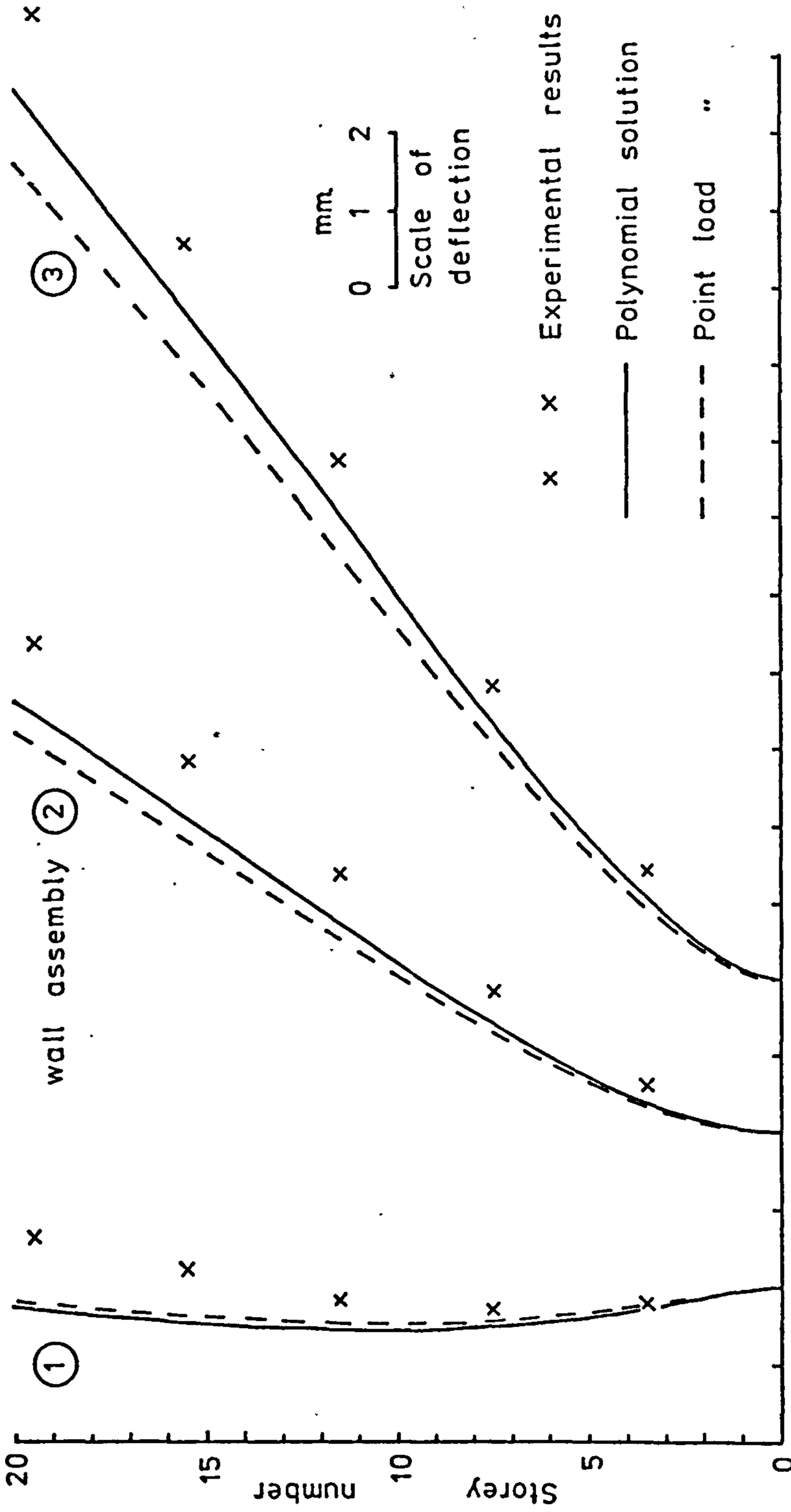

Test number 16 - Deflections

Figure 8.74

F 8.75

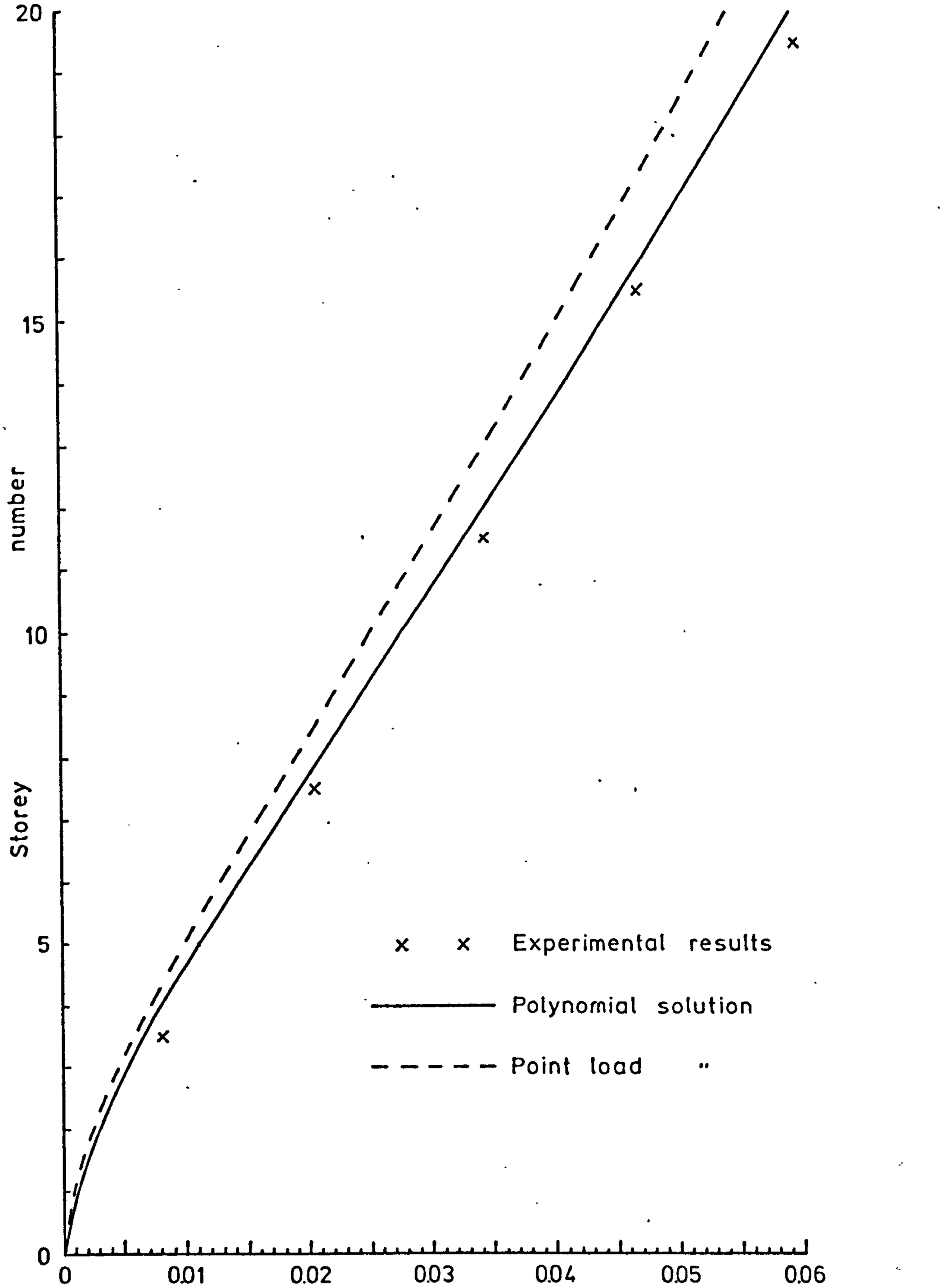

Test number 16 - Rotations

Figure 8.75

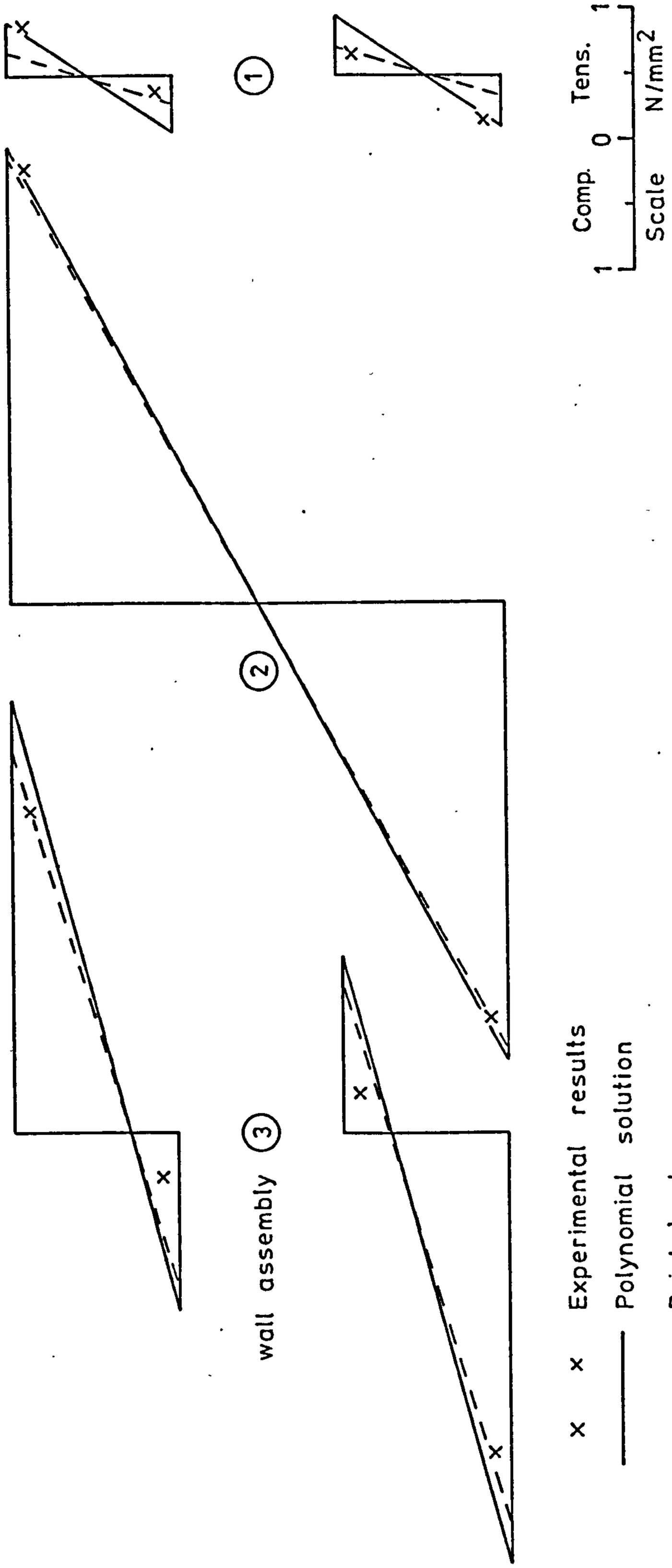

Figure 8.76 - Stresses

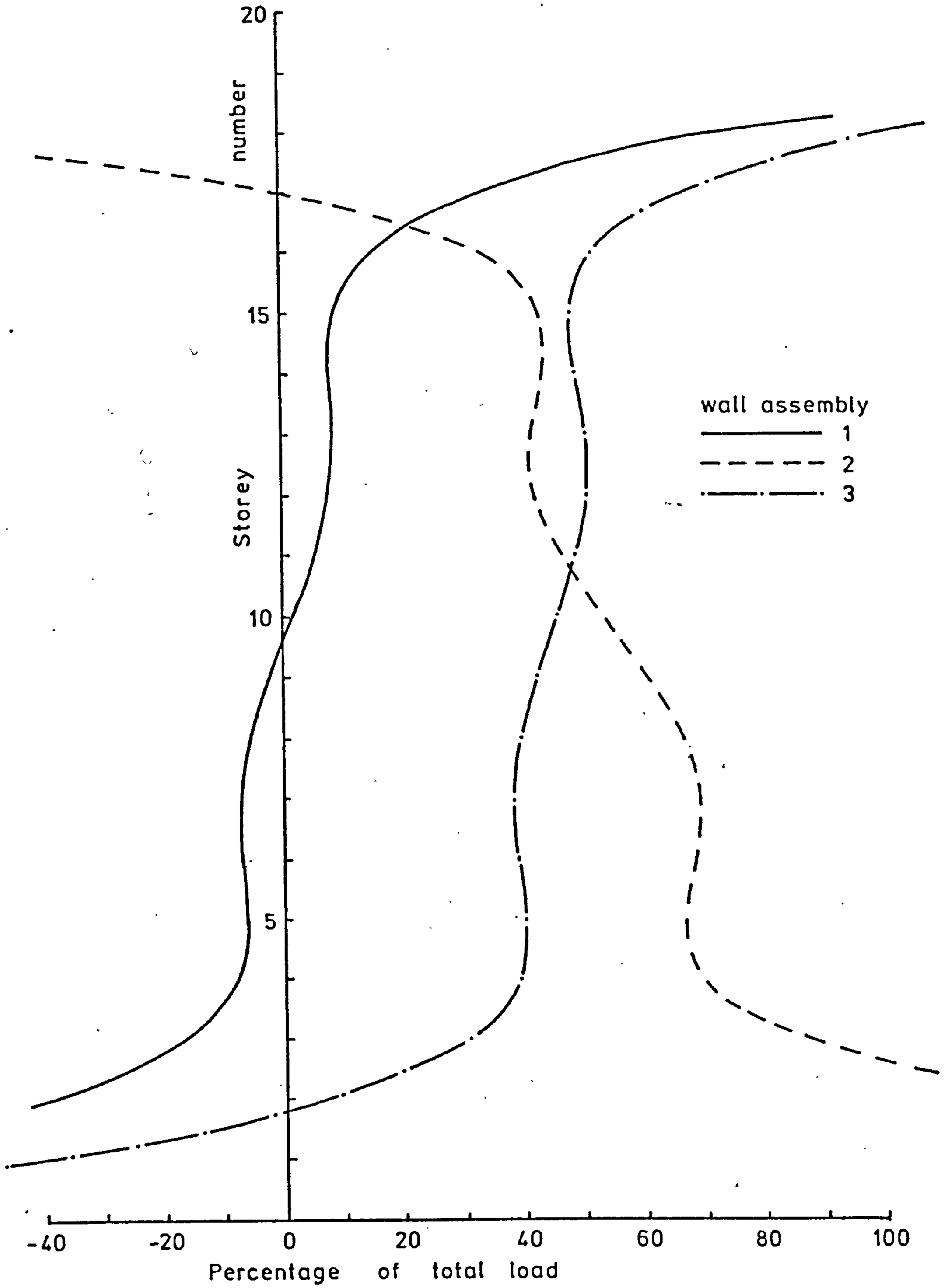

Test number 16 - Load distribution - Polynomial solution

Figure 8.77

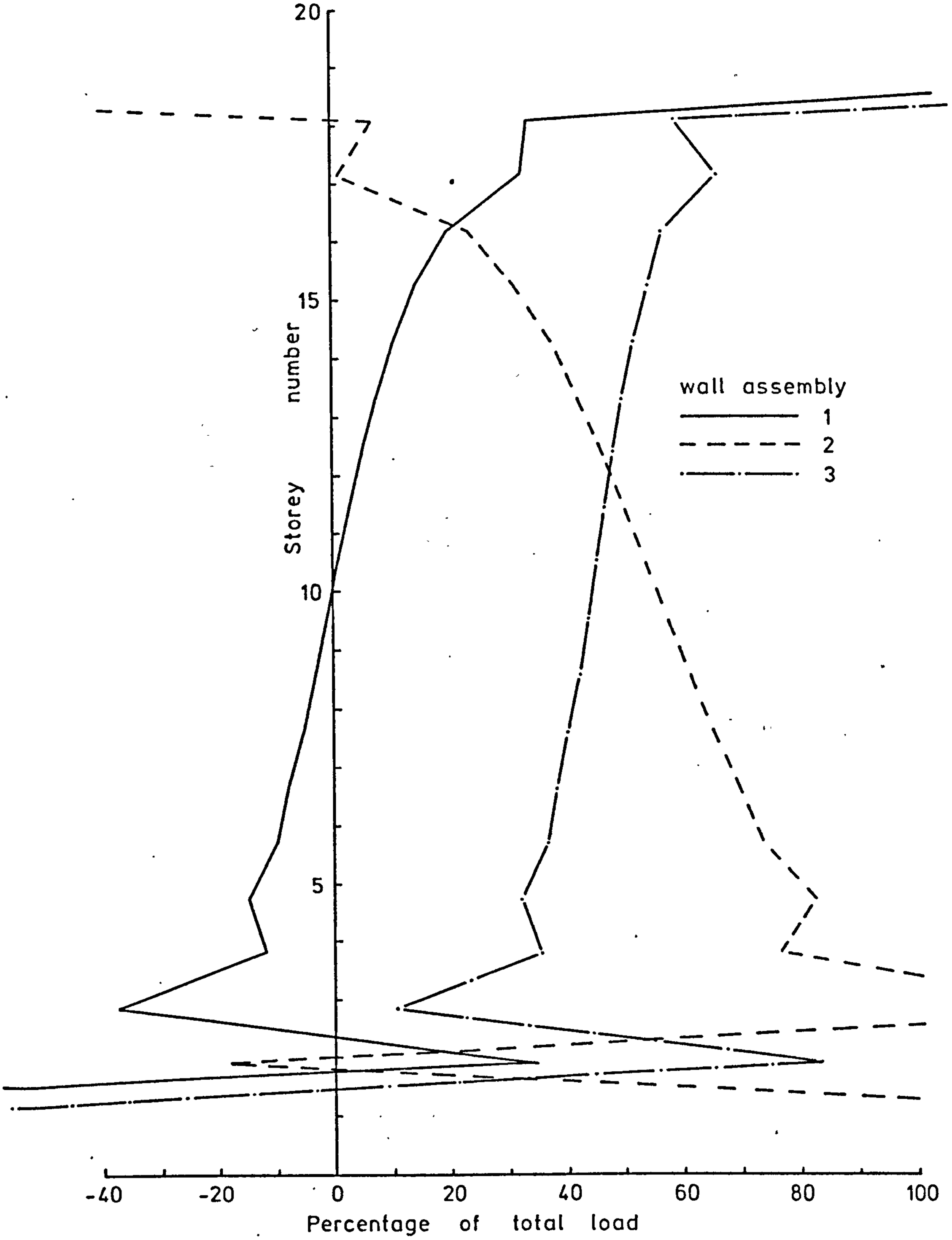

Test number 16 - Load distribution - Point load solution

Figure 8.78

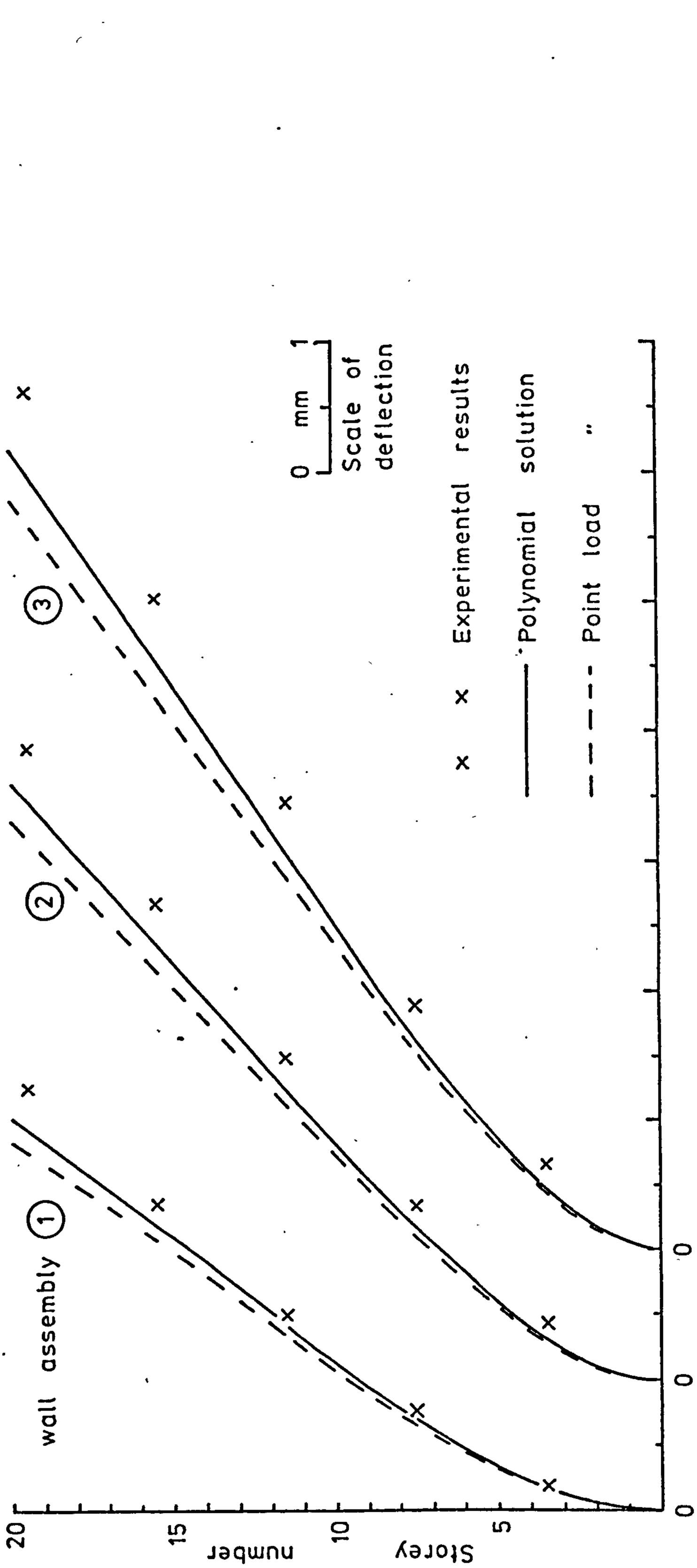
Deflections
Test number 17 - 8.79
Figure 8.79
Deflection mm.
0
0
Storey number
5
10
15
20
wall assembly (1)
(2)
(3)
x Experimental results
Polynomial solution
Point load "
0
Scale of deflection
mm 1

F 8.80

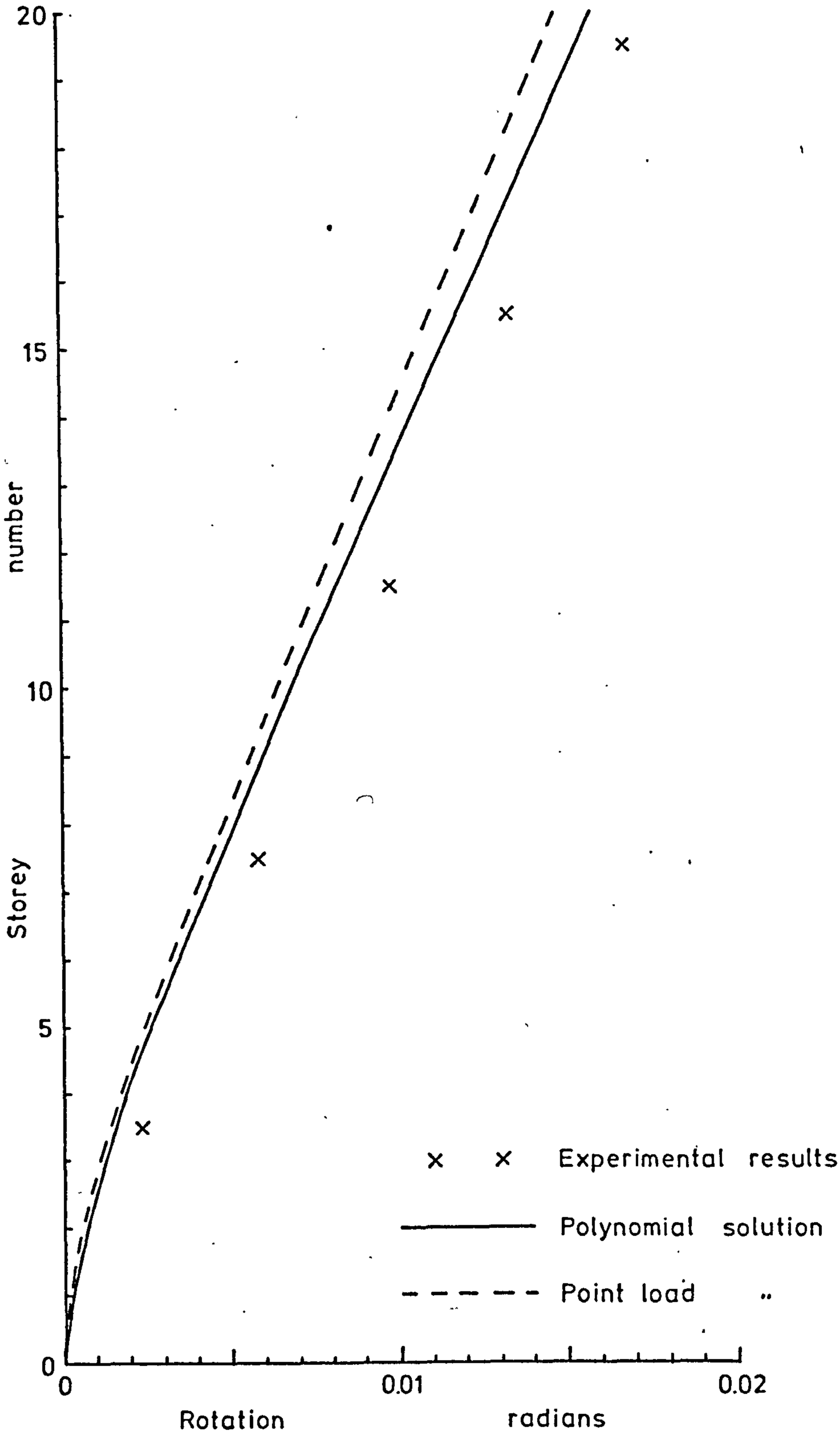

Test number 17 - Rotations

Figure 8.80

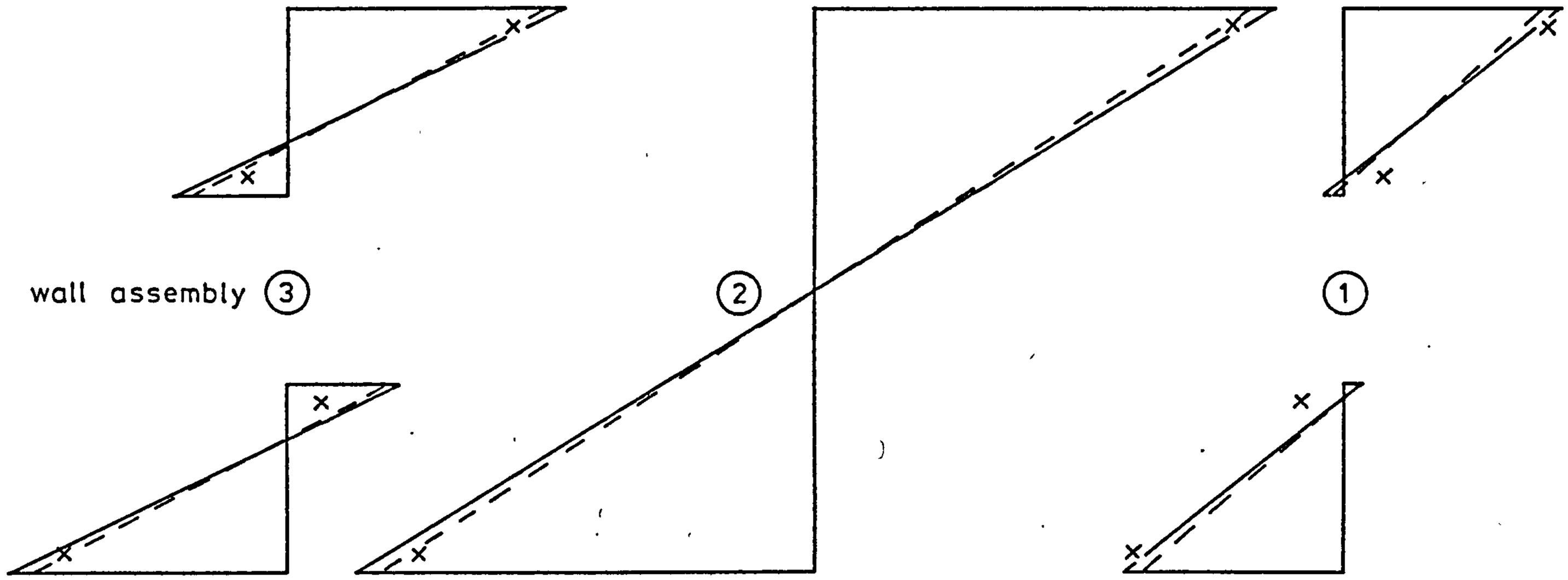

Test number 17 - Stresses

Figure 8.81

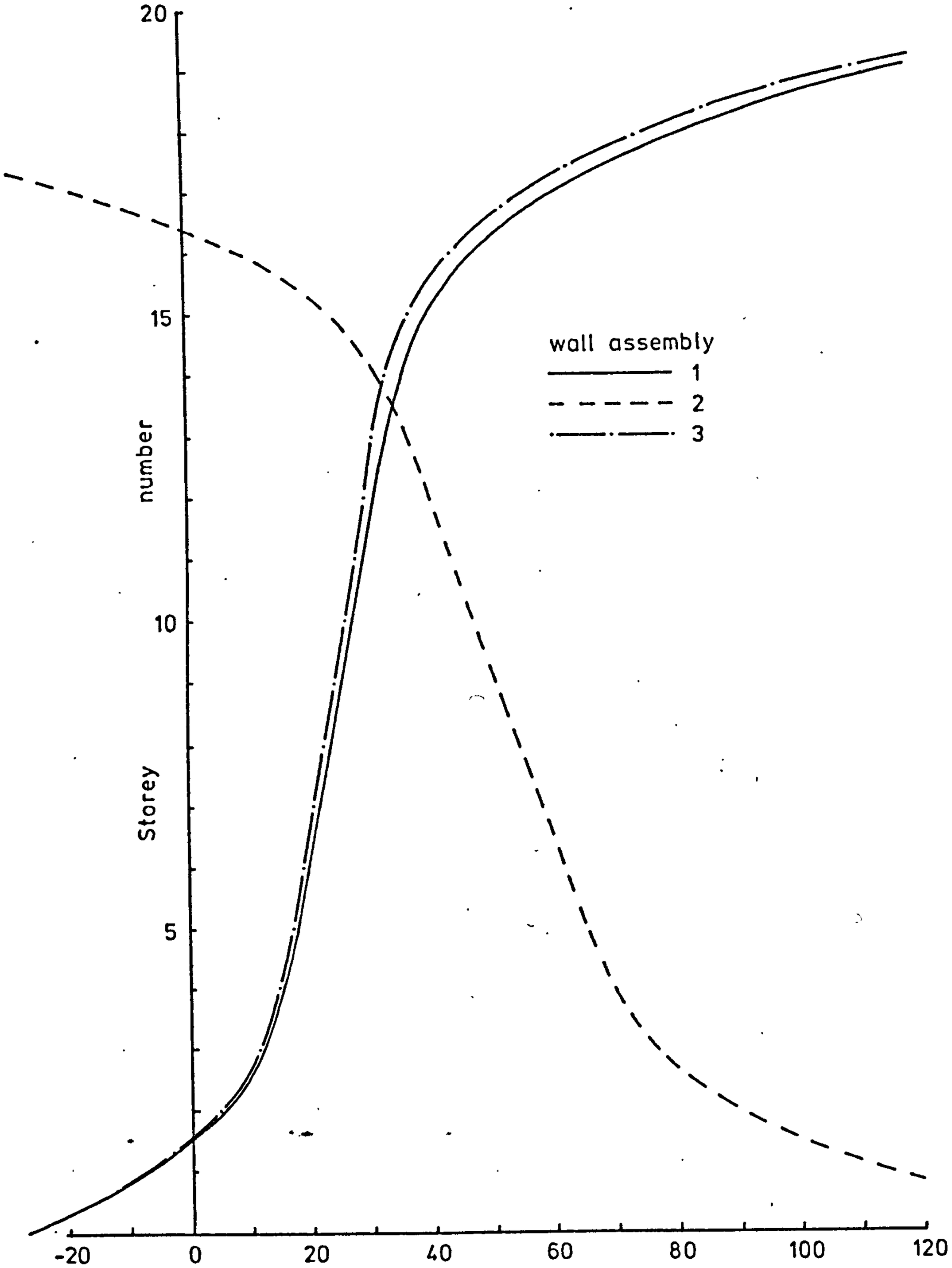

Test number 17 - Load distribution - Polynomial solution

Figure 8.82

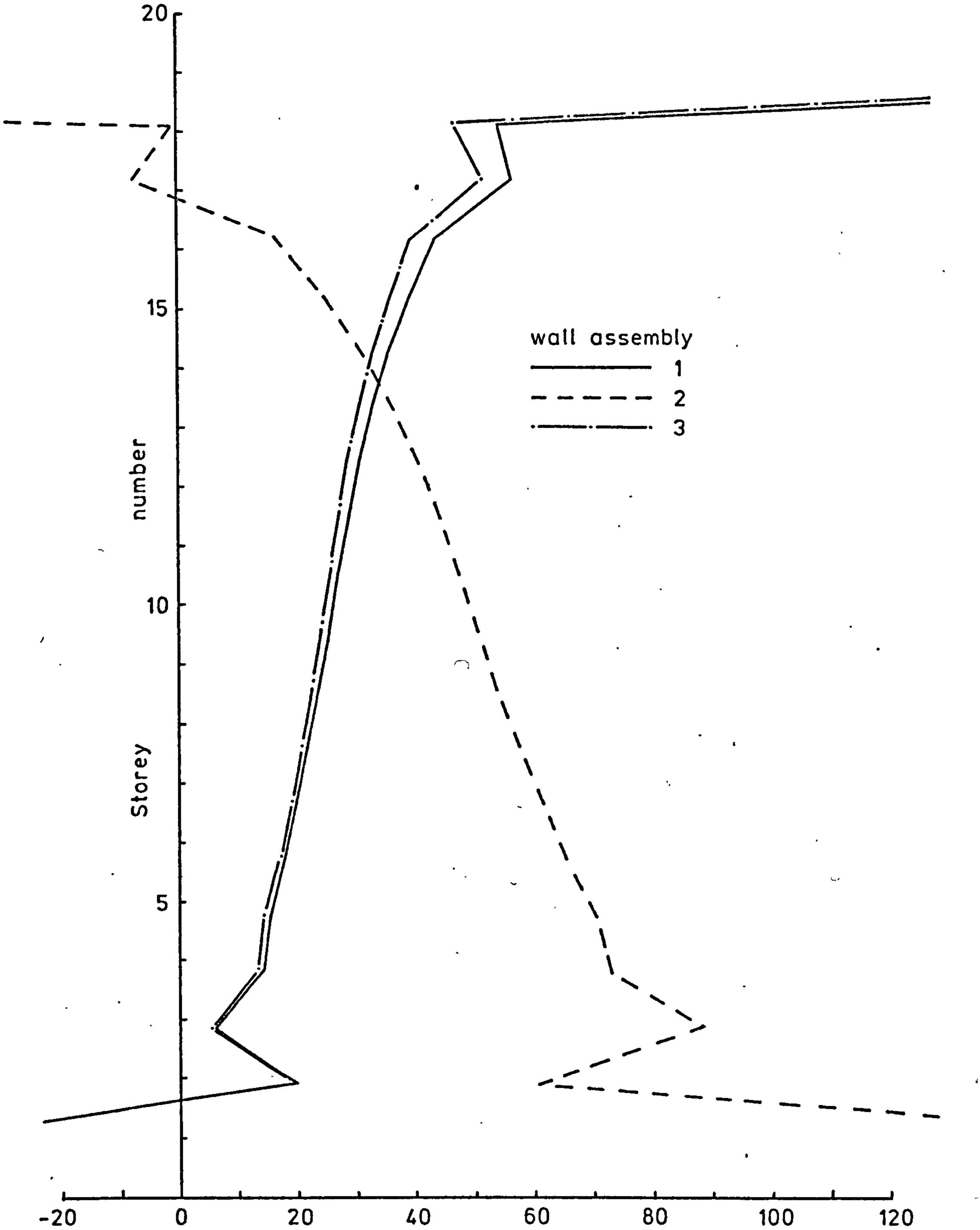

Test number 17 - Load distribution - Point load solution

Figure 8.83

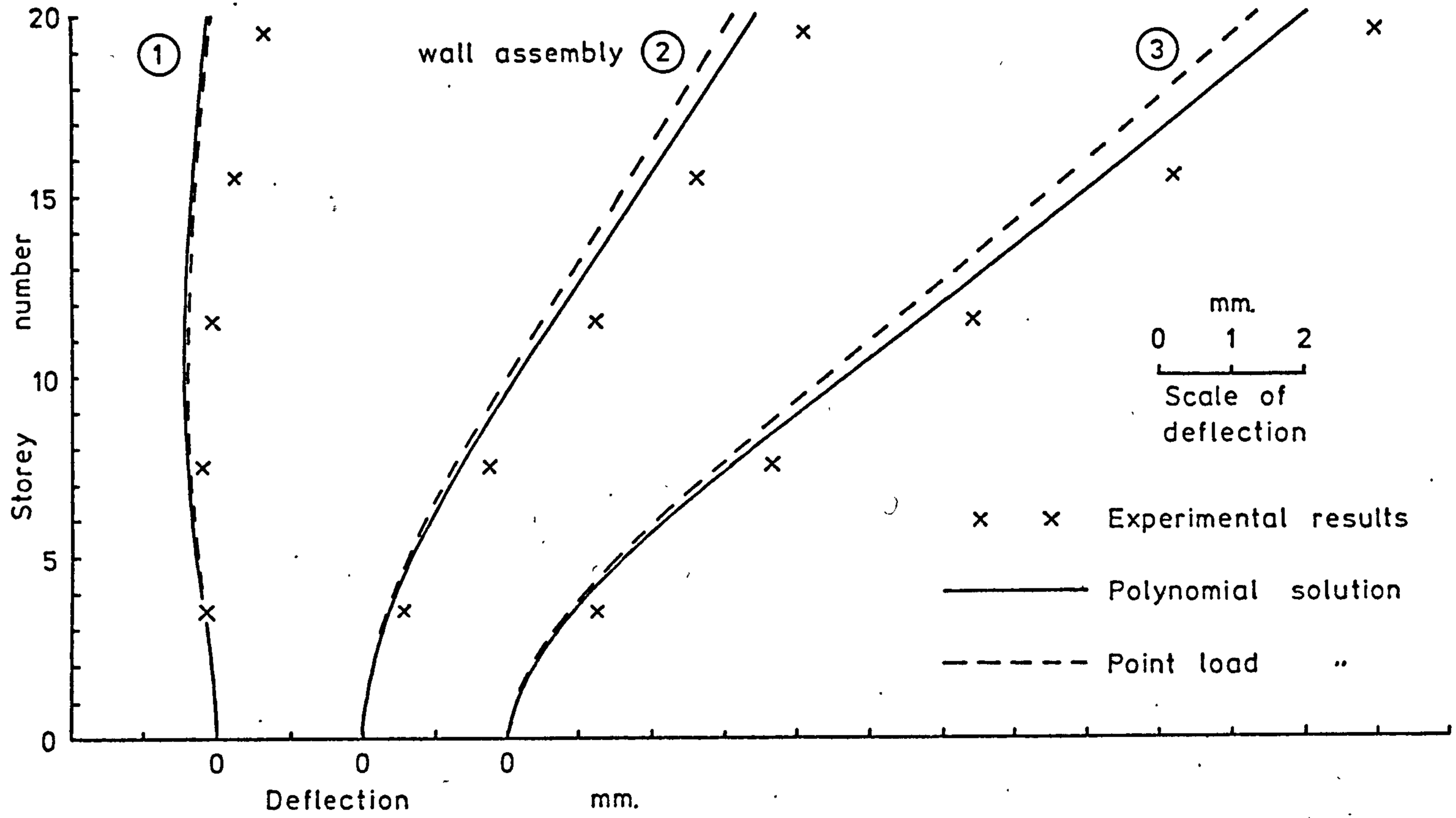

Test number 18 - Deflections

Figure 8.84

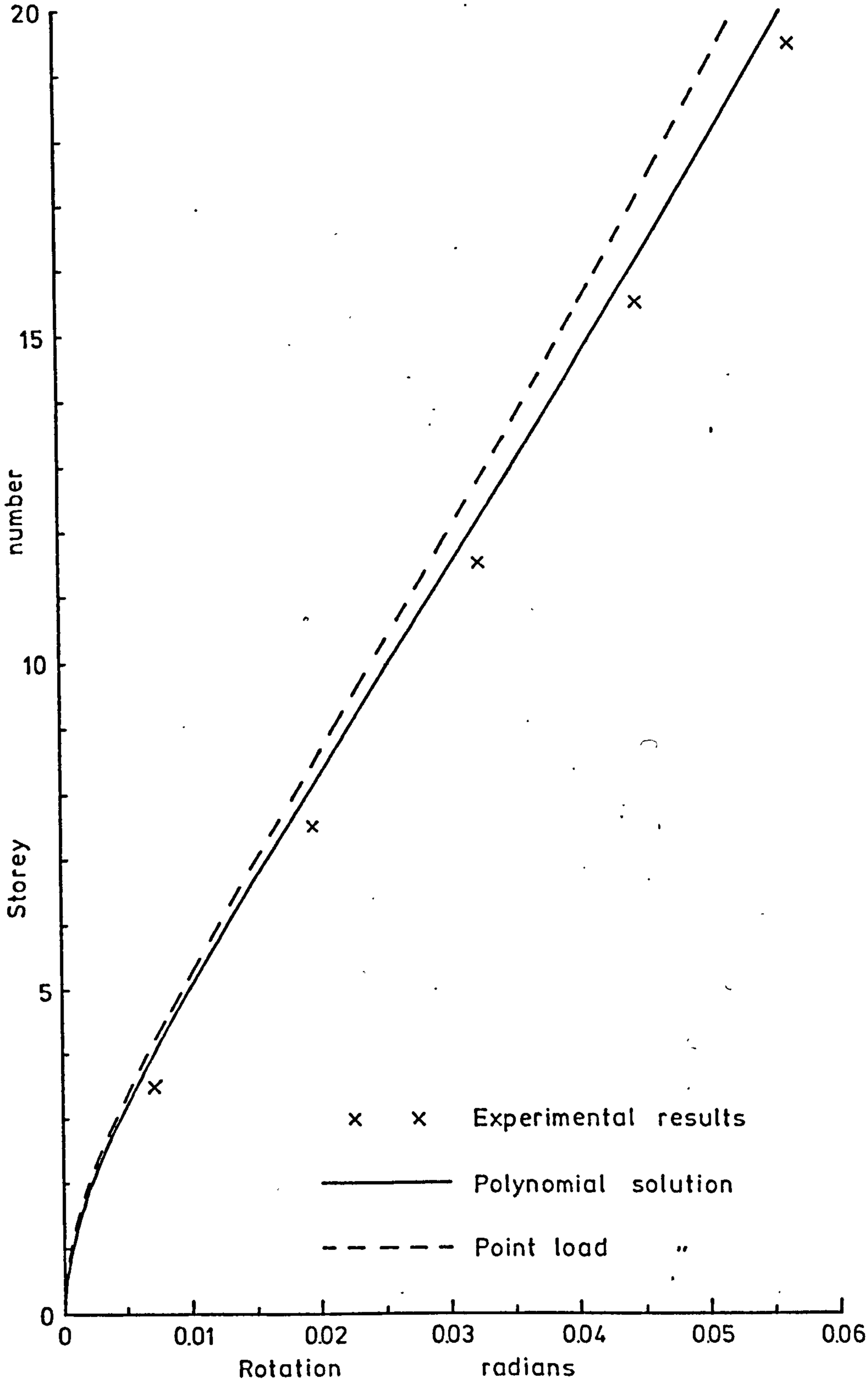

Test number 18 - Rotations

Figure 8.85

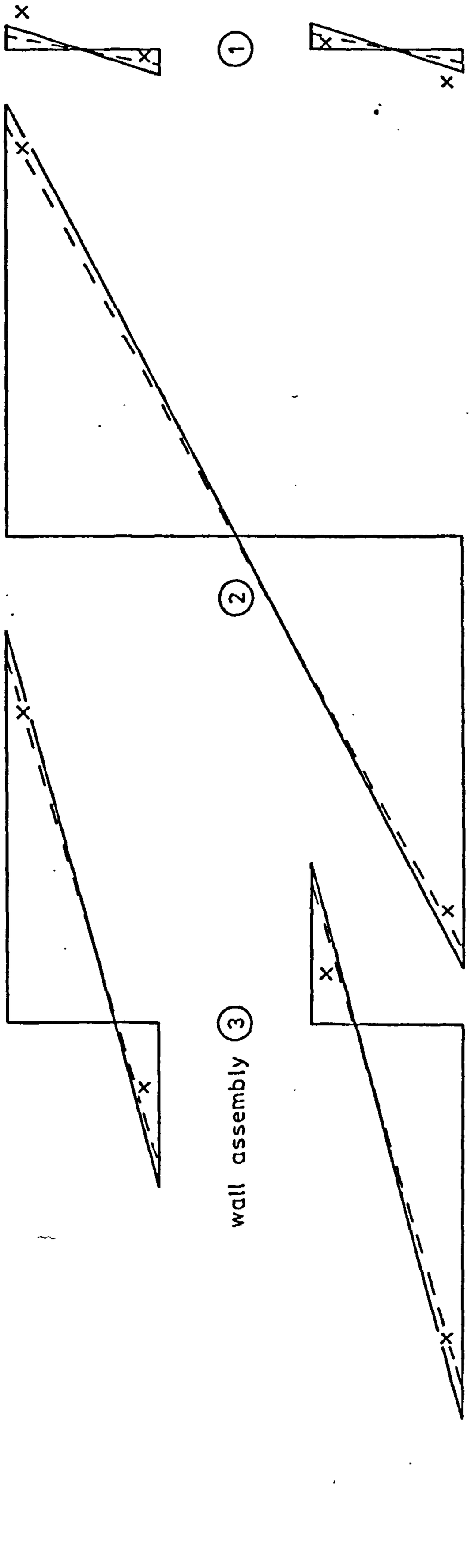

Figure 8.86 - Stresses

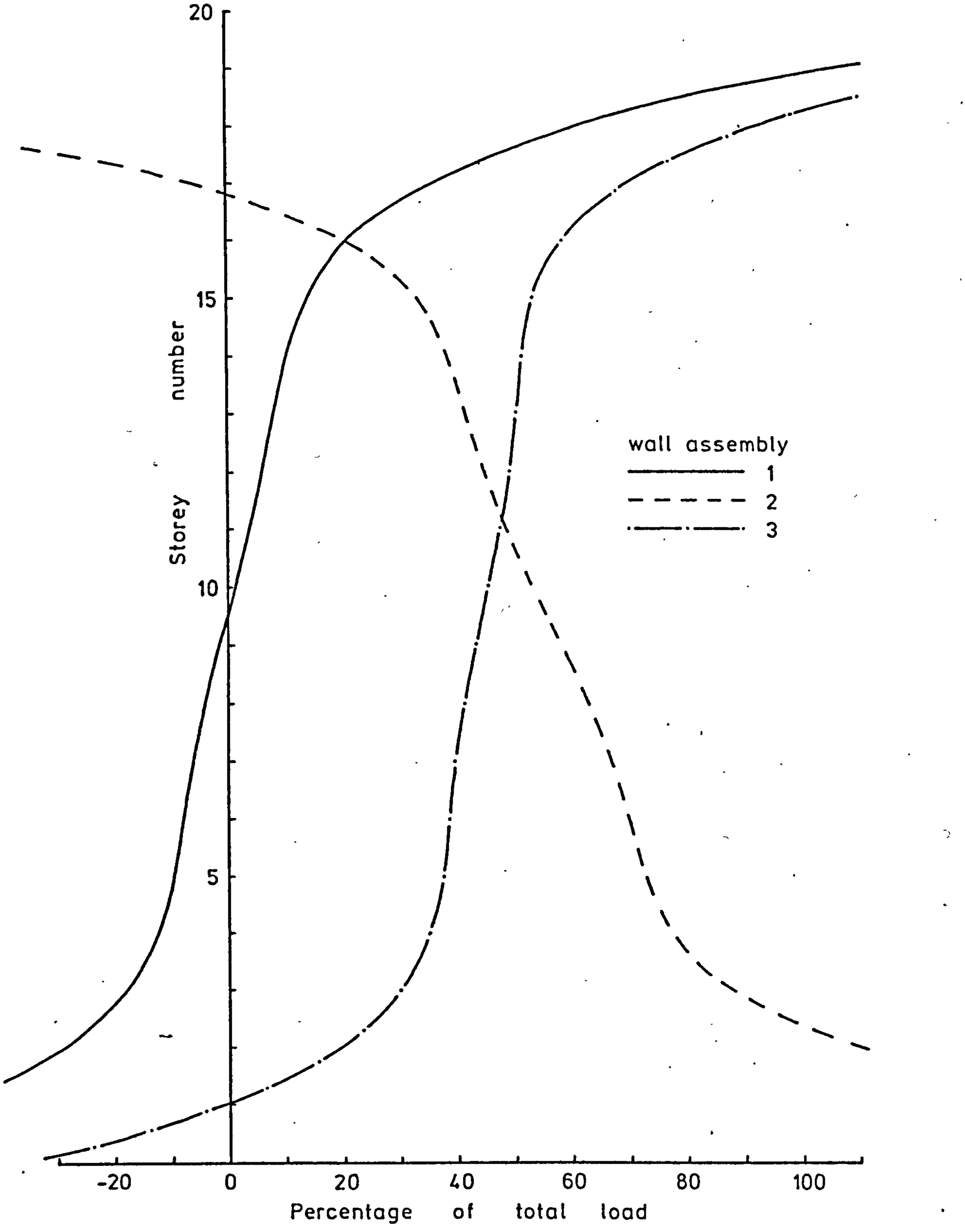

Test number 18 - Load distribution - Polynomial solution

Figure 8.87

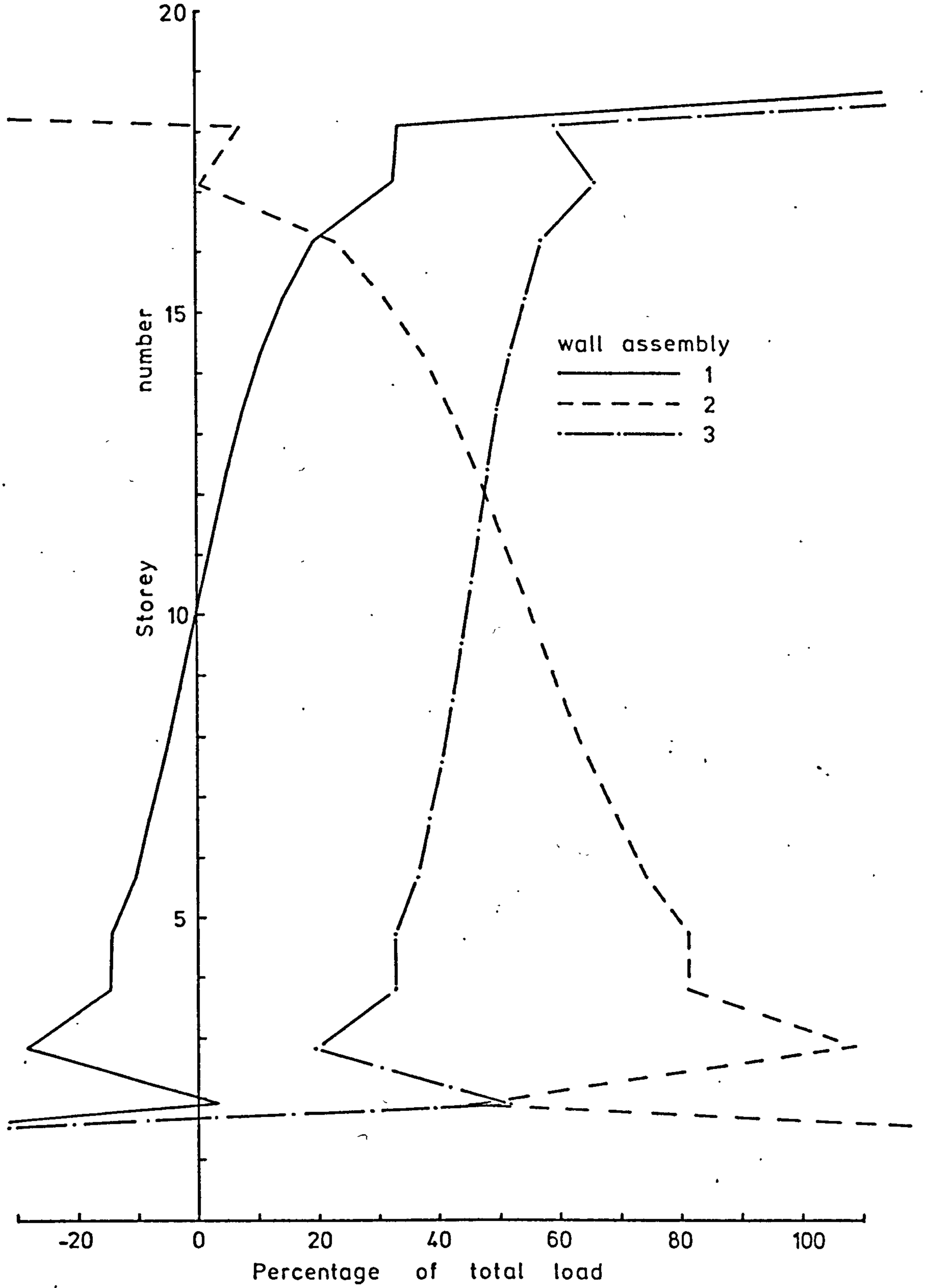

Test number 18 - Load distribution - Point load solution

Figure 8.88

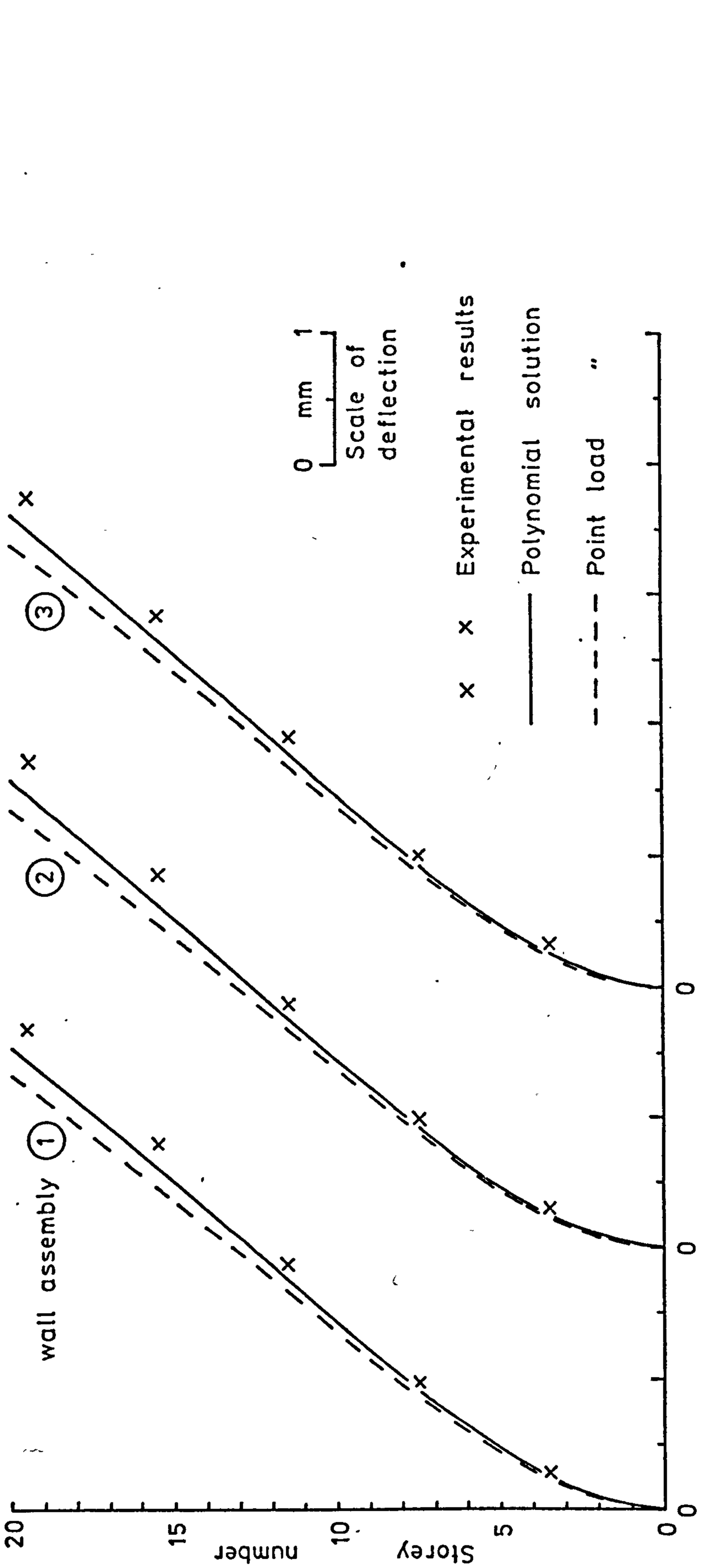
Storey number
20
15
10
5
0
Deflection
0
mm.
1
Scale of deflection
Test number 19
wall assembly ①
②
③
x Experimental results
Polynomial solution
Point load "
Deflections

Figure 8.89

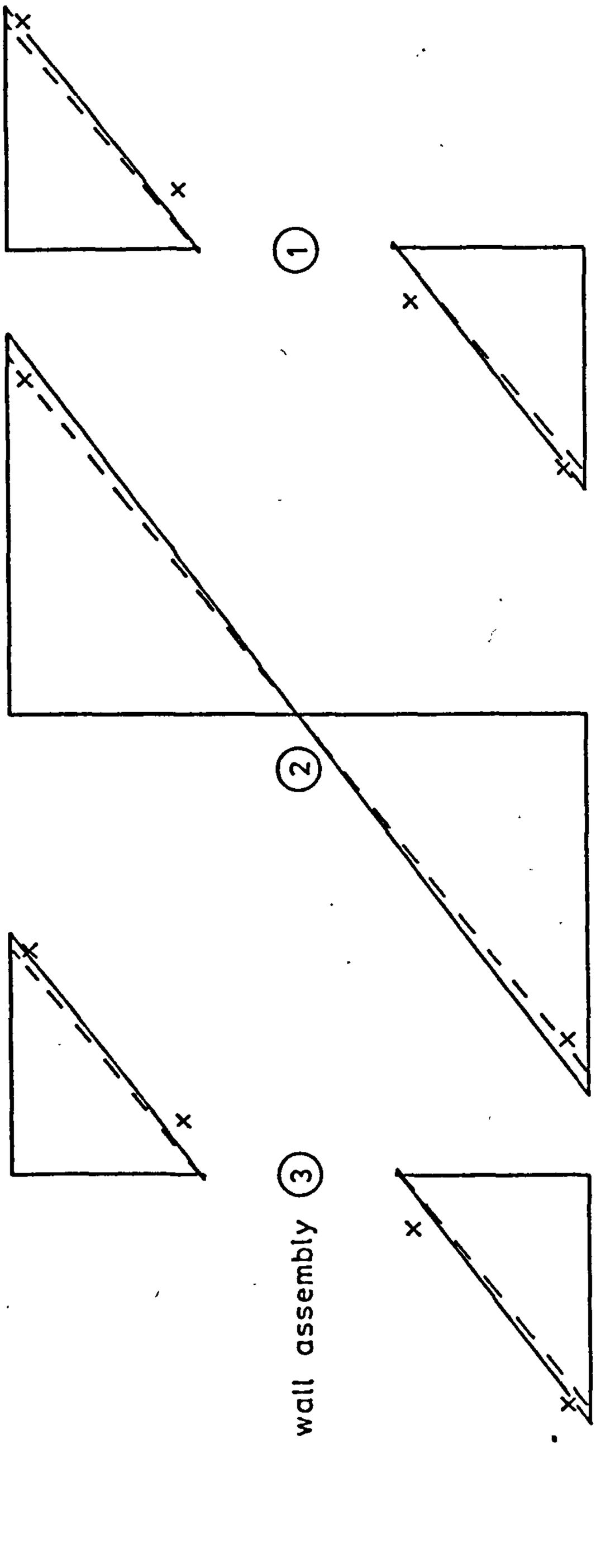
Comp. 0 Tens.
1 1
Scale N/mm2
Stresses
Experimental results
Polynomial solution
Point load "
Test number 19
Figure 8.90
wall assembly
1
2
3

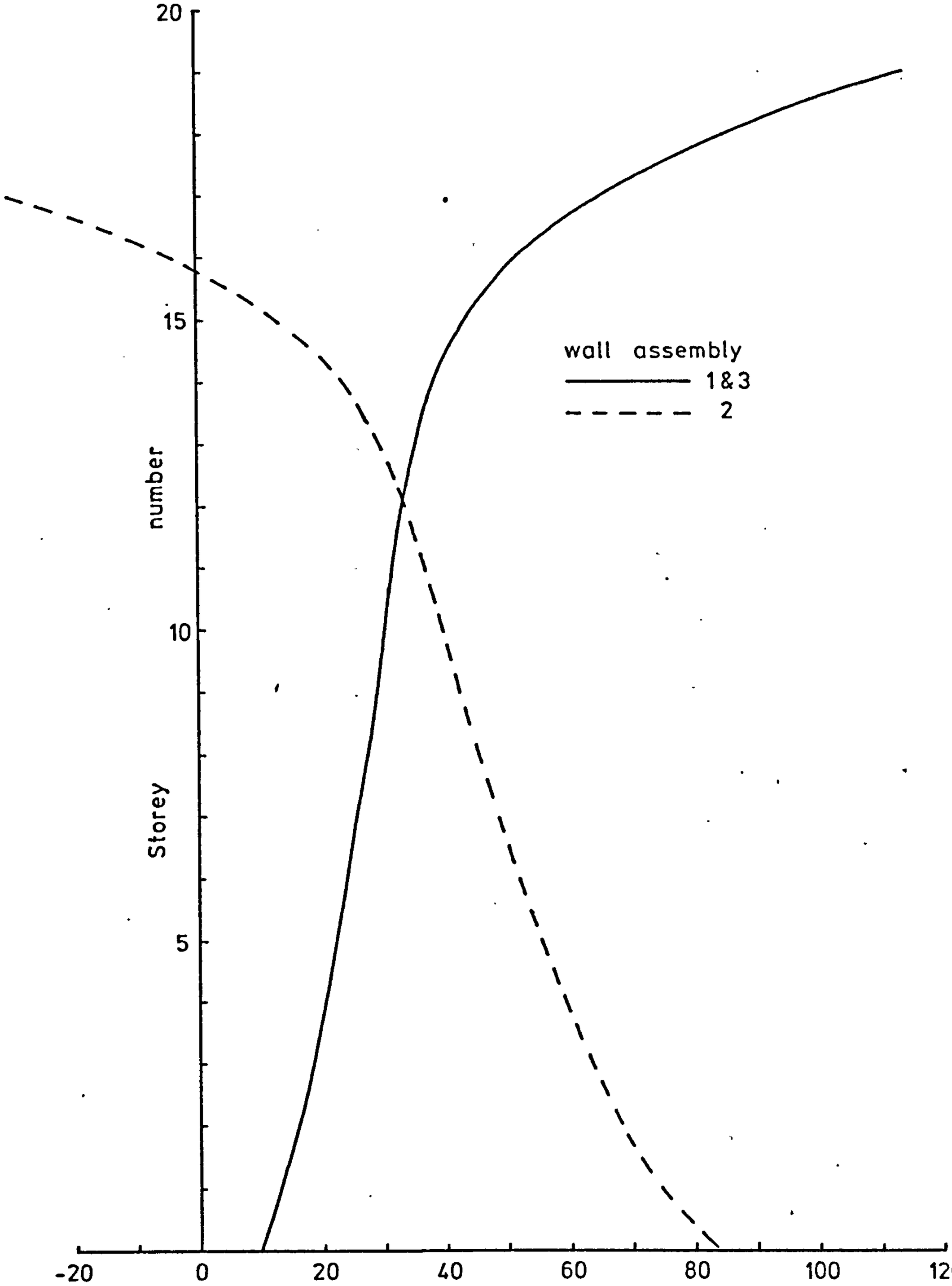

Test number 19 - Load distribution - Polynomial solution

Figure 8.91

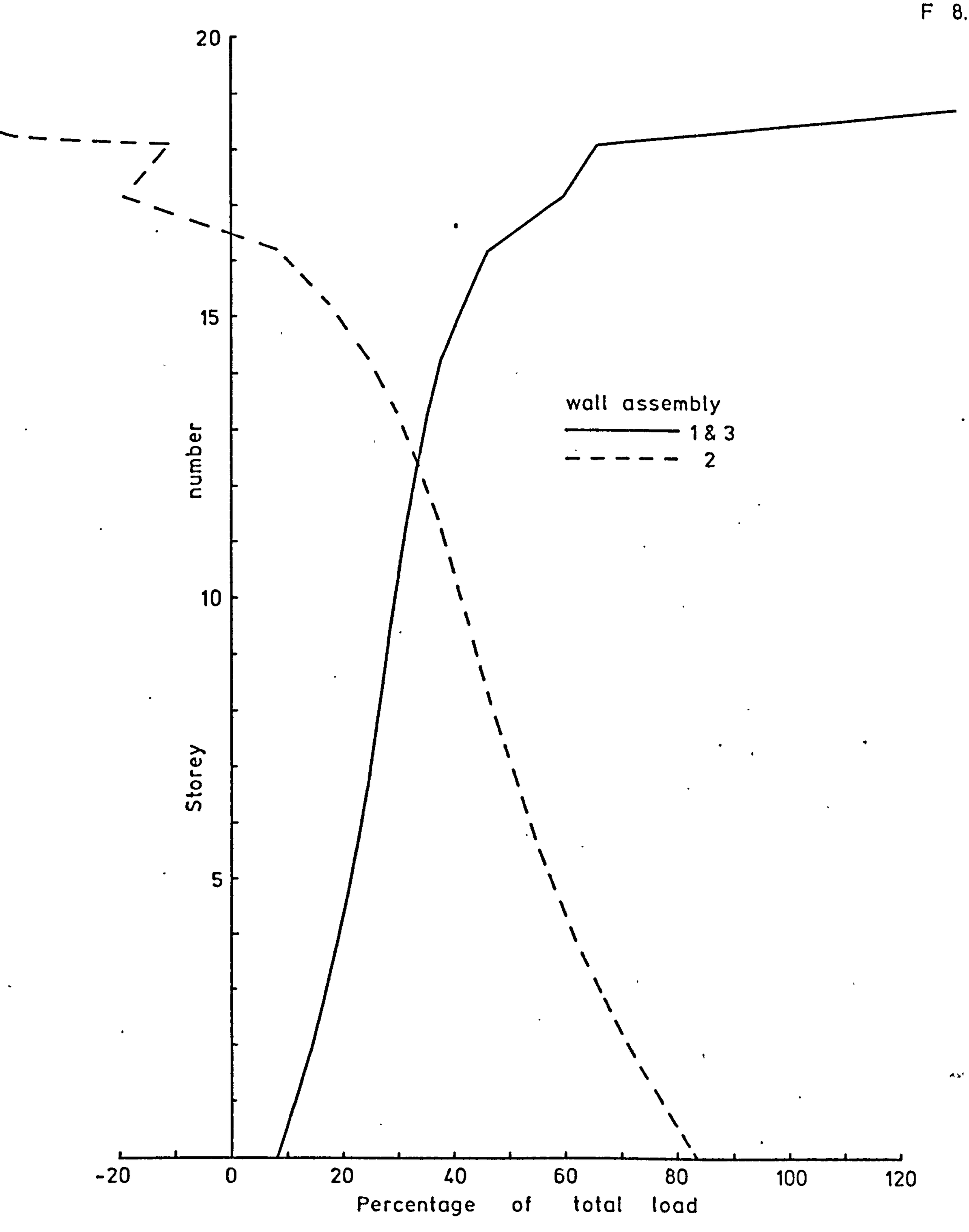

Test number 19 - Load distribution - Point load solution

Figure 8.92

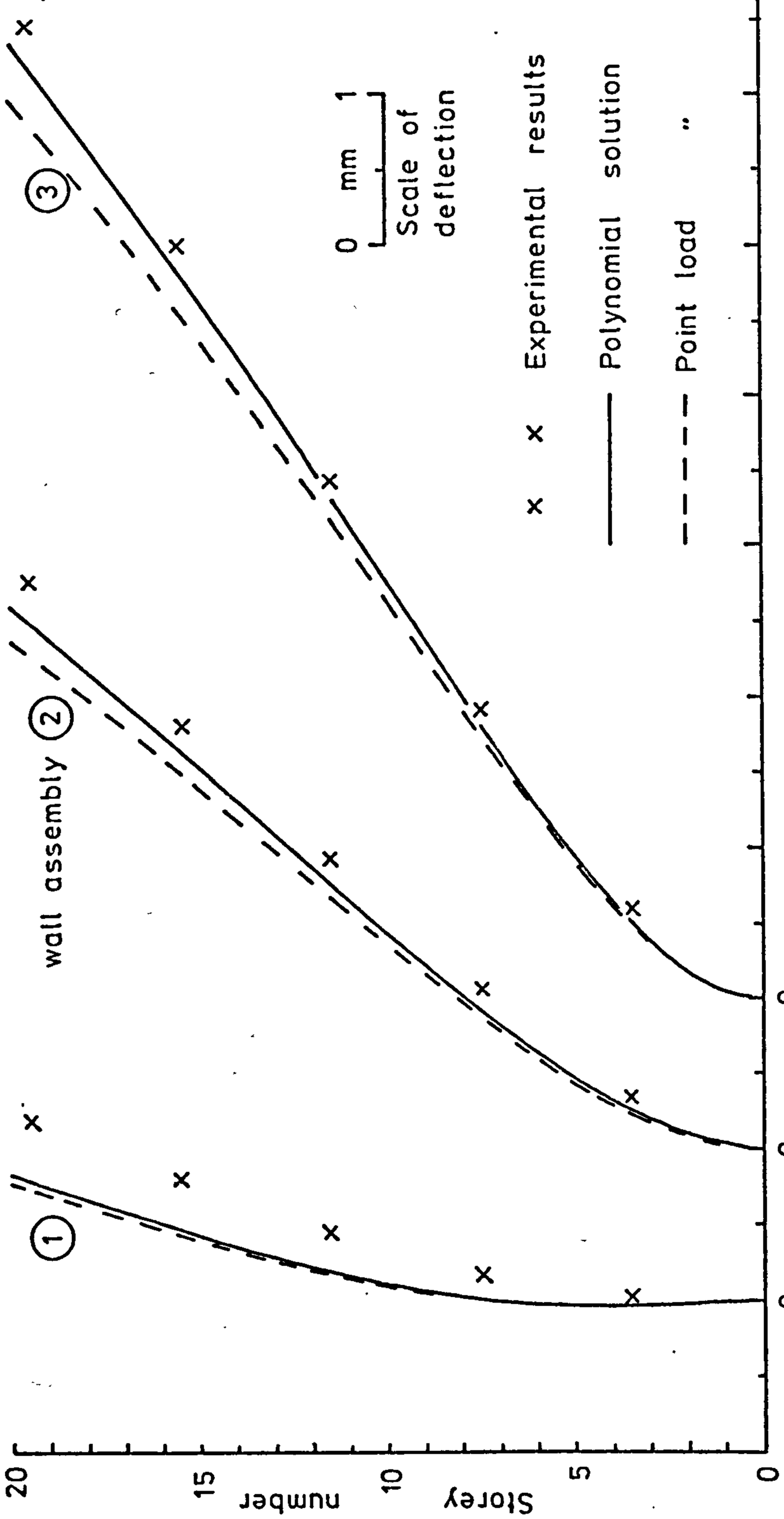
Storey number
20
15
10
5
0
Deflection
0
0
0
mm
Test number 20 - Deflections
8.93
wall assembly ①
wall assembly ②
wall assembly ③
0 mm 1
Scale of deflection
x x Experimental results
—— Polynomial solution
- - - - Point load "

Figure

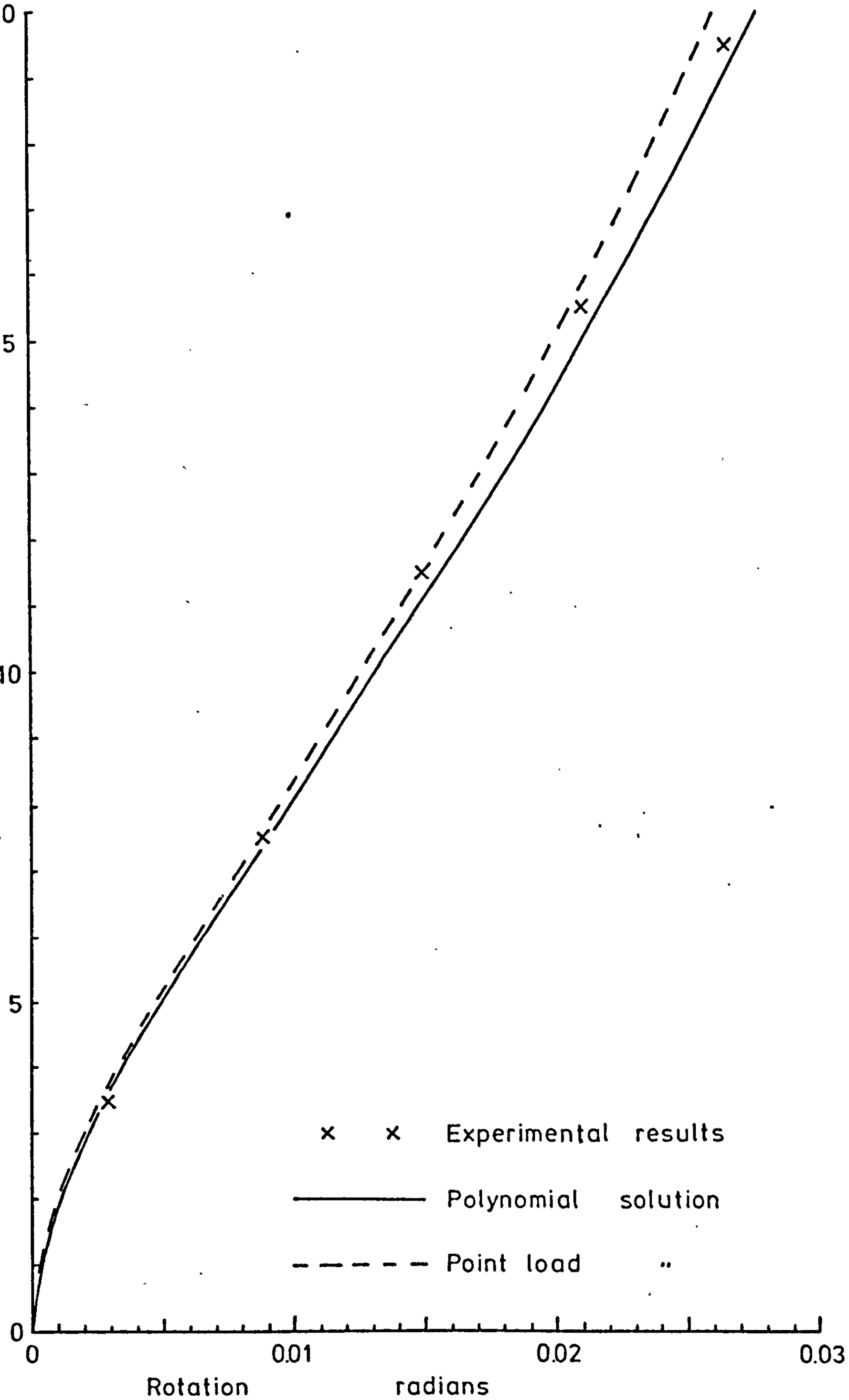

Test number 20 - Rotations

Figure 8.94

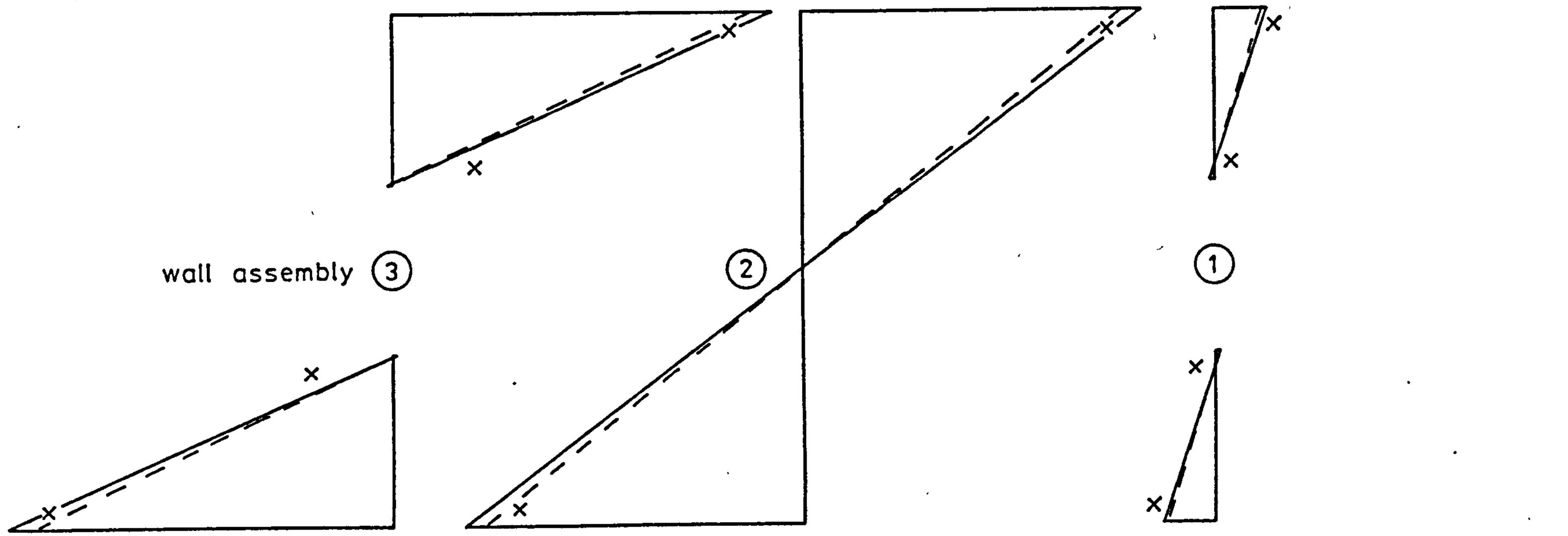

Test number 20 - Stresses

Figure 8.95

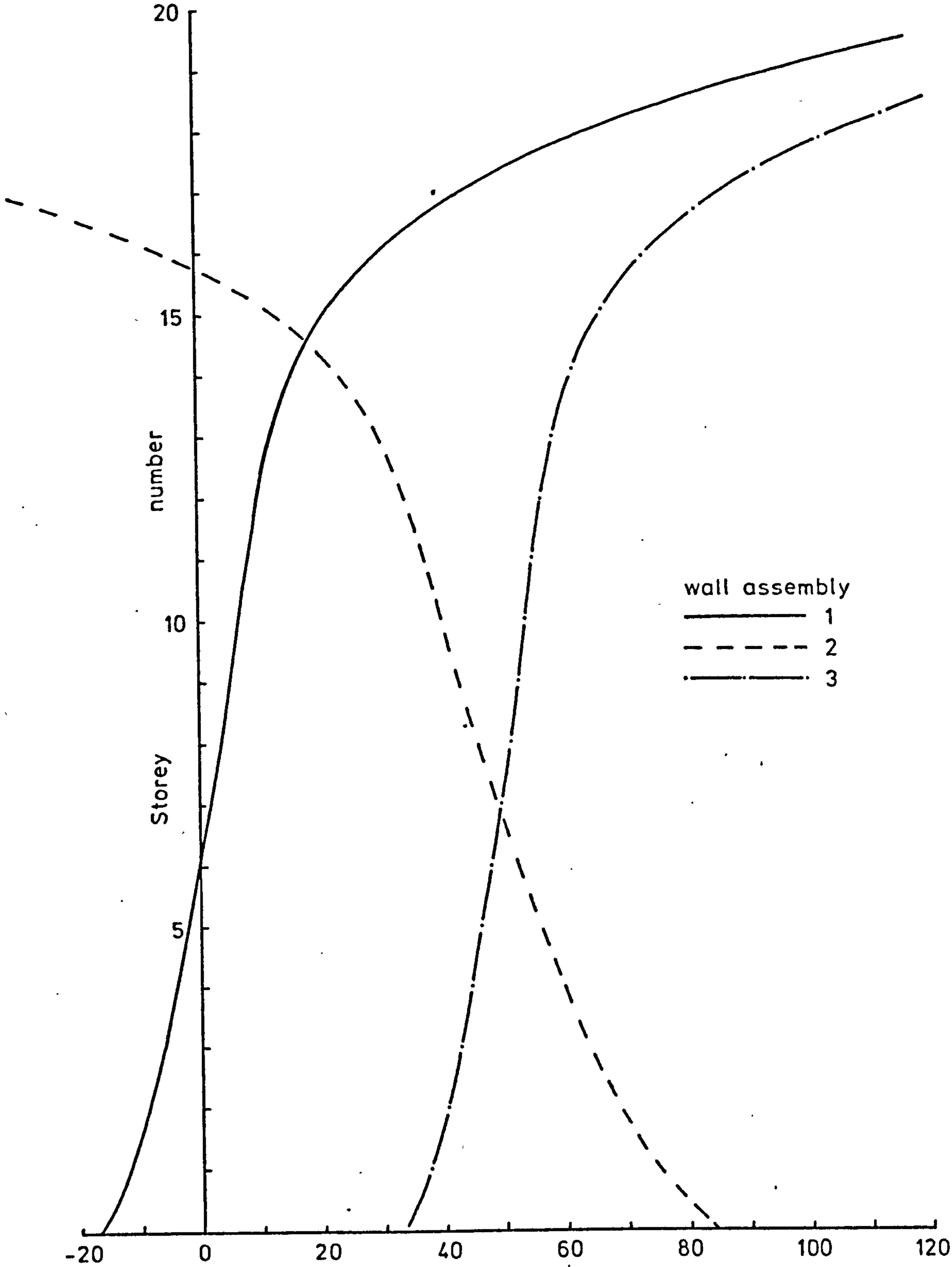

Test number 20 - Load distribution - Polynomial solution

Figure 8.96

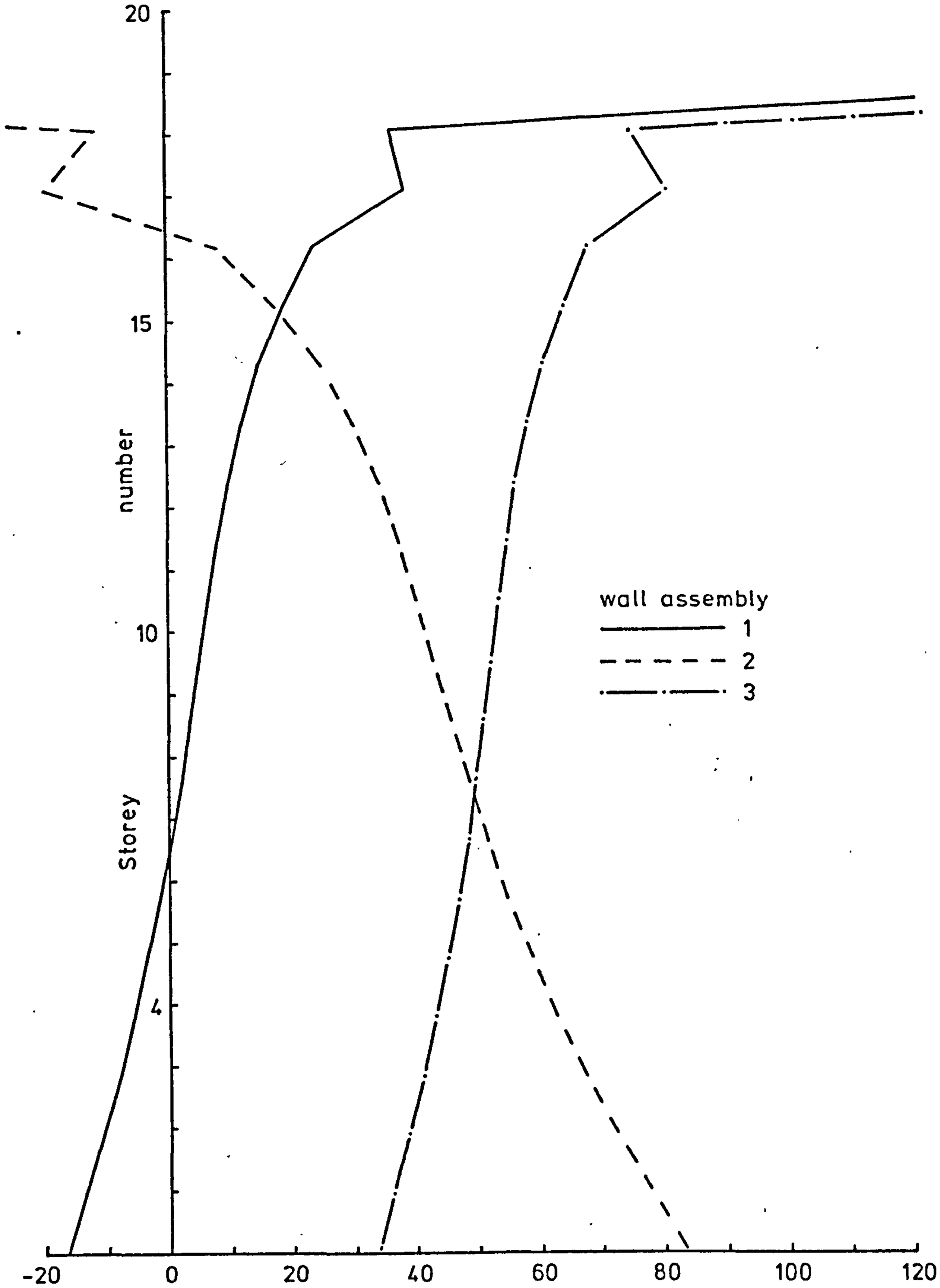

Test number 20 - Load distribution - Point load solution

Figure 8.97

Test Number	Model Number	Load Position	Effective length of foundation cantilevers mm		Foundation flexibility coefficients	
			Rotational	Vertical	Rotational K_θ radians/Nmm	Vertical K_v mm/N
1	1	1	40	30	0.0607×10^{-6}	0.370×10^{-3}
2	1	2	40	30	0.0607×10^{-6}	0.370×10^{-3}
3	1	1	80	30	0.364×10^{-6}	0.370×10^{-3}
4	1	2	80	30	0.364×10^{-6}	0.370×10^{-3}
5	1	1	80	80	0.364×10^{-6}	4.586×10^{-3}
6	1	2	80	80	0.364×10^{-6}	4.586×10^{-3}
7	1	1	40	80	0.0607×10^{-6}	4.586×10^{-3}
8	1	2	40	80	0.0607×10^{-6}	4.586×10^{-3}
9	1	1	Base built in		0	0
10	1	2	Base built in		0	0
11	2	1	40	30	0.0607×10^{-6}	0.370×10^{-3}
12	2	2	40	30	0.0607×10^{-6}	0.370×10^{-3}
13	2	1	80	30	0.364×10^{-6}	0.370×10^{-3}
14	2	2	80	30	0.364×10^{-6}	0.370×10^{-3}
15	2	1	80	80	0.364×10^{-6}	4.586×10^{-3}
16	2	2	80	80	0.364×10^{-6}	4.586×10^{-3}
17	2	1	40	80	0.0607×10^{-6}	4.586×10^{-3}
18	2	2	40	80	0.0607×10^{-6}	4.586×10^{-3}
19	2	1	Base built in		0	0
20	2	2	Base built in		0	0

Foundation conditions at wall assembly number 3 and load position as used in tests on model structures

Table 8.1

Test Number	Height Above Base mm	Horizontal deflection of wall assemblies mm			Rotation of Structure radians
		Wall 1	Wall 2	Wall 3	
1	175	0.421	0.485	0.545	0.00062
	375	1.262	1.368	1.526	0.00132
	575	2.153	2.349	2.54	0.00199
	775	3.01	3.28	3.60	0.00295
	975	3.83	4.14	4.42	0.00295
3	175	0.396	0.538	0.676	0.00140
	375	1.213	1.44	1.69	0.00239
	575	2.14	2.46	2.79	0.00325
	775	2.97	3.42	3.83	0.00430
	975	3.78	4.30	4.81	0.00515
5	175	0.282	0.645	1.015	0.00367
	375	0.951	1.725	2.57	0.0081
	575	1.719	2.94	4.20	0.01241
	775	2.45	4.14	5.75	0.0165
	975	3.16	5.20	7.25	0.02045
7	175	0.305	0.596	0.773	0.00234
	375	1.001	1.64	2.293	0.00646
	575	1.774	2.81	3.875	0.01051
	775	2.56	3.94	5.32	0.0138
	975	3.30	4.99	6.745	0.01723
9	175	0.379	0.387	0.378	-
	375	1.163	1.173	1.17	-
	575	2.065	2.03	2.035	-
	775	2.86	2.88	2.87	-
	975	3.65	3.67	3.65	-

Model number 1 - Load position number 1

Deflection of wall assemblies and rotation of structure

Table 8.2

Test Number	Height Above Base mm	Horizontal deflection of wall assemblies mm			Rotation of Structure radians
		Wall 1	Wall 2	Wall 3	
2	175	0.062	0.551	1.009	0.00474
	375	0.298	1.473	2.68	0.01193
	575	0.563	2.47	4.40	0.0192
	775	0.783	3.45	6.15	0.0268
	975	1.144	4.36	7.67	0.0326
4	175	0.039	0.603	1.167	0.00564
	375	0.259	1.548	2.92	0.0133
	575	0.512	2.60	4.66	0.0208
	775	0.751	3.55	6.43	0.0284
	975	1.073	4.54	8.12	0.0353
6	175	-0.045	0.867	1.795	0.0092
	375	0.050	2.213	4.383	0.0217
	575	0.204	3.75	7.10	0.0345
	775	0.407	5.167	9.81	0.0470
	975	0.617	6.537	12.43	0.0591
8	175	0.0	0.753	1.497	0.00749
	375	0.144	1.999	3.87	0.01863
	575	0.363	3.36	6.33	0.0298
	775	0.539	4.783	8.95	0.0421
	975	0.785	6.05	11.31	0.0526
10	175	0.1215	0.404	0.676	0.00277
	375	0.386	1.198	2.013	0.00814
	575	0.702	2.057	3.46	0.01378
	775	1.025	2.92	4.86	0.0192
	975	1.334	3.68	6.06	0.0236

Model number 1 - Load position number 2

Deflection of wall assemblies and rotation of structure

Table 8.3

Test Number	Height Above Base mm	Horizontal deflection of wall assemblies mm			Rotation of Structure radians
		Wall 1	Wall 2	Wall 3	
11	175	0.245	0.329	0.413	0.00084
	375	0.905	1.079	1.240	0.00168
	575	1.744	1.995	2.24	0.00248
	775	2.65	2.96	3.33	0.00341
	975	3.48	3.96	4.365	0.00441
13	175	0.225	0.333	0.445	0.00110
	375	0.867	1.103	1.265	0.00199
	575	1.679	2.04	2.25	0.00285
	775	2.52	2.98	3.41	0.00446
	975	3.385	3.92	4.41	0.00513
15	175	0.145	0.433	0.720	0.00288
	375	0.686	1.387	2.019	0.00667
	575	1.436	2.536	3.64	0.0110
	775	2.319	3.73	5.18	0.0143
	975	3.15	4.94	6.78	0.0182
17	175	0.178	0.434	0.650	0.00236
	375	0.748	1.344	1.909	0.00582
	575	1.501	2.496	3.46	0.0098
	775	2.364	3.67	5.03	0.0133
	975	3.25	4.88	6.61	0.o168
19	175	0.282	0.304	0.309	0.00014
	375	0.984	0.996	1.009	0.00013
	575	1.862	1.876	1.904	0.00021
	775	2.79	2.83	2.85	0.00031
	975	3.69	3.72	3.77	0.0004

Model number 2 - Load position number 1

Deflection of wall assemblies and rotation of structure

Table 8.4

Test Number	Height Above Base mm	Horizontal deflection of wall assemblies mm			Rotation of Structure radians
		Wall 1	Wall 2	Wall 3	
12	175	-0.084	0.375	0.844	0.00464
	375	-0.035	1.187	2.396	0.0122
	575	0.155	2.190	4.16	0.020
	775	0.438	3.115	6.02	0.0279
	975	0.819	4.10	7.75	0.0347
14	175	-0.124	0.390	0.914	0.00519
	375	0.004	1.212	2.498	0.0125
	575	0.063	2.187	4.28	0.0212
	775	0.328	3.13	6.09	0.0288
	975	0.707	4.13	7.79	0.0354
16	175	-0.200	0.635	1.454	0.00827
	375	-0.276	1.886	3.85	0.0206
	575	-0.142	3.40	6.72	0.0343
	775	0.241	4.85	9.60	0.0468
	975	0.636	6.39	12.56	0.0596
18	175	-0.159	0.592	1.276	0.00718
	375	-0.211	1.774	3.70	0.0195
	575	-0.065	3.25	6.44	0.0325
	775	0.272	4.63	9.21	0.0447
	975	0.687	6.12	11.98	0.0565
20	175	0.026	0.344	0.603	0.00289
	375	0.178	1.062	1.938	0.0088
	575	0.445	1.930	3.43	0.0149
	775	0.798	2.825	5.02	0.0211
	975	1.204	3.77	6.49	0.0265

Model number 2 - Load position number 2

Deflection of wall assemblies and rotation of structure

Table 8.5

Test Number	Strain gauge position	Stresses on horizontal plane 175 mm above base N/mm^2		
		Wall 1	Wall 2	Wall 3
1	A	+1.394	+1.523	+1.50
	B	+0.257	+0.573	+0.368
	C	-0.432	-0.423	-0.228
	D	-1.537	-1.452	-1.285
3	A	+1.425	+1.515	+1.403
	B	+0.315	+0.616	+0.453
	C	-0.334	-0.511	-0.315
	D	-1.505	-1.419	-1.25
5	A	+1.387	+1.78	+1.331
	B	+0.224	+0.759	-0.082
	C	-0.226	-0.691	+0.109
	D	-1.408	-1.77	-1.25
7	A	+1.351	+1.81	+1.48
	B	+0.242	+0.714	-0.138
	C	-0.351	-0.544	+0.243
	D	-1.48	-1.72	-1.30
9	A	+1.462	+1.407	+1.394
	B	+0.386	+0.372	+0.375
	C	-0.378	-0.376	-0.395
	D	-1.439	-1.419	-1.41

Tensile stresses positive

Model number 1 - Load position number 1

Stresses in wall assemblies

Table 8.6

Test Number	Strain gauge position	Stresses on horizontal plane 175mm above base N/mm^2		
		Wall 1	Wall 2	Wall 3
2	A	+0.505	+1.50	+2.26
	B	+0.010	+0.639	+0.484
	C	-0.105	-0.513	-0.423
	D	-0.609	-1.42	-2.12
4	A	+0.576	+1.426	+2.15
	B	0	+0.689	+0.599
	C	-0.026	-0.656	-0.645
	D	-0.557	-1.439	-2.13
6	A	+0.354	+1.89	+2.058
	B	-0.149	+0.917	-0.323
	C	+0.089	-0.904	+0.206
	D	-0.503	-1.918	-2.075
8	A	+0.380	+1.936	+2.32
	B	-0.120	+0.840	-0.319
	C	-0.057	-0.666	+0.337
	D	-0.495	-1.828	-2.145
10	A	+0.479	+1.364	+2.33
	B	+0.137	+0.358	+0.616
	C	-0.156	-0.384	-0.629
	D	-0.492	-1.357	-2.32

Tensile stresses positive

Model number 1 - Load position number 2

Stresses in wall assemblies

Table 8.7

Test Number	Strain gauge position	Stresses on horizontal plane 175 mm above base N/mm^2		
		Wall 1	Wall 2	Wall 3
11	A	+1.49	+2.28	+1.478
	B	+0.324	-	+0.260
	C	-0.262	-	-0.274
	D	-1.43	-2.215	-1.467
13	A	+1.47	+2.315	+1.395
	B	+0.271	-	+0.292
	C	-0.279	-	-0.345
	D	-1.48	-2.16	-1.44
15	A	+1.452	+2.74	+1.422
	B	+0.279	-	-0.195
	C	-0.214	-	+0.160
	D	-1.36	-2.64	-1.438
17	A	+1.363	+2.78	+1.504
	B	+0.269	-	-0.254
	C	-0.274	-	+0.233
	D	-1.378	-2.63	-1.473
19	A	+1.473	+2.15	+1.475
	B	+0.371	-	+0.355
	C	-0.341	-	-0.351
	D	-1.438	-2.11	-1.484

Tensile stresses positive

Model number 2 - Load position number 1

Stresses in wall assemblies

Table 8.8

Test Number	Strain gauge position	Stresses on horizontal plane 175 mm above base N/mm^2		
		Wall 1	Wall 2	Wall 3
12	A	+0.462	+2.42	+2.43
	B	+0.043	-	+0.374
	C	+0.004	-	-0.451
	D	-0.448	-2.30	-2.44
14	A	+0.537	+2.36	+2.33
	B	-0.066	-	+0.495
	C	+0.075	-	-0.551
	D	-0.444	-2.29	-2.36
16	A	+0.364	+3.285	+2.42
	B	-0.129	-	-0.353
	C	+0.146	-	+0.291
	D	-0.368	-3.13	-2.41
18	A	+0.305	+3.18	+2.54
	B	-0.065	-	-0.521
	C	+0.049	-	+0.403
	D	-0.274	-3.06	-2.57
20	A	+0.435	+2.21	+2.47
	B	+0.121	-	+0.601
	C	-0.158	-	-0.591
	D	-0.467	-2.085	-2.51

Tensile stresses positive

Model number 2 - Load position number 2

Stresses in wall assemblies

Table 8.9

Test Number	Rotation at base of walls radians			Relative vertical deflection at base of walls mm		
	Experimental Results	Polynomial Solution	Point Load Solution	Experimental Results	Polynomial Solution	Point Load Solution
1	0.00058	0.00057	0.00051	0.0820	0.0781	0.0737
2	0.00101	0.00099	0.00087	0.1490	0.1332	0.1257
3	0.00185	0.00182	0.00137	0.0997	0.0847	0.0782
4	0.00319	0.00315	0.00238	0.1588	0.1446	0.1335
5	0.00301	0.00295	0.00217	0.495	0.541	0.492
6	0.00508	0.00507	0.00374	0.814	0.923	0.839
7	0.00079	0.00088	0.00077	0.453	0.476	0.448
8	0.00129	0.00151	0.00133	0.733	0.812	0.764
11	0.00044	0.00029	0.00024	0.0680	0.0670	0.0630
12	0.00082	0.00066	0.00054	0.1149	0.1212	0.1146
13	0.00128	0.00078	0.00051	0.0679	0.0690	0.0641
14	0.00247	0.00176	0.00114	0.1203	0.1263	0.1170
15	0.00215	0.00130	0.00083	0.451	0.427	0.392
16	0.00410	0.00272	0.00172	0.794	0.782	0.716
17	0.00056	0.00048	0.00039	0.436	0.407	0.382
18	0.00107	0.00100	0.00081	0.765	0.739	0.694

Comparison of experimental results and theoretical solutions for rotation and deflection of foundations of wall assembly number three

Table 8.10

CHAPTER 9

CONCLUSIONS

Approximate analytical methods have been presented for the solution of structural problems concerning laterally loaded two- and three-dimensional multi-storey shear wall systems, whose structural form consists of parallel assemblies of shear walls and box cores. The methods may have wider application in more complex systems since it is frequently possible, for analytical purposes to divide them into discrete units whose form approximates to that for which the analysis was developed.

Two-dimensional assemblies consisting of a pair of shear walls coupled by a regular array of lintel beams or floor slabs have been analysed using the widely accepted continuous connection technique to provide explicit solutions suitable to be incorporated into the three-dimensional analysis. Single shear walls or isolated box cores have been analysed by means of elementary bending theory. Solutions were given both for any polynomial load distribution and for any system of discrete point loads acting in the plane of the wall assembly. Provision was included in both solutions for elastic deformations to take place in the foundations of the walls and cores.

The three-dimensional analysis was achieved by satisfying the conditions of equilibrium and compatibility of the structure at a discrete number of reference levels throughout the height of the structure, whereby the load resisted by each two-dimensional wall assembly may be evaluated in either of the forms employed for the two-dimensional analysis. These loads may then be used to evaluate the stresses and deflections at any point on the constituent wall assemblies in the structure by employing the relevant expressions from the two-dimensional analysis. The method is general in that any load form acting on a structure parallel to the wall assemblies may be solved using any suitably spaced system of reference levels.

Although the analysis has been presented such that the load distributed to two-dimensional wall assemblies takes the form of

either a polynomial distribution or a system of point loads the method may be extended to include any load form for which an explicit solution for the horizontal deflection of an assembly may be found at any level. However, either of the above load forms will yield an adequate solution in the majority of cases. The method may also be extended to encompass any structural form for which the above explicit solution for deflection may be derived.

The results of the two-dimensional analysis for coupled shear wall assemblies have been adapted to produce expressions whereby design curves have been drawn for the rapid semi-graphical evaluation of stresses and deflections. These design methods were developed previously using rigid foundation conditions for the cases of a uniform load distribution[8], a triangular load distribution[9] and a load distribution in the form of any term in the polynomial series[20]. In the present thesis the methods have been expanded to include elastic foundation conditions and, with reservations, the additional load form, namely a point load at any height.

The design methods do not deal with elastic foundation conditions entirely satisfactorily since a complete set of curves is required for each combination of foundation flexibilities. The number of curves required for a design where foundation conditions are doubtful would therefore become prohibitive. The amount of work involved in compiling a comprehensive set of curves in such a case would negate the advantages of time and labour savings derived from using the curves, unless a large number of structures were involved. A practical solution to this problem has been put forward in Chapter 3, namely that the initial designs to determine the layout and dimensions of a structure may be carried out graphically using a standard set of curves based on the assumption that walls have rigid foundations. Thereafter the structure may be checked for the effects of possible foundation deformations using the computer programs.

The design method put forward in Chapter 3 for the graphical evaluation of the stress distribution in a pair of coupled shear walls is not suitable where walls are loaded with a system of point loads. Since the parameters for the evaluation of the stresses at any level are expressed as a percentage of the total moment acting at that level the method is unable to take account of the effects of those

point loads which act below the level under investigation. The method could therefore only deal effectively with levels immediately above the base and below the position of the lowest load point. There is scope therefore for an alternative method to deal with a system of point loads. Such a method might be achieved by expressing the parameters either as a proportion of the moment induced at the level under consideration by a unit point load at the top or as a proportion of the moment at the base caused by the load acting at its point of application.

The application of the analytical methods to obtain numerical solutions for three-dimensional multi-storey shear wall structures subject to any system of lateral loads has been discussed in Chapter 5. In order that the analysis may be applied to solve any structural problem successfully it must be ensured that the values which are substituted for the various parameters of the analytical expressions adequately represent the behaviour of the structure under consideration. To this end it is important that the precise nature of all the lateral load bearing systems within a structure may be accurately defined. Three of the problems which are most often encountered in the determination of the strength of such systems have been stated, namely the proportion of the flange which may be considered as effective in a wide flanged wall system; the effects of local deformations at beam- and slab-to-wall connections; and the width of a floor slab which is effective in the coupling action between shear walls. The latter case has been illustrated by an example in section 6.2 whereby the importance of accurately determining the true coupling effects of floor slabs has been shown. There is scope for further investigation into these parameters particularly in the case of the coupling effect of floor slabs since previously published investigations on the subject are not in agreement.

The methods of analysis may be used both for preliminary design calculations and for more detailed calculations at a later stage. Depending on the degree of accuracy required, any number of reference levels may be used, and if only a limited number of levels are employed the computation may be performed using a desk calculator. Of the two the polynomial solution is the more suitable for use with a desk calculator since reliable results may be obtained using very

few reference levels, thus keeping the amount of computation to a minimum. Even where a large number of reference levels are used the calculations required to find a solution may be performed in a short time using a small capacity computer. In this context the point load solution is more suitable since the results obtained by its use converge towards a stable value as more reference levels are employed, whereas the polynomial solution becomes unstable when more than seven or eight levels are used.

The reference levels may be positioned at any suitable levels to take account of variations in the lateral load on the structure. Irrespective of the positions of the reference levels used, the forces, deflections, etc. on the two-dimensional wall assemblies may be evaluated at any desired level.

The numerical examples of sections 6.4 and 6.5 have been presented to illustrate various effects of elastic foundations on multi-storey shear wall structures. Within a two-dimensional coupled shear wall assembly it was found that where any foundation system became more flexible to one mode of deformation, i.e. rotation or vertical movement, the proportions of the applied moment carried by bending moments and direct axial forces in the shear walls changed to compensate. In three-dimensional structures in which elastic foundations are present there is a general redistribution of lateral load form the more flexible foundations to other more securely founded systems. In a case of extreme flexibility of a foundation virtually no load may be resisted by that foundation. Even in this latter case, however, the majority of the redistribution caused by the foundation conditions takes place within the lowest few storeys and at higher levels the distribution of the load is only slightly affected by the foundation conditions.

The results of the experimental investigation followed a consistent pattern which was generally in reasonable agreement with the analytical solutions. The experimental deflections of the models were typically in excess of the analytical solutions. While the stress distribution measured on the models was not in agreement with the analytical solutions at the inner edges of coupled walls, the maximum stresses, which occurred at the outer edges, were in close agreement throughout.

Since the models were specifically designed to test the validity of the assumptions made in the analysis the form adopted for the models was necessarily a compromise between theory and reality. It cannot therefore be claimed that the experimental investigation enables any direct conclusions to be drawn about real structures. However it is considered that the methods may be used with confidence for the rapid analysis of the regular structures of the type considered, particularly in the early stages of design. Because of their speed in use, either with a desk calculator or a small computer, the methods lend themselves to an iterative approach to design, enabling more economical schemes to be decided upon before recourse is made to a more complex, and more costly analysis by, for example, finite elementtechniques. Bearing in mind the degree of accuracy to which the expected wind forces may be predicted, it may be the case that the continuous connection technique, carefully applied, could yield results of sufficient accuracy to enable final designs to be prepared. If these analytical methods were suitable for use in this context it would represent considerable cost savings in such projects. There is scope therefore for comparison studies between the various methods of analysis available to determine, on the bases of accuracy and economy, the full potential of the continuous connection technique as a design aid.

The major potential of the continuous connection technique lies in the investigation of the behaiour of two- and three-dimensional shear wall systems particularly where interaction with deformable foundations is involved. With the aid of the computer wide ranging parameter studies may be undertaken whereby qualitative assessments of shear wall behaviour may be made without the use of experimental investigation. Practical tests, which are both time consuming and expensive, particularly when deformable foundations are involved may then be reserved to check the validity of the analytical findings for a small number of critical configurations.

The application of the methods to the design of realistic structures is limited by the fact that the analysis was developed on the assumption of regular systems throughout the height of the structure. With difficulty a very limited number of changes in structural configuration may be allowed for in the analysis but the resultant expressions would be extremely cumbersome. The

analytical methods, therefore, may only be used with success for regular structural systems or for those which may be assumed regular for analytical purposes.

REFERENCES

1. KHAN, F.R. and IYENGAR, H.S.,
"Optimisation approach for concrete high-rise buildings", "Response of multi-story concrete structures to lateral forces", A.C.I. Publication SP-36, 1973, pp.61-74.

2. COULL, A. and STAFFORD SMITH, B.,
"Analysis of shear wall structures (A review of previous research)", Tall Buildings, Pergamon Press, 1967, pp.139-156.

3. "Response of buildings to lateral forces",
Journal of A.C.I., Proceedings, Vol. 68, No. 2,
Feb. 1971, pp.81-106.

4. STAMATO, M.C.,
"Three dimensional analysis of tall buildings",
Proceedings, International conference on planning and design of tall buildings, Lehigh University, U.S.A., 1972, Vol. 3, Report 24-4, pp.683-699.

5. COULL, A.,
"Coupled shear walls subjected to differential settlement", Building Science, Vol. 6, 1971, pp.209-212.

6. COULL, A.,
"Interaction of coupled shear walls with elastic foundations", Journal of A.C.I. Proceedings, Vol. 68, 1971, pp.456-461.

7. MICHAEL, D.,
"The effect of local wall deformations on the elastic interaction of crosswalls coupled by beams", Tall Buildings, Pergamon Press, 1967, pp.253-270.

8. COULL, A. and CHOUDHURY, J.R.,
"Stresses and deflections in coupled shear walls",
Journal of A.C.I., Proceedings, Vol. 64, No. 2,
Feb. 1967, pp.65-72.

9. COULL, A. and CHOUDHURY, J.R.,
"Analysis of coupled shear walls", Journal of A.C.I.,
Proceedings, Vol. 64, No. 9, Sept. 1967, pp.587-593.

10. TIMOSHENKO, S.,
"Strength of materials", Vol. 1, Third edition,
Van Nostrand, 1955, pp.217-219.

11. DEN HARTOG, J.P.,
"Advanced strength of materials", McGraw Hill, 1952.

12. MICHAEL, D.,
"Torsion coupling of core walls in tall buildings",
Structural Engineer, Vol. 47, 1969, pp.67-71.

13. POPOFF, A. Jr.,
"What do we need to know about the behaviour of
structural concrete shear walls", "Response of
multi story concrete structures to lateral forces",
A.C.I. Publication SP-36, 1973, pp.1-12.

14. QADEER, A., and STAFFORD SMITH, B.,
"The bending stiffness of slabs connecting shear walls",
A.C.I. Journal, Proceedings V. 66, No. 6, June 1969,
pp.464-473.

15. COULL, A.,
"Tests on a model shear wall structure",
Civil Engineering and Public Works Review, Vol. 61,
No. 722, Sept. 1966, pp.1129-1133.

16. BARNARD, P.R., and SCHWAIGHOFER, J.,
"Interaction of shear walls connected solely through slabs",
Tall Buildings, Pergamon Press, 1967, pp.157-173.

17. BRITISH STANDARDS INSTITUTION
CP3, "Code of basic data for the design of buildings", Chapter V. Loading, Part 2, Wind Loads, 1972.

18. IRWIN, A.W.,
"Analysis of shear wall structures", Ph.D. Thesis, University of Strathclyde, 1970.

19. COULL, A.,
"Interaction between coupled shear walls and cantilevered cores in three-dimensional regular symmetrical cross-wall structures", I.C.E., Proceedings, Part 2, Vol. 55, Paper 7658, 1973, pp.827-840.

20. COULL, A. and ADAMS, N.W.
"A simple method of analysis of the load distribution in multi-story shear wall structures", "Response of multi story concrete structures to lateral forces", A.C.I. Publication SP-36, 1973, pp.187-216.

APPENDIX 1

DESIGN CHARTS

Design charts, prepared using the expressions developed in Chapter 3, are presented in figures A.1 to A.51 inclusive for ranges of both polynomial and point load cases. The charts, for the semi-graphical evaluation of wall stresses, forces in connecting beams and maximum deflection, are given for the case in which the foundations of both walls of the coupled wall assembly are rigidly built in. For polynomial loads a separate chart is presented for each exponent from 0 to 6 inclusive. In the case of point loads charts are given to cover single point loads acting at ten levels evenly spaced throughout the height of the walls.

The charts are arranged as follows:-

Figure

A.1 to A.7 Variation of wall bending stress factors, K_1 and K_2 - Polynomial load (1 - 7)

A.8 to A.17 Variation of wall bending stress factors, K_1 and K_2 - Point load (1 - 10)

A.18 to A.24 Variation of connecting medium shear stress factor, K_3 - Polynomial load (1 - 7)

A.25 to A.34 Variation of connecting medium shear stress factor, K_3 - Point load (1 - 10)

A.35 to A.41 Variation of maximum deflection factor, K_4 - Polynomial load (1 - 7)

A.42 to A.51 Variation of maximum deflection factor, K_4 - Point load (1 - 10)

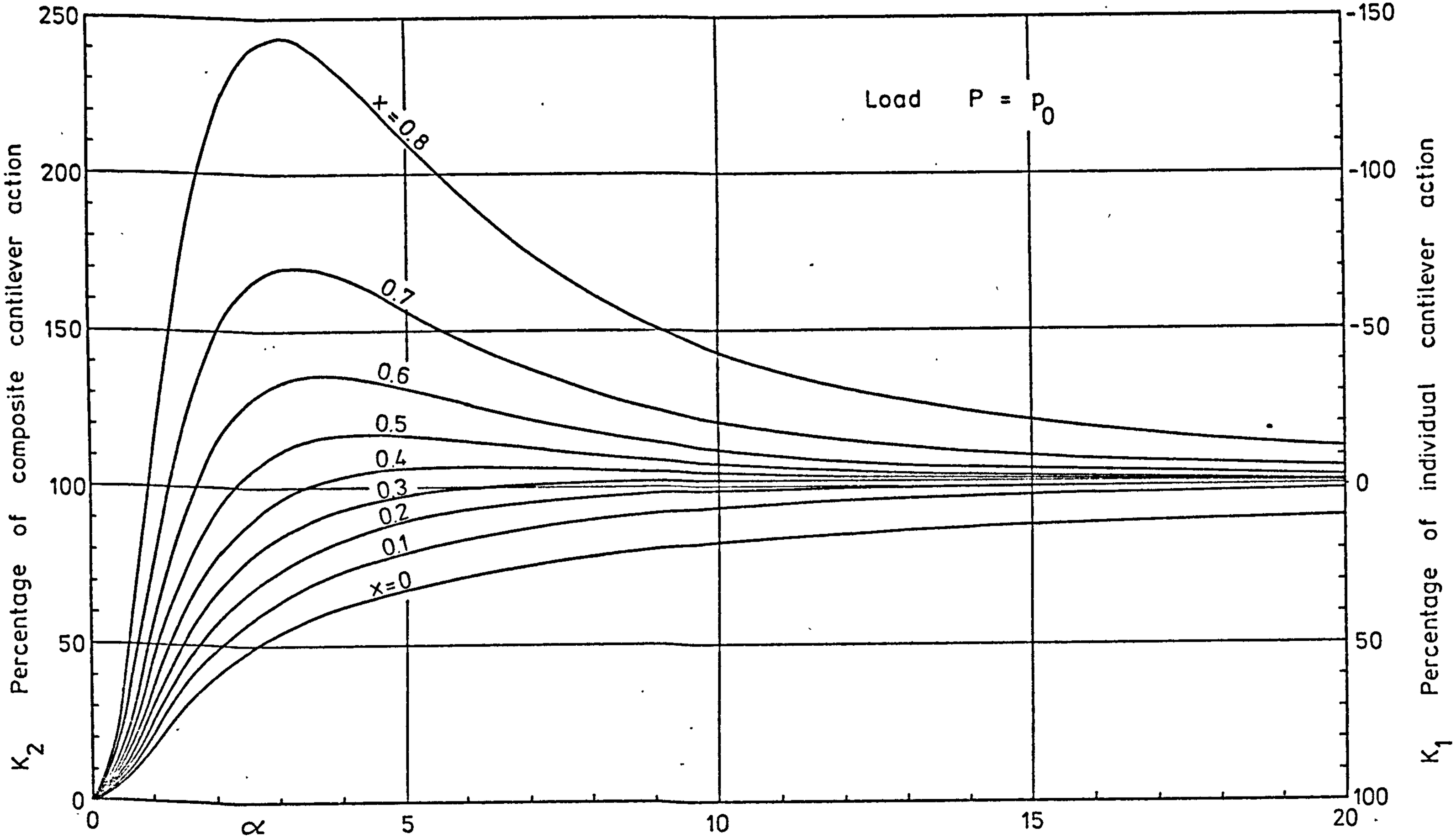

Variation of wall bending stress factors, K_1 and K_2 - Polynomial load (1)

Figure A.1

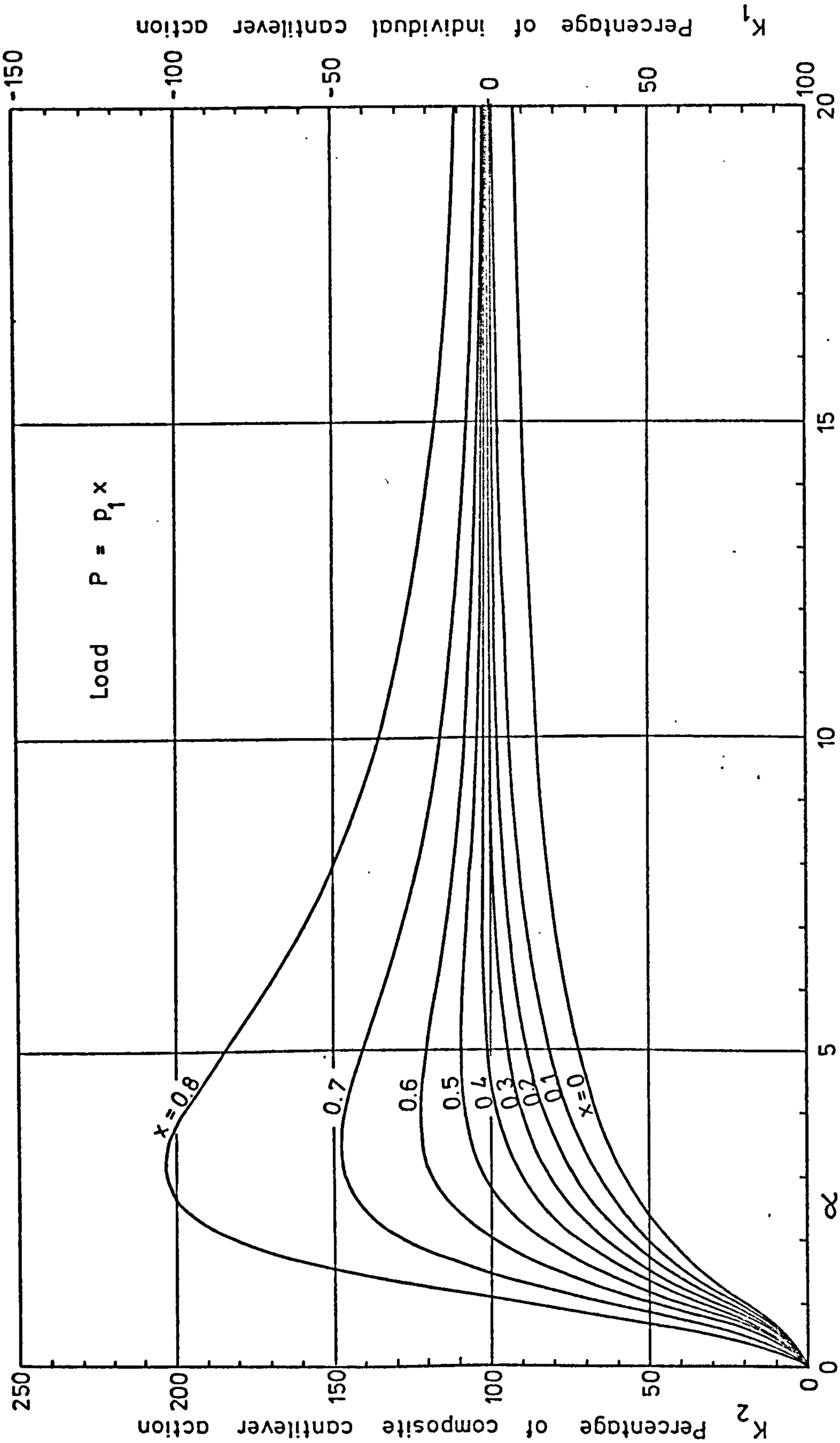

Variation of wall bending stress factors , K_1 and K_2 - Polynomial load (2)

A.2

Figure

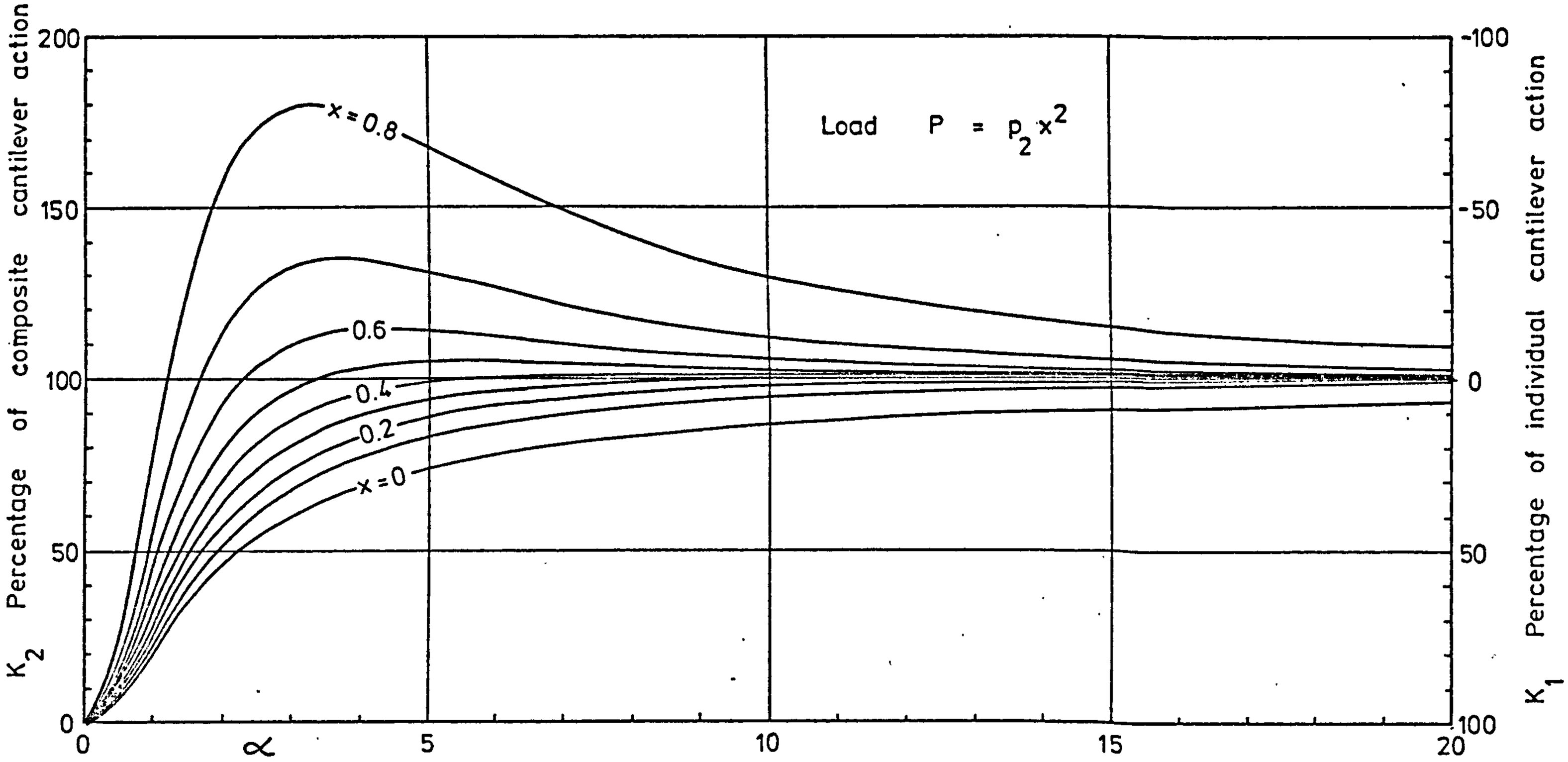

Variation of wall bending stress factors . K_1 and K_2 - Polynomial load (3)

Figure A.3

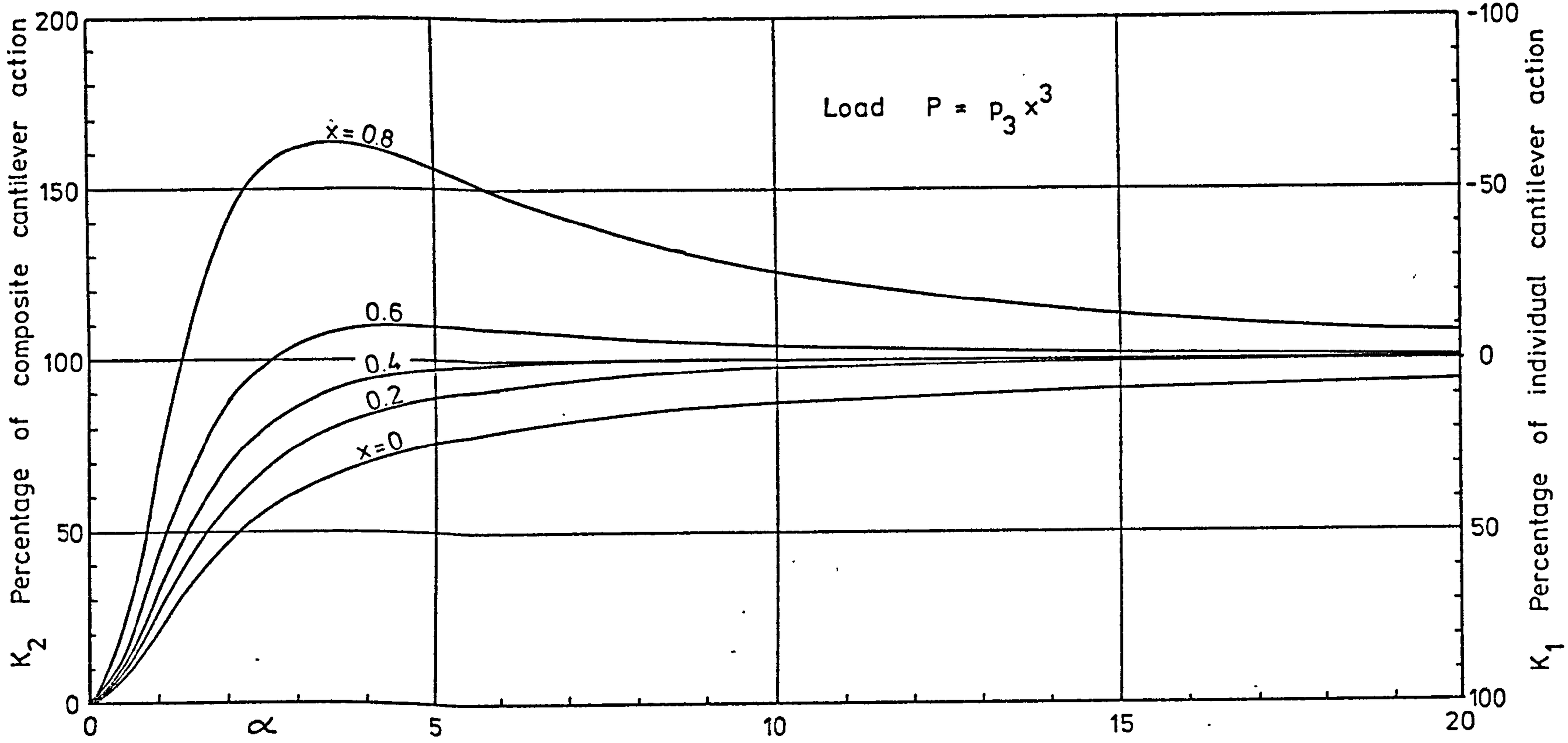

Variation of wall bending stress factors , K_1 and K_2 - Polynomial load (4)

Figure A.4

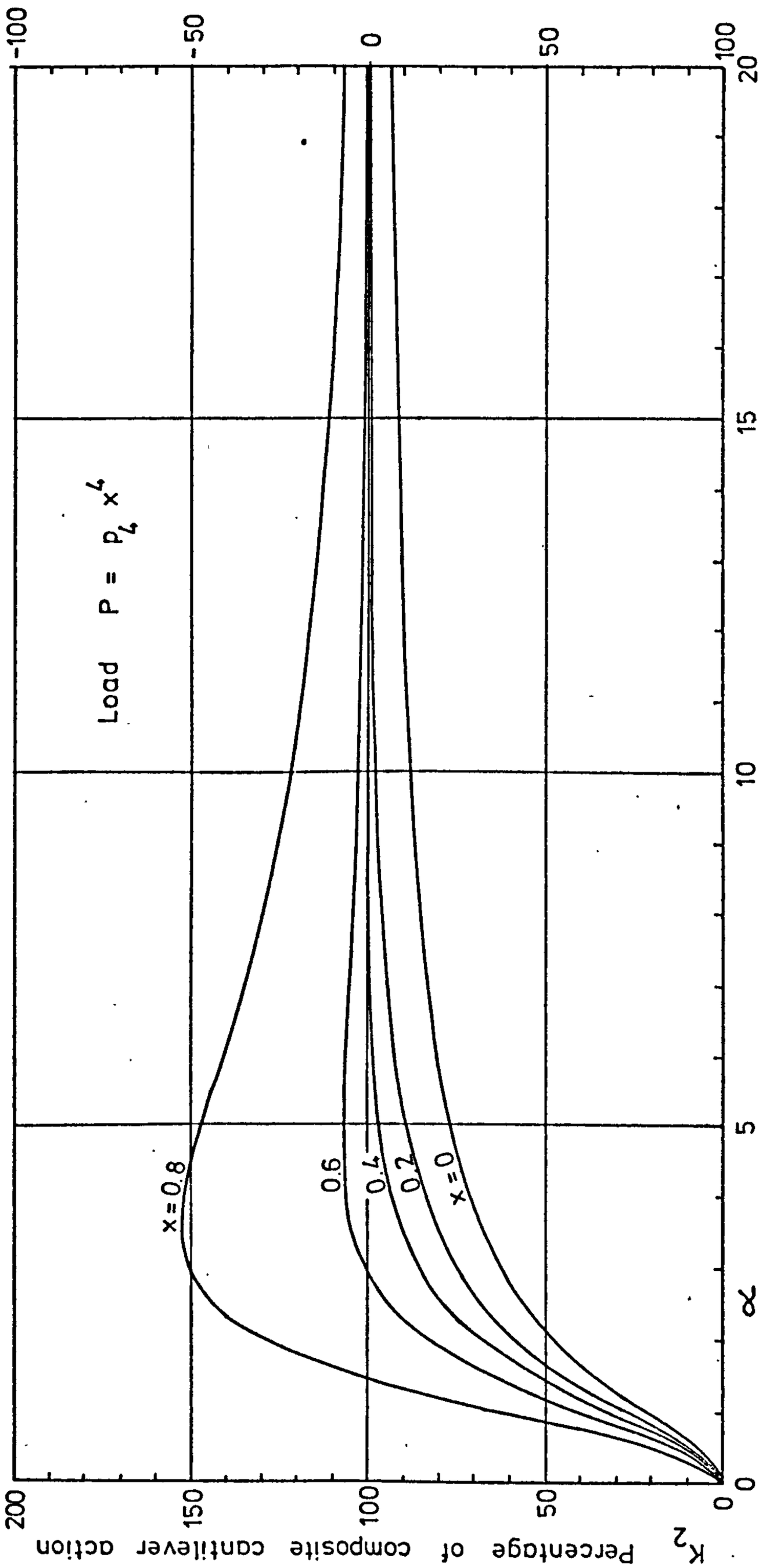

Variation of wall bending stress factors K_1 and K_2 - Polynomial load (5)

A.5

Figure

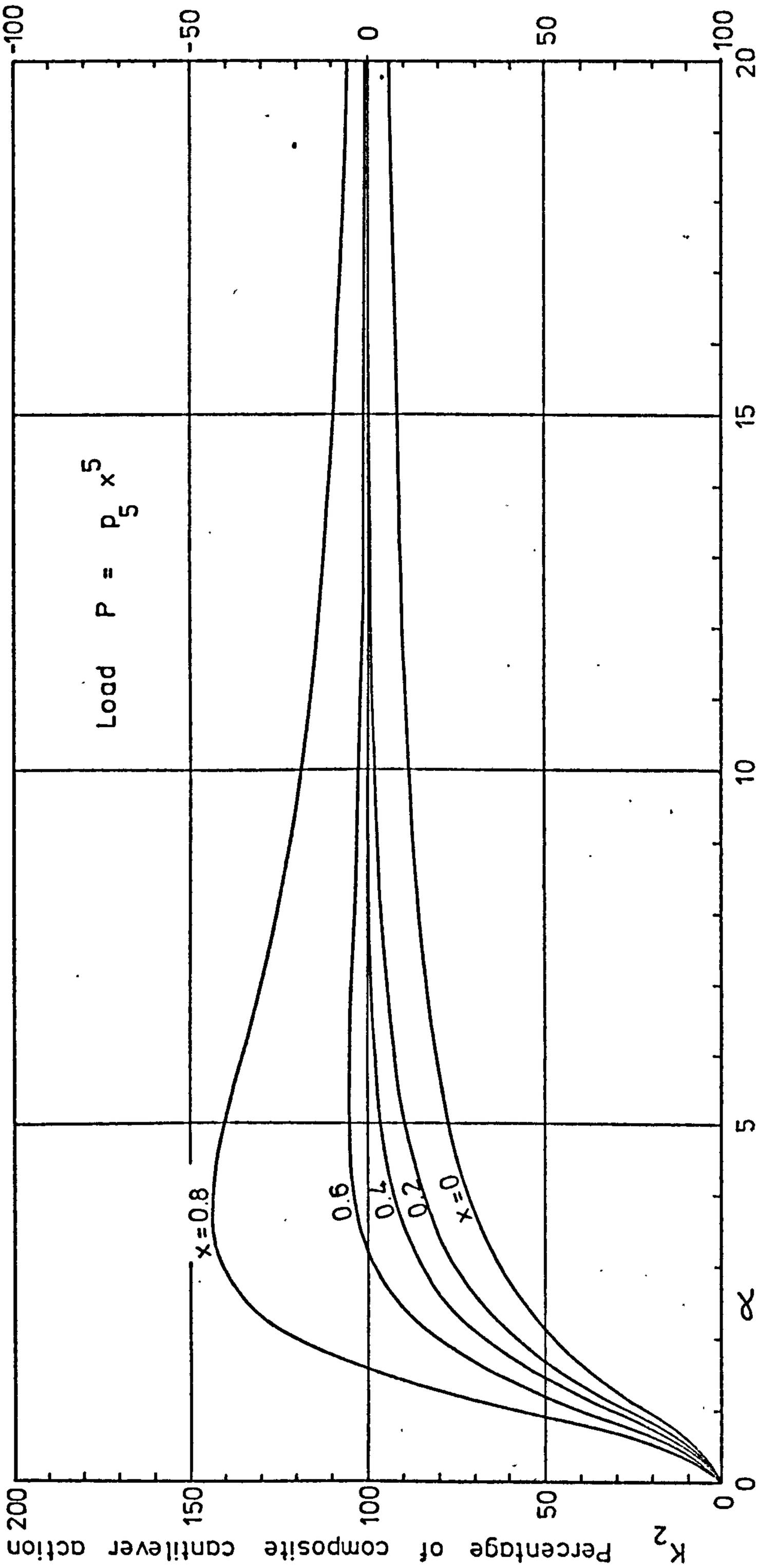

Variation of wall bending stress factors K_1 and K_2 - Polynomial load (6)

A.6

Figure

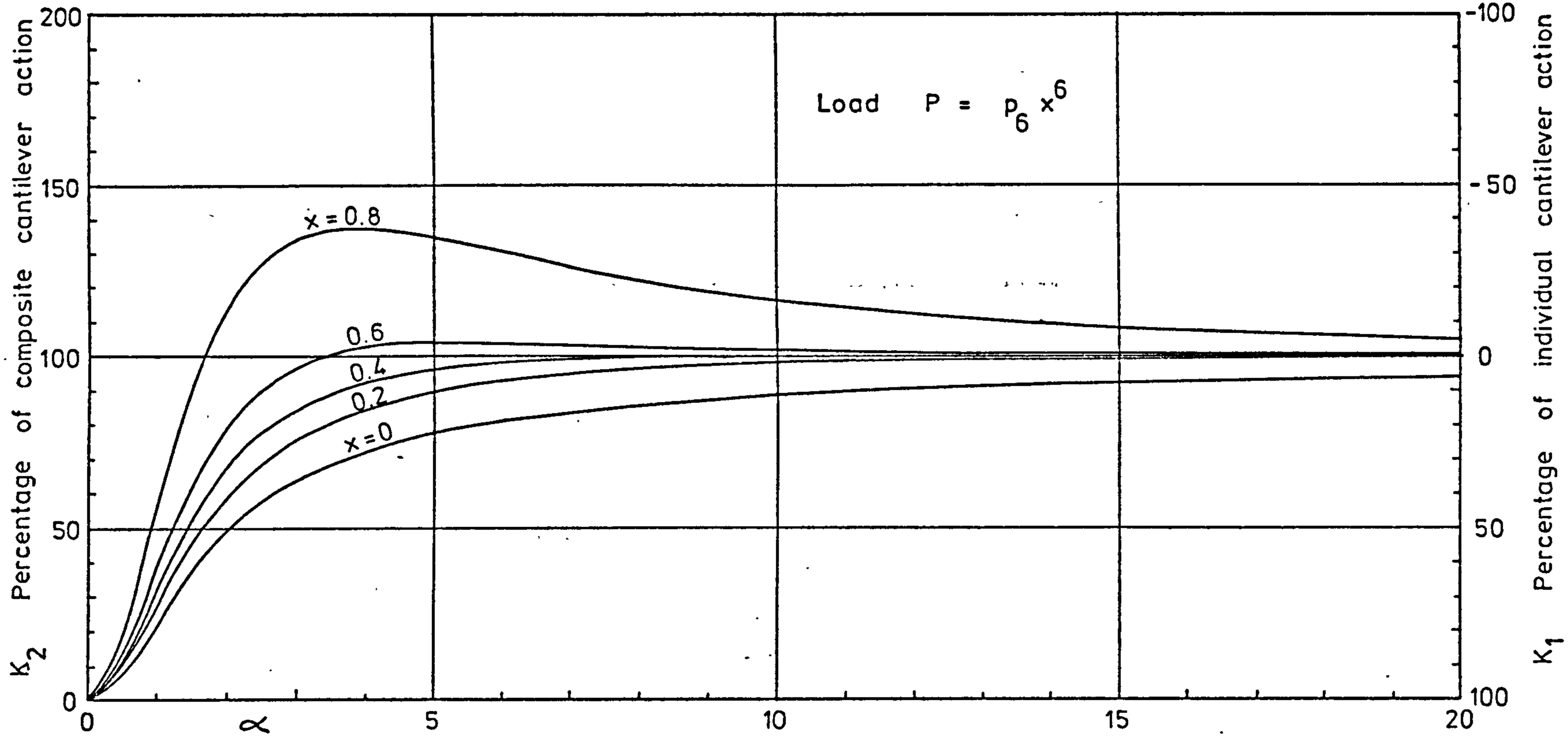

Variation of wall bending stress factors , K_1 and K_2 - Polynomial load (7)

Figure A.7

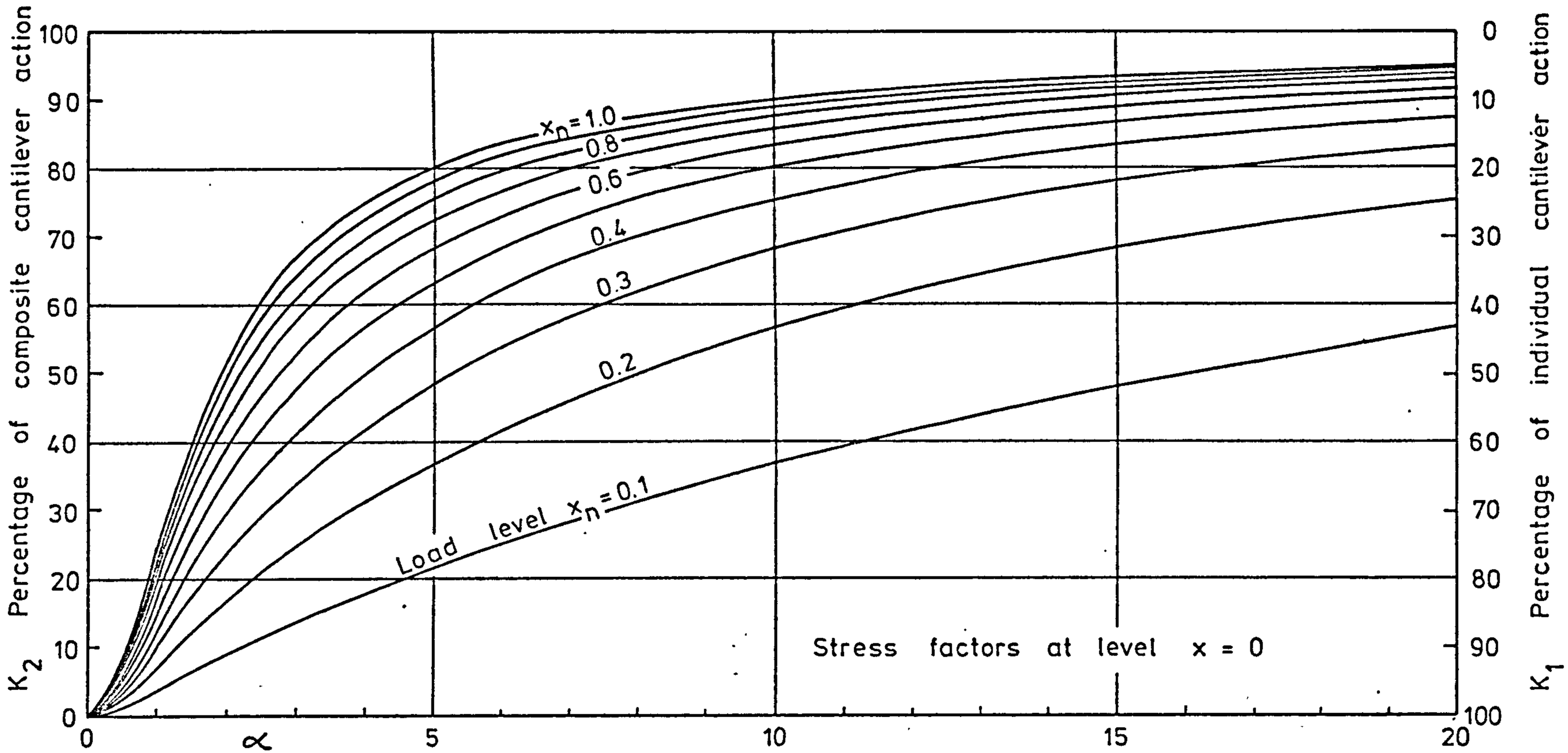

Variation of wall bending stress factors , K_1 and K_2 - Point load (1)

Figure A.8

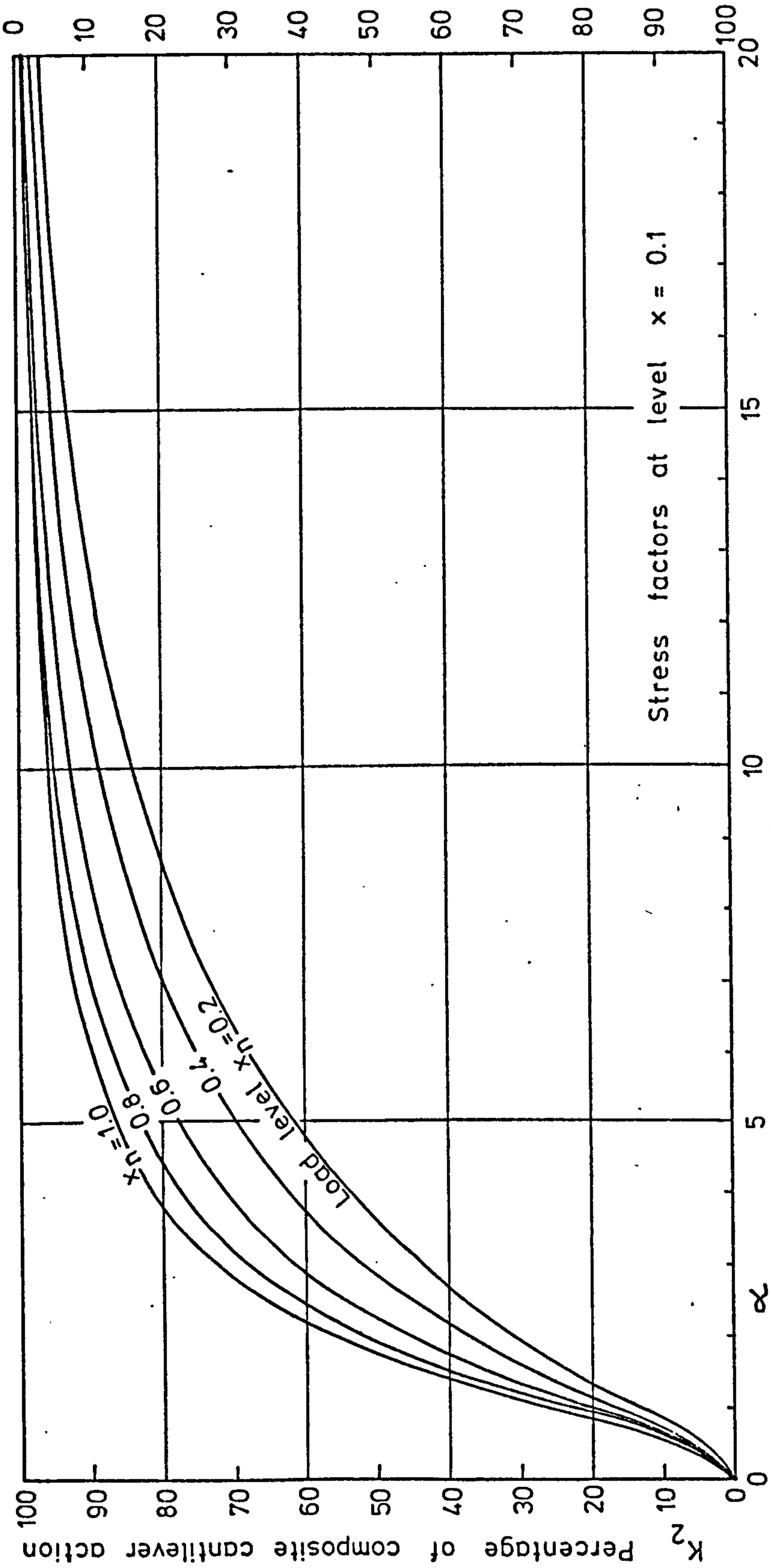

Variation of wall bending stress factors . K_1 and K_2 - Point load (2)

Figure A.9

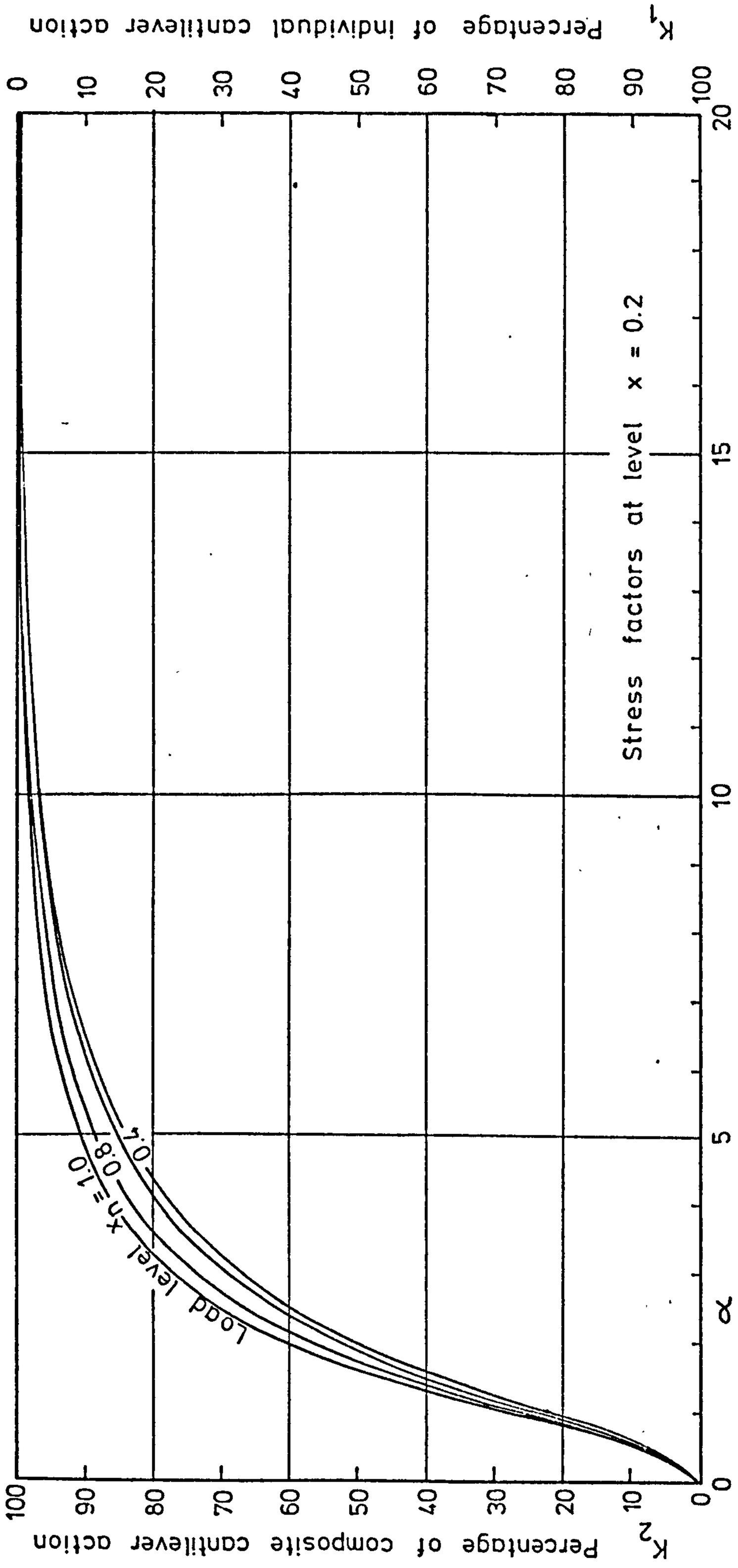
K_1 Percentage of individual cantilever action
0
10
20
30
40
50
60
70
80
90
100
20
15
10
5
0
Stress factors at level x = 0.2
K_1 and K_2 - Point load
A.10
Variation of wall bending stress factors .
Figure
K_2 Percentage of composite cantilever action
100
90
80
70
60
50
40
30
20
10
0
Load level xn = 1.0
0.8
0.4
α

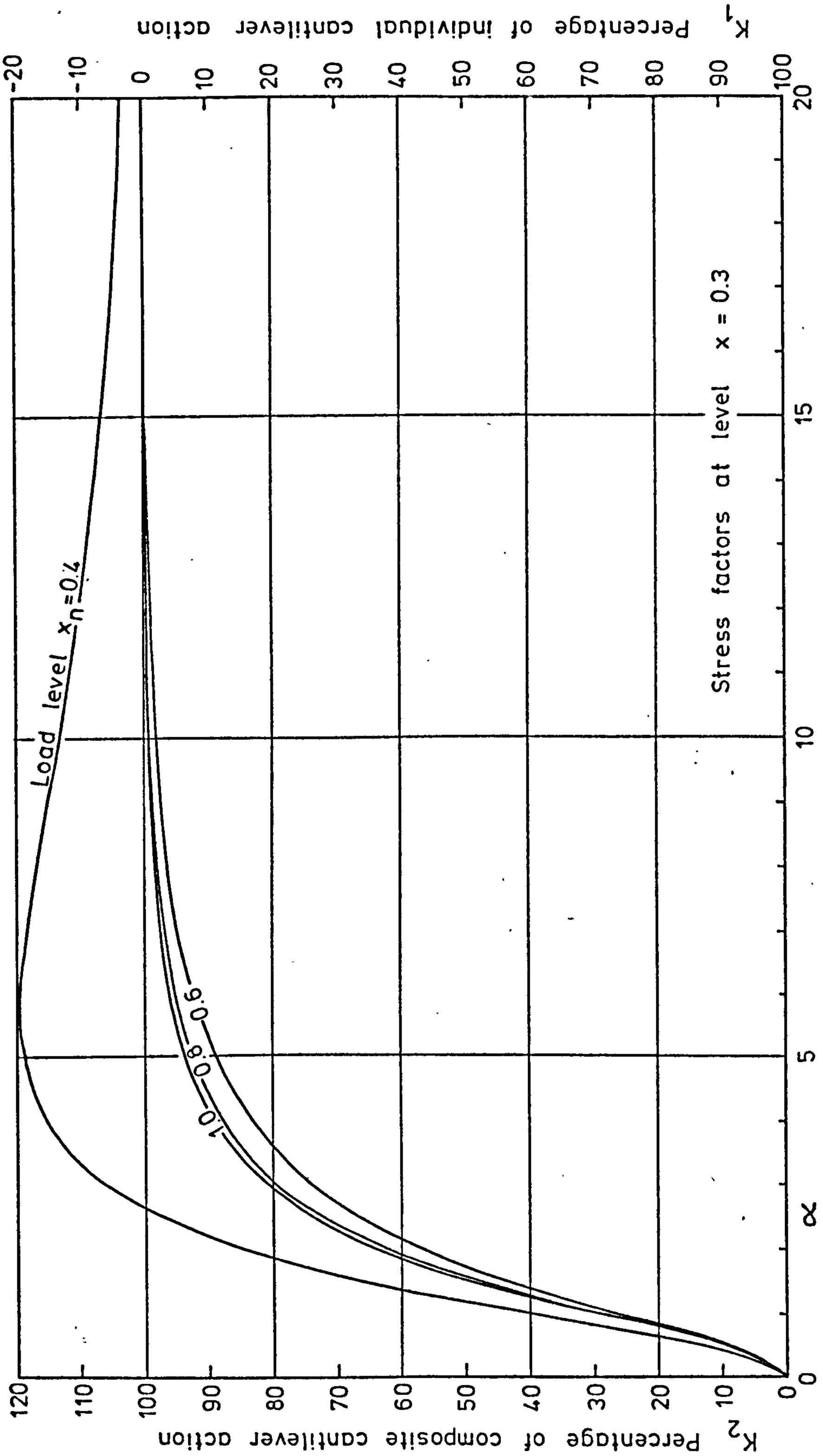
K_1 Percentage of individual cantilever action
-20
-10
0
10
20
30
40
50
60
70
80
90
100
Stress factors at level x = 0.3
20
15
10
5
0
Load
Load level x_n=0.4
0.6
0.8
1.0
K_2 Percentage of composite cantilever action
120
110
100
90
80
70
60
50
40
30
20
10
0
Variation of wall bending stress factors K_1 and K_2 - Point load (4)
Figure A.11
α

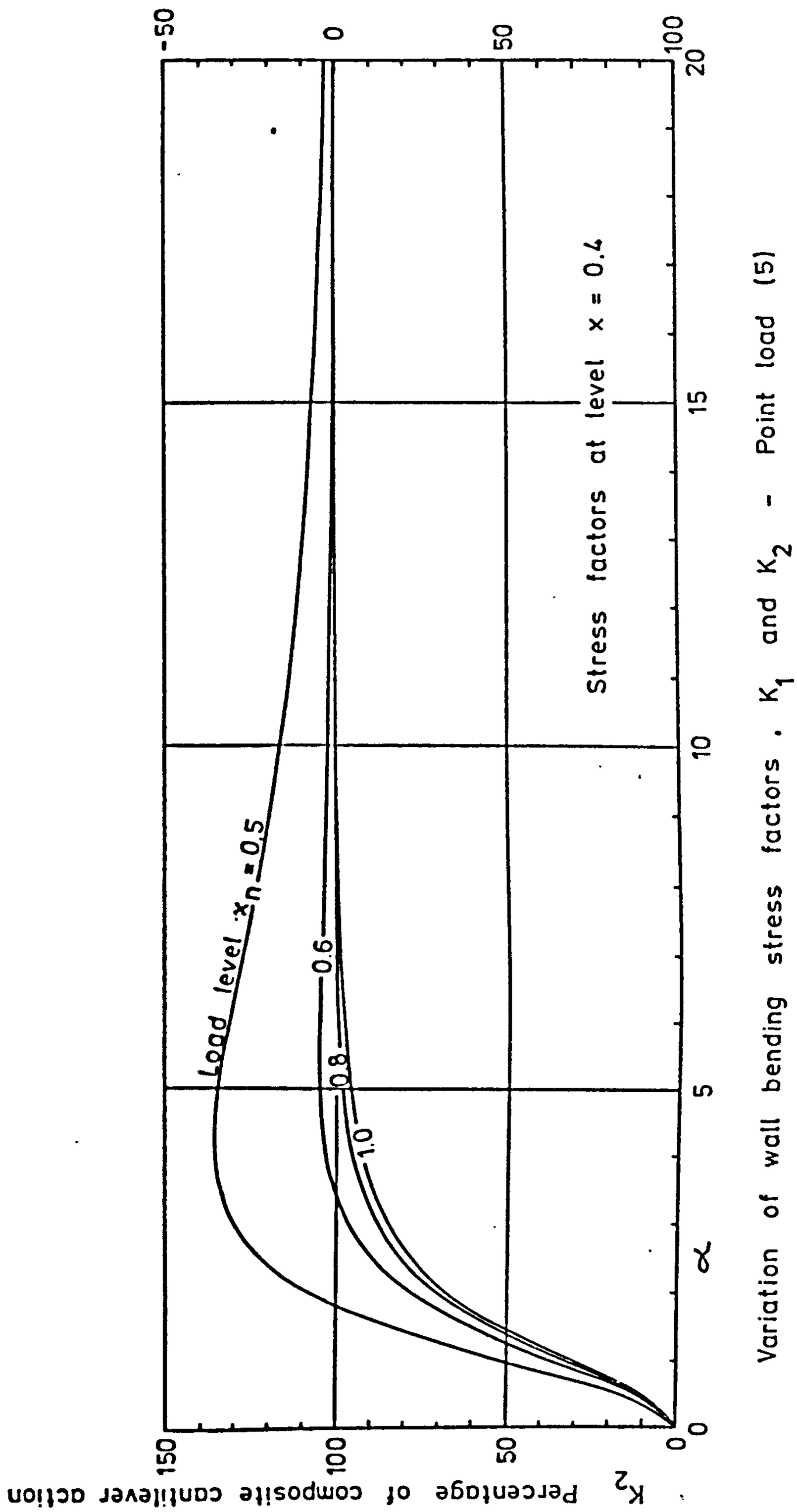

Variation of wall bending stress factors . K_1 and K_2 - Point load (5)

Figure A.12

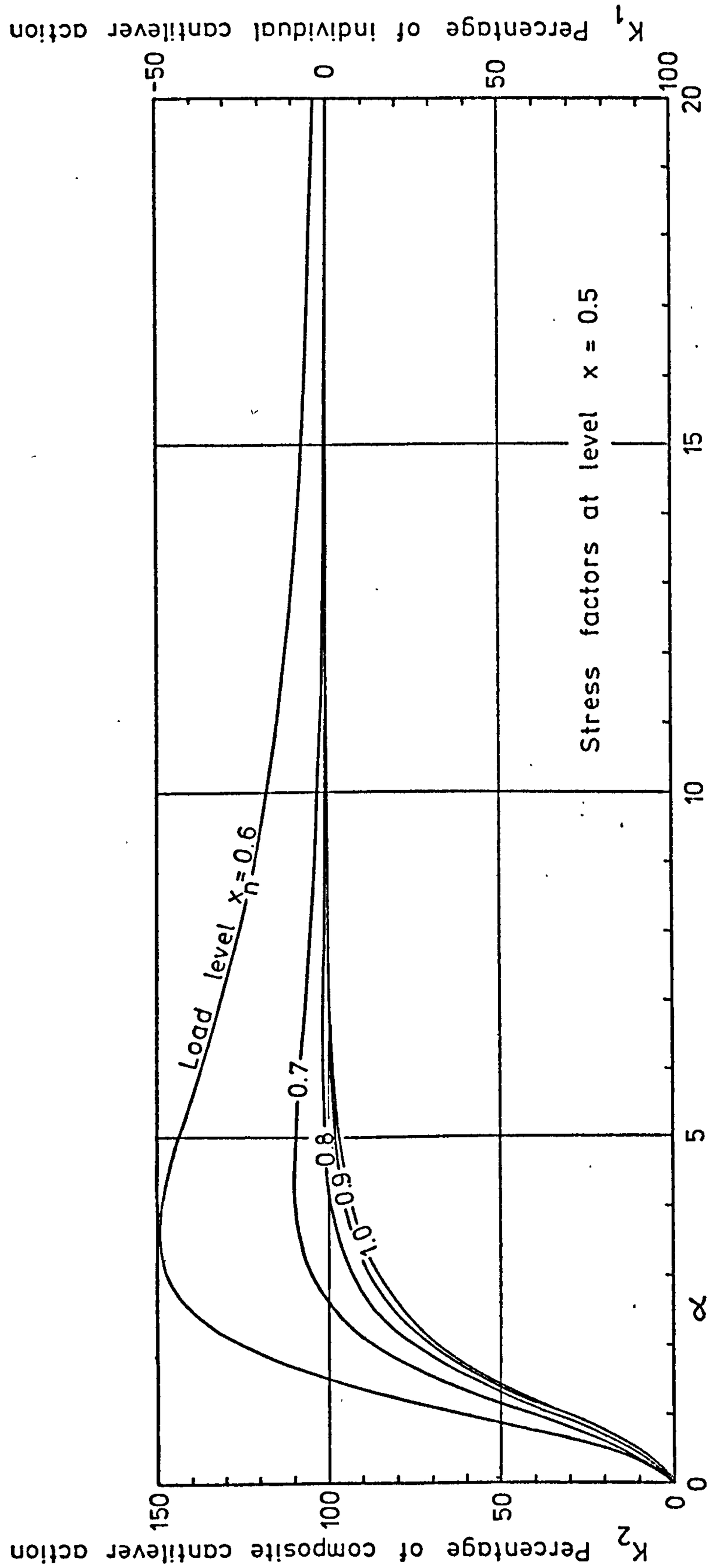

Variation of wall bending stress factors. K_1 and K_2 - Point load (6)

Figure A.13

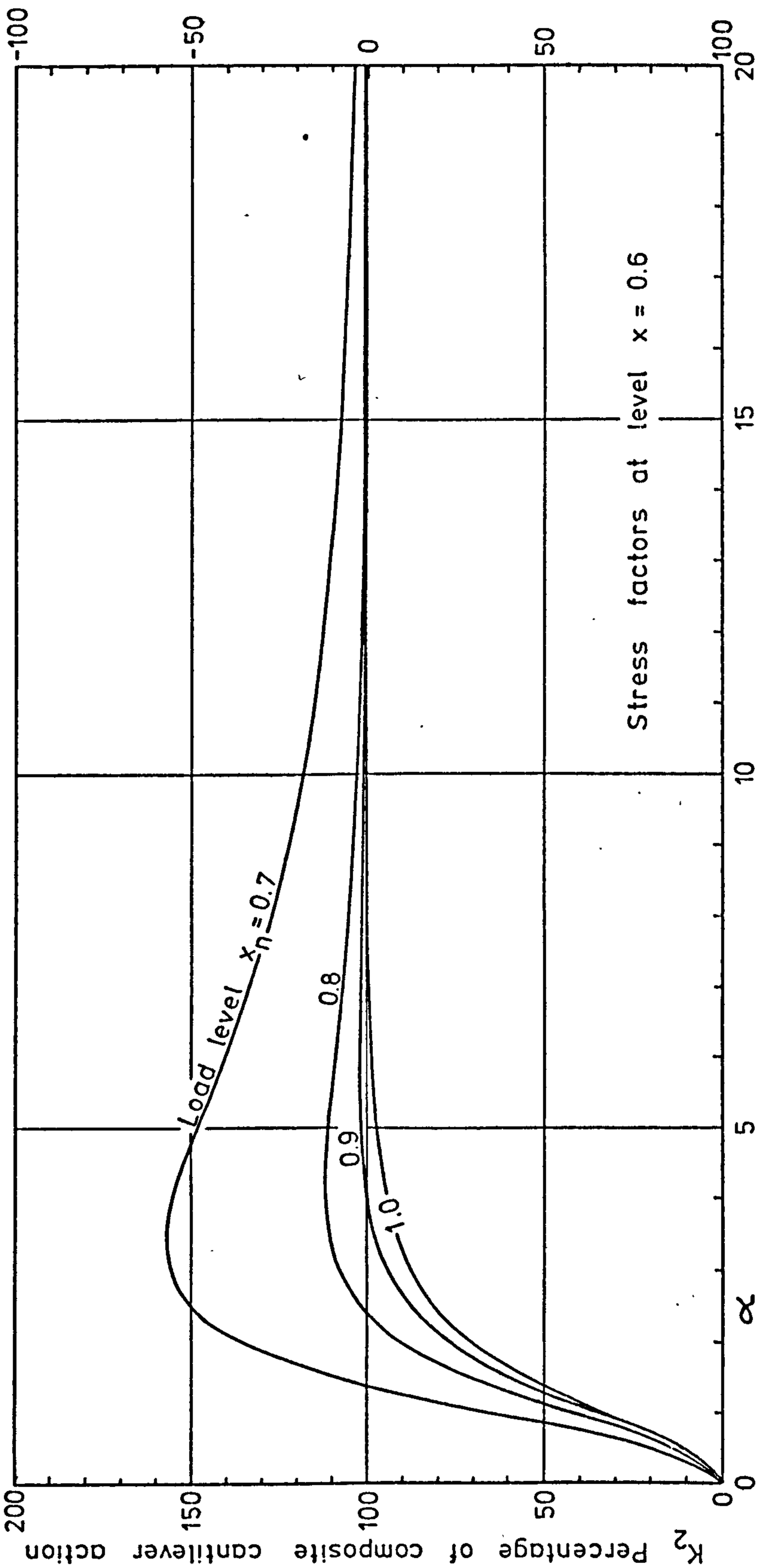

Variation of wall bending stress factors K_1 and K_2 - Point load A.14

Figure

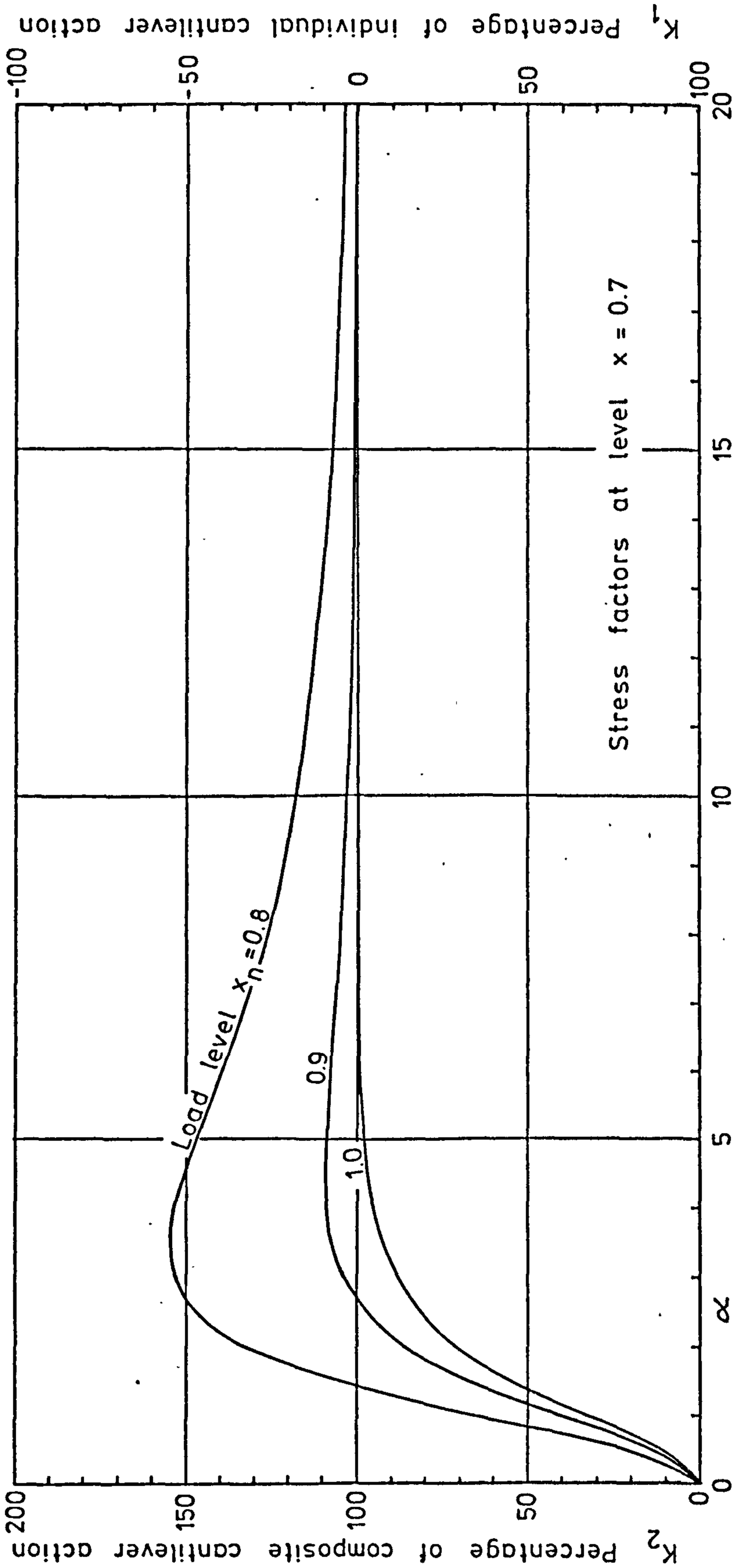

Variation of wall bending stress factors K_1 and K_2 - Point load (8)

Figure A.15

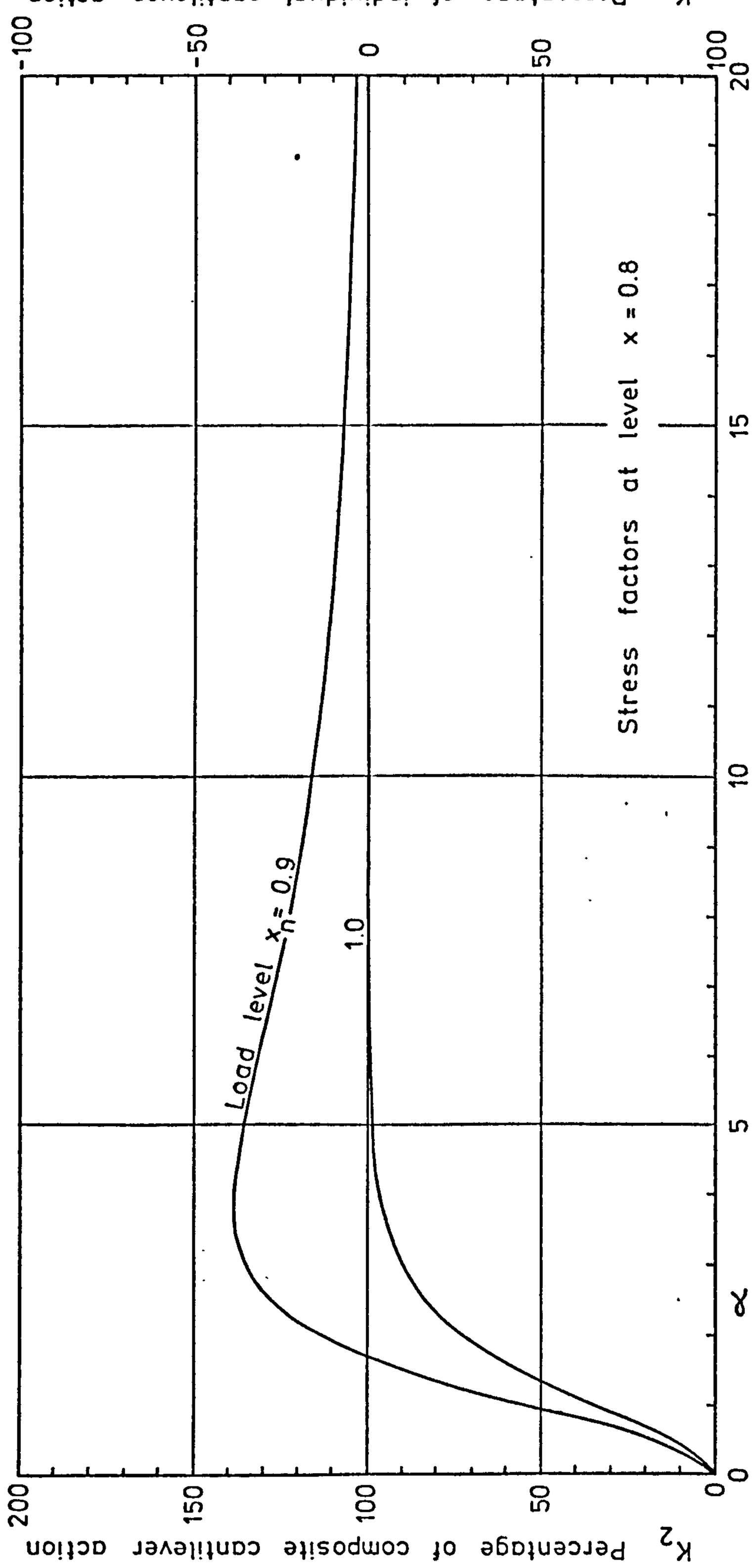

Variation of wall bending stress factors . K_1 and K_2 - Point load

Figure A.16

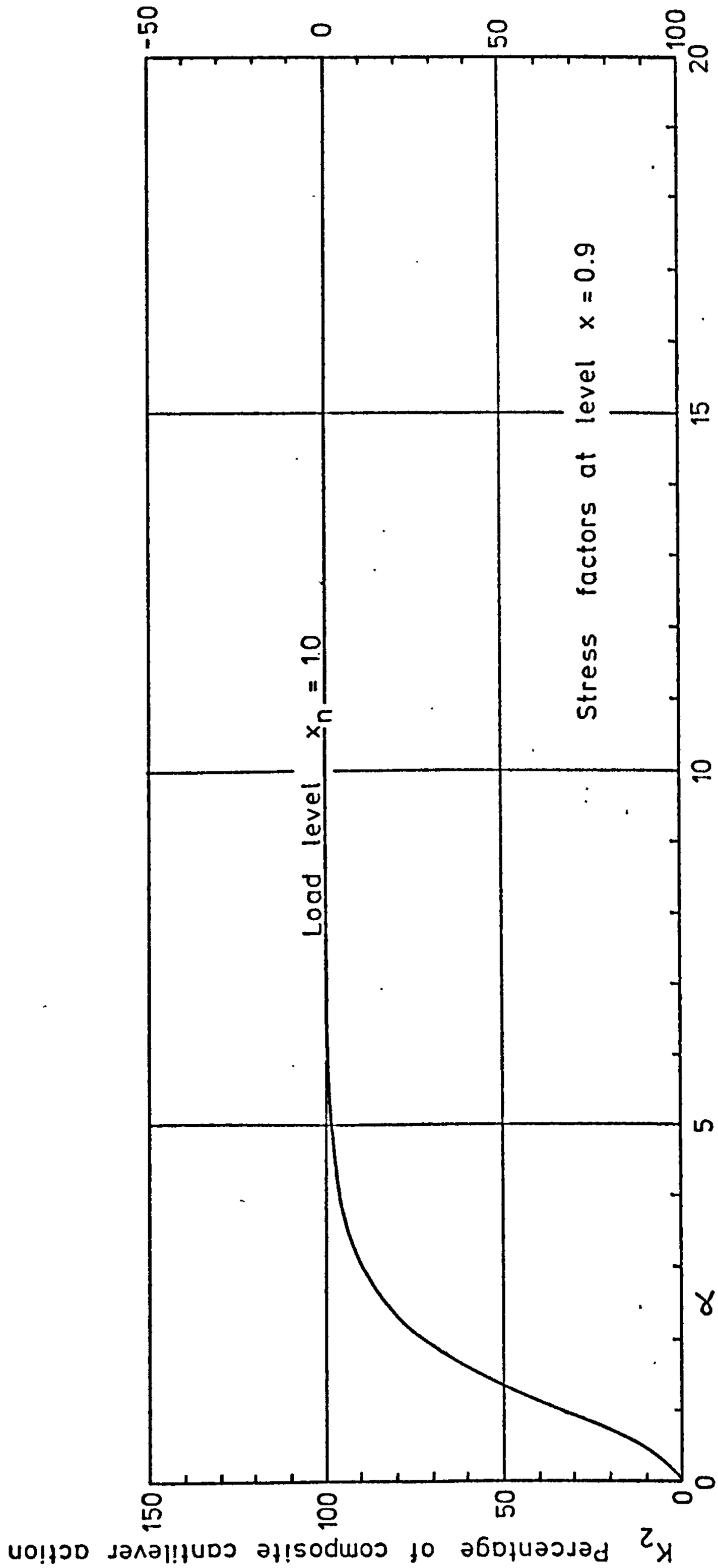
K_1 Percentage of individual cantilever action
-50
0
50
100
20
15
10
5
0
Load
level x_n = 1.0
level x = 0.9
Stress factors at
Point load (10)
Variation of wall bending stress factors . K_1 and K_2 - Po
K_2 Percentage of composite cantilever action
150
100
50
0
0
∝

Figure A.17

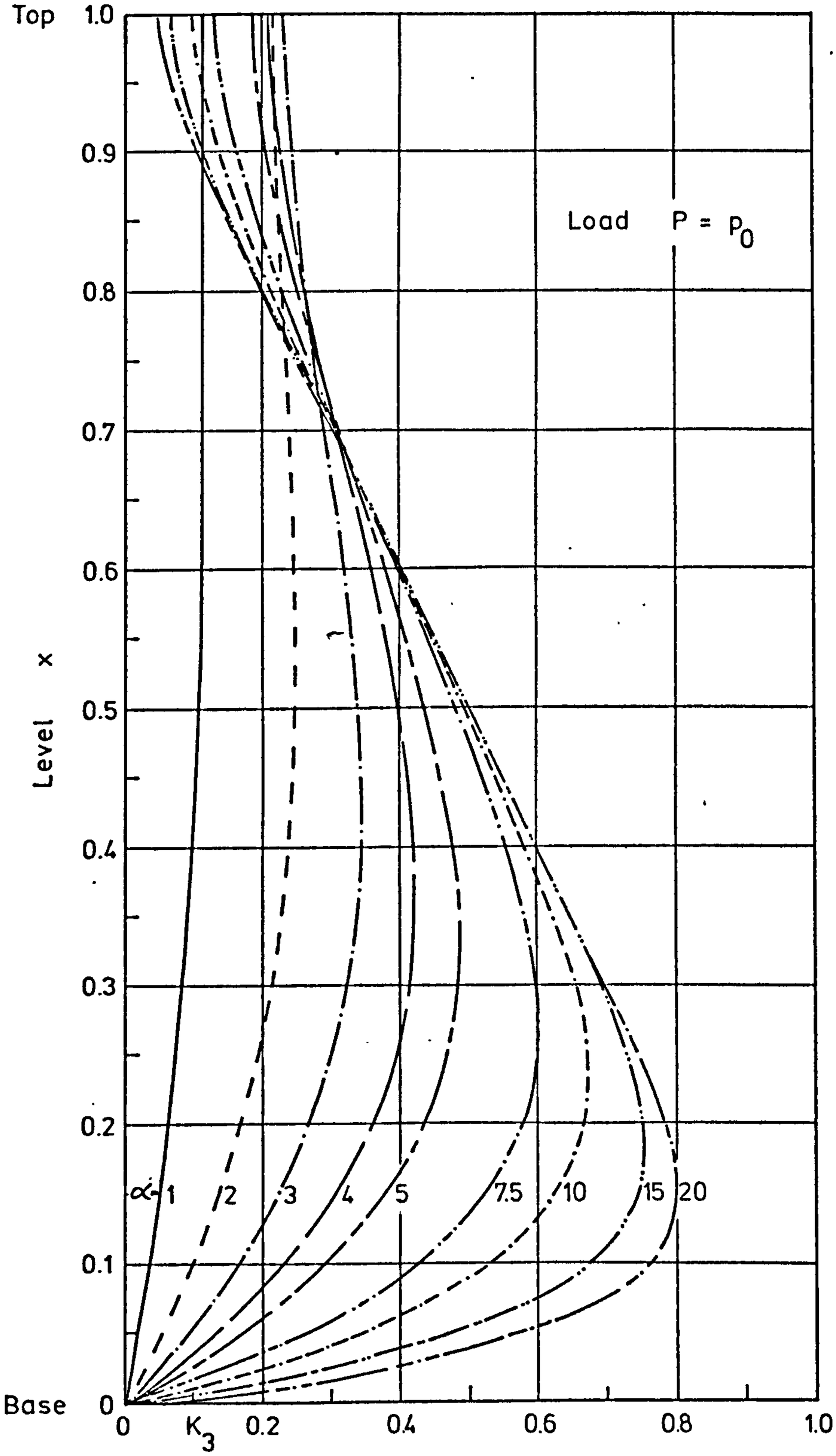

Variation of connecting medium shear stress factor, K_3
- Polynomial load (1)

Figure A.18

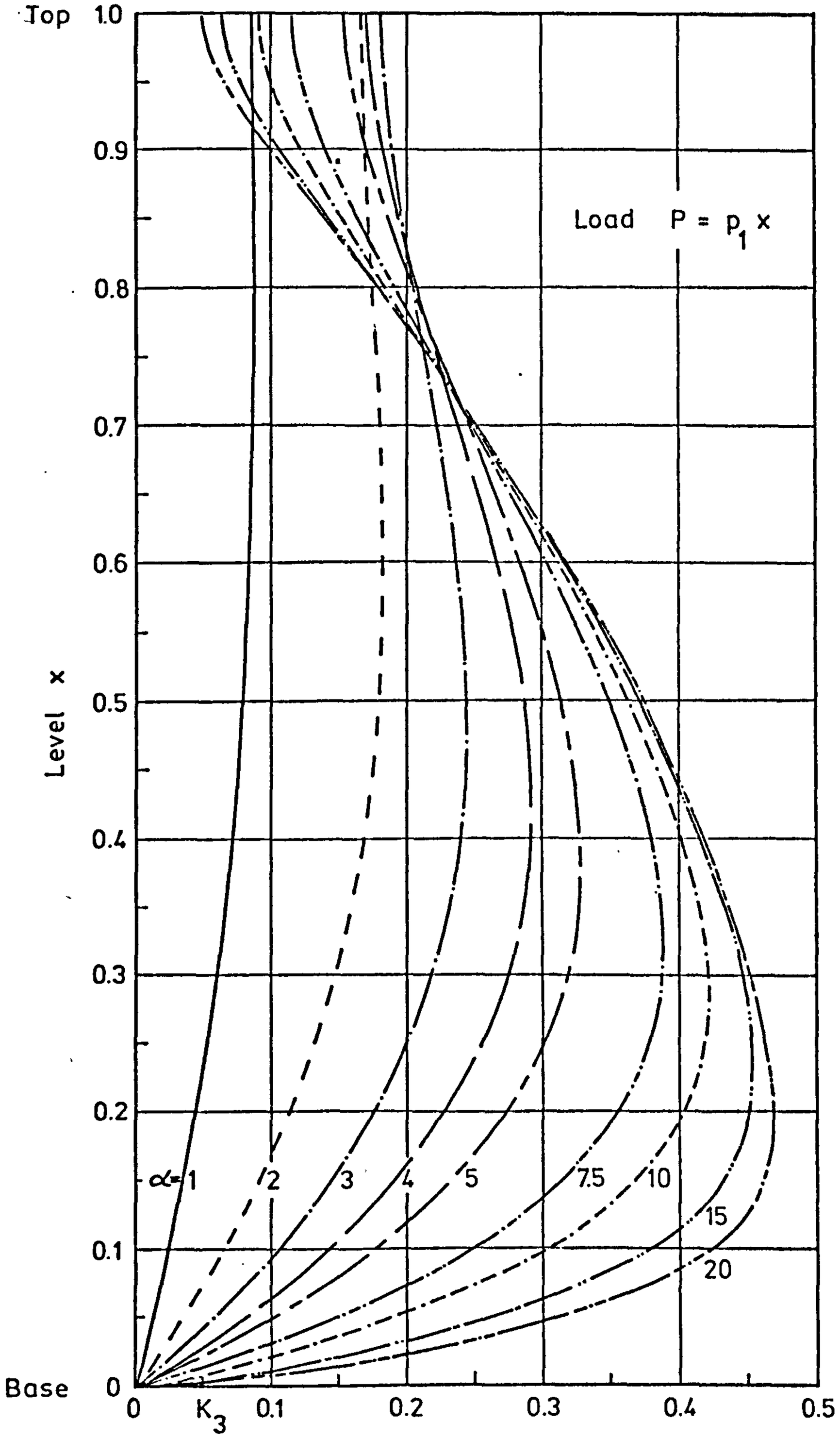

Variation of connecting medium shear stress factor, K_3
- Polynomial load (2)

Figure A.19

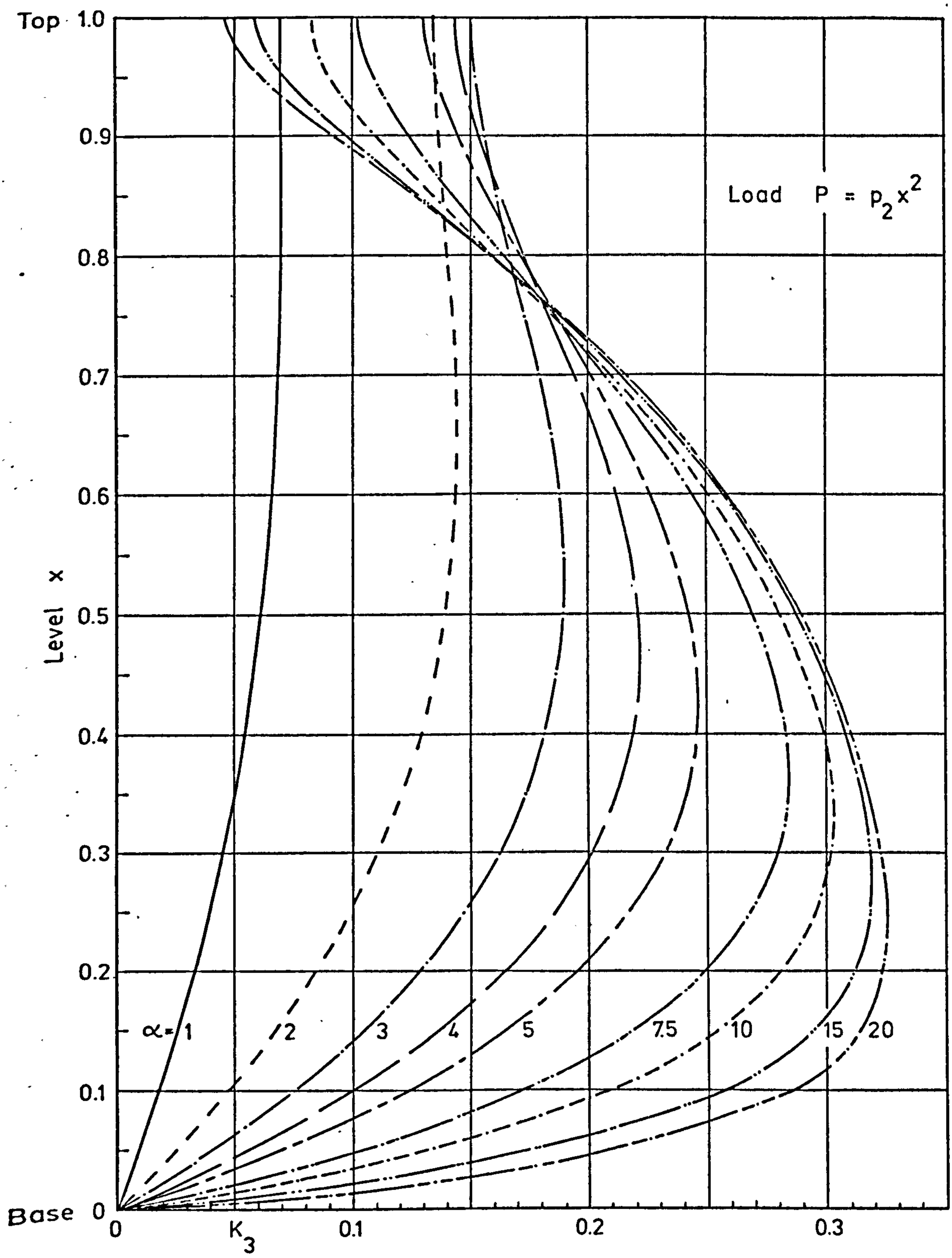

Variation of connecting medium shear stress factor, K_3
– Polynomial load (3)

Figure A.20

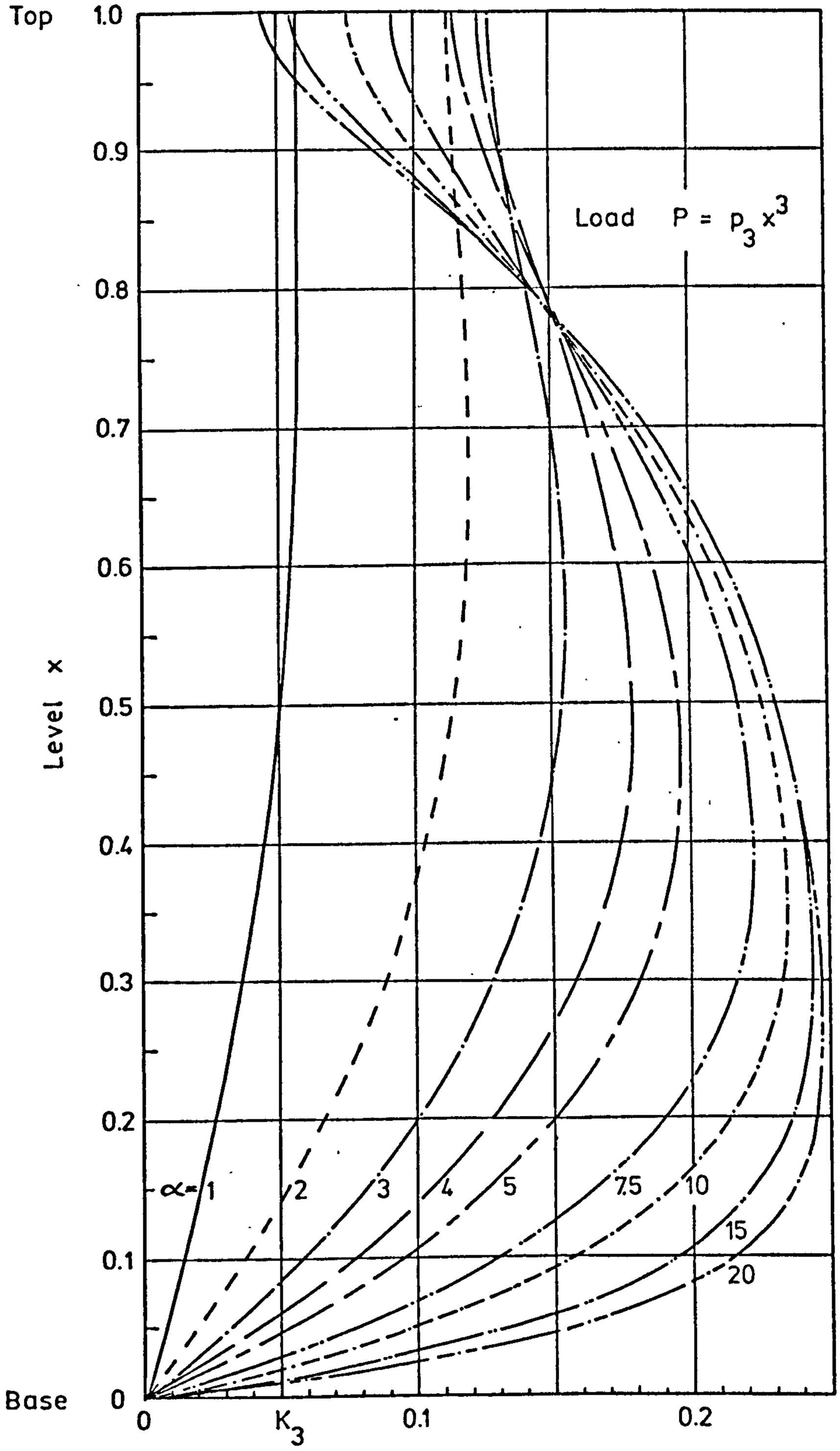

Variation of connecting medium shear stress factor, K_3 - Polynomial load (4)

Figure A.21

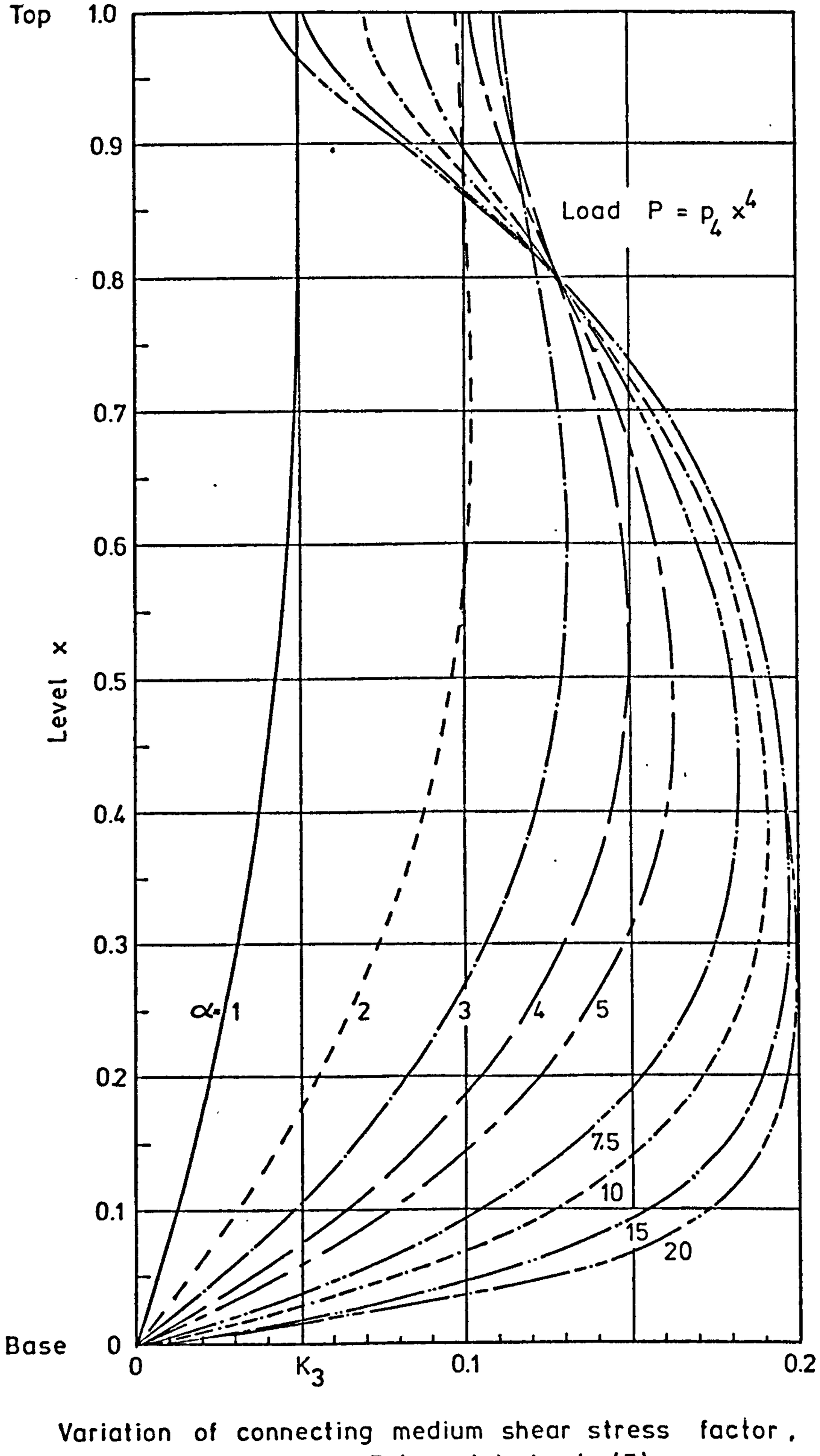

Variation of connecting medium shear stress factor, K_3
- Polynomial load (5)

Figure A.22

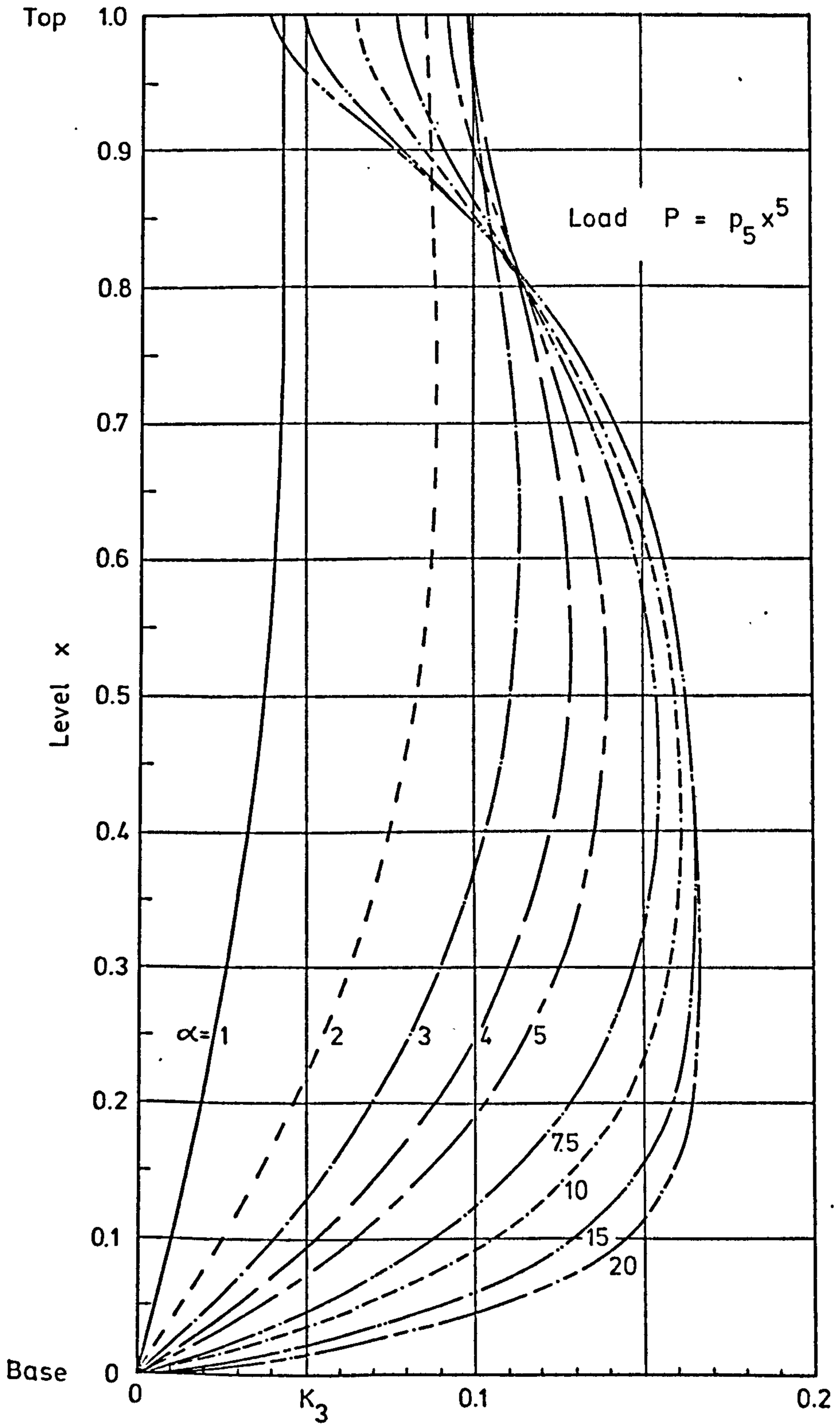

Variation of connecting medium shear stress factor , K_3
- Polynomial load (6)

Figure A.23

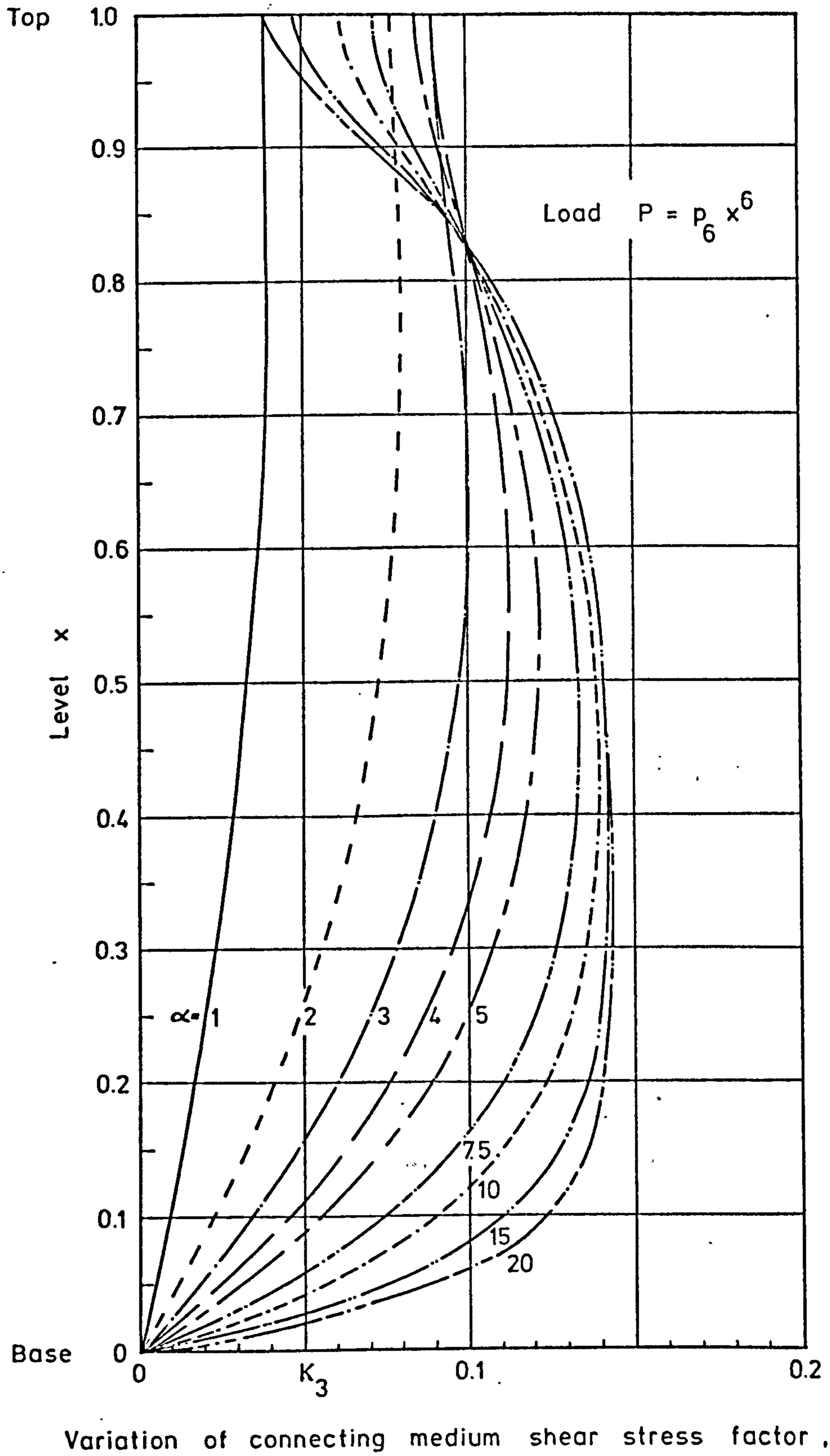

Variation of connecting medium shear stress factor , K_3
- Polynomial load (7)

Figure A.24

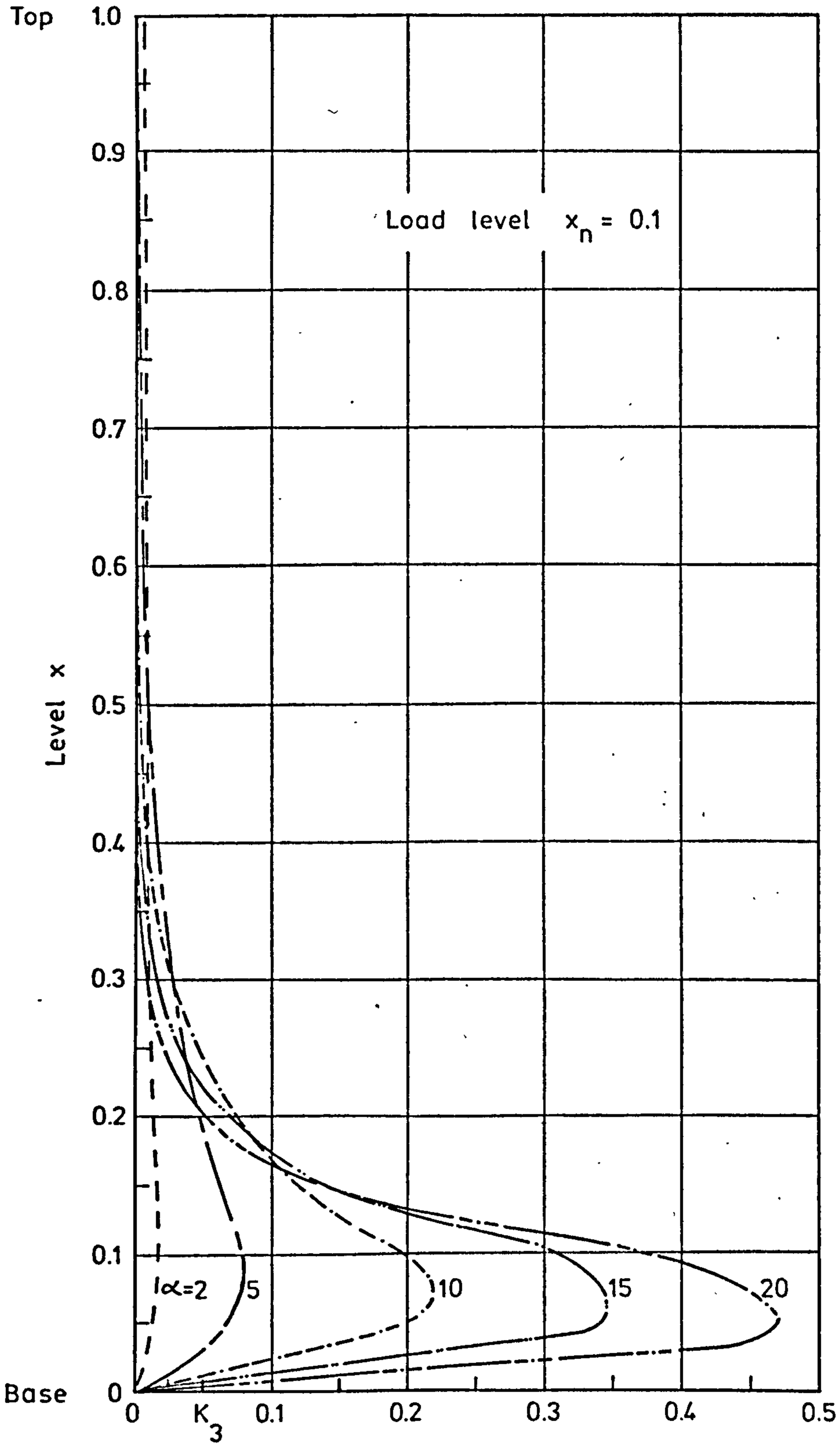

Variation of connecting medium shear stress factor, K_3 - Point load (1)

Figure A.25

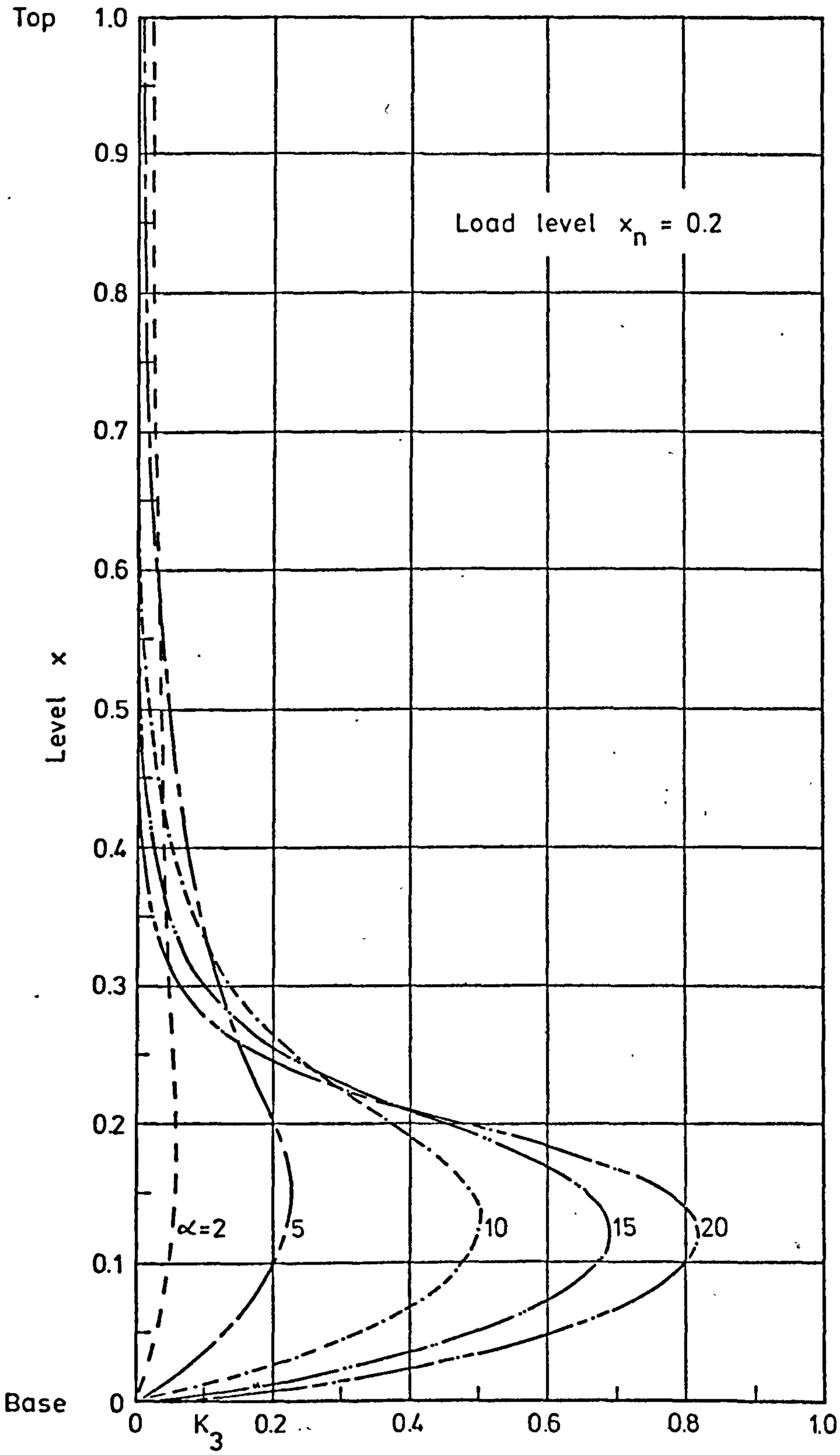

Variation of connecting medium shear stress factor , K_3
- Point load (2)

Figure A.26

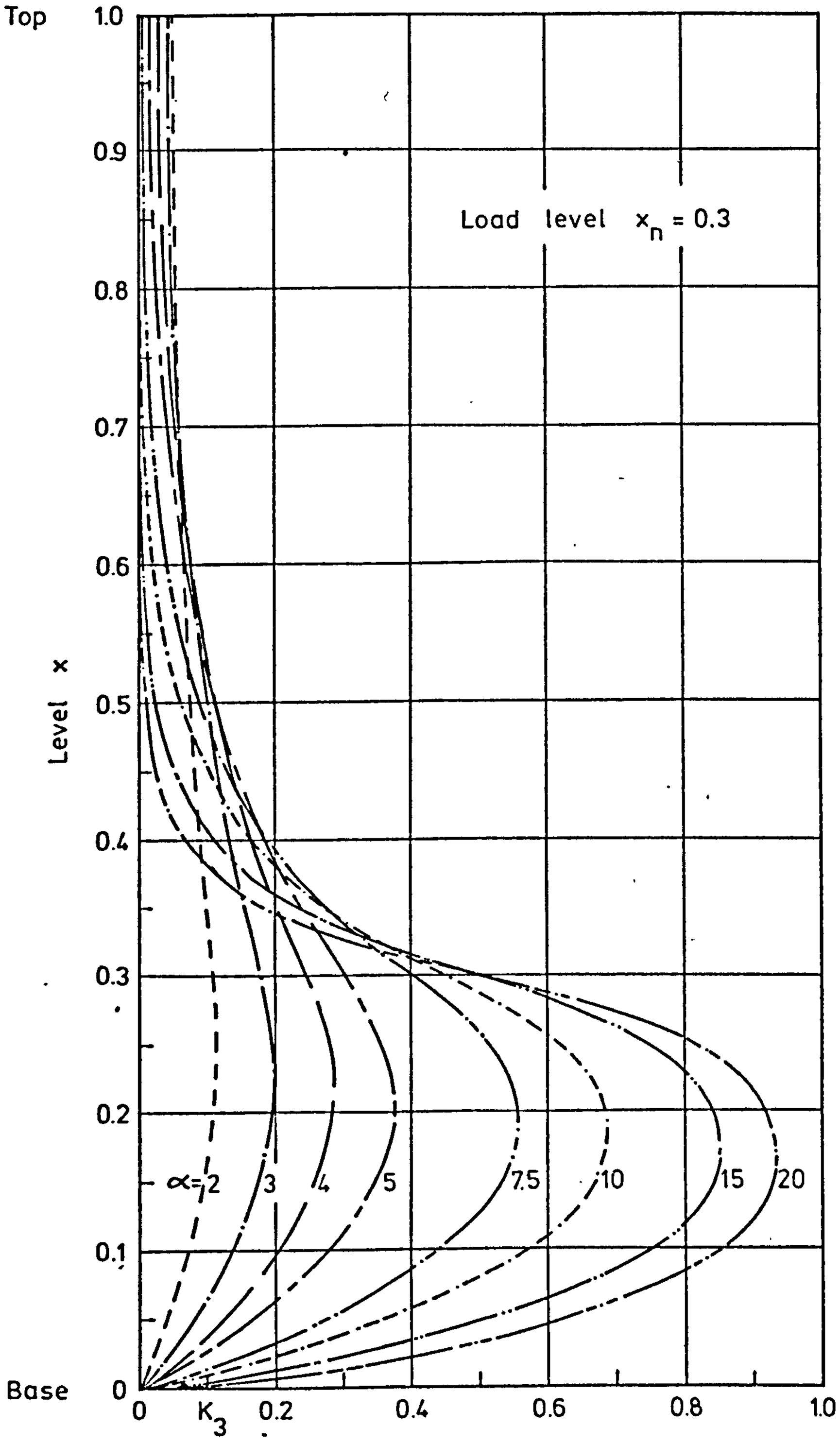

Variation of connecting medium shear stress factor, K_3 - Point load (3)

Figure A.27

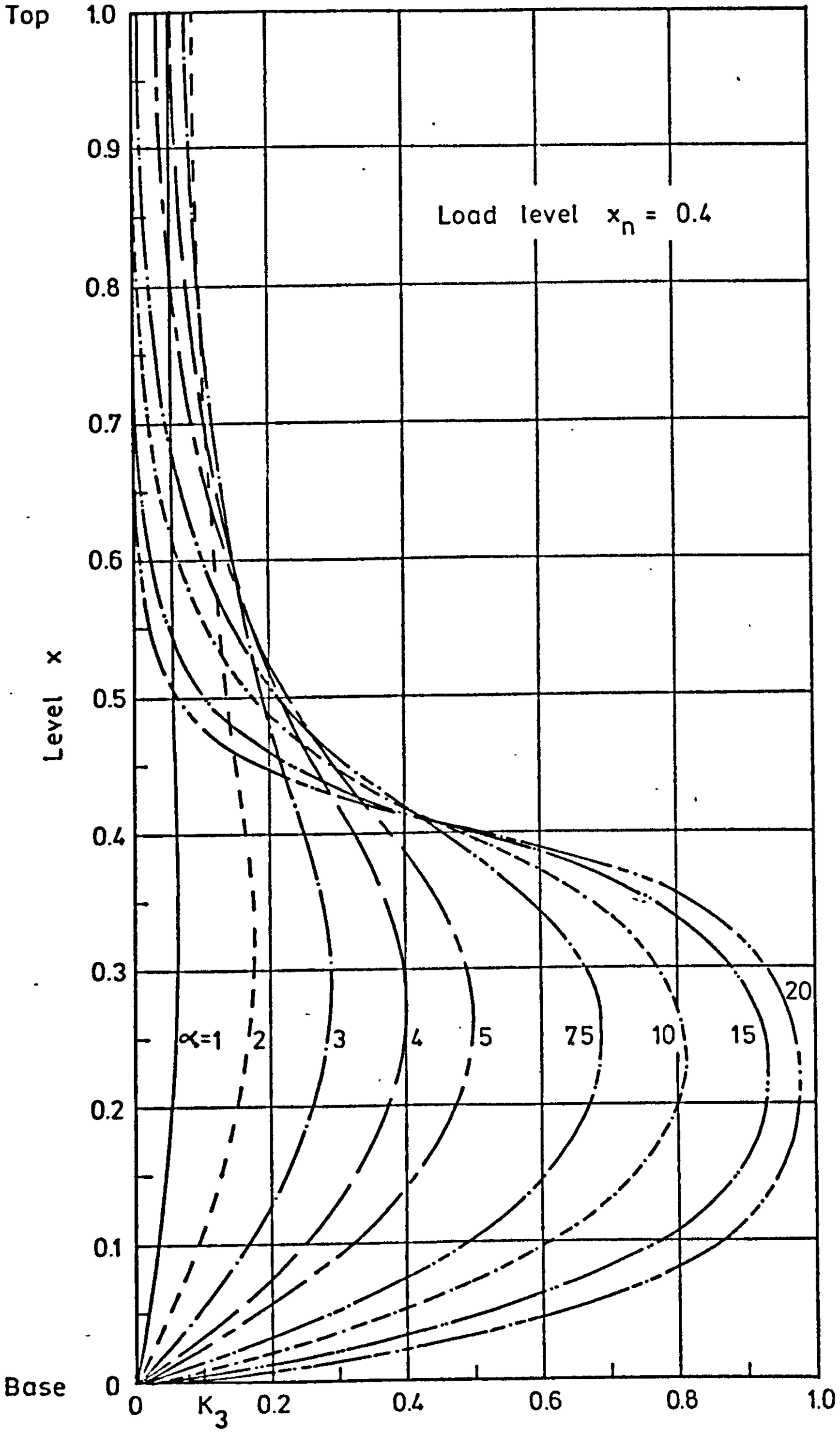

Variation of connecting medium shear stress factor , K_3
- Point load (4)

Figure A.28

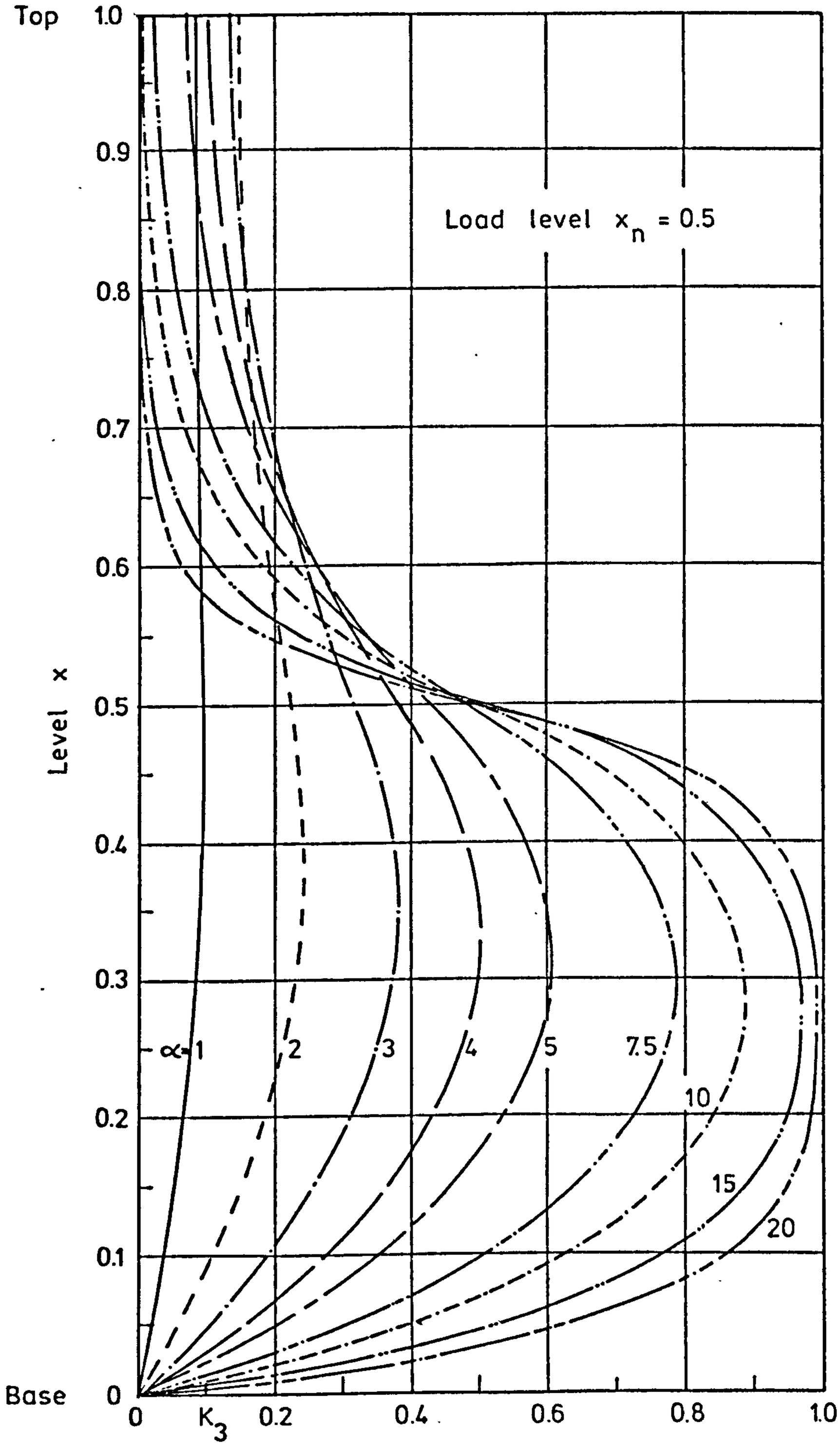

Variation of connecting medium shear stress factor , K_3
- Point load (5)

Figure A.29

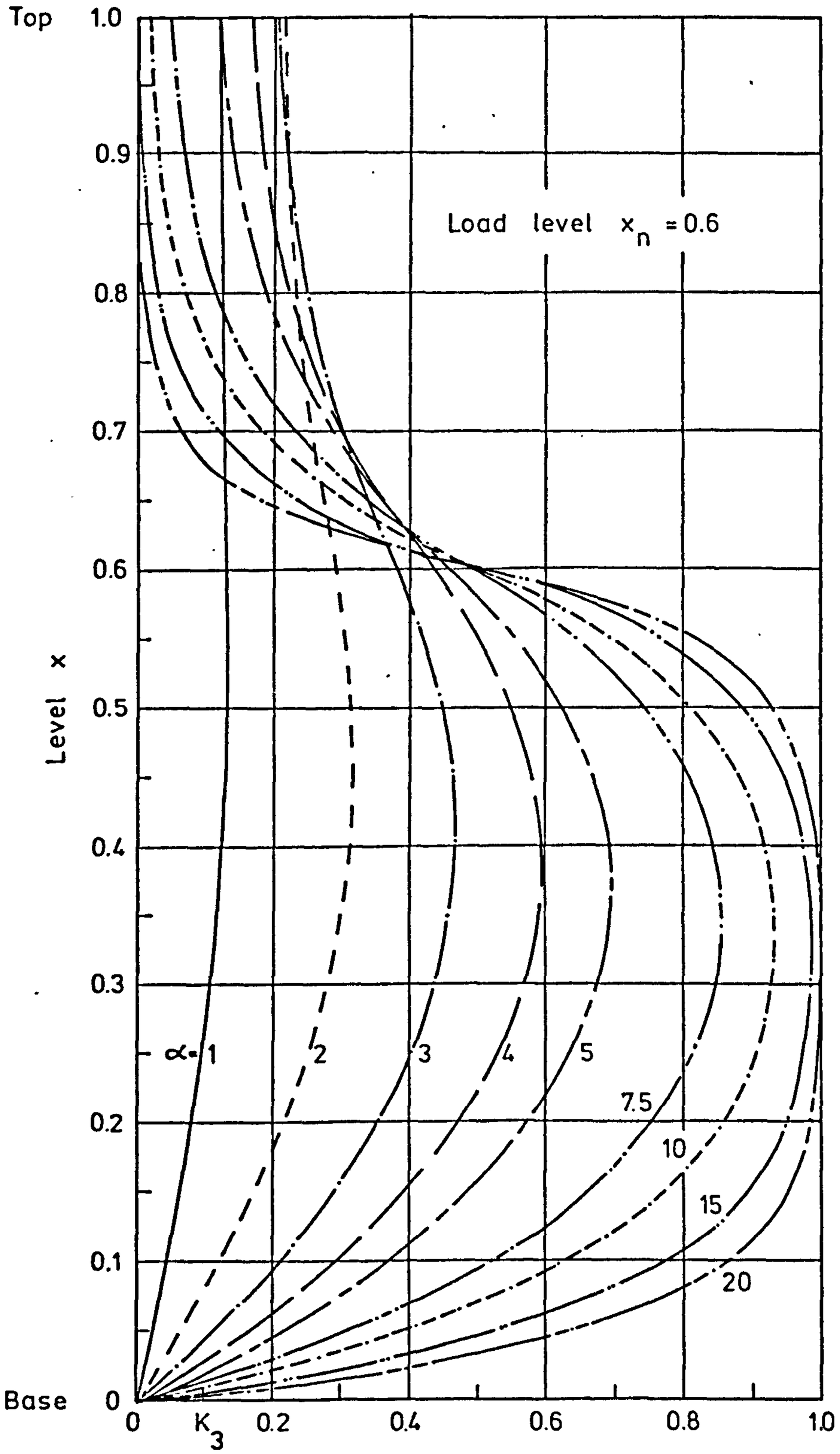

Variation of connecting medium shear stress factor, K_3 - Point load (6)

Figure A.30

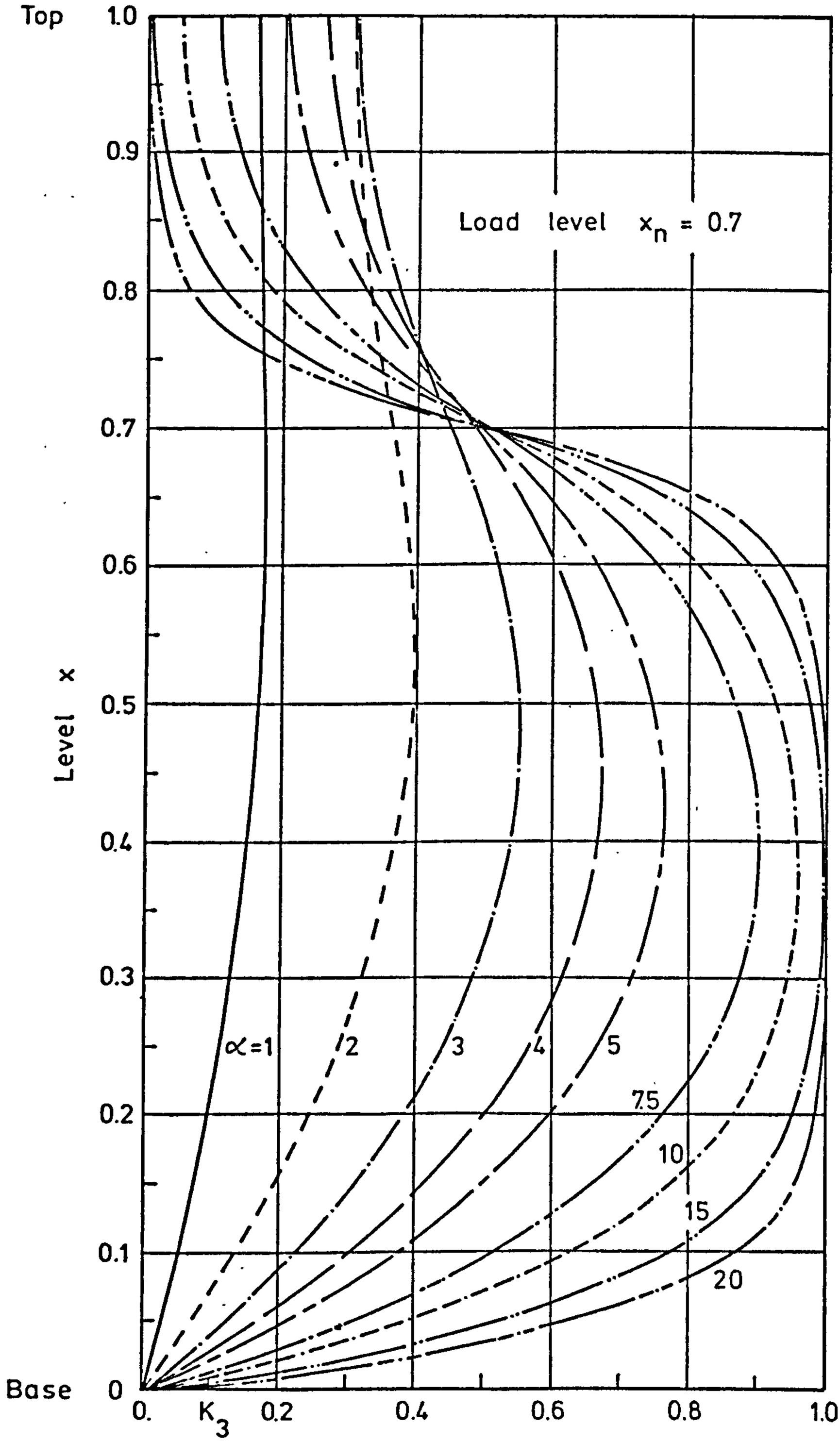

Variation of connecting medium shear stress factor , K_3
- Point load (7)

Figure A.31

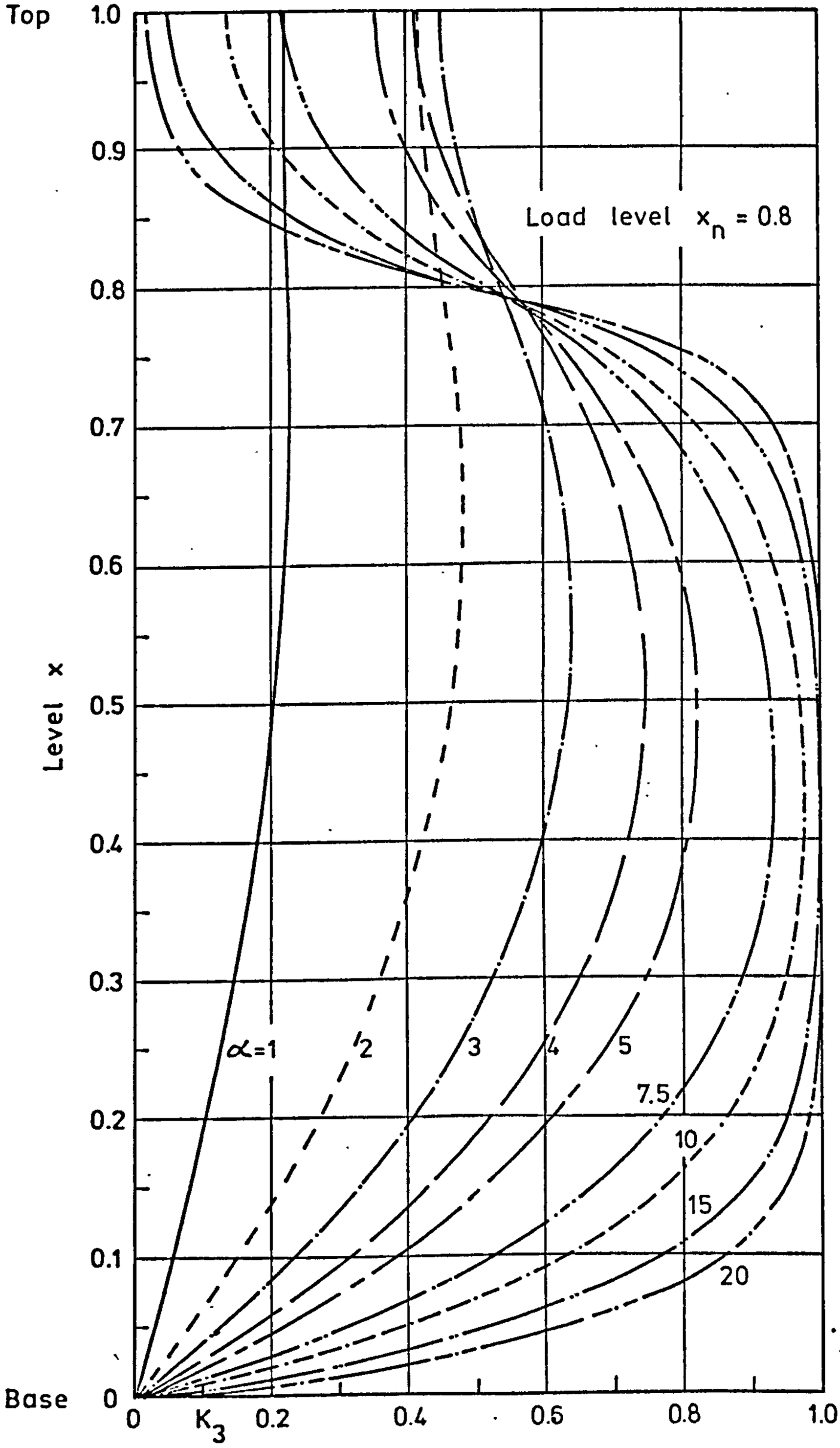

Variation of connecting medium shear stress factor , K_3
- Point load (8)

Figure A.32

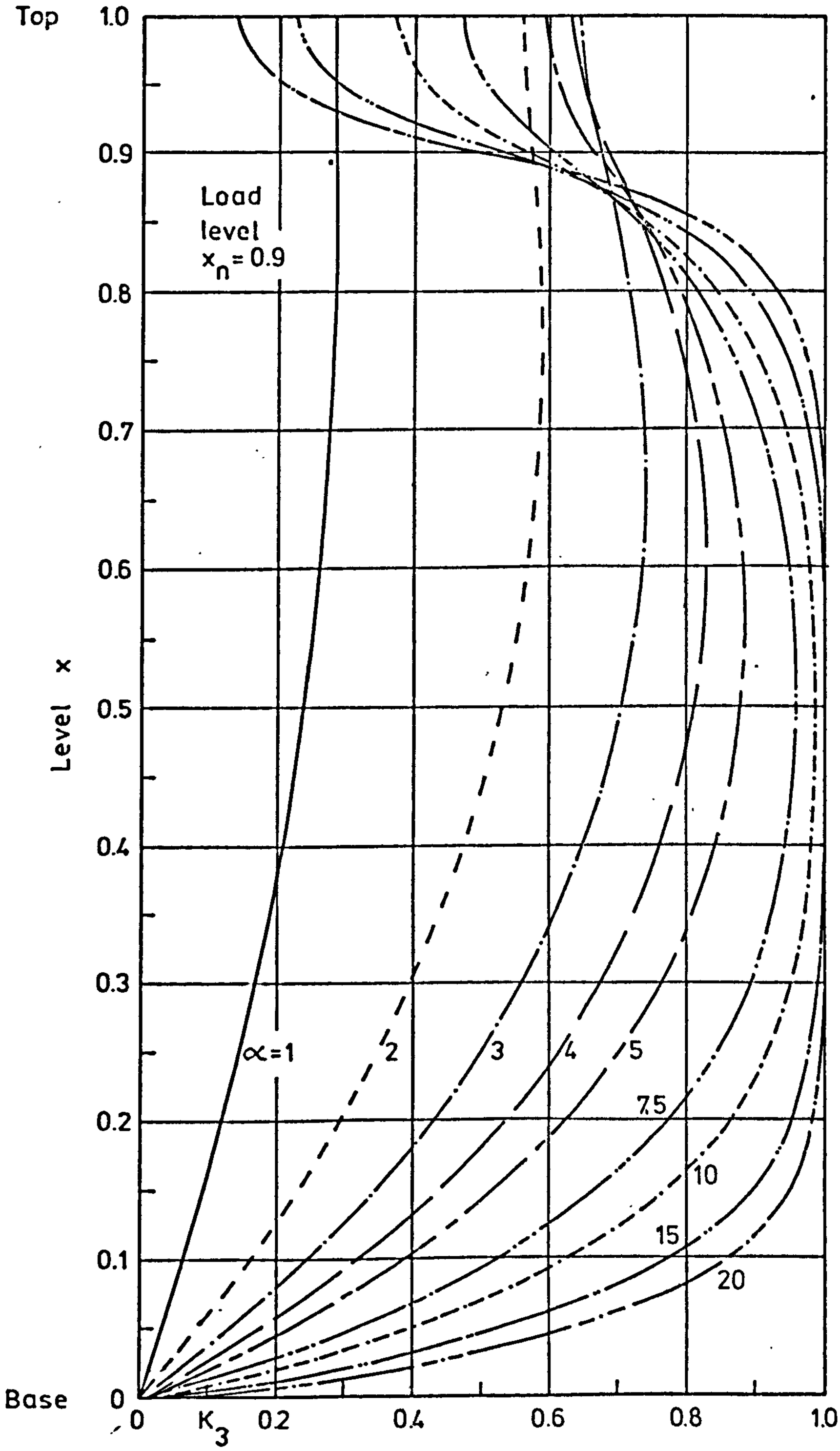

Variation of connecting medium shear stress factor , K_3
- Point load (9)

Figure A.33

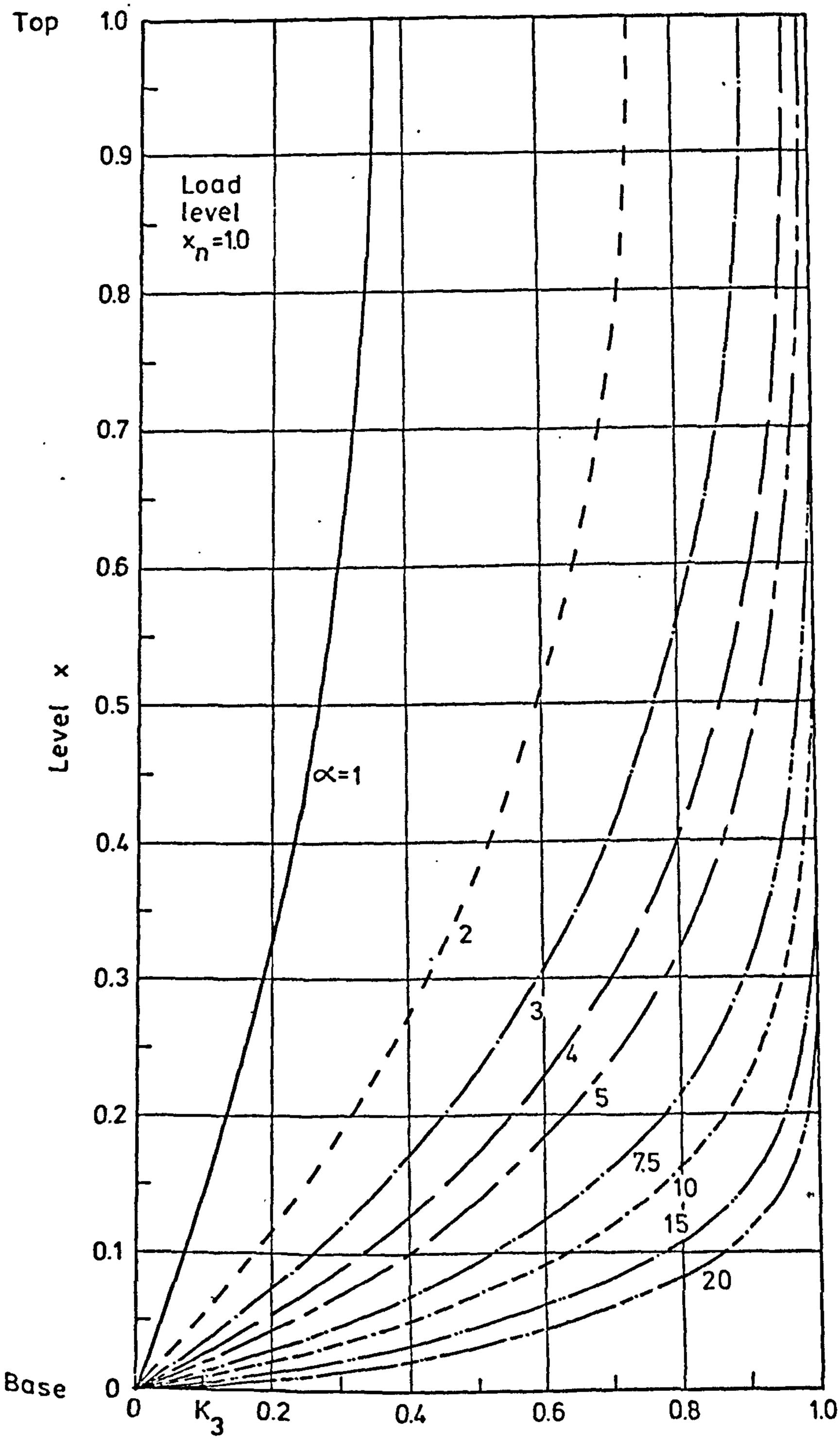

Variation of connecting medium shear stress factor , K_3 - Point load (10)

Figure A.34

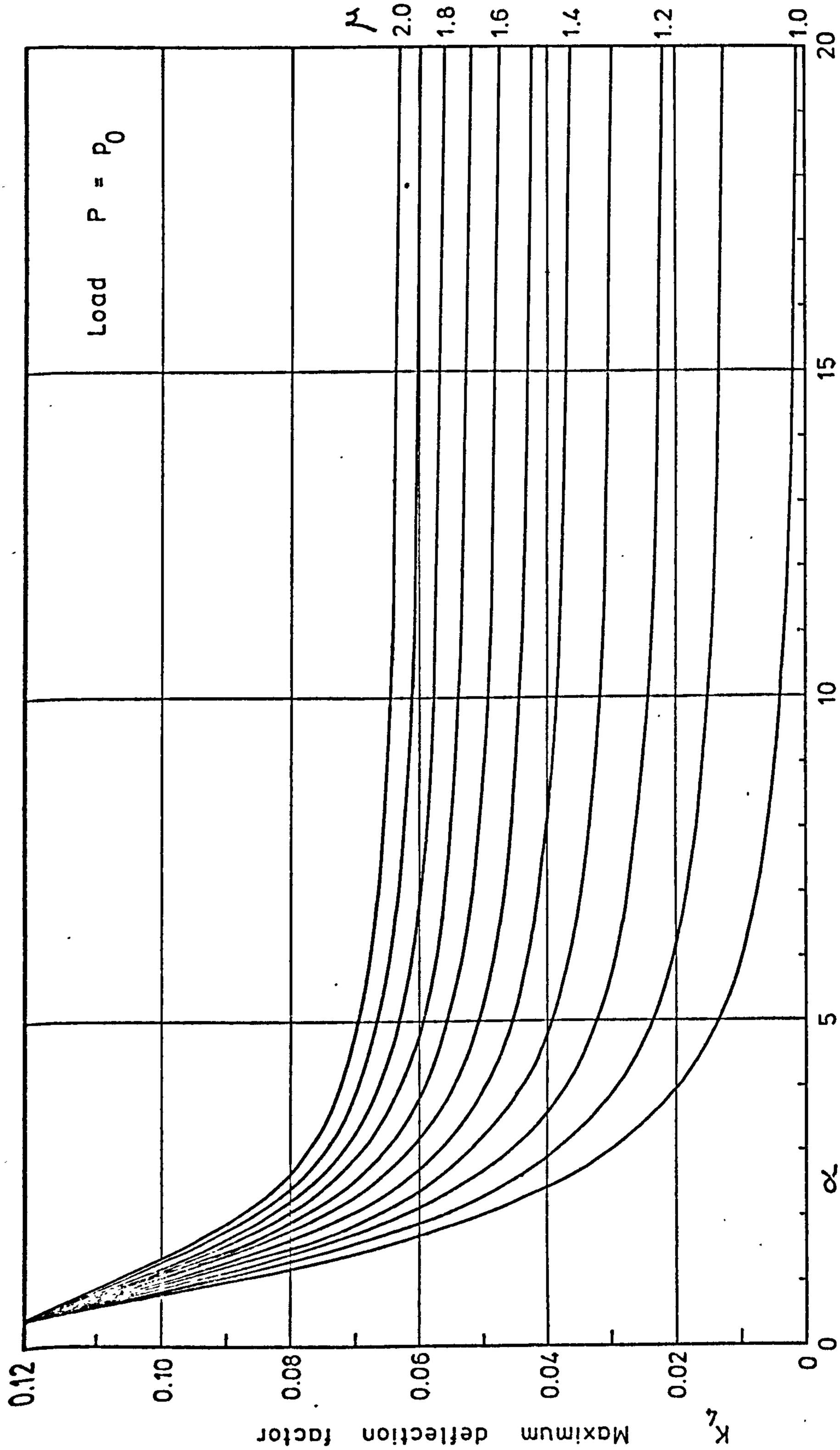

Variation of maximum deflection factor , K_4 - Polynomial load (1)

Figure A.35

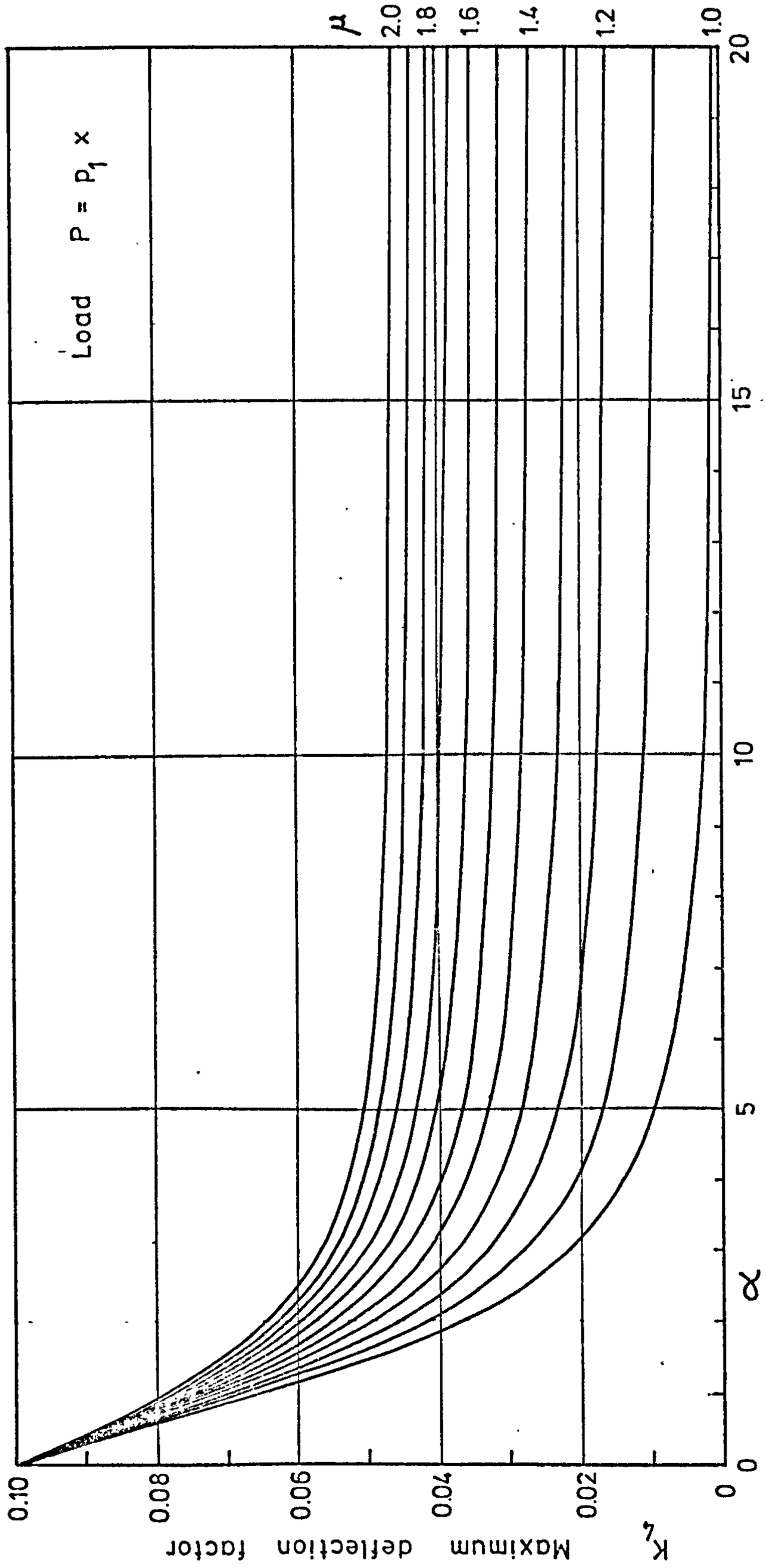

Variation of maximum deflection factor , K_4 - Polynomial load (2)

Figure A.36

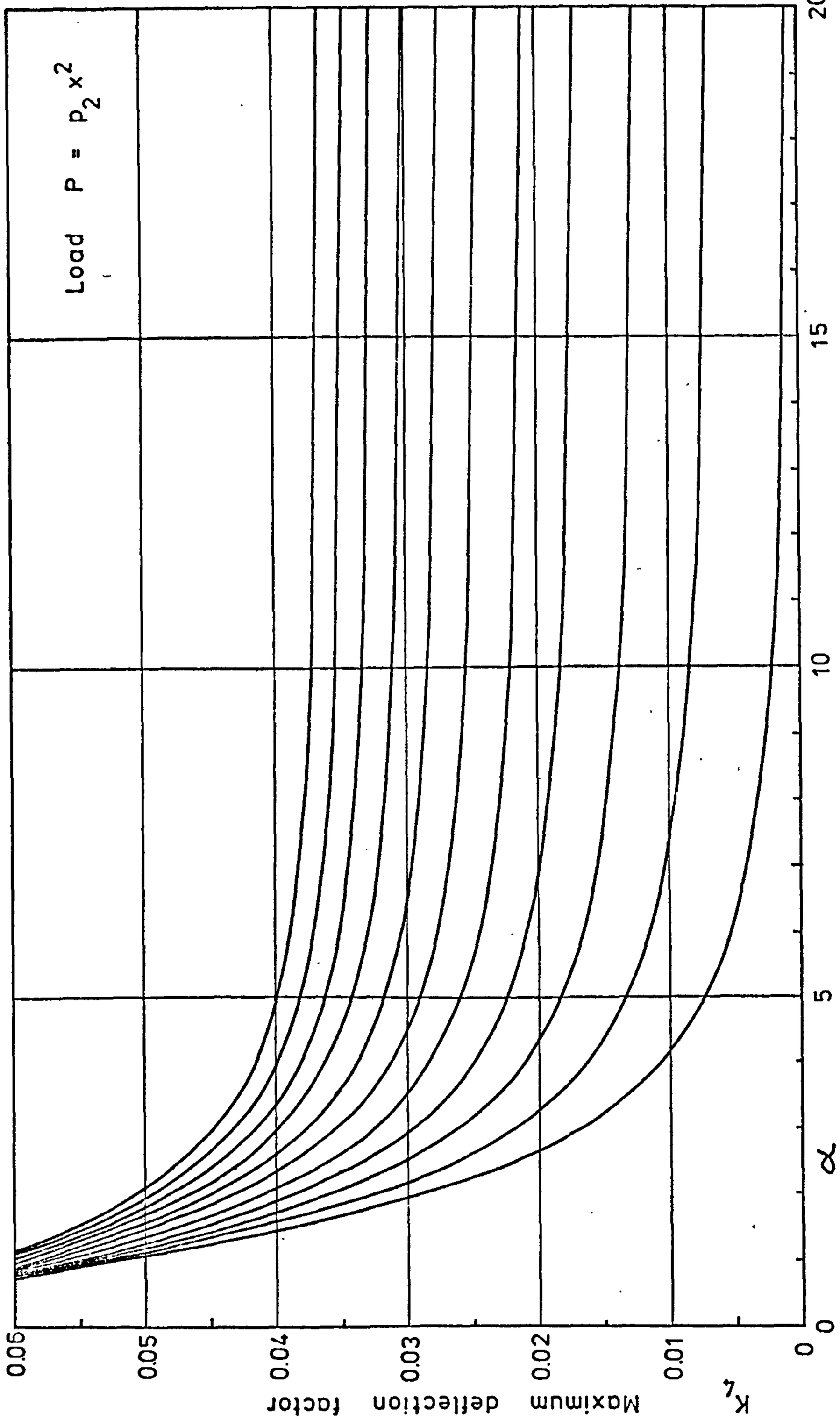
Load P = $p_2 x^2$
μ
2.0
1.8
1.6
1.4
1.2
1.0
20
15
10
5
0
α
0.06
0.05
0.04
0.03
0.02
0.01
0
K_4
Maximum deflection factor
Variation of maximum deflection factor , K_4 - Polynomial load (3)

Figure A.37

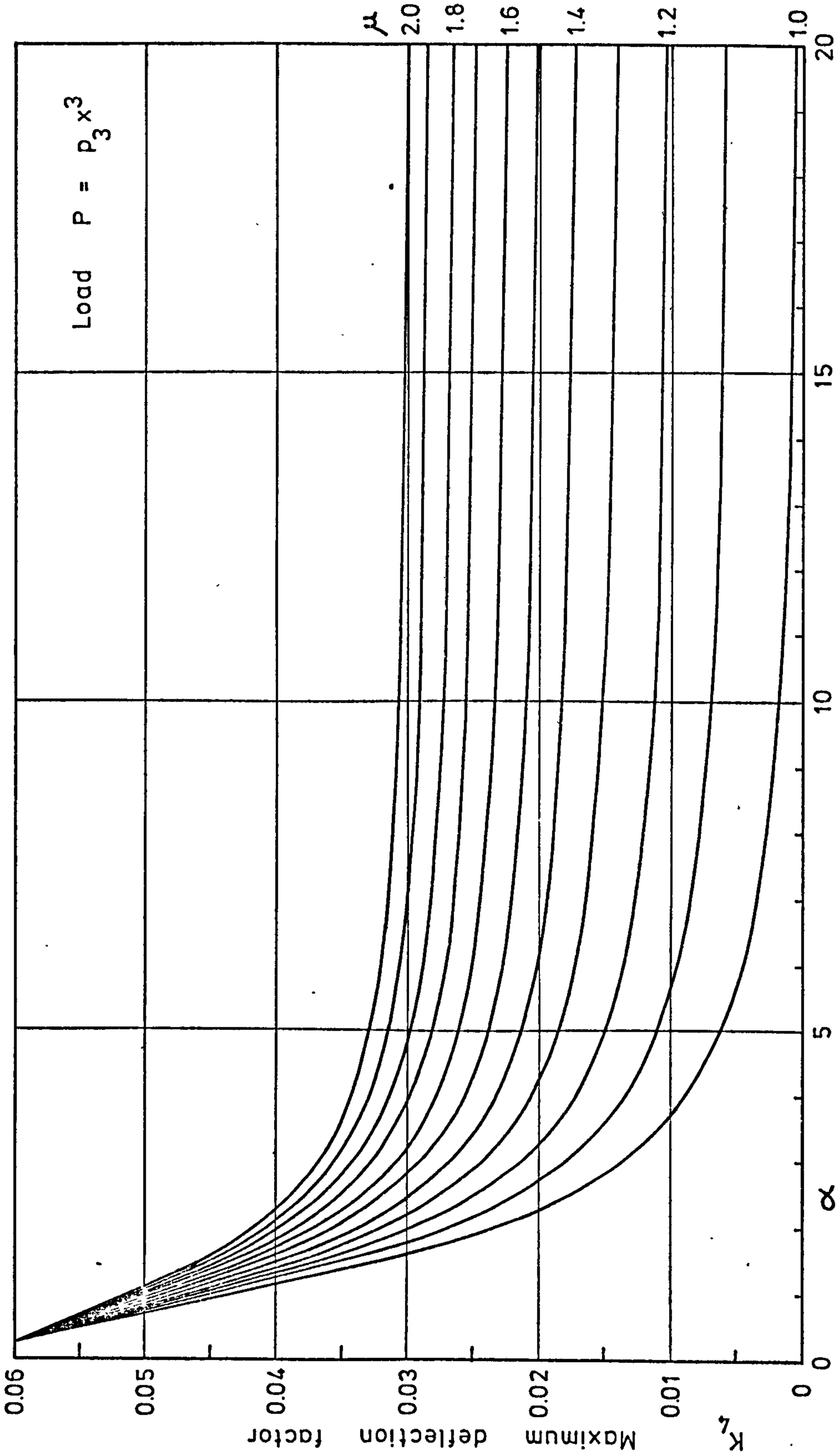

Variation of maximum deflection factor . K_4 - Polynomial load (4)

Figure A.38

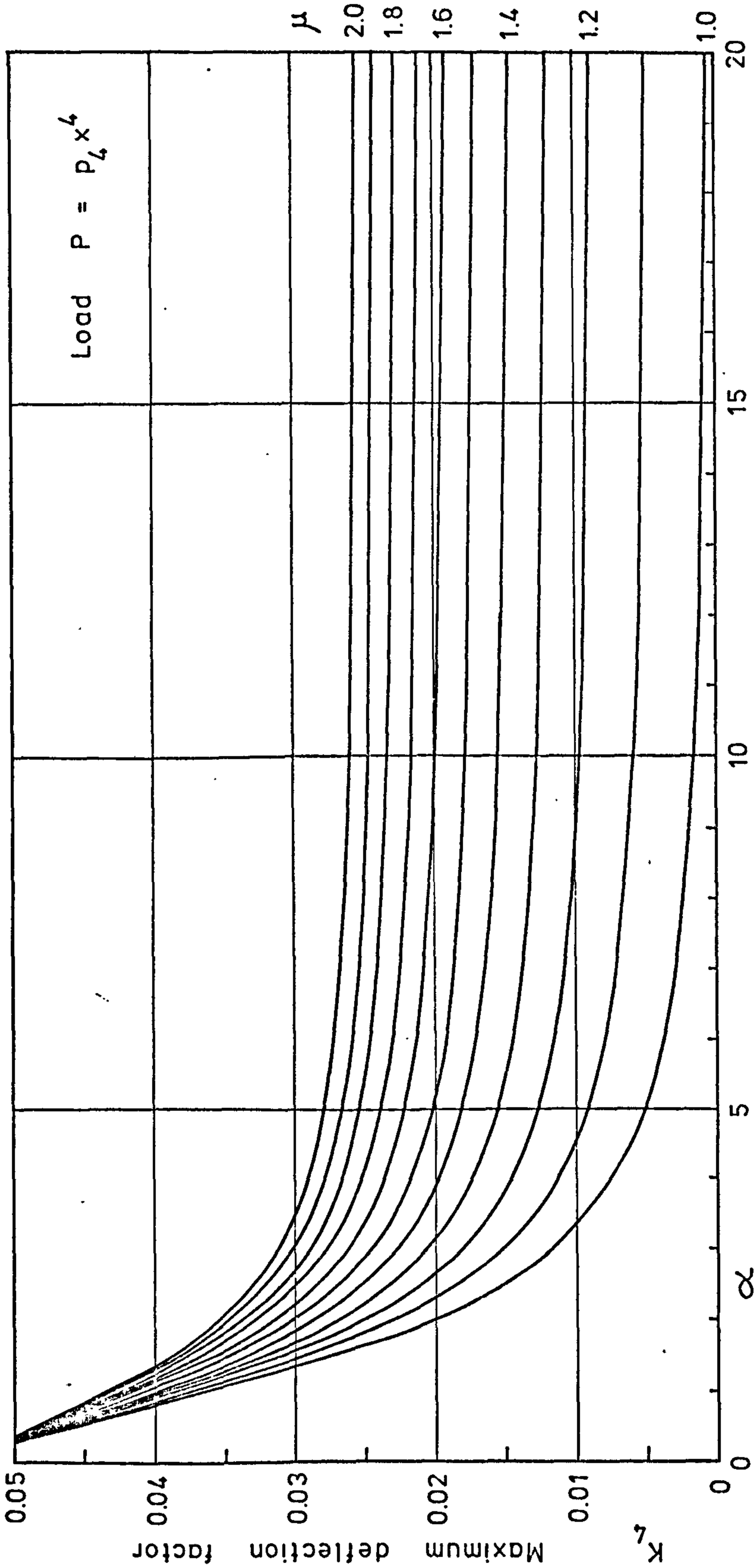

Variation of maximum deflection factor , K_4 - Polynomial load (5)

Figure A.39

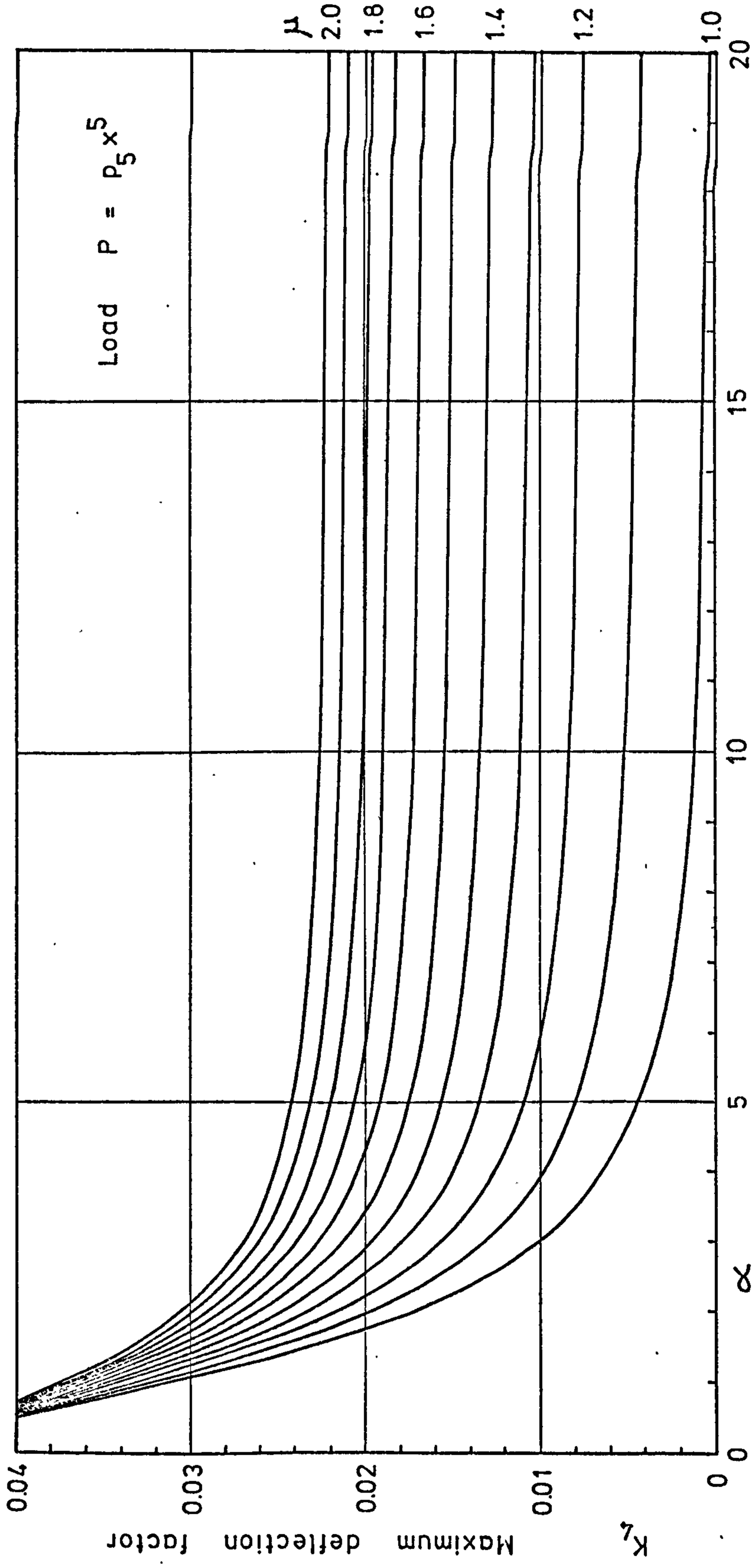
Load P = $p_5 x^5$
μ
2.0
1.8
1.6
1.4
1.2
1.0
20
15
10
5
0
α
0.04
0.03
0.02
0.01
0
K_4
Maximum deflection factor
Variation of maximum deflection factor , K_4 - Polynomial load (6)

Figure A.40

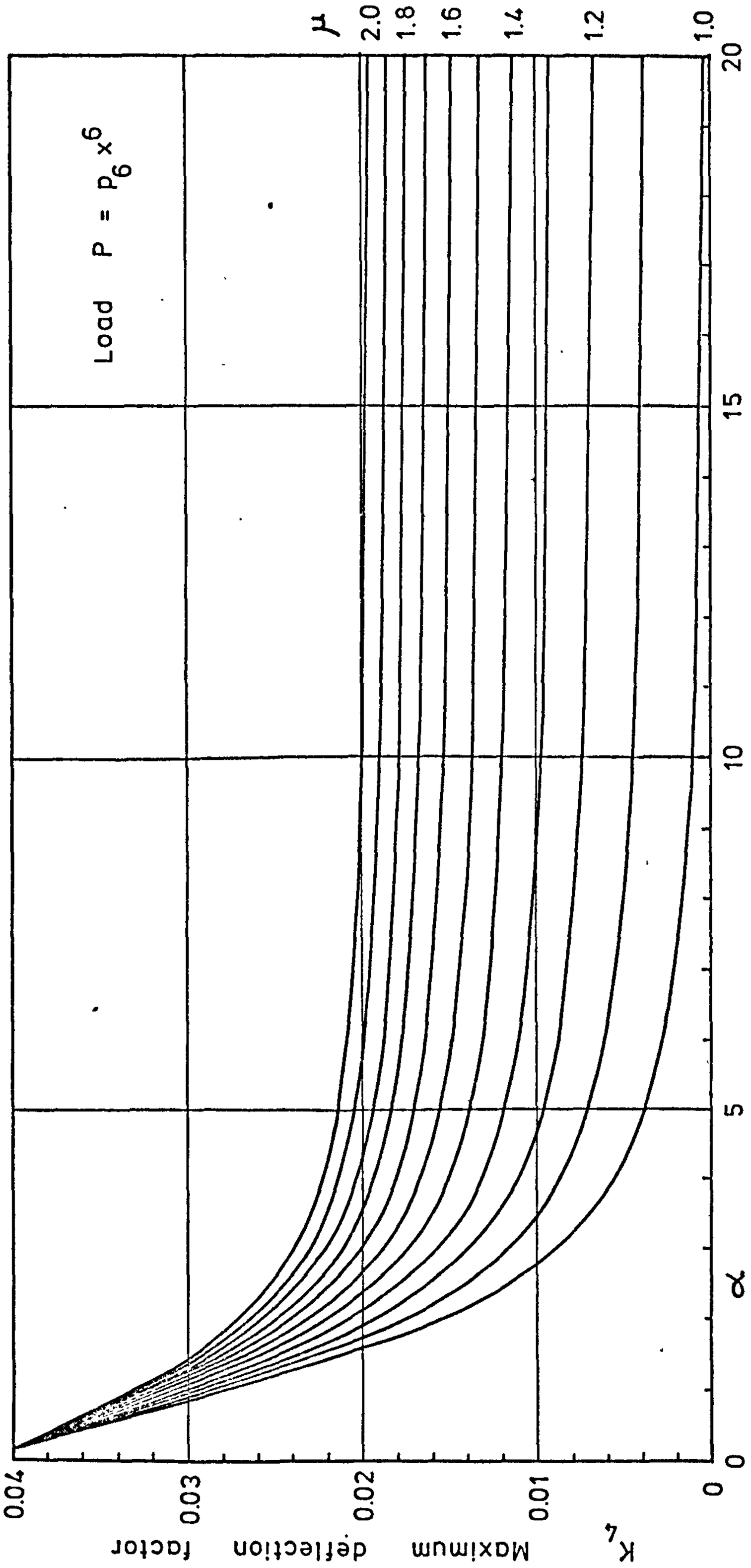

Variation of maximum deflection factor . K_4 - Polynomial load (7)

Figure A.41

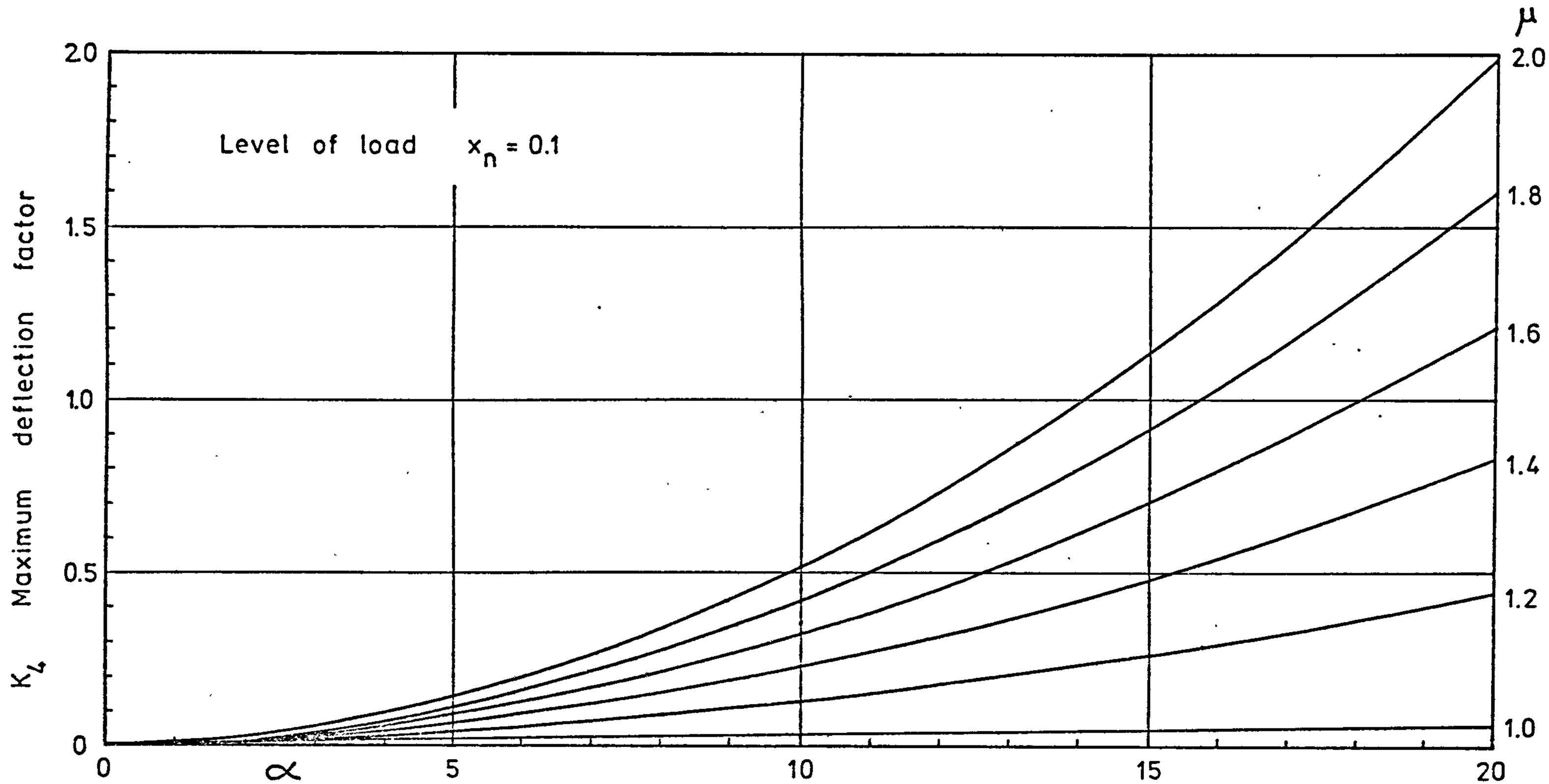

Variation of maximum deflection factor , K_4 - Point load (1)

Figure A.42

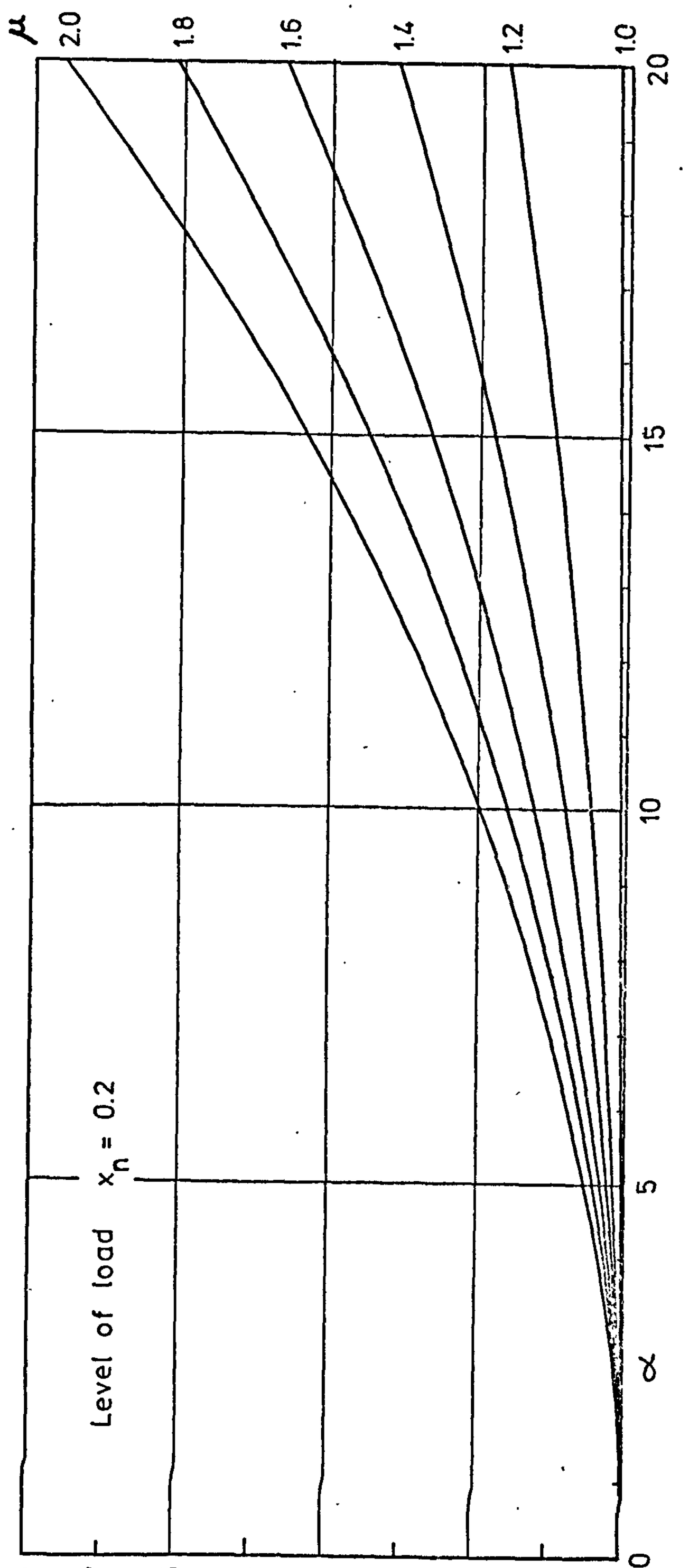

Variation of maximum deflection factor . K_4 - Point load (2)

Figure A.43

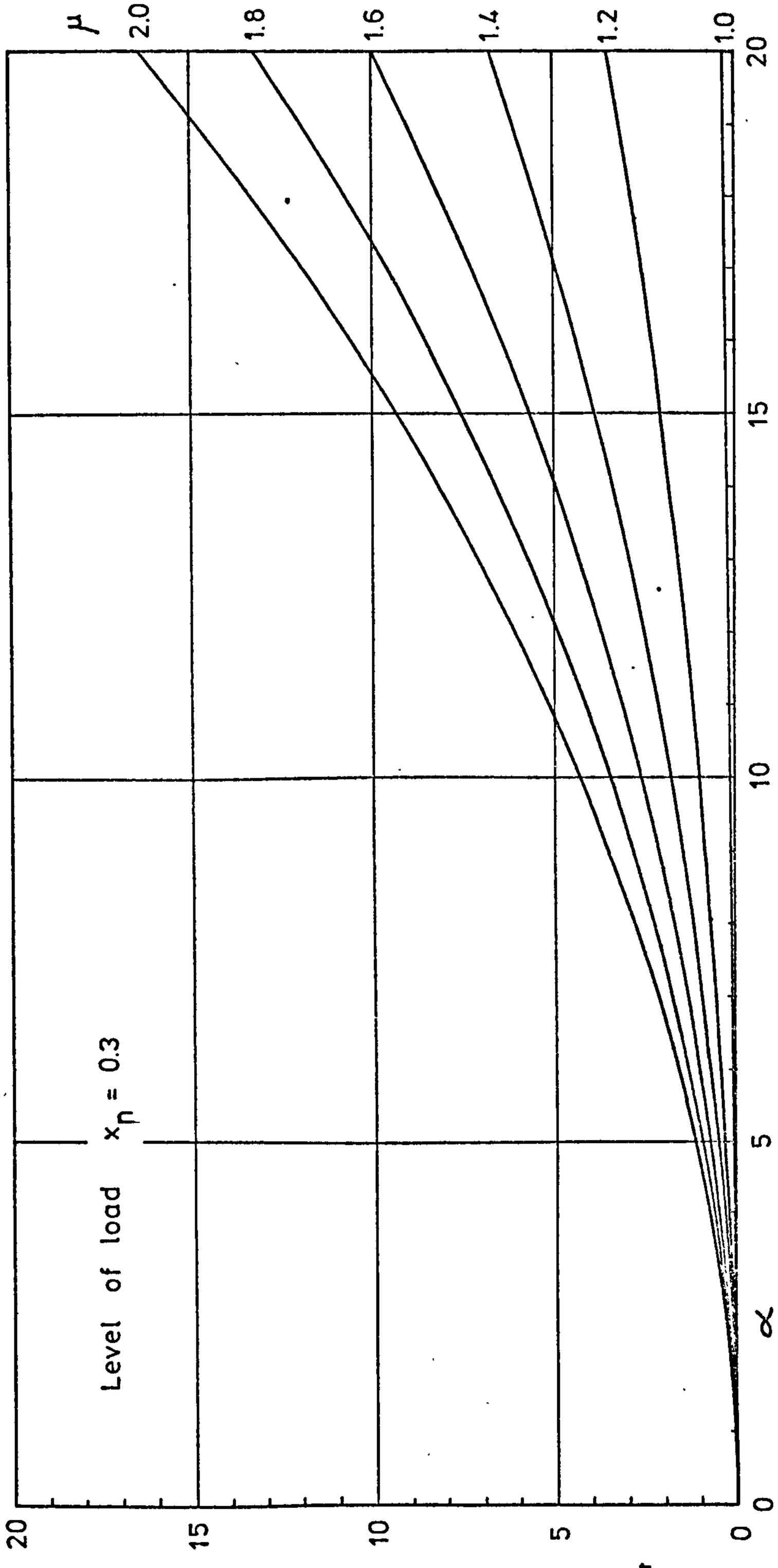
μ
2.0
1.8
1.6
1.4
1.2
1.0
20
15
10
5
0
Level of load x_n = 0.3
Variation of maximum deflection factor , K_4 - Point load (3)
K_4 Maximum deflection factor
α

Figure A.44

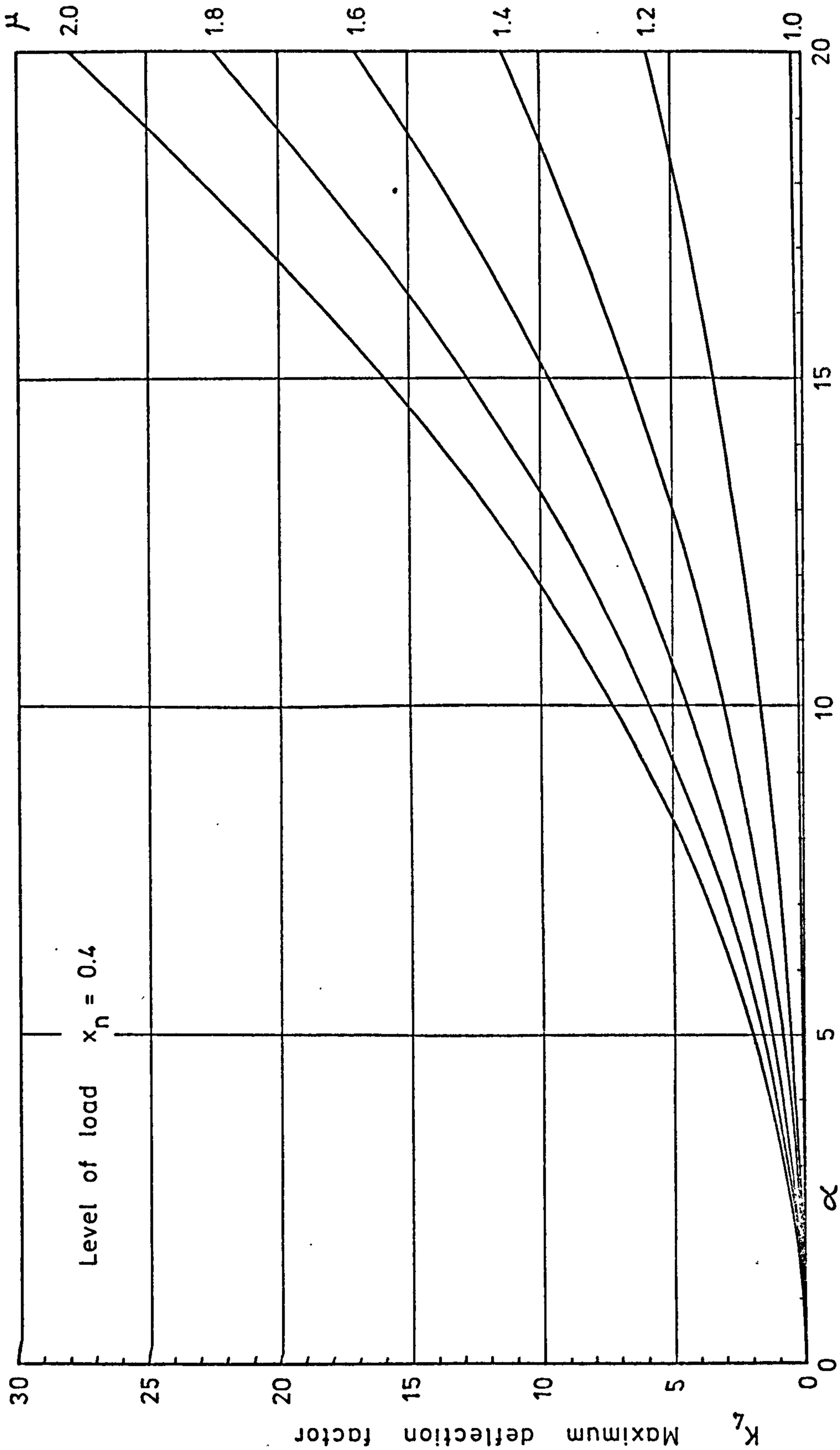
μ
2.0
1.8
1.6
1.4
1.2
1.0
20
15
10
5
0
Level of load x_n = 0.4
α
Variation of maximum deflection factor . K_4 - Point load (4)
K_7 Maximum deflection factor
30
25
20
15
10
5
0

Figure A.45

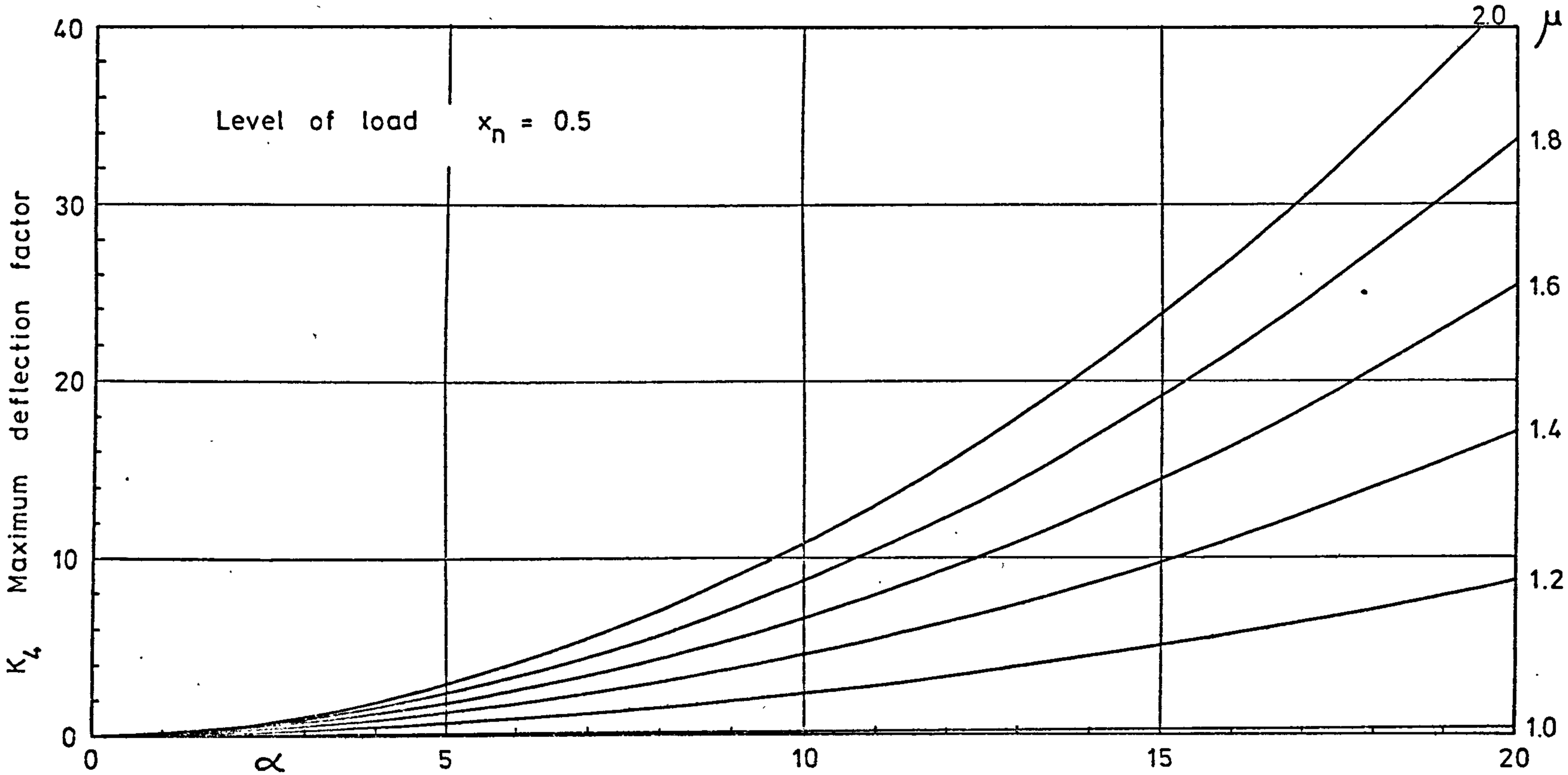

Variation of maximum deflection factor , K_4 - Point load (5)

Figure A.46

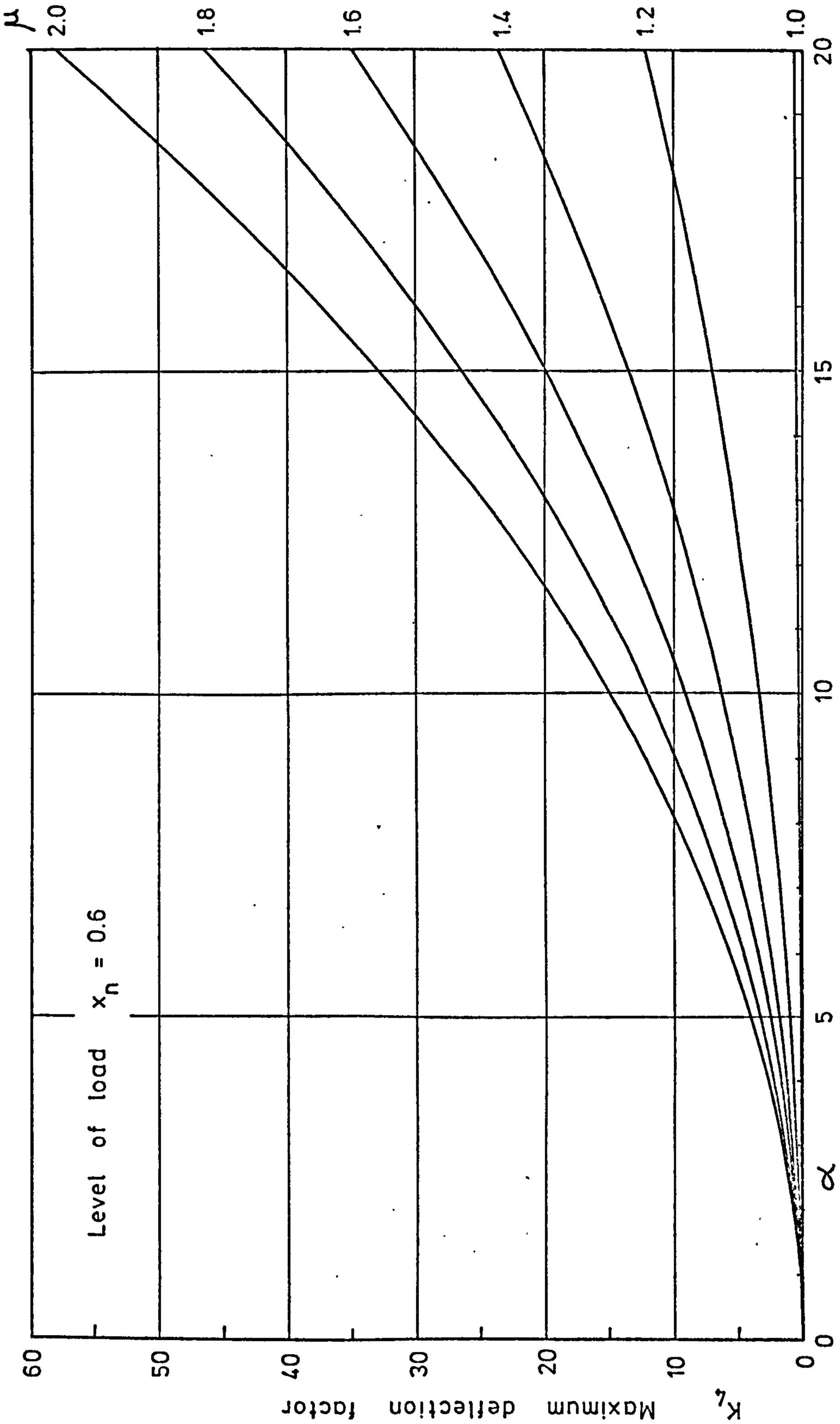

Variation of maximum deflection function . K_4 - Point load (6)

Figure A.47

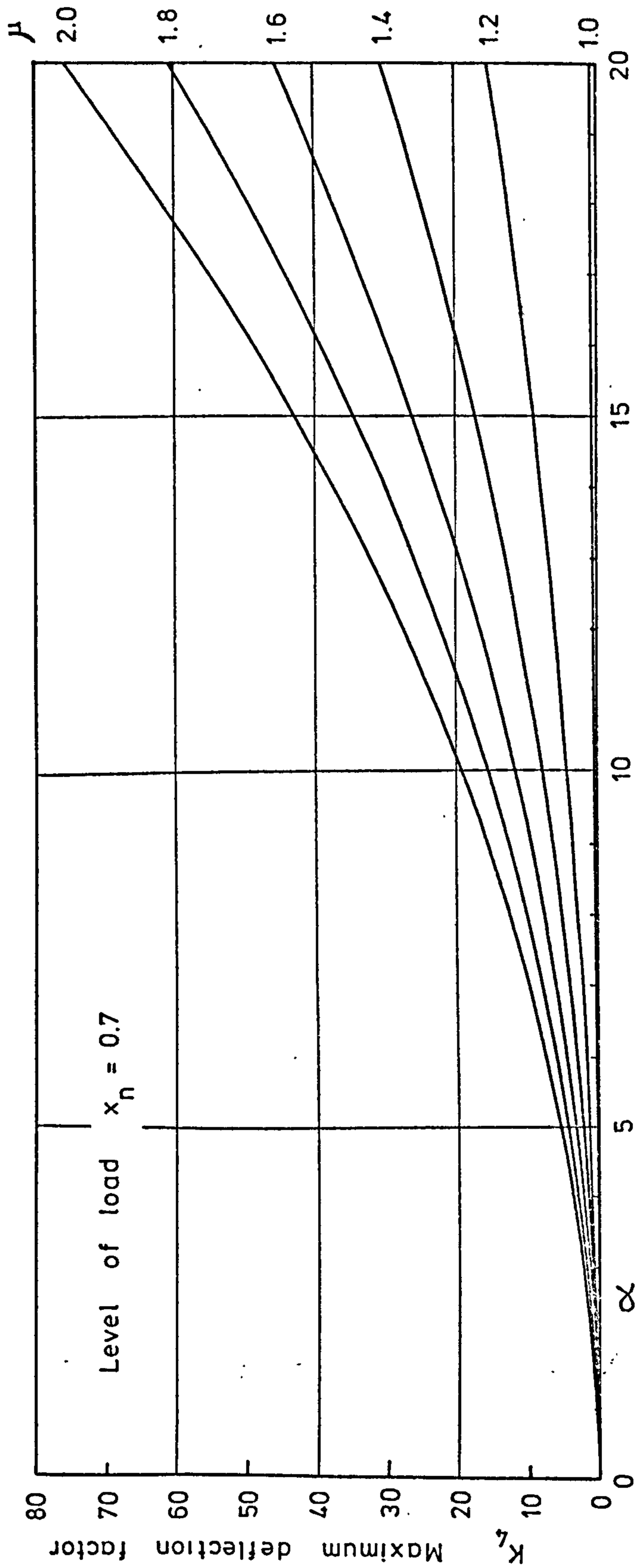
μ
2.0
1.8
1.6
1.4
1.2
1.0
20
15
10
5
0
Level of load x_n = 0.7
Variation of maximum deflection factor , K_4 - Point load (7)
α
0
10
20
30
40
50
60
70
80
K_4 Maximum deflection factor

Figure A.48

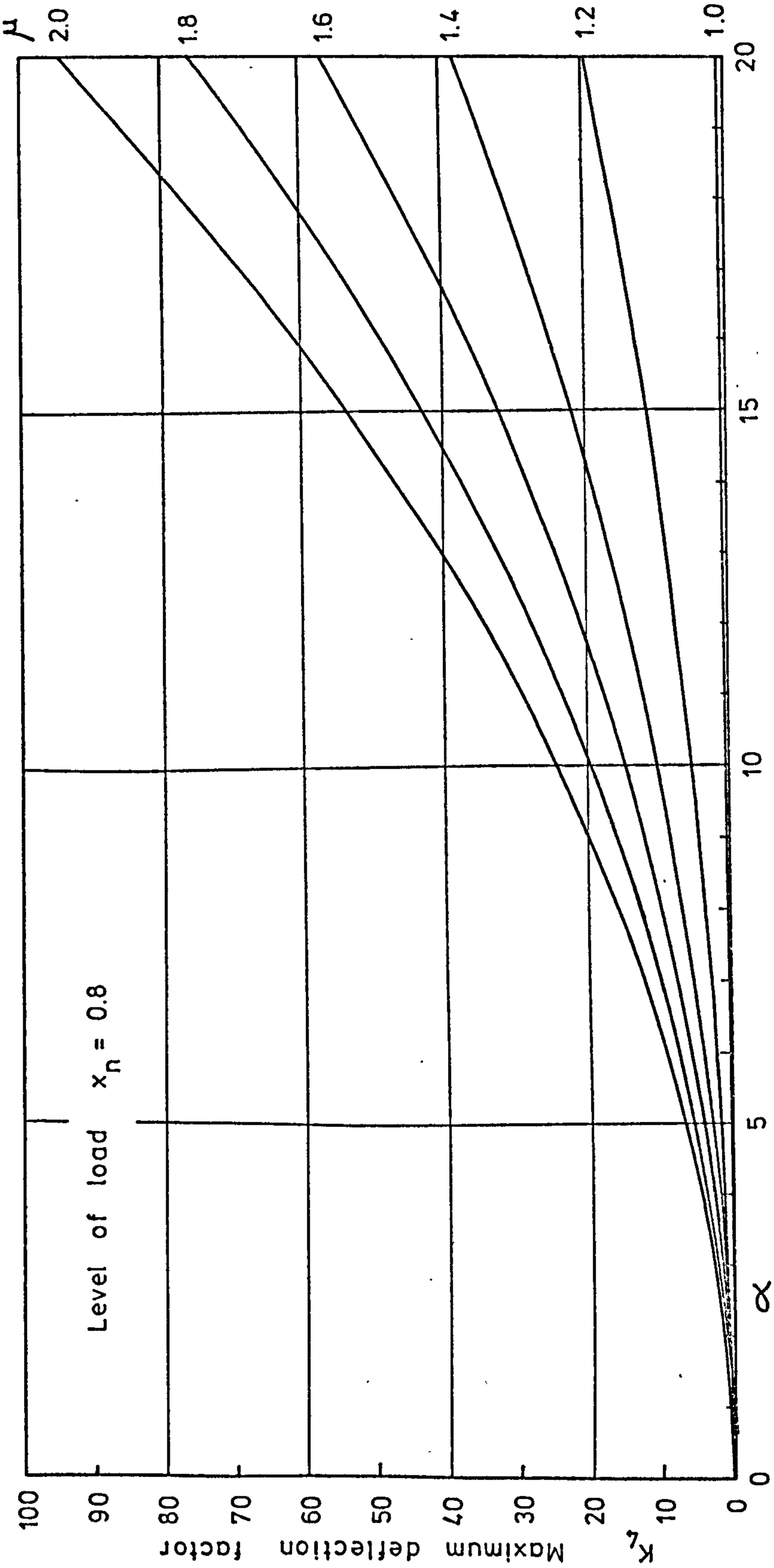

Variation of maximum deflection factor , K_4 - Point

Figure A.49

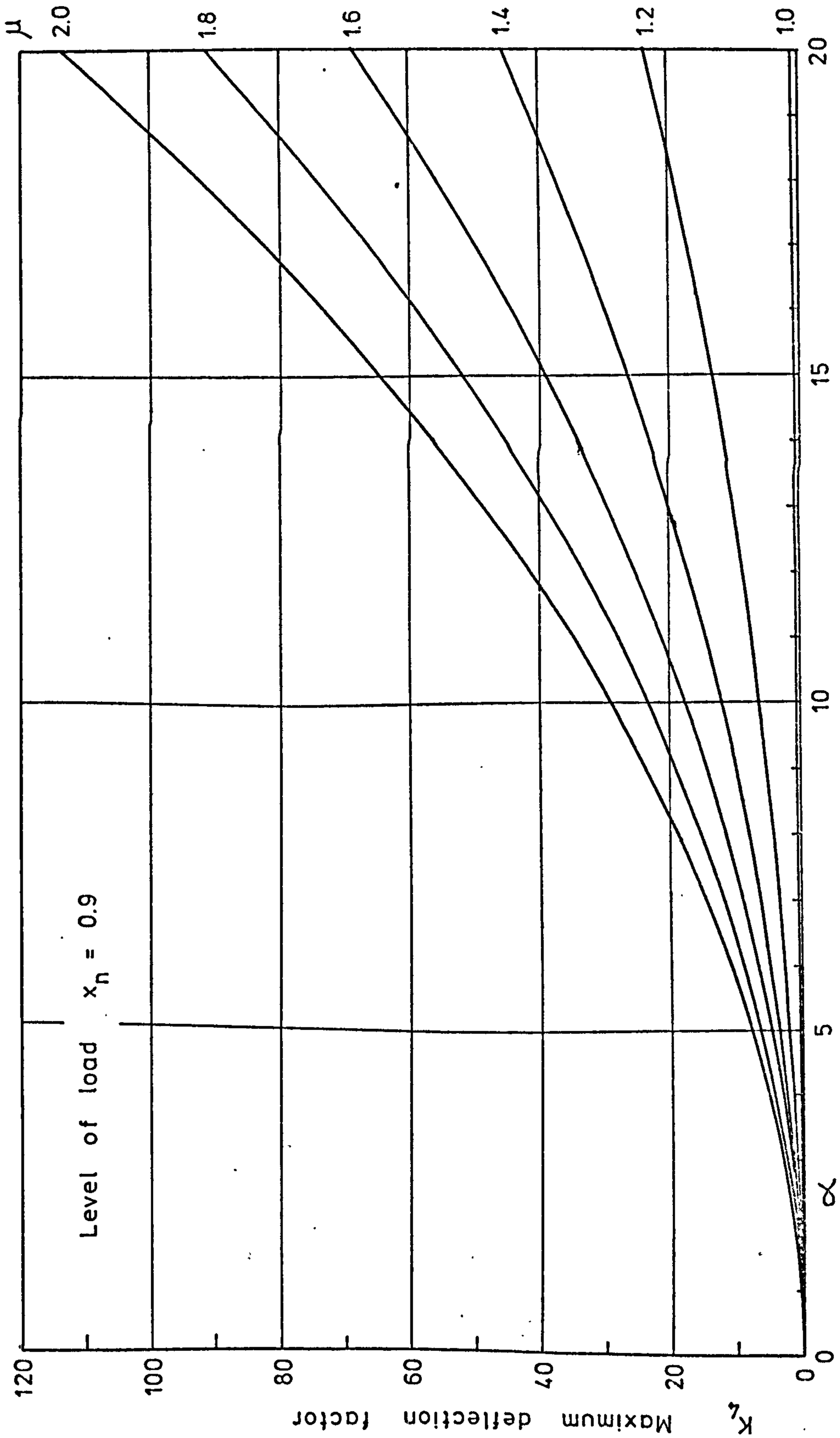
μ
2.0
1.8
1.6
1.4
1.2
1.0
20
15
10
5
0
Point load (9)
Variation of maximum deflection factor , K_4
Level of load x_n = 0.9
α
120
100
80
60
40
20
0
K_4 Maximum deflection factor

Figure A.50

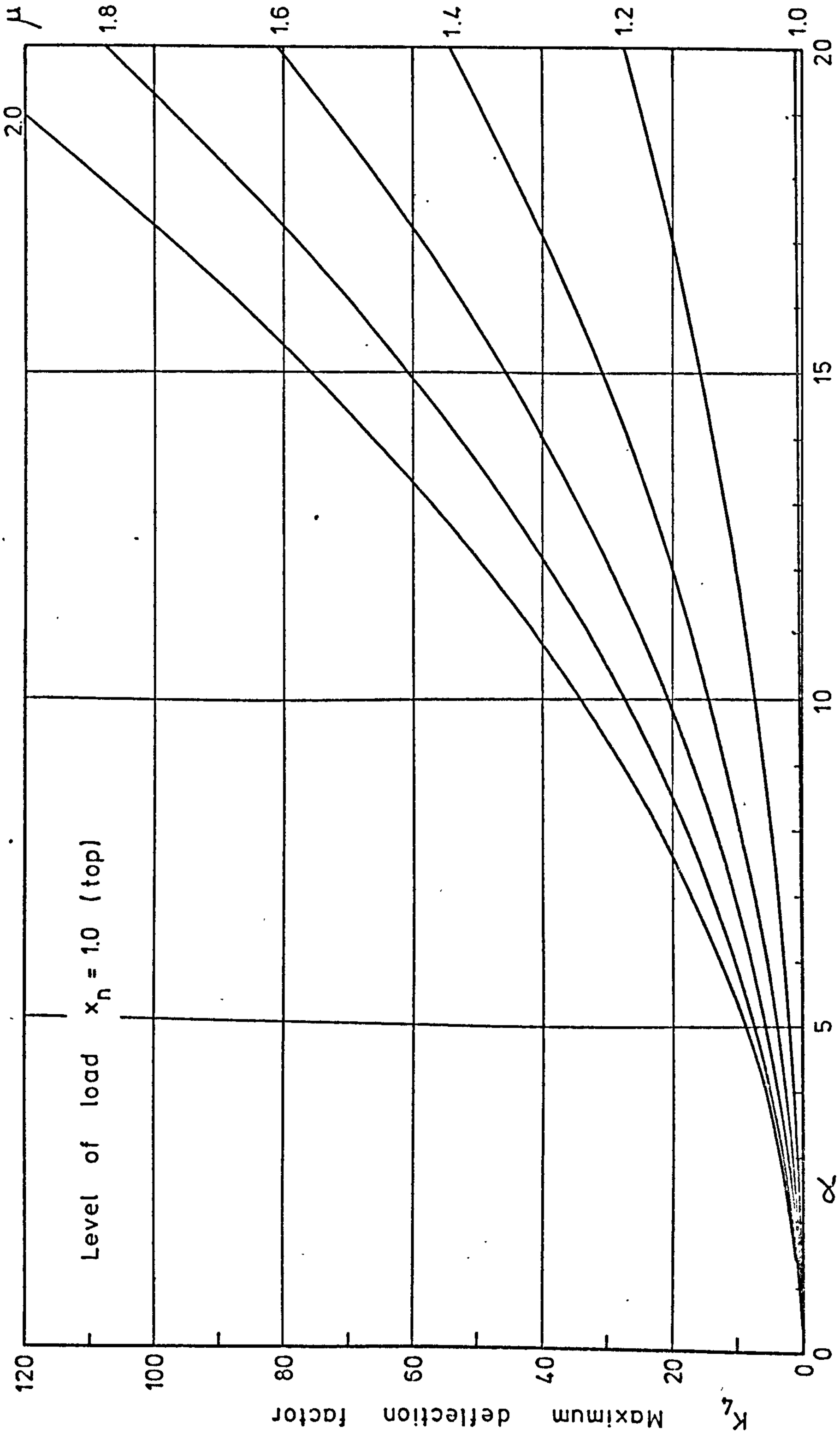
μ
1.8
1.6
1.4
1.2
1.0
2.0
20
15
10
5
0
Point load (10)
Level of load x_n = 1.0 (top)
Variation of maximum deflection factor , K_4 - α
K_4 Maximum deflection factor
120
100
80
60
40
20
0

Figure A.51